

Uranium exploration data and techniques applied to the preparation of radioelement maps

*Proceedings of a Technical Committee meeting
held in Vienna, 13–17 May 1996*



INTERNATIONAL ATOMIC ENERGY AGENCY

IAEA

The IAEA does not normally maintain stocks of reports in this series.
However, microfiche copies of these reports can be obtained from

INIS Clearinghouse
International Atomic Energy Agency
Wagramerstrasse 5
P.O. Box 100
A-1400 Vienna, Austria

Orders should be accompanied by prepayment of Austrian Schillings 100,—
in the form of a cheque or in the form of IAEA microfiche service coupons
which may be ordered separately from the INIS Clearinghouse.

The originating Section of this publication in the IAEA was:

Nuclear Fuel Cycle and Materials Section
International Atomic Energy Agency
Wagramerstrasse 5
P.O. Box 100
A-1400 Vienna, Austria

URANIUM EXPLORATION DATA AND TECHNIQUES APPLIED TO
THE PREPARATION OF RADIOELEMENT MAPS

IAEA, VIENNA, 1997
IAEA-TECDOC-980
ISSN 1011-4289

© IAEA, 1997

Printed by the IAEA in Austria
November 1997

FOREWORD

The earth's natural environment is determined by the underlying geology and its derivatives, modified by the local biosphere and climatic conditions. Reliable baseline information provides a better understanding of the diversified environment and can help monitoring the environment.

The treatment of exploration data is a discipline which is improving rapidly with the emerging geographic integrated system and satellite imagery. Progress made in the radiometric survey and geochemistry of radionuclides, allowing measurement of minute amounts of material and their integration with other data, provides a better understanding and knowledge of the natural distribution and background of various elements in different geological formations. It is now possible to understand different environmental situations and locate anomalous areas that are due to a natural phenomenon or are produced by human activities.

For many years the IAEA has been involved in the treatment of exploration data and their multiple applications related to mineral commodities, environmental assessment, siting of NPPs or agricultural application.

With the implementation of stricter environmental regulations imposed on the mining industry after the Chernobyl accident it became evident that geochemical and geophysical surveys carried out for the purpose of resource exploitation were multidisciplinary in nature and could be used in other disciplines, particularly in the monitoring of the environment. It is with this appreciation and the recognition that techniques and methods are progressing very fast that the IAEA convened a second Technical Committee meeting with the purpose of bringing together experts in uranium exploration, geophysics and geochemistry to discuss and exchange information on the treatment of exploration data, their use and relevance for other disciplines and the techniques used to collect these data as well as the multiple use of the data.

The Technical Committee Meeting to Review the Advantage and Pitfalls of Using Uranium Exploration Data and Techniques as well as Other Methods for the Preparation of Radioelement and Radon Maps for Baseline Information in Environmental Studies and Monitoring was held in Vienna from 13 to 17 May 1996 and was attended by 62 participants from 30 countries representing government organizations, universities and private industry. The 47 papers provided information on the distribution of radioelements, airborne and ground radiometric surveys, radon mapping and artificial isotopes released into the environment.

The IAEA is grateful to those participants who contributed papers and took part in the discussion. Special thanks are extended to F. Barthel (Germany), A.G. Darnley (Canada) and G. Åkerblom (Sweden) who chaired the sessions.

The IAEA staff member responsible for the organization and implementation of the meeting was J.-P. Nicolet of the Division of Nuclear Power and the Fuel Cycle.

EDITORIAL NOTE

In preparing this publication for press, staff of the IAEA have made up the pages from the original manuscripts as submitted by the authors. The views expressed do not necessarily reflect those of the IAEA, the governments of the nominating Member States or the nominating organizations.

Throughout the text names of Member States are retained as they were when the text was compiled.

The use of particular designations of countries or territories does not imply any judgement by the publisher, the IAEA, as to the legal status of such countries or territories, of their authorities and institutions or of the delimitation of their boundaries.

The mention of names of specific companies or products (whether or not indicated as registered) does not imply any intention to infringe proprietary rights, nor should it be construed as an endorsement or recommendation on the part of the IAEA.

The authors are responsible for having obtained the necessary permission for the IAEA to reproduce, translate or use material from sources already protected by copyrights.

CONTENTS

Summary	7
Uranium exploration data and global geochemical baselines: The need for co-ordinated action ... <i>A G Darnley</i>	9
Terrestrial radiation — A project for central and eastern Europe (<i>Abstract</i>) <i>M Matolin, G Sideris</i>	17
The Marna Project <i>E. Suarez Mahou, J.A Fernandez Amigot</i>	19
Construction of radioelement and dose rate baseline maps by combining ground and airborne radiometric data <i>L Rybach, F Medici, G.F. Schwarz</i>	33
Background radiation map of Thailand <i>P Angsuwathana, P. Chotikanatis</i>	45
Terrestrial gamma dose rate maps, their compilation and verification — radiometric map of the Czech Republic <i>M Matolin</i>	53
Compilation, back-calibration and standardization of aerodiometric surveys from Namibia, southern Africa <i>A Duffy, D.G Eberle, R.L Grasty, D G Hutchins, W.E.S Urquhart</i>	59
Airborne gamma ray spectrometry in certain areas of the Islamic Republic of Iran and its results — correlation to the other usages <i>Gh. Soleimani, F.Sh Yegani</i>	67
Correlation between natural gamma activity and the geological means in the province of Salamanca <i>E Suarez Mahou, J.A Fernandez Amigot</i>	77
Natural background radiation in Jordan <i>M N Daoud</i>	91
Radiometric maps of Israel — Partial contribution to the understanding of potential radon emanations <i>D. Vulkan, H Shirav</i>	119
Distribution of natural (U, Th and K) and artificial (Cs-137) radioelements in the flood plain deposits of northern Hungary <i>L Ódor, I Horváth, H Fügedi, J Renner</i>	125
Spatial distribution of ^{40}K , ^{228}Ra , ^{226}Ra , ^{238}U and ^{137}Cs in surface soil layer observed at small areas <i>D. Barišić, S. Lulić, E. Prohić, M. Čulinović</i>	135
Radioecological mapping of the territory of Belarus on the base information of radiation monitoring <i>M G Guermentchuck, O.M Zhukova, E.D Shagalova, I I Matveencko</i>	153
Mapping of post-Chernobyl environmental pollution in Poland <i>R. Strzelecki, S. Wolkowicz, P. Lewandowski</i>	163
Use and results of the aerial gamma mapping system during the international exercise R.E.S.U.M.E. 95 (Rapid environmental surveying using mobile equipment) in Finland ... <i>Ch Bourgeois, J. Bresson, R. Chastel, Th Chiffot,</i> <i>L Guillot, J.-C Kruajutch, C. Bergey</i>	173
Quantitative Cs-137 distributions from airborne gamma ray data <i>G Oberlercher, W. Seiberl</i>	181
Field Ge gamma spectrometry for on site measurements of some parameters characterizing radon-222 exhalation rates from soils and covers <i>P Zettwoog, I Kobal, J.F Pineau</i>	193
Application of sensitive and supersensitive radon detectors for radon flux density and radon concentration in environmental monitoring <i>W Zahorowski, S Whittlestone</i>	223

Mapping of groundwater radon potential	237
<i>G. Åkerblom, J. Lindgren</i>	
The role of house surveys in geological radon potential mapping	257
<i>K. Ball</i>	
Airborne and truck-borne "radiation footprints" of areas producing, storing, using or being exposed to nuclear materials	269
<i>B. Pavlik, F. Bottas, P.J. Cuneen, P. Jurza, V. Hoeschl</i>	
Environmental monitoring system based on airborne gamma ray spectrometry developed at Geoinstitut Beograd	279
<i>M. Milojević, V. Štrumberger</i>	
Airborne gamma ray spectrometry — an efficient method for finding and mapping pollution with radioactive elements from uranium extraction and ore mining	299
<i>L.M. Kerbelov, R. Rangelov</i>	
Airborne gamma anomalies in the Elbe Valley near Königstein, Germany — origin and variation with time	305
<i>G. Ruhrman, B. Schemeling, M. Schauer, R. Gatzweiler</i>	
The distribution of radionuclides in the upper soil horizons in Lower Saxony, Saxony and Thuringia, Germany	319
<i>F. Barthel, V. Thoste, K.H. Borsdorf</i>	
Use of isotopic signature of radionuclides released from uranium mines and mills to discriminate low levels of environmental impact against natural background levels	337
<i>P. Zettwoog, N. Lemaitre, S. Bernhard, Y. Vauzelle</i>	
The dispersion of radon in the Stráž-Hamr area in the Czech Republic as an effect of uranium mining and related activities	353
<i>R. Smetana, J. Novák</i>	
New approach to airborne monitoring of radioactive pollution	365
<i>V. Höschl, P. Jurza, B. Pavlik</i>	
Estimate of the radiological state of the "Eleshnitza" uranium deposit, Bulgaria	373
<i>I. Bojkov, T. Tzenov</i>	
The use of uranium exploitation techniques in the selection of a candidate site for Cs-137 radioactive waste from the Goiânia accident	377
<i>S. Saad</i>	
Environmental implications of the laboratory gamma ray spectrometric measurements made on the black sand beach deposit of the Abu Khashaba radioactive prospect, Rosetta, Egypt	389
<i>A.M. Elsirafe, H.A. Hussein, R.A. Elsayed, A.M. Sabri</i>	
Spectrometric aerial survey as a new tool for geological survey and mining prospecting	403
<i>R. Cambon</i>	
Definition of prospective terrains for industrial polymineralic placers in the Mississippi embayment region by use of uranium exploration data	409
<i>A.E. Grosz, W.J. Greenwood, P.G. Schruben, J.N. Grossman</i>	
Advantages of integration of uranium exploration data in GIS and models as tools for decision support	425
<i>M.C.L. Tusveld</i>	
Some practical aspects of computer processing of uranium exploration data for environmental purposes	433
<i>V. Štrumberger, M. Milojević, A. Štrumberger</i>	
Uranium concentration in building materials used in the central region of Egypt	443
<i>R.H. Higgy, M.S. El-Thahawy, A. Ghods</i>	
Preliminary use of uranium exploration data in environmental studies in Greece	455
<i>N. Karistineos</i>	
List of Participants	457

SUMMARY

The meeting was attended by 62 participants from 30 countries, representing government organizations, universities and private industry. A total of 47 papers were given by 29 country representatives. The wide spectrum of subjects has demonstrated the present knowledge on the behaviour of radioelements of natural and artificial origin.

The papers provided information on general aspects of the distribution of radioelements as well as on specific topics. It was pointed out that sustainable development of the world's growing population can only be achieved with a sustainable environment. There is a growing need of a healthy environment where people can live, which provides them with food and appropriate space for housing. The growing need for energy must be satisfied cheaply and with a minimum impact on the environment. The concentration of natural radioelements in our environment is generally in limits below hazard to public health. Careful monitoring is, however, necessary once the radioelements are released by industrial activities. As demonstrated in various examples artificial radioisotopes may have a serious impact on the environment if they are released by accidents at nuclear facilities. Various papers have demonstrated the role of geoscientific research how to manage problems once such accidents happen. Still a number of problems remain to be investigated but geoscientists should inform the public on the results of their research in order to provide a better understanding.

The meeting also showed examples of pitfalls from which one can learn and on which future research can be guided. There is a need for standardization of methods for the determination of background radiation in the various geological environments.

The presentations can be grouped into three major categories:

- radiometric data (airborne and ground total count and spectrometric surveys)
- radon mapping
- artificial isotopes.

Radiometric data can be used for various purposes regardless of how they were generated, e.g. by airborne radiometry and spectrometry or by ground methods. They can be used to produce maps of the natural background of radioelement concentration, e.g. on a worldwide basis as geochemical maps and atlases. They are applied for planning purposes or as baseline information for new mining projects (e.g. environmental impact studies). In various cases they have been proved useful for monitoring programmes. Such maps are applied to detect pollution caused by past and recent uranium mining and for the correlation with the natural (geological) background. In various countries airborne and ground mapping of radioelements are used for dose rate maps.

The recompilation of old airborne data by means of modern techniques has proved to be an effective method and for the conservation of otherwise useless data. Examples given at the meeting have shown the necessity of improvement. Airborne and ground gamma spectrometric data can also be applied for the detection of non-radioactive element concentration such as placer deposits. They certainly would be useful on other types of deposits too if appropriate techniques are applied. This method of data interpretation may be applied for resource management on a general scale. Gamma spectrometry can be used for determination of radioelement concentrations in building materials.

It was demonstrated that uranium exploration data in combination with the Geographic Information System (GIS) are applicable in remediation programmes for uranium mines. Isotopic fingerprints from mines and mills can help to understand the behaviour of radioelements once they are released to the environment.

Radon mapping and its aspect for the ecology has been another subject of great interest. Presentations given on the correlation of Rn concentration with the geology have shown how much is understood about this specific problem, demonstrated by examples of Rn measurements in soil gas and groundwater. Examples were given for Rn pollution due to uranium mining. However, non-uranium mines may also release considerable Rn emanation to the environment. The relevance of careful measurement and data interpretation was one of the important issue in most of the presentations. Rn mapping is applied for the investigation of the concentration of natural radioelements, however, Rn maps are available only in a small number of countries.

Artificial isotopes released to the environment can be measured with various techniques as demonstrated in examples from various countries. The accident at the Chernobyl nuclear power station in 1986 showed how far artificial isotopes can be transported through the atmosphere. The isotope Cs-137 is still present in measurable concentrations in areas affected after the accident. In many European countries maps on the distribution of Cs-137 have been prepared. Immediately after the accident various techniques have been tested on how to detect the fallout e.g. by airborne and ground investigations. Advantages, problems and pitfalls on the methods to measure Cs-137 and Cs-134 in various substances have been discussed as well as the need of calibration.

As the meeting has shown, various surveys to collect data on the distribution of natural and artificial radioelements have been made in many countries. Some, if not most of the data of surveys in the past are still in a form that are not suitable for using them as baseline maps and for other purposes. At present techniques are available to transform old data and prepare appropriate maps to match modern requirements. Effort to preserve old survey data would include (1) to locate the availability of the data and what techniques are required to improve their quality, (2) to preserve the data in a form that information can be retrieved, and (3) to reprocess the data with modern techniques. It was recommended that national organizations be encouraged to ensure data conservation and obtain funds for their appropriate reprocessing. Such a programme could be used for a better understanding of the Earth's environment in view of the increasing needs of the world's growing population for sustainable development.



URANIUM EXPLORATION DATA AND GLOBAL GEOCHEMICAL BASELINES: THE NEED FOR CO-ORDINATED ACTION

A.G. DARNLEY¹

Geological Survey of Canada,
Ottawa, Ontario,
Canada

Abstract

Public concern about environmental problems continues. The consequences of an expanding population, increasing industrialization, and greater demands for food production, raise serious questions about the ability of the earth's natural life-support systems to sustain present trends. In order to assess the magnitude of potential problems it is necessary to have comprehensive information. The absence of quantitative geochemical data to map the surface composition of the earth is one of the major information gaps in present day environmental (and earth) science. An IAEA Technical Committee meeting held in November 1993 reviewed the uses of uranium exploration data for environmental purposes. Most attention was focussed on data involving radiation measurements. Uranium exploration programmes conducted since 1970 in many countries collected a considerable amount of geochemical survey data, providing information about the distribution of *non-radioactive* elements in the natural environment. Canada is one of several countries where such data provided the foundation for national geochemical mapping; other countries could benefit from similar actions. Increasing importance is being attached by governments to the need to enact effective environmental legislation concerning "safe levels" of many chemical substances. Such legislation requires geochemical variations in the natural environment. It is becoming necessary to make quantitative comparisons of element abundances across national boundaries, and from continent to continent. In 1995 the IAEA, with other organizations, supported UNESCO to publish a report concerned with the establishment of a Global Geochemical Reference Network. This is designed to provide a framework to connect all types of geochemical survey, to move towards international compatibility of data. The report contains recommendations relating to the standardization of field and laboratory methods; the use of the most sensitive analytical techniques; and standardization of data management. Ground and airborne gamma ray spectrometry, and nuclear laboratory techniques are all discussed. Following the publication of the report, the International Union of Geological Sciences has now established a Working Group on Continental Geochemical Baselines, to coordinate implementation of the recommendations in the UNESCO report. National atomic energy organizations are invited to participate. The need for multi-agency co-operation and the support of the IAEA is discussed.

INTRODUCTION

This paper is written as a follow-up to two papers [1,2] presented in November 1993 at the previous meeting in this series concerned with uranium exploration data and the environment. In the intervening 30 months the world's environmental problems have continued to accumulate. Population growth, widely accepted as the major underlying cause of many of the problems, has not been checked, and relatively little progress has been made to mitigate the consequences.

At the previous meeting it was pointed out [1] that in order to react intelligently to global environmental problems it is necessary to possess comprehensive data concerning present conditions. It was pointed out that geochemical baseline data are (or should be) a major component of such a dataset and that uranium exploration data and related exploration methods are a vital subcomponent. For the reasons indicated, the need to acquire baseline data is increasing, not diminishing, and all possible sources and methods must be examined. Uranium exploration data constitute one of the largest existing reservoirs of information as far as the natural geochemical environment is concerned. The only reason not to use these data is if their quality is unsatisfactory. Factors affecting data quality

¹ Co-leader, International Union of Geological Sciences, Working Group on Continental Geochemical Baselines

include considerations such as the use of proper calibration procedures, standardization of measurements, adequate sensitivity, low detection limits, etc. It may be possible, by some additional work, such as selective re-analysis of retained samples, or back-calibration (see [3]), to remedy known deficiencies and avoid the necessity of repeating earlier large-area surveys. The scientific and technical literature relating to uranium exploration methods and related data, much of it generated as a result of the activities of the IAEA, is voluminous, and steps should be taken to ensure it is carefully reviewed before commencing new work.

There are both economic and environmental reasons why baseline information grows in importance with each successive year. For example, many governments are introducing legislation affecting society's use and disposal of many types of materials. Regulations are being established defining "safe-levels" of many substances, including naturally-occurring elements and metal-bearing compounds. Unless these decisions are based on adequate information concerning the variability of the natural environment, there could be excessive and unnecessary "clean-up" costs totaling billions of dollars, which, directly or indirectly, will be a cost to society as a whole. Hence the importance of comprehensive and reliable baseline information.

In recent years "sustainable development" has been identified as an international political and economic objective. It is open to question whether sustainable development will be possible if the human population continues to grow. Even with unlimited and pollution-free energy supplies, there would seem to be practical limits to the ability to provide a steady improvement in economic and social conditions for an expanding population. Unless the present natural environment can be sustained the long-term future for mankind must be regarded as potentially precarious, and efforts to pursue economic development without paying attention to potential detrimental effects upon the environment are a recipe for disaster. To the extent that sustainable development is achievable, it should not be pursued in the absence of an adequate database to describe and monitor current conditions.

The President of the International Union of Geological Sciences recently summarised the environmental problems facing mankind [4]. Essentially they are as follows. Time is not on the side of mankind. (Since the previous Technical Committee meeting in this series, world population has increased by about 250 000 000, equal to the population of the USA; world population is increasing at the rate of 10 000 per hour). Largely as a result of increasing population pressure, the quality of the soil, fresh water, forest cover, and biological diversity of the Earth's land surface (140 000 000 km²) is deteriorating. The 1992 UN Conference on Environment and Development in Rio de Janeiro recognised the scale of the problems. Unfortunately, so far, the reactions of most governments can only be described as modest. Regrettably few public authorities are yet willing to assign priority to the need for an adequate data base about environmental or other similar matters. Good decisions on any subject cannot be taken in the absence of relevant information. Systematic data collection is a basic prerequisite for achieving a sustainable environment. Nuclear research institutions and nuclear scientists can play a key role in gathering the necessary data.

THE EXISTING URANIUM EXPLORATION DATABASE

The 1993 meeting reviewed the uses of uranium exploration data for environmental purposes. Most attention was focussed on data involving radiation measurements, as shown by the following list of principal topics:

- standardization of old gamma ray data, from car-borne and airborne surveys;
- calibration of gamma ray measuring systems;
- use of gamma ray spectrometry to map natural background variations and accidental emissions of radioactivity;
- use of uranium survey data for the assessment of radon hazards;
- the use of gamma ray survey data to provide reference levels to correlate other multielement geochemical surveys.

The 1993 meeting devoted relatively little attention to the considerable amount of conventional (e.g. drainage sediment and soil) geochemical survey data acquired in the course of many uranium exploration programs. Many national and industry-sponsored uranium exploration programs, and also some sponsored by the IAEA, deliberately collected data about non-radioactive elements (a) to assist in overall interpretation and (b) because of the small incremental cost of obtaining data about other commodities. As a result much useful information about the distribution of non-radioactive elements in the periodic table was obtained and in a number of countries (e.g. Canada, Germany, USA), the foundation was laid for national geochemical mapping programs. For a bibliography, see [5]. In nearly every case the initial motivation was for economic mineral resource purposes, but subsequently the datasets obtained have provided a base for environmental mapping.

It was pointed out in 1993 that the division of environmental concerns into those pertaining to the radioactive as distinct from non-radioactive elements is arbitrary and undesirable from several points of view. It is particularly unfortunate because there is no international organization comparable to the IAEA with a mandate to gather data concerning the distribution of non-radioactive elements in the natural environment. The radioactive elements, both natural and man-made, are part of a single geochemical continuum and subject to the same chemical and physical processes as non-radioactive elements. For many reasons their spatial distribution should be studied and recorded as part of a common database. Not only are the non-radioactive elements essential constituents of the natural environment (associated in many cases with their own specific hazards), their distribution has a bearing on problems relating to radioactive elements, particularly in nuclear accident situations (e.g. uptake of Cs, I, by ruminants).

Since 1993, very little new uranium exploration data has been gathered. Compared with the period extending from 1970 into the 1980s, data acquisition in most countries has been negligible. The author is aware of some compilations of large blocks of existing airborne survey data, for example in Namibia, and plans to make similar compilations elsewhere. As a result of the almost universal reduction in funding for scientific research there has been little new research on topics relating to calibration, gamma ray mapping, and radon. Undoubtedly the knowledge that there is already an extensive literature in this field has contributed to the reluctance to undertake new work. There have been some interesting advances in the UK in the use of multi-parameter map displays to indicate radon hazard, reported elsewhere in this meeting.

TOWARDS A GLOBAL GEOCHEMICAL DATABASE

The International Geochemical Mapping (IGM) project, sponsored by the International Union of Geological Sciences (IUGS) and UNESCO, was described at the 1993 meeting by Darnley [1]. The reasons underlying the project were described. This project was started in 1987 to look into the possibility of preparing a global geochemical map. The project was a logical extension of IAEA-sponsored activities focussed upon nuclear raw materials. From the outset the IGM project was designed to gather data about the surface distribution patterns of all elements in the periodic table, not merely those which are radioactive. The IAEA was an active participant in the project, collecting data and organizing meetings and preparing reports containing the latest information pertinent to mapping both natural and anthropogenic radioelements.

The results of the IGM project were published in 1995 by UNESCO on behalf of IUGS, the Royal Society of London, the IAEA and other organizations ("A global geochemical database for environmental and resource management", [5]). Following a review of the existing state of geochemical mapping worldwide, this report contains recommendations concerned with the establishment of a Global Geochemical Reference Network. There are many components to the work, involving the collection and preparation of standard reference materials from a variety of representative natural sample media; standardization of analytical methods, with emphasis on ultra-low detection limits combined with stringent quality control; and standardized comprehensive data management. The geochemical reference network is intended to ensure international compatibility of

data between all the principal types of geochemical survey, for both environmental and resource purposes. It will allow quantitative comparisons of element abundances to be made across continents, and from region to region. Analytical methods are recommended according to their suitability for the particular element and media concerned.

The report had a favourable reception upon publication and within 3 months of its release all copies in UNESCO's stock in Paris had been distributed. The IAEA was responsible for sending out copies to national nuclear institutions. In response to continuing demand the report is now being reprinted.

RECOMMENDATIONS IN THE UNESCO REPORT

The following requirements summarise the essential prerequisites of a global geochemical database suitable for environmental baseline purposes:

- commonly available representative sample media, including surface water, collected in a standardized manner;
- continuity of data across different types of landscape;
- adequate quantities of the designated sample media for future reference and research requirements;
- analytical data for all elements of environmental or economic significance;
- the lowest possible detection limits for all elements;
- determination of the total amount of each element present, and
- tight quality control at every stage of the process.

Chapter 7 in the UNESCO report is devoted exclusively to radioelement mapping. Several sections of the extensive appendices relate to nuclear analytical techniques. Special attention is given to gamma ray spectrometry because of its suitability for identifying and quantifying radioactive elements, either by in situ measurements at fixed sites, or from a moving vehicle or aircraft. The radioelements are unique in that it is possible to obtain continuous profiles of their abundance across any type of terrain, using airborne gamma-ray spectrometry (AGRS). With properly calibrated systems, quantitative correlation of airborne and ground data can be assured within definable limits.

It was pointed out in [2], that as a consequence of different methods and lack of standardization, neighbouring blocks of conventional geochemical data in many parts of the world exhibit pattern and level discrepancies. In the absence of any confirmatory evidence it may not be possible to judge whether these discrepancies are real or apparent. Thorium and potassium surface abundance profiles, derived from widely spaced gamma ray transects, can provide an independent reference level against which discontinuities in other datasets can be assessed. These transects can contribute to more reliable and comprehensive baseline data for all elements, and simultaneously provide data about the natural radiation environment.

THE ESTABLISHMENT OF GLOBAL GEOCHEMICAL BASELINES

The project steering committee which prepared the UNESCO report realised that it was not sufficient merely to make scientific and technical recommendations. Given the importance attached to the subject it was considered necessary to comment on the practical aspects of implementing and managing the work. Most of the required steps were outlined in [1], and they are given in full in the UNESCO report [5]. Following from its publication, there have been several encouraging developments. The International Union of Geological Sciences approved in 1995 the formation of a new coordinating committee (Working Group on Continental Geochemical Baselines), reporting directly to the Board of IUGS, with responsibility to take whatever steps seem appropriate to begin implementation of the recommendations in the UNESCO report. Discussions are currently taking

place with a number of organizations with a view to securing funding to cover basic operational and administrative expenses.

Work is already in hand to initiate the establishment of global geochemical baselines in four regions of the world. These are China, Brazil, Europe, and Russia. The Australian Geological Survey Organization is currently carrying out an aerogeophysical survey of the entire country and this includes gamma-ray spectrometry, which constitutes a component of the Continental Geochemical Baselines project.

Floodplain sampling of large (1000 to 6000 km²) drainage basins is recommended in the UNESCO report for preliminary reconnaissance purposes in regions where access is difficult. Floodplain sampling has been carried out over all of China. In Brazil floodplain sampling has been carried out over an area of 625 000 km² in NE Brazil.

In Europe, the Forum of European Geological Surveys (FOREGS), representing 29 countries, has published a Geochemistry Task Group Report [6], recommending the preparation of a geochemical database for Europe, based on the sampling of both large and small (< 100 km²) drainage basins, as set out in the UNESCO document. Plans are now being prepared for field work to commence in some countries in 1996/97.

Responding to proposals from Greece and the Czech Republic, encouraged by the concepts of the International Geochemical Mapping project, the European Union has financed and published [7] an inventory of "Regional gamma-ray data in central and eastern Europe", relating to nine countries. A series of recommendations have been made involving back-calibration and recompilation of gamma-ray data for the whole region and ultimately the compilation of a gamma-ray dose map for the whole of Europe. Preparation of radioelement maps for the whole of Europe would be a logical continuation of this work in the near future.

THE FUTURE — THE NEED FOR COORDINATED ACTION

The Global Geochemical Baselines project is a multi-disciplinary task. Implementation of the project requires the support and participation of leading scientific institutions with active field and laboratory programs. Although the project has made a beginning, because of very limited financial resources (essentially restricted to what individual countries are willing to commit) there is a serious risk that different countries will make their own limited selection of the recommended methods because this is all they can afford. This may represent an advance on the disparity of methods used in the recent past, but it will fall far short of the aims of the project. Thus some countries may not have access to recommended analytical methods and some countries may not have access to mobile gamma ray spectrometry equipment.

For the project to succeed it is essential that there should be worldwide coordination of the following activities:

- overall strategy and planning;
- sample collection procedures and sample management;
- gamma radiation surveys;
- analytical procedures;
- data management;
- training and quality control;
- public dissemination of scientific information.

This degree of coordination cannot take place in the absence of a technically qualified secretariat with an adequate budget.

Regional cooperation is also essential. The tasks which have been identified for coordination at the international level should also be coordinated regionally amongst groups of countries with common borders, as is taking place in Europe through the Forum of European Geological Surveys, in conjunction with the European Union. With regard to less developed parts of the world, expertise, if it is not already available, must be built up in regional centres.

The usefulness of the data obtained depends in the first instance upon the reliability of the field work, both sample collection and field measurements. If these components of the work are not performed according to the specifications, the defects cannot be remedied and subsequent analytical work would be misleading. For this and other logistical reasons field sampling must be undertaken by trained personnel thoroughly familiar with the region in which work is being undertaken. In order to standardize the work to the greatest degree possible, training sessions should be provided for all local personnel, even those with experience.

In many countries the national atomic energy organizations often possess the best trained analytical staff and the best equipped laboratories. In some countries these organizations possess an extensive earth science database relating to radioactive minerals. It would benefit the countries concerned, and facilitate the establishment of a comprehensive global geochemical database if these national atomic energy organizations were willing to contribute their expertise to the Continental Geochemical Baselines project, e.g., by providing field gamma ray spectrometry equipment and, if necessary, personnel. As explained in the UNESCO report and in [2], gamma ray spectrometry measurements, taken in conjunction with conventional geochemical sampling, provide a method not only of monitoring the natural radiation background but also of monitoring the consistency of other non-radioactive element datasets. It should be noted that national nuclear laboratories may be the only establishment in a country to possess analytical techniques (e.g. neutron activation analysis, ICP-MS) capable of achieving the low detection levels required for the acquisition of baseline data for some of the non-radioactive elements. High quality datasets are an essential starting point for all types of environmental monitoring and the geochemistry of the earth's surface poses a multitude of questions and opportunities for further research.

It was pointed out in 1993 that the IAEA is one of the few, if not the only international Agency with experience in the coordination of the type of activities outlined above. The IAEA has established an enviable reputation with respect to technical assistance for both regional and national organizations, which, as indicated, is essential for the acquisition of global geochemical baselines.

It is important to emphasize that the IAEA has already provided a variety of support to the geochemical baselines project, including:

- over a 20+ year period, the infrastructure for the buildup of a worldwide database on the distribution of uranium;
- over a 30+ year period, the development of nuclear and related techniques which are now widely used for (non- radioactive element) geochemical analysis;
- technical assistance (provision of equipment and training) for the collection of radiometric and multielement data, some of which is now incorporated in the existing (limited) global geochemical database.
- text for inclusion in the UNESCO report, and a contribution to the cost of its publication.

The project could not have progressed as far as it has without this mostly indirect, low-key, support. For the project to go forward, to establish continental geochemical baselines as a datum for sustainable environment, more active support is now required. The Director General of IAEA, in his recent address to the 50th General Assembly of the UN, has affirmed the Agency's intention of assisting developing countries to achieve sustainable development. The IAEA currently has formal involvement in projects relating to food production, water resources, and human health. Geochemical baseline data pertain to each of these concerns. Given the Agency's participation in the evolutionary stage of the "baselines" project, it is to be hoped that the IAEA will see fit to make a formal

commitment to continuing support through the implementation stage of this project, within the limits of the IAEA mandate.

CONCLUDING REMARKS

Whereas nuclear energy and nuclear power are treated with suspicion by many members of the public, the use of nuclear data and techniques to mitigate environmental problems is not contentious. Uranium exploration data, nuclear techniques, and a spectrum of related specializations are essential components of global environmental data and the IAEA can provide an essential clearing-house for their utilization. In doing so it cannot fail to create goodwill in the community at large. The existing geochemical database needs to be expanded as a matter of some urgency, using the latest field and analytical techniques, to provide reliable quantitative baselines to ensure that the natural environment is not irreparably damaged by human activities.

REFERENCES

- [1] DARNLEY, A.G., "Uranium exploration data, international geochemical mapping and the environment", Application of uranium exploration data and techniques in environmental studies, IAEA-TECDOC-827, IAEA, Vienna (1995) 9-23.
- [2] DARNLEY, A.G., "The relevance of airborne and ground gamma ray spectrometry to global geochemical baselines", Application of uranium exploration data and techniques in environmental studies, IAEA-TECDOC-827, IAEA, Vienna (1995) 47-58.
- [3] INTERNATIONAL ATOMIC ENERGY AGENCY, Application of uranium exploration data and techniques in environmental studies, Proceedings of a Technical Committee meeting held in Vienna, 9-12 November 1993, IAEA-TECDOC-827, Vienna (1995) 352pp.
- [4] FYFE, W.S., The role of Earth sciences in society, UNESCO Nature & Resources, v. 30, nos. 3 & 4 (1995) 4-7.
- [5] DARNLEY, A.G., BJÖRKLUND, A.J., BØLVIKEN, B., GUSTAVSSON, N., KOVAL, P.V., PLANT, J.A., STEENNFELT, A., TAUCHID, M., XIE XUEJING, A global geochemical database for environmental and resource management: recommendations for international geochemical mapping, Earth Science Report 19, UNESCO Publishing, Paris (1995) 122pp.
- [6] PLANT, J.A., KLAVER, G., LOCUTURA, J., SALMINEN, R., VRANA, K., Forum of European Geological Surveys (FOREGS) Geochemistry Task Group Interim Report, August 1995, Technical Report WP/95/14R, Applied Geochemistry Series, British Geological Survey, Nottingham (1995) 60pp.
- [7] SIDERIS, G.N., MATOLIN, M., Study of regional gamma-ray data in Central and Eastern Europe, Final Report, DG XII/B European Union, Brussels (1994) 22pp.

NEXT PAGE(S) left BLANK



**TERRESTRIAL RADIATION — A PROJECT
FOR CENTRAL AND EASTERN EUROPE**
(Abstract)

M. MATOLÍN
Faculty of Science,
Charles University,
Prague, Czech Republic

G. SIDERIS
Institute of Geology and Mineral Exploration,
Athens Greece

Data on natural radiation are applicable in environmental studies, protection of population against ionizing radiation, raw materials exploration and regional geochemical investigations. Terrestrial radiation, causing substantial component of the natural radiation environment, is variable with the geological setting and space. Radiometric maps indicate the radiation level and distribution. Under the support of the European Union, a project of compilation of a terrestrial gamma dose rate map of Central and Eastern Europe has been initiated. Ten countries participate in the project: Poland, Czech Republic, Slovak Republic, Austria, Hungary, Slovenia, Romania, Bulgaria, Albania and Greece. Three stages of research activities have been planned. A project "Study of Regional Gamma-ray Data in Central and Eastern Europe", realized in 1993–1994, provided information on the available regional radiation data in participating countries. The study has shown the range of coverage of individual countries by the radiometric geophysical investigations 10–100% and the variability of applied instruments, their calibration, methods of measurement, data processing and reporting. Despite this fact, radiation data acquired in long time systematic geophysical investigations are of high value. A project "Unification of Gamma-ray Data in Central and Eastern Europe" has been submitted in 1996. Unification of gamma dose rate data in a region of a continental scale is planned for two years and implies the application of the gamma-ray spectrometry, selection of a reliable calibration facility, calibration of portable and airborne gamma-ray spectrometers, intercomparison measurement of all participating countries, selection and back calibration of national terrestrial radiation reference sites, verification and completion of gamma-ray data in border areas, airborne gamma-ray spectrometry tie lines, and levelling of national terrestrial gamma dose rate data to standard established level. The third stage of the activity implies complementary measurements in uncovered areas of some countries and compilation of standardized terrestrial gamma dose rate maps of separate countries and of the Central and Eastern European region. It is expected, that realization of the project of a continental extent will introduce new scientific problems, which solution will enrich the professional experience and will contribute to the development of monitoring of the radiation environment.

**NEXT PAGE(S)
left BLANK**

THE MARNA PROJECT

E. SUAREZ MAHOU
CSN

J.A. FERNANDEZ AMIGOT
ENUSA

Madrid, Spain

Abstract

The MARNA Project is developed within the framework of an agreement established between the Spanish Nuclear Safety Council (CSN) and ENUSA. It consists of two phases, of which the first one has already been concluded successfully in December 1995. The final objective of the first phase of the project was the elaboration of the Natural Gamma Radiation Map of Spain on a scale of 1:1 000 000. For the preparation of this map radiometric data were generated during the thirty years the old National Uranium Exploration and Investigation Plan (PNEIU), mainly through airborne, car-borne and by foot surveys and those generated within the MARNA Project. Previously, four pilot maps on the scale of 1:50 000 had been prepared for four radiometric zones of special interest. The total surface of these four zones add up to about 2500 km² and 10 000 radiometric data which were used in the elaboration of the maps. Further were prepared on the scale of 1:200 000: the radiometric Atlas of the Autonomous Communities of Extremadura and Castilla-Leon which covers an area of 130 000 km². The radiometric data extracted plus the generated applicable to such a surface add up to 120 000. This large data base has permitted to verify important quality controls in the technologies of data extraction and the elaboration of maps on various scales. The goal of the second phase, initiated in January 1996, is to complete the National Radiometric Atlas on the scale of 1:200 000 of a similar quality as the one obtained in Extremadura and Castilla-Leon and also to improve the Map 1:1 000 000. In this paper, the characteristics and more relevant results of the MARNA Project at the end of its first phase are presented.

1. INTRODUCTION

This report follows on from the one drawn up by the same authors in November 1993 and which was titled "The Use of Uranium Airborne Survey Data in the Preparation of a Radiometric Map of Spain", published by IAEA-TECDOC-827, pages 109-125 [13].

In December 1991 the Nuclear Safety Council of Spain (CSN) and the URANIUM NATIONAL ENTERPRISE S.A. (ENUSA), signed an agreement for carrying out the MARNA Project with the target of produce the following maps:

- A natural radiation pilot map and a dosimetric map, on a 1:50 000 scale, of four particularly interesting areas of Spain.
- A natural radiation pilot map and a pilot dosimetric map on a 1:200 000 scale of two Spanish regions in which sufficient data are available prior to carrying out the Project.
- A natural radiation map and a dosimetric map of Spain on a 1:1 000 000 scale.

The first stage of the MARNA Project was ended in December 1995.

The mesh radiometric cover of one kilometre of Spanish territory, generated by the former PNEIU, is approximately as shown in Fig. 1.

The Project in general was carried out in accordance with the forecast chronogram, and the pre-established objectives were achieved [13].

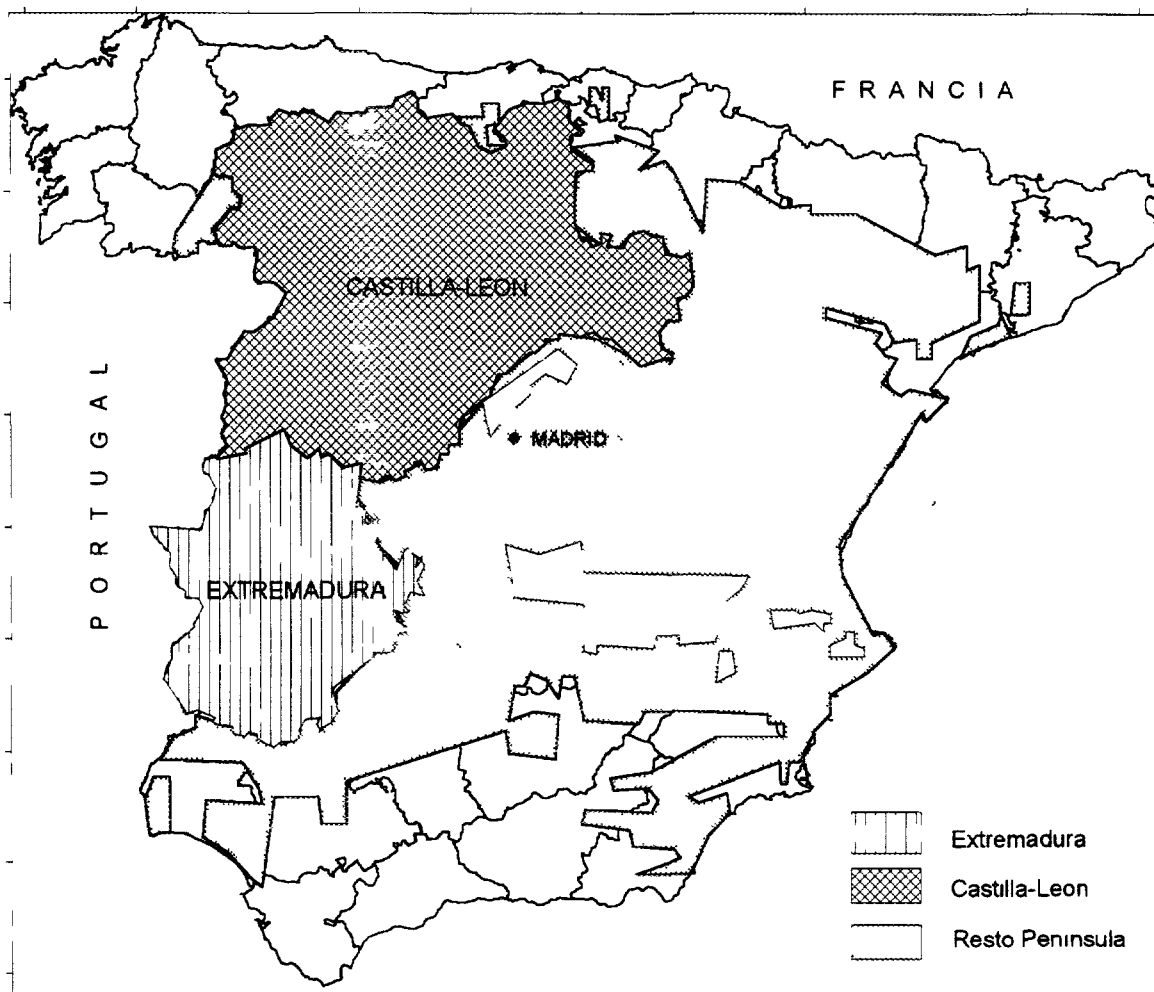


FIG. 1. Map of Spain with air-borne survey (PNEIU)

A notable feature of the first stage of the Project was the extent of university collaboration since, in addition to staff from ENUSA and CSN, eleven lecturers and several scholarship holders from various universities and departments, mainly Geology, Physics, Computer Science and Surveying, took part. Ongoing validation work on techniques and methodology has been carried out, and this is expected to be continued throughout the second stage of the MARNA Project.

2 BASIC PROBLEMS REGARDING THE MARNA PROJECT

Bearing in mind the size of the Spanish airborne radiometric cover (around 275 000 km²), as well as the varying nature of the apparatus used, the first problem was how to solve the relationship between airborne radiometry (cps) and ground radiometry ($\mu\text{R/h}$). Once this problem had been satisfactorily solved the feasibility of the project was ensured.

The ways to solve this problem were as shown in the outline below:

- Airborne radiometry \rightarrow eU, eTh and eK \rightarrow Coefficients \rightarrow $\mu\text{R/h}$
- Airborne radiometry, total counts (cps) \rightarrow Coefficients \rightarrow $\mu\text{R/h}$
- Airborne radiometry, total counts (cps) \rightarrow point-to-point empirical correlation \rightarrow $\mu\text{R/h}$
- Airborne radiometry, total counts (cps) \rightarrow radiometric plateaus-to-air empirical correlation \rightarrow $\mu\text{R/h}$

After various studies had been performed the empirical procedure was chosen with very good results being achieved both as regards point-to-point correlations and by way of the study of radiometric plateaus.

Finally, the latter procedure was chosen for operational reasons, among others.

Complementary to this technology, the following were also developed [13]:

- Correlations in the air between different kinds of flights:
- Hunting Flights — Geodata Flights
- Hunting Flights — JEN Flights
- JEN Flights — Geodata Flights
- Measurements systems:
 - Gauging control
 - Statistical fluctuation correction
 - Correlation between apparatus
- Data-extraction systems in the different airborne surveys:
 - Statistical control
 - Graphic control of data extraction
 - Data-processing control
- Computing systems
 - Map production systems
 - Base grid

3. ORGANIZATION OF THE EXISTING DATA BANK

The organization of the existing data bank is summarized in Fig. 2. In accordance with data-extraction technologies, and with what is laid down in the CSN-ENUSA agreement, data extraction in the Extremadura and Castilla-León regions reached about 525 per 1:50 000 sheet, the equivalent of one piece of data per square kilometre. (A 1:50 000 surveying sheet is understood as being a surface area determined by 20' by 10' meridians and parallels). This meant extracting around 40 000 pieces of data for the Extremadura region Fig. 4 and around 80 000 pieces of data for the Castilla-León region Fig. 1. File organization was carried out in DB3P on the basis of one file per 1:50 000 sheet.

4. THE GENERATED DATA BANK

At the same time as the above operations were being performed a new data bank was being generated through car-borne and foot surveys Fig. 3.

The car-borne surveys were performed by the University of Salamanca (Dpt. of Geology) and the basic aims of these were to:

- validate the data-capturing system in accordance with the available equipment
- fill in the radiometric blanks in the Castilla-León region
- carry out a radiometric control of certain geological formations.

Although continuous recording was carried out during the car-borne surveys (Mount Sopris apparatus), the following precautions were taken among others:

- They were performed along roads which had not been filled in by allochthonous materials.
- In addition to the Mount Sopris a switched-on scintillometer was always carried in the car.

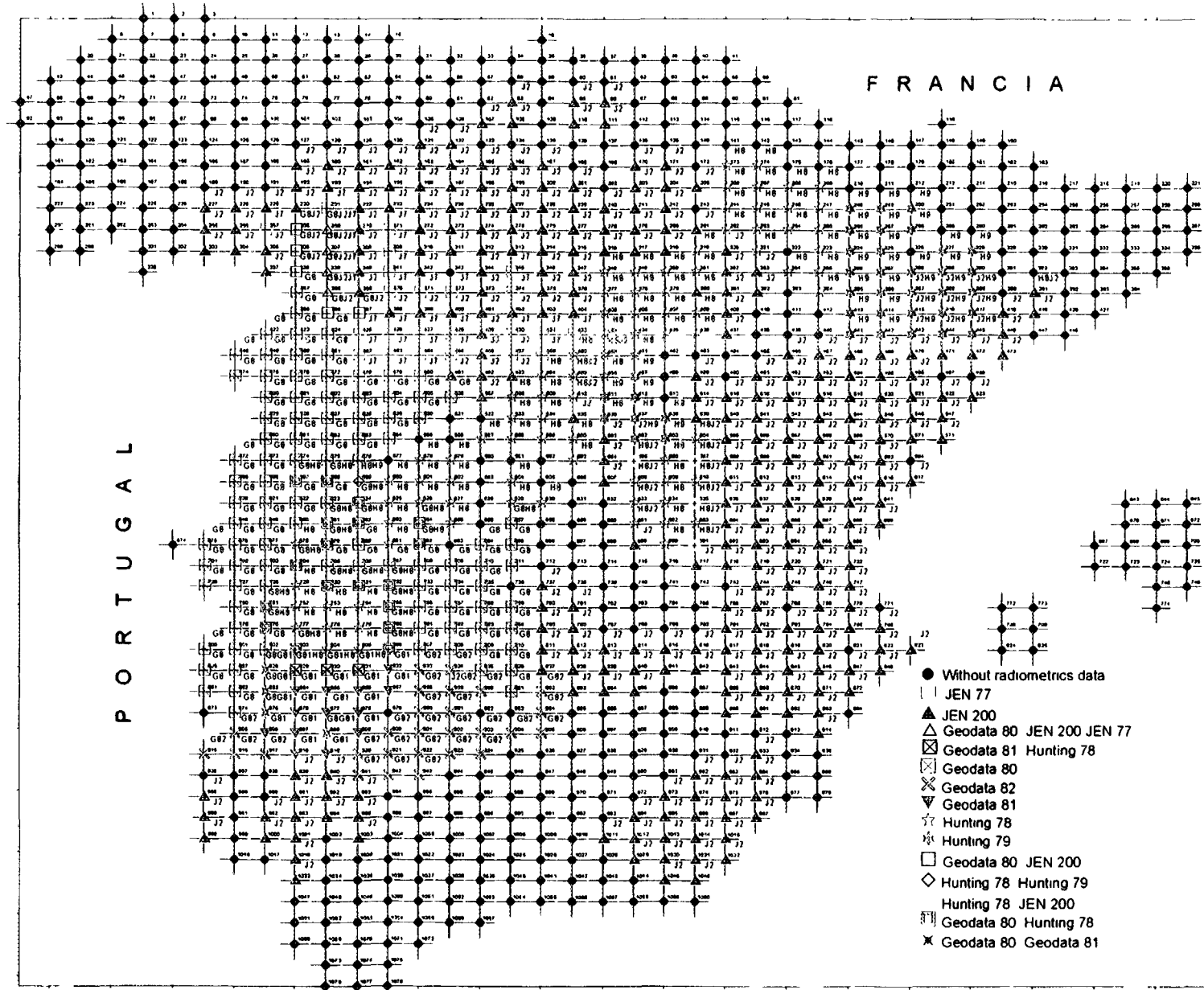


FIG. 2. Inventory radiometric map of Spain (PNEIU)

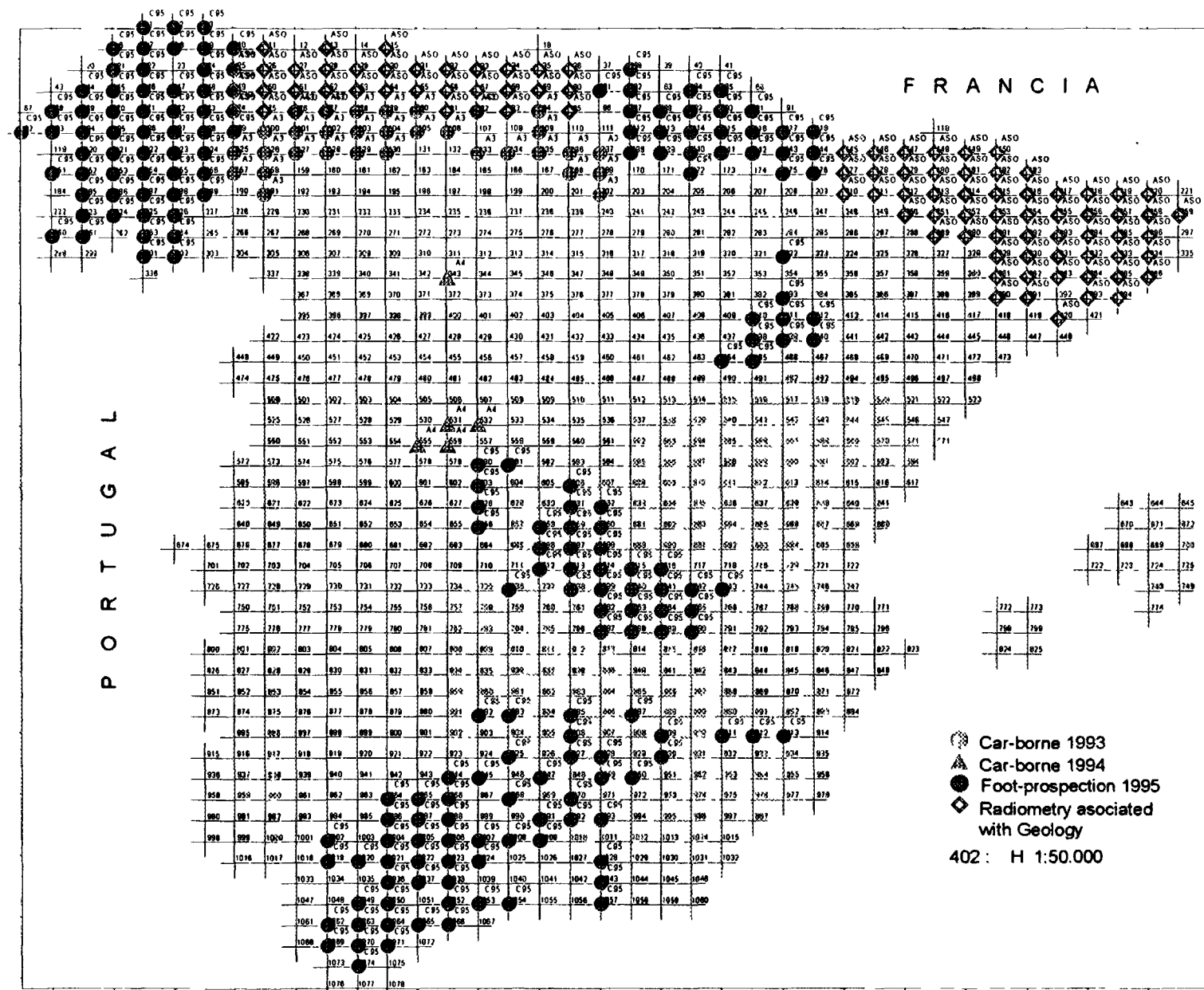


FIG. 3. Inventory radiometric map of Spain (MARNA Project)

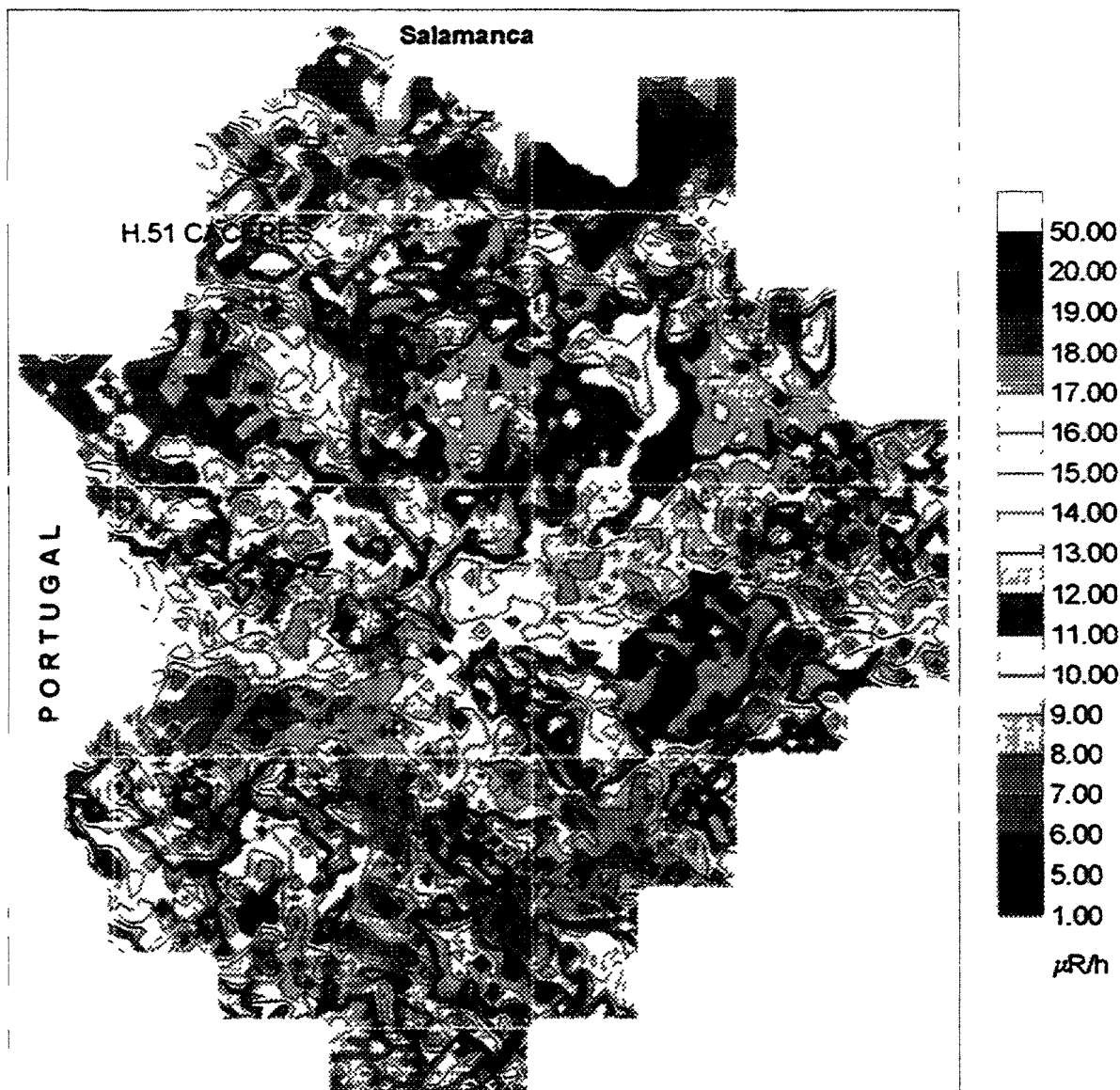


FIG. 4. Radiometric map of Extremadura.

- Stops were made on a kilometre basis in order to check the radiometry of outcrops and/or soils. Measurements were taken at these points, in accordance with the system established, by means of two correlated items of apparatus and in $\mu\text{R/h}$.

The accumulated experience will be described in another publication which is currently being drawn up. The surveys carried out on foot had a threefold aim:

- to extend the number of plateaus studied in Extremadura for the purpose of gauging, in other provinces, the earth-air correlations established for Extremadura.
- Radiometric data capturing in geologically pre-selected areas.
- Filling-in of radiometric blanks in areas where few or no radiometric studies had been made.

This data bank meant performing a radiometric control of 150 additional plateaus, as well as a geological control of 1700 outcrops and/or soils, and it provided radiometric extrapolation in some areas where it had not yet been possible to perform the necessary radiometric filling-in.

5. EXPERIMENTS IN DRAWING UP MAPS ON 1:50 000 AND 1:200 000 SCALES

1:50 000 Scale [13]:

The four pilot maps that were made affected the 1:50 000 sheets:

623. Malpartida de Plasencia (overlapping area of Geodata and Hunting flights).
525. Ciudad Rodrigo; 475. Lumbrales; 476. Villavieja de Yeltes.

The later three are located in Salamanca province where Spain's major uranium mines and radioactive anomalies are to be found.

Approximately 2500 pieces of data were extracted from each sheet. The study of the data from sheet 623 made it possible to establish the methodology and technology for the air-air correlations between different types of flights, which was then successfully applied in other parts of Spain. The study of the other three sheets made it possible to determine:

- the data-extraction quality in the base grid [13],
- an exceptional quality as regards the reconstruction of 1:50 000 maps with one piece of data per 0.5 km².
- A good reconstruction of the 1:50 000 sheets for extracting one piece of data per km² (graphic control). Colour tests were likewise performed for the reconstruction of vectorial maps and bitmaps.

1:200 000 Scale:

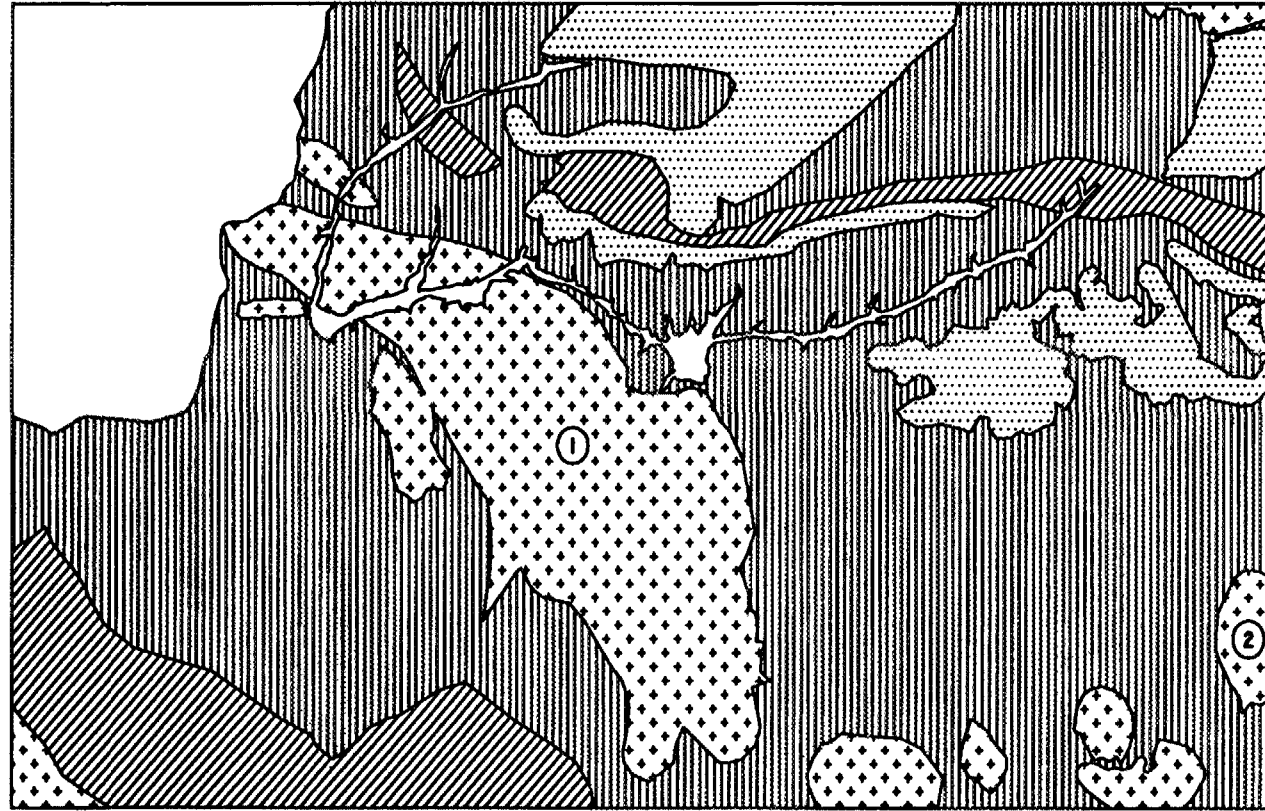
On a 1:200 000 scale the data were extracted with a density of 1/1 km² in the Extremadura and Castilla-León regions Figs. 1 and 4. For the Extremadura region Fig. 4 we have chosen 1:200 000 Sheet no. H-51 (Cáceres) in order to observe how maps drawn up on this scale had evolved, on the basis of the various radiometric resolutions. In Fig. 5 the geological macroformations of Sheet no. H-51 may be seen (a surface area equivalent to 4 × 4 1:50 000 sheets, in other words about 8500 km²). Fig. 6 shows Sheet no. H-51 with resolutions of 1/1; 1/4; 1/9; 1/25 and 1/100 km². The images are sufficiently expressive.

On a 1/1 resolution all the macroformations represented radiometrically can be clearly observed, and even the spread of the Alcántara reservoir may be seen over tens of kilometres. This radiometric low (lineal anomaly) soon becomes blurred as the map's resolution diminishes where, with a resolution of one piece of data per 100 km², only the batholithic forms of Cabeza de Araya may be seen while granitic stocks and other formations are lost. Likewise in this resolution an accurate value over water (coloured blue) becomes an apparently uncertain large radioactive depression. This series of figures shows us that, in order to achieve a good representation on a 1:200 000 scale, resolutions of between 1/1 and 1/9 pieces of data per km² must be used, at least in a geological context similar to the one we are involved in.

6. THE NATURAL RADIATION MAP ON A 1:1.000.000 SCALE (Fig. 8)

This map is governed by the following conditions:

- Previously acquired experience
- The terms of the CSN-ENUSA agreement
- The base grid pre-established by the CSN
- The isocurves



LEYENDA :



BATOLITOS Y STOCKS GRANÍTICOS



ORDOVICICO



① CABEZA DE ARAYA



≈ PANTANO DE ALCANTARA



CAMBRICO



TERCIARIO Y CUATERNARIO



② TRUJILLO

FIG. 5. H.51 Caceres. Simplified geologic map

On a 1:1 000 000 scale for a pixels representation it is advisable to have as great a resolution as possible. Such a density is inoperative as far as representing the isocurves map of Spain is concerned, since there would be so many isocurves for the required intervals of 1 $\mu\text{R/h}$ that to actually represent it would be an impossible task.

As regards representations with isocurves (interval of 4 to 20 $\mu\text{R/h}$), we saw in the 1:200 000 maps that good representations were obtained even with 1 piece of data per 9 km^2 . A resolution on a 1:1 000 000 scale homothetic to the above would in principle have 1 piece of data per 45 km^2 . When using a resolution of 1 piece of data/35 km^2 , Fig. 8, we must be within a good range of representation on a 1:1 000 000 scale.

Fig. 7 shows a geological scheme of Spain. The main features of which are easily seen in the National Natural Radiation Map with a resolution of 1/35, Fig. 8. These features rapidly become blurred with smaller resolutions.

Fig. 9 and Table I show the radiometric histogram of Spain. For this histogram, the most relevant parameters are the following: Sample size, average, median and standard deviation.

TABLE I. RADIOMETRIC HISTOGRAM OF SPAIN

Sample size	16 744
Average	8.702 828
Median	7.755 145
Standard deviation	3.968 093

7. THE GEOGRAPHIC PROBLEM

Reducing all the units to UTM's was done by means of two programs, one of which was produced by ENUSA in order to turn cms into UTM's. The other program is the same as that used by the Technological and Geomining Institute of Spain and the Polytechnic University of Extremadura for converting geographic units into UTM's and for changing time zones. This unit conversion has made it possible to homologate the MARNA Project coordinates with those of other bodies for the purpose of superposing information layers.

8. QUALITY OF THE 1:1 000 000 MAP

- Areas with a resolution of 1 piece of data per km^2 :
These correspond to Extremadura (40 000 km^2) and Castilla-León, Figs. 1 and 4 (90 000 km^2). For these two regions 900 radiometric maps of different types have been interpreted and/or computerized.

The data corresponding to the base grid (7 per 5 km^2) of the 1:1 000 000 map Fig. 8, as well as for other tests, have been extracted from this data bank.

- Areas with a basic resolution close to 1 piece of data per 35 km^2 :
These correspond to the 145 000 km^2 taken up by the areas outside the Extremadura and Castilla-León regions and which have airborne radiometric cover, Fig. 1. The degree of computerization expected to be achieved by 1996 is equivalent to 1 piece of data per km^2 .

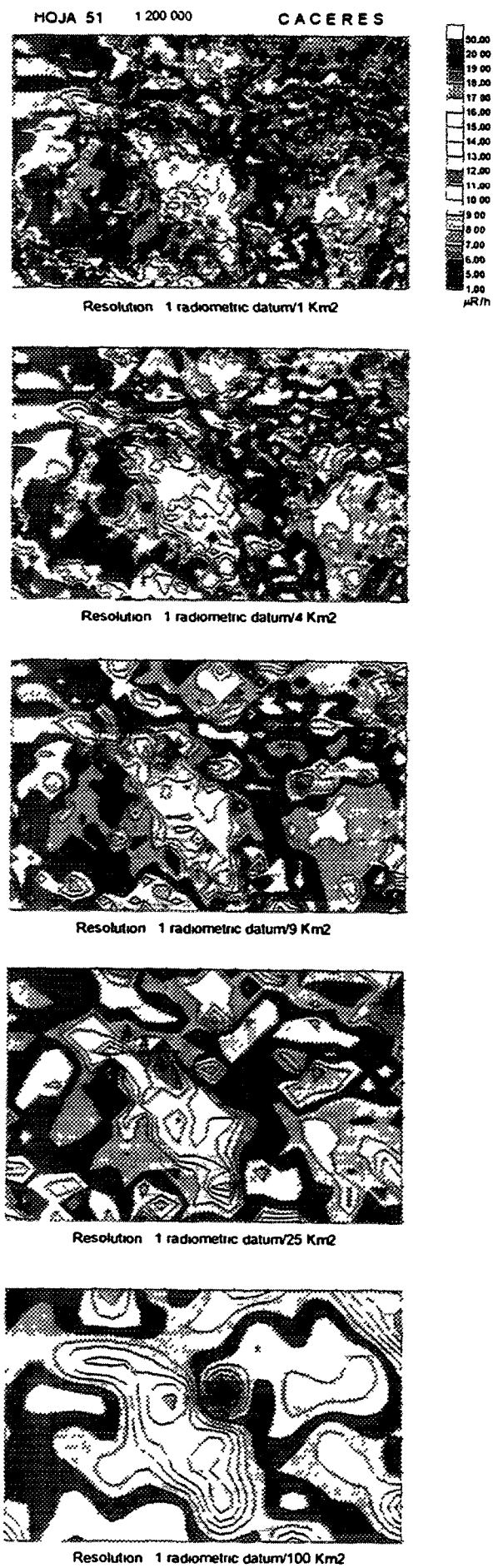


FIG. 6 H 51 Caceres. Radiometric map with different resolutions

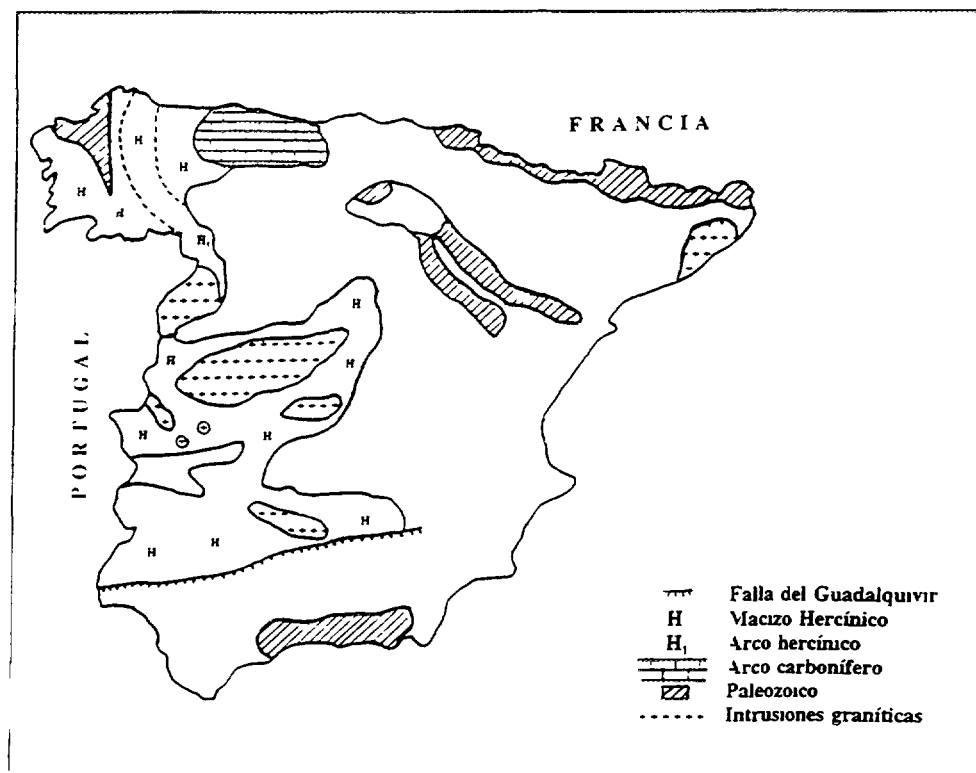


FIG. 7. *Peninsular geological scheme.*

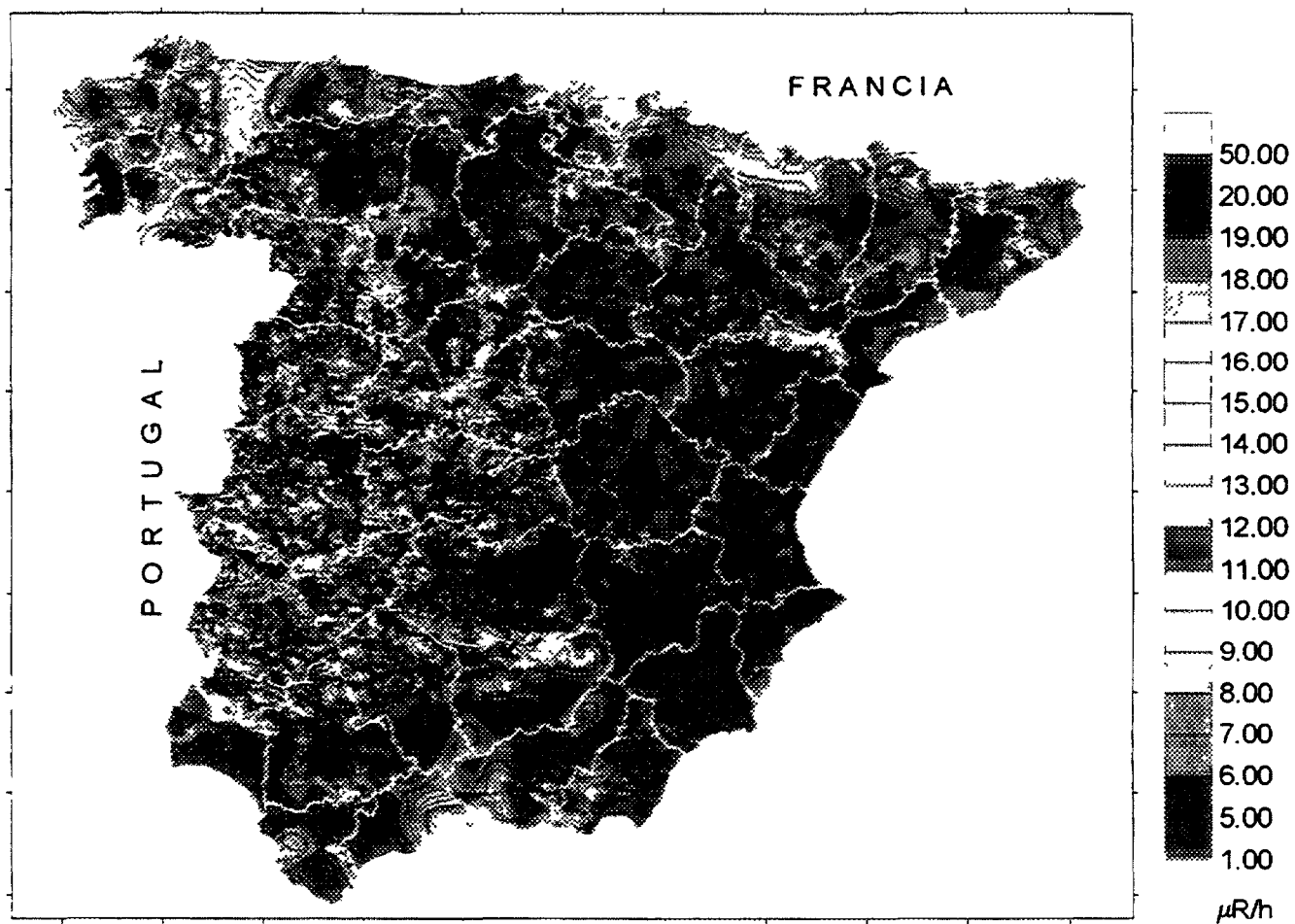


FIG. 8. *Radiometric map of Spain*

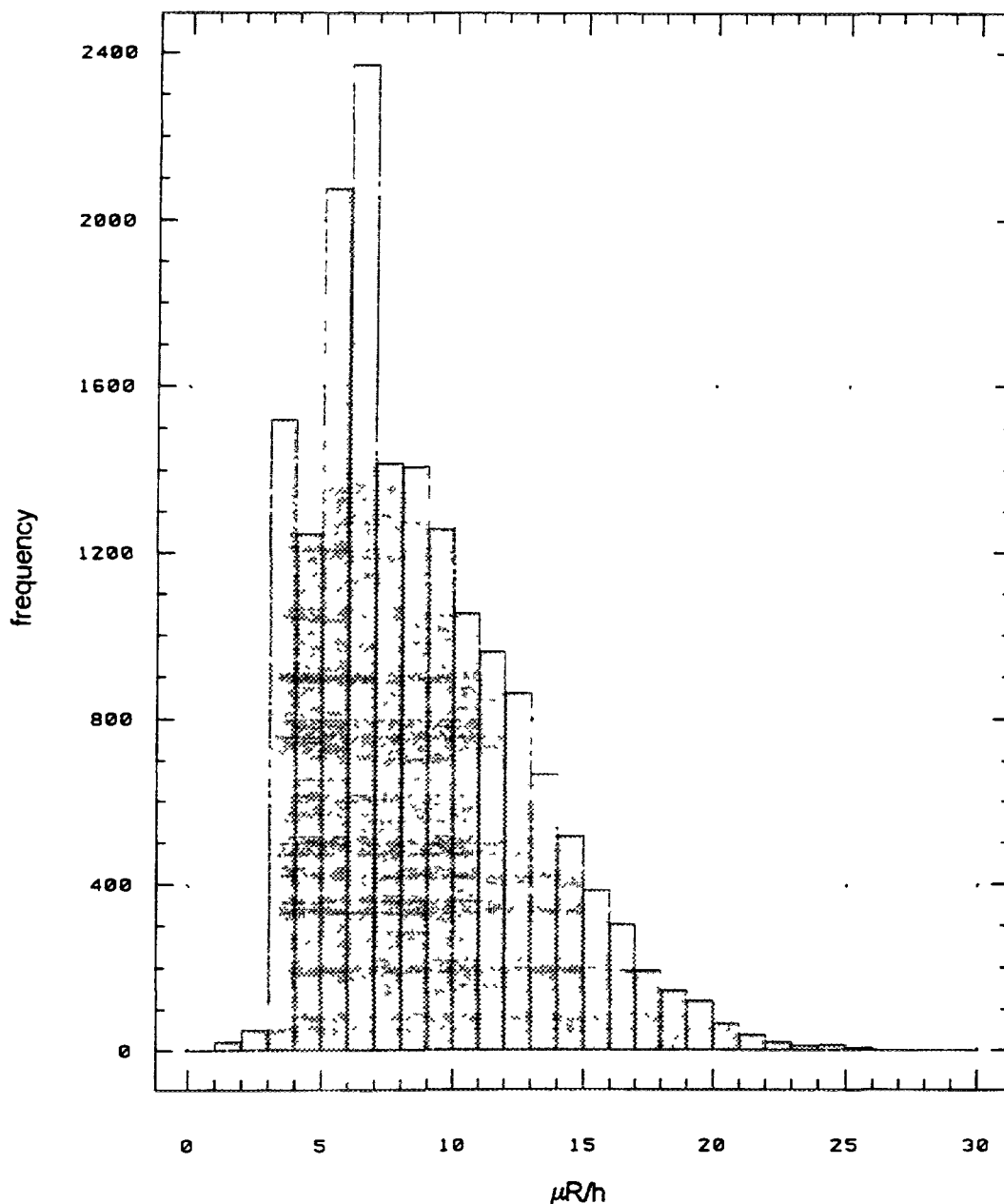


FIG. 9. Radiometric histogram of Spain

- Rest of peninsular Spain Fig. 1:
The degree of resolution is variable, being around 1 piece of data per 20 km² in the central areas, 1 piece of data per 500/1000 km² in Galicia and the Basque Country and Andalucia and geological cover in the rest of the northern fringe.

9. FUTURE ACTIVITIES

From a technical standpoint, all the initial uncertainties displayed by the MARNA Project have been satisfactorily solved within confidence limits quantified and laid down by the CSN. These technologies have likewise been validated by various universities.

Abundant additional documentation regarding car-borne surveys has been located in relation to Galicia. The experience gathered during the 1993 and 1994 surveys, Fig. 3, will be applied to this documentation.

The technology devised for the earth-air correlations will be used to interpret former radiometric flights carried out by private firms in the Ebro valley. The checking and, if pertinent, modification of earth-air correlations, both as regards the type of flight and geology, and even topography, may be regarded as being an ongoing activity.

Predictive experiments regarding the radiometric map of Galicia will be performed using the experience gained in geology/radiometry correspondences and this, furthermore, will soon be the subject of a new publication.

10. THE MARNA PROJECT-2

In view of the good results achieved during the first stage of the MARNA Project, the CSN and ENUSA have signed a new agreement to extend the Natural Radiation Atlas for the Extremadura and Castilla-León Regions on the scale 1:200 000 to the rest of Spain. Initially, this project will cover 95 000 km² and will subsequently be extended to the whole of Spain.

11. CONCLUSIONS

The quality of the technology and methodology used in the MARNA Project have allowed it to be successfully completed according to what was foreseen in the CSN-ENUSA agreement. The creation of a specific file and the volume of data will, in the immediate future, make it possible to generate a large number of multidisciplinary publications, chiefly through universities and bodies interested in the subject.

REFERENCES

- [1] ÅKERBLOM, G., "The use of airborne radiometric and exploration surveys data and techniques in radon risk mapping in Sweden", Application of uranium exploration data and techniques in environmental studies, IAEA-TECDOC-827, IAEA, Vienna (1995) 159.
- [2] DARNLEY, A.G., "The relevance of airborne and ground gamma ray spectrometry to global geochemical baselines", Application of uranium exploration data and techniques in environmental studies, IAEA-TECDOC-827, IAEA, Vienna (1995) 47.
- [3] Atlas of Natural Radiation Levels in the European Communities. Phase II. Final Report — Nov. 1988. CEC Contract Nr 85, 420.
- [4] BAEZA, A., et al., Estudio comparado de dos métodos para la evaluación de los niveles de tasas de dosis ambientales en la provincia de Cáceres (Relación Interna) Mayo 1994.
- [5] BROWN, et. al.; Radon en España, Forum Atómico Español, Madrid (1992).
- [6] GRASTY, R. L., "Environmental monitoring by airborne gamma ray spectrometry,-experience at the Geological Survey of Canada", Application of uranium exploration data and techniques in environmental studies, IAEA-TECDOC-827, IAEA, Vienna (1995) 93.
- [7] GREEN, B.M.R., Atlas of natural radiation levels in the European Community Pilot Study, Report to the CEC, Oct. 1986.
- [8] LOWDER, W., External terrestrial and cosmic radiation, Proceeding of the Fifth International Symposium on the Natural Radiation Environment, Salzburg (1991).
- [9] MORO, M^a.C., PEREZ DEL VILLAR, L., Estudio de la distribución de K, U, y Th en el batolito de Cabeza de Araya mediante prospección aéreo-radiométrica, Implicaciones petrogenéticas y metalogenéticas, Libro Jubilar de Figuerola L.D. Omega, Madrid (1988).
- [10] SCHWARZ, G. F., RYBACH, L., KINGELE, E.E., "Data processing and mapping in airborne radioactivity surveys", Application of uranium exploration data and techniques in environmental studies, IAEA-TECDOC-827, IAEA, Vienna (1995) 61.
- [11] SUAREZ MAHOU, E., CERRAJERO H., J., CREGO, A., Relación Interna JEN, Prospección aérea sistemática de la zona de Badajoz, Madrid (1967).

- [12] SUAREZ MAHOU, E., FERNANDEZ AMIGOT, J. A., Proyecto MARNA (Mapa de Radiación Natural y Dosimétrico de España) XIX Reunión Anual SNE, Cáceres (Oct. 1993)
- [13] SUAREZ MAHOU, E., FERNANDEZ AMIGOT, J. A., "Use of uranium airborne survey data in the preparation of radiometric map of Spain", Application of uranium exploration data and techniques in environmental studies, IAEA-TECDOC-827, IAEA, Vienna (1995) 109.
- [14] SUAREZ MAHOU, E., FERNANDEZ AMIGOT, J. A., The Radiometrics Map of Spain (MARNA PROJECT), IX Congreso internacional de Minería y Metalurgia, León (1994)
- [15] TORRES, L. M., GRASTY, R. L., "The natural radioactivity map of Portugal", Application of uranium exploration data and techniques in environmental studies, IAEA-TECDOC-827, IAEA, Vienna (1995) 127.



CONSTRUCTION OF RADIOELEMENT AND DOSE RATE BASELINE MAPS BY COMBINING GROUND AND AIRBORNE RADIOMETRIC DATA

L. RYBACH, F. MEDICI

Institute of Geophysics,
ETH-Hoenggerberg,
Zurich

G.F. SCHWARZ

Swiss Federal Nuclear Safety Inspectorate,
Würenlingen

Switzerland

Abstract

For emergency situations like nuclear accidents, lost isotopic sources, debris of reactor-powered satellites etc. well-documented baseline information is indispensable. Maps of cosmic, terrestrial natural and artificial radiation can be constructed by assembling different datasets such as ground and airborne gamma spectrometry, direct dose rate measurements, and soil/rock samples. The in situ measurements were calibrated using the soil samples taken at/around the field measurement sites, the airborne measurements by a combination of in situ, and soil/rock sample data. The radioelement concentrations (Bq/kg) were in turn converted to dose-rate (nSv/h). First, the cosmic radiation map was constructed from a digital terrain model, averaging topographic heights within cells of $2 \text{ km} \times 2 \text{ km}$ size. For the terrestrial radiation a total of 1615 ground data points were available, in addition to the airborne data. The artificial radiation map (Chernobyl and earlier fallout) has the smallest data base (184 data points from airborne and ground measurements). The dose rate map was constructed by summing up the above-mentioned contributions. It relies on a data base which corresponds to a density of about 1 point per 25 km^2 . The cosmic radiation map shows elevated dose rates in the high parts of the Swiss Alps. The cosmic dose rate ranges from 40 to 190 nSv/h, depending on altitude. The terrestrial dose rate maps show general agreement with lithology: elevated dose rates (100 to 200 nSv/h) characterize the Central Massifs of the Alps where crystalline rocks give a maximum of 370 nSv/h, whereas the sedimentary northern Alpine Foreland (Jura, Molasse basin) shows consistently lower dose rates (40–100 nSv/h). The artificial radiation map has its maximum value in the southern part of Switzerland (90 nSv/h). The map of total dose rate exhibits values from 55 to 570 nSv/h. These values are considerably higher than reported in the Radiation Atlas ("Natural Sources of Ionising Radiation in Europe") published by the Commission of the European Communities. The most frequent radiation range in Switzerland is 85–115 nSv/h (total dose rate outdoors).

1. INTRODUCTION

Radioactivity is part of our physical environment. The largest contribution to the radiation field is of natural origin: it is due to cosmic rays, the natural radioactivity of the ground and the radioactive decay products of radon in the air. Artificial radioactivity is emitted by nuclear power plants, industrial plants and research facilities. These emissions are very small in normal operation, although large amounts of radioactivity can be released to the environment through accidents.

Maps of terrestrial gamma radiation, when converted to dose rate distribution, are indispensable for various purposes: they provide basic information for the effects of low doses and a well documented reference base for accident and emergency situations (release from nuclear power plants, lost radioactive sources, debris from fission-powered satellites). Furthermore, they can aid geological mapping and/or prospecting for raw materials (e.g. by locating potassium alteration). Gamma radiation maps are especially needed on the scale of whole countries. We summarize here the methodology followed to establish a set of ground gamma radiation maps for Switzerland [1].

2. INPUT DATA

No single nationwide dataset of radioactivity in Switzerland was available with sufficient areal density. Therefore four different datasets have been combined for map generation (Fig. 1):

- Airborne gamma-ray spectrometric measurements: About 10% of Switzerland has been surveyed by helicopters. The selected regions are mainly located in the Swiss Alps.
- In situ gamma-ray spectrometric measurements: At 166 sites high precision in-situ gamma spectrometric measurements have been carried out with a portable germanium detector.
- Dose rate measurements: Together with the in situ measurements a dose rate determination with a Reuter-Stokes ionization chamber was carried out at every site. In addition, 282 sites of an earlier survey were also included. Finally, data collected with Geiger-Mueller counters during emergency preparedness training (389 sites) were added to the data set.
- Laboratory measurements on surface rock and soil samples: Over the last 30 years many surface rock and soil samples have been examined with both sodium iodide and germanium detectors, mainly for geochemical and geothermal studies (612 samples).

The aim of this project was to compile and combine these datasets to create a radiometric map of Switzerland. In a somewhat similar effort, the usefulness of combining airborne gamma spectrometric survey data with radiogeological ground data in estimating gamma-ray dose rates was demonstrated in California [2].

2.1. Airborne gamma-ray spectrometric measurements

The Swiss Geophysical Commission (SGPK) performed the mapping of selected regions with elevated natural radioactivity within the framework of the Swiss National Geophysical Survey [3]. Attention was principally given to the crystalline rocks of the Central Massif of the Swiss Alps because of their relatively high natural radioactivity. Selected areas with typical lithology (Mesozoic limestones, Tertiary Molasse sediments and Quaternary deposits) have also been surveyed. The area covered by this survey is about 3000 km². In addition, an area of about 50 km² surrounding each of the four nuclear power plants (Beznau, Goesgen, Leibstadt and Muehleberg) and the Swiss nuclear research facility (Paul Scherrer Institute) have been surveyed annually for the past four years (financed by the Swiss Federal Nuclear Safety Inspectorate (HSK)). The measurements aim to monitor the dose-rate distribution and to provide a documented reference base [4].

The measuring system consists of a helicopter-borne gamma-ray spectrometer with data control and storage and flight positioning instrumentation. The spectrometer covers the gamma-ray energy range of 40 keV to 3000 keV with 256 channels. An additional channel is used for the registration of high energy cosmic radiation. The detector used for the survey consists of a package of four 4" × 4" × 16" prismatic, thallium-doped, sodium iodide crystals (total volume 16.8 L). A PC-based data acquisition system synchronizes and controls the measurements. The spectrometer data are collected every second together with radar altitude, time, barometric pressure, outside air temperature and aircraft attitude angles. Positioning is done with the satellite navigation system GPS [5].

Processing covers the common calibration and reduction procedures (cosmic and background correction, spectral stripping, altitude correction) extended with an additional topographical correction to account for the effects of the rugged topography in the Swiss Alps. The data processing procedures adopted in this project, in particular for reducing the effects of topography on airborne gamma-ray spectrometry measurements, are described in [3] and [6].

2.2. In situ gamma-ray spectrometric measurements

The in situ gamma spectrometric data were collected by the Branch for Radioactivity Surveillance of the Federal Office of Public Health (SUEr). A total of 166 points are monitored for environmental radioactivity, particularly in the neighbourhood of nuclear installations and factories handling, processing or producing radioactive material ([7] and [8]).

The measuring instrument consists of a portable germanium detector system with 4096 channels. In addition to the in situ measurement, which lasts for about two hours, soil samples were collected from different depths for subsequent laboratory analysis.

2.3. Dose rate measurements

At the time of the in situ spectrometric measurements, a dose rate measurement with a Reuter-Stokes ionization chamber (RSS 111) was taken at every location. Many more measurements were made subsequently (especially inside houses) to give a more detailed map [9].

Data from 282 sites reported from an older survey with a 25 L, air-filled ionisation chamber instrument were also included [10]. Recent emergency preparedness exercises of the Swiss National Emergency Operation Centre (NAZ) with Geiger-Mueller (GM) counters contributed 389 additional points. The instrument used was the Automes 6150 AD2, calibrated to measure the total dose rate, and the measuring time was one hour [11].

2.4. Laboratory measurements

Since the late 1960s, 612 surface rock and soil samples have been analysed for the natural radioelements, potassium, uranium and thorium, with a laboratory sodium iodide system at the Geophysics Institute, ETH. The aim of these measurements was mainly to determine heat production ([12], [13] and [14]). Since 1990 these measurements have been performed with a modern high purity germanium system from Intergamma (efficiency 26%) with 4096 channels.

3. CALIBRATION

When combining these datasets, it is essential to account for the fact that they have been acquired with different methods. In particular, the representative volumes are different. An airborne measurement represents the topmost 50 cm in an area of about 300 m x 300 m. An in situ or dose rate measurement represents a much smaller area of 10 m x 10 m. The smallest volume is represented by the sample measurements which are normally carried out on 0.5 kg of material.

The in situ measurements were calibrated using the soil samples taken with every set of measurements. Experience showed that five to ten samples per site were enough for the calibration. Since the artificial isotopes are not distributed homogeneously in the soil a depth profile is taken to determine their distribution. The error of an in situ gamma spectrometric measurement can be estimated at about $\pm 20\%$ for each isotope.

The airborne data were calibrated using a combination of in situ measurements and rock sample data. Since the airborne measurements cover a much larger sample area, an average of four in situ measurements and 50 rock samples in different lithological units were used for the calibration. Table I lists the calibration factors obtained.

The ground activities in Becquerels per kilogram have been converted to dose rates in nanoSieverts per hour using the following conversion factors (in nSv/h per Bq/kg): 0.05 for ^{40}K , 0.51

for ^{214}Bi , 0.71 for ^{208}Tl and 0.17 for ^{137}Cs [8]. Other isotopes (^{134}Cs , ^{60}Co , ^7Be , etc...) occur only in traces and were neglected for this application. In the uranium and thorium decay chains, equilibrium up to the isotopes ^{226}Ra , ^{228}Ac , respectively, was assumed.

TABLE I. CALIBRATION FACTORS FOR THE AIRBORNE SYSTEM (CALCULATED FROM COUNT RATES MEASURED WITH THE AIRBORNE SYSTEM AT 120 M FLIGHT ALTITUDE AND ACTIVITY DETERMINATIONS IN BQ/KG AT GROUND)

Isotope	^{137}Cs	^{40}K	^{214}Bi	^{208}Tl
cps in window per Bq/kg	0.500	0.090	0.268	0.418

4. COLLATION/INTERPOLATION/MAPPING

The radiation at a point is composed of three components:

- Cosmic background: The intensity of the radiation due to cosmic rays depends mainly on the thickness of the atmosphere above the measurement location, and therefore mainly on altitude above sea level. Neglecting the effects of air pressure, the cosmic background can be considered constant in time.
- Natural terrestrial radiation: Terrestrial radiation is mostly produced by the decay of the four natural radio isotopes ^{235}U , ^{238}U , ^{232}Th and ^{40}K .
- Artificial terrestrial radiation: Sometimes contributions of long-lived decay and activation products from nuclear weapon tests and/or nuclear facilities (mainly ^{137}Cs) add to the natural contributions. The artificial radiation at the surface varies with time due to decay and downward migration of caesium.

The cosmic contribution of the radiation was calculated from a digital terrain model averaging topographic heights within a cell size of $2\text{ km} \times 2\text{ km}$ using the relation:

$$D_{\text{cosmic}} [\text{nSv/h}] = 37.0 \cdot \exp (0.38 \cdot \text{altitude} [\text{km}]) \quad [8]$$

which yields a map of the cosmic background in Switzerland (Fig. 2).

The map of the natural terrestrial radiation assembles the airborne gamma-ray spectrometry, in situ gamma-ray spectrometry and rock/soil sample data. In addition to the airborne data, a total of 1615 ground data points were available for the map production.

The variations in the natural dose rate (terrestrial and cosmic) due, for example, to radon washout, soil humidity, snow cover and sun activity are around 25%, and were neglected for this work. The artificial part of the radiation poses a specific problem. Since this contribution is not constant in time, the value depends on the time of the measurements.

In particular, data recorded in 1986 are strongly influenced by the fallout from Chernobyl. The map of the artificial radiation was therefore produced only using data from in situ and airborne spectrometric measurements taken after 1987, which yielded 167 data points. Laboratory measurements on rock samples could not be used for the map of artificial radiation, since they are usually taken from an unweathered (covered) part of a rock, and are therefore devoid of any artificial radioactive isotopes. This map (Fig. 4) has the smallest data base.

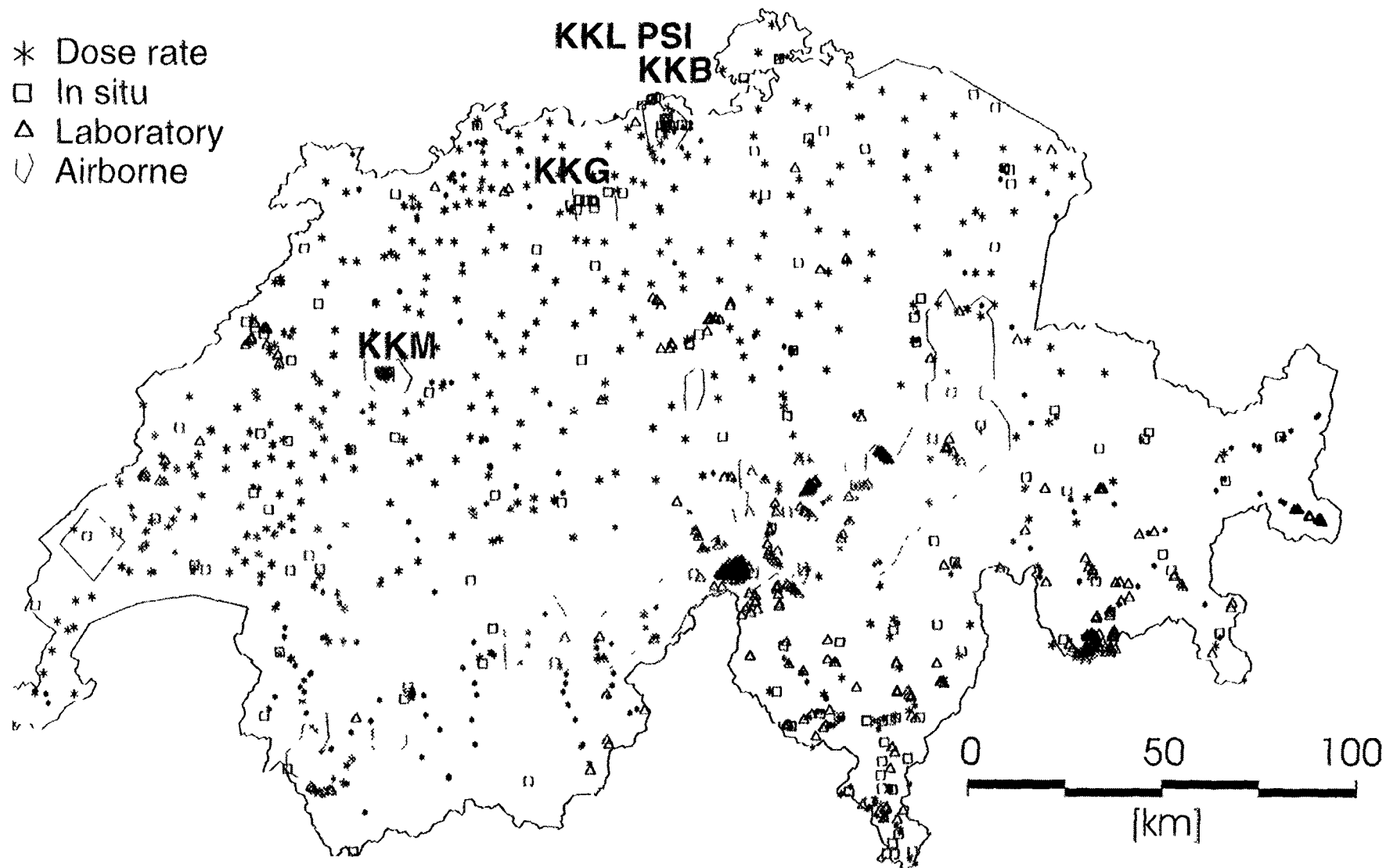


FIG. 1. Distribution of the input data. Hatched areas have been surveyed by airborne gamma ray spectrometry. Swiss nuclear facilities: KKB = nuclear powerplant Beznau, KKG = nuclear powerplant Gßsgen, KKL = nuclear powerplant Leibstadt, KKM = nuclear powerplant Mühleberg, PSI = Paul Scherrer Institute.

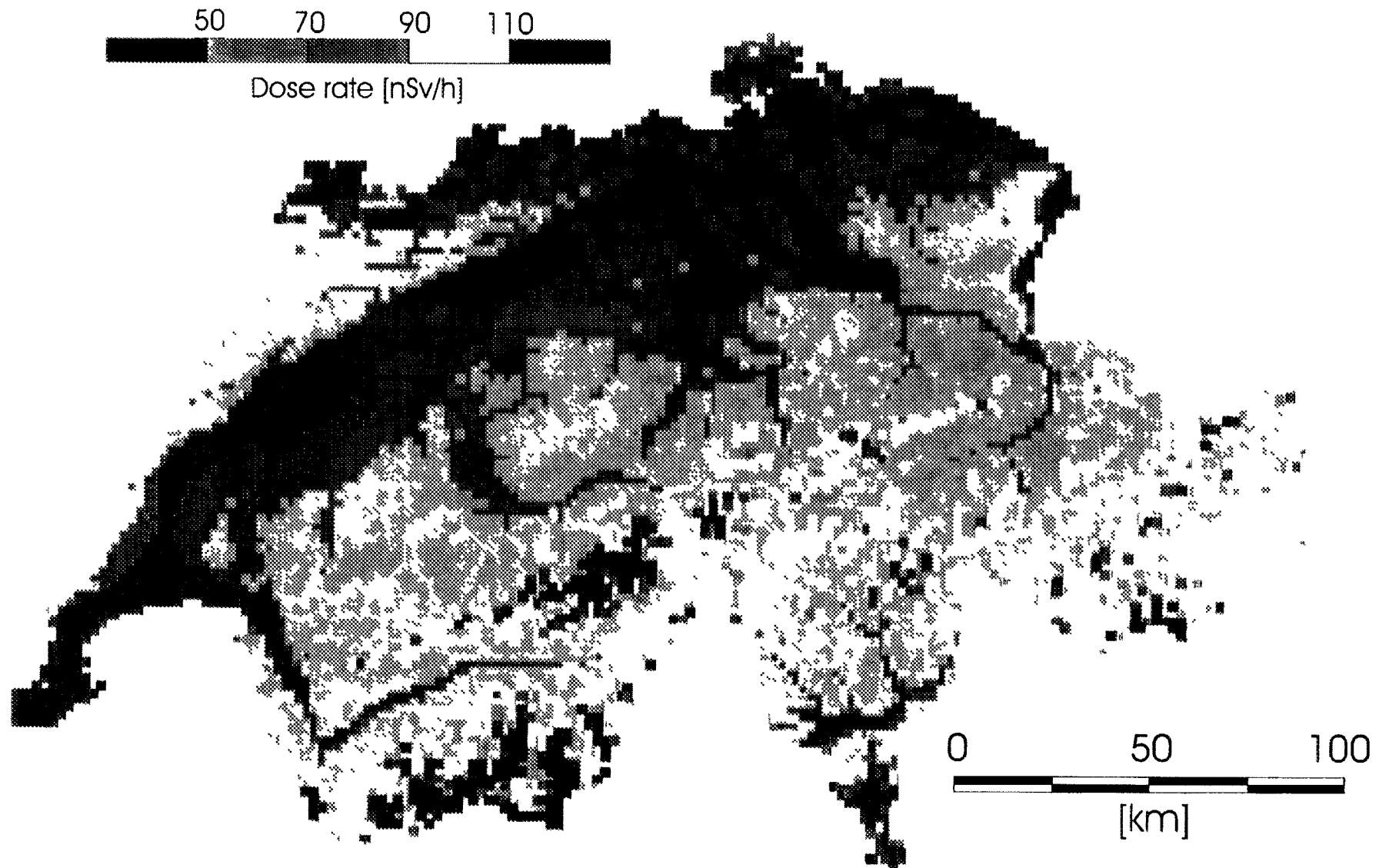


FIG 2. Cosmic dose rate map (in nSv/h) of Switzerland Min. value: 40 nSv/h, Max. value 191 nSv/h, Average value: 64 nSv/h, Std. deviation 22 nSv/h

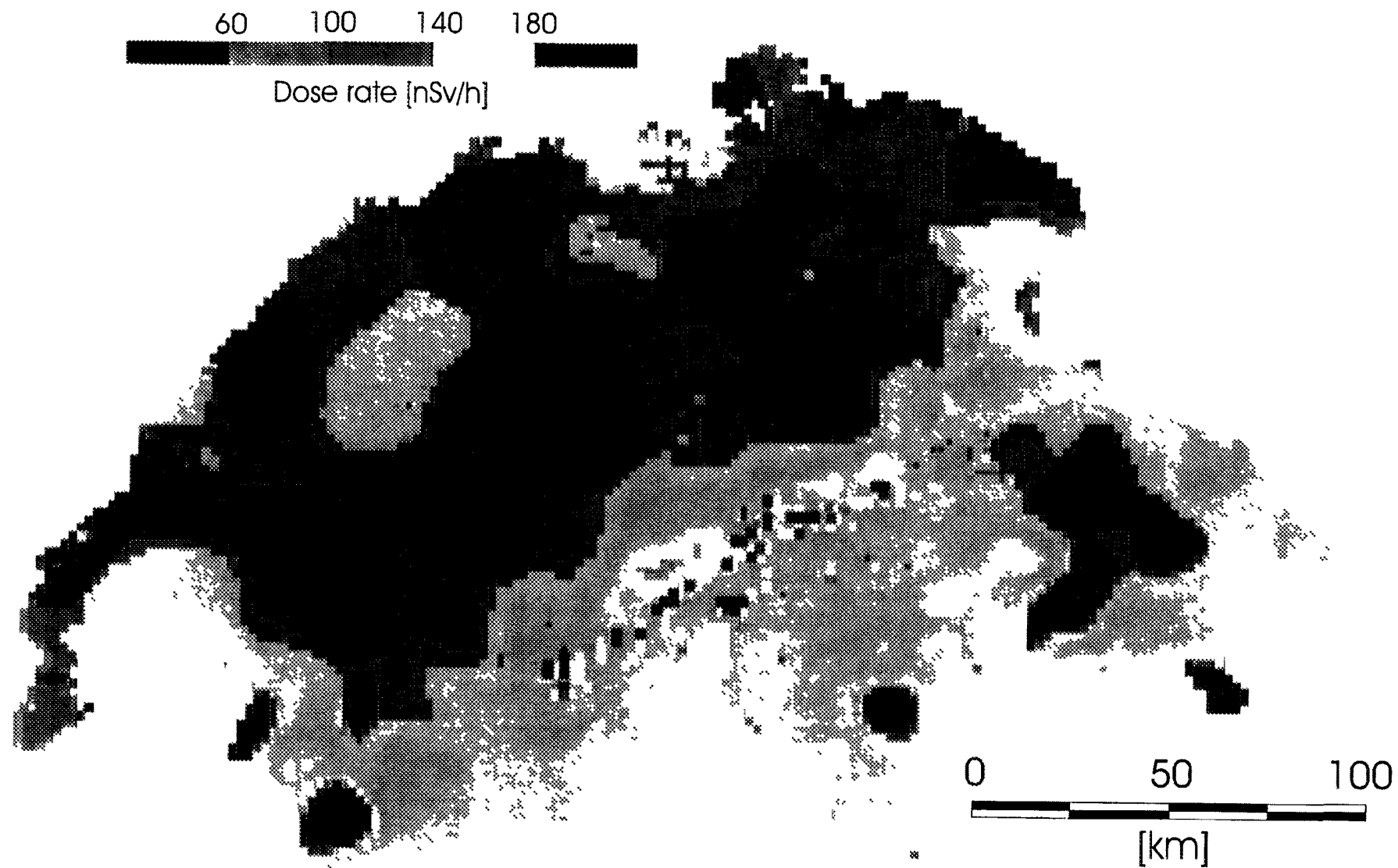


FIG. 3. Natural terrestrial dose rate map (in nSv/h) of Switzerland. Min. value: 6 nSv/h; Max. value: 368 nSv/h; Average value: 68 nSv/h; Std. deviation 35 nSv/h.

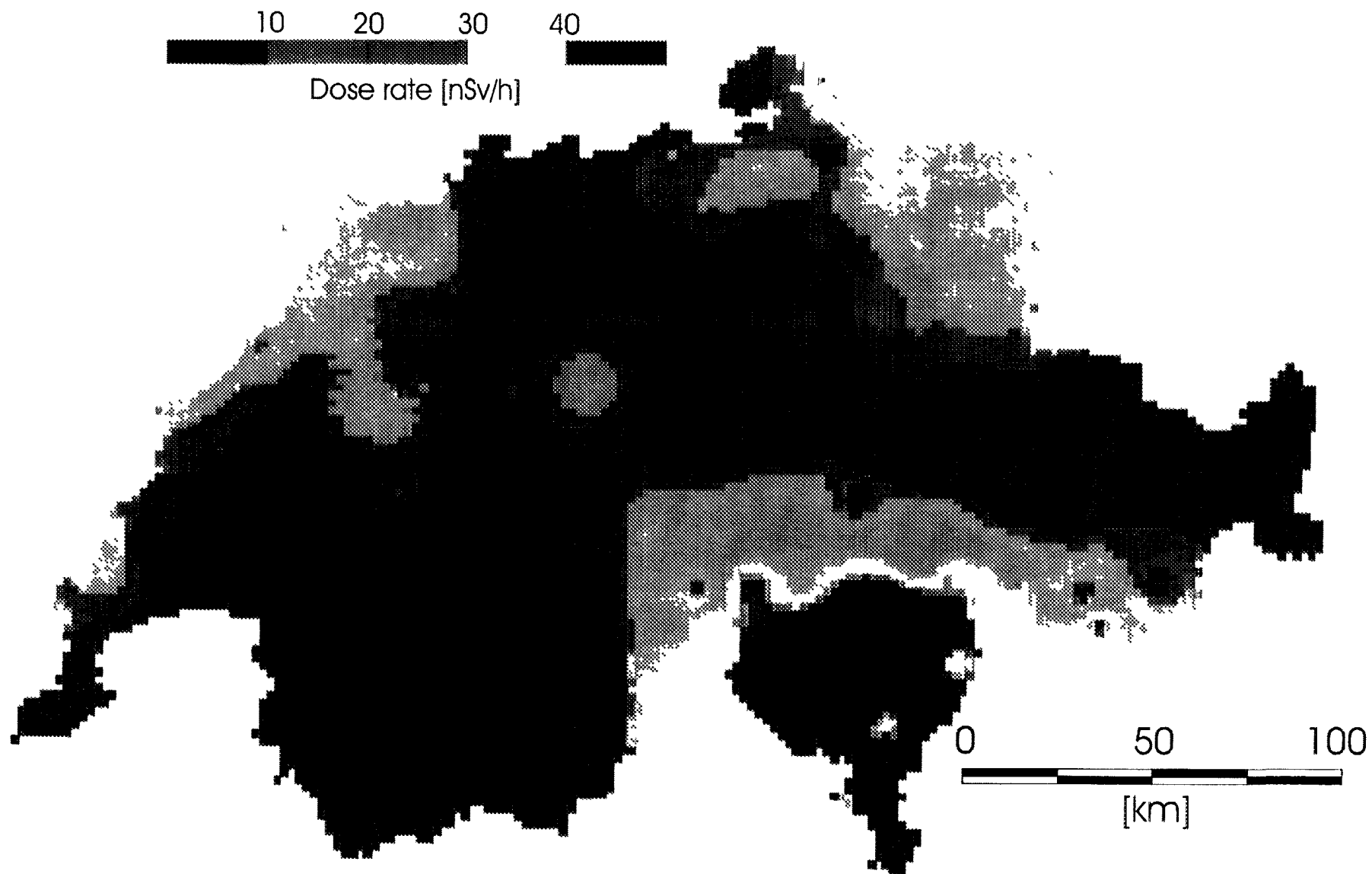


FIG. 4. Artificial dose rate map (in nSv/h) of Switzerland. Min. value: 1 nSv/h; Max. value: 91 nSv/h; Average value: 11 nSv/h; Std. deviation 14 nSv/h.

The total dose rate map of Switzerland was calculated by summing the previously described maps (cosmic, natural terrestrial and artificial dose rate).

For the interpolation of the maps, a simple inverse distance method with a search radius of 12 km and cell size of $2\text{ km} \times 2\text{ km}$ was chosen. In areas with airborne data coverage the search radius was decreased to 2 km to give better spatial resolution.

Because of the generally large statistical errors in radiometric data, the sharp changes in radioactive field intensities and the inhomogeneous data point distribution the classical isoline representation was abandoned and the pixel representation was used (for details see [3] and [15]). The values on the maps are given in a 25-grade linear color scale (blue \rightarrow cyan \rightarrow green \rightarrow yellow \rightarrow red: increasing values). The color ranges are given on the respective figures, along with the maximum, minimum, and mean value with standard deviation.

5. RESULTS AND CONCLUSIONS

By assembling different ground radiation datasets and after appropriately converting the measured values, a dose rate map of Switzerland could be constructed. It relies on a data base which corresponds to a density of about 1 point per 25 km^2 .

The map of the cosmic radiation (Fig. 2) shows elevated dose rates in the high parts of the Swiss Alps. The cosmic dose rate ranges from 40 to 190 nSv/h, according to the altitude.

The terrestrial natural dose rate map presented in Fig. 3 shows general agreement with lithology: elevated dose rates (100 to 200 nSv/h) characterize the Central Massifs of the Alps where crystalline rocks give a maximum dose rate of 370 nSv/h, whereas the sedimentary northern Alpine Foreland (Jura, Molasse Basin) shows consistently lower dose rates (40–100 nSv/h). The ground radiation can show short-term changes. After rainfall, the short-lived daughter products of atmospheric radon are deposited on the ground; they can increase the dose rate for about a day by several tens of nSv/h.

The artificial radiation map (Fig. 4) has its maximum value in the southern part of Switzerland (90 nSv/h). In this region it rained soon after the Chernobyl accident, so the airborne aerosols with radioactive isotopes were washed out and deposited.

And finally the map of the total dose rate of Switzerland is presented (Fig. 5), which corresponds roughly to the sum of the above three maps (with additional data points from the dose rate measurements). The values range from 55 to 570 nSv/h. The dose rate frequency distribution derived from the total dose rate map by counting the pixels in each interval is shown in the histogram of Fig. 6. The predominance of the dose rate range 85–115 nSv/h is evident.

These values are considerably higher than reported in the Radiation Atlas ("Natural Sources of Ionising Radiation in Europe") published by the European Communities (60–70 nSv/h).

In summary, by properly treating the non-uniform data base available, a consistent ground radiation map of Switzerland has been established. The results indicate the dose rate varies over about one order of magnitude and the most frequent radiation level is in the range 85–115 nSv/h (total dose rate outdoors).

ACKNOWLEDGEMENTS

This mapping study was performed within the project framework of the Swiss Federal Nuclear Safety Inspectorate. We thank Dr. S. Prêtre and W. Jeschki (Würenlingen) for continuous support and valuable discussions. Contribution no. 913, Institute of Geophysics ETH Zurich.

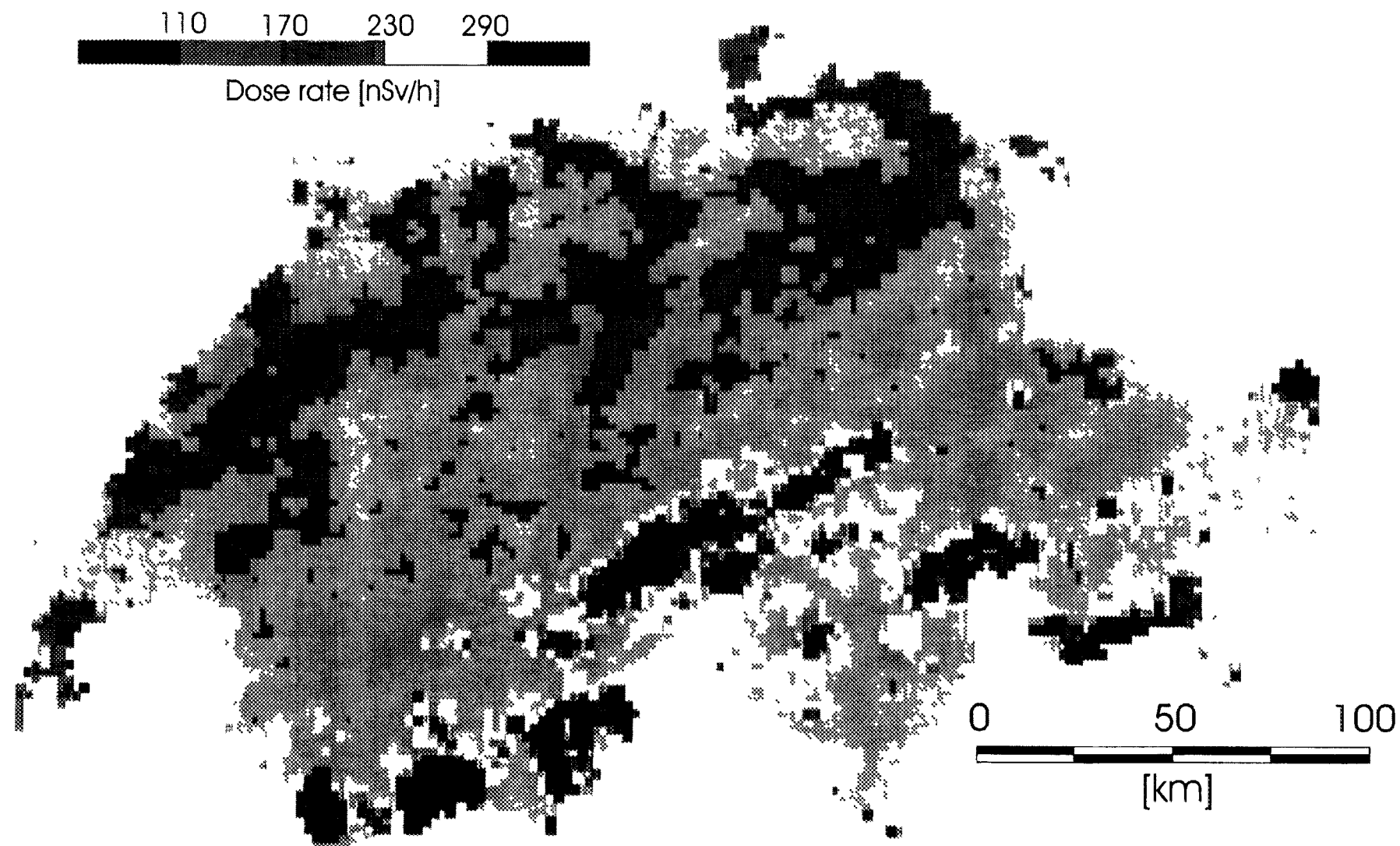


FIG. 5 Total dose rate map (in nSv/h) of Switzerland Min value: 55 nSv/h; Max value: 569 nSv/h, Average value: 147 nSv/h, Std deviation 59 nSv/h

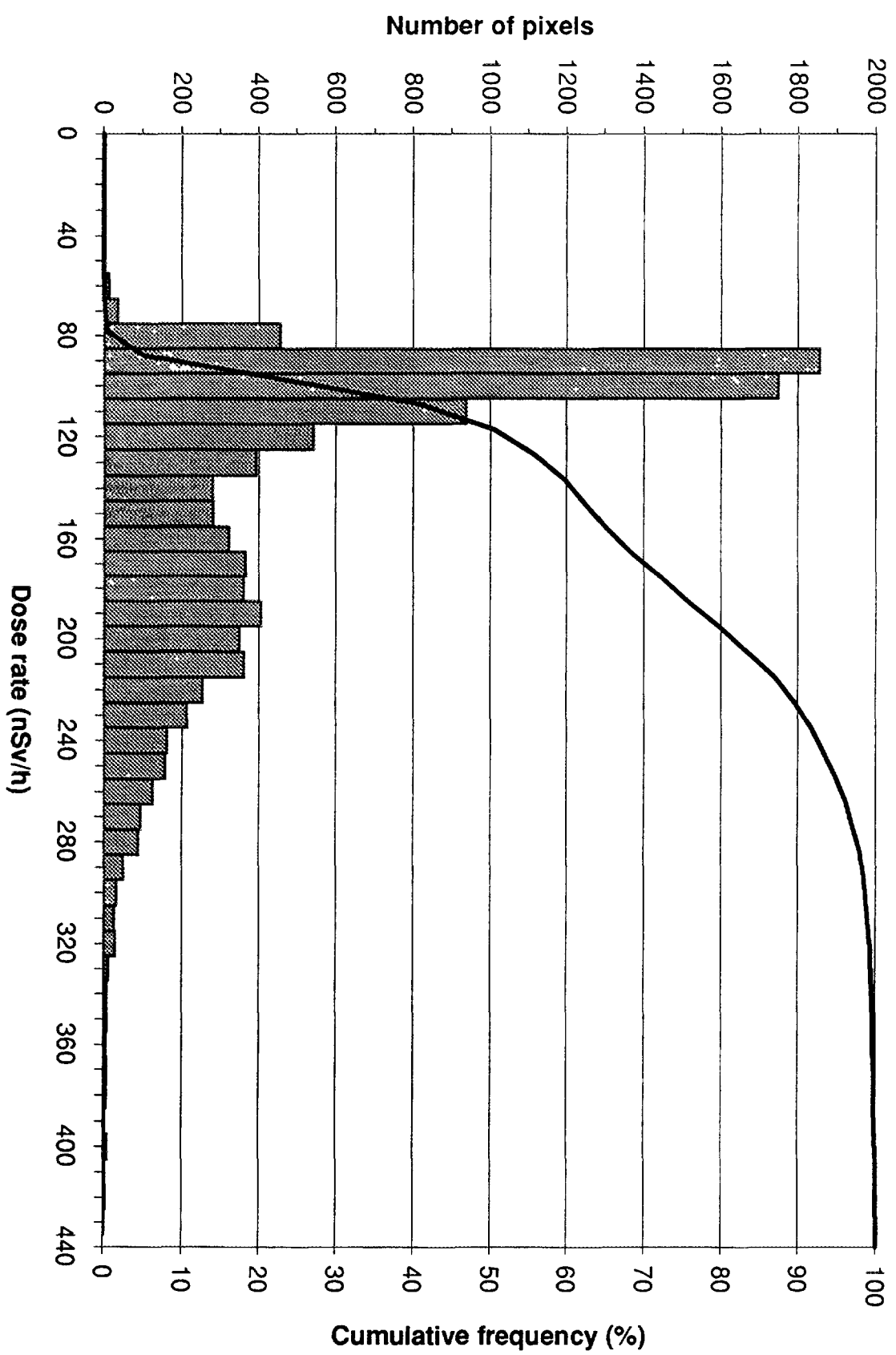


FIG. 6. Dose rate frequency distribution in Switzerland.

REFERENCES

- [1] RYBACH, L., SCHWARZ, G.F., Ground gamma radiation maps: processing of airborne, laboratory and in situ spectrometry data, *FIRST BREAK* 13 (1995) 97–104.
- [2] WOLLENBERG, H.A., REVZAN, K.L. and SMITH, A.R., Application of airborne gamma spectrometric survey data to estimating terrestrial gamma-ray dose rates: An example in California, *Health Physics* 66 (1994) 10–16.
- [3] SCHWARZ, G.F., KLINGELE, E.K., RYBACH, L., Airborne radiometric mapping in Switzerland. Beiträge zur Geologie der Schweiz, Geophysik Nr.25. Schweizerische Geophysikalische Kommission, Institut für Geophysik der ETHZ, Zürich (1992).
- [4] SCHWARZ, G.F., KLINGELE, E.K., RYBACH, L., Aeroradiometrische Messungen in der Umgebung der schweizerischen Kernanlagen, Berichte zuhanden der Hauptabteilung für die Sicherheit der Kernanlagen (HSK), Interne HSK-Berichte, Hauptabteilung für die Sicherheit der Kernanlagen, Villigen, Switzerland (1989, 1990, 1991 and 1992).
- [5] SCHWARZ, G.F., RYBACH, L., BAERLOCHER, C.K., KLINGELE, E.E., "Development and calibration of an airborne radiometric measuring system", *Application of Uranium Exploration Data and Techniques in Environmental Studies*, IAEA-TECDOC-827, IAEA, Vienna (1995) 25–34.
- [6] SCHWARZ, G.F., RYBACH, L., KLINGELE, E.K., How to handle rugged topography in airborne gamma-ray spectrometry, *First Break* 10 (1992b) 11–17.
- [7] MURITH, C., VOELKLE, H.R., SURBECK, H., PILLER, G., BAERISWIL, L., BEURET P., FERRERI, G., GOBET, M., GURTNER A., RIBODRY, L., Mesures in situ — mesures aéroradiométrie dans le voisinage du PSI, Interner SUeR-Bericht, Bundesamt für Gesundheitswesen, Sektion zur Überwachung der Radioaktivität, Fribourg, Switzerland (1991).
- [8] MURITH, C., GURTNER A., "Mesures in situ et irradiation externe", *Environmental Radioactivity and Radiation Exposure in Switzerland*, Annual Reports 1990, 1991, 1992 and 1992, BAG-Bericht. Bundesamt für Gesundheitswesen, Abteilung Strahlenschutz, Bern, Switzerland (1990, 1991 and 1992).
- [9] JOHNER, H.U., VOELKLE, H.R., "Die natürliche terrestrische und kosmische Strahlung im Hausinnern", *Environmental Radioactivity and Radiation Exposure in Switzerland*, Annual Report 1993, Bundesamt für Gesundheitswesen, Abteilung Strahlenschutz, Bern, Switzerland (1993).
- [10] HALM, E., HERBST, W., MASTROCOLA, A., Messung des natürlichen Strahlenpegels in der Schweiz, *Bulletin des Eidg. Gesundheitsamtes*, Beil. B Nr. 6 (1962) 133–167.
- [11] RAUBER, D., Übung NARACH der Nationalen Alarmzentrale (NAZ), *Allgemeine Schweizer Militär-Zeitschrift* (Verlag Huber & Co, Frauenfeld) 11 (1993) 498–500.
- [12] SCHÄERLI, U., Geothermische Detailkartierung (1:100 000) in der zentralen Nordschweiz mit besonderer Berücksichtigung petropysikalischer Parameter, Dissertation ETH Nr.8941, Eidgenössische Technische Hochschule, Zürich (1989).
- [13] RYBACH, L., LABHART, T.P., Regelmässigkeiten der Radioaktivitätsverteilung in granitischen Gesteinskörpern (Beispiele aus den Schweizer Alpen), *Schweizerische Mineralogische und Petrographische Mitteilungen* 53 (1973) 379–385.
- [14] LABHART, T.P., RYBACH, L., Abundance and distribution of uranium and thorium in the syenite of Piz Giuv (Aar-Massif, Switzerland), *Chemical Geology* 7 (1971) 237–251.
- [15] SCHWARZ, G.F., RYBACH, L., KLINGELE, E.E., "Data processing and mapping in airborne radioactivity systems", *Application of Uranium Exploration Data and Techniques in Environmental Studies*, IAEA-TECDOC-827, IAEA, Vienna (1995) 61–70.



BACKGROUND RADIATION MAP OF THAILAND

P. ANGSUWATHANA, P. CHOTIKANATIS

Department of Mineral Resources,
Ministry of Industry,
Bangkok, Thailand

Abstract

The radioelement concentration in the natural environment as well as the radiation exposure to man in day-to-day life is now the most interesting topic. The natural radiation is frequently referred as a standard for comparing additional sources of man-made radiation such as atomic weapon fallout, nuclear power generation, radioactive waste disposal, etc. The Department of Mineral Resources commenced a five-year project of nationwide airborne geophysical survey by awarding to Kenting Earth Sciences International Limited in 1984. The original purpose of survey was to support mineral exploration and geological mapping. Subsequently, the data quantity has been proved to be suitable for natural radiation information. In 1993 the Department of Mineral Resources, with the assistance of IAEA, published a Background Radiation Map of Thailand at the scale of 1:1 000 000 from the existing airborne radiometric digital data. The production of Background Radiation Map of Thailand is the result of data compilation and correction procedure developed over the Canadian Shield. This end product will be used as a base map in environmental application not only for Thailand but also Southeast Asia region.

INTRODUCTION

In the last few years there has been increasing public concern regarding the natural radiation environment. The natural radiation we received is due almost to gamma radiation and cosmic radiation. The natural radiation is therefore frequently referred as a standard for comparing additional sources of man-made radiation such as atomic weapon fallout, nuclear power generation, radioactive waste disposal. In order to evaluate the significance amount of these additional man-made radiation, the levels of natural background radiation must be known.

Since a nearly entire part of the Kingdom of Thailand has been covered by airborne gamma ray measurement. The main outputs from the survey are maps and profiles of total count, potassium, equivalent uranium, equivalent thorium and either uranium to thorium or thorium to potassium ratio.

It was recommended by IAEA technical officer that the radiometric digital data should be further processed to produce background radiation map. With the assistance of IAEA, the project THA/3/004 was approved in 1993. However, the limitation of software and computer facilities at that time, the productions of background radiation map and ternary radioactivity map of Thailand as part of this project were contracted to Urquhart Dvorak Limit of Canada.

AIRBORNE GEOPHYSICAL SURVEY

In 1984, the Department of Mineral Resources of Thailand commenced a five-year project of nationwide airborne geophysical survey. The contract was awarded to Kenting Earth Sciences International Limited (KESIL), a Canadian company, with the support of the Canadian International Development Agency (CIDA) and the Geological Survey of Canada (GSC).

The objective of the survey was to establish a completely systematic geophysical database for both the government and the private sector in mineral resources exploration and investment. Three different types of surveys were designed:

- 1) Aeromagnetic Survey was flown by fixed wing aircraft using high resolution magnetometer in survey area A at various altitudes ranging from 305 m (1000 ft) to 2286 m (7500 ft) with

line spacing 1 km in north-south direction covering an area approximately 440 000 km² (86 % of the country).

- 2) Airborne Radiometric Surveys were flown using high sensitivity gamma-ray spectrometer system with a sodium iodine detector of 50 litres, magnetometer and VLF-EM in survey areas B and C at 122 m (400 ft) mean terrain clearance with line spacing of 1,2,5 km in east-west direction (Fig. 1). The difference between survey areas B and C was the type of aircraft being used, survey area B was flown by twin-engine fixed wing aircraft over low relief terrain while survey area C was flown by helicopter over rugged terrain covering an area approximately 430 000 km² (35 and 50% respectively).
- 3) Airborne Electromagnetic Survey was flown by helicopter using EM and magnetometer in follow-up survey at 60 m mean terrain clearance with line spacing 400 m in the direction perpendicular to the geological trend covering area approximately 18 000 km² (3.5%).

PROCESSING OF RADIOMETRIC DATA

The processing methods were designed for airborne radiometric survey data by Data Plotting Services International Limited in co-operation with the GSC.

The energy windows used to monitor gamma rays are tabulated in Table I.

TABLE I. SPECTRAL WINDOWS USED TO MEASURE GAMMA RAYS

Element	Isotope Used	Energy Window (Mev)
Potassium	⁴⁰ K	1.36–1.56
Uranium	²¹⁴ Bi	1.66–1.86
Thorium	²⁰⁸ Tl	2.42–2.82
Total count		0.40–2.82

Calibration of airborne and ground spectrometers was necessary to obtain accurate ground concentration from the survey. To deal with the problems of calibration, large radioactive calibration pads were constructed, under the guidance of R.L. Grasty, at U-Tapao Airport, Rayong province, eastern Thailand and airborne test range was established at Lam Takhong reservoir, 200 km northeast of Bangkok.

Data collected by airborne gamma ray spectrometry have been processed and presented as five different maps: potassium (K), equivalent uranium (eU), equivalent thorium (eTh) concentrations, uranium to thorium (eU/eTh) or thorium to potassium (eTh/K) ratio and total count.

In order to relate the airborne count rate from the three windows to radioelement concentrations of the ground, the data processing are necessary. These are :

- 1) removal of background radiation;
- 2) spectral stripping procedure;
- 3) altitude correction ; and
- 4) conversion of the corrected count rate data to ground concentration.

ad 1) Removal of Background Radiation

There are three sources of background radiation; the radioactivity of the aircraft and its equipment, cosmic radiation, and radioactivity in the air arising from daughter products of radon gas in the uranium decay series. The technique used to remove the effect of these three sources of background radioactivity has been traditionally applied by measuring total radioactivity contribution over water. In the areas where no water is available, high level background is accepted for background observation. An alternate method of determining background is a test line measurement.

Since cosmic background is well controlled and the aircraft background is small and constant, background errors are due to improper estimates of the radon component. Variation caused by radon emanating from the ground in the north of Thailand is strong therefore de-corrugation filtering is approved.

ad 2) Spectral Stripping Procedure

Due to the characteristic of the airborne gamma ray spectrum measured by sodium iodine detectors, gamma rays originating from one particular radioelement may be detected in any of the three windows. To correct for this interference, a spectral stripping procedure must be carried out. This is achieved by determining the gamma ray spectra of the respective radioactive concrete calibration pads. The stripping procedure used to derive the corrected counts in each window that originate from the respective radioelement has been described by Grasty [2].

ad 3) Altitude Correction

In the range of altitudes normally encountered in airborne survey operations the stripped and background-corrected count rate in each window is found to be related to the aircraft altitude by a simple exponential expression of the form :

$$N = Ae^{\mu h}$$

where attenuation coefficient (A) and attenuation rate (μ) are determined experimentally over the calibration range [1]. This exponential curve is used to correct the count rates in each window for deviations from the planned survey altitude.

ad 4) Conversion of corrected count rate data to ground concentration

After the window count rates are normalized to a standard condition of measurement, they are simply converted to equivalent ground concentrations by application of the sensitivities of the airborne gamma ray spectrometer. The sensitivity factors are determined over calibration range of known radioelement concentration as shown in Table II.

TABLE II. SENSITIVITY FACTORS USED TO CONVERT GROUND CONCENTRATION

Element	Normal Sensitivity
Total count	174 cps/ur
Potassium	100 cps/%
Uranium	10.9 cps/ppm
Thorium	6.8 cps/ppm

PRODUCTION OF BACKGROUND RADIATION MAP

In 1989, KESIL delivered radiometric maps, stacked profiles and digital data on tapes. Map products include radioactivity colour pixel map of Thailand at the scale of 1:1 000 000 and radiometric contour maps at the scale of 1:250 000. These maps are presented as total count, potassium (K), equivalent uranium (eU), equivalent thorium (eTh) and either uranium to thorium or thorium to potassium ratio.

The airborne radiometric digital data of 301 162 line km stored on nine-track tapes were transferred to backup tapes using Computer Centre facility within the Department. The productions of Background Radiation Map and Ternary Radioactivity Map of Thailand were assigned to IAEA selected sub-contract, Urquhart Dvorak Limited of Canada in 1993.

All the data were compiled and reprocessed to produce Background Radiation Map of Thailand at the scale of 1:1 000 000 and presented in exposure rate unit of micro roentgens per hour (uR/h) (Fig. 2).

The relationship between radioelement concentration and exposure has been calculated by Beck et al and Lovborg and Kirkegaard. Grasty et al [3] derived the contribution of potassium, uranium and thorium to the exposure from those experiments and assigned the value as shown in Table III.

TABLE III. CALCULATE CONTRIBUTION OF POTASSIUM, URANIUM AND THORIUM TO THE EXPOSURE 1 M ABOVE THE GROUND

Exposure Rate (uR/h)	
	Assigned Value
1 % K	1.505
1 ppm U	0.625
1 ppm Th	0.310
$E = 1.505 K + 0.625 eU + 0.310 ETH$	

CONCLUSION

Ground level exposure rates can be determined by airborne gamma ray spectrometry. A total of 301 162 line km of airborne radiometric data were compiled and reprocessed to produce Background Radiation Map of Thailand. This map shows a very good correlation with geological features. In situ gamma ray measurement confirms that the areas of high radioactivity are generally related to granitic rocks. The lowest radioactive areas are found to be associated with sandstone.

The Background Radiation Map of Thailand will be a particularly effective tool for environmental study in the country. Furthermore, it is expected that this map will also contribute to the production of Natural Radioactivity Map of the World.

ACKNOWLEDGEMENTS

The writers wish to acknowledge Mr. Pricha Attavipach, the Director General of the Department of Mineral Resources for permission to publish this paper. More specifically to Mr. Suvit Sampattavanija, the Director of Economic Geology Division for his encouragement and advice. The

technical and financial assistance of the IAEA through the project THA/3/004 with the support of Mr. Mohamad Tauchid are gratefully acknowledged.

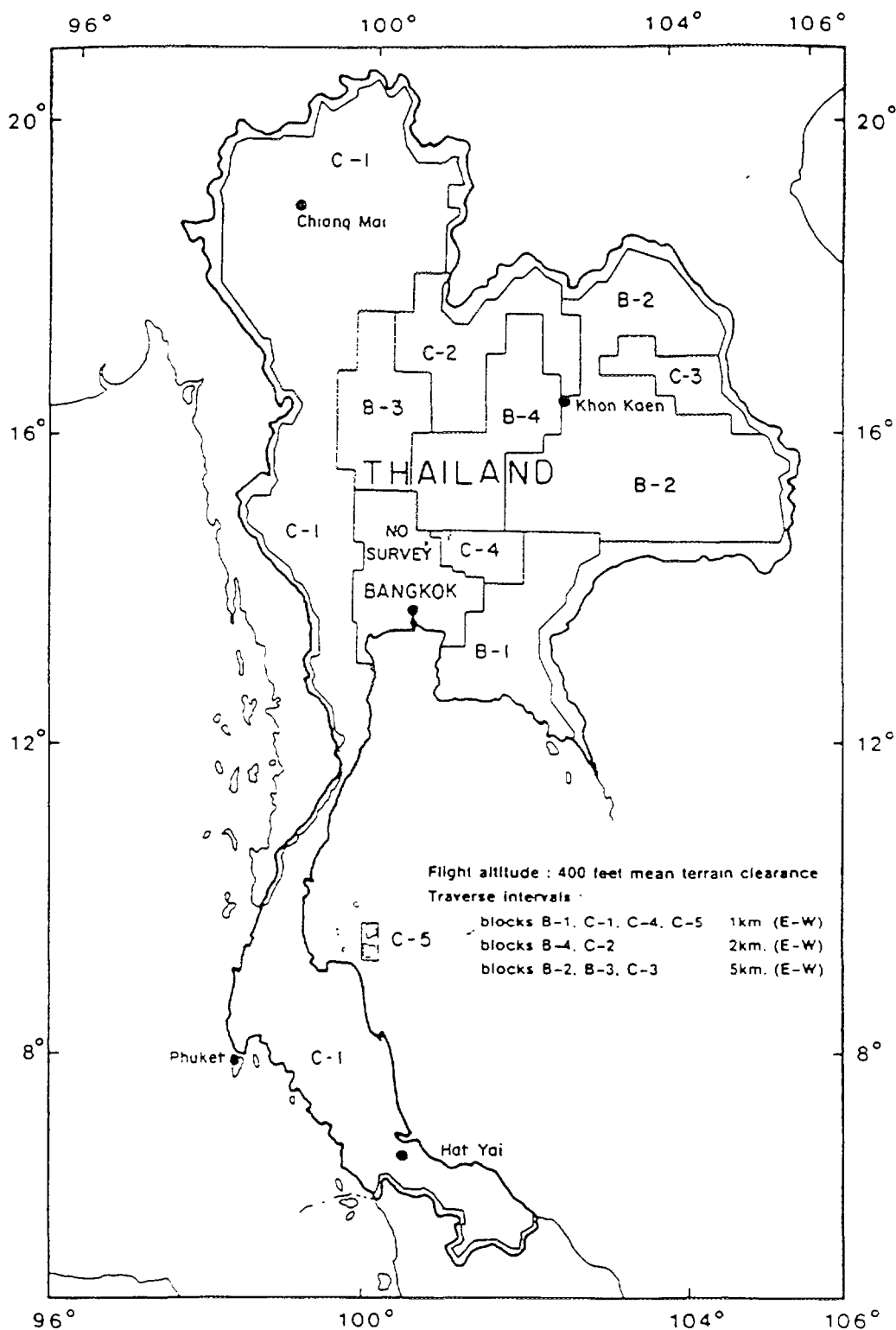


Fig. 1. Map of Thailand showing airborne radiometric survey areas B and C.

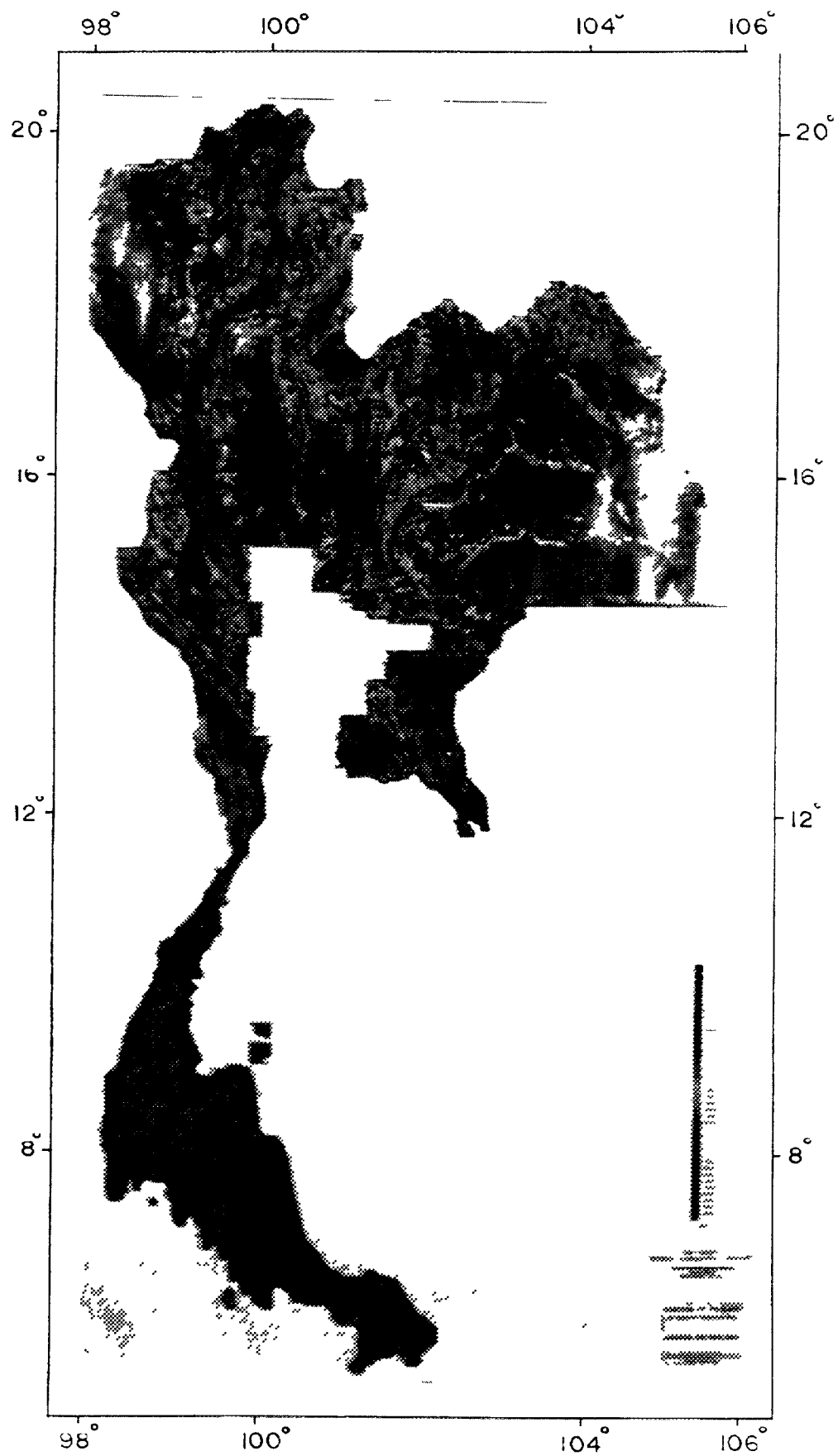


Fig 2 Background Radiation Map of Thailand at 1 1 000 000 (reduced to fit page)

REFERENCES

- [1] DARNLEY, A.G., BRISTOW, Q., AND DONHOFFER, D.K., "Airborne gamma-ray spectrometer experiments over the Canadian Shield", Nuclear Techniques and Mineral Resources (Proc. Conf. Buenos Aires, 1968), IAEA, Vienna (1969) 163-186.
- [2] GRASTY, R.L., A calibration procedure for an airborne gamma-ray spectrometer: Geological survey of Canada, Paper 76-16 (1976) 1-9.
- [3] GRASTY, R.L., CARSON, J.M., CHARBONNEAU, B.W. AND HOLMAN, P.B., Natural background radiation in Canada: Geological Survey of Canada, Bull. 360 (1984) 39 p.
- [4] GRASTY, R.L., TAUCHID, M. AND TORRES, L.M. de M., "Standardization of old gamma ray survey data", Application of uranium exploration data and techniques in environmental studies, IAEA-TECDOC-827, IAEA, Vienna (1995) 35-46.
- [5] KENTING EARTH SCIENCES INTERNATIONAL LIMITED, Technical Reports for Airborne Geophysical Survey, Surveys B and C, for the Department of Mineral Resources, Ministry of Industry, Kingdom of Thailand, Ottawa (1989).

**NEXT PAGE(S)
left BLANK**



TERRESTRIAL GAMMA DOSE RATE MAPS, THEIR COMPILATION AND VERIFICATION — RADIOMETRIC MAP OF THE CZECH REPUBLIC

M. MATOLÍN
Faculty of Science,
Charles University,
Prague, Czech Republic

Abstract

Maps of terrestrial gamma dose rate, usually expressed in nGy.h^{-1} , specify the natural radiation environment. Technique of measurement, data processing and compilation of radiometric maps contribute to resultant data deviations. Substantial influence on results may have technical parameters of used instruments, calibration facilities and method of instrument calibration, geometry, density and the mode of field radiometric measurement, data processing, data levelling and their graphical presentation. If maps are used for the assessment of the natural radiation environment, reliability of reported gamma dose rate values must be acceptable and should be checked. Radiometric map of the Czech Republic 1:500 000, published in 1995, expressed in gamma dose rate, is based on regional and detailed airborne total count (1957–1959) and gamma ray spectrometry (from 1976 onward) measurement, completed by ground investigations. Back calibration was applied to convert the data to dose rate and to level the map. Regional terrestrial radiation in the Czech Republic, formed by magmatic, sedimentary and metamorphic rocks, is in the range $6\text{--}245 \text{ nGy.h}^{-1}$, with the mean $65.6 \pm 19.0 \text{ nGy.h}^{-1}$. Preliminary verification of data reported in the radiometric map, carried out by ground gamma ray spectrometry regional traverses, showed a good map data levelling, while the mean deviation $\pm 13.8 \text{ nGy.h}^{-1}$ illustrates expected differences at individual sites and geological setting.

1. MAPS OF THE NATURAL RADIATION ENVIRONMENT

Terrestrial radiation, causing substantial component of the natural radiation environment, varies with the geological setting at the earth surface. Potassium, uranium and thorium are fundamental sources of radioactivity of rocks. Radiometric maps of terrestrial gamma dose rate are used in geological investigations, exploration of radioactive raw materials, environmental studies, delimitations of regions of radon risk, estimation of absorbed radiation dose from terrestrial radiation and they provide a base, against which man made radiation can be determined. A series of radiometric maps has been published [1].

2. CAUSES OF RADIOMETRIC DATA DEVIATIONS

Terrestrial gamma dose rate can be well determined at particular stations by means of pressurized ionization chambers. Standard geophysical equipment, its regional survey application and methods of data processing may yield deviations from local dose rate values. There are several factors influencing resultant radiometric data.

The field of gamma radiation, with natural abrupt changes, due to uneven distribution of natural radionuclides in rocks, is by routine technique determined as spatial average value, in dependence on the method of measurement.

Gamma total count instruments and their response to terrestrial gamma radiation are fundamentally sensitive to type and size of used detectors and equipment energy discrimination threshold. Small size NaI(Tl) scintillation detectors and low (30–100 keV) energy discrimination thresholds are mostly used. Response of these instruments to gamma radiation of K, U and Th in rocks need not to be proportional to the dose rate. The deviations depending on equipment parameters and on the ratios of K, U, Th in rocks, can be up to 20% relatively [2]. The range of deviations can

be estimated by equipment uranium equivalents of potassium and thorium with respect to ideal values 2.3 ppm U/1 % K and 0.44 ppm U/1 ppm Th [2, 3]. Range of deviations has been calculated and analyzed [4]. Calibration of total count instruments by means of a ^{226}Ra point source generally results in an overestimation of reported dose rates. Calibration over small size calibration pads, that do not generate adequate air downward backscattered radiation, does not correspond to radiation of natural infinite plane source.

Gamma ray spectrometers, determining concentrations of K, U, Th in rocks, that can be converted to gamma dose rate [2], are used in airborne and ground measurements. Calibration facilities and calibration procedures are essential for the correctness of field results. Intercomparison measurement of calibration pads in various countries showed the differences and inaccuracy in their reported concentrations of radionuclides [5]. Further, correction for the geometry of small size calibration pads can be critical. Inconvenient material for their construction may result in gradual internal geochemical changes, pad decomposition, radon escape and instability in radiation. Instability of equipment function, causing gamma energy spectrum shift, contributes to instrument output data errors. Sensitivity of airborne gamma ray spectrometers play an important role in depression of radioactivity fluctuations and statistical data processing. Large volume NaI(Tl) scintillation detectors are preferable for regional airborne gamma ray spectrometry, though semiconductor detectors has been also tested [6].

Geometry of gamma ray detection and width range play an important role for compilation of regional terrestrial radiation maps. Flight height and line spacing of airborne measurement determine the percentage of area covered. Climatic changes, affecting the variation of air density and air radon concentration may result in inconsistency of data measured in various periods. Attenuation of gamma rays by biomass, soil moisture and water planes is essential namely for the airborne measurement, and may contribute to deviations of tens of percent relatively [7].

Unlike to simple processing of ground gamma ray measurement, the airborne data processing, implying steps of data filtering, background correction, air radon correction, stripping, altitude correction and conversion to element concentration, depends on series of introduced constants [8].

Compilation of radiometric maps may imply digitalization, gridding, filtering, interpolation of digital data and their graphical presentation, realized by contour lines or pixels [9].

Though the theory of radiometric measurement, field procedures and data processing has been intensively studied and developed in the last 30 years, the nature of observed physical field and a series of input and correction constants may affect resultant values of dose rate reported in radiometric maps.

3. RADIOMETRIC MEASUREMENT OF THE CZECH REPUBLIC

Airborne and ground radiometric measurement were applied for uranium exploration and radiometric mapping in the Czech Republic in past decades. Regional 1:200 000 (flight lines separation 2000 m, flight height 100 m, period 1957–1959) and detailed 1:25 000 (flight lines separation 250 m, flight height 80 m, period 1960–1971) airborne gamma total count measurement covered the whole area of the country. Airborne equipment was calibrated by means of a ^{226}Ra point source and the maps of contour lines were expressed in exposure rate ($\mu\text{R/h}$). Detailed 1:25 000 airborne gamma ray spectrometry (from 1976 onward) with digital, spectrum stabilized airborne spectrometers DiGRS 3001 of 14800 cm³ NaI(Tl) volume and GR 800D of 33 600 cm³ NaI (Tl) volume at flight height 80 m covered 50% of the country. The instruments were calibrated by calibration standards and at airborne natural calibration strips. Maps of total count and K, U, Th concentrations and their ratios were compiled. Car-borne, ground, logging and laboratory radiometric measurements were used too.

4. BACK CALIBRATION

Original total count airborne maps, checked and completed by airborne gamma ray spectrometry, were back calibrated in order to level the data and to convert them into gamma dose rate. A ground portable gamma ray spectrometer GS-256 was calibrated at calibration facilities Bratkovice (Czech Republic) and Langenlebern (Austria) and verified by intercomparison measurement (in Berlin 1992) with a Geological Survey of Canada gamma ray spectrometer GR-256, calibrated in Canada. 122 regional traverses 1–5 km long, evenly distributed in the area of the Czech Republic, situated in low, medium and highly radioactive rocks, were measured and results were expressed in gamma dose rate ($\text{nGy}\cdot\text{h}^{-1}$). Regression analysis between these data and data of airborne measurement, converted into dose rate ($1\ \mu\text{R}/\text{h} = 8.69\ \text{nGy}\cdot\text{h}^{-1}$), determined multiplication correction constant 0.85 for data of the original airborne map. Correction constant reflects the inconsistency in geometrical conditions and gamma energy spectra of ^{226}Ra airborne total count equipment calibration, and the field measurement. Coefficient of correlation 0.933 showed acceptable agreement of airborne and ground data sets used in regression.

5. COMPILATION OF THE RADIOMETRIC MAP OF THE CZECH REPUBLIC

Original airborne exposure rate maps of contours, on the scale 1:200 000, has been converted to vector form by digitizing and expressed by 871652 data in a regular grid $300 \times 300\ \text{m}$ over the territory. Digital data were converted into dose rate and the multiplication correction constant 0.85 was applied. The new terrestrial gamma dose rate map, on the scale 1:500 000, was compiled by computer processing with the step of contours $10\ \text{nGy}\cdot\text{h}^{-1}$. The map has been published in 1995 [10]. Regional radioactivity of rocks of the Czech Republic, formed by magmatic, sedimentary and metamorphic rocks, is in the range $6\text{--}245\ \text{nGy}\cdot\text{h}^{-1}$, with the mean $65.6 \pm 19.0\ \text{nGy}\cdot\text{h}^{-1}$ (Fig. 1).

6. RADIOMETRIC MAP DATA VERIFICATION

A series of factors, which have been described in the paragraph 2, affect resultant data of radiometric maps. In 1995, reported data in published radiometric map of the Czech Republic were preliminary checked by comparison with ground gamma ray spectrometry measurement of 81 regional traverses 1–5 km long, situated in the whole area of the Czech Republic. Ground gamma ray measurement was carried out with calibrated spectrometer GS-256 at 761 sectors of 200 m length in dynamic mode. Results were expressed in dose rate, averaged for each traverse, and compared to dose rate values of the map 1:500 000, read with the step of $5\ \text{nGy}\cdot\text{h}^{-1}$. The average difference of compared data sets $2.1\ \text{nGy}\cdot\text{h}^{-1}$ shows a good procedure of regional dose rate data levelling, while the mean deviation $\pm 13.8\ \text{nGy}\cdot\text{h}^{-1}$ illustrates expected differences at individual sites and geological setting. Coefficient of correlation of compared data sets ($N = 81$) is 0.942.

Analysis of dose rate data verification must take into consideration the limited width range of ground measurement, which is compared with integrated data of airborne measurement and map data interpolation, resulting in filtered regional average values. Magnitude of determined mean deviation, and its statistical significance, is a measure of accuracy, with which the radiometric map can be used for the assessment of the radiation environment.

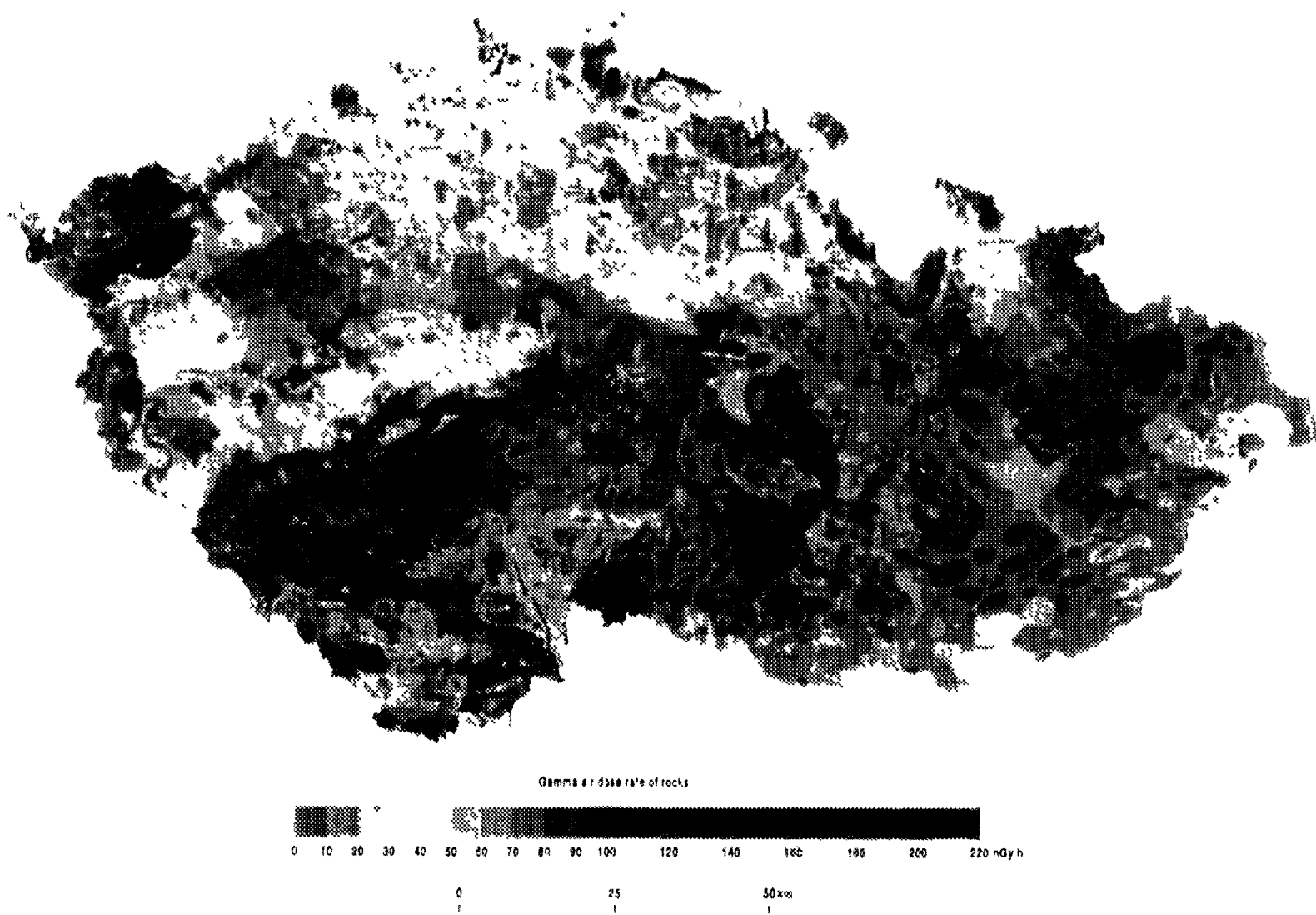


FIG 1 Map of terrestrial gamma dose rate of the Czech Republic

REFERENCES

- [1] INTERNATIONAL ATOMIC ENERGY AGENCY, Application of uranium exploration data and techniques in environmental studies, IAEA-TECDOC-827, Vienna (1995).
- [2] INTERNATIONAL ATOMIC ENERGY AGENCY, The Use of Gamma Ray Data to Define the Natural Radiation Environment, IAEA-TECDOC-566, Vienna (1990).
- [3] LOVBORG, L., The Calibration of Portable and Airborne Gamma Ray Spectrometers — Theory, Problems and Facilities, Riso-M-2456, Riso (1984).
- [4] MATOLÍN, M., DĚDÁČEK, K., The Causes of Differences in the Maps of Total Gamma Ray Activity of Rocks, Acta Universitatis Carolinae-Geologica, 4, Prague (1974) 371–383
- [5] LOVBORG, L., Monitoring of Pads in Various Countries for the Calibration of Portable and Airborne Gamma Ray Spectrometers, Riso-N-02-82, Riso (1982) 35 p.
- [6] SANDERSON, D.C.W., ALLYSON, J.D., TYLER, A.N., "Environmental Applications of Airborne Gamma Ray Spectrometry", Application of uranium exploration data and techniques in environmental studies", IAEA-TECDOC-827, IAEA, Vienna (1995) 71–91.
- [7] RUBIN, R.M., LEGGET, D., WELLS, M., Effects of Overburden, Biomass and Atmospheric Inversions on Energy and Angular Distribution of Gamma Rays from U, K, Th and Airborne Radon Sources, Radiation Res. Associates, Report-GJBX-141 81, Fort Worth (1980) 259 p.
- [8] INTERNATIONAL ATOMIC ENERGY AGENCY, Airborne Gamma Ray Surveying, Technical Reports Series No. 323, IAEA, Vienna (1991).
- [9] SCHWARZ, G.F., RYBACH, L., KLINGELÉ, E.E., "Data processing and mapping in airborne radioactivity surveys", Application of uranium exploration data and techniques in environmental studies, IAEA-TECDOC-827, IAEA, Vienna (1995) 61–70.
- [10] MANOVÁ, M., MATOLÍN, M., Radiometric map of the Czech Republic 1:500 000, Czech Geological Survey, Prague (1995) 19 p.

**NEXT PAGE(S)
left BLANK**



COMPILATION, BACK-CALIBRATION AND STANDARDIZATION OF AERORADIOMETRIC SURVEYS FROM NAMIBIA, SOUTHERN AFRICA

A. DUFFY, D.G. EBERLE, R.L. GRASTY,
D.G. HUTCHINS, W.E.S. URQUHART
High-Sense Geophysics Ltd,
Toronto, Canada

Abstract

During 1992 and 1993 select portions of existing government airborne radiometric data covering almost 91 000 km² of central Namibia were compiled into a master digital data set. This compilation involved the interactive, semi-automated digital recovery of approximately 42 000 line kilometres of original analogue chart traces. A further 49 000 line kilometres of digital data were also reprocessed. Available data represented ten different surveys collected over 12 years with a variety of spectrometers, spectral windows and survey parameters. Preliminary digital grids of each radioelement were compiled, verified and used to select representative sites for ground measurements within each survey block. Results obtained from the ground program were used to back-calibrate the airborne data, standardize the various surveys and convert airborne measurements into equivalent ground concentrations of uranium, thorium and potassium. The quality and consistency of final map products conclusively demonstrates that existing analogue radiometric data, in various states of preservation, can be successfully recovered, combined with modern digital data, and utilized to assist exploration, mapping and environmental studies.

1. INTRODUCTION

Airborne geophysical data have been collected over much of Namibia since 1968. Although these government sponsored regional surveys were generally of good quality, data collected prior to 1977 were not in a digital format. Furthermore, in the case of radiometric data, existing map products were neither consistent in form (ranging from simple redball anomaly selections and stacked profiles to contour presentations) nor particularly suited for mineral exploration, geological interpretation or environmental applications. The different map presentations also hindered geophysical and geological correlation between survey blocks.

In an attempt to overcome this problem, the Geological Survey of Namibia (GSN), in conjunction with the Bundesanstalt für Geowissenschaften und Rohstoffe (BGR, Germany), selected an area of central Namibia (Fig. 1) from which all available airborne radiometric data would be recovered, standardised and compiled into a master digital data set. This digital data would then be used to produce maps of a) exposure rate, b) ground concentrations of potassium, uranium and thorium, c) elemental ratios and d) ternary images. A contract for radiometric data recovery, compilation, back-calibration and map plotting was awarded to UDL (Urquhart Dvorak Limited, Canada) in conjunction with DMT (Gesellschaft für Forschung und Prüfung mbH, Germany). The project was funded by the German Government in a technical cooperation agreement with the Government of Namibia, and jointly supervised by BGR and GSN geophysicists.

2. SURVEY AREAS AND DATA SOURCES

The selected area consists of four (4) 1:250 000 scale map sheets — namely 2014 Fransfontein, 2016 Otjiwarongo, 2114 Omaruru and 2116 Okahandja. Covering almost 91 000 km² of west central Namibia, the area includes varied physiographic regions (coastal plain (Namib desert), escarpment and highlands), typical geological environments and a representative sampling of the different types of radiometric data.

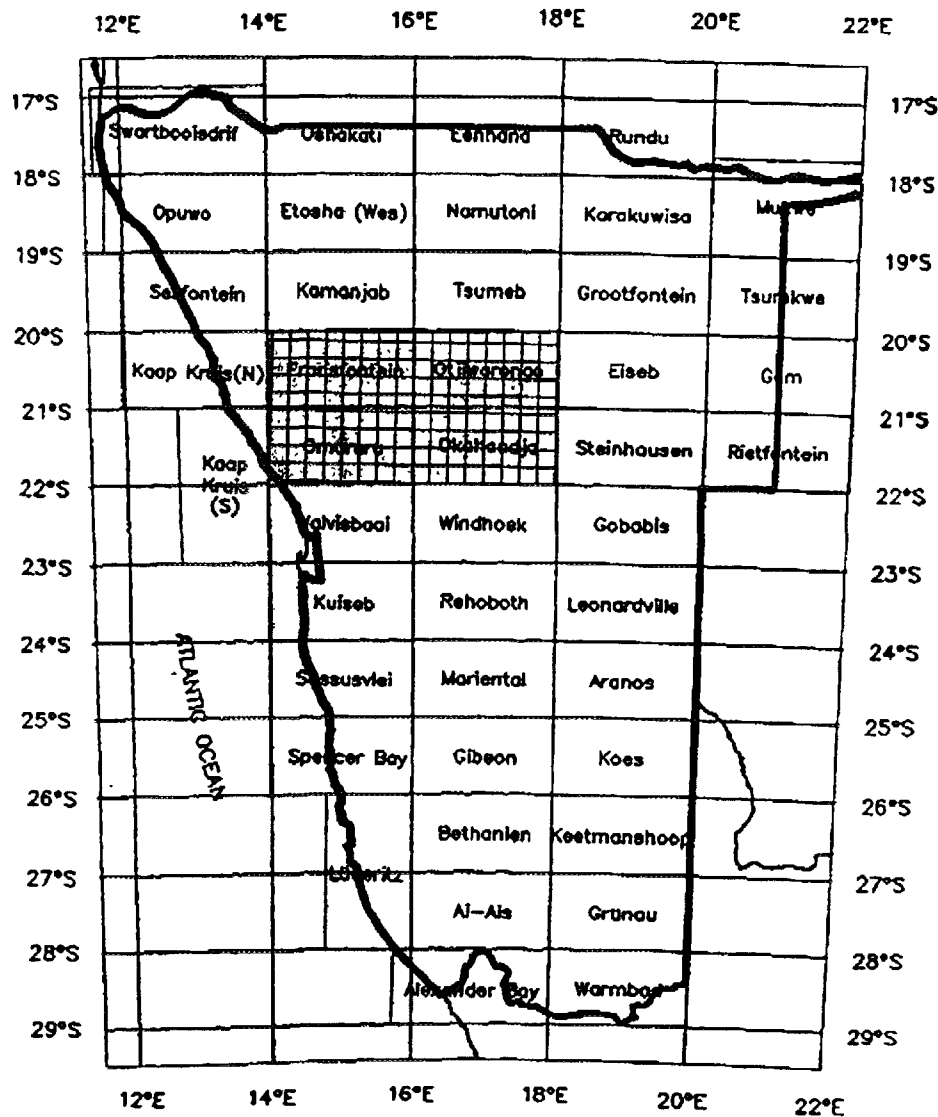


FIG. 1. Project location — Namibia.

This radiometric data resource comprises ten different surveys flown between 1968 and 1980; approximately 42 000 line kilometres of analogue chart records and about 49 000 line kilometres of digital data. Flight line orientation and mean terrain clearance vary, but line spacing remains constant at 1000 m (Fig. 2). Although each survey recorded four radiometric data channels, the contractor, survey equipment, detector crystal volume, energy windows, sensitivities and calibration procedures varied from year to year and survey to survey (see Table I for a summary). In addition to these known variations, it became apparent that parameters were occasionally changed during the course of a single survey (e.g. survey aircraft, equipment, location of calibration sources, correction coefficients, etc.). Unfortunately, in some cases (particularly the older surveys) only incomplete records of survey procedures were available.

3. DATA RECOVERY, BACK-CALIBRATION AND PROCESSING

Original analogue chart records (approximately 46% of the total line kilometres) were digitized with a proprietary interactive trace recovery procedure (RE-TRACE) developed by UDL. This interactive, semi-automated system scans and vectorizes each pen trace, capturing a perfect digital reproduction of both high and low frequency components, thereby ensuring profile fidelity for

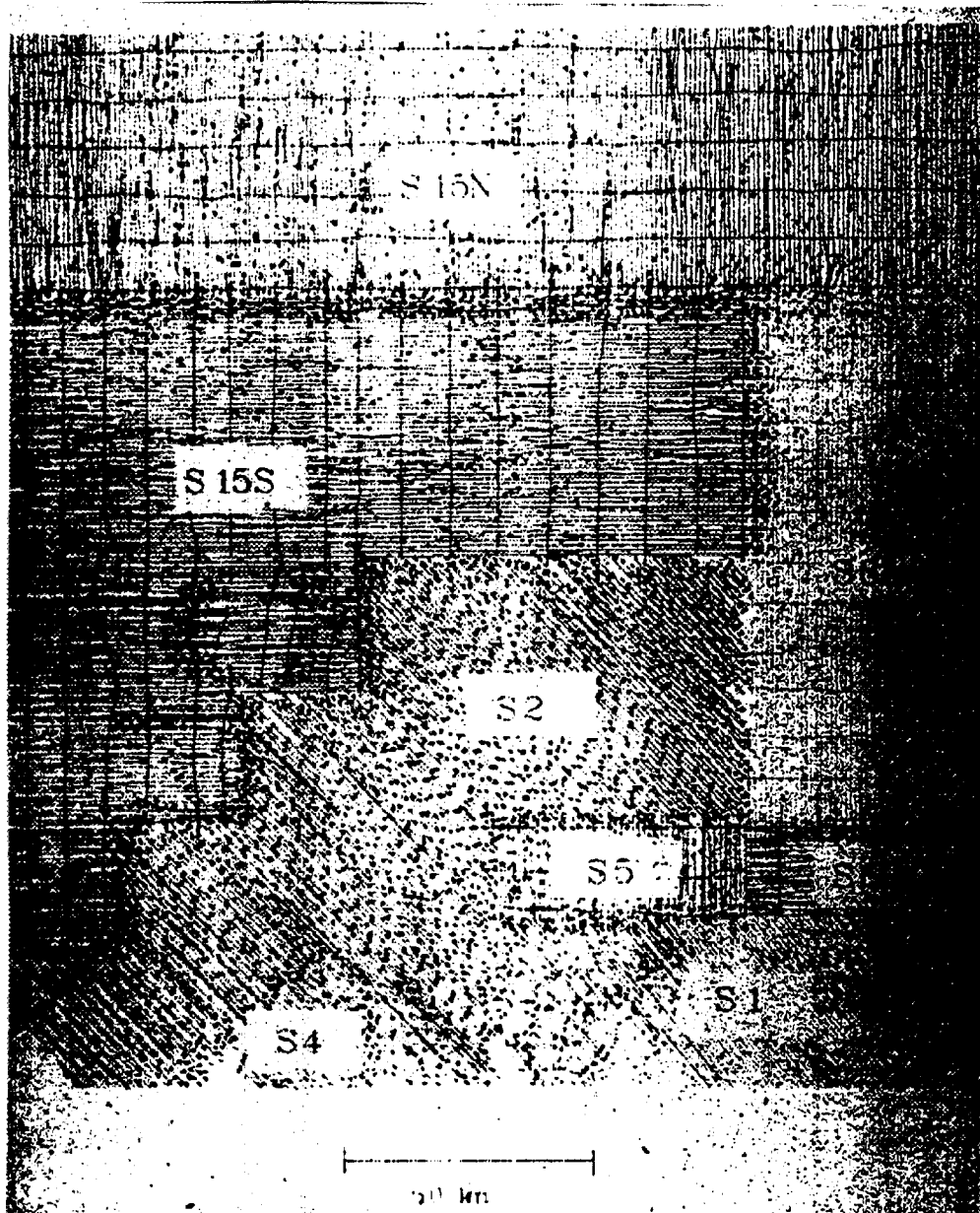


FIG. 2. Typical flight path coverage.

all radiometric channels plus the altimeter information. Analogue data recovery formed the main thrust of this project. Raw digital data was recovered from the original survey tapes, reformatted and written to databases. The degree of early data manipulation (stripping, etc.) done by the initial contractor varied from survey to survey for both analogue and digital data sets.

Processing commenced once the recovery stage was complete, and can be divided into two main parts, an initial data verification phase followed by a second, intensive processing phase. Initial data verification consisted of preparing rough maps that were used to check completeness of the recovered databases for each survey area. Radiometric anomaly positions were compared with known locations of river valleys and granitic bodies. These rough maps were also used to identify data errors, adjust for failings in the original surveys and to determine back-calibration sites.

Back-calibration of radiometric data is based on the comparison of airborne counts rates with ground concentrations measured beneath the flight path by a calibrated portable gamma-ray

TABLE I. SUMMARY OF AIRBORNE SURVEY ACQUISITION PARAMETERS

Survey Number	Year Flown	Digital/ Analogue (a or d)	Line Direction	Line Spacing (metres)	Flight Height (metres)	Crystal Volume (litres)
S1	1968	a	NW/SE	1000	??	??
S2	1971	a	NW/SE	1000	150	??
S4	1973	a	NW/SE	1000	150	??
S5	1973	a	N/S	1000	150	??
S6	1974	a	N/S + E/W	1000	125	11.12
S7	1975	a	N/S + E/W	1000	100	16.68
S10	1977	a*	E/W	1000	100	16.68
S13	1979	d	E/W	1000	100	16.68
CDM80	1980	d	N/S	1000	100	16.68
S15	1980/81	d	N/S + E/W	1000	100	16.68

?? No Documentation Available

* Digital data collected for area S10 was not available

spectrometer [2]. Aircraft sensitivity factors calculated by this technique can be used to correlate survey results obtained from radiometric systems with different detector crystal volumes and, to a lesser extent, energy windows.

Systematic ground radiometric measurements in Namibia were made at 20 calibration sites within each of the ten airborne survey areas. Preferred ground calibration sites were situated at the intersection of flight lines and roads, in areas of uniformly elevated radiometric signatures and subdued topography. By choosing calibration sites located at the same features used by the survey aircrews for navigation (fiducial markers recorded on flight records) good data correlation was assured. Each site was evaluated with respect to potential cultural disturbance or physiographic influences prior to taking ground concentration readings. Four measurements were made at every calibration site; two on either side of the road and typically 25 m apart. A laptop computer was used to store the full digital site spectrum measured by the portable spectrometer. Preliminary databases for each survey area (generated during the data verification stage) were available on the same computer, allowing each days ground data to be processed, evaluated and compared with the airborne results while the field crew was still in the area.

Navigation in the field was via published 1:50 000 scale topographic maps, assisted by satellite GPS (Global Positioning System). GPS readings were used to verify location at each calibration site, and provided positioning control in areas of featureless terrain (e.g. Namib desert). A typical series of ground calibration sites are shown in Fig. 3.

Airborne count rates at the different calibration sites showed variations in radioactivity. Airborne and ground measurements were therefore compared separately at each site to derive potassium, uranium and thorium sensitivities. Sensitivity errors were computed from the calculated statistical error, based on the mean value of the airborne count rates and the four ground

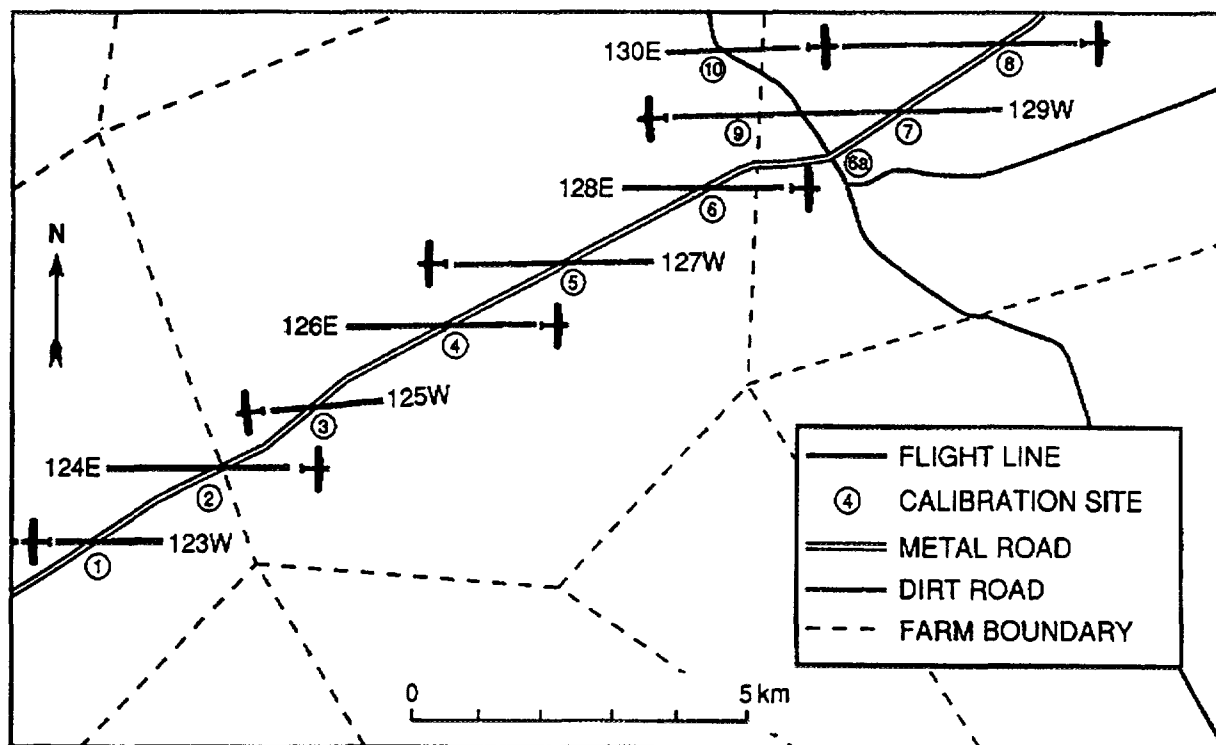


FIG. 3. Ground calibration sites with corresponding flight path (survey area S10).

measurements. The total count channel was calibrated by comparing the airborne measurements with the calculated exposure rate derived from the ground concentrations of potassium, uranium and thorium using the following standard relationships [1]:

$$1 \text{ percent K} = 1.505 \text{ uR/h}, 1 \text{ ppm eU} = 0.625 \text{ uR/h}, 1 \text{ ppm eTh} = 0.31 \text{ uR/h}$$

Table II provides an example of the preliminary total count sensitivities for survey S10. The final sensitivity was calculated from the individual sensitivities, taking into consideration errors associated with calibrations at each measurement location. Fig. 4 graphically compares the exposure rates (uR/h) at each of the calibration sites. During the final intensive stage of data processing, individual surveys were fine-levelled using a variation of microlevelling adapted for radiometrics. Each survey was processed independently following standard radiometric correction procedures consisting of background determination and removal, Compton stripping (where required — some analogues were already stripped) and altimeter correction. All surveys were continued to a common flight height of 150 m above terrain. Optimal radiometric filters were applied to reduce noise effects. Intermediate grids of each survey area were prepared throughout the process, and checked for internal consistency with an imaging program.

Airborne sensitivities were recalculated for each survey area, and applied to generate equal area ground concentration grids for each component. Individual survey areas were merged together on central meridians of 15 and 17° at a 500 m grid cell size. Decorrugated [3] of the data was used as a guide, with any discrepancies between the pre and post decorrugation mitigated by the earlier application of fine levelling.

4. FINAL PRODUCTS

The back calibration and re-processing of the radiometric data facilitated merging of the individual survey data to provide a master digital grid, for each of the components (potassium,

TABLE II. SAMPLE CALIBRATIONS DERIVED FOR TOTAL COUNT DATA
(SURVEY AREA S10)

Site #	Calculated Exposure Rate($\mu\text{R/hr}$)	Airborne Total Count(cps)	Sensitivity (cps/ $\mu\text{R/hr}$)
2	11.6 \pm 0.8	301 \pm 24	26.0 \pm 2.7
3	17.9 \pm 2.9	258 \pm 30	14.4 \pm 2.9
4	18.3 \pm 0.7	536 \pm 33	29.3 \pm 2.1
5	18.6 \pm 0.7	574 \pm 35	30.9 \pm 2.2
.	.	.	.
.	.	.	.
.	.	.	.
16	17.8 \pm 1.2	566 \pm 44	31.8 \pm 3.3

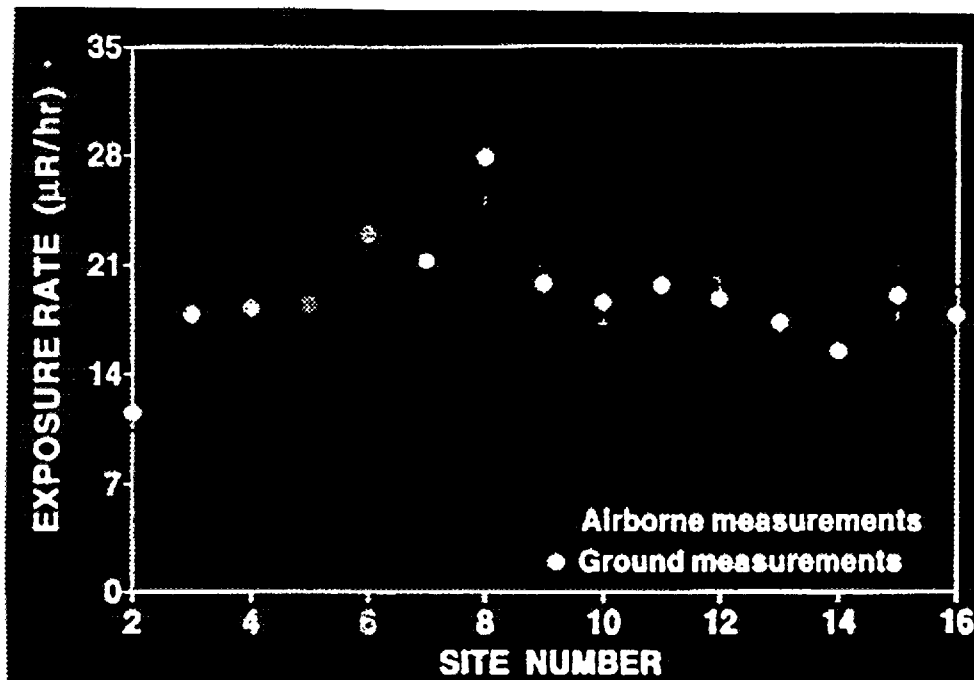


FIG. 4. Comparison of airborne and ground exposure rates (survey area S10).

uranium, thorium and exposure rate). This data was plotted as 1:250 000 scale colour contour and ternary maps, providing a valuable, hitherto unavailable, radiometric map series to compliment aeromagnetic maps and aid in geological interpretation.

Some residual effects from errors and imperfections inherent in the original data can be seen in the final products. Nevertheless, the resultant radiometric maps enable correlation between surveys, and across the selected area. Results from this project have demonstrated that analogue and digital radiometric data collected from a series of surveys flown over a long time span and at different specifications can be successfully and economically recovered, back calibrated and re-processed, providing valuable map products to assist mineral exploration, geological mapping and environmental studies.

REFERENCES

- [1] GRASTY, R.L., CARSON, J.M., CHARBONNEAU, B.W. AND HOLMAN, P.B., Natural background radiation in Canada, Geological Survey of Canada, Bulletin 360 (1984) 39 p.
- [2] GRASTY, R.L., WHITTON, R.M. AND DUFFY, A., Back Calibration and reprocessing an airborne gamma-ray survey, Malaysia, Paper presented at Society of Exploration Geophysicists, 62nd Annual Meeting, New Orleans, October 25-29. Abstract published in Technical Program (1992) 550-551.
- [3] URQUHART, W.E.S, Decorrugation of enhanced magnetic field maps, Paper presented at Society of Exploration Geophysicists, 55th Annual Meeting, Anaheim, October 25-29, Abstract published in Technical Program (1988).

**NEXT PAGE(S)
left BLANK**

AIRBORNE GAMMA RAY SPECTROMETRY IN CERTAIN AREAS OF THE ISLAMIC REPUBLIC OF IRAN AND ITS RESULTS — CORRELATION TO THE OTHER USAGES



XA9745938

GH. SOLEIMANI, F. SH. YEGANI
Atomic Energy Organization,
Tehran, Islamic Republic of Iran

Abstract

Airborne survey can be utilized as a multipurpose data in different fields such as exploration, health physics, environmental studies and so on. The well known advantages of airborne survey include rapidity, more extent of surveyed area, the possibility of application in inaccessible regions where no other methods can be utilized. More than one third of Iran territory i.e. about 600 000 km² has been surveyed by magnetic and spectral gamma ray airborne. This survey is one of the largest and most highly specified survey of its type ever attempted. Extremely large quantities of data were generated during the survey which can be used as a baseline information.

1. INTRODUCTION

A large part of Iran has been surveyed by airborne radiometric and magnetic techniques focusing on uranium exploration during the years 1976–78, by three companies; Austirex, Prakla Seismos, General de Geophysics (CGG), in different areas as shown in Fig. 1 and Table I. Exploratory areas mostly cover eastern and northwestern parts of Iran, which exceed 600 000 km² including 960 000 km flight lines. This survey is one of the largest and most highly specialized surveys of its type ever attempted. The selection of promising areas which might be favorable for uranium occurrence was based on geological information and mineralization trends.

The advantages of geophysical airborne survey include different aspects such as; economy, largeness of area, time saving, monitoring inaccessible areas, etc. Only airborne survey can record such an extremely huge data in a vast region during an acceptable time, considering economical problems. This method is able to get a comprehensive potential view on the country in the first phase, then determining interested zones for further detailed works in the next phase. In other words fairly constant and lower counts (radioactivity) may indicate absence of radioactive mineral enrichments, and such areas can be eliminated from further surveys, then such a procedure can save time and expenditure.

2. TECHNICAL SPECIFICATION OF AIRBORNE SURVEY

2.1. Flight Data

The airborne survey has been carried out at 0.5, 1.0, 2.0 km line spacing and mean terrain clearance of 120 m. Flight lines were in direction N40W in the eastern part, N40E in the central part and N/S in the northwestern part of IRAN according to the geological trends. Also some flights were made along tie lines in the spacing ten times more than flight spacing, i.e. 5, 10 or 20 km perpendicular to the flight lines. Sample interval was 1 sec. while the maximum aircraft speed was 70 m/sec.

2.2. Data Acquisition Equipment

Magnetometer System: Varian V85 proton precession magnetometer for auto tune in fields varying from 25 000 to 100 000 nT with 1 nT sensitivity. Gamma ray Spectrometer: Using 50 lit. NaI (Tl) crystal as a main crystal detector with a 256 channels spectrometer in four windows TC, K, U, Th ranging 0.32–2.9 Mev (TC), 1.36–1.56 Mev (K), 1.66–1.76 Mev (U), 2.42–2.90 Mev (Th).

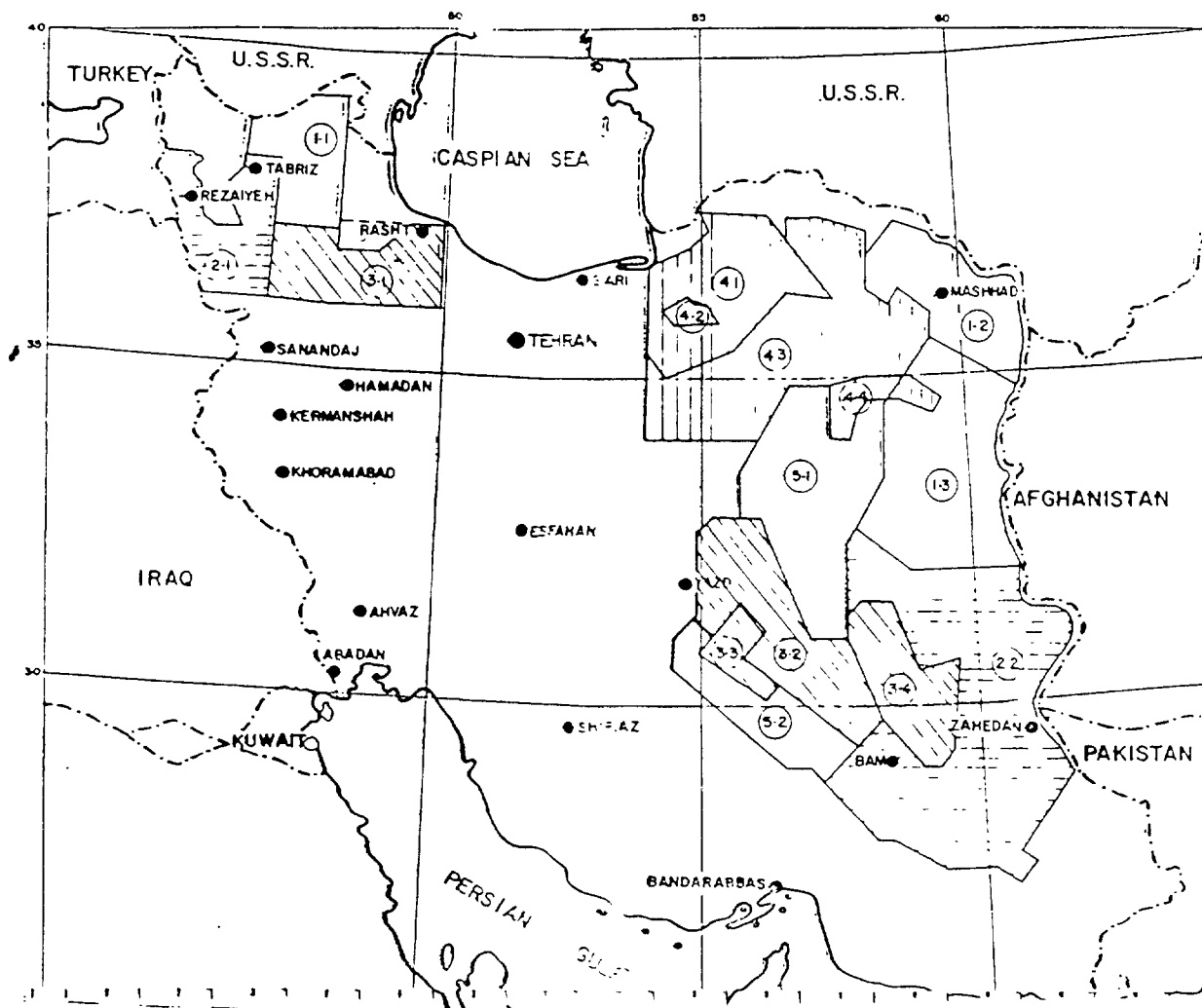


FIG. 1. Airborne surveyed areas.

TABLE I. EXTENT OF FLIGHT AREAS

	Flight area code	Flight line (km)	Surveyed area
Austirex	1.2	310 000	290 000
Prakla	3.5	450 000	216 300
CGG	4	150 000	148 500

3. WORK PROCEDURES

3.1. Calibration

The spectrometer system was to be calibrated over especial test pads constructed at Tehran airport consisting five pads; uranium, thorium, potassium, mixed and background as static calibration, and along test ranges extending 10 km long and 1 km width as dynamic calibration.

3.2. Data Acquisition

Geophysical data was recorded digitally on the magnetic tapes in addition to analogue chart.

3.3. Flight Path Recovery

The geophysical values are assigned to the recovered points of flight tracks.

3.4. Data Processing

Using peripheral hardware (digitizer, plotter,...) and Geopak software, plotted maps, after doing some correction, gridding, contouring are produced.

3.5. Interpretation

interpretation of geophysical data is essentially is an iterative process, with ground truth as it becomes known fed back into the interpretation loop, and new models generated to allow for the latest knowledge. The steps attempted at this stage consist of:

3.5.1. Image Processing

An alternative approach to the analysis of geophysical data is to present it in image rather than graphical format. Geophysical data is transformed, or scaled, from physical units to a number between 0 and 256, and either a grey scale or colour value is assigned to the transformed value. RTICAD software operates on grid files so as to produce pseudo-coloured image to show various physical potentials like magnetic field intensity and radioactivity for the following geophysical parameters: total count, U, Th, K, Mag, filtered mag, colour composite of U,Th,K and ratios; (U/Th,U/K,Th/K).

3.5.2. Quantitative Interpretation

The discovery of uranium resources, emphasis in the interpretation has been placed on the radiometric data, so in these maps by defining the background level and anomaly amplitude, it is possible to reject the values less than anomaly limit, then anomalies are recognizable.

3.5.3. Data Compilation

Compiling complementary data from different aspects could be lead to a comprehensive idea on the interested area, therefore contour maps, pseudo coloured maps, geology map, stacked profiles and remote sensing data were compiled together.

3.5.4. Qualitative Interpretation

The last stage of interpretation for finding out the results, is carried out considering the following:

- migration of uranium;
- ratios maps; sometimes uranium deposits produce identifiable ratio anomalies without producing simple uranium channel anomalies;
- results of field checking, mineralization, alteration and so on;
- recognizing of pseudo-anomalies arising from leaching, facies changes and concentration of radon gas.

4 DATA PRESENTATION

Data is presented as a raw processed and interpreted one in form of

- digital on the magnetic tapes,
- analogue strip chart records of all survey flights, test lines and calibrations,
- stacked profiles at 1 250 000 scale of the following geophysical parameters, total count(c/s), K(c/s), U(c/s), Th(c/s), Bi-214(air), U/Th ratio, U/K ratio, Th/K ratio, total magnetic field and radar altitude (Fig 2),
- contour maps at scales of 1 50 000 and 1 250 000 of the following geophysical parameters, total count (Ur)¹, uranium equivalent(ppm), thorium equivalent(ppm), potassium(percent) and the three isotope ratios U/Th, U/K, Th/K (Fig 3),
- pseudo coloured maps at scales 1 100 000 and 1 250 000 of the above mentioned parameters Fig 4 shows radioactive potential in area flown by Austirex, i e z40 eastern part of Iran As it is observed, in scales about 1 50 000 the background radiation level varies from one area to the other one, but in general view it is about 8 Ur The maximum value is about 20 Ur Fig 5 shows magnetic field intensity in the same area Sometimes there is a correlation between magnetic complexes and uranium channel response, and it will be more observable in scales about 1 100 000 Some information on geological structures, lineaments, faults, basement, could be found out from magnetic map and the filtered one
- interpreted maps for interested areas, showing uranium anomalies classification and geological structures

5 LIMITATION AND DISADVANTAGES OF AIRBORNE SURVEY

In spite of numerous advantages of geophysical airborne survey which are impossible to be obtained by the other methods, there are some insufficiencies as follows

- high topographic regions,
- covered areas,
- straight sampling

Sometimes, presence of a facies among the other ones having different gamma radiation, leaching of radioactive mineral, concentration of radon gas in traps may lead to pseudo anomaly

6 CONCLUSION

As it is mentioned the well known advantages of airborne survey include rapidity, more extent of surveyed area, relative simplicity of use and in some cases, the possibility of application in inaccessible regions where no other methods can be utilized

Such an extremely large information can be applied in different ways as a multi-purpose data bank in addition to uranium exploration, for instance

- mineral exploration,
- corresponding and correcting geology maps,
- identifying high radiation areas for various purposes, (exploration, health physics, environmental studies,),
- registering the background of radiation as a reference for each area and comparing it in the future for probable nuclear events, (natural and man-made) and variation of radioactive pollution

¹ Ur Universal radiation 1 Ur = 1 ppm eU = 0.6 R/h

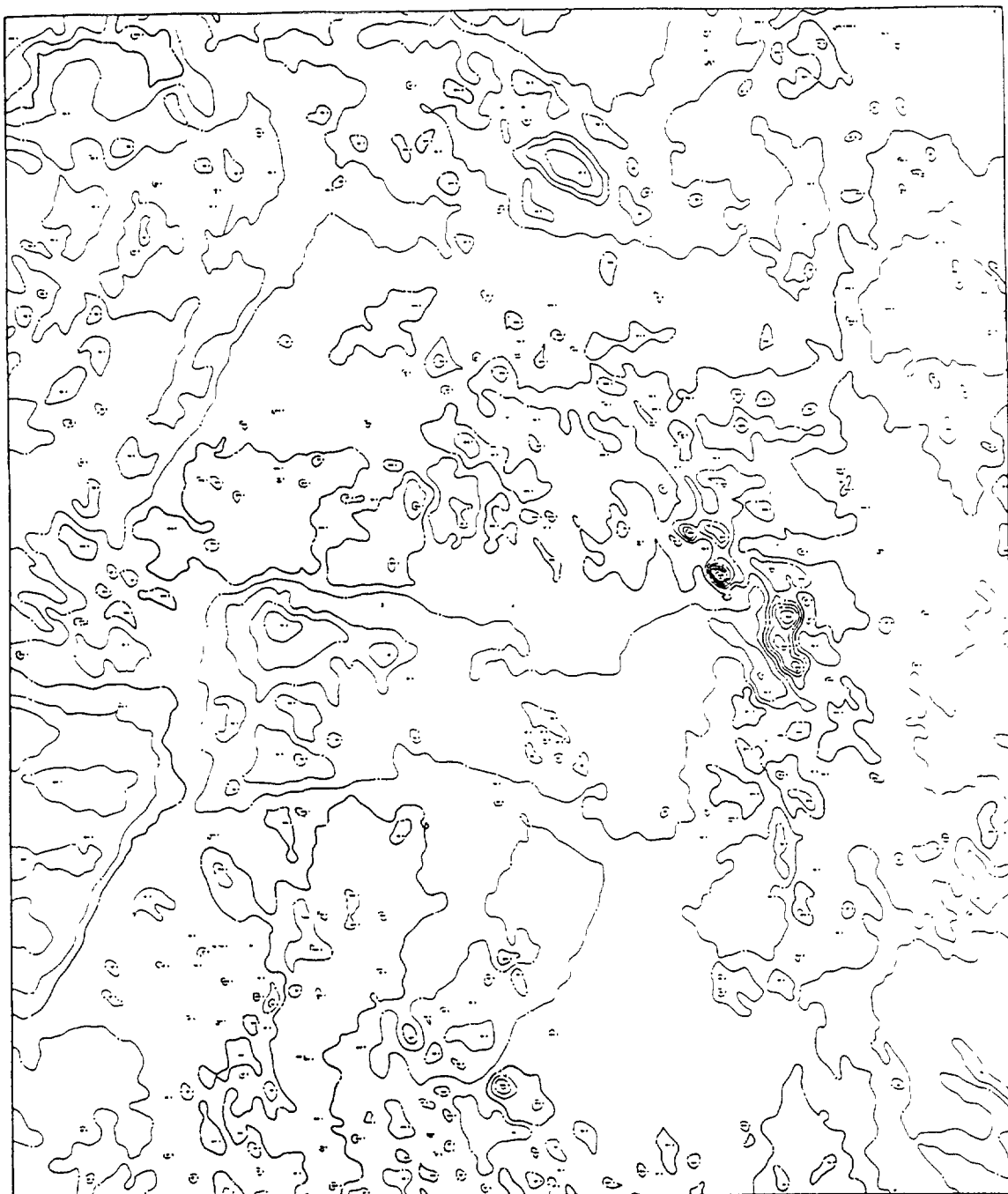


FIG. 3. Total radioelement concentration contour map (ur).

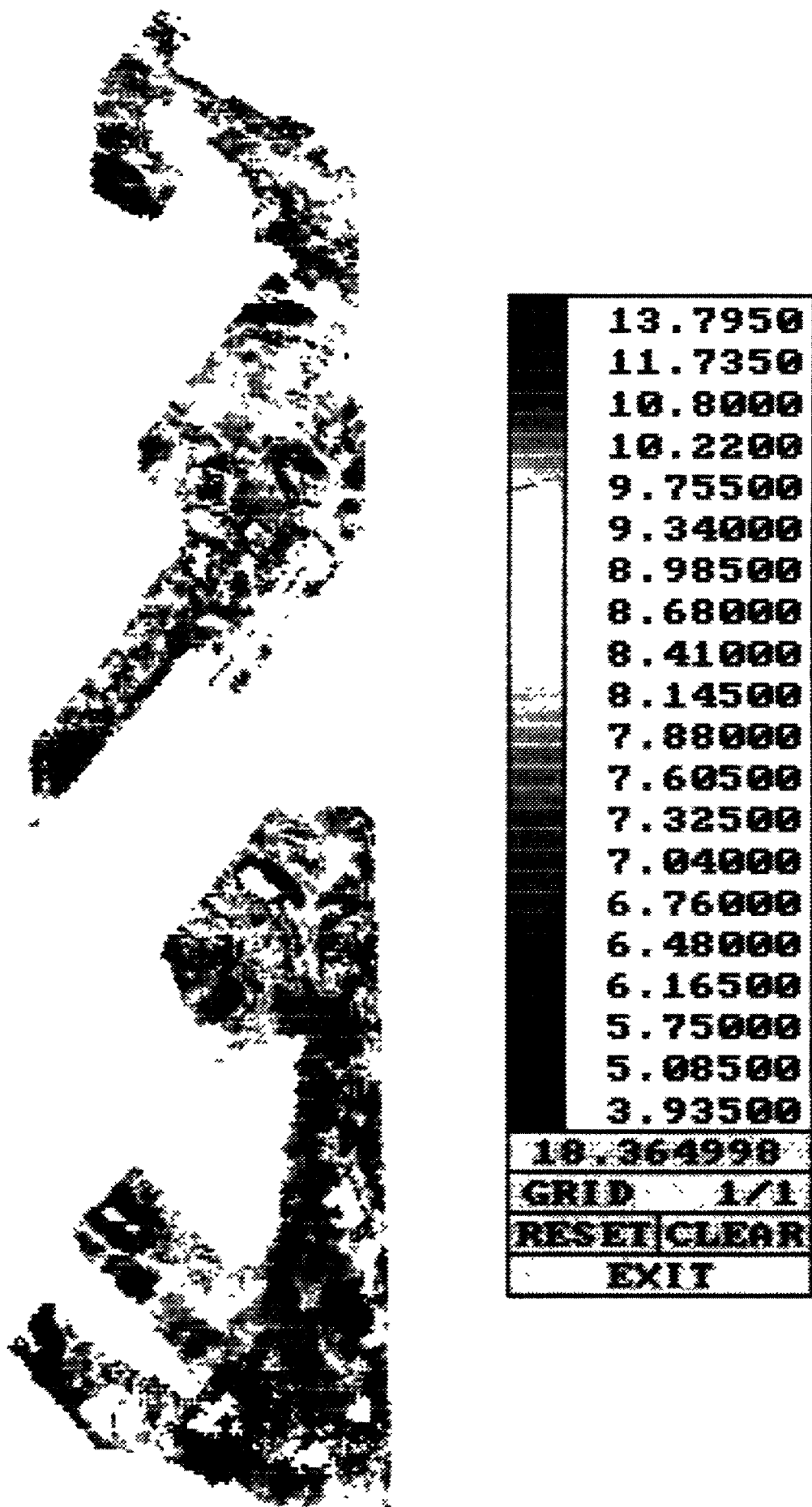


FIG. 4. Total count image.



184.300
61.4000
9.70001
-22.100
-46.500
-66.400
-82.700
-97.300
-109.90
-121.60
-133.10
-145.10
-158.40
-172.70
-189.70
-210.10
-235.40
-265.50
-312.30
-413.50
456.70001
GRID 1/1
RESET CLEAR
EXIT

FIG 5 Magnetic field intensity image

REFERENCES

- [1] UWAH,E.J., Analyses and Interpretation of Air-borne Gamma-ray Survey Data for Radioactive Mineral Recovery, Nucl. Geophys, Vol 7, No.1 (1993) 97–107.
- [2] LEONHARDT, J.W., IAEA-SM-229/235 (1991).
- [3] AUSTIREX INTERNATIONAL LIMITED, Final Geophysical Report, Iran project (1985).
- [4] ASHTIANI,A., Spectral and Magnetic Airborne Survey and its Results for Mining in Iran (1993).
- [5] AEOI, Technical Specification of Airborne Survey (1997).

NEXT PAGE(S)
left BLANK



CORRELATION BETWEEN NATURAL GAMMA ACTIVITY AND THE GEOLOGICAL MEANS IN THE PROVINCE OF SALAMANCA

E. SUAREZ MAHOU
CSN

J.A. FERNANDEZ AMIGOT
ENUSA

Madrid, Spain

Abstract

The purpose of this work is to analyse on a surface of 15 000 km² some of the existing correlations between activity and geology. Approximately 90% of the studied zone has been covered by radiometric airborne surveys with a grid of 1 km using multichannel spectrometers for the uranium, thorium and potassium discrimination. The total gamma accounts records have been translated to micro Röntgen/hour at the soil level, using the air-land correlations obtained by empirical procedures. Numerous field works have been carried out for the acquisition of data, as well as for the elaboration of maps into a geological mean known. Within this context some of the historical cases that have served as guides for the elaboration of maps are also analysed on various scales.

1. RADIOACTIVITY IN NATURE

Radioactivity in nature is basically emitted by the elements uranium, thorium and potassium. Within the potassium series the only radioactive isotope is K-40 which usually exists in a proportion of 0,019%. 90% of the K-40 emission is beta radiation and approximately 10% corresponds to gamma radiation with an energy of 1.460 kiloelectron Volts (keV).

Uranium gamma radiation in nature is basically emitted by Bi-214, which is the uranium family gamma radiation emitter. The radioactive energies of this element are 609, 1120 and 1761 keV. Thallium-208, belongs to the thorium-232 decay series. Several gamma energies in the interval 300-3000 KeV. The most important among them at 583 and 2620 keV.

The foregoing means that, as regards an approximate conversion to percentages for the purpose of gamma radioactivity emissions, for an average-type granite containing 4% of K20, 4 ppm of U and 13 ppm of Th, the radioactive balance takes place as follows: 23% of the gamma rays would come from the K-40, 25% from the U and 51,5% from the Th.

The natural radioactivity of different rocks and their average geochemical uranium content is variable according to their origin and composition. Roughly we have the following contents in ppm:

Igneous rocks with a high silica content	4-5 ppm
Igneous rocks with an average silica content	2-3 ppm
Igneous rocks with a low silica content	1 ppm
Sedimentary rocks	2 ppm
Sea water	0.002 ppm
Underground water	0.0002 ppm
Oil	0.1 ppm

As far as natural gamma radioactivity is concerned, if we take as coefficient 1 that corresponding to a siliceous sandstone, it will vary from the form given below for the rocks taken into consideration: alluvium 0,8; siliceous sandstone 1; detrital rocks 1, 1-2; metamorphic series 1,8-2; gneisses 2-3; calc-alkaline granites; alkaline granites >4.5.

These coefficients are merely an indication of radiometric variability. The measurements were taken with a duly gauged SPP-2 scintillometer (cps) and with an ES-3 ($\mu\text{R/h}$) (Table I). The average uranium content of surface rocks varies between 1 and 2 ppm. Far more abundant is thorium which can reach proportions 3 and 4 times higher than those of uranium. Both thorium and uranium are in a tetravalent state, but whereas the $\text{U}+4$ ion in an oxidizing atmosphere becomes hexavalent thorium does not change its valency. In oxidizing conditions hexavalent uranium forms the uranium ion (UO_2^{++}) which may give rise to a number of minerals.

Thus it can be seen that uranium and thorium go their separate ways quite soon (in geological terms), and this will inevitably condition the form of the deposits and the geochemical content of the rocks in these elements.

Thorium, due to its being highly resistant to meteorization, will be located exclusively in its original rocks or mechanical concentrations of its minerals during transport, whereas uranium will partly follow its cycle leached by water until it encounters deposit conditions, and another part may remain in its original rocks.

The problem raised by speculation as to the average contents (ppm) of radioactive elements in rocks is clear, as are some of the reasonings which have led us to an empirical system of earth-air radiometric correlations.

2. GEOLOGY OF THE PROVINCE OF SALAMANCA

The province of Salamanca covers a surface area of around 15 000 km^2 of which approximately 40% is taken up by Hercynian granitic outcrops, 20% by Palaeozoic metasediments, 20% by Tertiary sediments and 10% by Plioquaternary sediments (Figs. 1, 2 and 3).

TABLE I. RADIOMETRY OF SOME LITHOLOGIC UNITS IN THE PROVINCE OF SALAMANCA ($\mu\text{R/h}$)

LITHOLOGY	MAX. ($\mu\text{R/h}$)	MIN. ($\mu\text{R/h}$)	AVERAGE ($\mu\text{R/h}$)(m_1)	(m_1-m_2)/ m_1
GRANITIC	>20	15	>17.5	>0.01
GNEIS	>20	13	>16.5	>10.7
SANDS	11	6	8.5	+13.3
SANDSTONES	14	6	10	+37.0
CLAY	11	7	9	-1.1
RAÑAS	9	6	7.5	+17.2
PHILITES	15	11	13	-2.3
SLATES	>15	11	>13	>-10.3
CUARCITICS	>14	7	>10.5	>10.5
GRAUWACKAS	15	11	13	-5.4
ARCOSICS	14	6	10	83.6

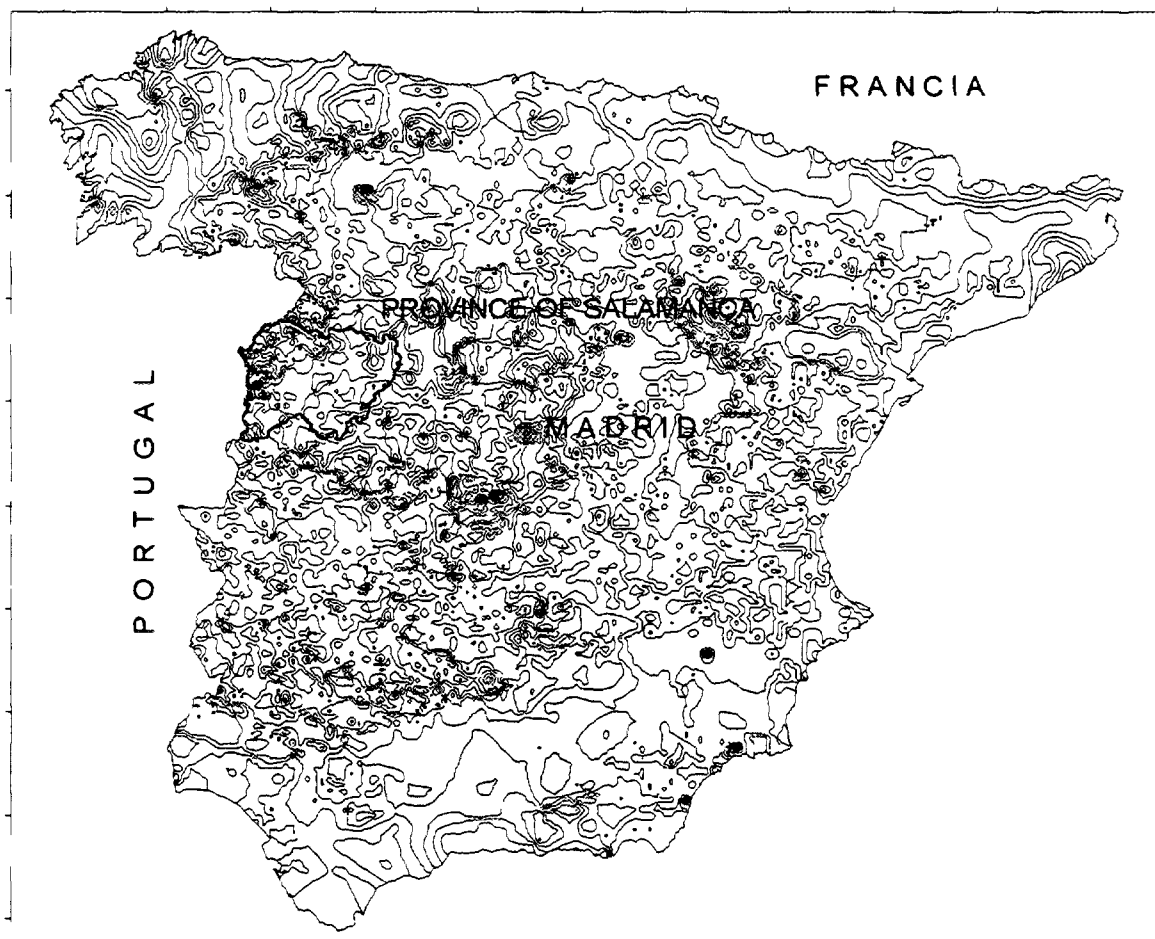


FIG. 1. Radiometric map of Spain. Province of Salamanca.

2.1. Granites

The granites in the northern zone (Fig. 2, nos. 3, 5 and 7) are from several generations and generally vary between granodiorites and quartzomonzonites as well as showing a small proportion of syenite outcrops, microgranites and phyllonian retinues typical of these intrusive rocks. As a general radiometric characteristic it may be said that they have high average potassium, thorium and uranium contents. With such geochemical features these granites have extremely high radioactive background, often showing radioactive veins with uranium minerals and also transmit strong radioactive gradients to the residual Palaeozoic rocks (Fig. 2 nos. 4, 6 and 8) which overlay or have lateral contact with them and which have undergone contact metamorphism during the granites' emplacement stage. Residual Quaternary (Fig. 2, nos. 9, 11 and 12) or Tertiary (Fig. 2, no. 13) terrains may also overlay on these granites.

The granites in the southern zone (Fig. 2, nos. 14, 16 and 17) cover a smaller surface area than those in the northern zone and show some local uraniferous anomalies close to the Portuguese border (Fig. 2 no. 14)

2.2. Palaeozoic

The Palaeozoic metasediments of the northern zone contain the same materials subsequently mentioned for the southern part. However, these materials have undergone a heavy additional contact

metamorphism which has transformed the lithologic units over great extensions, and we thus find andalusitic and cordieritic cornubianites, micacites, quartzites and two-mica gneisses. Over these formations are to be found many radioactive anomalies, and the most important Spanish uranium mines (Fe, D, Alameda, Caridad, etc. mines).

The Palaeozoic of the southern block (Fig. 2, no. 15) is more massive and is basically made up of predominantly clay and quartz phyllites, although these may be sericitic, graphitic, etc., graywackes, the odd conglomerate and Ordovician quartzites. There also exist some local contact metamorphisms generated by the emplacement of the granites in this zone (Fig. 2, nos. 14 and 16), but with little radioactive influence and extension.

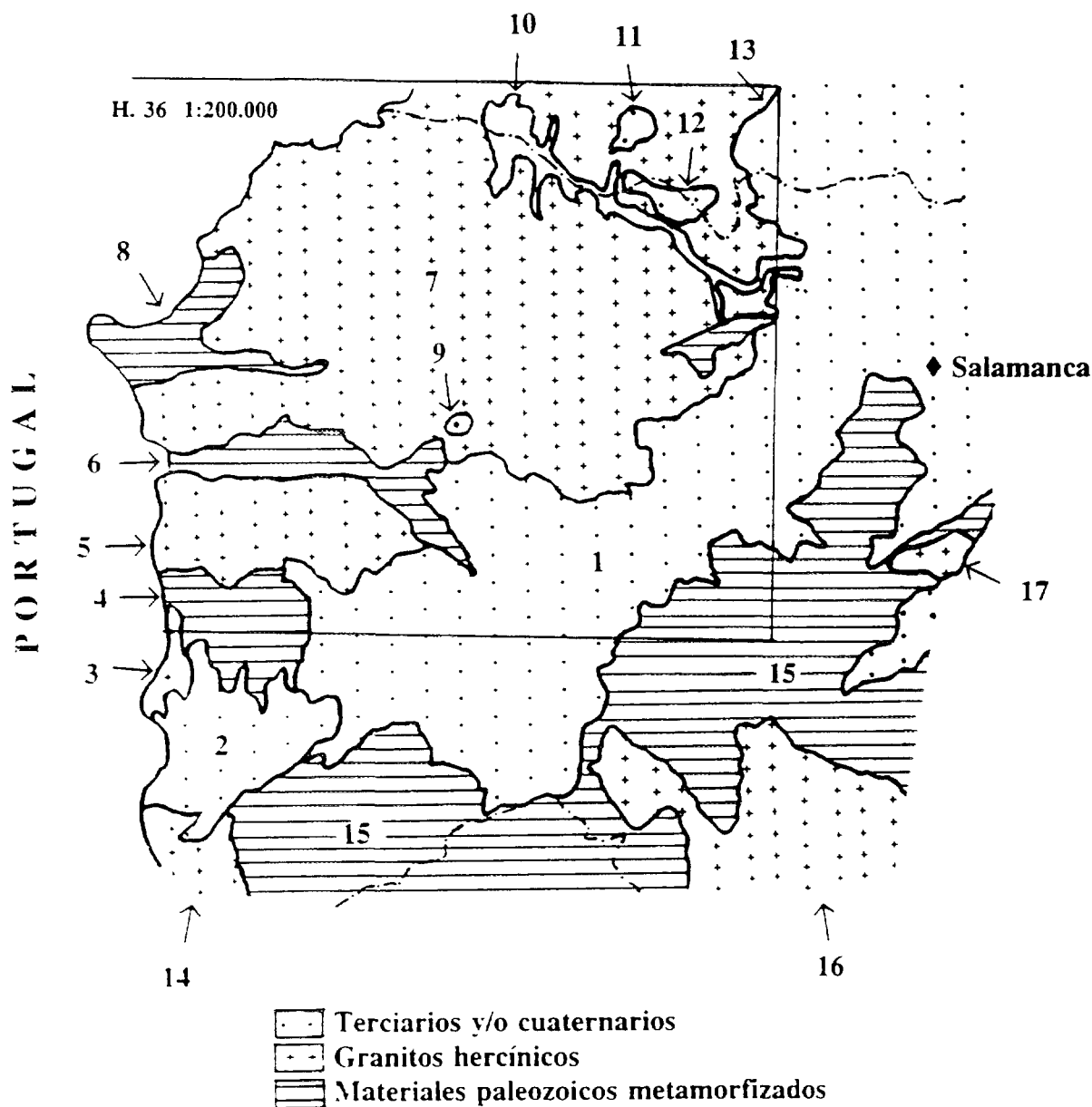


FIG. 2. Partial geological scheme of the Province of Salamanca.

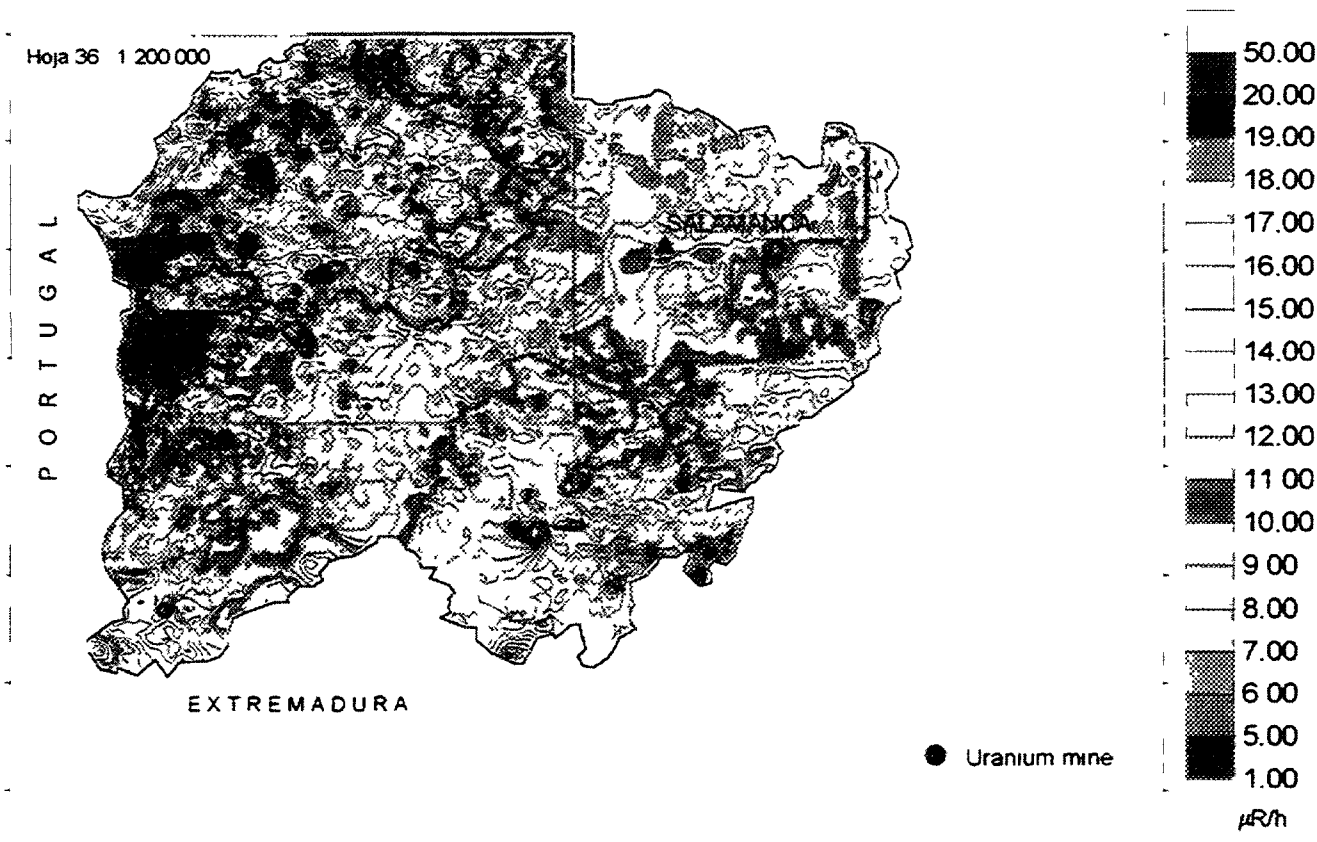


FIG. 3. Radiometric map of the Province of Salamanca. Resolution: 1 Radiometric datum/1 km².

2.3. Tertiary sediments

These form a basin running in a NE-SW direction and which is about 150 km long and 15-20 km wide (Fig. 2, nos. 1 and 2). Topographically speaking, this basin descends from Salamanca in a south-westerly direction as far as Ciudad Rodrigo and reaches into part of Portugal. Both the basin itself and the area to the north are peneplains, whereas the topography to the south is abrupt due to the uplift of the tectonic horst forming the Sierra de Gata. The basin has been filled in by the neighbouring materials and therefore shows ranges of sedimentation and lateral facies evolutions that vary between arkosic types, clay types and high-energy sediments. From a radiometric standpoint the materials show a diminished uranium content due to the leaching undergone by this element during the erosion, transport and sedimentation stages of the parent rocks, as well as showing thorium losses from the clay phyllites and clays except in the south-western area (Fig. 2, no. 2) where the granitic extension and the proximity of the uranium deposits has raised its radiometric backgrounds.

In the northern part of Sheet H-36 (Vitigudino) (Fig. 2, no. 10) we can see the great morphological irregularity caused by the Almendra dam over the River Tormes. This reservoir is at its widest just upstream from the dam (over 50 km²) and stretches out more narrowly over tens of kilometres.

2.4. Quaternary

Finally, to the north of the Almendra reservoir (Sheet H-36, Fig. 2, nos. 11 and 12) one can see two clay, detrital quaternary tracts, known as *rañas*, with surface areas of 40 and 60 sq km. These sediments, which show little evolution, chiefly consist of large quartzite stones, poorly classified quartz sands, silt and clays with a low radioactive component.

3. RADIOMETRIC INTERVALS OF THE LITHOLOGIC UNITS IN THE PROVINCE OF SALAMANCA IN RELATION TO THOSE OF THE REST OF SPAIN

Ever since the MARNA Project began, ENUSA has been checking and tabulating the radiometries of most of the geological formations in Spain in $\mu\text{R/h}$. Over 1 700 points have been catalogued and these are currently at an advanced stage of classification and study. As far as the lithologic units of Salamanca province are concerned, their behaviour with regard to those in the rest of Spain is shown in Tables I and II.

As can be seen, the percentages of the differences between average radiometries remain within very acceptable limits. In some cases one can see the regional influence of the uraniferous metallogenetic province (maximum values of the arkoses on the south-west edge of the Ciudad Rodrigo basin, gneisses and slates), whilst the constants are quite well maintained in the Ordovician quartzite despite the frequent variation of its thorium content.

TABLE II. RADIOMETRY OF SOME SPANISH LITHOLOGIC UNITS ($\mu\text{R/h}$)

LITOLOGY	MAX. ($\mu\text{R/h}$)	MIN. ($\mu\text{R/h}$)	AVERAGE ($\mu\text{R/h}$) (m_2)	VARIANCE	N° OF DATA
GRANITIC	27	10.2	17.5	11.32	48
GNEIS	19.4	11.4	14.9	8.49	6
SANDS	14.4	3.8	7.5	4.42	139
SANDSTONES	18	3	7.3	10.29	88
CLAY	21	3.7	9.1	10.99	153
RAÑAS	17.4	1.9	6.4	6.38	115
PHILITES	14	12.6	13.3	0.33	3
SLATES	19.4	7.6	14.5	10.49	30
CUARCITICS	13.3	5.6	9.5	4.99	30
GRAUWACKAS	14	13.3	13.7	0.12	2
ARCOSICS	5.4	5.4	5.4	0	1

4. DRAWING UP OF MAPS

4.1. Analysis of the surface unit-geology factor in its relationship with the extraction and drawing-up of data

A radiometric study may be approached with multidisciplinary aims. In our case we shall focus on geology although the bases to be used are, in our opinion, common for this type of study. Anyone, when faced with a radiometric study, will ask questions such as the following: What radiometric support (surface) must be chosen in order to represent the area to be worked on? What is the accuracy of its radiometry? Can we quantify the radiometric appraisal of the area under study? If we can answer these questions we shall be able to programme and delimit the system for extracting data or taking samples.

The problem will have been reduced to defining the financial optimization of the project for an acceptable quantification of its parameters. The problem becomes simpler if, for each support unit (surface), we are able to determine the number of samples (radiometries) in order to obtain a radiometric knowledge with an acceptable predetermined error. In geology the surface to be studied may be very variable, depending on the objectives.

We may go from a radiometric macro representation of a country's geology with a surface area of, for example, 500 000 km² such as that of Spain to locating uranium deposits of a predetermined size, for example 2 km², and even giving a radiometric description of a sublayer or geological structural projection such as a fault with lineal characteristics and a thickness between decimetric and metric.

Thus it can be seen that geological variability may be very great, depending on the aims of the area under study. In Spain, for example, a horizontal Pontian limestone may appear as a single outcrop over tens and even hundreds of sq km, whereas in some metamorphosed Palaeozoic sediments petrographic and radiometric variations may occur several times in only a few metres.

4.2. Practical case of the Marna Project

- a) Direct problem: We have a series of radiometric data (maps) generated by surveys (airborne) and we want to have a radiometric knowledge, with a predetermined accuracy, of each surface unit chosen as a radiometric support. What must be the minimum data-extraction mesh?
- b) Opposite problem: We have no radiometric data for the area to be studied. What must be the minimum data-capturing mesh in order to achieve a predetermined accuracy?

Statistically speaking the two cases are practically identical and are reduced to the analysis of a series of samples over a surface. Within the context of this publication we give the summary of the study carried out for a 35 sq km base grid (support) over Spanish territory. For another specific problem the error resolution will be done by means of a simple variance composition.

In the MARNA Project a base grid was defined as a being a quadrilateral with sides approximately proportional to those of a 1:50 000 sheet and a surface equivalent to 1/16 of such a sheet (the 1:50 000 sheet is equivalent to a quadrilateral of 20 by 10 minutes of geographic coordinates and the base grid represents a surface area of almost 35 km²).

The Nuclear Safety Council (CSN) dictated that the radiometry of each base grid should be known with an error of less than 1 μ R/h for data extracted from airborne survey maps. Eleven base grids representative of the radiometric variability of two flight campaigns (Hunting and Geodata) were chosen, and 10 data-extraction meshes were made over each grid.

The criteria chosen in the data-extraction meshes were as follows:

Mesh L1 Four points corresponding to the vertices of the grids.

Mesh L2 Four points corresponding to the centres of the grid's sides.

Mesh L3 Four points corresponding to the centres of the four quadrilaterals resulting from dividing a grid into four subgrids.

Mesh L4 Is a mesh with 12 points per grid corresponding to the middle points of the subgrids.

C Centring of a mesh.

The basic characteristics of surface representativeness are given in Table III, while the statistical data for one of the base grid are given in Table IV.

TABLE III. MAIN CHARACTERISTICS OF THE DIVERSE GRINDS

Grid	Enclosed Area Km ²	Surface which represent Km ²	N° of points per Based Grid	N° of data per sheet 1:50.000	N° of points per Km ²
L ₁	33.0	33	4	25	0.11
L ₁ +C	33.0	33	5	41	0.15
L ₂	16.5	33	4	40	0.11
L ₂ +C	16.5	33	5	56	0.15
L ₁ +L ₂ +C	33.0	33	9	81	0.26
L ₃	8.25	33	4	64	0.11
L ₃ +C	8.25	33	5	80	0.15
L ₁ +L ₂ +L ₃ +C	33.0	33	13	145	0.37
L ₄	33.0	33	12	144	0.34
L ₁ +L ₂ +L ₃ +L ₄ +C	33.0	33	25	289	0.71

TABLE IV. STATISTICAL DATA FOR ONE OF THE BASE GRID

Flight	Base Grid	Grid	N° of Points	Points per Km ²	Average	Standar desviation Sn	Sn-1	Variation rate	Freedom grade	Confidence limit
GEO-80	16	L-1	4	0.11	2380	739.13	365.02	36.3	3	709.32
		L-1 (C)	5	0.15	2224	739.12	926.37	37.2	4	565.43
		L-2	4	0.11	2230	604.73	698.28	31.3	3	572.59
		L-2 (C)	5	0.15	2104	596.71	667.14	31.7	4	489.3
		L1/L2	9	0.26	2226.67	682.67	724.09	32.5	8	337.91
		L-3	4	0.11	2022.5	426.05	491.96	24.3	3	403.41
		L-3 (C)	5	0.15	1938	416.86	466.07	24	4	341.83
		L1/L2/L3	13	0.37	2163.85	622.4	647.81	29.9	12	244.35
		L-4	12	0.34	2080	572.01	597.45	29.7	11	234.56
		L1.L4 (C)	25	0.71	2123.6	600.21	612.58	28.8	24	161.72

Much could be written on the analysis of the above table, the way of representing the results and the evolution thereof. If we take as a basic criterion the fact that any measurement of the grid must be known with a confidence limit of less than $1 \mu\text{R/h}$, mesh L1+L2+L3+L4+C, that is the 25-point mesh, is the first one to fulfil this condition in all the circumstances being studied, even in grid no. 16 of Geodata-80 flight which has a variation coefficient of 28.8, since for an average of 2,123.6 cps, $1 \mu\text{R/h}$ means about 234 cps which is a much higher figure than the confidence limit of 161.72 cps.

This macro conclusion shows us that "an extraction method with 25 or more points per grid with a regular mesh will almost always (and possibly always) fulfil the basic criterion". On account of the foregoing the decision was taken to perform the data extraction of the Hunting and Geodata flights by means of a bicentimetric mesh (one point per square kilometre of 1:50 000 Sheet or 35 per base grid).

Afterwards, the quality of the extractions was finally ascertained by means of a simple program in case it might be necessary to close the extraction meshes in some cases. This circumstance did not arise.

4.3. Analysis of the resolution of radiometric maps

Using the aforementioned characteristics the radiometric map of Salamanca province was drawn up with the same resolution as the national map (1 piece of data per 35 km^2), Fig. 4. The same map with a resolution of $1/100 \text{ km}^2$ may be seen in Fig 5.

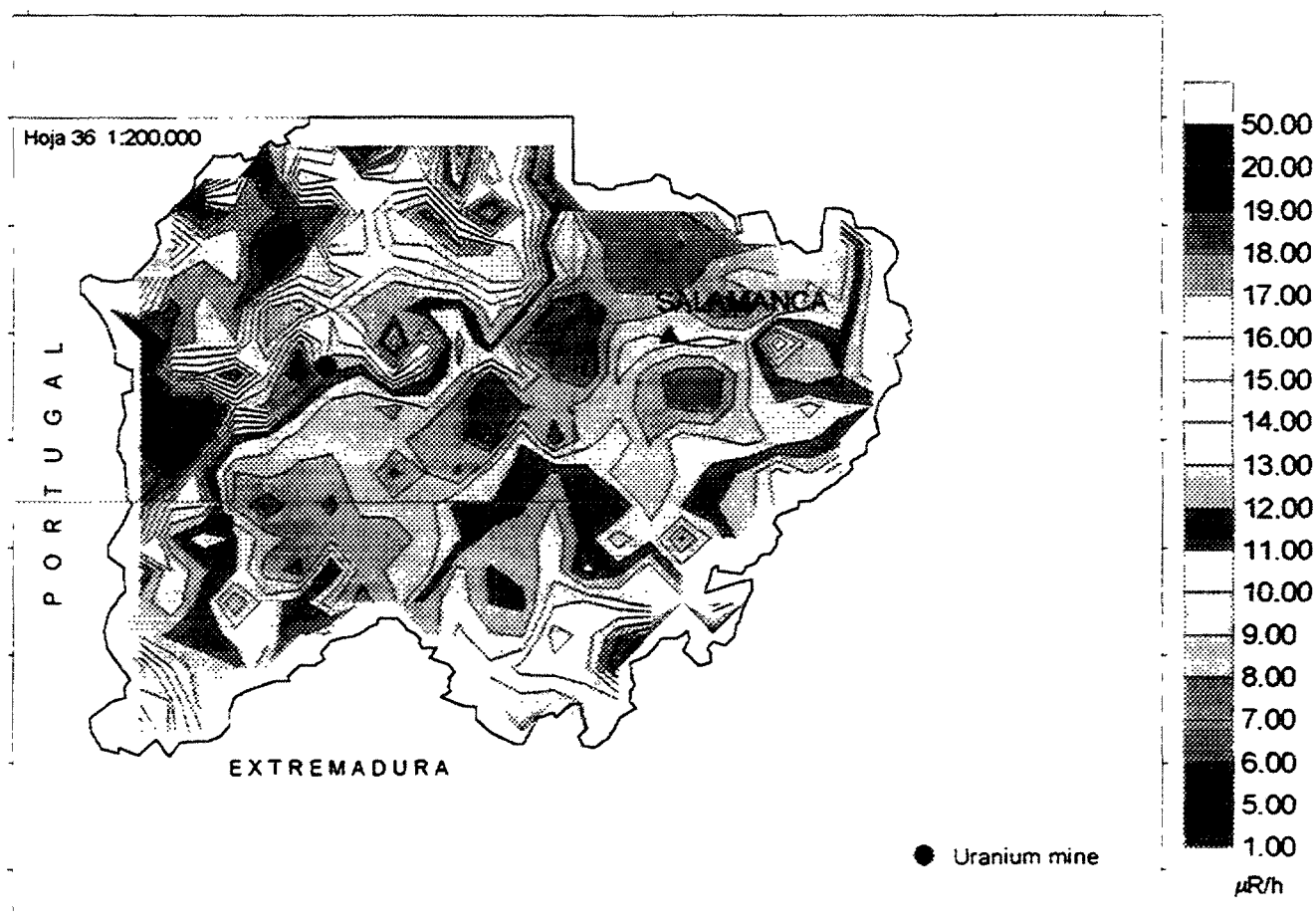


FIG. 4. Radiometric map of the Province of Salamanca. Resolution: 1 Radiometric datum/ 35 km^2 .

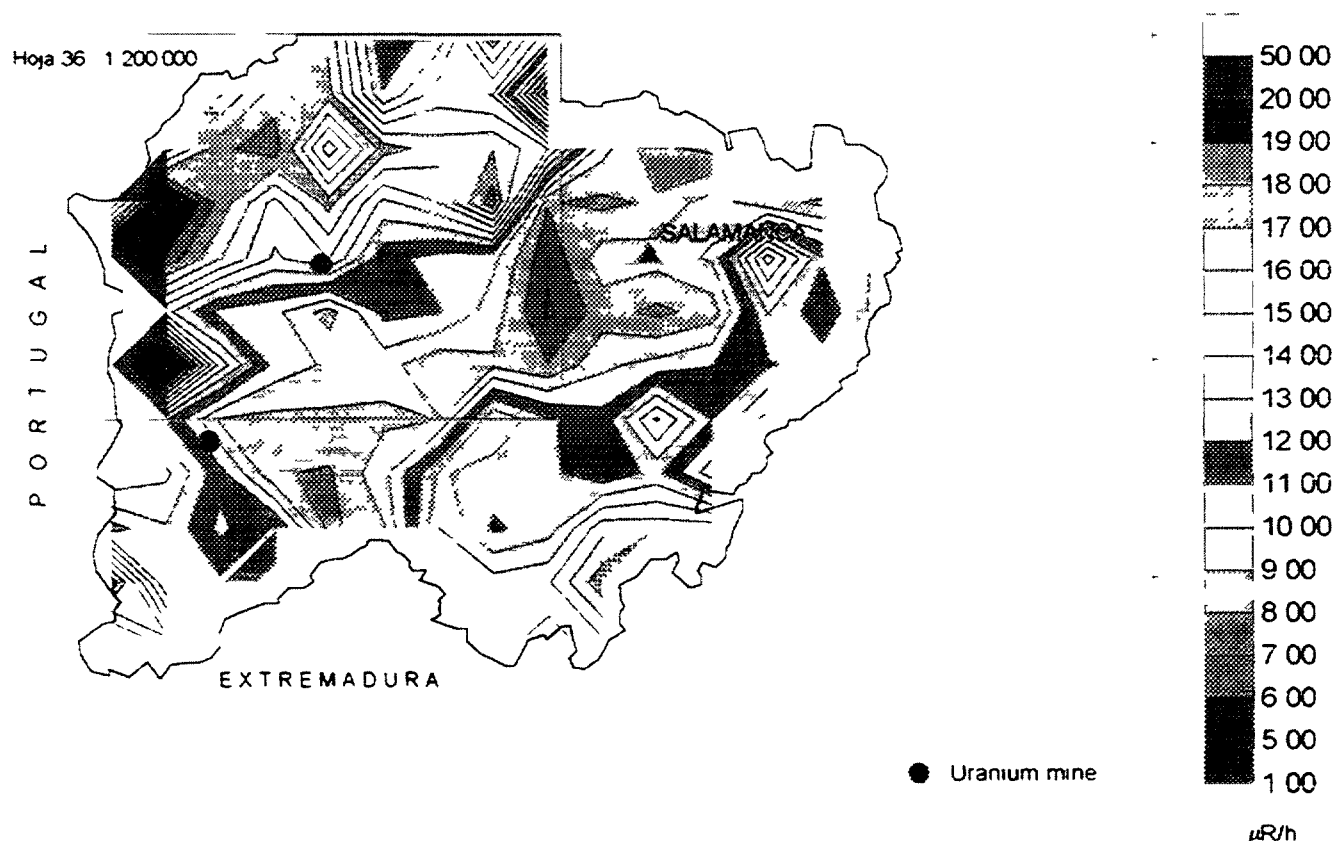


FIG 5 Radiometric map of the Province of Salamanca Resolution 1 Radiometric datum/100 km²

If both maps are compared with the geological scheme in Fig 2 it can be seen that, in the first case, the geological macroformations (entities of over 100 km²) are quite well drawn, whereas in the second case only the limits of these macroformations can be seen approximately (Ciudad Rodrigo basin, northern zone of Lumbrales and southern zone, Sierra de Gata)

Fig 6, shows the sheet no H-36 (Vitigudino) 1 200 000, with resolutions of 1/4, 1/9, and 1/25, (one 1 200 000 sheet is made up of 4 × 4 1 50 000 sheets)

From a comparative analysis with the geological sketch in Fig 2 it is deduced that

- With a 1/1 resolution the position of the uranium mines (Fe and Retortillo mines), the Almendra reservoir and its extension over a great distance, minor (quaternary north of the reservoir) and major geological formations, clear edges between radiometrically well characterized geological formations, and even the influence of the metamorphic gradient over the residual Palaeozoic of the northern part of the Ciudad Rodrigo basin are perfectly in evidence
- With a 1/4 resolution the tail of the reservoir disappears and the Retortillo mine has not been captured
- With a 1/9 resolution the foregoing details can still be seen, albeit more faintly

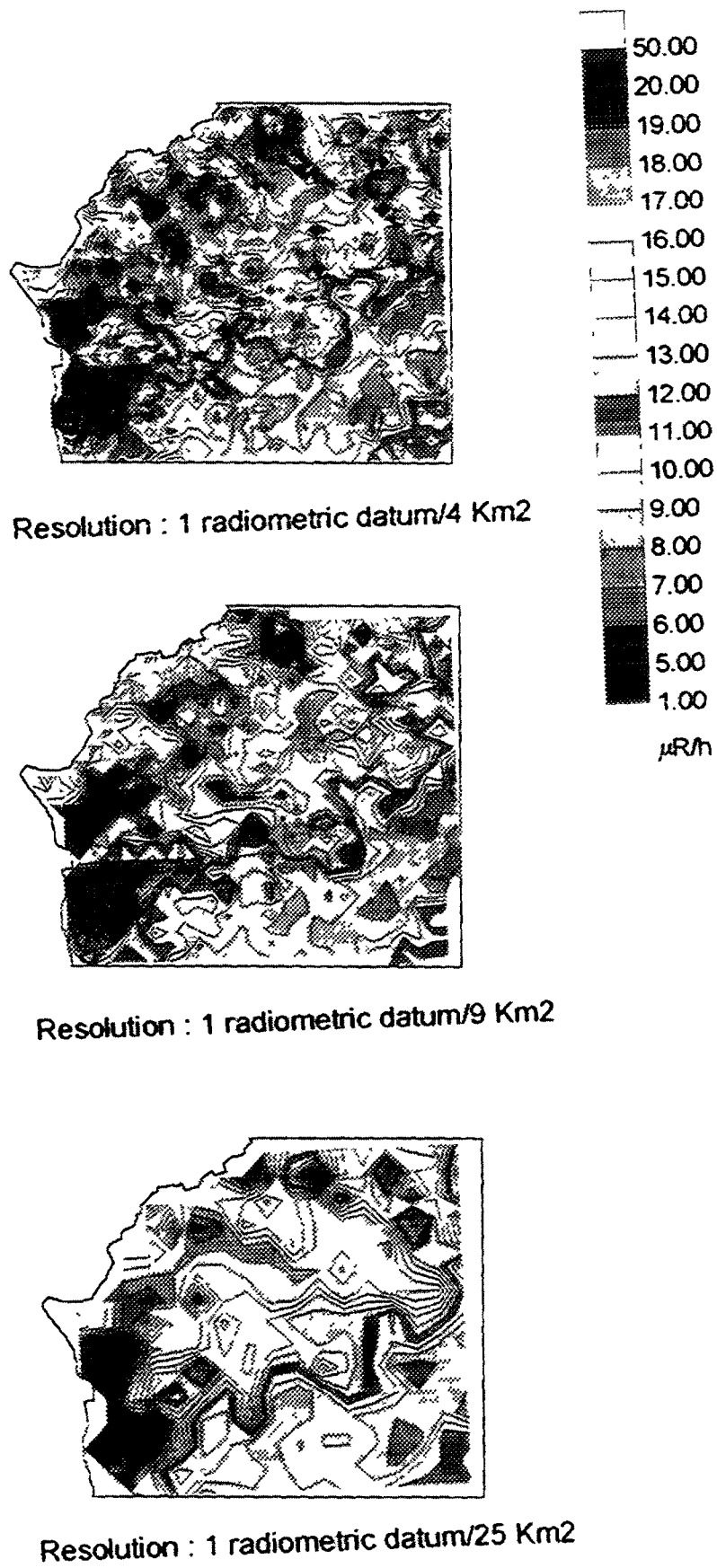


FIG 6. Radiometric map of the H. 36 Vitigudino 1: 200 000 with different resolutions.

- With resolutions of 1/25 and 1/35 the radiometric contacts become fainter and fainter. Anomalies of less than 25-35 km² might not be captured and if they are they offer a sharpening of kilometric forms

5 CONCLUSIONS

With regard to data extraction

- The problem with the data-extraction mesh in our MARNA Project is similar to that of the calculation of the optimum sampling
- Each surface factor must be studied statistically and the number of data increased until an acceptable confidence limit is reached in all cases. Should any of the samples fail to fulfil the error limit, the mesh on its surface will be closed until the confidence limit can be brought down to within acceptable or admissible margins, otherwise the item of data will be dispensed with

With regard to the drawing-up of maps

On a 1 200 000 scale

From the experience gained in drawing up maps on 130 000 km² of Spanish territory, it is inferred that for resolutions included between 1/1 and 1/9 km² very acceptable resolutions are obtained, versus geology and orography [15], [16], [17]

On a 1 1 000 000 scale

A resolution of 1/35 km² is very acceptable, and a resolution of 1 100 km² deforms important geological and geographic irregularities

With regard to the geology/radiometry correlation

- Very good with the resolution 1/1 km² (mines detected)

With regard to the quantitative determination of contaminations

- Once the preoperational radiometric map has been drawn up, an eventual contamination may be quantified by means of similar comparative methods
- The extension and variability in intensity of the contamination will govern the size of the sampling

REFERENCES

- [1] ALLYSON J L , TYLER, A N , "Rapid quantification and mapping of radiometric data for anthropogenic and technologically enhanced natural nuclides", Application of uranium exploration data and techniques in environmental studies IAEA-TECDOC-827, IAEA, Vienna (1995) 197
- [2] ANDJELOV, M , TOMŠIČ, J , PEČNIK, M , "Natural background radioactivities and geochemical map of Slovenia", Application of uranium exploration data and techniques in environmental studies, IAEA-TECDOC-827, IAEA, Vienna (1995) 217

- [3] BAEZA, A., et al., Estudio comparado de dos métodos para la evaluación de los niveles de tasas de dosis ambientales en la provincia de Cáceres (Relación Interna) (Mayo 1994).
- [4] BALL, T.K., CAMERON, D.G., COLMAN, T.B., ROBERTS, P.D., "The use of uranium exploration data for mapping radon potential in the U.K. — advantages and pitfalls" Application of uranium exploration data and techniques in environmental studies, IAEA-TECDOC-827, IAEA, Vienna (1995) 139.
- [5] BARNET, I., "The role of airborne gamma spectrometric data in the radon programme of the Czech Republic", Application of uranium exploration data and techniques in environmental studies, IAEA-TECDOC-827, IAEA, Vienna (1995) 151.
- [6] COX, J.R., "Radiation detection of buried shielded sources in vehicles loaded with scrap steel", Application of uranium exploration data and techniques in environmental studies, IAEA-TECDOC-827, IAEA, Vienna (1995) 315.
- [7] GUNDERSEN, L.C.S., OTTON, J.K., SCHUMANN, R.R., REIMER, G.M., DUVAL, J.S., "Uranium resources assessment and exploration data for geological radon potential assessment in the United States, Application of uranium exploration data and techniques in environmental studies, IAEA-TECDOC-827, IAEA, Vienna (1995) 135.
- [8] MELLANDER, H., "The role of mobile gamma spectrometry in the Swedish emergency response programme for nuclear accidents — experience and future plans", Application of uranium exploration data and techniques in environmental studies, IAEA-TECDOC-827, IAEA Vienna (1995) 187.
- [9] MORO, M^a.C., PEREZ DEL VILLAR, L., Estudio de la distribución de K, U, y Th en el batolito de Cabeza de Araya mediante prospección aéreo-radiométrica, Implicaciones petrogenéticas y metalogenéticas. Libro Jubilar de Figuerola L.D, Omega, Madrid (1988).
- [10] MULTALA, J., "Airborne Gamma-ray measurements in radioactive cloud — Experience at the Geological Survey of Finland", Application of uranium exploration data and techniques in environmental studies, IAEA-TECDOC-827, IAEA, Vienna (1995) 103.
- [11] OTTON, J.K., NIELSON, K.K., BROWN, R.B., ZWICK, P.D., SCOTT, T.M., "Quantitative modelling of radon potential in Florida and the use of aeroradiometric data", Application of uranium exploration data and techniques in environmental studies, IAEA-TECDOC-827, IAEA, Vienna (1995) 181.
- [12] SANDERSON, D.C.W., ALLYSON, J.D., TYLER, A.N., SCOTT, E.M., "Environmental application of airborne gamma spectrometry", Application of uranium exploration data and techniques in environmental studies, IAEA-TECDOC-827, IAEA, Vienna (1995) 71.
- [13] SIDERIS, G.N., PAPAConstantinou, K.N., PAPADOPOULOS, N.N., "The contribution of applied geophysics for the estimation of the radioelement contamination of the environment", Application of uranium exploration data and techniques in environmental studies, IAEA-TECDOC-827, IAEA, Vienna (1995) 281.
- [14] SUAREZ MAHOU, E., CERRAJERO H.J., CREGO, A., Relación Interna JEN, Prospección aérea sistemática de la zona de Badajoz, Madrid (1967).
- [15] SUAREZ MAHOU, E., FERNANDEZ AMIGOT, J.A., Proyecto MARNA (Mapa de Radiación Natural y Dosimétrico de España) XIX Reunión Anual SNE, Cáceres (Oct. 1993)
- [16] SUAREZ MAHOU, E., FERNANDEZ AMIGOT, J.A., "Use of uranium airborne survey data in the preparation of radiometric map of Spain, Application of uranium exploration data and techniques in environmental studies, IAEA-TECDOC-827, IAEA, Vienna (1995) 109.
- [17] SUAREZ MAHOU, E., FERNANDEZ AMIGOT, J.A., The Radiometrics Map of Spain (MARNA PROJECT), IX Congreso internacional de Minería y Metalurgia, León (1994).
- [18] TORRES, L.M., GRASTY, R.L., "The natural radioactivity map of Portugal", Application of uranium exploration data and techniques in environmental studies, IAEA-TECDOC-827, IAEA, Vienna (1995) 127.
- [19] VULKAN, U., SHIRAV, M., SHILONI, Y., "Radon levels of rock formations in Israel" Application of uranium exploration data and techniques in environmental studies, IAEA-TECDOC-827, IAEA, Vienna (1995) 197.

**NEXT PAGE(S)
left BLANK**



NATURAL BACKGROUND RADIATION IN JORDAN

M.N.S. DAOUD

National Resources Authority,
Ministry of Energy and Mineral Resources,
Amman, Jordan

Abstract

An Airborne Gamma Ray survey has been accomplished for Jordan since 1979. A complete report has been submitted to the Natural Resources Authority along with field and processed data "digital and analogue". Natural radioelements concentration is not provided with this report. From the corrected count rate data for each natural radioelement, Concentrations and exposure rates at the ground level were calculated. Contoured maps, showing the exposure rates and the dose rates were created. Both maps reflect the surface geology of Jordan, where the Phosphate areas are very well delineated by high-level contours. In southeastern Jordan the Ordovician sandstone, which contain high percentage of Th (around 2000 ppm in some places) and a moderate percentage of U (about 300 ppm), also show high gamma radiation exposures compared with the surrounding areas. Comparing the values of the exposure rates given in ($\mu\text{R/h}$) to those obtained from other countries such as United States, Canada, Germany, etc. Jordan shows higher background radiation which reach two folds and even more than those in these countries. More detailed studies should be performed in order to evaluate the radiological risk limits on people who are living in areas of high radiation such that the area of the phosphatic belt which covers a vast area of Jordan high Plateau.

1. INTRODUCTION

The natural environment is the major source of radiation exposure to man. This natural radiation could be used as a standard for comparing additional sources of man made radiation such as those produced by medical sources of X rays, atomic weapons, fallout, nuclear power generators and radioactive waste disposal. To assess the significance of these additional sources of man-made radiation, the levels of natural background radiation and its variation must be known. Radiation exposure is considered as internal when it is taken by breathing or swallowing such as ^{40}K or ^{222}Rn and it is considered as external when it is received by the surface of the body such as cosmic rays and natural radioactive elements principally ^{40}K and uranium and thorium decay series occurring in the ground, in building materials and in the air.

The external radiation can vary considerably according to many things such as the geological environment, the elevation above the sea level, the temperature, humidity, moisture, type of living and accommodation, etc.

The natural radionuclides decay through emission of alpha particles, beta particles and gamma radiation. Alpha particles are very heavy and cannot travel more than few centimeters through the air. Beta particles which are much lighter can travel about one metre in the air. While gamma rays which have almost no mass can travel several hundred metres through the air. Cosmic rays which are very energetic can travel long distances from stars and penetrate the whole earth's atmosphere down to the ground surface. While lungs and respiratory tract are the most affected organs to alpha and beta particles which are present in the air, except that the human body is exclusively exposed to gamma and cosmic radiation.

This report deals with the effects of gamma radiation, emitted only by the natural radioelements of potassium and uranium and thorium and their decaying series, on the whole body and is not concerned with alpha and beta particles which affect only specific parts of the body. Different kinds of techniques were used to evaluate the natural background radiation in different parts of the world; these techniques have involved the use of ionization chambers, portable and airborne scintillometers, laboratory analysis of the radioactive elements in soil samples, etc. None of these above methods was capable to carry out a representative sampling on a country wide basis because

of the variation of the ground radioactivity from place to place and because of the limited number of measurements that could be taken.

Because of the large areas that could be covered and the huge amounts of data that could be collected, airborne survey is considered as unchallenged method in the point of view representation. Very considerable improvements were achieved since the first airborne radiometric surveys until recent airborne gamma ray spectrometer surveys. Improvements did not involve only the equipment, where powerful computers control the whole parameters of the flight with very sophisticated equipment on board, but the procedure as well which includes the construction of large radioactive concrete calibration pads and the establishment of airborne calibration range such that of Breckenridge strip near Ottawa in Canada. Now it is possible to estimate the concentration of the natural radioelements at the ground level with high accuracy.

2. GEOCHEMISTRY OF RADIOELEMENTS

It is important to know the distribution of the natural radioelements in nature in order to know which rock type is responsible of the most contribution of gamma radiation to the environment. This will lead us to have a certain knowledge about the abundance of these radioelements in nature.

2.1. Abundance in crustal rocks

Table I indicates the concentration of the three radioelement in common rock types. All three elements are oxyphile and have relatively large ionic radii, these two factors play a role in the crystal chemistry. Within igneous rocks, the abundance of the three radioelements increases with increasing silica content. The difference in geochemical behaviour becomes apparent under strongly oxidizing conditions which may exist beyond the stage of pegmatite formation, or under supergene conditions. Uranium and Thorium behave in a similar way when uranium exists in a quadrivalent state which is the characteristic of uranium, and form several isomorphous mineral series, but uranium behaves differently in the hexavalent state. Both elements may occur as accessory minerals in granitoid rocks or be concentrated in pegmatite.

TABLE I. RADIOELEMENTS CONCENTRATIONS IN CRUSTAL ROCKS
[Adapted from Clark et al. (1966)]

Rock type	K %	U (ppm)		TH (ppm)		Th/U	
	average	average	range	average	range	average	range
crustal average	2.1	3		12		4	
mafic igneous	0.5	1	0.2-3	3	0.5-10	3	3-5
intermediate igneous	1-2.5	2.3	0.5-7	9	2-20	4	2-6
acid igneous	4	4.5	2-23	28	5-20	4	2-10
arenaceous sediment	1.4	1	0.5-2	3	2-6	3	
argillaceous sediment	2.7	4	1-13	16	2-47	4	1-12
limestone	0.3	2	1-10	2	-	1	
black shales	2.7	8	3-250	16	-	2	wide
laterites	low	10	3-40	50	8-132	5	wide
metamorphics		depend on rock type					

2.2. Uranium Geochemistry

The relative concentration of uranium compared to both thorium and potassium is an important factor in the recognition of possible uranium deposits using gamma ray survey. In the hexavalent state, uranium is ready to form the soluble uranyl ion (UO_2^{++}) and become very mobile. This permits the segregation and, under favourable conditions, the concentration of the uranium. More commonly, uranium moves in solution as the uranyl complex with carbonate, sulphate and chloride ions. Under reducing conditions, the uranyl is precipitated as primary complex oxide compounds by organic matter or insoluble hydroxides of iron or manganese. Under oxidizing conditions, secondary uranium minerals are precipitated by evaporation of uranium bearing solutions, and with copper, calcium, potassium or other metals may form as phosphates, arsenates, vanadates or silicates. Black shales and marine phosphates are commonly enriched in uranium and may contain in excess of 100 ppm. Gamma ray measurements of uranium abundance usually depend upon the gamma emission of its daughter product, ^{214}Bi , which is the ninth decay product in the series. Radon and radium are very important in geochemistry exploration because of their mobility. Radium is only mobile in sulphate free, neutral or acid solutions and is ready to be precipitated by gypsum, anhydrite, barite, hydroxides of iron, manganese and aluminium. Radon on the other hand is an inert gas with a short half-life time but is easily dissolved in water and can escape to the atmosphere through permeable rocks. The displacement of uranium, radon or radium from the mother radioactive source will cause disequilibrium, leading to erroneous gamma ray estimations of the uranium concentration in the source, and may create confusing secondary exploration targets in the vicinity.

2.3. Thorium Geochemistry

There is similarity of geochemical behaviour for both uranium and thorium under hypogene conditions. Thorium is not susceptible to leaching under most supergene conditions, and its principal mode of occurrence is in the refractory heavy minerals, which under supergene conditions may become concentrated as residual residue in laterite cappings, or in placers deposits. In primary igneous rocks some carbonatites are strongly enriched in thorium, which is indicative of the presence of other rare earth's.

2.4. Potassium Geochemistry

The geochemistry of potassium is well known and may need to add this comment. Certain types of uranium mineralization are accompanied by sodium metasomatism mineralization. Under these conditions sodium initially replaces potassium in rock forming minerals and further exaggerates the U/K ratio which always increases where there is significant uranium mineralization.

3. AIRBORNE RADIATION SURVEY OF JORDAN

3.1. Survey planning

The survey, which covered the entire Kingdom of Jordan, was divided into three zones as illustrated in Fig. 1. All lines were flown in an east northeast/west southwest direction as indicated on the flight path map Fig. 2. Survey lines were planned to terminate 8 kilometers from the international borders. Area A is only a magnetic survey area which covers the Wadi al Araba-Jordan Rift and the highlands east of the rift, including the outcropping basement rocks of the southern mountainous desert. The flight altitude was kept constant for each traverse within area A varying between 1500 and 2000 metres above sea level, depending on the maximum height of the topography beneath the flight line. ENE traverses were spaced at 1 km intervals with NNW control lines flown at 20 km spacing. Control lines were also flown along the western and southern perimeters of the

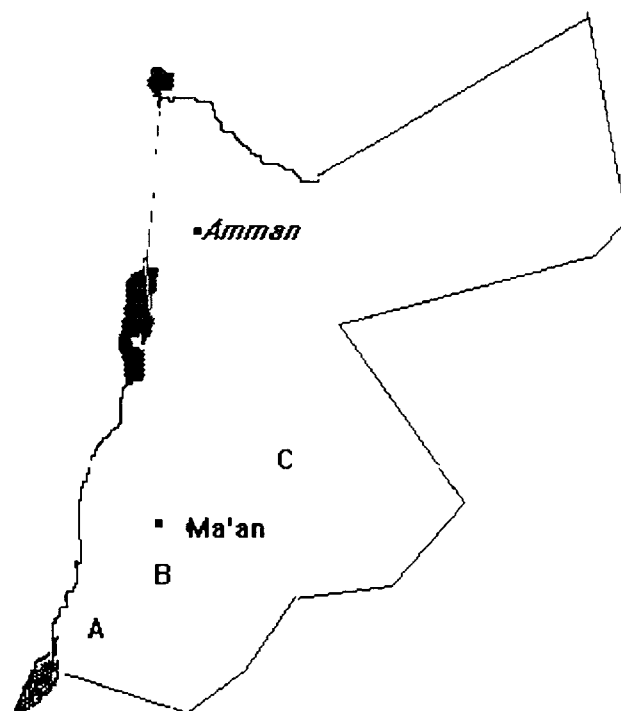


FIG. 1. Location map of the survey area

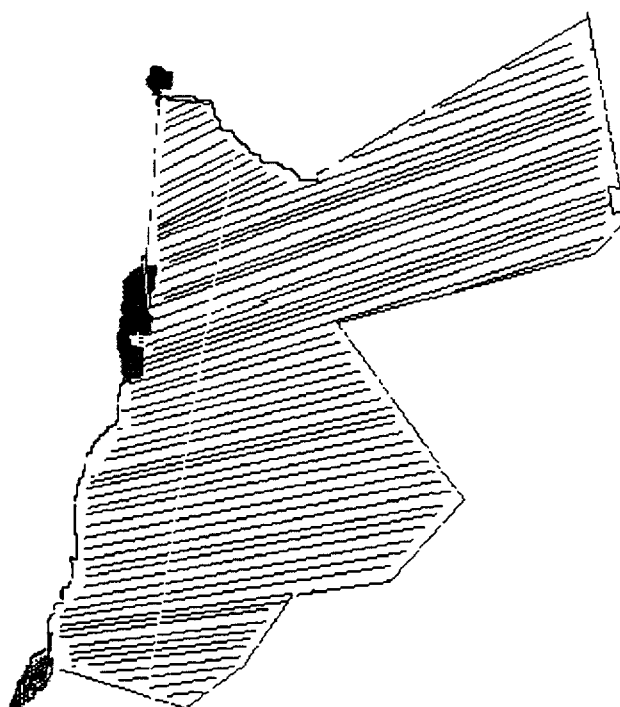


FIG. 2. Flight path map

area. Area B, as depicted in Fig. 1 is a magnetic and gamma radiation survey area. A survey altitude of 120 metres terrain clearance was maintained except over a small section in the north-west corner where rugged topographic features necessitated flight altitudes of 800 to 1050 metres above sea level in order to ensure safe aircraft operations. ENE traverses were spaced at 1 km intervals with NNW control lines at 10 km interval in the northern section of the area and 20 km intervals in the southern

portion. Three NS traverses were flown along the western boundary of the survey area, from the southern end of the Dead Sea to the northern survey limit in order to ensure complete survey coverage.

Area C, a magnetic and gamma radiation survey area, covered the largest portion of the Kingdom of Jordan as shown in Fig. 1. A survey altitude of 120 meters terrain clearance was maintained for the entire area. ENE traverses were spaced at 2 km intervals with NNW control lines flown at 20 km spacing and 2 perimeter control lines were flown across the northern boundary. The bases of the survey operation were Amman for the northern portion of the survey and Aqaba for the southern portion. The survey aircraft was a twin-engine Douglas DC-3 with registration C-FITH.

The equipment on board the aircraft used for the purpose of the survey are described as list-1.

List 1: Airborne Survey Equipment

- Airborne Magnetometer-Geometric Model G803 proton precession magnetometer with sensor mounted in a tail stinger. The magnetometer resolution was 0.5 gauss with a sampling interval of 1.0 second.
- Crystal Detectors- 8 Harshaw polycrystalline $10.2 \times 10.2 \times 40.6$ cm Sodium Iodide (Thallium activated) crystal. Total crystal volume of 33567 cubic centimeters.
Geotrex MADACS digital data acquisition computer system. Basic components are an Interdata Model 6/16 minicomputer, a crystal clock, a Nuclear Data Model 560 analogue/digital converter and custom designed operating system.
- Digi Data Model 1600, 9 track, 800 BPI magnetic tape transport.
- Gulton Model TR-888, 8 channel analogue chart recorder (4 cm/channel).
- Moseley Model 7100B, 2 channel analogue chart recorder (25.4 cm width).
- Geotrex Model 75-SF, 35 mm frame, tracking camera.
- Sperry Radar Altimeter, Model RT-220.
- Geotrex custom magnetometer compensation unit.
- Bendix DRA-12C Doppler navigation system.

3.2. Data Acquisition

Doppler navigation was employed in addition to visual navigation through the use of topographic map flight strips. Visual navigation alone has been impractical as a large portion of the survey area was desert area devoid of identifiable features.

The recording of all of the airborne survey parameters was controlled by a command signal from the MADACS unit. MADACS is the name of a Geotrex designed software controlled system built around a 16-bit minicomputer. This unit controlled and synchronized the recording of all the parameters through a crystal clock. The spectrometer system recorded the radiometric counts in 256 channels for energies in the range 0.0 to 3.0 Mev.

Also recorded were four channels of summed "window" data for the energy ranges as indicated in Table II.

TABLE II. 4 GAMMA- RAY WINDOWS RECORDED BY GEOTERREX SPECTROMETER SYSTEM

Window	Photo Peak	Energy Range (Mev)
Thorium	Thallium 208	2.42–2.82
Uranium	Bismuth 214	1.66–1.86
Potassium	Potassium 40	1.36–1.56
Total Count	—	0.8–2.82

The spectrometer magnetometer, radar altimeter and barometric altimeter data were recorded in both analogue and digital formats with no corrections applied. On the 8 channel analogue recorder, each channel is 4 cm and the chart speed was 6.0 cm/minute. A sample of an 8 channel analogue record is contained in Fig. 3. The parameters recorded and their full scale deflections, arranged in order of chart top to chart bottom, are described as list 2

List 2. Survey parameters and their full scale deflections

Integer Fiducials	every 10 samples (10 seconds)
Barometric Altimeter	1000 feet deflection (305 metres)
Radar Altimeter	1000 feet deflection
Magnetics(coarse scale)	2000 gamma deflection
Magnetics (fine scale)	200 gamma deflection
Total Counts	2000 counts/second deflection
Potassium	500 counts/second deflection
Uranium	200 counts/second deflection
Thorium	200 counts/second deflection

The Doppler measurements, recorded in digital format only, were the instrument output before processing through the Doppler navigational computer. Hence they were not subject to any changes made by the pilot in his instrument settings. The two parameters recorded digitally were the distance traveled and the track direction, in each one second measuring interval.

3.3 Survey Procedures

3.3.1. Geophysical Equipment Tests

The following tests of the geophysical survey instruments were made: Prior to departure for Jordan the radiometric instruments had been calibrated on the radiometric test pads and over the range near Ottawa, Canada. The results are included with Phoenix report. After arrival in Jordan, on the ground and before each survey flight, a radiometric balance check and adjustment was performed under control of the MADACS operating system.

3.3.2. Flight Tests

Prior to the commencement of flying the actual survey portion of a flight and just after, a series of short tests were performed for the purpose of monitoring the equipment stability and for calibration. A common test line, which was selected for repeatability of navigation and geophysical responses was flown with all survey equipment in operation. While based in Amman, the test line was over a railroad line just south of Amman ending just before the new airport under construction. While

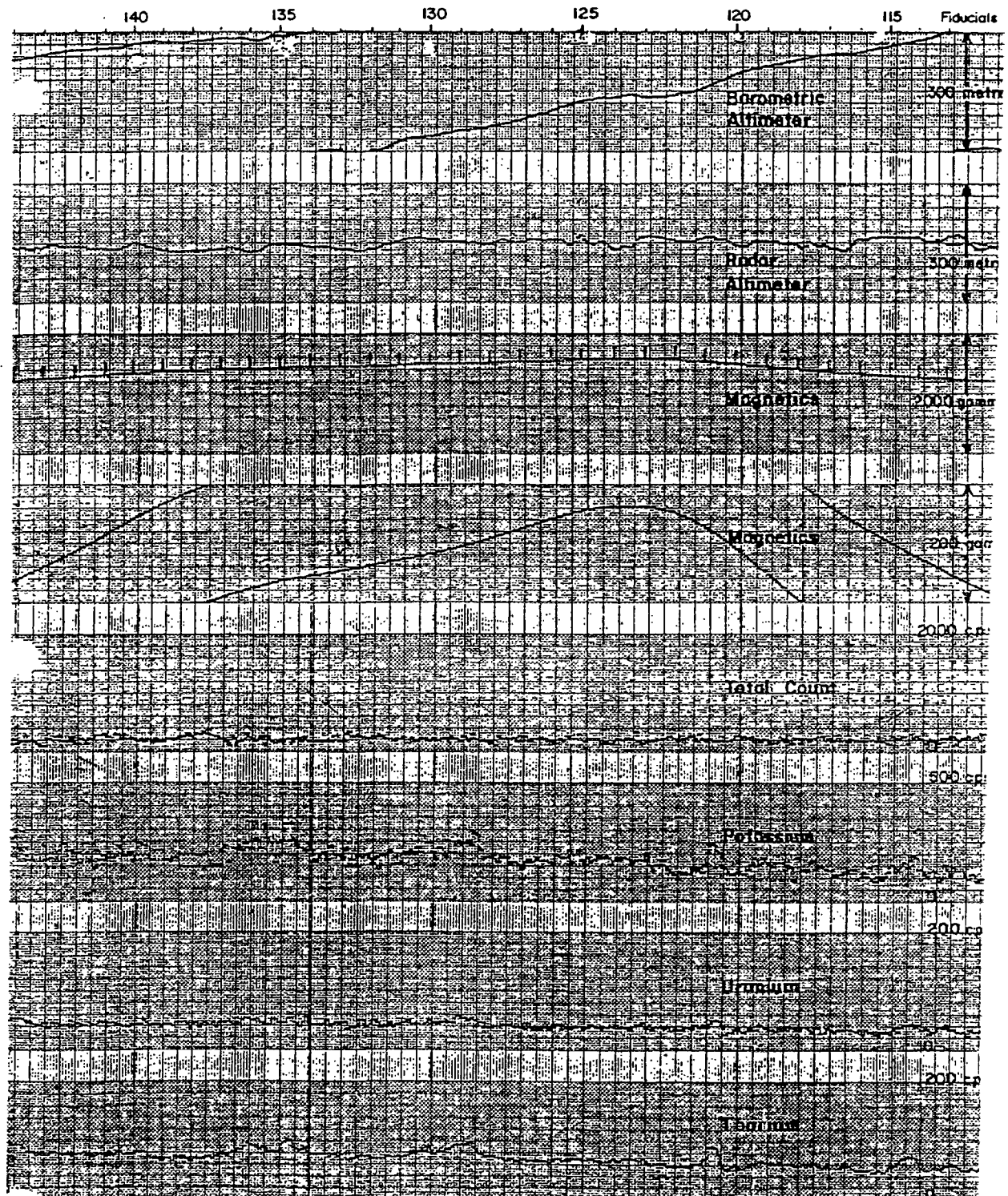


FIG. 3. Sample of eight channel analogue record (not fit to scale).

based at Aqaba airport the test line was flown over the gulf of Aqaba. Backgrounds are best determined by flying over a large body of water at survey altitude but in the north this was impossible. General checks for the proper functioning of all inputs to the MADACS system (barometric altimeter, radar altimeter, tracking camera, Doppler, radiometric sensors) were made before commencement of surveying.

The MADACS system, under control of the operator, was capable of providing on-line multichannel display of accumulated natural Potassium and Thorium photopeaks.

3.3.3. Post flight Procedures

Upon completion of a flight, the 35 mm tracking was developed. The actual flight path was proved by identifying points from the film on the topographic map flight strips. Flight log and analogue records were checked to ensure the satisfactory data had been obtained. The radiometric source tests and test line results were analyzed to check the stability of the spectrometer system. All original survey data, analogue or digital, have been delivered to Natural Resources Authority.

3.4. Aeroradiometric Data Reduction and Compilation

In order to relate the airborne count rates of the three windows to radioelement concentrations of the ground four distinct steps are necessary: the removal of background radiation; the spectral stripping procedure; altitude correction; with temperature and pressure correction; and the conversion of the corrected count rate data to ground concentration.

3.4.1. Removal of Background Radiation

Three sources of background radiation exist in any airborne radioactivity measurements:

the radioactivity of the aircraft and its equipment; cosmic radiation; and the radioactivity in the air arising from daughter products of radon gas in the uranium decay series. To remove the effect of these three sources, it will be enough to take measurements over a large body of water. Unfortunately large bodies of water are not available except the Dead Sea and Aqaba Gulf.

When the survey was based in Aqaba, the background calibrations were made at survey altitude over the gulf of Aqaba. While the survey based in Amman, the aircraft flew at high altitude. The backgrounds, which were subtracted from the survey data, were determined linearly interpolating on a time basis from the pre-flight to the post-flight background levels.

3.4.2. Stripping Procedure (Compton Stripping Factors)

Due to the characteristics of the airborne gamma ray spectrum measured by sodium iodide detectors, gamma rays emitted from one particular radioelement may be detected in the other two windows. To correct for this interference, a spectral stripping procedure must be carried out. This is achieved by calibrating the aircraft and equipment over a set of large radioactive concrete pads which were constructed at Uplands Airport in Ottawa, Canada. The calibration pad measurements were carried out on August 31, 1979. Mean total system count rates observed in the Total Count, Potassium, Uranium and Thorium are summarized in Table III. These mean values were used for the calculation of the stripping constants.

The Compton stripping coefficients are (α , β , γ , a, b and g) and error analyses of these values were computed using the mean window count rates previously described. Calculations of the above coefficients were performed after the Tammenmaa program utilizing a weighted fit to all six stripping ratios, the matrix used in the calculation is having the following form.

K3	a	b	B1
α	K2	g	B2
β	γ	K1	B3

Where K represents the test pad sensitivities;
 β represents the window background estimates;
1, 2, 3 represent Potassium, Uranium and Thorium windows respectively.

The compton stripping coefficients extracted from running this programme are:

α (Th into U) = 0.36648
 β (Th into K) = 0.44650
 γ (U into K) = 0.76596
a (U into Th) = 0.01742
b (K into Th) = 0.01110
g (K into U) = 0.01398

TABLE III. LIVE TIME NORMALIZED COUNT RATES

Test pad number	Total Count (cps)	Potassium (cps)	Uranium (cps)	Thorium (cps)	Recording Time (sec)
1	1782.8	443.8	95.8	85.9	610
2	2784.3	619.6	118.9	119.7	641
3	2974.7	598.9	165.3	221.1	611
4	3753.9	657.9	208.6	339.6	631
5	3242.0	667.3	248.5	122.3	609

3.4.3 Altitude Correction

One of the factors that affects the number of gamma rays detected per second in each window (N) is the altitude of the aircraft above the ground. It is found experimentally that the stripped and background-corrected count rate in each window is to be related to the aircraft altitude (H) by a simple exponential expression of the form:

$$N = A e^{(-\mu H)} \quad (1)$$

where A and μ are constants.

Fig. 4 shows the stripped and background-corrected potassium count rate variation with aircraft altitude over the GSC airborne gamma ray spectrometer calibration range at Breckenridge 30 km west of Ottawa, flown by Douglas DC-3 on August 31, 1979. The exponential curve given by the above equation is also shown. This curve is used to correct the count rates in each window for deviations from the planned survey altitude. The detailed description of the algorithm used in the reduction of the Jordanian radiometric data is shown in Annex No. 1. It takes into consideration the previous corrections.

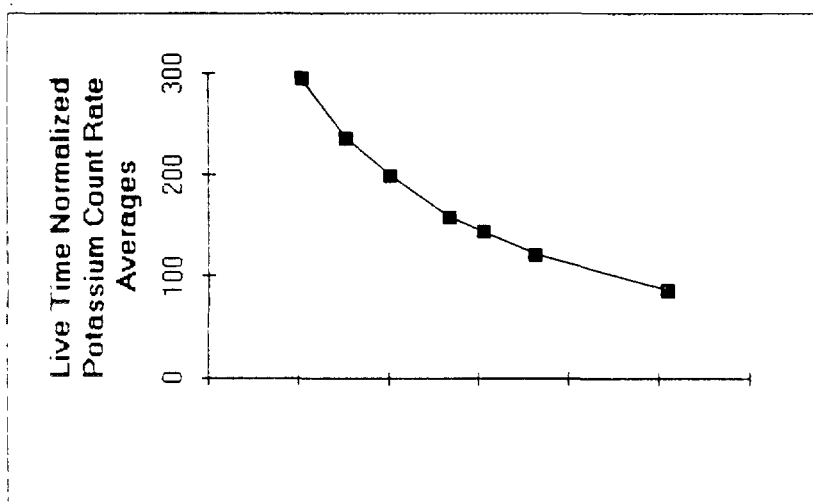


FIG. 4. Potassium count rate variation with aircraft altitude.

From the measured ground radioelement concentration of the calibration range the sensitivity of the airborne gamma ray spectrometer in terms of counts per unit time per unit concentration of potassium, uranium and thorium may be determined at the nominal survey altitude, thus allowing the ground concentration to be evaluated over unknown area. As the twin-engined Douglas DC-3 aircraft flew over the GSC airborne calibration range at different altitudes on August 31, 1979 which has a known concentration, it was possible to establish a relationship between the stripped background-corrected count rates and the concentrations of the natural radioelements at the ground level.

In an attempt to establish a relationship between the field measurements and laboratory analyses; 70 soil samples were collected at seven sites along the 10 km length of the strip [Grasty, 1975]. These samples were then sealed in metal cans, stored 4 weeks to allow the gamma ray activity of ^{214}Bi to reach equilibrium, and analysed in the laboratory by gamma ray spectroscopy for potassium, uranium and thorium. These results are presented in Table IV, together with the results of a detailed ground gamma ray spectrometer survey carried out with a portable spectrometer calibrated on the radioactive concrete calibration pads at Uplands Airport in Ottawa [Charbonneau and Darnley, 1970] concrete calibration pads at Uplands Airport in Ottawa [Charbonneau and Darnley, 1970].

TABLE IV. RADIO-ELEMENT CONCENTRATION OF THE BRECKENRIDGE AIRBORNE CALIBRATION RANGE

Type of measurement	Number of analyses	Potassium (%)	Uranium ¹ (ppm)	Thorium ¹ (ppm)
Laboratory (sealed can assay)	70	2.03 ± 0.04	0.92 ± 0.09	7.70 ± 0.28
Field	27	1.8 ± 0.1	0.5 ± 0.1	8.0 ± 0.4
Assigned value		2.03 ± 0.04	0.5 ± 0.04	7.70 ± 0.28

¹ Assuming radioactive equilibrium

Field and laboratory measurements show good agreement for potassium and thorium. Contrary to the uranium laboratory assays which are considerably higher than the field measurements. These results could be explained by a loss of ^{222}Rn from the surface soil of the calibration strip and a corresponding decrease in the ^{214}Bi activity. In the case of laboratory assays the radon and associated ^{214}Bi activity is allowed to build up and reach equilibrium because the cans are sealed and the radon gas cannot escape. Exposure rate above the ground, due to gamma rays emitted by the uranium series, is better estimated by field gamma ray spectrometer measurements rather than laboratory assays on sealed samples which can indicate an artificially high gamma ray activity. The equivalent uranium concentration of the test strip was therefore assigned the field value of 0.5 ± 0.1 ppm. Thorium and potassium laboratory were considered more reliable than the field measurements because of the greater number of samples analysed (see Table IV). Based on the potassium, uranium and thorium count rates recorded over the strip and the calibration pads, the sensitivities of the 8 Harshaw polycrystalline Sodium Iodide (Thallium activated) crystal were evaluated by Phoenix and values are given in Table V including other two detectors from GSC for comparison of the sensitivities of the two GSC detectors with the Harshaw detector supplied by Phoenix.

TABLE V. SENSITIVITY FOR DIFFERENT TYPES OF SODIUM IODIDE CRYSTALS

System	Potassium per K%	Uranium (ppm)	Thorium (ppm)
12 (22.9×10.2 cm) Cylindrical detector	78.9 ± 4.2	19.1 ± 4.8	6.1 ± 0.4
12 ($12.2 \times 10.2 \times 40.6$) Prismatic detector	90.9 ± 1.8	16.2 ± 0.9	7.0 ± 0.1
8 ($10.2 \times 10.2 \times 40.6$) Prismatic detector Harshaw	$66.5 \pm ?$	$7.7 \pm ?$	$4.8 \pm ?$

4. RADIATION DOSES UNITS

All people are exposed to gamma radiation resulting from radioactivity, and it should be recognized that the biological long-term effects of such an exposure are unknown and may be detrimental. Units of radioactivity can be confusing. This confusion originating from the fact that an ionizing field of radiation cannot be defined uniquely, such as the case of almost all fields of science, since it can consist of radiation with a complete range of energies and angular distributions. One way of comparing radiation fields is by means of an ionization chamber which measures the quantity of electrical charge released in a gas through absorption of the radiation. This type of measurement is most useful for the health physicist since it may be related to the physical damage that will occur in living cells. The radiation intensity at a given place is termed its "Exposure" (E) and is measured by its ability to produce ionization at that place; the unit of exposure is the roentgen. One roentgen is defined as the quantity of X or gamma radiation that produces one electrostatic unit of charge of either sign in 1 ml of air at standard temperature and pressure. The unit of "absorbed energy" or "dose" is the energy imparted by ionizing radiation to 1 gram of any material at the particular point of interest. The unit of absorbed dose is the "rad" (Radiation Absorbed Dose) which is deposition of an energy of 100 ergs per gram. In expressing the absorbed dose, the particular absorbing material under consideration must always be given. Environmental radiation measurements are normally presented as absorbed dose rates in air or as exposure rates. The relation between the air absorbed dose rate (Da) and exposure rate is given by:

$$Da = aE \quad (2)$$

where a has the value 0.869 rad/R

O'Brien (1978) has calculated the conversion factors between exposure and absorbed dose for various organs and tissues of the body. The relationship between exposure and whole-body dose (d) measured in rad, is given by:

$$D = 0.6E \quad (3)$$

Different types of radiation cause different effects in biological tissues. For this reason, in comparing the effects of radiation on living systems, a derived unit, the roentgen equivalent man, or rem is used. One rem is the dose from any radiation that produces effects in man equivalent to one rad of X rays. The dose in rems is the product of the dose in rad and a factor which depends on the Relative Biological Effectiveness (RBE) of the radiation considered. This unit of dose is commonly called dose-equivalent (D.E.). Therefore

$$D.E. \text{ (rems)} = RBE \times \text{rad} \quad (4)$$

X rays and gamma rays, which are the principal concern in this report, have an RBE value = 1. In recent years quantities used in radiation protection have more commonly been expressed in System International units; these SI units are the Gray (GY) and the Sievert (Sv). The Gray is the unit of absorbed dose corresponding to the rad and is the energy imparted by ionizing radiation to material corresponding to one joule/kg. The relation between the gray and the rad is:

$$1\text{Gy} = 100 \text{ rad} = 1 \text{ Joule/kg} \quad (5)$$

The Sievert is the SI unit for dose-equivalent corresponding to the rem, the relation is given by

$$1 \text{ Sv} = 100 \text{ rem} \quad (6)$$

5. THE RELATIONSHIP BETWEEN RADIOELEMENT CONCENTRATION AND EXPOSURE

It is extremely difficult to evaluate the radiation exposure 1 m above the ground for radioelements of known concentration because the energy distribution of the gamma ray flux of each of the three radioelements must be calculated and there are several hundred gamma ray energies involved by this flux, each with different attenuation coefficients and with multiple scattering occurring both in the ground and air. This difficulty has been overcome with the advent of high speed computers and the energy and angular distribution of both the direct and scattered gamma ray components can now be determined. Beck and de Planque (1968) carried out these calculations at the Environmental Measurements Laboratory in New York for the purpose of evaluating the exposure rate from natural gamma radiation and fallout from nuclear weapons tests. Independently, Kirkegaard (1972) and Lovborg and Kirkegaard (1975) have carried out similar calculations to aid in the interpretation of gamma ray survey for exploration and arrived at similar solutions. Both calculations solve the Boltzman transport equation for two semi-infinite homogeneous media, one being the ground with a uniform distribution of gamma ray emitters, and the other being the air.

Table VI shows the contribution from potassium, uranium and thorium to the exposure rate 1 m above the ground. The agreement between the results of Beck et al. (1972) and Lovborg and Kirkegaard (1974) is a good indication that the energy distribution of the gamma ray flux can be derived reliably.

TABLE VI. CALCULATED CONTRIBUTION OF POTASSIUM, URANIUM AND THORIUM TO THE EXPOSURE RATE 1M ABOVE THE GROUND

	Exposure Rate ($\mu\text{R/h}$)		
	Beck et al. 1972	Lovborg, Kirkegaard 1974	Assigned value
K%	1.49	1.52	1.505
1 ppm U ¹	0.62	0.63	0.625
1 pm Th ¹	0.31	0.31	0.31
Assuming radioactive equilibrium			

In order to verify the validity of the content of the above Table, Reuter Stokes carried out measurements at four sites along the airborne gamma ray spectrometer calibration range utilizing ionization chamber. Radiation measurements were also taken by a boat on the Ottawa River nearby, to estimate the combined background radiation exposure due to cosmic radiation, airborne radioactivity, and any small component of instrument background. Soil moisture measurements were taken at each site because of the dependence of the gamma ray exposure rate on the moisture content of the soil. Utilizing the assigned radioelement concentration of the Breckenridge of airborne calibration range, the average exposure rate along the test strip due solely to potassium, uranium and thorium was calculated to be $5.7 \pm 0.12 \mu\text{R/h}$. This calculated value, however, will vary with the moisture content of the soil. The reduced exposure rate (E) over soil with W per cent soil moisture by dry weight compared to the value E_0 over dry soil, can be considered to be the result of a decrease in radioactive concentration and is given by

$$E = \frac{100 E_0}{100 + 1.11 W} \quad (7)$$

The factor 1.11 arises because water has 1.11 times as many electrons per gram as most rock material and therefore is more effective in attenuating gamma radiation by Compton scattering, which is the predominant attenuation process above about 0.4 Mev.

6. A BRIEF ABOUT JORDAN GEOLOGY

Jordan is situated on the northwest flank of the Nubo-Arabian shield, along the eastern flank of the Dead Sea Rift, and on the southern shore of the ancient Tethys Ocean (Fig. 5). The oldest known rocks of Jordan outcrop in its southwestern corner. Since Pre-Cambrian times this granitic shield has remained predominantly a land surface, ringed around by seas which received the erosion product from the land. The shield has pulsed up and down in epeirogenic movement. Minor down beats permitted small ingressions of the sea; the rare major descents resulted in marine transgressions reaching far into the heart of the continent.

The age of these oldest rocks is imprecisely known, they are classified as Proterozoic, they include metamorphosed to unmetamorphosed mafic to felsic igneous rocks and associated sedimentary to metasedimentary assemblages. These are unconformably overlain by Late Precambrian metasedimentary rocks which are intruded by granitic bodies of varying sizes. Unmetamorphosed Cambrian to Silurian sedimentary rocks unconformably overlie the Precambrian. These rocks are predominantly marine but continental sediment occur within the Cambrian, Lower Ordovician and Upper Silurian sequence which dips gently north and northeastward beneath the Mesozoic and Cenozoic sequences. The Paleozoic section consists mostly of clastic, probably derived from the southeast and east. Some relatively thin carbonates occur to the northwest in the Cambrian section

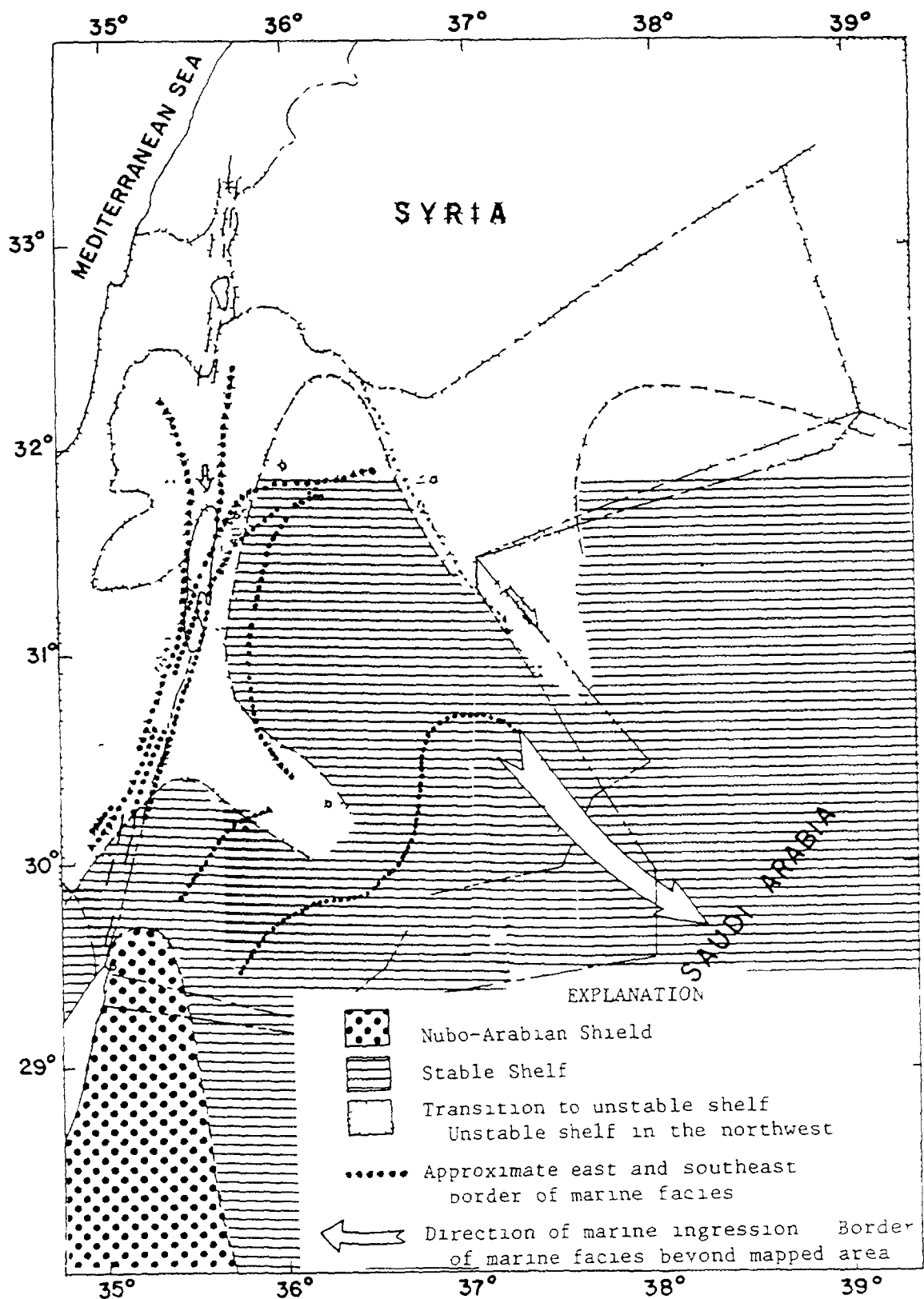


FIG 5 Regional tectonic setting of survey area (after Bender, 1975)

not far above the base of the sequence, probably representing an abortive attempt to establish a carbonate bank in the early Paleozoic. Younger Paleozoic (Devonian, Carboniferous and Permian) sequences are not known in Jordan.

The post-Paleozoic unconformity bevels the entire section from the exposed Silurian down to the Precambrian. The oldest rocks found above the unconformity are Lower to Middle Triassic rocks representing the first vestige in Jordan of the Mesozoic marine transgression of the Tethys Ocean from the north. Uppermost Triassic rocks are not existing everywhere, and the overlying Jurassic is separated partly from the Triassic by an unconformity, but the sequence are dominated by marine carbonates and clastics. Lower Cretaceous rocks overlie Triassic to the south and the former overlie the Paleozoic and Precambrian further south suggesting extensive uplifting and erosion following the earlier initial marine transgression from the north and northwest during the Triassic and Jurassic. Following the beveling of the pre-Cretaceous rocks, a clean quartz sandstone marked the continental facies of Cretaceous transgression in the southwest, delineating the shoreline over a broad area. Other lithologies occur along the base of the unit farther north and it grades into a coarse brown sandstone to the southeast. Lithologic similarities and the lack of other evidences make it difficult to recognize the unconformity in several places. The widespread deposits of the Upper Cretaceous including a variety of marls, limestones, dolostones and dolomitic limestones are representing the most extensive and dominating northwest to southeast transgression of the Tethys Ocean to date. Carbonate deposition continued until well into the Oligocene. However, widespread deposition of clastics with some calcareous occurred in central, eastern and southern Jordan until the Cenomanian. The widespread phosphate-bearing sediments of economic importance in central and southern Jordan were deposited in a Campanian-Maestrichtian transgression overlap the lower parts of the Upper Cretaceous. Sediments consist of fossiliferous phosphatic limestone and silicified material (both limestone and phosphate), are considerably less silicified than the unit below. Despite its fossiliferous nature there is disagreement about the exact age of this unit. Some place it in the Maestrichtian, while others feel it should be classed as Campanian. Field correlation indicate it is a time-transgressive unit in either case, becoming younger toward the southeast. Some of southeasternmost phosphorite deposits are found in the Paleocene.

Transgressions in the northwest to southeast directions were repeated several times during the Mesozoic as the Tethys Ocean inundated the region and then retreated. The uppermost Cretaceous-lowermost Tertiary thins toward the southeast and becomes a sandier littoral facies. Local thickenings are found in basins having a north to northwest elongation.

Volcanic activity occurred in the western part of Jordan between middle Jurassic and early Cretaceous time. Other mafic to felsic dykes and sills are found in the Wadi Araba region cutting Mesozoic sedimentary rocks, but they could be much younger (Bender, 1974, p.105).

Deposition of limy sediments continued in uninterrupted way from the Cretaceous into the Tertiary. Coarse lenticular-unsorted conglomerates (lower Syntectonic Conglomerates) begin to appear in the section overlying Upper Cretaceous or Tertiary units in the eastern Wadi Araba area. They are in an unconformable relationship in some areas and fossil evidence from several localities indicates their ages may range from Upper Oligocene to Lower Miocene. They are significant that they indicate uplift and probably tectonic activity nearby. A similar conglomerate (Upper Syntectonic Conglomerate) overlies unconformably the lower conglomerate or the older Cretaceous or Tertiary units, always in Wadi Araba region. The age of these upper conglomerates is uncertain and could range from Miocene to Middle Pleistocene (Bender, 1974, p. 92). Their tectonic significance is the same as that of the lower conglomerates. Both sets of deposits probably are related to initial subsidence and block faulting along the Dead Sea Rift. Considerable thickness of marine sediments were deposited throughout the Tertiary in Jordan. However, in some areas uplifting above sea level occurred and brackish water, lacustrine and fluvial deposits were laid down. Also, as part of the Dead Sea Rift opened, over 3.5 km of evaporates were deposited, probably during the late Miocene to early Pleistocene (Bender, 1974, p. 90-91).

Deposits of quaternary age in Jordan reflect continuous uplifting and retreating of the marine environment. More lacustrine and fluvial occur in this interval than in older sequences. Considerable thicknesses of conglomerates were deposited in and near the Rift during this time. Extensive mafic volcanic and shallow intrusive activity occurred in Jordan and the remainder of the Arabian Peninsula during the Quaternary. While there are four principal modes of occurrence of Quaternary mafic rocks, their locus is Dead Sea Rift. They occur as localized flows and plugs, some tuffs, and as plateau flood of basalts. The latter make up an extensive basalt plateau that crosses northeast Jordan from Syria and continues well into Saudi Arabia.

Basalts which may be directly associated with the Rift are chemically primitive and appear to reflect rapid propagation of fractures into the mantle, then rapid extrusion [Barberi et al., 1979].

7 NATURAL RADIOELEMENTS OCCURRENCE IN JORDAN

7.1. Uranium

The best occurrence of uranium minerals is that of the phosphorite unit which covers a large part of the Jordan plateau and parts of the highlands as shown on the location map (Fig. 6). The phosphorite section reaches 70 metres in thickness in some locations. It contains disseminated uranium minerals, from which the following have been identified:

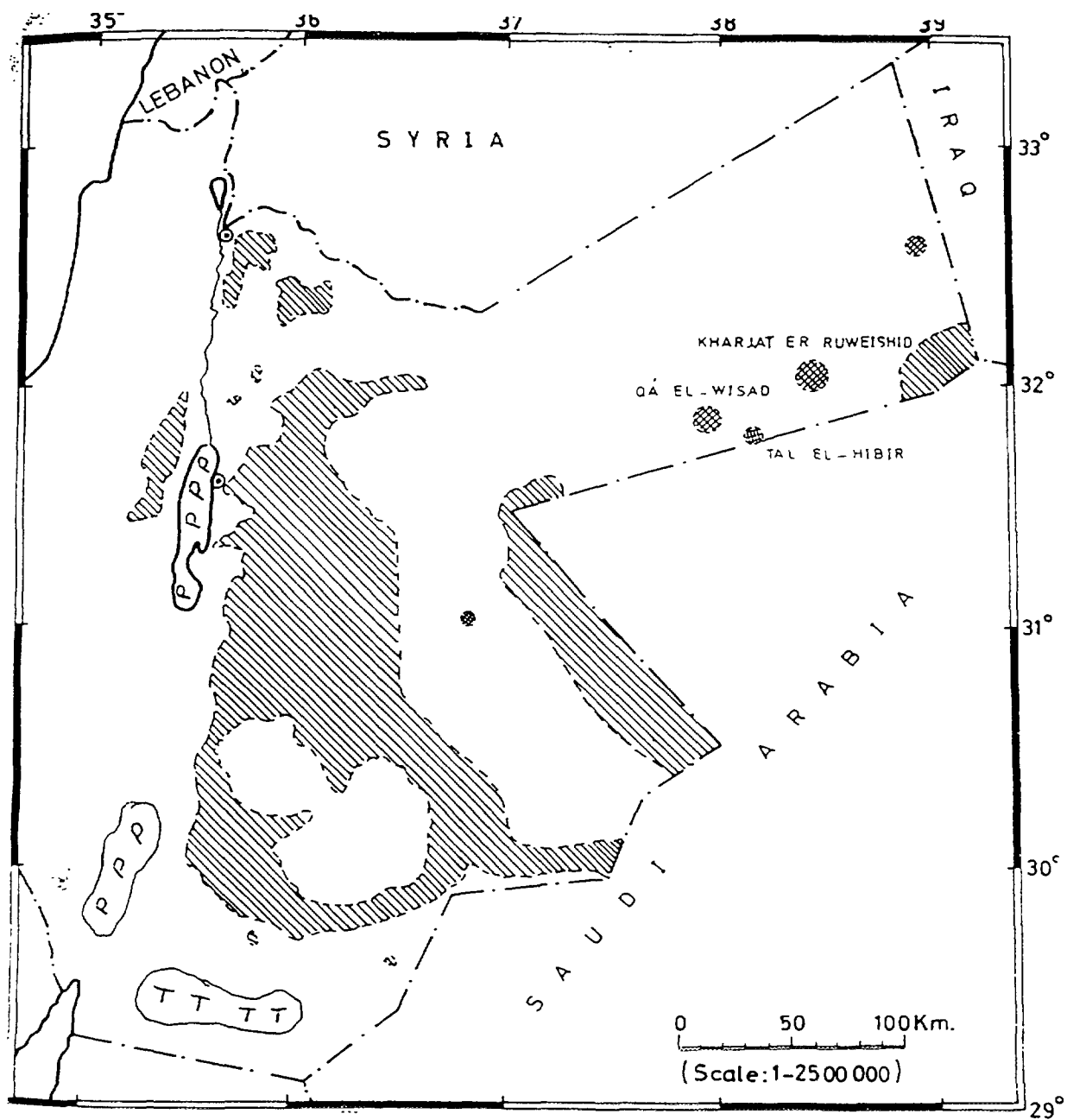
Meta-Autunite $\text{Ca}(\text{UO}_2)_2(\text{PO}_4)_2 \cdot 8\text{H}_2\text{O}$
 Metatuyamunite $\text{Ca}(\text{UO}_2)_2(\text{VO}_4)_2 \cdot 3-5\text{H}_2\text{O}$
 Uranophane $\text{Ca}(\text{UO}_2)_2(\text{SiO}_3)_2 \cdot (\text{OH})_2 \cdot 5\text{H}_2\text{O}$

Uranium minerals are distributed vertically through the whole phosphorite section. But their concentration varies with depth and lithology, although generally the highest concentrations are in the uppermost phosphate beds.

Hundreds of samples have been analysed on the basis of gamma ray of logging and scintillometric measurements and a relationship between gamma radiation and uranium oxide has been established accordingly, as indicated in (Fig. 7). The zoning in the uranium content is also correlated with lithology.

The phosphorite section of Fig. 8 represents most of the upper-Cretaceous (Campanian-Maestrichtian) in east Jordan. This cross-section is divided into the following zones according to their radioactivities:

- 1 The moderate radioactive zone I (M R Z I). It consists of marl that overlies the phosphate, sometimes it is completely eroded, its age is estimated as Danian-Paleocene. Its U_3O_8 in average is 95 ppm.
- 2 The strong radioactive zone (S R Z). It is the upper minable phosphate series and contains a thin marl band on its top. Its U_3O_8 in average is about 204 ppm.
- 3 The moderate radioactive zone II (M R Z II). It consists of the lower part of the upper U_3O_8 ab-The very low radioactive zone (V L R Z). It consists of oyster beds that phosphate series and the intercalated marl. Its U_3O_8 is about 90 ppm.
- 4 The very low radioactive zone (V L R Z). It consists of oyster that have been reworked and is known as the coquina beds of variable thickness about 24 metres. Its average is 90 ppm.
- 5 The lower phosphate series (M R Z III) which underlies the coquina beds. Its U_3O_8 is about 100 ppm.








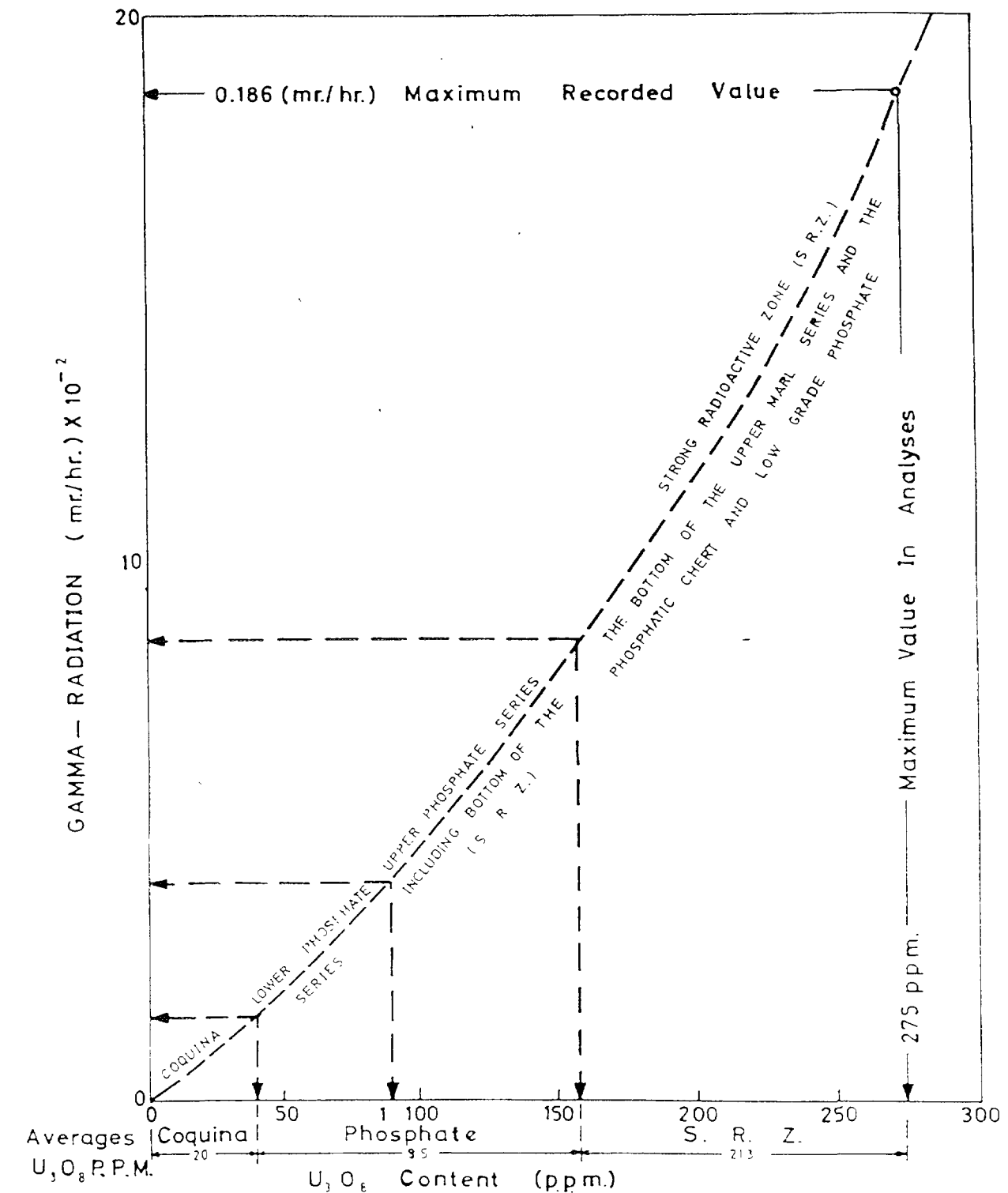
- | | |
|---|--|
|  | Location Area of Uranium Occurrences in Phosphate and Phosphatic Strata |
|  | Location of Radium Concentrations in Fault Zone Associated with Hot Mineral Springs and Basaltic Eruptions |
|  | New Phosphate Discoveries |
|  | Area of Thorium Occurrence |
|  | Area of Potassium Occurrence |

FIG. 6. Natural Radioelements Occurrence in Jordan

URANIUM EQUIVALENTS IN EL-HASA PHOSPHORITE UNIT

(AN INTERPRETATION OF GAMMA - RAY LOGS AND THE X - RAY FLUORESCENCE ANALYSES OF BORE SAMPLES



Note: THIS DIAGRAM IS AN APPROXIMATE MATCHING OF AVAILAB DATA CALCULATED ERROR IN RADIATION . 2
CALCULATED ERROR IN EQUIVALENT U_3O_8 PPM = 14%.

FIG. 7. Uranium equivalents in El-Hasa phosphorite unit (from Abu Ajamieh 1974).

CHARACTERISTIC SUBSURFACE SECTION

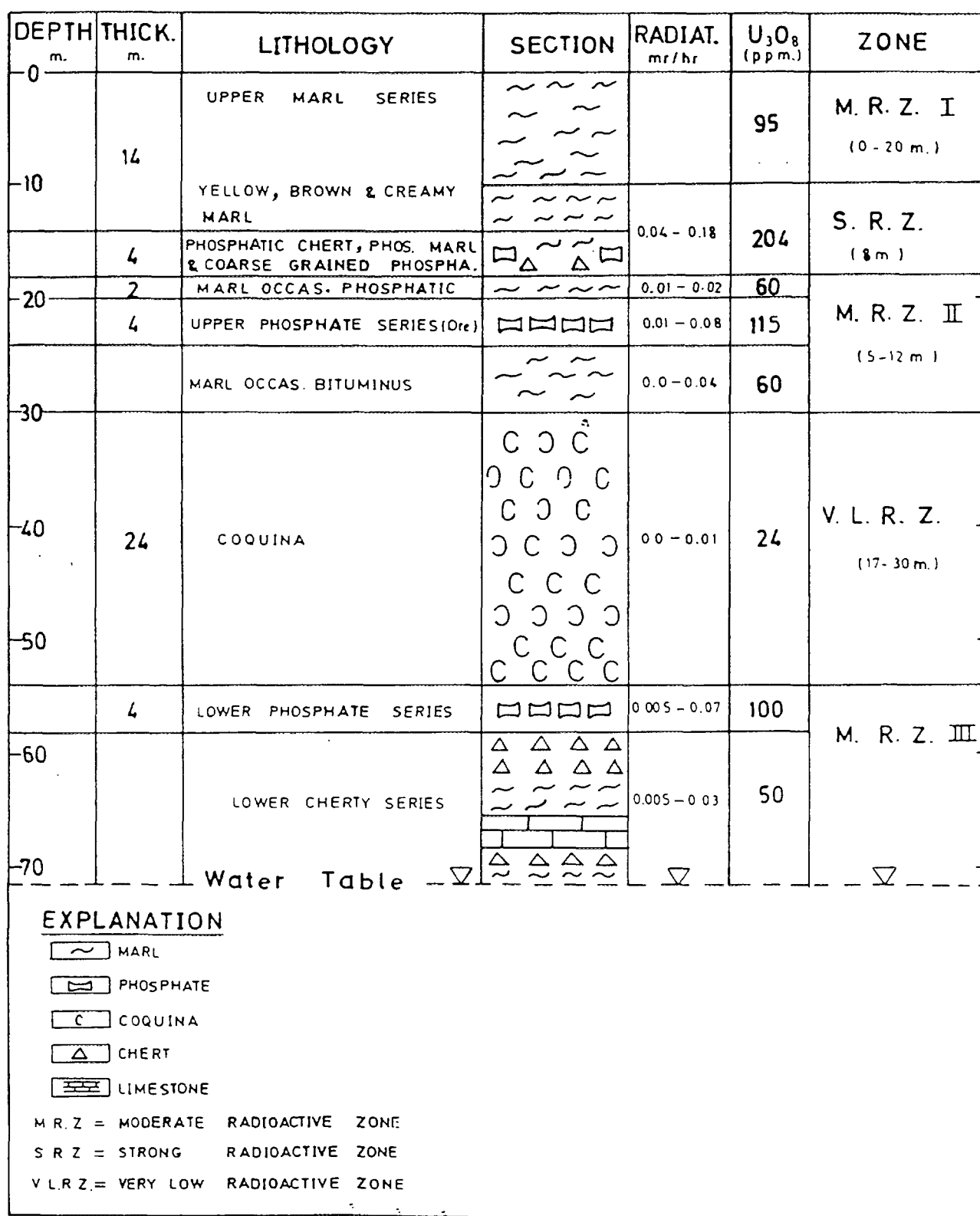


FIG. 8. Average cross section of subsurface geological and radiometric analyses data in the area between Suwaqa and Jurf Addarawish (from Abu Ajamieh 1974).

6. The lower cherty series: which consists of an alternation of chert, limestone and marl or thin low grade phosphate. Its U_3O_8 is about 50 ppm. This zone is the top of the regional aquifer.

7.2. Thorium

Thorium is typically present in crustal materials in concentrations of between 3 to 4 ppm. However, Phosphate mineral is poor in thorium concentrations as the case of Jordan Phosphate. Thorium is present in Jordan within the Paleozoic section in southeastern Jordan. It occurs within the fine-grained marine sandstone and shale unit of Llanvirn age in the Ordovician. It is found associated with uranium and zircon mineral in a metamict state. Its concentration reaches sometimes 2000 ppm.

7.3. Potassium

Potassium has a simple form of radioactive decay, only ^{40}K of several natural isotopes of potassium is radioactive. It has a relative isotopic abundance of only 0.018%.

The average concentration of potassium in crustal rocks ranges from 0.1 to 5% Jordan is rich in this element. The concentration of this element reaches about 7.5% in the Dead Sea salty water. It is present as KCl mineral. Potassium also exist in southern Jordan, it is found with associated with orthoclase feldspar (K feldspar).

TABLE VII. DIGITAL ARCHIVE TAPE

Digital Archive Tape	
Tape density	9 Track, 1600 BPI
Code	EBCDIC
Physical Blocksize	17600 bytes (fixed)
Logical record length	176 bytes

Content of a single logical record — Format (2218)

1. Identifier = flight $\times 10 \exp 6$ + line $\times 10 \exp 2$ + part	11. IGRF value (gamma $\times 100$)
2. Fiducial	12. Raw total count (cps)
3. Time (seconds $\times 10$ past midnight)	13. Raw potassium (cps)
4. Residual magnetics (gamma $\times 100$)	14. Raw uranium (cps)
5. X (UTM)	15. Raw thorium (cps)
6. Y (UTM)	16. Final total count (cps)
7. Radar altimeter (metres)	17. Final potassium (cps)
8. Barometric altimeter (gamma $\times 100$)	18. Final uranium (cps)
9. Raw magnetics (gamma $\times 100$)	19. Final thorium (cps)
10. Compensation value (gamma $\times 100$)	20. uranium/thorium
	21. uranium/potassium
	22. thorium/potassium

8. DATA VALIDATION AND EXPOSURE AND DOSE RATES CALCULATION

The whole field data (raw and processed) are available at Natural Resources Authority archives. The processed data are as described in Table VII, they are recorded on residual archive

tapes which contain the counts/second and the ratios for K, U, and Th. The tapes were down loaded to the Unix system and then the wanted columns (coordinates and corrected counts/second for K, U, and Th) are extracted from other data by using an appropriate program.

The data were checked to find any possible error in coordinates or values using the Geosoft software, some points were rejected because of wrong coordinates and many of data were rejected because of negative counts/second values.

Assumed that the data is now free of errors the counts per second were divided by 7.7, 4.8 and 66.5 which represent the sensitivity of the Harshaw crystal for U, Th and K respectively (see Table V). The results obtained by these divisions are the concentrations at the ground level expressed in ppm for uranium and thorium and in percentage for potassium.

In order to find the exposure rate expressed in μ R/h; the ground concentrations for K, U and Th are multiplied by the factors 1.505, 0.625 and 0.31 respectively as indicated in Table VI. The values obtained were added together and the total exposure rate due to the natural radioelements is thus obtained.

In order to find the dose rate expressed in μ Sv/h, the exposure rate is divided by 100 and multiplied by 0.6 as indicated by equation (3).

9. MAP CONTOURING

The values of exposure rate and dose rate were gridded with grid cell size equal 500 m using the Geosoft software. Values were smoothed using two passes of Hanning filter in order to get rid of noisy values which due to bad topography or difficulty in maintaining the same aircraft altitude or due to equipment noise or other sources of errors. The exposure rate reached a value as high as 46 μ R/h in El-Hasa area where there are Phosphate mines and dose rate equivalent to 0.276 μ Sv/h, these values are corresponding to 380 mR/y and 2.3 mSv/y, see exposure rate and dose rate map for Jordan.

10. MAP ANALYSIS

In spite of that the map represent the contribution of the three natural radioelements all together but it reflects the surface geology of Jordan where the phosphate deposition is very well delineated by the high radiation contours in the central part of Jordan. Jordan phosphate contain about 200 ppm of uranium with practically no thorium and very low content of potassium and covers almost the whole the eastern high plateau of Jordan. In eastern Jordan parallel to Saudi Arabia borders, the exposure radiation map does not show good indication of the phosphorite occurrence in this region because the phosphate has low uranium content in this region. In northern Jordan, the phosphate deposition is very well indicated by the radiation exposure map, while in the far north east of Jordan the exposure map is less indicative of phosphate occurrence in this region, this because the recent sedimentation covers the phosphorite units and prevent gamma radiation from escaping into the space and therefore less detection by airborne radiometric survey, also the exposure rate map Fig. 9 shows medium two high radiation areas, one at the eastern coast of the Dead Sea, this because of Main and Zara hot springs which is caused by radon emanation carried by underground circulating waters through different rock types.

The other one in southern Jordan between Quweira and Mudawwara villages at Dubeidib area. This area proved the existence of high concentration of thorium in the Ordovician sandstones which reach about 2000 ppm in some locations associated with a medium to high concentrations of uranium (100 to 500) ppm in a metamicts state.

Comparing Fig 9 with Fig 6, good match is noticed between the two maps, which means high concentration in one of the three radioelements leads to the contribution of high radiation exposure to the environment of results

11 DISCUSSION OF RESULTS

Jordan shows high radiation exposure in its central part of Jordan where the phosphate deposition occur. Most of Jordan phosphates are covered by recent sedimentations, such as oil shale and chalky marl depositions of Upper Cretaceous age their thicknesses reach about 15 to 20 metres in some locations. The detected radiation by airborne survey are only those which outcropping in some places or uncovered by phosphate mining. The level of radiations already high despite the fact that the survey lines were separated of 2 km from each other which might lead not passing over the Phosphate Mines or missing many of open casts of Phosphate Mines in the phosphate mining area and also without taking into considerations the effect of radiation caused by cosmic rays or caused by internal radiation as discussed early in this report. Off the total of 343 894 measurements were taken by airborne survey, there are about 500 readings exceeding $20 \mu\text{R/h}$ and about 13 300 measurements exceeding the value 10 and there are several readings as much high as $45 \mu\text{R/h}$, all these readings are found in the vicinity or around the Phosphate Mines.

Comparing these results to those obtained in some other countries such as the United States, Germany, Poland, Italy, etc (see Fig 10, the exposure rate in Jordan is higher than those of other countries).

12 CONCLUSION AND RECOMMENDATIONS

Airborne radiometric survey proved to be a very good tool in estimating the ground level exposure rate easily and with an accepted accuracy especially after the creation of very voluminous sodium iodide crystals and the establishment of the calibration concrete pads and with the continuous improvements of signal to noise electronic devices. The airborne radiometric survey is very representative to the area under studying because of the enormous amount of data that cover a wide area. As it is shown previously Jordan has high background radiation. This high background radiation is related to the effect that a vast areas of Jordan high plateau are covered by phosphate deposition which has about 150 ppm in average of uranium. The maximum value of uranium concentration registered in phosphates unit according to Abu Ajamieh (1974) was 275 ppm. Recently in the areas surrounding the Phosphate belt, new investigations proved the existence of high uranium concentration of about 1000 ppm in the recent sedimentations of chalky marl type that overlie the phosphorous and oil shale layers, according to the exposure rate map shows an average exposure rate value of about $20 \mu\text{R/h}$ in Phosphate belt and the surrounding areas, this corresponds to a dose equivalent of about $0.12 \mu\text{Sv/h}$ or about 1 mSv/y . This value does not consider the area of open mines after uncovering the overlying sedimentations where the thickness of these overlying layers have a thickness of about 30 metres in some locations. Now if we imagine that the whole phosphate belt is outcropping as the case of open cast mines, simple calculations lead us to the conclusion that an extending superficial of Phosphate area with a concentration in uranium of 150 PPM of uranium will contribute an exposure rate to the environment, and according to the table no (6), of about $97 \mu\text{R/h}$ neglecting the contributions coming from other radioelements which will be very low because Jordan Phosphate has low concentrations in thorium and potassium. The $97 \mu\text{R/h}$ corresponds to a dose rate of about 5 mSv/y . This figure without doubt is detrimental to human being. If we return back to the figure $20 \mu\text{R/h}$, this figure is neglecting any other contributions coming from cosmic rays which is expected to be high because of dry weather in Jordan which permits to the cosmic rays to penetrate the atmospheric cover with less attenuation, or because of the inhalation of the radon gas during breathing (especially the dry climate help radon gas to be emanated and collided to the dust particulates which are abundant in dry countries) or taking any kind of radioactive elements contained with food or water. Comparing the value of $20 \mu\text{R/h}$ to those obtained from other countries such that the United

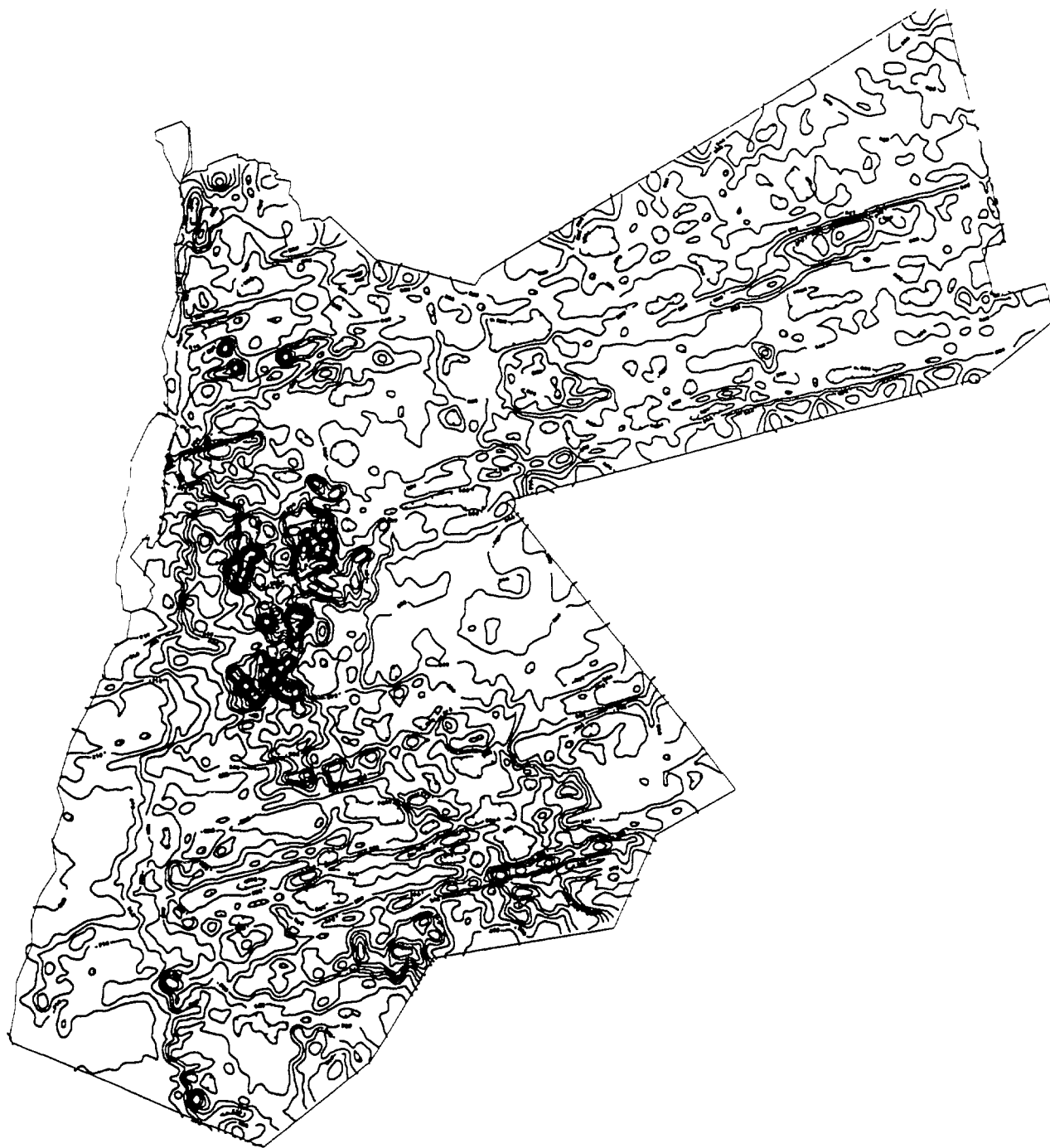


FIG. 9. Radiation exposure rate map of Jordan. Scale 1:2 500 000. MINISTRY OF ENERGY AND MINERAL RESOURCES, Nuclear Energy Directorate, Natural Radiation Exposure Rate Map, Jordan, Radiation Unit: $\mu\text{R/h}$, Contour Interval 1 $\mu\text{R/h}$.

States, Germany, Italy, Canada, etc. (see Fig. 10). Jordan shows higher radiations than all other countries.

This study illustrated the following to be recommended:

- More detailed studies should be presumed in Jordan so as to determine the radiation exposure rates originating from the external and internal resources.

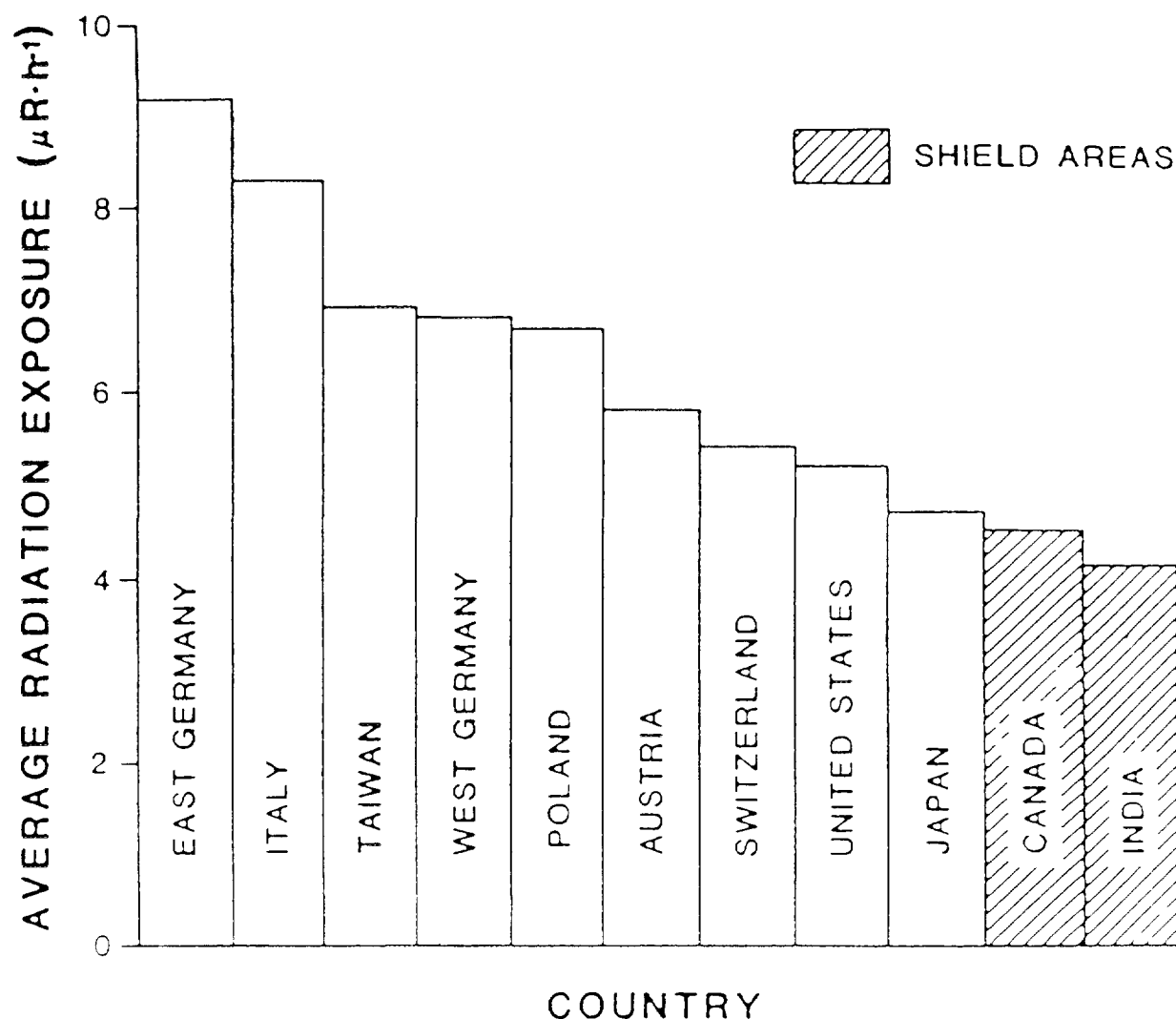


FIG 10 Outdoor exposure rates for some countries

- The radiations from every individual natural radioelement should be calculated separately in order to make better estimation to the radiations originated from the uranium which is the primary responsible of high background radiation in Jordan and more care should be paid to the ratios between the three different radioelements because these ratios are good control of the reliability of the data
- Radiological risks studies should be made on those people who are residing in the Phosphate belt which extends over a vast area in Jordan and detailed studies should be done on those people who are working in Phosphate Mines

ACKNOWLEDGEMENTS

I am particularly grateful to thank the Director of the Nuclear Energy Director of the Ministry of Energy and Mineral Resources of Jordan for his fruitful suggestions and help I am also grateful to thank the following for their great help Geophysicist Abdulrahman Abu El-Adas, Geophysicist Hami Akrabawi, Geophysics Eng Wajdi El-Tamimi

BIBLIOGRAPHY

ABDULKADER M. ABED, Geology of Jordan (1982).

BENDER, F. et al., "Geology of Jordan" Berlin, Gebrüder Borntraeger (translated by M. K. Khdeir, D.H. Parker, and U. Wilkening), (1969).

BURDON, D.J., Handbook Of the Geology Of Jordan (1959).

GRASTY, R.L., CARSON, C.M., CHARBONNEAU, B.W., HOLMAN, P.B., Natural Background Radiation in Canada, Bulletin 360 (1980).

INTERNATIONAL ATOMIC ENERGY AGENCY, Construction and Use of Calibration Facilities for Radiometric Field Equipment, Technical Report Series No. 309, Vienna (1989).

INTERNATIONAL ATOMIC ENERGY AGENCY, Gamma Ray Surveys in Uranium Exploration, Technical Reports Series No. 186, Vienna (1979).

MOHAMMAD ABU AJAMIEH, Uranium Reserves in Jordan (1974).

PHOENIX CORPORATION, A comprehensive Airborne Magnetic/Radiation Survey of the Hashemite Kingdom of Jordan (1980).

APPENDIX 1.

Algorithm of Calculations

A) Normalize all recorded radiometric channel data to 1 second sampling interval.

$$TC_n = TC_r \times 1 / L_T$$

$$K_n = K_r \times 1 / L_T$$

$$U_n = U_r \times 1 / L_T$$

$$Th_n = Th_r \times 1 / L_T$$

L_T - recorded live time in milliseconds

Subscript "r" refers to raw recorded data

Subscript "n" refers to normalized data

B) Reduce terrain clearance to the effective value at zero Celsius degree

$$\Delta H2 = H \times 273 / (T + 273) - H_p$$

$$\Delta H1 = H \times 293 / (T + 273) - H_p$$

where $\Delta H1$ = departure from planned survey height, H_p corrected to 20 Celsius degrees for correcting of U/Th stripping ratio,

$\Delta H2$ = departure from planned survey height, H_p corrected to 20 celsius degrees for attenuation corrections.

H = terrain clearance in feet or meters

T = ambient temperature in celsius degrees

H_p = planned survey height.

C) Correction for Background

$$TC_b = TC_n - B_{TC}$$

$$K_b = K_n - B_k$$

$$U_b = U_n - B_u$$

$$Th_b = Th_n - B_{th}$$

B_{TC} , B_k , B_u , B_{th} -background values for TC,K,U,Th

Subscript "b" refers to background corrected data

Subscript "n" refers to normalized data

The background value at any time is linearly interpolated between known background corrected segments.

D) Altitude correction of stripping coefficients

Geoterrex practice has been to correct one stripping coefficient, $ALPHA(\alpha)$, for latitude following the technique outlined by Grasty.

$$ALPHA_H = ALPHA + 0.0373 + 0.000076 \times \Delta H1$$

$ALPHA$ - Th into U stripping ratio at ground level

$ALPHA_H$ - Height corrected $ALPHA$

0.0373 and 0.000076 -constants theoretically determined by the Geological Survey of Canada.

E) Spectral Stripping

$$U_s = (U_b - \text{ALPHA} \times Th_b) / (1 - a \times \text{ALPHA})$$

$$Th_s = (Th_b - a \times U_b) / (1 - a \times \text{ALPHA})$$

$$K_s = K_b - \gamma \times U_s - \beta \times Th_s$$

$$TC_s = TC_b$$

Subscript "b" refers to background corrected data

Subscript "s" refers to stripped data

a = U into Th backstripping ratio

β = Th into K stripping ratio

γ = U into K stripping ratio

F) Altitude Correction of the Data

$$TC_a = TC_s \times e^{(\mu_{TC} \times \Delta H_2)}$$

$$K_a = K_s \times e^{(\mu_K \times \Delta H_2)}$$

$$U_a = U_s \times e^{(\mu_U \times \Delta H_2)}$$

$$Th_a = Th_s \times e^{(\mu_{Th} \times \Delta H_2)}$$

where μ_{TC} , μ_K , μ_U , μ_{Th} are total count, Potassium, Uranium and Thorium attenuation coefficients

Subscript "s" refers to stripped data.

Subscript "a" refers to attenuated data.

The data submitted by Phoenix Corporation To Natural Resources Authority were not reduced to indicate %K, ppm U and ppm Th, but were compiled in counts per second(cps) response. The ratios of U/Th, U/K and Th/K were computed.

**NEXT PAGE(S)
left BLANK**



RADIOMETRIC MAPS OF ISRAEL — PARTIAL CONTRIBUTION TO THE UNDERSTANDING OF POTENTIAL RADON EMANATIONS

U. VULKAN
Soreq Nuclear Research Centre,
Yavne

M. SHIRAV
Geological Survey of Israel,
Jerusalem
Israel

Abstract

An airborne radiometric survey over parts of Israel was carried out in 1981. The system was comprised from 10 NaI 4" × 4" × 16" detectors, arranged in 4, 4 and 2 sensors, with total volume of 1560 inch³, and one 4" × 4" × 16" uplooking NaI detector. All the data, including 2 full spectra (0–3 MeV), air temperature and pressure, time and altitude, were recorded by GAM-2001 (Scintrex) on tapes. Ground projections of the flight lines were obtained by video recording using Panasonic wide angle camera and VTR. Synchronized fiducial markings were generated at 1 sec⁻¹ frequency at both the radiometric data and video tapes. Flight nominal height was 400 feet, line distances were 1 km and line tie every 20 km. Data analysis took place using the eU, eTh and K region of interest, the data was corrected for cosmic radiation, Rn in the air, background and altitude, stripped and the terrestrial concentration of eU, eTh and K were calculated [1]. The radiometric concentrations were smoothed using 1/4; 1/2; 1/4 3 points moving average and every point was checked for statistical acceptance. The radiometric data was calculated on a grid using the minimum curvature method with SURFER for Windows (version 6) and presented on the maps using the 0, 25, 50, 75, 90, 95 and 100 percentiles. Statistical radiometric signature of all exposed rock formations was accomplished using a GIS system. It was found that the Mount Scopus Group (of Senonian origin) is the main source for high uranium — phosphoritic rocks of this group contain up to 150 ppm U. Comparing the eU radiometric map with a map of potential radon emanation from rock units [2], reveals a fair correlation — high radon emanations usually follow the distribution of the Mount Scopus Group in Israel. The correlation between the two maps is excellent over arid terrain where soil cover is missing, whereas over semi-arid — humid areas (western and northern Israel), where soil and cultivation covers are developed, the eU levels over Mount Scopus Group's outcrops are much lower due to absorption of the radiation, and do not depict the full radon potential. Detailed mapping of radon hazards usually exhibit poor correlation between airborne eU data and direct pore radon measurements, even in arid terrain. This phenomenon is attributed to the fact that a radon "source rock" (e.g. phosphorite) could be covered with a few up to some tenths of meters of uranium-barren rock. About 0.5 meter cover is enough to absorb all radiation, causing very low airborne eU readings, while the radon free way in this rock is about 10 meters, yielding high pore radon levels when directly measured.

1. THE RADIOMETRIC SURVEY

An airborne radiometric survey over parts of Israel was carried out in 1981. The system was comprised of 10 NaI(Tl) 4" × 4" × 16" detectors (4 π), arranged in 4, 4 and 2 sensors, with total volume of 40 liters, and one 4" × 4" × 16" uplooking NaI(Tl) detector with 4 liters volume (2 π). All the data, including 2 full spectra (0–3 MeV), air temperature and pressure, time and altitude, were recorded by GAM-2001 (Scintrex) on tapes. Ground projections of the flight lines were obtained by video recording using Panasonic wide angle camera and VTR. Synchronized fiducial marks were generated at 1 sec⁻¹ frequency at both the radiometric data and video tapes. The flight was carried out using a Piper Navajo Chieftain on nominal height of 400 feet. Line spacing was 1 km and line tie was done every 20 km.

Calibration of the airborne system was done using calibration pads, specially built near the Soreq Nuclear Research Center. Background and cosmic rays contribution was calibrated by high altitude flights over the Mediterranean sea. Details of the calibration and fluctuation analysis for the airborne system can be found in Aviv and Vulkan [1].

Data analysis took place using the eU, eTh and K region of interest. Table I shows the windows for the Region of Interest in keV.

TABLE I. THE WINDOWS SETTING

Name of region	Isotope	Photopeak Energy (MeV)	Energy interval (KeV)	Energy width (keV)
Total count (4π)			398 – 2984	2586
K (4π)	^{40}K	1.461	1357 – 1569	211
U (4π)	^{214}Bi	1.764	1661 – 1860	199
Th (4π)	^{208}Tl	2.615	2410 – 2820	410
Total count (2π)			1661 – 2984	1323
U (2π)	^{214}Bi	1.764	1661– 1860	199
Th (2π)	^{208}Tl	2.615	2410 – 2820	410

The data was corrected in this order:

1. Background and cosmic radiation subtraction.
2. Radon in the air subtraction.
3. Stripping of the mutual contribution the elements.
4. Altitude correction, taking into account the air temperature and pressure.
5. Terrestrial concentration of eU, eTh and K calculation [1].
6. Statistical test for "acceptance/not acceptance" detection level, based on net count being higher than 1.5 the square root of the background (raw counts — net counts).

The radiometric concentrations were smoothed using 1/4; 1/2; 1/4 3 points moving average, to exclude irregularity of data points. The radiometric data was calculated on a grid using the minimum curvature method with SURFER for Windows (version 6) and presented on the maps using the 0, 25, 50, 75, 90, 95, and 100 percentiles [3].

2. GEOLOGICAL SETTING

The outcropping rock sequence in Israel is built mainly of sedimentary rocks, ranging from Paleozoic sandstones up to recent soils. Precambrian igneous and metamorphic rocks can be found only in the southern part, at the vicinity of the Gulf of Eilat. Young basalts are covering quite large areas in the northern part of Israel. The prominent rock formations that cover over 70% of the area belong to three groups:

Judea Group: The Judea Group is built of Cenomanian carbonate rocks — limestones, dolomites, chalks and marls — usually without any clastic components. As a result of magmatic activity during the Cenomanian, some tuffs and basalts can be found in the Mount Carmel area.

Mount Scopus

Group: The Senonian-Paleocene Mount Scopus Group is characterized by a wide transgression of a nutrient-rich sea which deposited chalks with a high content of phosphate. Under shallow conditions, a sequence of alternating chalks and cherts was

deposited, in many places including economic phosphorite layers. The Mount Scopus Group is divided into three formations (described from bottom to top):

- Menuha Formation* — massive chalk, usually covered by a caliche crust;
- Mishash Formation* — alternating chalks, cherts and phosphorites. The Mishash Formation attains its maximal thickness in synclinal basins in the northern Negev, where the economic phosphorite layers are most developed and utilized for the fertilizers industry. The P_2O_5 content in these layers is usually 24–35 %;
- Ghareb Formation* — chalk, marly chalk and marl; a metamorphosed analogue of this formation is the Hatrurim Fm.

Avedat

Group: Comprised of a thick sequence of chalks, limestones and marls of Eocene time, with chert lenses in some places.

Since the Mount Scopus Group contains high content of phosphate with appreciable amounts of uranium (90–150 ppm [4]), this group's outcrop was a target for a more detailed study concerning radon emanations.

3. CONSTRUCTING A RADON "RISK" MAP

As part of the on-going effort of producing baseline data maps for Israel, a map of potential radon emanation from rock units was accomplished by the Soreq Nuclear Research Center and the Geological Survey of Israel. The map (on a 1:500 000 scale) is based on direct measurements of radon within the rock/soil pore space, coupled with the known local stratigraphy and sub-surface geology [2].

A modified alpha-track detection system was implemented for direct measurements of radon in soil/rock pore gas, as described in [5 and 6]. The instrumental assemblage is installed in a PVC pipe which makes it easy and convenient to insert the system in shallow (~ 50 cm) drillholes. The measurements were conducted in 70 sites, representing all outcropping rock formations in Israel. In each site, 15 to 35 films were buried, usually on a 20 × 20 m grid, for up to 28 days (according to the expected radon level). After removal, the foils were electrochemically etched and track densities measured. Calibration of the track density versus absolute activity was accomplished by a special designed calibration cell with a known radon source.

Nearly all stratigraphic units which were studied exhibit low average radon levels (3,000–8000 Bq/m³). On the other hand, the Mount Scopus Group yielded high average radon levels (10 000 –140 000 Bq/m³), with the Mishash Formation showing very high levels (up to 300 000 Bq/m³) due to its high phosphorite content.

The outcropping rock units were divided into three categories and accordingly mapped:

Category III — high radon

average ²²²Rn concentrations higher than 50 000 Bq/m³. This category includes the Mishash Formation in the Judea Desert and southern Israel, where phosphate-rich layers are mostly developed. It was observed that a chalky overburden of up to 20 m above a phosphorite layer yields radon concentrations which fall into this category. Hence, the relevant areas were mapped accordingly.

Category II — moderate radon

average radon concentrations between 10 000 to 50 000 Bq/m³ are attributed to the Mount Scopus Group in central and northern Israel, Menuha and Ghareb Formations in southern

Israel. Areas in which a thin layer of alluvial material or soil cover rocks of the Mount Scopus Group were classified into this category.

Category I — low radon

average radon concentrations lower than 10 000 Bq/m³. This category includes all other rock units and alluvial soils.

The area along the Dead Sea Rift was separately mapped due to high radon emanations from sediments [7] and water sources in the area [8], and the presence of alluvial fans of large wadis (ephemeral streams) which drain outcrops of phosphate-rich Mount Scopus Group rocks.

4. COMPARISON BETWEEN THE RADIOMETRIC AND RADON MAPS

Statistical radiometric signature of all exposed rock formations was accomplished using the data gathered during the radiometric survey and the GIS system of the Geological Survey of Israel, in which all exposed rock units are coded. It was found that the Mount Scopus Group is the main source for high uranium — the average eU levels ranges between 5–10 ppm for this group, while for other rock units the range is 1.3–4 ppm (Fig. 1). Based on these data, a "cut-off" value of 4 ppm was used for a comparison between the radiometric and radon maps.

Comparing parts of the eU radiometric map with that of potential radon emanation from rock units (both on a regional scale of 1:500 000), reveals a fair correlation. The radiometric map in Fig. 2 represents data above 4 ppm eU which usually follow the distribution of the Mount Scopus Group in Israel, depicting the outline of the radon map which is based on the known geology of the region. The correlation between the two maps is high over arid terrain where soil cover is missing, whereas over semi arid — humid areas (western and northern Israel), where soil and cultivation covers are developed, the eU levels over Mount Scopus Group's outcrops are much lower due to absorption of the radiation, and do not depict the full radon potential.

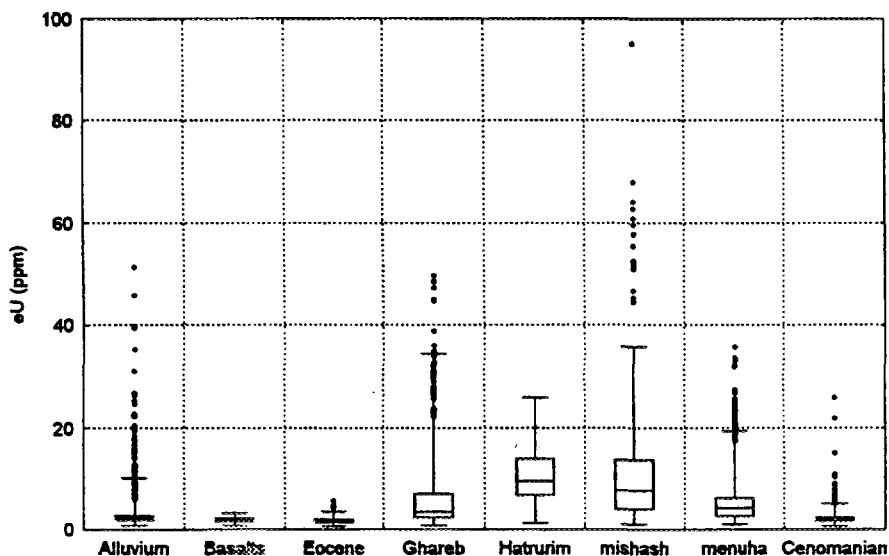


FIG. 1. Box plots indicating eU concentrations in main rock formations in Israel. The horizontal spread of each box represents 50% of the data, between the 25th and 75th percentiles; the vertical line in each box is the median. Horizontal lines extending from the boxes are bound at the 1st and 99th percentiles. Dots are extremes.

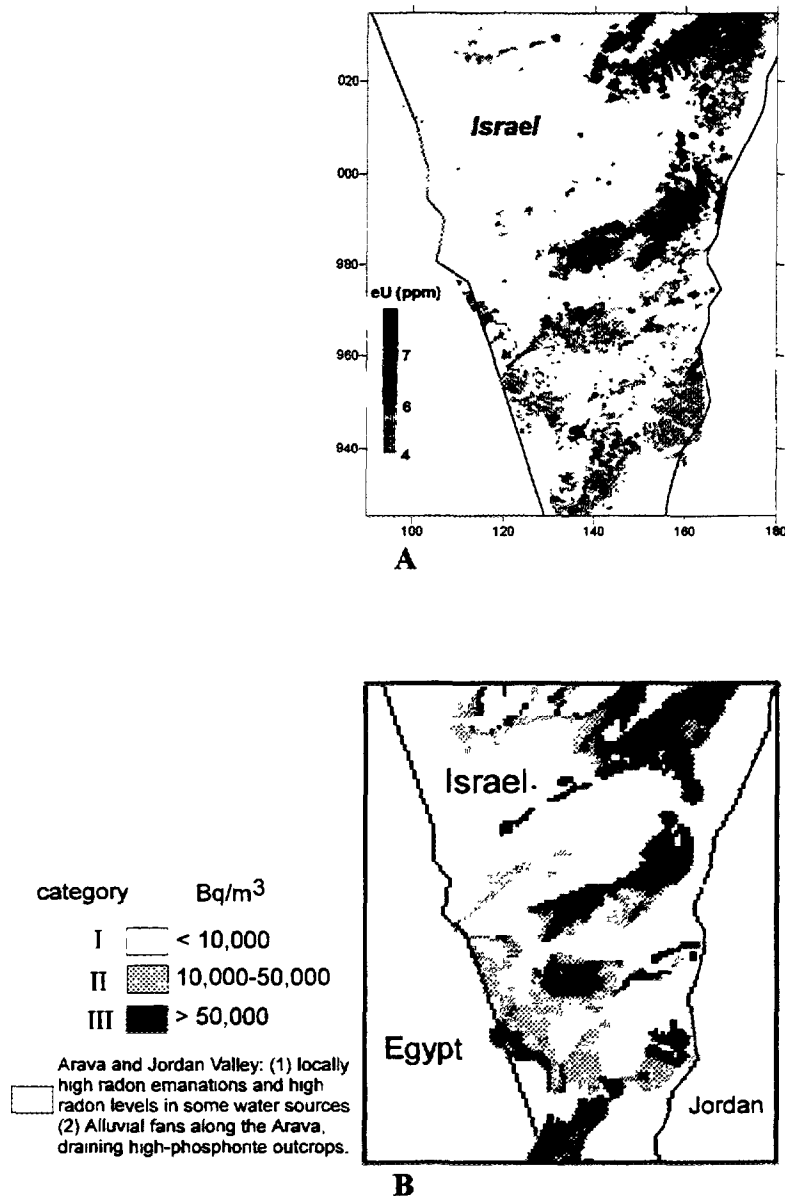


FIG. 2. Comparison between eU radiometric map (A) and a radon map (B) over part of the Negev Desert, Israel. The original scale is 1:500 000.

Detailed mapping of radon hazards usually exhibit poor correlation between airborne eU data and direct pore radon measurements, even in arid terrain. This phenomenon is attributed to the fact that a radon "source rock" (e.g. phosphorite) could be covered with a few up to some tenths of meters of uranium-barren rock. About 0.5 meter cover is enough to absorb all radiation, causing very low airborne eU readings, while the radon free way in this rock is about 10 meters, yielding high pore radon levels when directly measured. The example displayed in Fig. 3 is taken from the vicinity of the town of Arad, northern Negev Desert. A detailed radon mapping for this area was carried out by Vulkan and others [9], based on numerous radon measurements and geological mapping in a 1:20 000 scale (Fig. 3A). The eU radiometric map for the same area (Fig. 3B), can only partly be correlated with the radon map, due, as mentioned, to local geological considerations (overburden above an uranium source) and the resolution between rock units which can not be achieved in a radiometric survey, compared with a very detailed geological map.

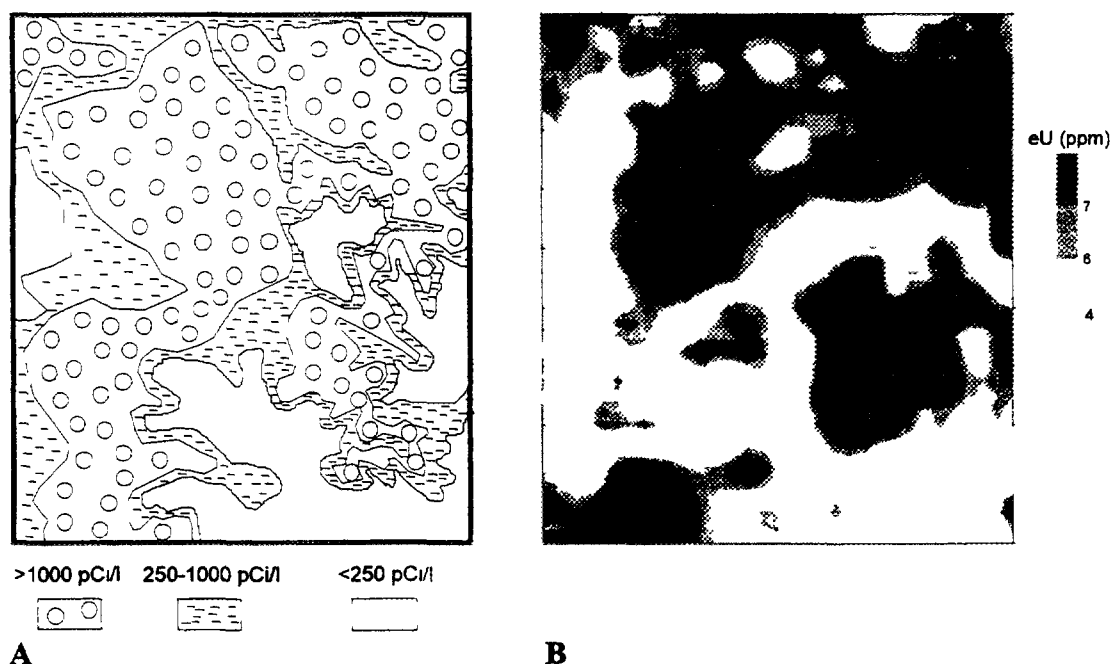


FIG. 3 Comparison between a detailed radon mapping in the vicinity of Arad, northern Negev Desert, Israel (A), and a radiometric map of the same area (B). The covered area is 8×9 km and the original mapping scale is 1:20 000.

REFERENCES

- [1] AVIV, R., VULKAN, U., Airborne gamma ray survey over Israel: the methodology of the calibration of the airborne system. SNRC Rep. ZD/58/82 (1983).
- [2] SHIRAV (SCHWARTZ,) M., VULKAN, U., ROSENSAFT, M., Map of Radon Emanation from Rock Units in Israel (1:500 000) (1993).
- [3] VULKAN, U., SHIRAV, M., AVIV, R., BAER, G., ITAMAR, A., LOUIS, S., Airborne radiometric map of Israel — eU concentrations, SNRC Rep. ZD/182/95 (1995).
- [4] NATHAN, Y., SHILONI, Y., RODED, R., GAL, I., DEUTCH, Y., The geochemistry of the northern and central Negev phosphorites, Geol. Survey of Israel Bull. No. 73 (1979) 41p.
- [5] STRULL, A., EVEN, O., ASSAEL, Y., ZAFRIR, H., New application of radon measurement by alpha-track technique over barren country rocks. Tran. Nuclear Soc. Israel Ann. Meeting 1986 (1986) pp 134–138
- [6] VULKAN, U., STEINITZ, G., STRULL, A., ZAFRIR, H., Long distance (+ 100 m) transport of radon in syenitic rocks at Makhtesh Ramon, Israel. Nucl. Geophys. 6:261–271 (1992).
- [7] STEINITZ, G., VULKAN, U., LANG, B., GILAT, A., ZAFRIR, H., Radon emanation along border faults of the rift in the Dead Sea area. Israel J. of Earth Sci. 41:9–22 (1992).
- [8] MAZOR, E., Radon and radium content of some Israeli water sources and a hypothesis on underground reservoirs of brines, oils and gases in the Rift Valley, Geochim. Cosmochim. Acta 26:765–786 (1962).
- [9] VULKAN, U., SHILONI, Y., GILAT, A., ZAFRIR, H., Radon levels in rocks in the vicinity of Arad — principles and mapping. Geol. Surv. of Israel Rep. No. GSI/36/91 (1991) 33 p (in Hebrew)



DISTRIBUTION OF NATURAL (U, Th AND K) AND ARTIFICIAL (CS-137) RADIOELEMENTS IN THE FLOOD PLAIN DEPOSITS OF NORTHERN HUNGARY

L. ÓDOR, I. HORVÁTH, U. FÜGEDI

Geological Institute of Hungary,
Hungarian Geological Survey

J. RENNER

Eötvös Loránd Geophysical Institute of Hungary

Budapest, Hungary

Abstract

Low density geochemical survey has been conducted in Hungary based on the flood-plain sediments of large catchment basins in order to establish regional baseline values for 30 elements including environmentally important ones like As, Hg, Cd, Pb, Zn, Cu and Cr. The geochemical background and the present state of the environment are characterised respectively by the use of the lower (50–60 cm) and upper (0–10 cm) samples of the flood-plain profiles. In addition to the determination of minor elements by ICP and AAS methods natural and artificial radioelements have also been determined in the laboratory in the samples coming from northern Hungary. Highly reliable background values of U, Th and K have also been established due to the use of naturally averaged fine-grained sediments. The individual values and the spatial distribution of radioelement Cs-137 can be used for monitoring purposes. These laboratory measurements have been made in a low-background lead shield using a high purity germanium semiconductor detector. A car-borne radioactive gamma spectra measuring system has also been established for monitoring in field circumstances.

1. INTRODUCTION

The Hungarian Geological Survey and the Eötvös Loránd Geophysical Institute of Hungary are working jointly on a large number of scientific programs. One of these is the National Geochemical Mapping project managed by the scientists of the Geochemical Department of the Hungarian Geological Survey and the Radiometric Department of the Geophysical Institute.

Geochemical surveys covering the whole country have not been conducted before in Hungary. The first low-density geochemical survey was carried out following the proposals and recommendations of both the IGCP International Geochemical Mapping project and the Western European Geological Surveys (WEGS). The aims of the project were to establish abundance data and background values and to determine the regional distribution patterns of elements for follow-up environmental studies. So it was reasonable to use the samples of this nation-wide survey to determine the natural and artificial radioelement contents of flood-plain deposits. The radioelement content has so far been determined only for the northern part of Hungary.

2. SAMPLING AND ANALYTICAL METHODS

Flood-plain and overbank deposits of large to medium sized drainage basins have been suggested as sampling media for low to reconnaissance scale geochemical surveys [1, 2, 3 and 4]. Regarding the geographic situation of Hungary, it is clear that in lowland areas individual catchment basins can not be delineated so the whole country can not be covered by this survey (Fig. 1). In regions with well-developed drainage systems the average size of sampled catchment basins, or "cells", is 400 km². 196 drainage basins have altogether been sampled. Two samples were collected at each sampling site not far from the active channel: one from 0–10 cm and another one from 50–60 cm depths. The composition of the latter is presumably close to that of the weathering products of pre-industrial times. The material of the upper 10 cm of the profile is expected to reflect the effects of human activity.

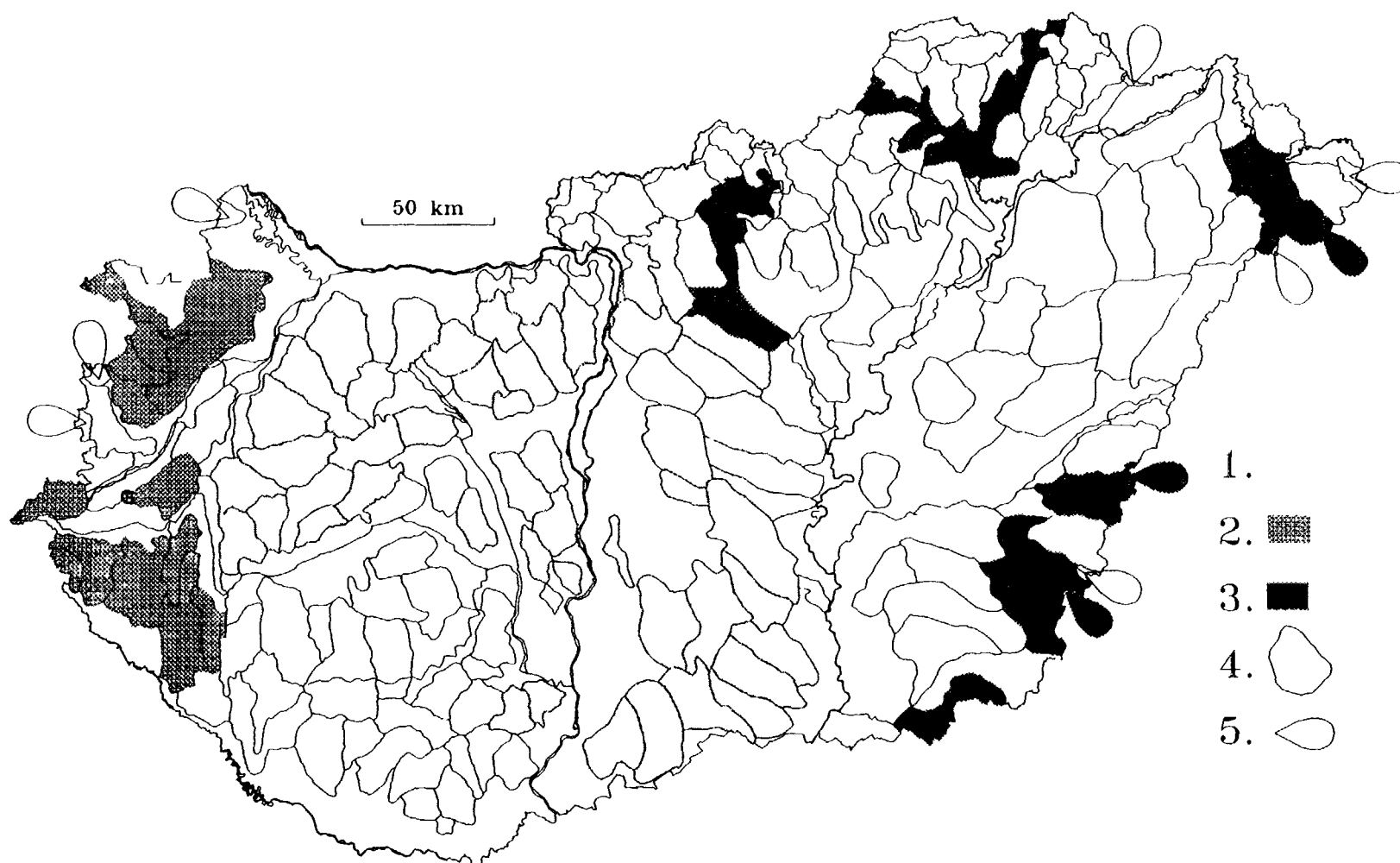


FIG. 1. Element associations in the flood-plain sediments of Hungary. 1) Ca - Mg - Sr - LOI, 2) Co - Cr - Ni - Fe, 3) Ag - As - Au - Cd - Cu - Hg - Pb - Zn, 4) catchment basins, 5) sources outside Hungary.

The samples were analysed by ICP and AAS techniques in two laboratories using different dissolution techniques (nitric acid leaching and aqua regia treatment). The samples collected in the north-eastern part of Hungary were submitted to radiometric analysis. (49 catchment basins were altogether represented by 22 individual and 67 subsamples). This have been achieved on a CANBERRA measuring system equipped with a liquid nitrogen cooled high purity Ge semiconductor detector. The energy resolution of it is 2,0 keV (measured on the 1330 keV line of Co-60). The detector is placed in a low background chamber. From 300 g to 1000 g of samples have been weighted in a special vessel which is covering the detector completely. While the radioactivity of the samples is very low, the characteristic measuring time was 60 000–80 000s.

The calibration and the calculation were carried out by means of 10 samples with well-known U, Th and K contents. In the case of U and Th the equivalent concentrations have been calculated. In case of Cs-137 the intensity values in nGy/h have been determined and mapped. We use SAMPO-90, the well known gamma spectrum analysis program for the quantitative evaluation of the above mentioned components.

3. STATISTICAL PARAMETERS

Medians were used to estimate expected values and anomalies were separated from background by the use of the frequency distributions and boxplot diagrams of the elements. Values of the geochemical background and the threshold have been determined for 25 elements in the low-density nation-wide survey [5] Table I shows the main parameters for some of the elements determined in the upper layer of flood-plain sediments.

TABLE I. MEDIAN AND MAX. VALUES FOR SOME OF THE ELEMENTS DETERMINED IN THE UPPER (0–10 CM) LEVEL OF FLOOD-PLAIN SEDIMENTS IN HUNGARY (Leached amounts in ppm)

Element	Median	Max. value
As	7.2	230
Cd	<0.5	12.8
Co	8.9	17.8
Cr	19.7	473
Cu	19.2	400
Hg	0.08	1.11
K (%)	1.78	5.48
Ni	21.2	58
Pb	16.9	286
Zn	63.3	2160

Medians and max. values for some of the elements determined in the upper (0–10 cm) level of flood-plain sediments in Hungary (leached amounts in ppm)

The following elements have been analysed by radiometric method: eU, eTh, K and Cs-137. Geochemical parameters are given in Table II.

TABLE II. MEDIANS AND MAX. VALUES FOR THE NATURAL AND ARTIFICIAL RADIOELEMENTS IN THE FLOOD-PLAIN SEDIMENTS OF NORTHERN HUNGARY (Sampling interval: u = upper level, 0–10 cm, l = lower level, 50–60 cm)

Element	Median	Max. value
eU (ppm) (u)	1.65	4.9
eTh (ppm) (u)	14.7	20.4
K (%) (u)	1.39	1.97
Cs-137 (nGy/h) (u) (u)		4.26
Cs-137 (nGy/h) (l) (l)		1.82

Medians and max. values for the natural and artificial radioelements in the flood-plain sediments of Northern Hungary. (Sampling interval: u = upper level, 0–10 cm, l = lower level, 50–60 cm).

For comparison previously established U and Th values are given in Table III for this part of Hungary, based on air-borne gamma spectrometric measurements [6].

TABLE III. U AND TH MEAN VALUES (PPM) FOR DIFFERENT FORMATIONS OF NORTHERN HUNGARY [5]

Formations	U	Th
Paleozoic	4.1	9.9
Mezozoic	4.5	12.0
Cenozoic	3.9	10.2

U and Th mean values for the different formations of northern Hungary [5].

4. DISTRIBUTION OF ELEMENTS

4.1. Distribution of minor elements and element associations

Based on the results of factor analysis the following element associations could be distinguished in the country-wide survey (Fig. 1.).

- Co–Cr–Fe–Ni — showing the effect of accumulation and leaching processes.
- Ca–Mg–Sr–LOI — this group contains the characteristic components of carbonate minerals. The anomalies of this association outline a large area in the middle of the country reflecting the presence of calcareous soils.
- Ag–As–Au–Cd–Hg–Pb–(Cu–Zn) — these are the characteristic elements of low to medium temperature hydrothermal ore processes. Most of the extreme values are found in the flood-plain deposits of the rivers entering from Transylvania. The effect of mining and ore processing can be clearly seen in the deeper horizons of these profiles too. The samples collected from the flood-plains of the rivers Zagyva, Sajó and Hernád (Northern Hungary) contain both the traces of ore material coming from Slovakia and the pollution products of heavy industry in the region.

4.2. The distribution of radioelements

The distribution of radioelements is shown on Figs 2, 3 and 4. The main aim of these maps is to give geochemical baseline information for regional studies. The flood-plain sediments as

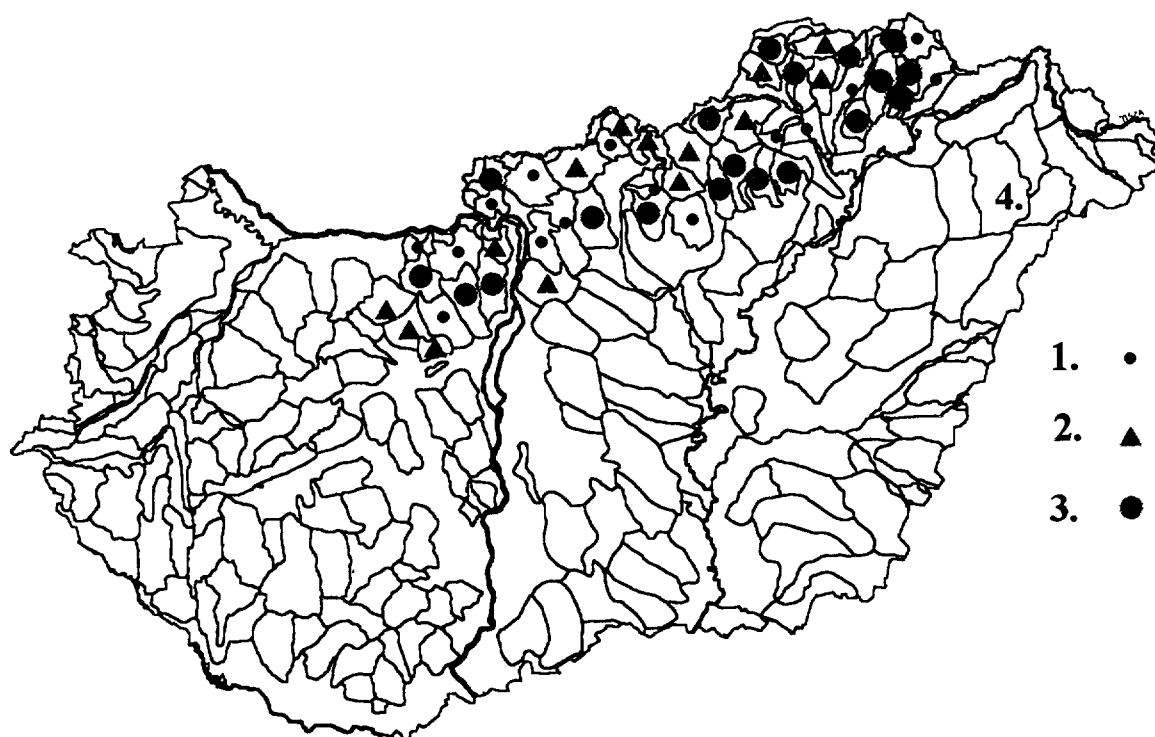


FIG. 2. Distribution of eU (ppm) in the flood-plain sediments of Hungary. (Sampling interval: 0–10 cm). 1) <1.4, 2) 1.4–2.0, 3) >2.0, 4) catchment basins.

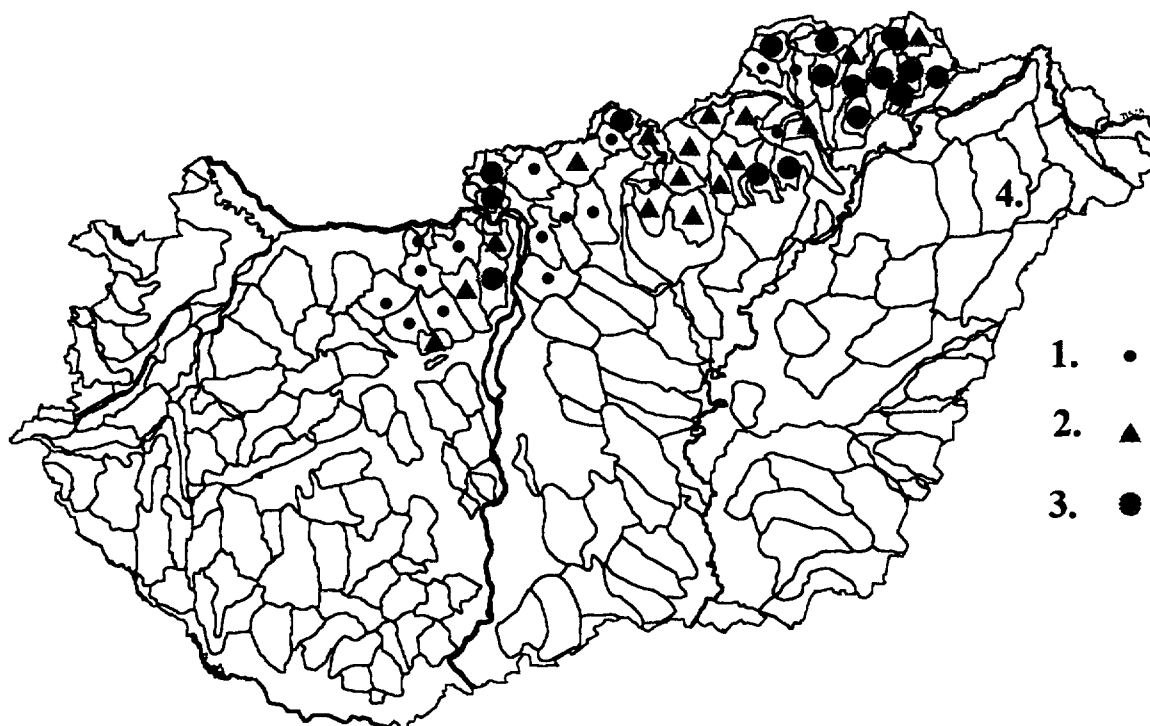


FIG. 3. Distribution of eTh (ppm) in the flood-plain sediments of Hungary. (Sampling interval: 0–10 cm). 1) <13.6, 2) 13.6–16.9, 3) >16.9, 4) catchment basins.

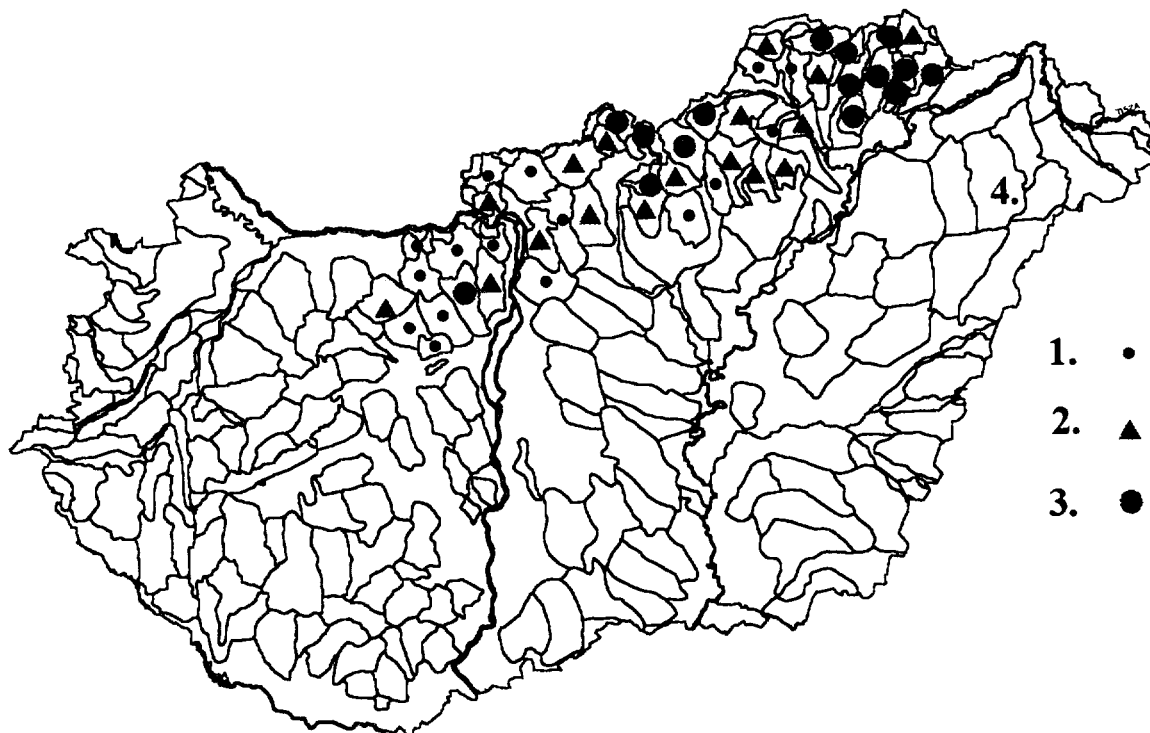


FIG. 4. Distribution of K (%) in the flood-plain sediments of Hungary. (Sampling interval: 0–10 cm), 1) <1.25, 2) 1.25–1.55, 3) >1.55, 4) catchment basins.

sampling media are highly reliable because of the mixing and averaging of the surface formations by natural processes. As a consequence radioelement can also be used in regional environmental studies and monitoring.

The well recognizable feature in the distribution of U, Th and K is the presence of comparatively high values in areas covered by andesitic, rhyolitic volcanites. There are only few anomalous values considering the frequency distribution of these elements.

Cs-137 ranges and nation-wide distributions are given on Fig. 5, representing the impact of the Chernobyl accident as early as in 1987. Intensity values measured in 1995 in the river and stream sediments on the flood-plains are shown on Fig. 6. In the majority of cases Cs-137 could not be detected or was of very low intensity in the deeper part (50–60 cm) of the sediment profile (Fig. 7). The details of the vertical distribution of Cs-137 were not so far investigated.

5. FIELD MEASURING POSSIBILITIES

In addition to the laboratory analysis a car mounted radioactive gamma spectra measuring system was established in the Geophysical Institute. It is also suitable for the measurement of the natural (U-Ra, Th, K-40) and artificial (e.g. Cs-137 of Chernobyl) gamma spectra in field circumstances.

The measuring car is a four-wheel-driven air-conditioned van. The basis of the measuring system is a portable, liquid nitrogen cooled, high purity germanium semiconductor detector. By the help of the built-in professional computer system, there is the possibility of the prompt analysis and report of the locally obtained spectra. This is independent of the electric network. In case of nuclear accidents this system can also work as a monitoring unit.

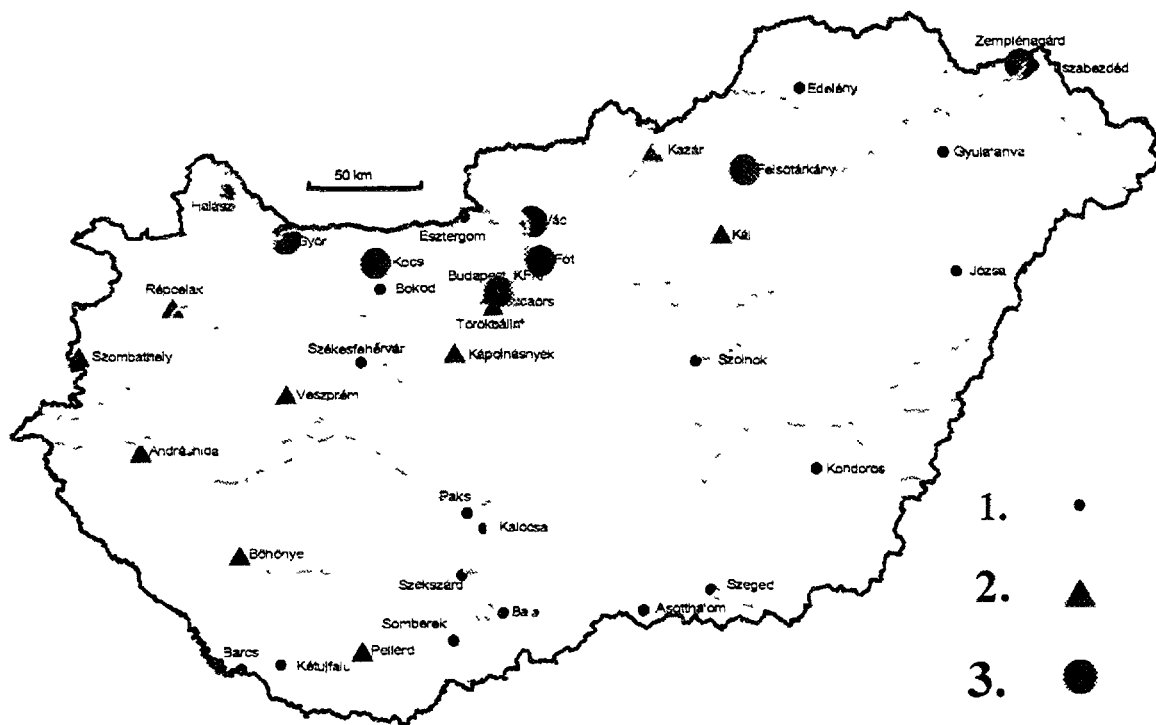


FIG. 5. Cs - 137. Estimated intensity values (nGy/h) – 1987-88. 1) 0– 40, 2) 40–80, 3) 80–170.

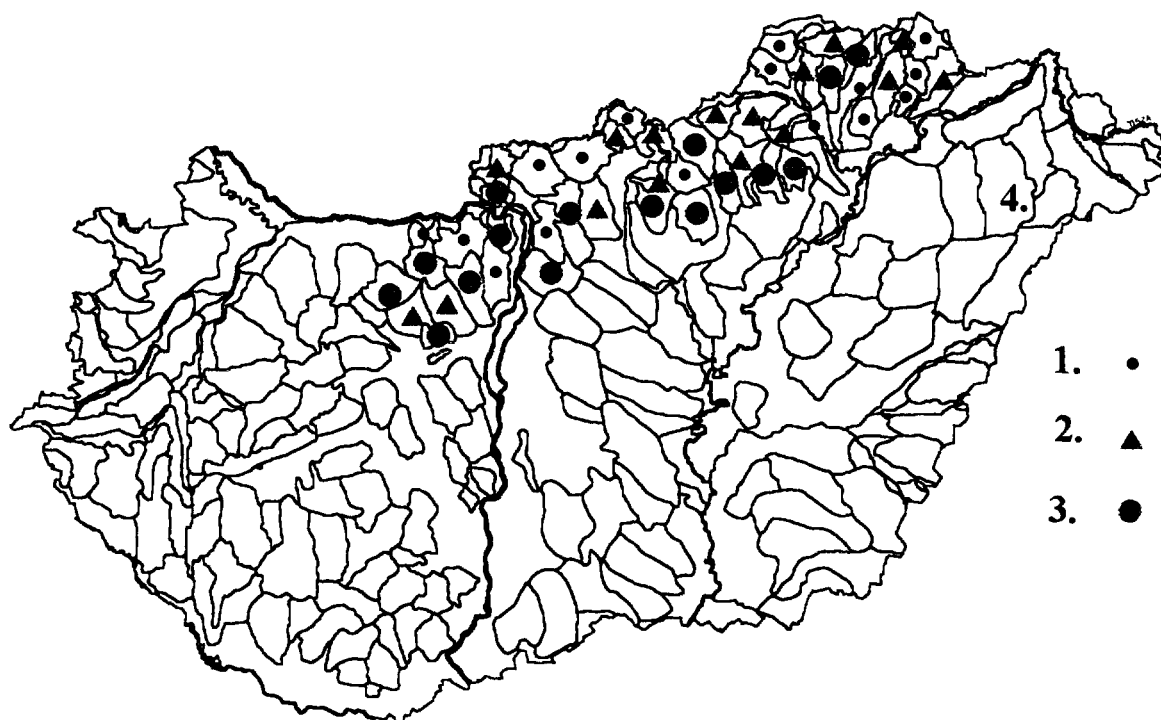


FIG. 6. Distribution of Cs-137 (nGy/h) in the flood-plain sediments of Hungary. (Sampling interval: 0–10 cm). 1) <1.0, 2) 1.0–1.78, 3) >1.78, 4) catchment basins.

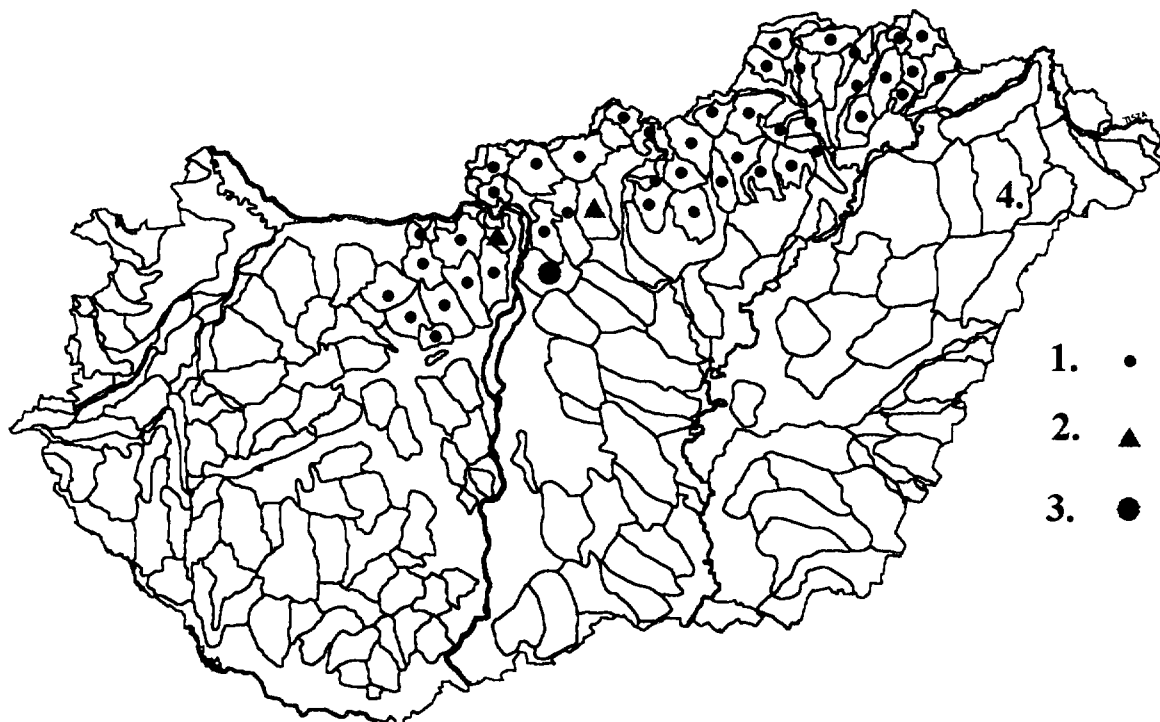


Fig. 7. Distribution of Cs-137 (nGy/h) in the flood-plain sediments of Hungary. (Sampling interval: 50-60 cm). 1) < 0.7, 2) 0.7-1.5, 3) > 1.5, 4) catchment basins.

6. CONCLUSIONS

The prime factor in low density surveys determining the geochemical pattern in Hungary is the surface predominance of young (Pleistocene or Miocene) clastic sediments over the older formations and basement rocks. The geochemical method used has the advantage to give regional surface background data outlining at the same time the areas of possible contamination. It also has the disadvantage of not being contrasty enough to differentiate geologically dissimilar areas.

At certain regions, the rate of sedimentation was fairly fast: the environmental effects of ore mining in Transylvania and in southern Slovakia as well as those of the heavy industry in northern Hungary can be observed even in the lower (50-60 cm) samples.

For the radioelements investigated highly reliable abundance data can be obtained for the surface environment. This approach gives no definite contrast in the distribution of the radioelements, only areas covered by the andesitic rocks can be outlined.

Catchment basins with anomalous values of e.g. Pb, Zn, As and Cd have been delineated but potentially dangerous concentration of radioelements have not so far been found in the investigated sediments.

ACKNOWLEDGEMENTS

This publication is partly sponsored by the U.S.-Hungarian Science and Technology Joint Fund in co-operation with the U. S. Geological Survey and the Hungarian Geological Survey under Project: J. F. No. 415.

REFERENCES

- [1] DARNLEY, A.G., International geochemical mapping: a new global project, *Journal of Geochemical Exploration* (1990) 39, 1–3.
- [2] XIE XUEJING, Some problems, strategical and tactical, in international geochemical mapping, *Journal of Geochemical Exploration* (1990) 39, 15–33.
- [3] DEMETRIADES, A., OTTESEN, R.T., LOCUTURA, J. (eds.), *Geochemical Mapping of Western Europe towards the Year 2000, Pilot Project Report, NGU Report* (1990) 90–105, 9 pages and 10 appendices.
- [4] DARNLEY, A.G. (CANADA), BJÖRKLUND, A. (FINLAND), BOLVIKEN, B. (NORWAY), GUSTAVSSON, N. (FINLAND), KOVAL, P.V. (RUSSIA), PLANT, J. A. (UK), STEENFELT, A. (GREENLAND), TAUCHID, M. (IAEA), XIE XUEJING (CHINA), with contributions by Garrett, R.G. and Hall, G.E.M. (Canada), *A Global Geochemical Database for Environmental and Resource Management, Recommendations for International Geochemical Mapping, Final Report of IGCP Project 259, UNESCO Publishing* (1995) Earth Sciences 19.
- [5] ÓDOR, L., HORVÁTH, I., FÜGEDI, U., Low-density geochemical survey of Hungary. *Environmental Geochemical Baseline Mapping in Europe, Abstracts* (1996) May 21–24, 1996 Spisska Nova Ves, Slovakia.
- [6] WÉBER, B., Az urán és tórium eloszlása az Északi Középhegység földtani képződményeiben légi gamma-spektrometriai mérések alapján, The distribution of U and Th in the geological formations of northern Hungary on the basis of air-borne gamma spectrometric measurements, *Földtani Közlöny*, (1975) 105/3., 309–319 (in Hungarian).

**NEXT PAGE(S)
left BLANK**



SPATIAL DISTRIBUTION OF ^{40}K , ^{228}Ra , ^{226}Ra , ^{238}U AND ^{137}Cs IN SURFACE SOIL LAYER OBSERVED AT SMALL AREAS

D. BARIŠIĆ, S. LULIĆ

Ruder Bošković Institute

E. PROHIĆ

Faculty of Natural Sciences,

University of Zagreb

M. ČULINOVIĆ

Ministry of Agriculture and Forestry

Zagreb, Croatia

Abstract

The main goal of this study is to give a more detailed insight into spatial radionuclide distribution in soils. It had been necessary in order to plan the future soil sampling procedure that would assure the representative soil samples for brother areas that are usually covered by in situ gamma-spectrometry measurements or aerial gamma-ray spectrometry. The spatial distributions of natural radionuclides and ^{137}Cs activity in surface soil layer were studied in five regular grids, consisting of 9 points each. The distances between sampled points were 30 cm (A grid), 2.45 m (B grid), 19.5 m (C grid), 156 m (D grid) and 312 m (E grid), respectively. Soil samples were dominantly taken at agricultural ploughed fields from areas of ca. 315 cm² (circle of a. 20 cm diameter), from surface up to 15 cm depth. The fraction of air-dried material that passed through a 0.5 mm sieve was reduced by quartering and dried at 105°C to the constant weight. The activities of ^{40}K , ^{228}Ra , ^{226}Ra , ^{238}U and ^{137}Cs were determined by the gamma-spectrometry method. The highest variations of ^{40}K activities are found in the E grid: 312–573 Bq/kg, the lowest are in the B grid: 318–338 Bq/kg. ^{40}K activities are found in ranges of 310–408 Bq/kg in 9 samples taken in the A grid, in an area of less than 0.65 m². Very high variations in ^{228}Ra activities are found in the E grid: 22–32 Bq/kg, while the lowest are in the A and B grid (22–24 Bq/kg). A very similar range of ^{226}Ra and ^{238}U activities are found in all observed grids; the lowest are in the A, B, and C grid (23–24 or 25 Bq/kg for ^{226}Ra , 22–24 or 25 Bq/kg for ^{238}U , respectively); the highest are in the D and E grid (21 or 22–31 Bq/kg for ^{226}Ra , 23–30 Bq/kg for ^{238}U , respectively). ^{137}Cs activities are found in a range of 17–37 Bq/kg in the E grid, a very high range was observed in the B grid (18–31 Bq/kg) and the lowest range (20–22 Bq/kg) in the A grid. It seems that variations of potassium concentration could be very high in areas of less than one square metre. The Average of ^{40}K activity in 38 taken samples was 368 Bq/kg: 359 in the A, 327 in the B, 340 in the C, 412 in the D and 414 Bq/kg in the E grid. Distribution of other observed natural radionuclides is relatively homogenous in areas which covered approximately 1500 m². The representative soil sample must cover the broader area to provide data that could be compared with data collected by aerial gamma-spectrometry. The average sample on each locality must be prepared from several point samples. It seems that the central point and four points, each at approximately 50–100 m N, S, E, and W from the central point, could be enough.

1. INTRODUCTION

The UNESCO International Geological Correlation Programme (IGCP) Project 259 — International Geochemical Mapping (IGM) was launched to address the problem of distribution of chemical elements, including radioactive ones, in the earth's surface materials. Airborne gamma survey has been applied and recommended for radiometric mapping of most national territories. Current researches are mostly based on aerial gamma-ray spectrometry measurements and data conversion into radionuclide concentration in soil. In the context of IGM project, the main function of ground gamma-ray spectrometry measurements is to provide a link between data gathered by conventional geochemical sampling and related airborne gamma-ray profiles. Many useful details about aerial gamma-ray spectrometry measurements have been published [1, 2], and regional geochemical maps of some primordial radionuclides are presented elsewhere.

Radiation from soil is the most important contributor to the external terrestrial radiation because bedrock is covered with soil in most areas of the world. It is a well-known fact that the

absorbed gamma dose rate in air is a function of radionuclide concentration in the first metre of the soil profile. Most recent conversion factors for the recalculation of dose rate in the air into potassium, uranium and thorium concentrations in the soil [3] assume the radiochemical equilibrium between radionuclides in ^{232}Th decay series as well as in ^{238}U decay series, and a homogeneous radionuclide concentration in the first metre of soil. Although all ^{232}Th decay products are often in radiochemical equilibrium with ^{232}Th , ^{238}U decay products are not in equilibrium with their precursors now and then. In the first few centimetres of carbonate derived soil the disequilibrium between ^{238}U and ^{226}Ra can be very high [4]. ^{226}Ra is precursor of the noble gas ^{222}Rn and its decay products, among which aerial gamma-ray spectrometry determination of ^{214}Bi is the base for ^{238}U assessment in the ground. Recalculation of ^{238}U decay series dose rate into ^{238}U concentration could be incorrect because the recalculated value presents ^{226}Ra activity [5].

Conventional geochemical sampling of the first 15 cm of A soil horizon or upper regolith, below O1 and Of horizons, if present, and laboratory gamma-ray spectrometry could provide the data for potassium, thorium, radium and uranium geochemical map construction. Models and databases for estimating the distribution of radioactivity in soil and associated external gamma doses above the soil surface have been presented in literature [5–9]. Identical sampling grid and determination of all elements in the single sample provide correct conditions for correlation of various elements reciprocally. Possible errors in ground component of natural background dose rate assessment, caused by radiochemical disequilibrium occurring in primordial radionuclides decay series or subseries are insignificant. Correlations between different non-radioactive and radioactive elements are also possible as the maps of radioactive elements could be constructed under same conditions. Unfortunately, the methods have not yet been used routinely in environmental dose rate assessment.

There are two main problems in correlation of data collected by aerial gamma-ray surveys or ground gamma spectrometry and data obtained by laboratory gamma spectrometry of samples collected during conventional geochemical sampling. First problem is very high difference in sampling scales, while second problem arises from significant differences in soil compartments from which information (signal) originated. The main goal of this study is to give more detailed insight into spatial radionuclide distribution in soils at relatively small areas in order to plan the future soil sampling procedure. Such a procedure must assure the soil sample of the same or similar soil types, naturally, that is representative for area usually covered by aerial gamma-ray surveys or ground gamma spectrometry.

2. SAMPLING AND METHODS

2.1. Sampling procedure

Soil was sampled by channel sampling the upper 15 cm of soil profile from area of cca 315 cm² (circle of 20 cm in diameter). The fraction of air-dried material that passed through a 0.5-mm sieve was reduced by quartering and dried at 105°C to the constant weight. The sampled soil types were luvisol on loess and luvisol on sand of agriculture areas that had been ploughed on a regular basis for more than a century.

Eight outer samples and the central sample were taken in the middle of the square in each of following regular grids: 0.3 × 0.3 m — A; 2.45 × 2.45 m — B; 19.5 × 19.5 m — C; 156 × 156 — D and 312 × 312 m — E grid with the randomly selected position of the central point of A grid. That central point is central point of B and C grid also. Randomly selected outer point of C grid was taken as a one of outer point of D grid. Similarly, randomly selected one of outer corner point of D was taken as a central point of E grid. In total, 38 soil samples were taken and analysed by gamma ray spectrometry method.

2.2. Gamma ray spectrometry

Dried soil samples were placed in the counting vessels of known geometry, sealed and stored at least for 4 weeks to allow ingrowth period of gaseous ^{222}Rn . At the end of the ingrowth period, the samples were counted on a HPGe detector joined to 4096 channel analyser. The detector system was calibrated using standards supplied by Amersham International, while precision and accuracy were checked by parallel measurement of IAEA-306 and IAEA-314 standards. Spectra were recorded 80 000 seconds. Recorded spectra were processed on PC using GENIE PC software. Activities of ^{40}K were calculated from the 1460.75 keV-peak, ^{137}Cs from 661.6 keV-peak, ^{226}Ra (as a mean value) from 609.3 keV-peak of its ^{214}Bi progeny and 352 keV-peak of its ^{214}Pb progeny, ^{228}Ra from 911.1 keV-peak of its ^{228}Ac progeny and ^{235}U from 186 keV-peak (after subtraction of the overlapping ^{226}Ra peak). Activities of ^{238}U were calculated from ^{235}U activity assuming the $^{235}\text{U}/^{238}\text{U}$ activity ratio of 0.04603 [10].

3. RESULTS AND DISCUSSION

Differences in radionuclides activity observed among central and other sampled points in grids, for A to E grid are given in Table I to V respectively. Measured values, together with accompanying counting errors, are shown for central points of grids as well as mean values of differences for ^{40}K , ^{228}Ra , ^{226}Ra , ^{238}U and ^{137}Cs . Mean of all measured values are shown as well as the means of two groups each consisting of 5 samples taken in cross scheme. First group comprehends central point and 4 nearest points (N, S, E and W) at distance of respective grid unit; second group comprehends central point and 4 the furthest points (NE, SE, SW and NW) at distance of respective grid unit diagonally.

As expected, the highest variation of ^{40}K activities are found in E grid: 312-573 Bq/kg, but variation in potassium concentration found in 9 samples of A grid at area of half square metre only, is unexpected. Near to all of considered means (of 9 or 5 points each) of ^{40}K activities in B and C

TABLE I. DIFFERENCES IN RADIONUCLIDES ACTIVITY (Bq/kg) OBSERVED IN A REGULAR GRID AMONG CENTRAL (0) AND OTHER POINTS IN GRID

POINT	^{40}K	^{228}Ra	^{226}Ra	^{238}U	^{137}Cs
1	1.1	-0.9	0.2	0.9	-1.7
2	9.0	-0.9	0.2	0.5	-1.2
3	-6.9	-1.2	0.4	1.6	-1.1
8	84.3	0.5	2.3	2.5	-2.7
4	-14.3	-0.8	0.5	0.9	-1.1
7	66.8	0.1	1.7	2.1	-2.1
6	56.4	0.0	1.1	1.3	-1.4
5	37.4	-0.4	0.7	0.7	0.1
0 ⁽¹⁾	324.0 ± 14.5	23.2 ± 1.4	23.2 ± 0.8	22.7 ± 3.0	22.3 ± 0.4
MEAN ⁽²⁾	26.0 ± 72.1 ⁽³⁾	-0.4 ± 1.2	0.8 ± 1.5	1.2 ± 1.6	-1.2 ± 1.8
*	350.0 ± 72.1	22.8 ± 1.2	24.0 ± 1.5	23.9 ± 1.6	21.1 ± 1.8
**	351.1 ± 83.1	23.0 ± 1.2	24.0 ± 1.9	23.7 ± 1.9	21.0 ± 1.9
***	343.7 ± 63.0	22.7 ± 1.1	23.8 ± 1.3	23.8 ± 1.6	21.3 ± 2.0

⁽¹⁾ measured value ± counting error; ⁽²⁾ mean value of differences; ⁽³⁾ mean value ± standard deviation of 2σ; * mean of all samples in grid; ** mean of central point and 4 points at d = 30 cm in cross scheme; *** mean of central point and 4 points at d = 42 cm in cross scheme

TABLE II. DIFFERENCES IN RADIONUCLIDES ACTIVITY (Bq/kg) OBSERVED IN B REGULAR GRID AMONG CENTRAL (0) AND OTHER POINTS IN GRID

POINT	⁴⁰ K	²²⁸ Ra	²²⁶ Ra	²³⁸ U	¹³⁷ Cs
9	-5.4	-0.2	0.3	0.6	-2.4
10	9.9	0.4	-0.1	-0.6	-2.7
11	12.4	-0.8	-0.4	1.1	-1.2
16	-5.9	-1.3	-0.2	-0.2	-4.8
12	-1.2	-0.2	0.1	0.8	0.7
15	7.1	0.0	0.3	1.5	3.9
14	-3.1	-0.5	-0.2	1.3	5.0
13	13.9	-0.2	0.2	0.6	8.9
0 ⁽¹⁾	324.0 ± 14.5	23.2 ± 1.4	23.2 ± 0.8	22.7 ± 3.0	22.3 ± 0.4
MEAN ⁽²⁾	3.1 ± 15.6 ⁽³⁾	-0.3 ± 1.0	0.0 ± 0.5	0.6 ± 1.4	0.8 ± 8.7
*	327.1 ± 15.6	22.9 ± 1.0	23.2 ± 0.5	23.3 ± 1.4	23.1 ± 8.7
**	323.9 ± 12.0	22.9 ± 1.3	23.1 ± 0.3	23.0 ± 1.5	21.9 ± 7.4
***	329.6 ± 16.4	23.0 ± 0.7	23.3 ± 0.6	23.5 ± 1.1	24.1 ± 4.6

⁽¹⁾measured value ± counting error; ⁽²⁾mean value of differences; ⁽³⁾mean value ± standard deviation of 2σ; *mean of all samples in grid; **mean of central point and 4 points at d = 2.45 m in cross scheme; ***mean of central point and 4 points at d = 3.5 m in cross scheme

TABLE III. DIFFERENCES IN RADIONUCLIDES ACTIVITY (Bq/kg) OBSERVED IN C REGULAR GRID AMONG CENTRAL (0) AND OTHER POINTS IN GRID

POINT	⁴⁰ K	²²⁸ Ra	²²⁶ Ra	²³⁸ U	¹³⁷ Cs
17	44.2	0.1	0.2	0.5	0.3
18	29.3	-2.4	0.1	0.9	5.6
19	24.7	0.0	0.2	0.7	-1.7
24	40.8	0.8	-0.5	-0.3	-2.4
20	-12.0	-1.4	0.3	1.4	-0.1
23	46.5	0.4	-0.5	0.2	-3.6
22	24.0	-1.2	-0.4	0.6	-2.9
21	28.6	-2.6	-0.5	1.5	-1.8
0 ⁽¹⁾	324.0 ± 14.5	23.2 ± 1.4	23.2 ± 0.8	22.7 ± 3.0	22.3 ± 0.4
MEAN ⁽²⁾	25.1 ± 39.4 ⁽³⁾	-0.7 ± 2.5	-0.1 ± 0.7	0.6 ± 1.2	-0.7 ± 5.5
*	349.1 ± 39.4	22.5 ± 2.5	23.1 ± 0.7	23.3 ± 1.2	21.6 ± 5.5
**	340.4 ± 43.5	22.4 ± 2.5	23.1 ± 0.7	23.2 ± 1.4	22.3 ± 6.7
***	352.8 ± 37.4	22.8 ± 2.5	23.1 ± 0.7	23.3 ± 1.2	20.9 ± 3.2

⁽¹⁾measured value ± counting error; ⁽²⁾mean value of differences; ⁽³⁾mean value ± standard deviation of 2σ; *mean of all samples in grid; **mean of central point and 4 points at d = 19.5 m in cross scheme; ***mean of central point and 4 points at d = 27.6 m in cross scheme

TABLE IV. DIFFERENCES IN RADIONUCLIDES ACTIVITY (Bq/kg) OBSERVED IN D REGULAR GRID AMONG CENTRAL (25) AND OTHER POINTS IN GRID

POINT	⁴⁰ K	²²⁸ Ra	²²⁶ Ra	²³⁸ U	¹³⁷ Cs
26	-92.4	0.0	-7.2	-3.9	0.3
19	-112.6	-1.8	-6.3	-5.9	0.3
27	-87.0	1.0	-3.1	-2.0	-1.1
32	-60.6	-0.2	-1.8	-2.6	-3.7
28	-147.0	-0.9	-8.8	-6.8	0.8
31	-37.9	2.3	-5.1	-4.1	0.1
30	25.1	3.6	-1.8	-0.6	8.2
29	67.7	6.9	1.4	0.3	1.3
25 ⁽¹⁾	461.3 ± 15.3	25.0 ± 1.4	29.7 ± 0.9	29.3 ± 3.2	20.3 ± 0.4
MEAN ⁽²⁾	-49.4 ± 139.2 ⁽³⁾	1.2 ± 5.4	-3.6 ± 6.9	-2.8 ± 5.1	0.7 ± 6.3
*	411.9 ± 139.2	26.2 ± 5.4	26.1 ± 6.9	26.5 ± 5.1	21.0 ± 6.3
**	402.3 ± 145.5	25.1 ± 4.1	26.0 ± 7.3	26.2 ± 6.1	21.4 ± 8.7
***	431.4 ± 132.9	27.0 ± 5.8	26.9 ± 7.1	27.4 ± 4.2	20.4 ± 0.7

⁽¹⁾measured value ± counting error; ⁽²⁾mean value of differences; ⁽³⁾mean value ± standard deviation of 2σ; *mean of all samples in grid; **mean of central point and 4 points at d = 156 m in cross scheme; ***mean of central point and 4 points at d = 220 m in cross scheme

TABLE V. DIFFERENCES IN RADIONUCLIDES ACTIVITY (Bq/kg) OBSERVED IN D REGULAR GRID AMONG CENTRAL (25) AND OTHER POINTS IN GRID

POINT	⁴⁰ K	²²⁸ Ra	²²⁶ Ra	²³⁸ U	¹³⁷ Cs
33	204.3	6.8	8.4	3.3	6.3
34	5.7	0.8	5.6	2.7	4.2
35	-56.9	-2.8	0.6	-2.4	-0.6
37	25.9	-0.3	5.0	1.8	-3.5
27	5.4	1.0	4.1	1.9	-1.4
36	6.6	1.4	4.2	1.6	16.3
31	54.5	2.3	2.1	-0.2	-0.2
29	160.1	6.9	8.6	4.2	1.0
26 ⁽¹⁾	368.9 ± 14.8	25.0 ± 1.4	22.5 ± 0.8	25.4 ± 3.0	20.6 ± 0.4
MEAN ⁽²⁾	45.1 ± 167.4 ⁽³⁾	1.8 ± 6.4	4.3 ± 6.1	1.4 ± 4.0	2.5 ± 11.9
*	414.0 ± 167.4	26.8 ± 6.4	26.8 ± 6.1	26.8 ± 4.0	23.1 ± 11.9
**	387.2 ± 45.0	25.8 ± 2.0	25.9 ± 4.6	26.6 ± 2.5	20.4 ± 5.6
***	431.7 ± 225.7	27.5 ± 8.6	26.9 ± 8.2	26.7 ± 5.3	25.2 ± 14.1

⁽¹⁾measured value ± counting error; ⁽²⁾mean value of differences; ⁽³⁾mean value ± standard deviation of 2σ; *mean of all samples in grid; **mean of central point and 4 points at d = 312 m in cross scheme; ***mean of central point and 4 points at d = 442 m in cross scheme

grids shows less aberration from A grid central point value, than mean value of A grid itself shows. In case of potassium, it seems that composite of few different samples taken at points inside circle with more than 20 metres radius could be more representative for the centre of half square metre area (area of central sample) than the same composite taken at points inside circle with less than half metre radius. Similarly differences in ^{137}Cs activity among central point and outer points are found in circles with 3.5 m and 220 m radius respectively. It seems that for ^{40}K and ^{137}Cs activity assessment in central point, composite sample acquiring in circle of some 150 metres radius could be the more important factor than sampling point position.

Relatively high range of ^{228}Ra activities was found in E grid: 22–32 Bq/kg, and D grid: 23–32 Bq/kg. Activity of ^{228}Ra in all of samples taken in A, B and C grid is the same practically. Activity that was higher for more than single counting error was found in one case only. Nearly identical spatial activity distribution show ^{226}Ra and ^{238}U . It seems than, in case of same or similar soil types, differences of uranium activities that are higher than corresponding double counting error could be rarely found in circle up to some 200 m radius. In the case of thorium, that radius is probably about 100–150 metres, and about hundred metres or less in case of ^{226}Ra . Maps of ^{40}K , ^{228}Ra , ^{226}Ra , ^{238}U and ^{137}Cs spatial activities distribution (Figs 1–5) are generated, by inverse distance Kriging method — quadrant data search, on the basis of data collected in D and E grid.

The signal recorded by gamma ray spectrometer, elevated above ground at 100 metres height, are spatially averaged over more than $1.5 \times 10^5 \text{ m}^2$, whereas conventional geochemical core soil samples represent perhaps few hundred cm^2 . Signal recorded by ground gamma spectrometry when detector is elevated at 1 metre height are spatially averaged over more than thousand m^2 . In fact, the differences of sampling scales could be of some 6–7 or 3–4 orders of magnitude. As shown previously, the very first insight into ^{40}K , ^{228}Ra , ^{226}Ra , ^{238}U and ^{137}Cs spatial activities distribution in soil at relatively small areas indicates that composite soil sample acquiring in cross scheme could be satisfactorily for activity assessment in central cross point up to distance of some 150 metres from cross centre. In that case, it seems that differences of sampling scales, which exist between conventional geochemical soil sampling and aerial gamma-ray surveys or ground gamma spectrometry, could be far less significant.

The second problem in correlation of data collected by aerial gamma-ray surveys or by ground gamma spectrometry and data obtained by laboratory gamma spectrometry of samples collected during conventional geochemical sampling arises from fact that conventional geochemical sampling provides homogeneous sample of the first 15 cm of soil profile. In the same time, the contribution of the first centimetre of soil profile in signal recorded by detector that is elevated at 100 metres height could be more than 12% (Fig. 6). If detector is elevated at 1 metre height, signals recorded from the first centimetre and from 15–100 cm soil depth compartment are equal (about 4% of total signal recorded) at distance of approximately 3.5 metres from point under detector (Fig. 7). If ground surface is plain, signal contribution from the first centimetre of soil profile could be even half of total signal received by detector elevated at 1 metre height. Contribution of signals from different soil compartments in total signal received by detector elevated at 1 m height above plain ground surface are shown in Fig. 8 in dependence on soil layer thickness as a function of distance from the point under detector. It is obviously that the first few centimetres of soil profile contribution in signal recorded by detector at 1 metre height is exceptionally high. In cases when ground surface is covered with vegetation, the first few centimetres of soil profile contribution in signal recorded by detector at 1 metre height is probably even unacceptably high.

Narrowing of the area wherefrom recorded signal originated is relatively easily achievable by lateral detector shielding. The information (signal) that originated from a first few centimetres of soil could be reduced significantly by lateral detector shielding in case of low elevated detector. Cumulative gamma doses distribution which are received by at 1 metre elevated shielded detector (shield reduce the received information at 5 metres radius circle) is shown in Fig. 9. Figure 10 present percentage contribution of signals from different soil compartments in total signal received

Gaus-Kruger projection

BELICA

POINT 0
measured:
324.0 Bq/kg
(mean values)

A grid: 350.0

B grid: 327.1

C grid: 349.1

D grid: 411.9

E grid: 414.0

M 1 : 5000

INSTITUTE
RUDJER BOŠKOVIĆ
CENTRE FOR MARINE
RESEARCH
DEPARTMENT ZAGREB
Laboratory for nuclear
chemistry and radioecology
1996

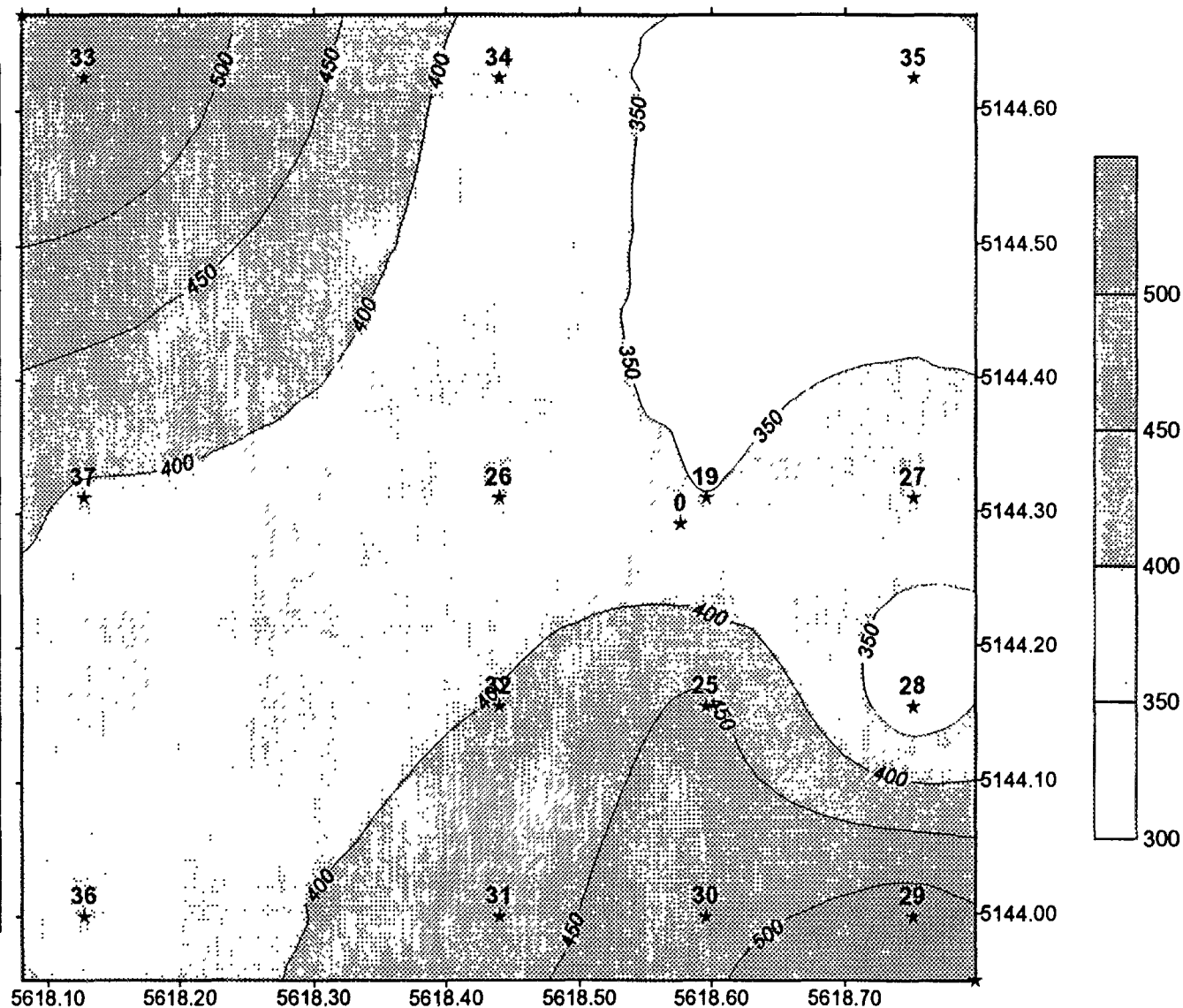


FIG. 1. ^{40}K spatial distribution in D and E grid (^{40}K activity in Bq/kg).

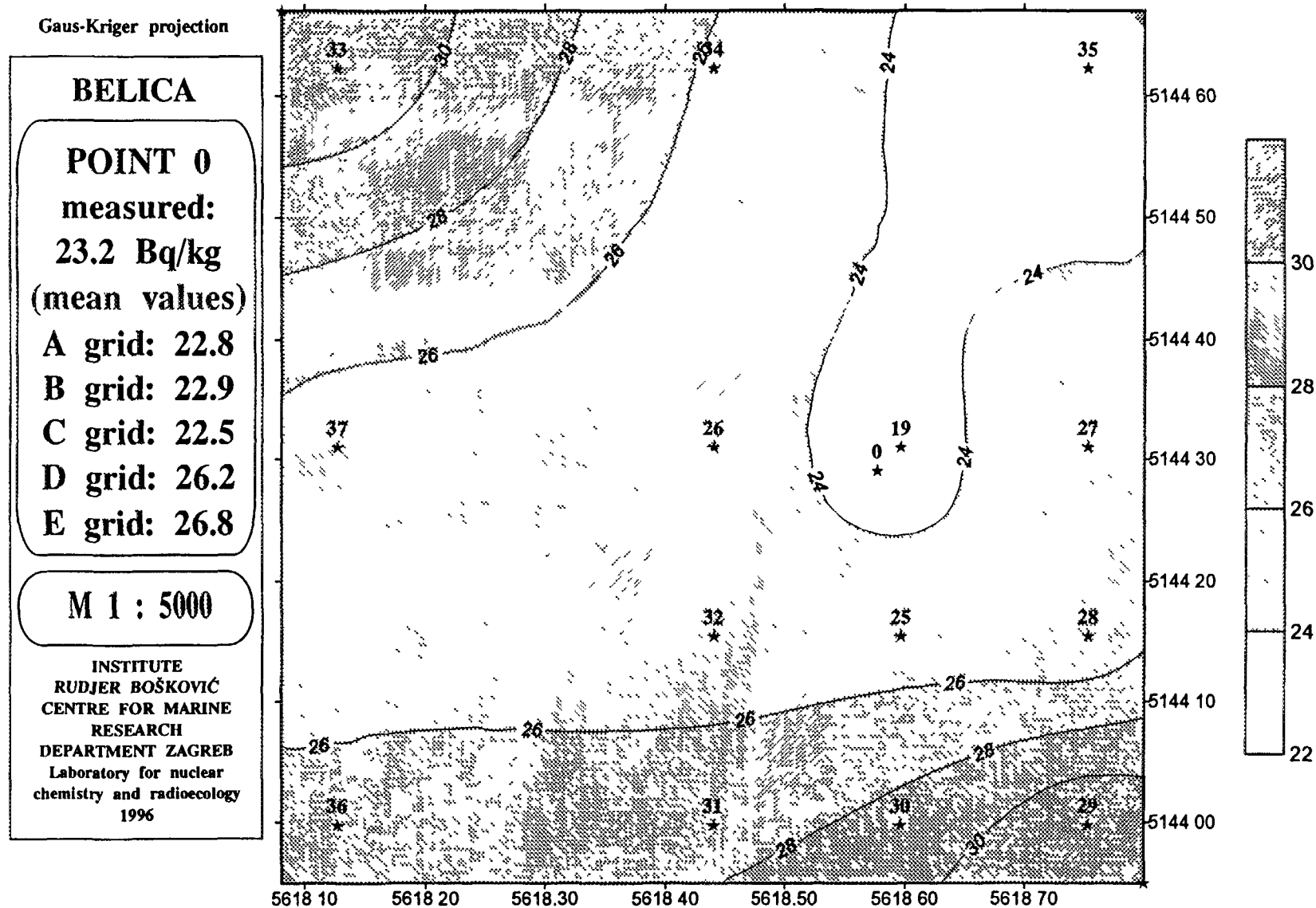


FIG. 2 ^{228}Ra spatial distribution in D and E grid (^{228}Ra activity in Bq/kg).

Gaus-Kruger projection

BELICA

POINT 0
measured:
23.2 Bq/kg
(mean values)

A grid: 24.0

B grid: 23.2

C grid: 23.1

D grid: 26.1

E grid: 26.8

M 1 : 5000

INSTITUTE
RUDJER BOŠKOVIĆ
CENTRE FOR MARINE
RESEARCH
DEPARTMENT ZAGREB
Laboratory for nuclear
chemistry and radioecology
1996

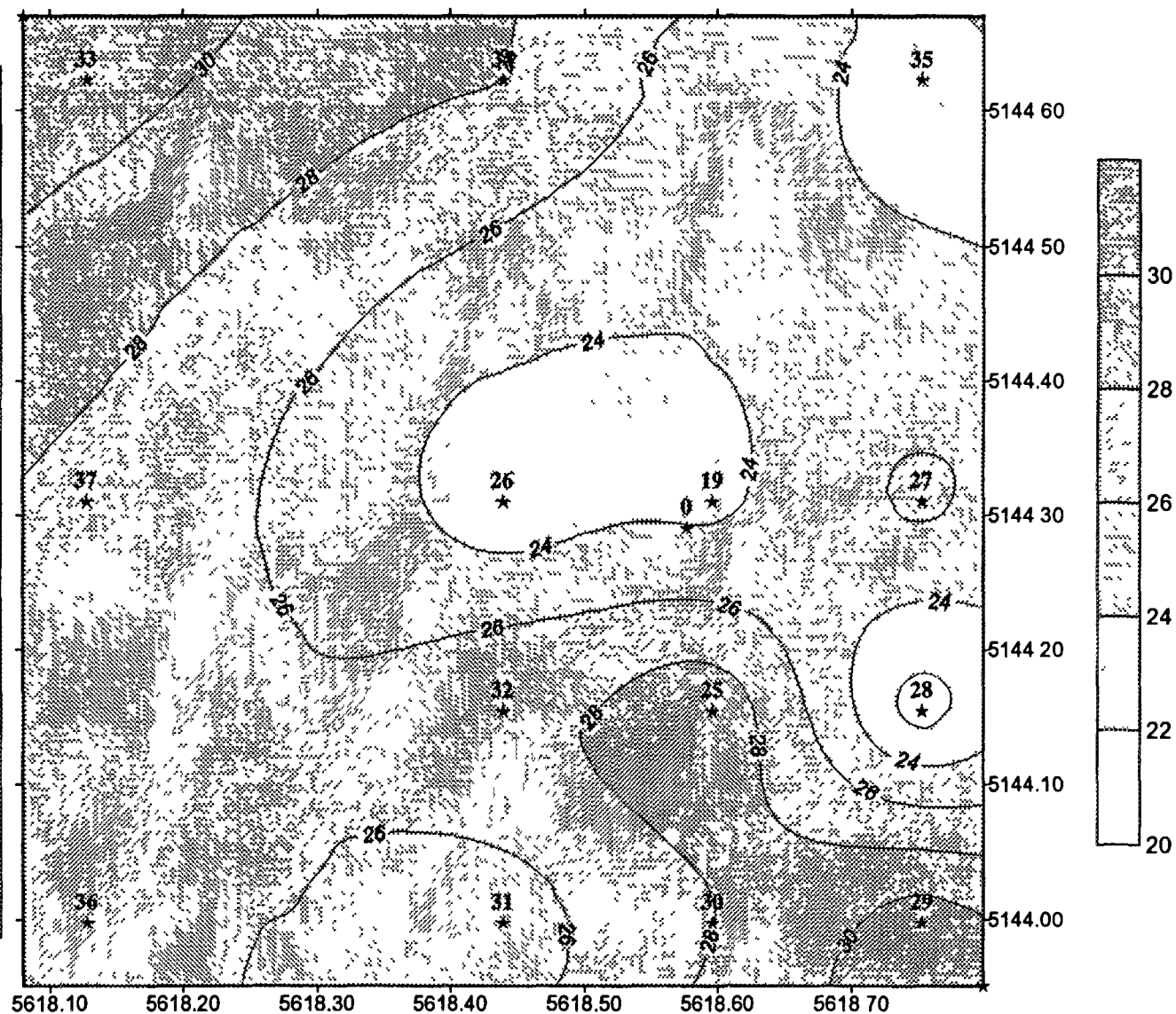


FIG. 3. ^{226}Ra spatial distribution in D and E grid (^{226}Ra activity in Bq/kg).

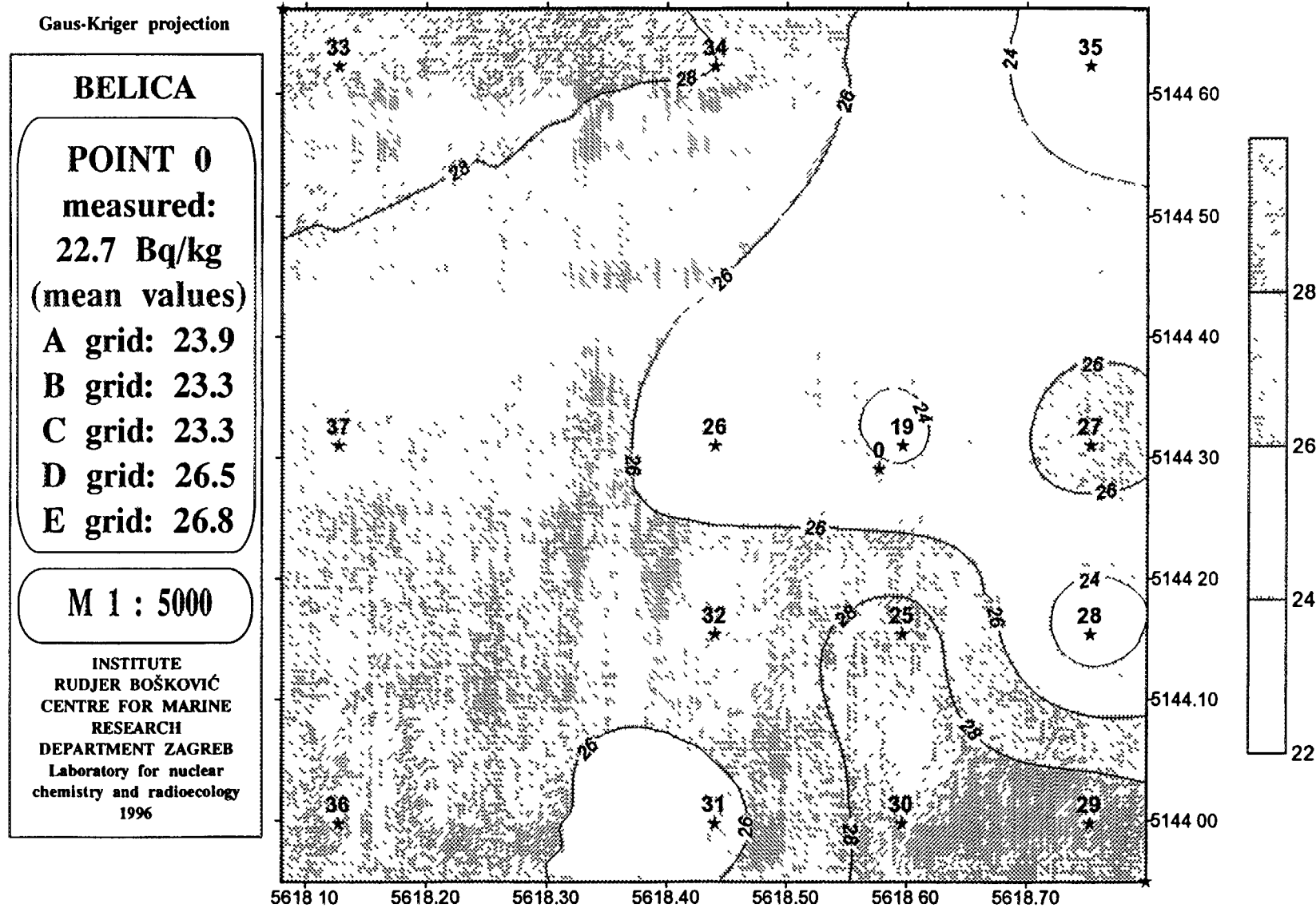


FIG 4. ^{238}U spatial distribution in D and E grid (^{238}U activity in Bq/kg).

Gaus-Kruger projection

BELICA

POINT 0
measured:
22.3 Bq/kg
(mean values)

A grid: 21.1

B grid: 23.1

C grid: 21.6

D grid: 21.0

E grid: 23.1

M 1 : 5000

INSTITUTE
RUDJER BOŠKOVIĆ
CENTRE FOR MARINE
RESEARCH
DEPARTMENT ZAGREB
Laboratory for nuclear
chemistry and radioecology
1996

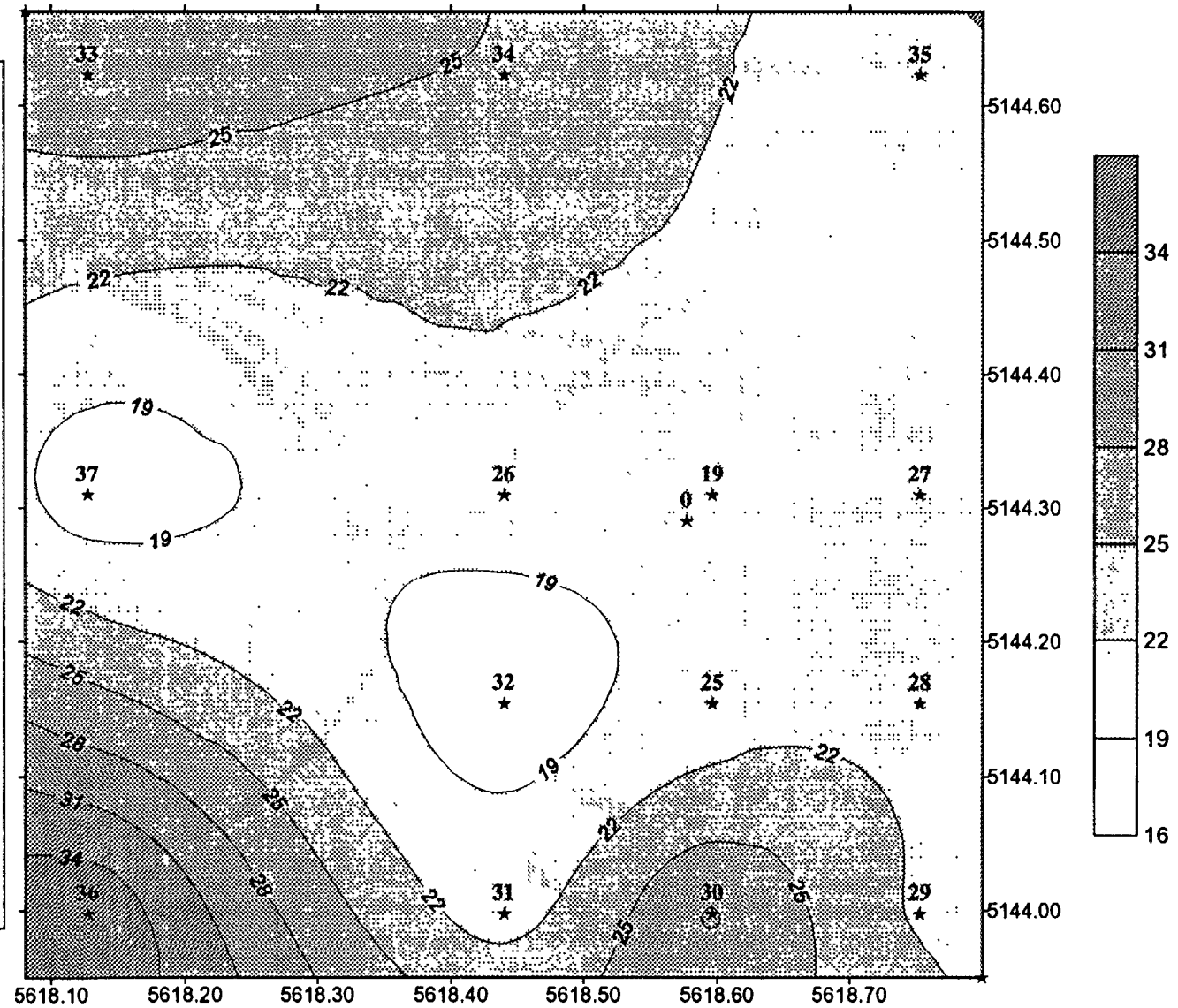


FIG. 5. ^{137}Cs spatial distribution in D and E grid (^{137}Cs activity in Bq/kg).

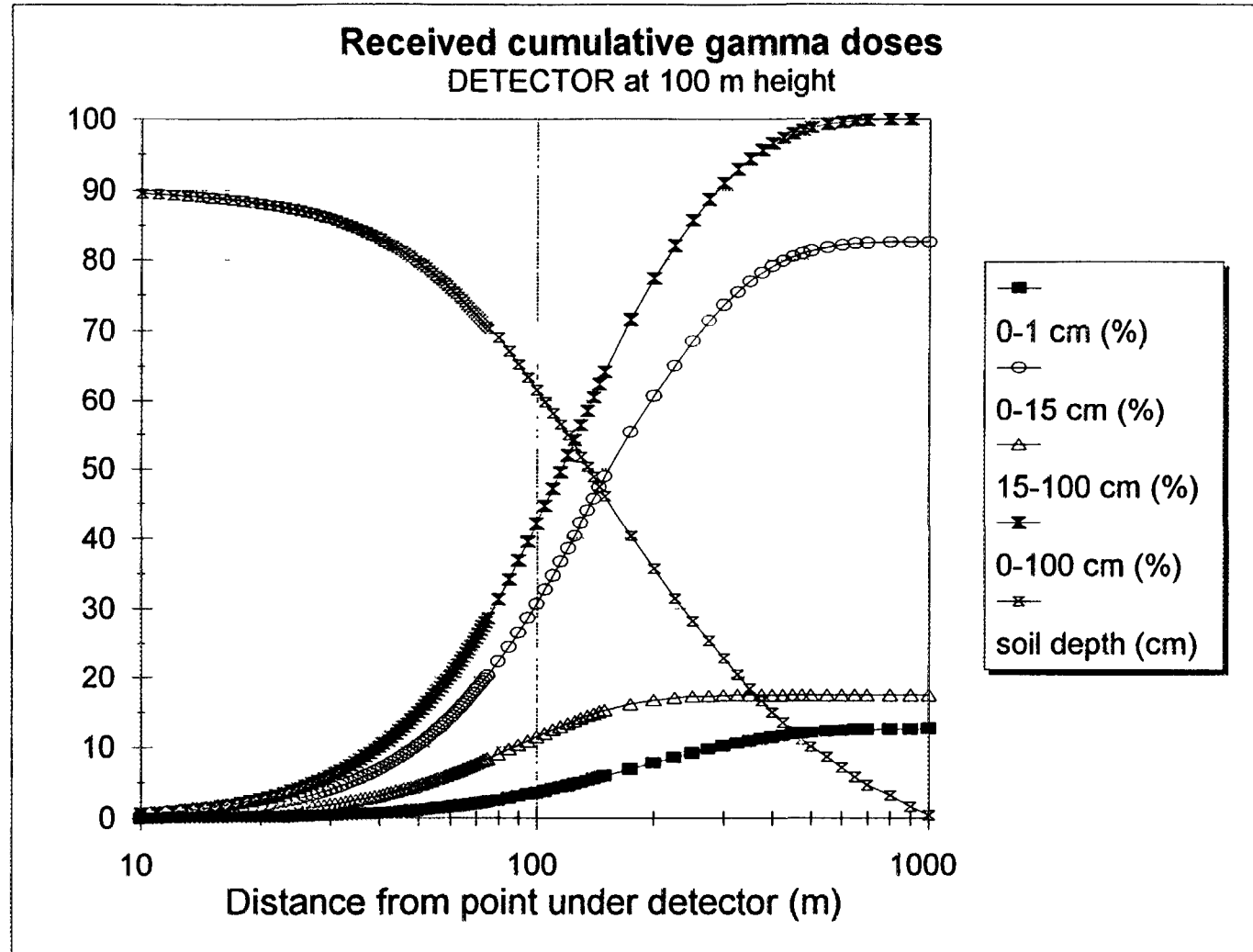


Fig.6. Cumulative gamma doses received by detector elevated in air at 100 meters height above plain ground surface in dependence on distance from point under detector

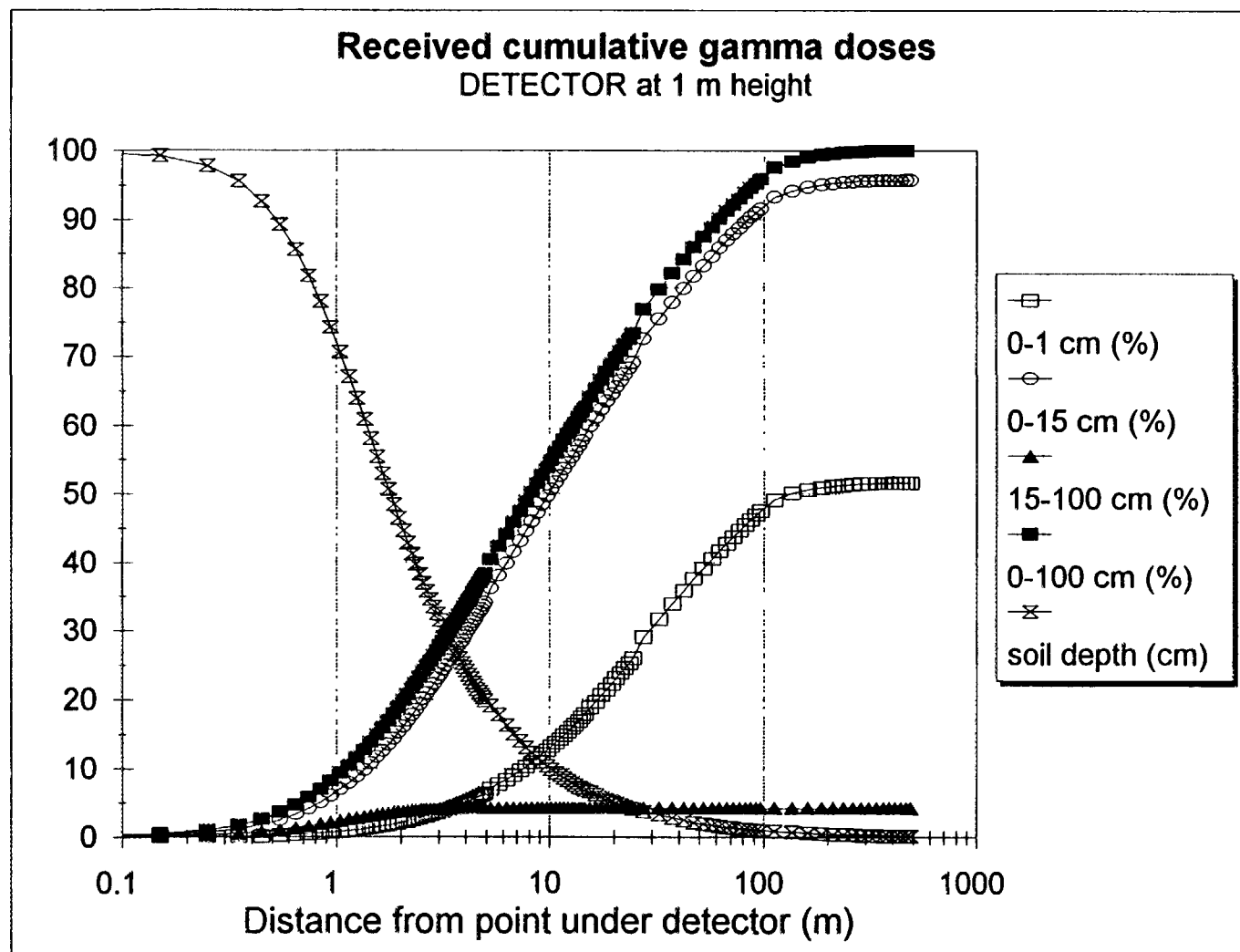


Fig.7. Cumulative gamma doses received by detector elevated in air at 1 meter height above plain ground surface in dependence on distance from point under detector

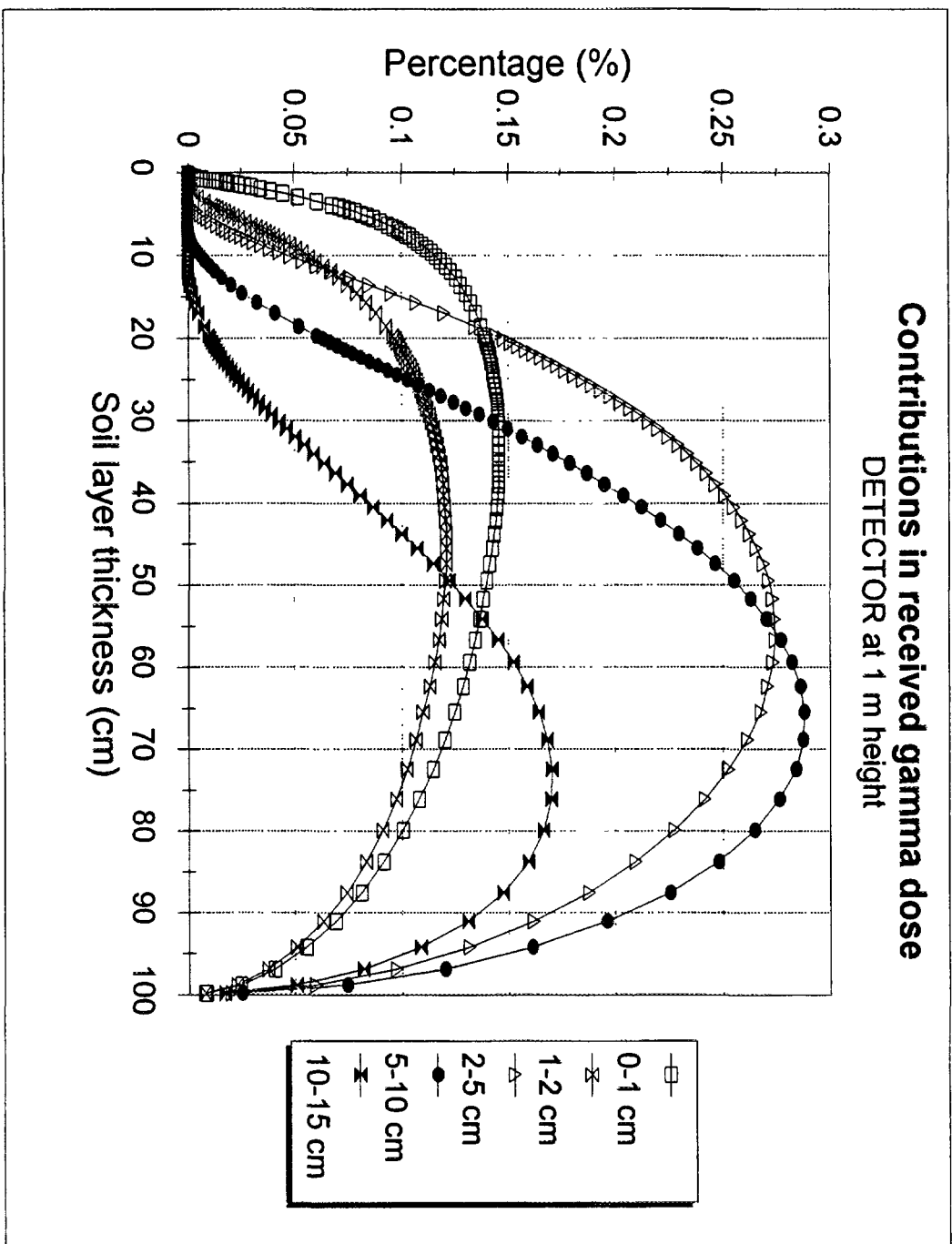


Fig.8. Percentage contribution of gamma dose that arise from different soil compartments in total gamma dose received by detector elevated in air at 1 meter height above plain ground surface in dependence on soil layer thickness as a function of distance from point under detector

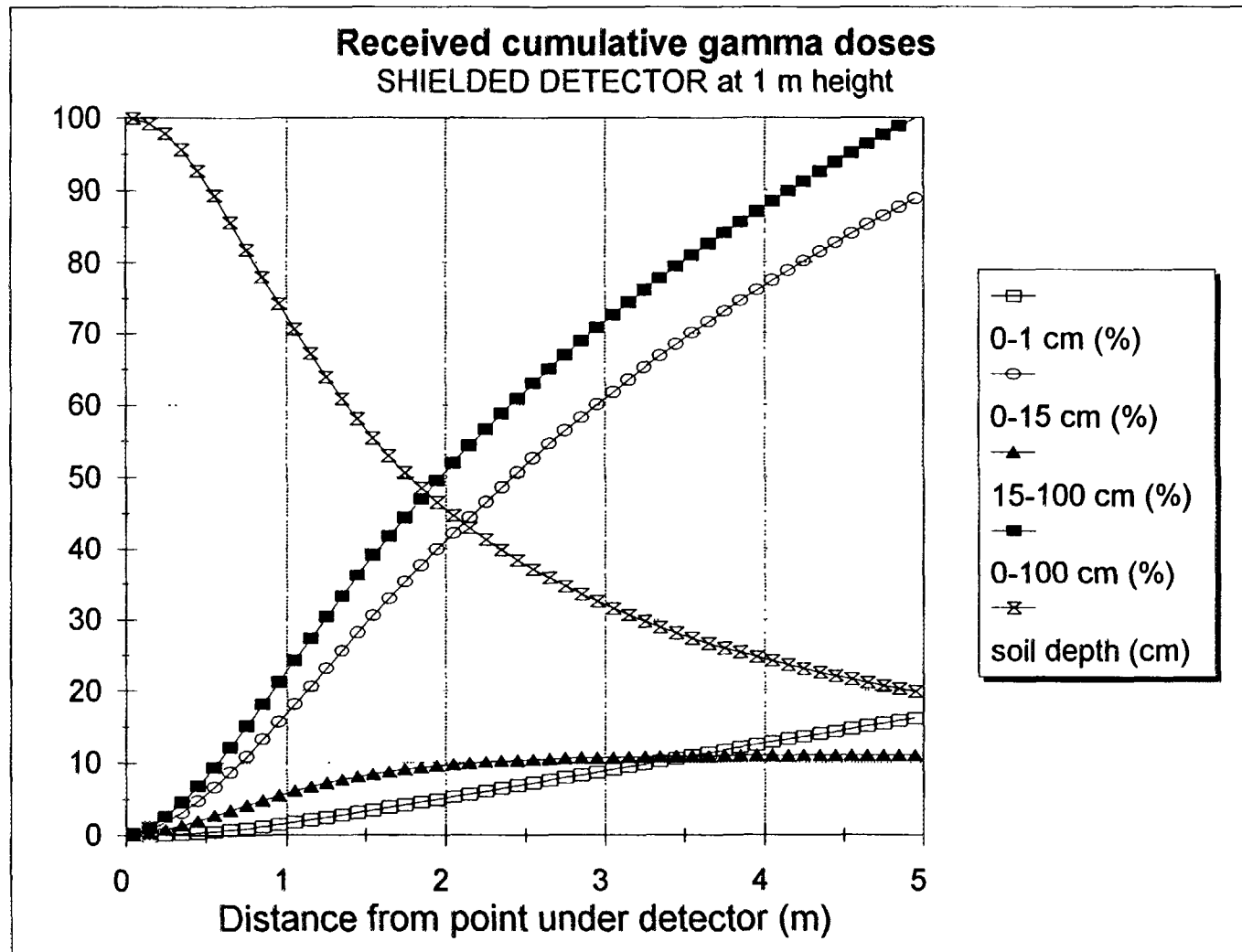


Fig.9. Cumulative gamma doses received by shielded detector (shield reduce the received signal at 5 meters radius circle) elevated in air at 1 meter height above plain ground surface in dependence on distance from point under detector

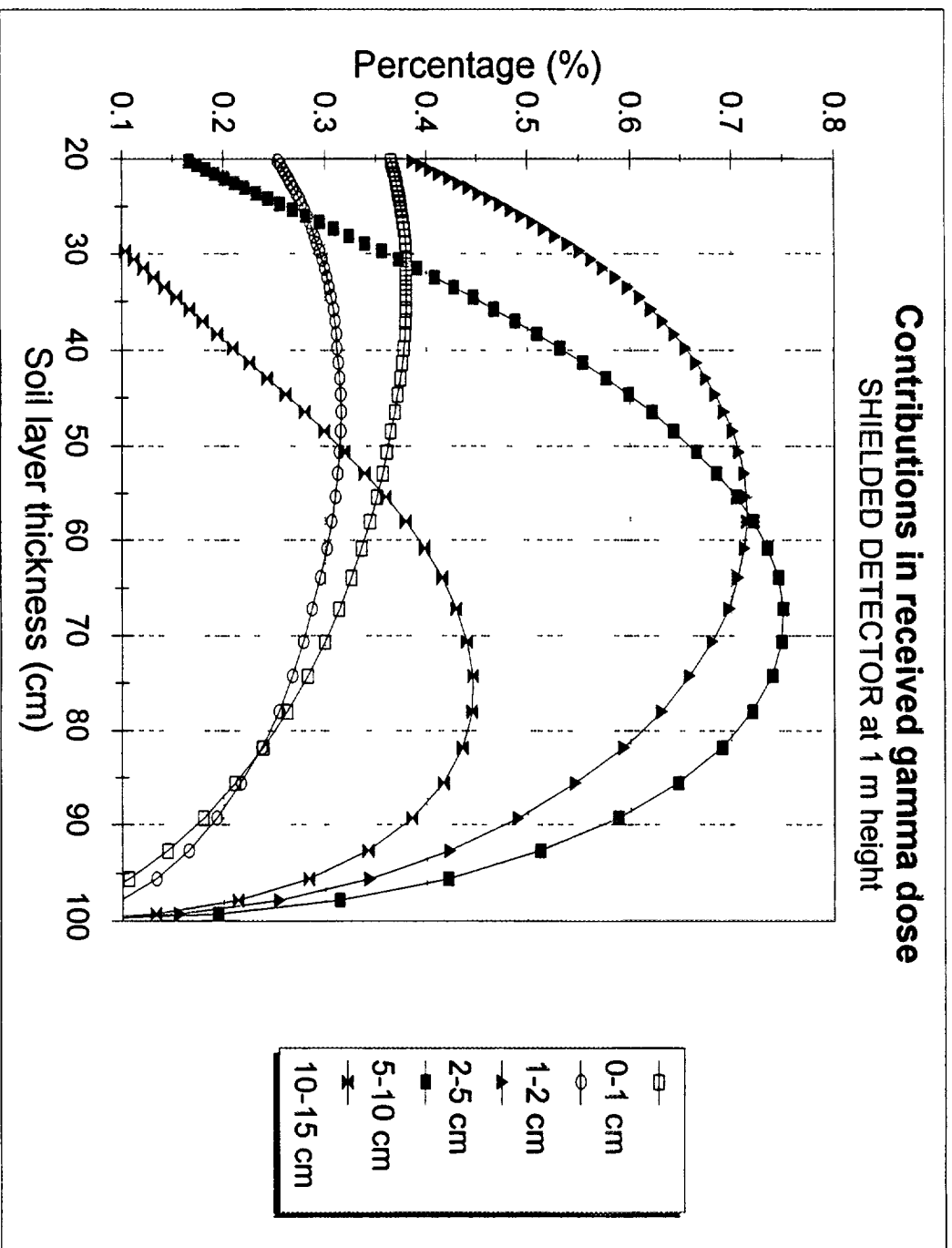


Fig.10. Percentage contribution of gamma dose that arise from different soil compartments in total gamma dose received by shielded detector (shield reduce signal at 5 meters radius circle) elevated in air at 1 meter height above plain ground surface in dependence on soil layer thickness as a function of distance from point under detector

by shielded detector elevated at 1 m height (shield reduce the received information at 5 metres radius circle) in dependence on soil layer thickness as a function of distance from the point under shielded detector. For detectors elevated at 100 metres height, that reduction is not significant as long as radius of circle under detector, reduced by detector shielding, overcomes some 300 metres, but it seems that reduction of that circle at some 150–200 metres radius could be reasonable when the ground surface is vegetation covered.

^{40}K and ^{137}Cs spatial activities distribution in soil observed at areas overlapped by A and B grid indicates that lateral shielded and at one metre elevated detectors are able to provide very quality information about potassium and caesium concentrations in soil. It seems that ground spectrometry measurements with lateral shielding of detectors (when shields reduce the received information at less than 5 metres radius circle) are able to provide information of better quality than conventional geochemical sampling assures. Conventional geochemical sampling has a preference in cases of ^{228}Ra and ^{226}Ra , but both methods are probably at an alike quality level. Due to possible radiochemical disequilibrium between ^{226}Ra and ^{238}U recalculation of any, in air measured gamma dose rate that comes from uranium decay chain — in fact from ^{226}Ra decay products mainly, into uranium concentration in soil is questionable.

Aerial gamma-ray spectrometry with high sensitivity spectrometers applied, provides the means to conducting large scale surveys describing the major spatial variation in radioactivity distribution on relatively large scale area. On the other hand, laboratory gamma spectrometry of samples collected by conventional geochemical sampling method provides quality data for uranium and thorium (less quality for potassium) concentrations on small scale area. It seems that composite sample acquiring could be recommended for future soil sampling procedure. Average soil sample on each locality could be prepared from five point samples taken in cross scheme inside some 50-150 metres radius circle.

4. CONCLUSIONS

Spatial distribution of ^{40}K , ^{228}Ra , ^{226}Ra , ^{238}U and ^{137}Cs activities was studied at relatively small areas in order to plan the future soil sampling procedure that would assure the soil samples representative for broader area that are usually covered by *in situ* gamma-spectrometry measurements or aerial gamma-ray spectrometry.

The very first insight into ^{40}K , ^{228}Ra , ^{226}Ra , ^{238}U and ^{137}Cs spatial activities distribution in soil at relatively small areas indicates that composite soil sample acquiring in cross scheme could be satisfactorily for caesium, potassium, uranium and, probably thorium, activity assessment in central cross point up to distance of some 150 metres from cross centre. For radium activity assessment in central cross point, the distance from cross centre could be about hundred metres or less. In case of composite soil sample acquiring in cross scheme, it seems that differences of sampling scales which exist between conventional geochemical soil sampling and aerial gamma-ray surveys or ground gamma spectrometry, could be far less significant.

Thorium, radium, uranium and caesium spatial activities distribution in soil samples, that were taken by conventional geochemical sampling method from less than square metre area, shows that any of analysed samples could represent ^{228}Ra , ^{226}Ra , ^{238}U and ^{137}Cs activities at that area. Very high variation of potassium concentrations, found in 9 samples taken at the same area, indicates that even each sample taken in suggested cross scheme needs to be sampled as one composite from one or few metres radius circle.

Additionally, unacceptably high contribution of gamma dose that originated from a first few centimetres of surface soil layer, occurring during field gamma-spectrometric measurements, could be reduced significantly by narrowing of the area wherefrom recorded signal originated (by lateral

detector shielding). *In situ* gamma-spectrometric measurements could be performed, similarly as composite soil sample acquiring, in the identical cross scheme or randomly selected (with the same central point) one.

REFERENCES

- [1] INTERNATIONAL ATOMIC ENERGY AGENCY, The use of gamma ray data to define the natural radiation environment, IAEA-TECDOC-566, Vienna (1990).
- [2] INTERNATIONAL ATOMIC ENERGY AGENCY, Application of uranium exploration data and techniques in environmental studies, IAEA-TECDOC-827, Vienna (1995).
- [3] UNSCEAR, Sources and Effects of Ionizing Radiation, United Nations Scientific Committee on the Effects of Atomic Radiation 1993 Report to the General Assembly, with Scientific Annexes, United Nations, New York (1993).
- [4] GREEMAN, D. J., ROSE, A. V., JESTER, W. A., Form and behaviour of radium, uranium, and thorium in central Pennsylvania soils derived from dolomite, *Geophysical Res. Lett.* 17 (1990) 833-836.
- [5] BARIŠIČ, D., Dose Rate Conversion Factors, Soil Thickness and their Influence on Natural Background Dose Rate in Air Above Carbonate Terrains, *J. Environ. Radioactivity*, 31 1 (1996) 51-70.
- [6] BECK, H.L., DE PLANQUE, G., The radiation field in air due to distributed gamma-ray sources in the ground, Health and Safety Laboratory, U. S. Atomic Energy Commission, HASL-195, New York (1968).
- [7] DICKSON, H.W., KERR, G.D., Dose rates from plane sources of gamma rays, *Health Phys.* 29 (1975) 131-136.
- [8] BECK, H.L., Exposure rate conversion factors for radionuclides deposited on the ground, Environmental Measurements Laboratory, U. S. Department of Energy, EML-308, New York (1980).
- [9] KOCHER, D.C., SJOREEN, A.L., Dose-rate conversion factors for external exposure to photon emitters in soil, *Health Phys.* 48 (1985) 193-205.
- [10] MURRAY, A.S., AITKEN, M.J., Analysis of low-level natural radioactivity in small mineral samples for use in thermoluminescence dating, using high-resolution gamma spectrometry, *Int. J. Appl. Radiat. Isot.* 39 2 (1988) 145-158.



RADIOECOLOGICAL MAPPING OF THE TERRITORY OF BELARUS ON THE BASE INFORMATION OF RADIATION MONITORING

M.G. GUERMENTCHUK, O.M. ZHUKOVA,
E.D. SHAGALOVA, I.I. MATVEENKO
State Committee for Hydrometereology,
Minsk, Belarus

Abstract

The accident at the Chernobyl nuclear power plant (NPP) is the largest technogenic accident of our time. The global consequences of this accident for the whole mankind will be of a larger significance with the course of time. An important problem which arose during the period following the accident was the evaluation of radioactive contamination of the territory of Belarus and the creation a specific monitoring system. Although the radioactive contamination caused by the Chernobyl accident affected the whole world, Belarus was subjected to the most intensive radioactive contamination. Around 23% (46 450 km²) of the territory of Belarus was subjected to more than 37 kBq/m² contamination by caesium-137. There are 27 cities and more than 3600 populated districts with a total population of 2.2 millions which were contaminated. The preparation of maps of the distribution of iodine-131 according to the situation on 10 May 1986, and ruthenium-106 and cerium-144 for 30 May 1986 has been carried out. Every three years, based on the results of the complex examination, maps of caesium-137, strontium-90 and plutonium isotopes in the soil are issued. Because of the non-uniformity of the radioactive contamination, 350 thousands of personal plots of land are examined, and radiation passports issued to their owners. This measure was taken for reasons of protection as well as an effort to reduce the dose loads, thus increasing the safety of the residents of the contaminated territories.

1. THE RADIATION MONITORING SYSTEM APPLIED IN BELARUS

In Belarus, radiation monitoring includes measurements in: atmospheric air, soil and surface water. At present, for the entire territory of Belarus, a broad network of the regular observation points are in operation. These are: 55 stations for power measurement of exposition gamma-emanation dose; 25 control points of radioactive pollution from the atmosphere; 6 control points of radio-dopi's content in the air; 181 reference sites for the study of radiation situation dynamics; 18 landscapes and geochemical grounds for the study of radionuclides migration in the soil; 5 control sites in the big rivers of Belarus for the radionuclides content of the surface waters.

All environment radioactive contamination data were stored in an automated database and processed using the geo-information system RECALL. It is used to estimate and forecast the situation and deduce the living conditions of a given area. The most complicated situation was observed during the first period after the Chernobyl nuclear power plant (NPP) accident, due to the great quantity of the deposited short-lived radionuclides and the radionuclides with half-lives of up to 1 year. It was suggested that the methodical approaches in evaluating the contamination of the territory of the Republic with these radionuclides should be done through the preparation of the reconstruction maps. The work on remediation of irradiation doses received by the population during the first few days after the accident needs to be continued for the planning and realization of preventive and medical measures.

2. THE RECONSTRUCTION AND MAPPING OF I-131, CE-144 AND RU-106 CONTAMINATION IN APRIL-MAY 1986

As a result of air movements to the north-western, northern and north-eastern directions during the initial period after the accident, a significant increase of the exposition dose rate was registered practically in the whole territory of Belarus. The levels of radioactive contamination by

short-lived iodine-131 in many regions of the Republic were so high, that the resulting irradiation of millions of people was considered as period of "iodine impact" (Fig. 1).

In April-May 1986, the highest levels of iodine-131 fall-out were registered in the nearest 10-30 km zone in the Bragin, Khoyniki, Narovlya areas of the Gomel region, where the content of iodine-131 in the soil reached 37 000 kBq/m² and in some cases even more. The exposition dose rates of the gamma-radiation were 25-100 mR/h. In the Chechersk, Kormyany, Buda-Koshelev, Dobrush areas, the levels of contamination reached 18 500 kBq/m². In the south-western regions, that is in the areas of Elsk, Lelchitsy, Zhitkovichi, Petricov of the Gomel region, and Pinsk, Luninets, Stolin areas of the Brest region, were significantly contaminated. High levels of contamination were also registered in the north of the Gomel and the Mogilev areas. For example, in a number of places of the Vetka area of the Gomel region, the content of iodine-131 in the soil was more than 20 000 kBq/m². In the Mogilev region, the highest contamination by iodine-131 was registered in the populated areas of the Cherkov and Krasnoàolye areas, where the level reached 5550-11 100 kBq/m².

The high level of contamination by iodine-131 has resulted in large doses of irradiation, first of all, on thyroid gland, that gave rise in the future to a significant increase of its pathology. As of January 1995, the number of thyroid cancer cases in adolescents was 379. For comparison, only 4 cases were registered in January 1986. However, as noted earlier, the contamination registered in the initial period after the accident was not only by iodine-131 but also by such short-lived radionuclides as molybdenum, technetium, lanthanum, barium, radioactive noble gases (xenon, krypton). This has caused high doses of irradiation in the population, which should be taken into account in evaluating values of received doses by the population, living in contaminated territories, those evacuated from the evacuation zone and personnel who participated in the elimination of the consequences of the accident.

The reconstruction of the distribution of iodine-131 according to the situation on 10 May 1986, ruthenium-106 and cerium-144 on 30 May 1986 has been carried out. At the initial stage of the accident, the main contribution to the contamination of the natural environment and the formation of dose loads on the population were the long-lived radionuclides caesium-137 (30 years), strontium-90 (29 years), plutonium-238 (88 years) plutonium-239 (24000 years), plutonium-240 (6537 years), plutonium-241 (14,4 year), caesium-134 (2 years), and the short-lived iodine-131 (8 days), lanthanum-140 (40 hours), neptunium-239 (2 days), barium-140 (13 days), molybdenum-99 (66 hours). Strontium-89 (50 days) including the number of radionuclides with the periods of half-lives up to 1 year (cerium-144: 284 days, ruthenium-106: 368 days).

The work on remediation of irradiation doses, received by the population in the first days after the accident needs to be continued for planning and realization preventive and medical measures. Radioactive releases outside the area of Unit-4 have resulted in significant contamination of distant districts, populated areas and water bodies. Increase of radioactivity as a result of the Chernobyl NPP accident has been registered at a distance of ten thousands of kilometers from the place of the accident.

3. PRESENT ESTIMATION OF CS-137, SR-90 AND PU-238, -239, -240 CONTAMINATION IN THE TERRITORY OF BELARUS AND CS-137 FORECAST

Data on environment Cs-137, Sr-90 and Pu-238, -239, -240 contamination are stored in an automated database and are processed using the geo-information system RECASS. This information is used to estimate and make forecasts of the situation and the expected living conditions (Figs. 2-5). In Belarus 46 450 km² of the territory were contaminated with Cs-137, where the content in the soil was equal to more than 37 kBq/m². Twenty seven cities and more than 3600 populated areas with a total population of 2.2 millions, which is more than 1/5 of the population of Belarus, were affected. As a result of the Chernobyl NPP accident, the Gomel, Mogilev and Brest regions appeared to be the most contaminated.

РАСПРЕДЕЛЕНИЕ ЙОДА-131 В ПОЧВЕ НА ТЕРРИТОРИИ РЕСПУБЛИКИ БЕЛАРУСЬ

по состоянию на 10 мая 1986 года (реконструкция)

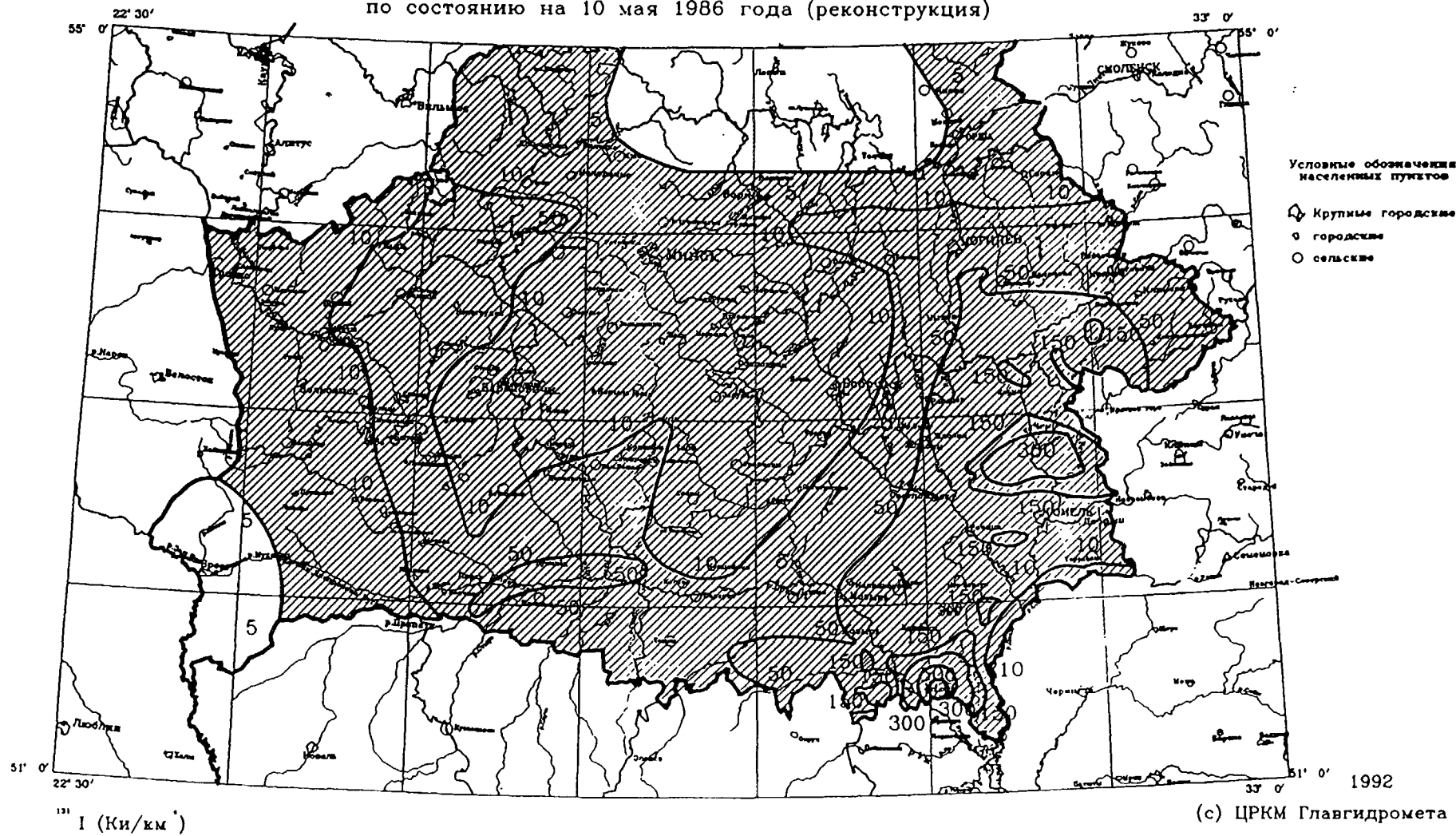


FIG. 1. Radioactivity contamination of I-131 in the soil of Belarus (10 May, 1988).

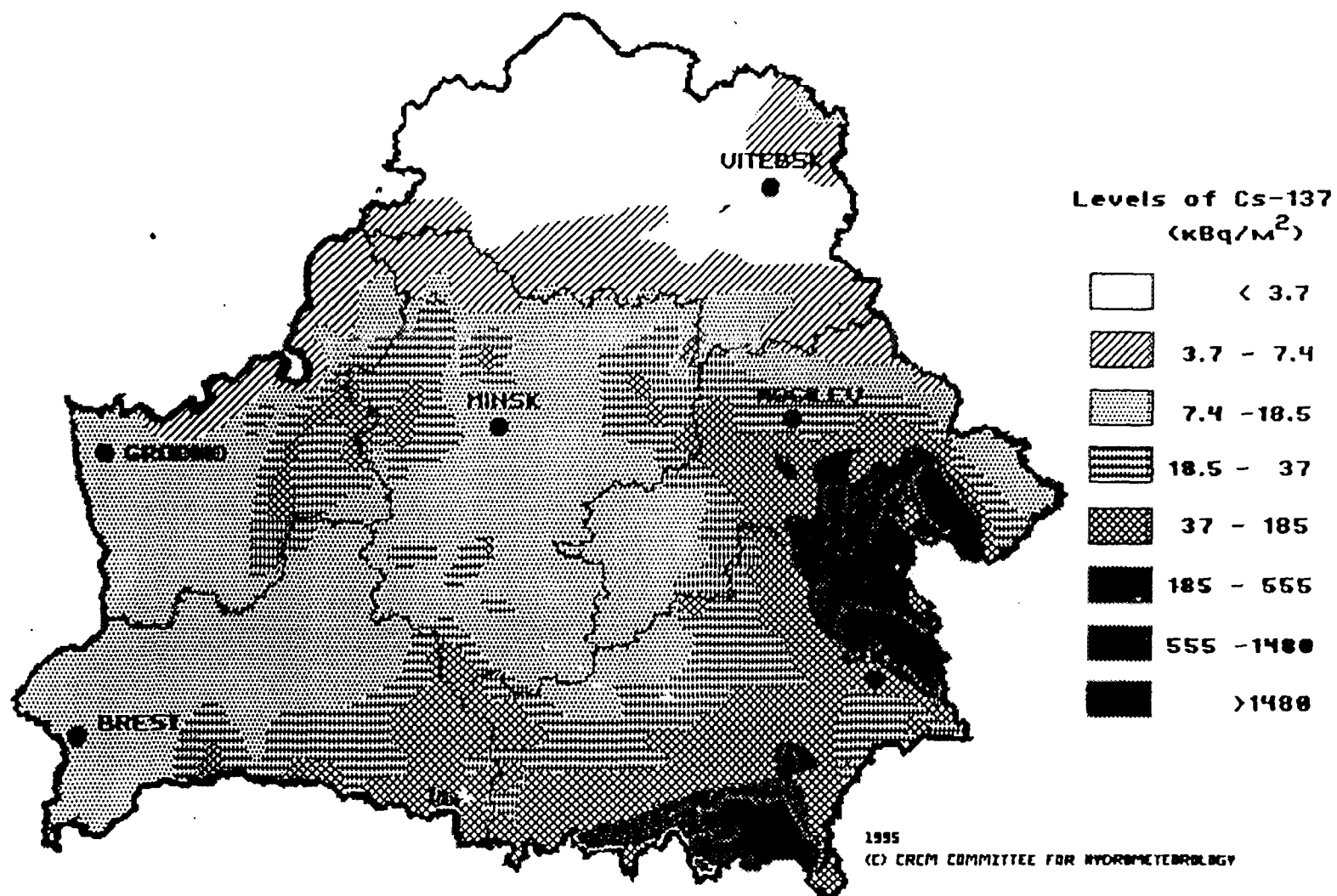


FIG. 2. Radioactivity contamination of Cs-137 in the soil of Belarus (1 January, 1995).

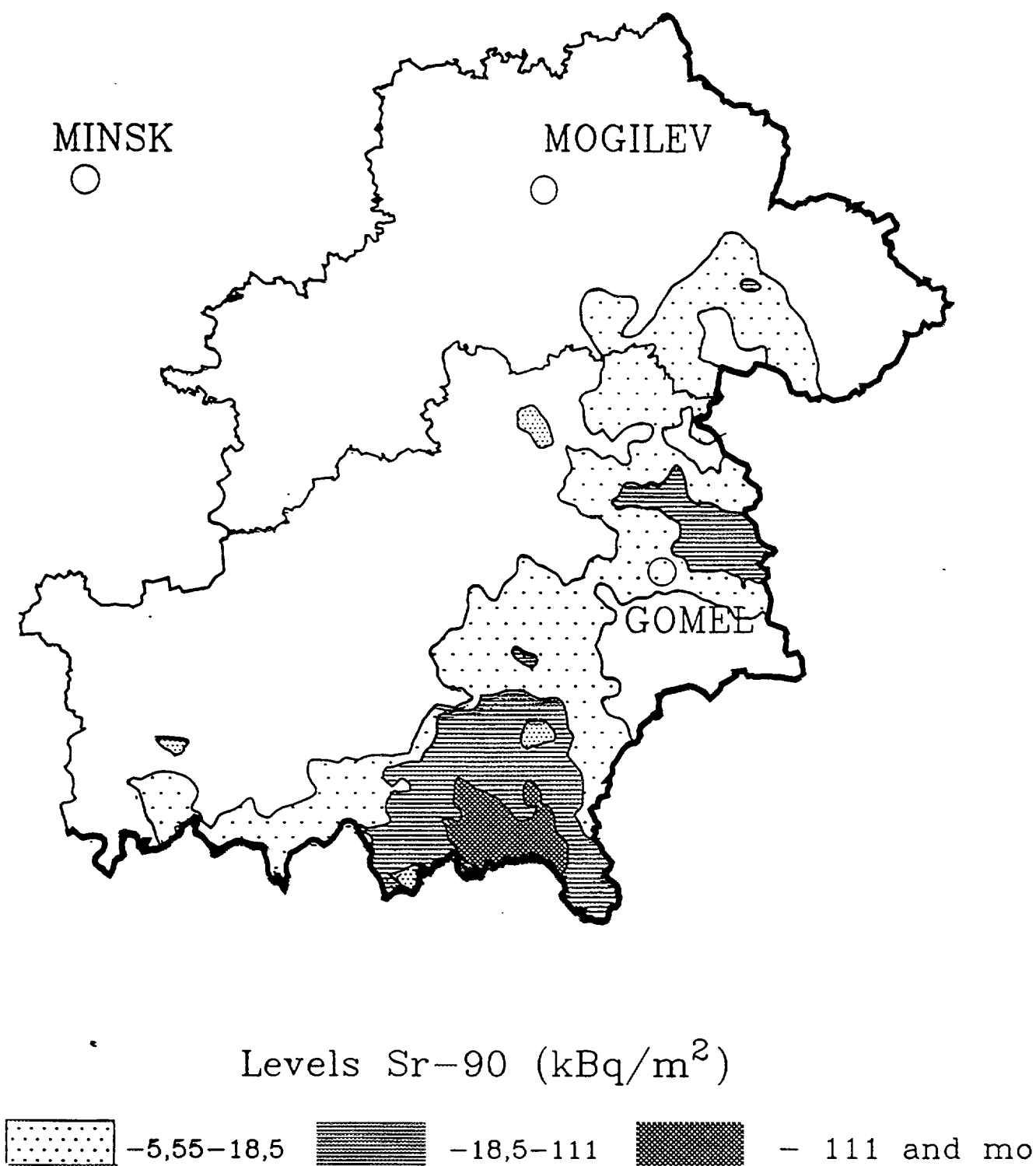


FIG. 3. Radioactivity contamination of Sr-90 in the soil of the Gomel and Mogilev Regions of Belarus (1 January, 1995).

There are cases, within the same populated area, where clean (uncontaminated) sites are found in the neighbourhood of highly contaminated places. The populated area Kolyban of the Bragin area of the Gomel region can be taken as an example, where the value of contamination by caesium-137 is in the range of 170 to 2400 kBq/m^2 . The maximum level of caesium-137 in the soil of the populated areas of the nearest zone to the Bragin area was 2600 kBq/m^2 , and in the distant zone, of some 250 km away, for instance, in the populated area Chudyany of the Chericov area in the Mogilev

region, levels of 51000 kBq/m² were registered. In the Brest region, in the south-eastern part, in 6 regions the content of caesium-137 in the soil range from 37 to 185 kBq/m², and the maximum levels reach 400 kBq/m². In the Minsk, Grodno areas and 4 populated areas of the Vitebsk region, the content of caesium-137 in the soil amounts to 37 kBq/m². In the other territories of Belarus, the levels of contamination of the soil by caesium-137 are higher in comparison to the values registered before the accident. Only in the north-western regions of the Vitebsk region they are comparable to the global fall-out levels.

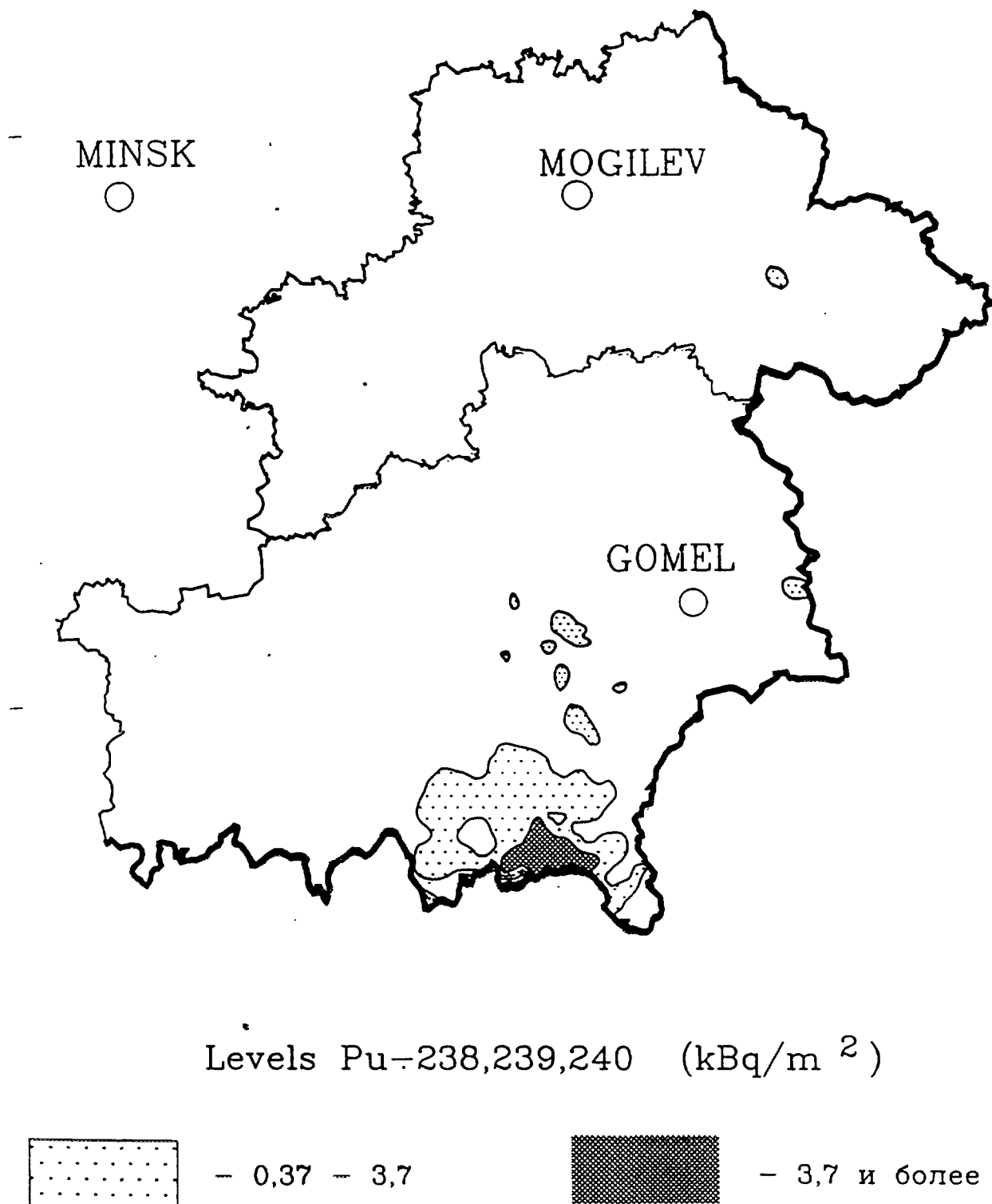


FIG. 4. Radioactivity contamination of Pu-238, 239, 240 in the soil of Belarus (1 January, 1995).

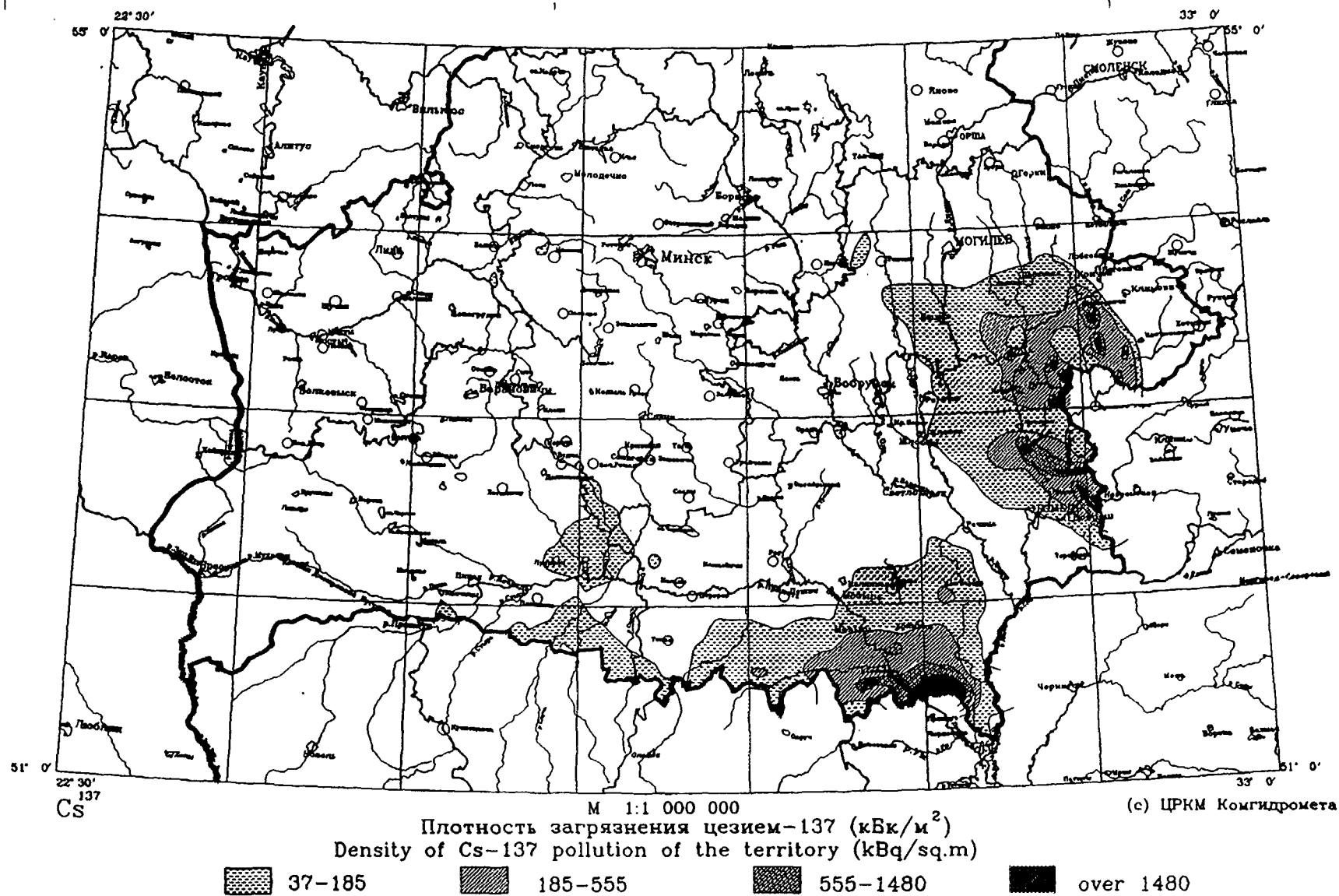


FIG. 5. Map of radiation projection of the area of the Republic of Belarus for 2016. Concentration of Cs-137 detected in the territory (kBq/m^2).

The contamination of the territory of the Republic with Sr-90 has a more local character. The levels of contamination of the soil with Sr-90 of more than 6.5 kBq/m² are found over an area of 21 100 km², i.e. 10% of the total area of the Republic. The maximum levels of Sr-90 in the soil in the populated areas of the nearest zone are found within the 30-km zones of the Chernobyl NPP, in the Khojniki area of the Gomel region, with 1800 kBq/m². The highest contents of Sr-90 in the soil of a distant zone (250 km away), were registered in the Cherikov area of the Mogilev region, were they amounted to 29 kBq/m². In the northern part of the Gomel region, Vetka area, amounts of 137 kBq/m² were registered.

The contamination of the soil by the plutonium isotopes amounting to more than 0.37 kBq/m² covers an area of nearly 4000 km², about 2% of the area of the Republic. These territories are predominantly located in the Gomel region and the Chechersk area of the Mogilev region. Contamination of the soil by plutonium isotopes of 0.37 up to 3.7 kBq/m² reached the highest levels in the Bragin, Narovlya, Khojniki, Rechitsy and Dobrush, Loev areas of the Gomel region. The contents of plutonium in the soil of 3.7 kBq/m² is characteristic for 30-km zones of the Chernobyl NPP. The highest levels of plutonium isotopes in the soil were registered in the Massany populated area of Khojniki area with values of more than 111 kBq/m².

4. ATLAS ON CAESIUM CONTAMINATION OF EUROPE AFTER THE CHERNOBYL NUCLEAR POWER PLANT ACCIDENT

The European Commission and Belarus, Ukraine and the Russian Federation took part in the preparation of the Atlas on caesium contamination of Europe after the Chernobyl NPP accident. The main purpose of the Atlas is:

- to present information on the spatial distribution of deposited Cs-137;
- to indicate how the levels of Cs-137 contamination after the Chernobyl NPP accident have increased compared to global deposition;
- to identify relatively "clean" territories the contamination of which is mainly related to global fallout;
- to present information on radioactivity contamination in Europe to scientist in different fields;
- to allow the estimation impact of accident.

A geographic information system (GIS), ARC/INFO, has been used for the preparation of the Atlas on caesium contamination in Europe. The analysis of Cs-137 data was the main problem. Our position related to the analysis of Cs-137 data, using ARC/INFO, should include the re-evaluation of:

- maximum values, quantity,
- initial range of isolines,
- number of points with absolute values of less than min-isolines.

The analysis of the absolute values should be carried allowing for the data on the global contamination around the points, which are dubious. The map of distribution of the contamination should be constructed, using various methods in case of different parameters. On the basis of the expert evaluation, the best method of interpolation of mapping should then be chosen. A GIS system will allow the evaluation of the distribution of the radioactive contamination in the territory of Europe and construct the isolines of the contamination by various methods. The following methods of interpolation are used:

- IDW (methods of inverse radii),
- TIN (methods of Delane triangulation),
- Kriging (methods of Kriging).

5. CONCLUSION

In connection with the presentation noted above it is necessary to emphasize the increased role of radiation control and monitoring of the contaminated territories, the result of which will permit the observation of changes to reveal additional sources of contamination, as well as to predict further development of the radiation-ecological situation. This forecast should be used as the basis for formulating the policy of protective measures.

BIBLIOGRAPHY

ASTAKHOVA, L., GERMENCHUK, M., NEDVECKAITE, T., FILISTOVICH, V., The particularity of human thyroid system radiation exposure by radioactive iodine isotopes in Byelorussia and Lithuania after the Chernobyl accident and analysis of possible medical diseases, *Visuomenes sveikata: abartis ir atitis Public health: present and future*, Kaunas (1993) p. 79-81.

GERMENCHUK, M., ZHUKOVA, O., SHAGALOVA, Eh., MATVEENKO, I., Distribution of Radioactive Iodine-131 (reconstruction) in the Territory of the Republic of Belarus, evaluation of Radiological Situation During the First Days after the Accident at ChNPP, Republican Conference "Hygienic and Psychological-Social Aspects of Accident at ChNPP", Gomel (1993).

GERMENCHUK M.G., MATVEENKO I.I., ZHUKOVA O.M., Assessment of radiation situation in the territory of the Republic of Belarus under conditions of pollution after the catastrophe in the Chernobyl nuclear power plant with the use of GIS RECASS, The Canadian conference on GIS — 1994, Proceedings, vol. 2. Ottawa, Canada (1994) p.1269-1280.

MATVEENKO, I.I., ZYUKOVA, O.M., GERMENCHUK, M.G., Dynamics of the radiation and rehabilitation of the environment of the Republic of Belarus territory after the catastrophe in Chernobyl NPP, Nuclear and hazardous waste management Spectrum'94, American Nuclear Society, Inc., Atlanta, GA, Illions 60525 USA, (1994) p. 2419-2424.

MATVEENKO, I.I., ZHUKOVA, O.M., GERMENCHUK M.G., SHAGALOVA, E.D., State and prognosis of radiation situation in the territory of the Republic of Belarus, Belarus — Japan Symposium "Acute and Late Consequences of Nuclear Catastrophes: Hiroshima — Nagasaki and Chernobyl, 3-5 October, Minsk (1994) p.173-183.

ZHUKOVA O.M., MATVEENKO I.I., GERMENCHUK M.G., Dynamics of radioactive pollution of atmospheric air on the territory of Belarus after the Chernobyl catastrophe, Proceedings of the Second International Meeting on Low-level Air Radioactivity Monitoring. 14-18 February 1994, Warsaw (1995) p.83-91.

**NEXT PAGE(S)
left BLANK**



MAPPING OF POST-CHERNOBYL ENVIRONMENTAL POLLUTION IN POLAND

R. STRZELECKI, S. WOLKOWICZ, P. LEWANDOWSKI

Polish Geological Institute,
Warsaw, Poland

Abstract

The accident at the Chernobyl nuclear plant considered as one of the greatest ecological disasters in the 20th century. It is responsible for a very negative public concern on the Polish nuclear power industry and became one of the most important reasons for stopping the construction of the first Polish nuclear power plant located in Żarnowiec near Gdansk (N Poland), although the construction has reached an advance stage. Never the less the feeling of strong pollution over the territory of Poland with post-Chernobyl radioisotopes and their negative impact on the environment and human health still dominates the country. Very few data have been released to the public up till the year 1990, mostly in the form of result of measurements carried out by the Central Laboratory for Radiological Protection that supported the population in their feeling of the negative impacts of the Chernobyl accident for the environment. Polish Geological Institute proposed in 1990 to the Ministry of Environmental Protection, Natural Resources and Forestry starting of a big mapping programme in order to recognize the spatial distribution of Cesium- and natural-radioisotopes using the equipment and work methodology previously applied in gamma-spectrometric survey for uranium prospection. Upon acceptance by the Ministry and a period of experimental studies, the field works have been started in 1992 and completed in 6 months period. The Cs distribution map at scale of 1:750 000 has been published in 1993. In 1994 more detailed studies have been carried over "anomalous" areas where besides detailed mapping 10 000 measurements also geochemical profiles used for describing Cs distribution in the soil depth profile and Cs bioaccumulation in the vegetation cover have been made. The above works are still in progress. Data obtained from the above studies allowed the compilation of maps on the distribution of natural uranium, thorium and potassium as well as maps of gamma-dose rate for the territory of the country.

WORK METHODOLOGY

Measurements were made applying the in situ methodology using the field gamma spectrometer GS-256 produced by "Geofizyka" Brno, Czech Republic. The equipment was calibrated based on the calibration pads in Bratkowice near Příbram, Czech Republic. Detailed work methodology applied for mapping has been presented in the IAEA Technical Committee meeting held in Vienna in November 1993 [1].

About 20 000 measurements have been made for the whole territory of the country. Measurement point have been located each 1000 m and the measurements have been made along N-S oriented profile lines spaced each 15 (about 17 km). In the case of counting above 5500 impulses in "Total Canal" the measurements have been made each 500 m.

In 1994 additional measurements have been made over areas characterised with Cs concentration above 15 kBq/m² what gave the density of observation equal to 1 point/1 km². Geochemical profiles of the soil and at the same points studies of Cs bioaccumulation in the plant cover have been made in the area of Opole (SW Poland) and Bialystok (NE Poland) regions. Analyses of Cs distribution in soils and in plants have been performed by the Central Laboratory for Radiological Protection, Warsaw using semiconductor detectors HPGE working together with Canberra-90 spectrometer. Soil analyses including granulometric composition, organic carbon content, pH in water and In KCI, base saturation of soils, sorption capacity have been made in soil laboratory.

RESULTS OF MAPPING

Average Cs content for the territory of Poland calculated on the basis of 19 528 measurements is equal to 4.7 kBq/m² with standard deviation of 5.5 kBq/m². The maximum observed value was equal to 96 kBq/m².

The biggest as to the area and highest as to intensity of Cs pollution is reported from SW part of Poland — East part of Sudetes Foreland and Silesia Lowland (Fig. 1 [2]). The above concentration is lying within the zone of pollution running from SW direction towards NE from the area of Polish-Czech border in the region of Kłodzko Valley up to the Warsaw region. Few areas characterized with higher level of pollution can be distinguished within this zone out of which the biggest anomaly is described as Opole anomaly and is covering the area of 4000 km² and showing the Cs concentration up to 96 kBq/m². Detailed studies carried within this anomaly showed presence of few smaller anomalous fields. Taking as the basis Cs concentration of 37 kBq/m² six separate anomalies can be distinguished covering in total the surface of 620 km² out of which the biggest one is located NE from Opole in the region of Olesno town (Fig. 2).

Radomsko and Warsaw anomalies are covering smaller areas and are showing lower Cs concentration. Increased Cs concentrations have been also reported from E part of the country - near to Polish/Byelorussia border where over small area of about 3 km² near Milejczyce village Cs concentrations higher than 75 kBq/m² and reaching even 112 kBq/m² has been recognized. The above anomaly is the part of long zone of pollution running from the area of Mazurian Lake District (N Poland) up to Siedlce Highland (E Poland) characterised with irregular shape of anomalous fields with dominating Cs concentration varying from 8–15 kBq/m², only locally reaching 25–30 kBq/m². Small anomaly covering the area of about 5 km² and showing Cs concentration of about 50 kBq/m² has been reported from NW Poland (W of Szczecin).

STATISTICAL ANALYSIS

Analysis of Cs average concentration made respecting the applied administrative division of the country — 49 voyevodships showed, that the highest Cs concentrations equal to 16.6 kBq/m² are reported from Opole voyevodship region (SW Poland), followed by Ostrołęka voyevodship (NE Poland) with Cs pollution value equal to 8.3 kBq/m². In Cs concentration higher than average value for the country equal to 4.7 kBq/m² is observed on the territory of 20 voyevodships. Distribution of frequency of Cs pollution over the territory of Poland is lognormal and does not show any significant disturbances. Its modal class is in the range of 1.7–3.5 kBq/m² (Fig. 3.A). More detailed where analyses distribution of Cs pollution in each voyevodship has been studied showed, that the above observed Cs distribution is the result of interference of few natural factors which impacted the spatial diversification of Cs concentration in environment over the Polish territory. Detailed analyses were based on data obtained from the voyevodships showing lowest pollution (Koszalin voyevodship) as well as highest pollution (Opole and Ostrołęka voyevodship) and from Warsaw voyevodship showing increased concentrations.

The distribution of Cs concentration over the area of Koszalin voyevodship is bimodal and slightly asymmetric (Fig. 3.B). Most probably it reflects the results of interference of 2 populations of Cs pollution — one of distribution similar to the normal and with average concentration value near to 0.6 kBq/m² and second characterised with normal distribution but showing higher standard deviation and of average value close to 3 kBq/m². The first one corresponds to Cs pollution related to pre-Chernobyl period and is the result of military nuclear weapon tests carried in the years 1959–1963 while the second one is the result of fall of radioactive dust migrating in the high atmospheric strata. After compilation the above distribution becomes unimodal, close to normal and showing slightly positive skewness (Fig. 3.C) with modal class of 1.2–2.2 kBq/m². It reflects the current Cs concentration background in Polish soil.

Cs frequency over the area of Warsaw voyevodship is quite different. It is bimodal and slightly asymmetric but its modal classes are varying between 5.2–7 and 9.8–11.6 kBq/m² (Fig. 3.D). The above distribution is most probably the result of interference of 2 populations of Cs, both showing distribution close to normal and average values dose to 3.5–4 and 12 kBq/m² (average values of the 2 populations are slightly shifted with respect to modal classes as in the case of interference of 2 populations occurring of the middle class is responsible for increasing of observed frequencies compared to real frequencies).



FIG. 1. Map of Caesium concentration in Poland.

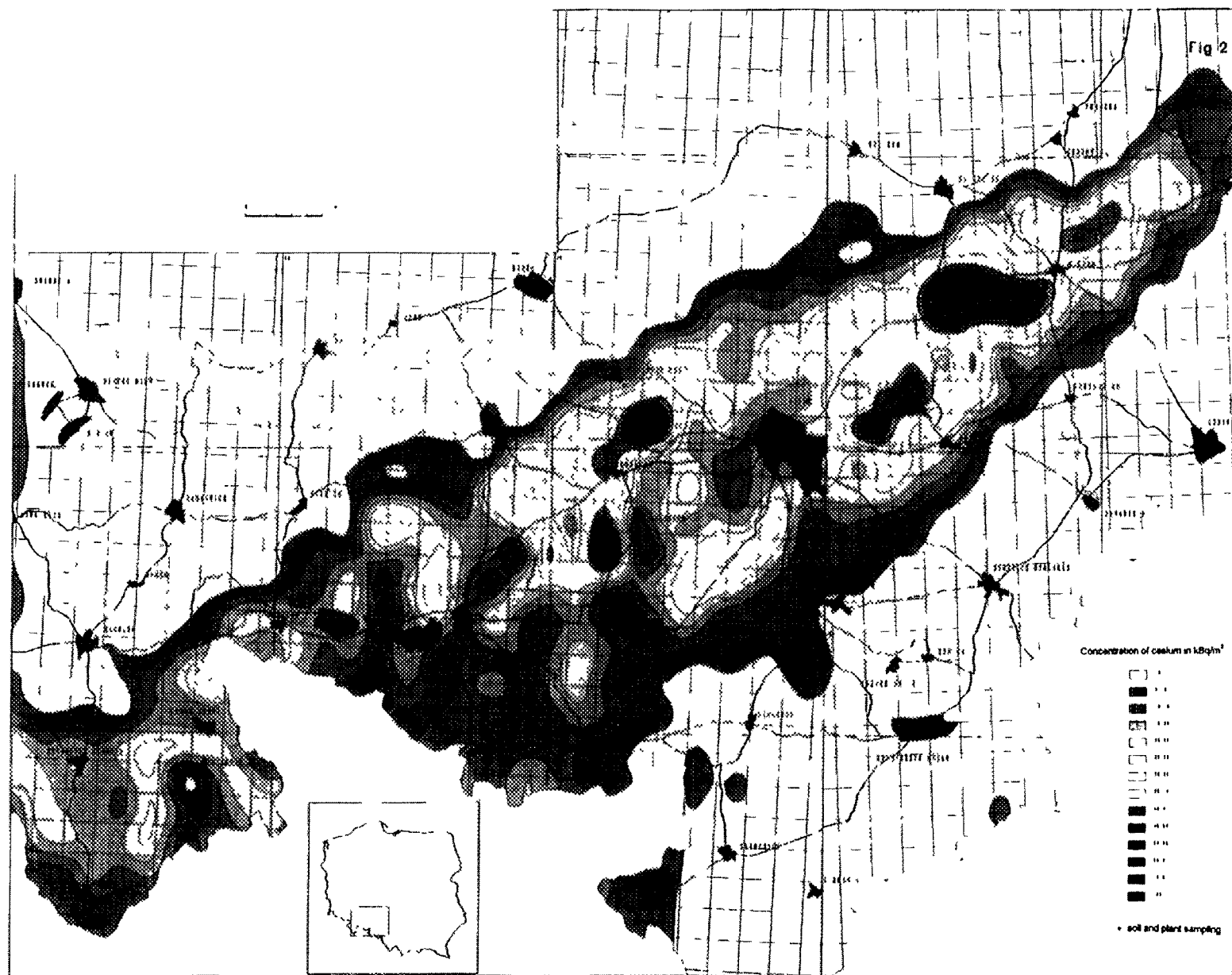


FIG. 2. Map of Caesium concentration in Opole Region.

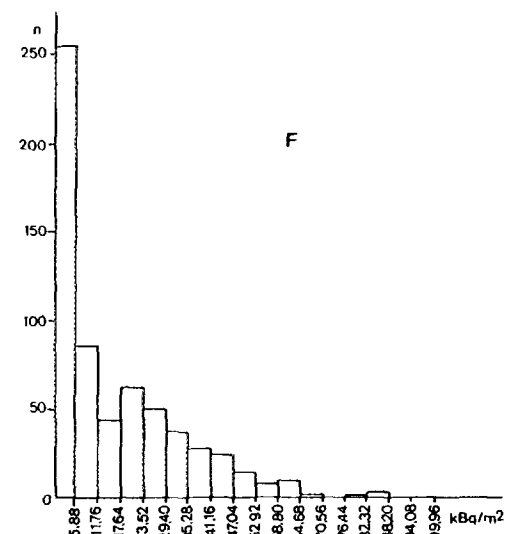
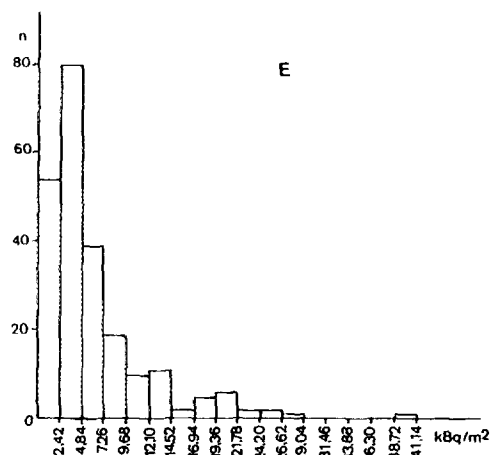
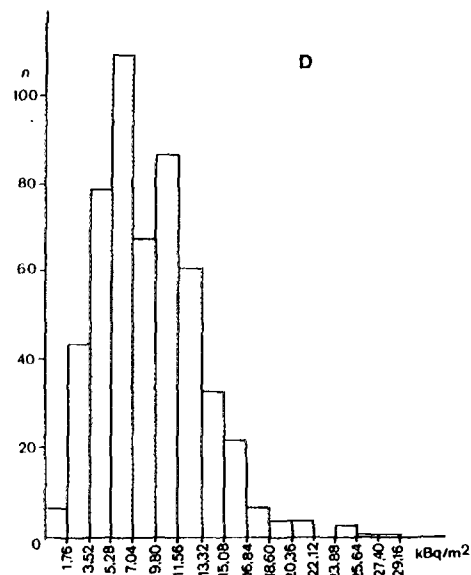
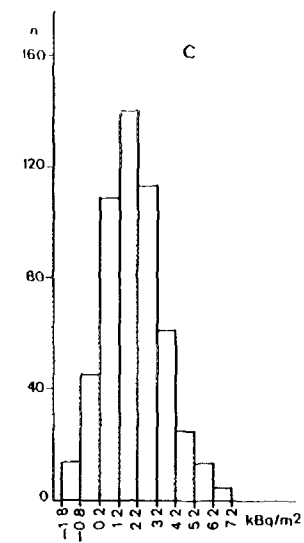
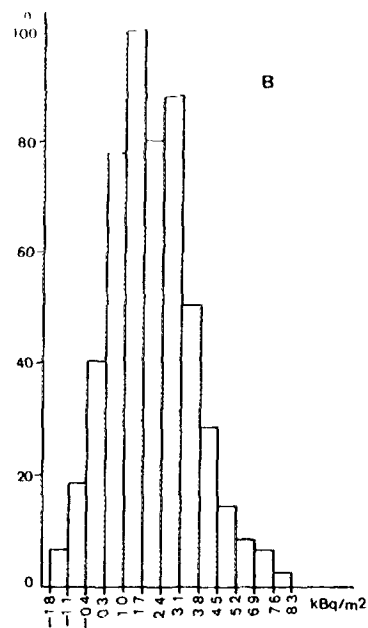
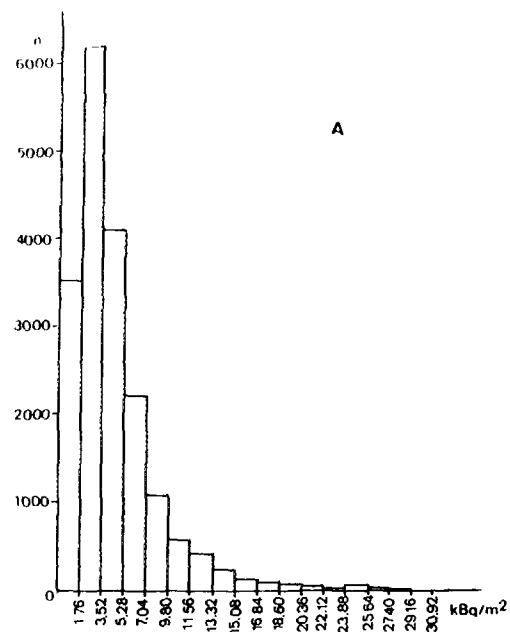


FIG. 3. Histograms of the distribution of cesium concentrations.

A - in Poland; B,C - in Koszalin voivodship; D - in Warsaw voivodship;
E - in Ostrołęka voivodship; F - in Opole voivodship

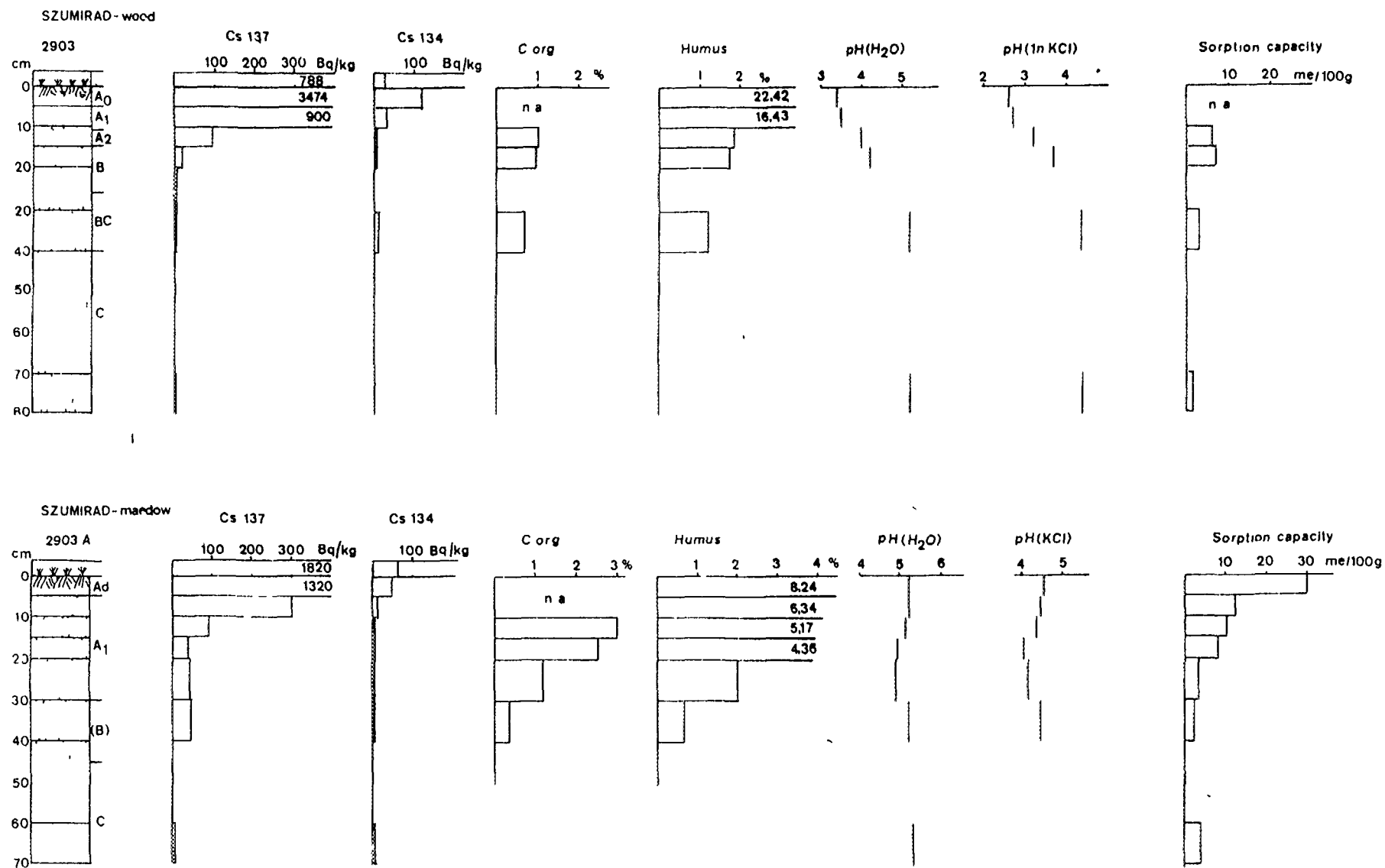


FIG. 4a. Distribution of Caesium radioisotopes in soil profiles.

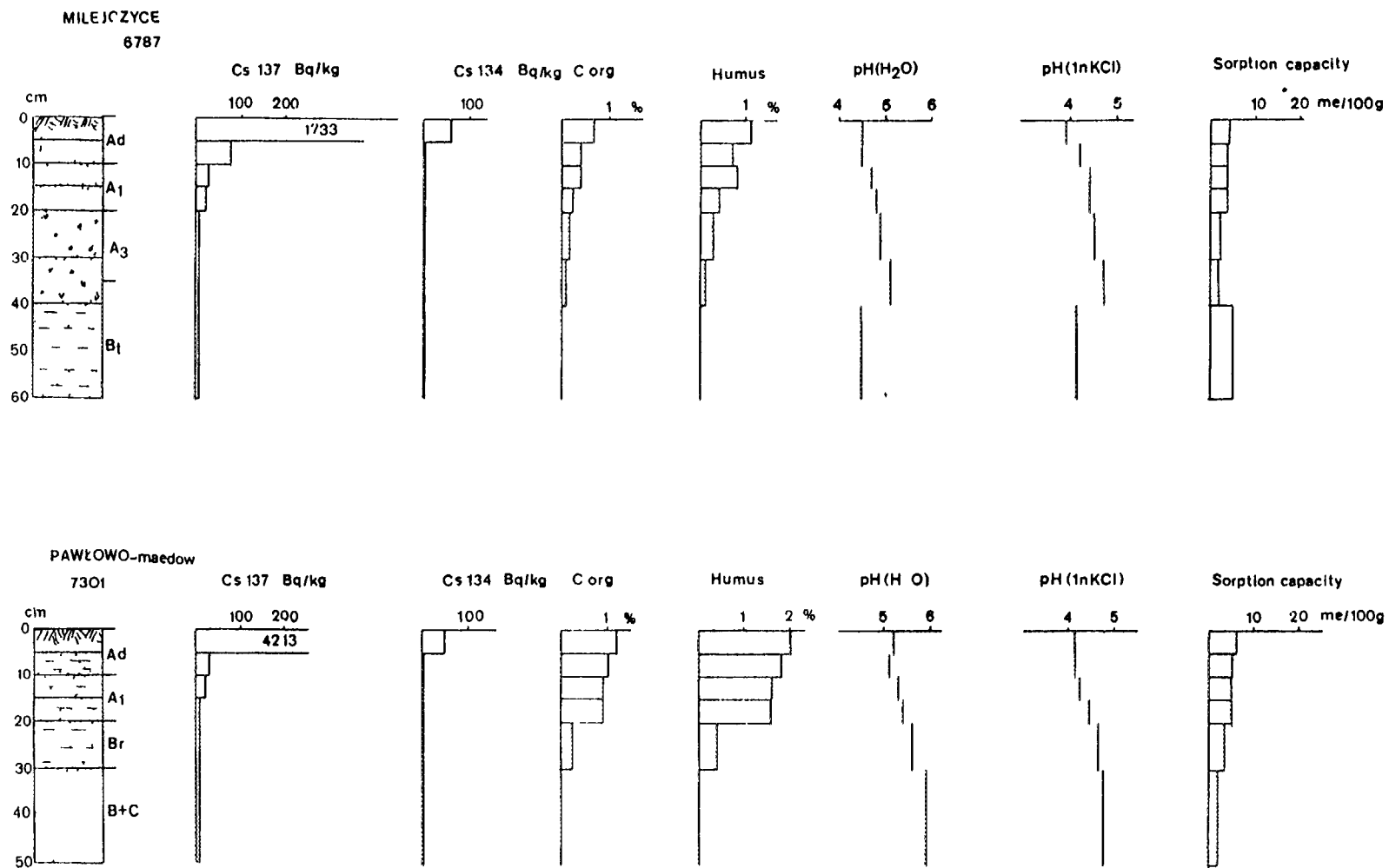


FIG 4b Distribution of Caesium Radioisotopes in soil profiles.

It can be assumed that the first population was formed, similarly as over the area of Koszalin voyevodship as the result of fallout of the radioactive dust migrating in high strata of atmosphere while the second as the result of radioactive fallout of dust migrating from the Chernobyl area in low atmospheric strata.

Distribution Cs concentration over the area of Ostroleka and Opole voyevodships are strongly disturbed, bimodal and are showing strong positive skewness (Fig. 3.E and F).

The 3–4 kBq/m² class is dominating over the area of the 2 mentioned voyevodships. Population of average Cs concentration equal to 20 kBq/m² is observed from the area of Ostroleka and Opole voyevodships and additional small population of average value dose to 84 kBq/m² is observed from the territory of Opole voyevodship. Distribution of frequency of above population is not well determined and it can be supposed, that it was formed as the result of rain fall containing radioactive dust. Their concentration and distribution is depending from intensity of the rain fall.

CESIUM GEOCHEMICAL DISTRIBUTION

Studies have been carried in the area of Opole anomaly — 12 profiles and 2 profiles in E Poland (Milejczyce village). Besides one, all profiles were running across meadows and forests in the soil cover not disturbed with agricultural activities. All the profiles (Figs 4a and 4b) are showing the presence of 90 % of Cs isotopes in the near-surface 5–10 cm zone, despite 8 year period from the date of Cs deposition. Cs concentration is dropping with the depth and below the humus zone Cs is found only in trace amounts. No correlation is observed between Cs and morphogenetic type of soil and its granulometric composition. Analysis of correlation indicator showed that pH H₂O and pH in KCl are showing negative correlation while significant correlation was observed between ¹³⁷Cs and ¹³⁴Cs content and organic carbon and humus content. The above high contents with small volumes of silty-fractions are the main factors deciding on sorption capacity of the soil, showing significant correlation with Cs. The above indicates the presence of adsorption process and immobilization of considerable amount of Cs with humus and organic carbon. Only small part of Cs is transported into deeper parts of the soil profile, most probably due to process of mechanical transportation by for example migrating surface waters.

Sample collected from the uppermost 25 cm zone of the cropland is showing Cs concentration of 400 Bq/kg. No Cs was found deeper what indicates mechanical mixing in the uppermost zone and absence of geochemical migration.

CESIUM BIOACCUMULATION IN THE PLANTS

Cs concentration studies carried by Central Laboratory for Radiological Protection for vegetables, fruits, mushrooms in the period of 1986–1994 showed the highest Cs concentration in mushrooms (*Xerocomus badius*) equal to 374 Bq/kg, average for the 1994, in blueberries — average value for 1994–37 Bq/kg. The above values are average for the territory of the whole country and can be not considered as average values for the anomalous areas.

Cs concentrations from samples collected from grass meadows (*Poa pratensis*, *Festuca rubra*, *Dactylis glomerata*, *Holcus lanatus*, *Deshapsia caespitosa*) in November 1994 has been determined from 11 samples and showed varying concentration of ¹³⁷Cs from 14.8 to 2170 Bq/kg and ¹³⁴Cs from 0.6 to 77.8 Bq/kg. Generally relation between intensity of Cs concentration in soils and its concentrations in the vegetation cover can be observed but due to small number of samples difference of bioaccumulation by different plant species is difficult to determine.

CONCLUSION

Intensity of pollution of the territory of Poland with post-Chernobyl Cs isotopes is smaller than supposed after preliminary studies. Over 90% of the territory Cs concentration is not higher than 8 kBq/m². Concentration above 37 kBq/m² has been recognized only on the surface of 700 km². In the soil profiles 8 years after the accident 90% of Cs is found in the uppermost 10 cm of the soil. The migration is very slow and most probably related to mechanical transportation by precipitation waters. Type of the soil and its granulometric composition does not impact the Cs distribution. Correlation between Cs organic carbon and sorption volume has been recognized. Small geochemical migration of Cs eliminates possibility of pollution of underground waters while possibility of Cs bioaccumulation in plants with small roots is possible. Preliminary samples collected from grasses showed Cs concentration up to 2170 Bq/kg. Further biogeochemistry studies will be conducted in order to determine intensity of Cs bioaccumulation in different plants.

REFERENCE

- [1] STRZELECKI, R., WOLKOWICZ, S., LEWANDOWSKI P., "Use of Gamma Ray Spectrometric Survey for Radioecological Mapping in Poland", Application of uranium exploration data and techniques in environmental studies, IAEA-TECDOC-827, IAEA, Vienna (1995).
- [2] STRZELECKI, R., WOLKOWICZ, S., LEWANDOWSKI, P., Radioecological Maps of Poland, Part I (1993).

**NEXT PAGE(S)
left BLANK**



USE AND RESULTS OF THE AERIAL GAMMA MAPPING SYSTEM DURING THE INTERNATIONAL EXERCISE R.E.S.U.M.E. 95 (RAPID ENVIRONMENTAL SURVEYING USING MOBILE EQUIPMENT) IN FINLAND

Ch. BOURGEOIS, J. BRESSON, R. CHASTEL,
Th. CHIFFOT, L. GUILLOT, J.-C. KRUAJITCH, C. BERGEY
Commissariat à l'Énergie Atomique,
Centre d'études de Valduc/HELINUC,
Is/Tille, France

Abstract

The French Atomic Energy Commission (C.E.A.) has developed an aerial gamma mapping system called HELINUC. The acquisition of a gamma spectrum and at the same time the corresponding coordinates of the aircraft is performed by the equipment aboard a light helicopter or an aeroplane. The data acquired in flight are processed on the ground by a specialized computer data processing system. Within a few minutes the system can produce a map with artificial colours showing the levels of natural or man-made activity and then superimpose it on a topographic map. HELINUC can, within a few hours, elaborate a map of radioactivity of areas spread over several square kilometres up to several tens of square kilometres and identify the radioelements in the range from natural radioactivity to a serious accidental situation. HELINUC has been operational for about 12 years and is part of the French nuclear emergency preparedness in the event of a civil or military nuclear accident. In August 1995, the exercise RESUME 95 was arranged in Vesivehmaa, 150 kilometres north of Helsinki by the Nordic Nuclear Safety Project, EKO-3. The main objective of this exercise was to compare results from survey measurements from airborne, car-borne and in situ measurements on the ground. Different areas and routes had been defined for survey purposes, and artificial point sources had been hidden. The main results of this exercise, particularly those concerning the gamma mapping of the area called II, contaminated by the Chernobyl's fallouts and the hidden sources are presented here. The cartography of area II shows that the levels of ^{137}Cs reaches 100 kBq/m^2 in small spots and the average value more than 60 kBq/m^2 . In the research of hidden sources, we discovered a point-source of cobalt 60 the activity of which was only 25 MBq (0.7 mCi). The results obtained with the HELINUC system during this exercise prove that the methods using uranium exploration data and techniques are rapid, powerful and efficient techniques for measuring and controlling the radioactivity in the environment of industrial or nuclear sites.

1. PRINCIPLE AND DESCRIPTION

The Commissariat à l'Énergie Atomique has developed an aerial gamma mapping system called HELINUC. This system makes it possible to establish, within a few hours, a map of radioactivity for areas (several dozen to several hundreds of hectares) by identifying the radioelements present, in a range from level of natural radioactivity to that of man-made radioactivity resulting from a large scale accident.

1.1. Experimental device

The helicopter borne device is composed of a NaI detector containing 16.8 litres which is connected to a spectrometer for signal analysis, with 512 channels, ranging from 30 to 3000 keV. At the end of sample time (1 to 3 seconds), a computer records the spectrum plus the average helicopter position (X, Y, Z) during the measurement.

The helicopter's position (X,Y) is computed by a G.P.S. or a transponder system used in Finland. The flight altitude is always accurately measured with a radio-altimeter.

Remarks: Since January 1996, the positioning has been achieved by a differential GPS. The helicopter (AS-350/B1), belonging to the French company "HELIFRANCE" came to Finland especially for the exercise.

1.2. Data collection

For a detailed site analysis, the following parameters are required: pattern size (length of profiles and distance between profiles), altitude, flight velocity and sample time (two seconds in Finland).

1.3. Data processing

The data collected and stored on a Bernoulli disk are processed by a dedicated ground-based computer. On the basis of the flight data records, colour maps are processed and overprinted on topographic maps. Such maps provide, in a very short time, the positions of contaminated areas or lost point-sources, the contamination levels and the nature of the radioelements. In the event of a nuclear incident, this information could be handed over to competent authorities for use.

2. MEASUREMENTS PERFORMED DURING R.E.S.U.M.E. 95

The following tasks were specified by the organisers:

- Mapping of area 2 (6 km per 3 km), localised between two villages: Vesijako and Auttoinen: This area should be covered by 21 profiles of 6 kilometres, spacing of 150 metres.
- Mapping of area 3 (5 km per 1 km) and real time detection of hidden point sources.

Both areas had to be flown in one flight.

2.1. Hidden sources detection

During the survey of area 3, 15 point sources were hidden, of different natures and activities. Fly conditions were free but the time over the area restricted to *only one* hour. The detection of "traces" averages that sources have been detected, but their contributions are too weak to conclude about their attendance. The activity of the point source Co3 which has been detected on the road between areas 2 and 3 was only 25 MBq. The following table (Table I) shows the detection results for each source:

TABLE I. DETECTION RESULTS FOR EACH SOURCE

<i>Nuclide</i>	<i>Code</i>	<i>Activity (mCi)</i>	<i>Results after detailed data processing</i>
⁶⁰ Co	Co1	7	yes
⁶⁰ Co	Co2	9 (strongly collimated)	traces
⁶⁰ Co	Co3	0.7	traces
⁶⁰ Co	Co 4 à 9	1 à 2 mCi linear source (~ 200 metres)	yes, detection of linearity
¹³⁷ Cs	Cs1	77	yes
¹³⁷ Cs	Cs2	50 (strongly collimated)	no
¹³⁷ Cs	Cs3	7.5	traces ?
¹³⁷ Cs	Cs4	14.6	traces
¹⁹² Ir	I	15000	yes
⁹⁹ Tc	T	30	yes

The following figures presents some screen hard copies showing the detection of some sources. The $^{99}\text{Tc}_m$ source has been clearly detected on spectrum 764 by the 140 keV emission ray (channel 25, Fig. 1).

The Cs3 and Co1 sources of close activities (7.5 and 7 mCi) were localised at the same place (Fig. 2). The evolution of channel 190 (1173 keV) shows clearly the cobalt source. The attendance of an anomaly can be seen at channel 110 (662 keV), but it is impossible to conclude about the attendance of a caesium source because these photons should have been emitted by the cobalt source and scattered by the atmosphere.

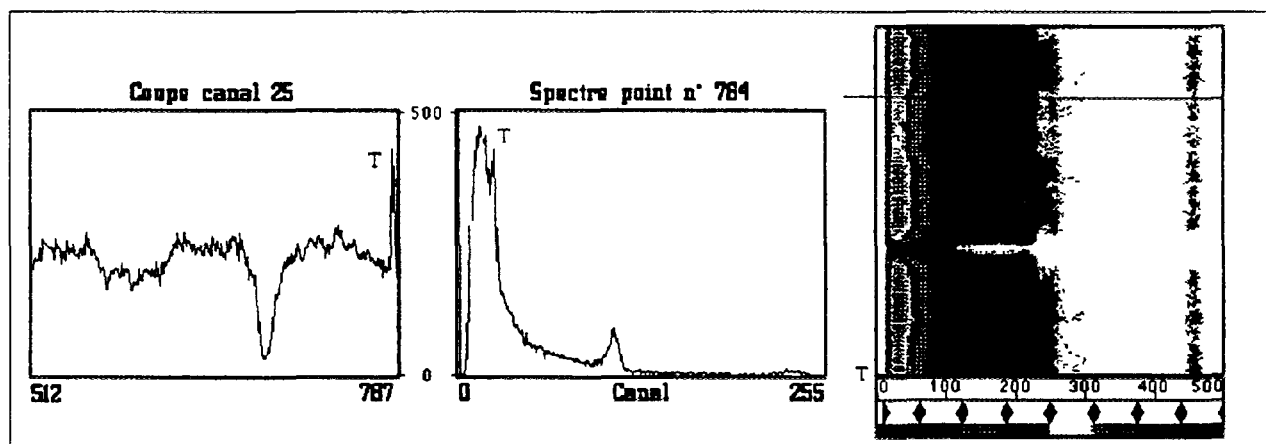


FIG. 1. $^{99}\text{Tc}_m$ source detection during survey of area 3.

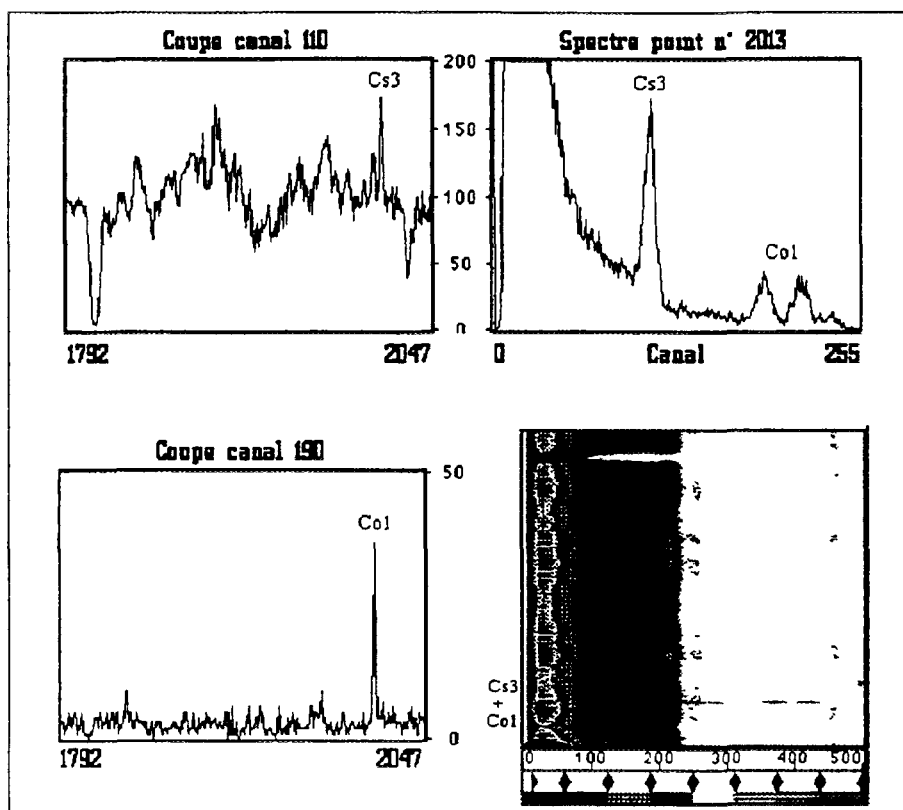


FIG. 2. Cs3 and Co1 detection during survey of area 3.

The detection limit is function of the natural background of the spot. For a caesium source the detection threshold was about 10 mCi on area 3, for a superficial concentration about 50 kBq/m². Therefore the Cs3 source was too little active for being detected with reliability. In France the ¹³⁷Cs background is about 1 to 2 kBq/m² and the detection threshold for a source is less than 1 mCi (40 MBq).

2.2. Isoactivity maps

2.2.1. Spectral analysis

Data processing is achieved by a new algorithm for spectral analysis, suitable AGRS operational conditions. This algorithm can detect and calculate full absorption peaks area associated to ground nuclides. The short sample time (2s. in Finland) and the detection altitude (about 50 m.) generate a poor counting statistic and a low signal/noise ratio.

Classical processing software are unusable in these conditions, and a specific algorithm has been developed by L. Guillot. The counting fluctuations are removed by the use of numerical filters which take into account peaks characteristics (gaussian shape, variation of FWHM with energy...). After filtering, peak detection is done by the study of first and second derivatives. Full absorption peaks area is computed after calculation and subtraction of the background (Fig. 3).

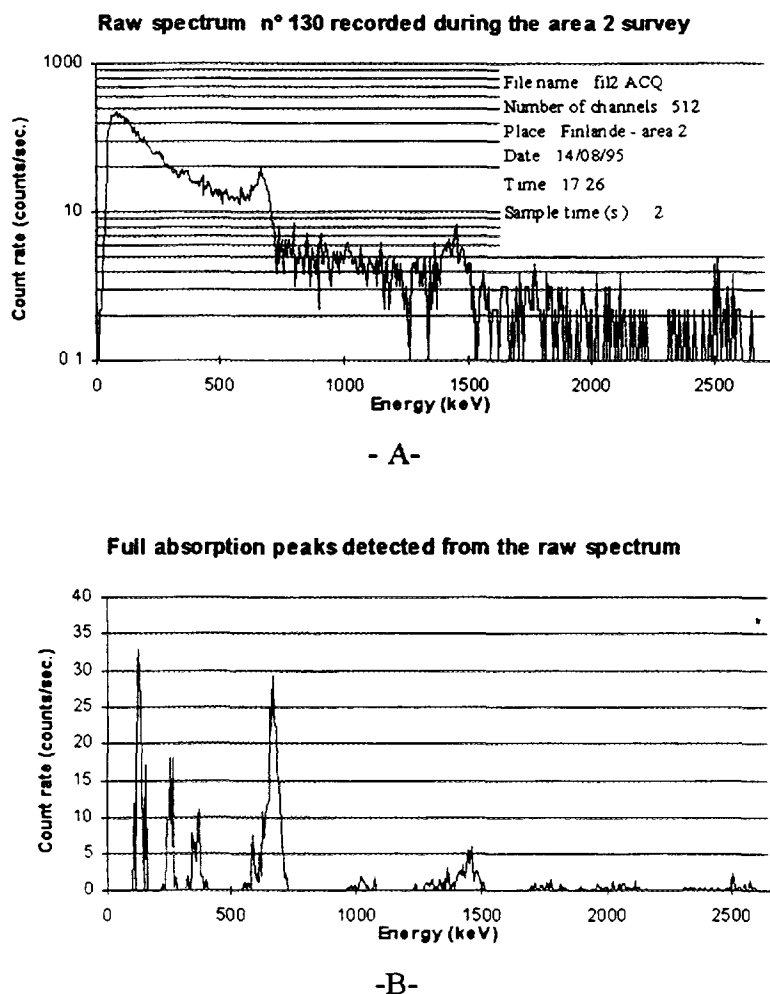


FIG. 3. Calculation of full absorption peaks (B) by processing of a raw spectrum(A).

Nuclides are identified in a reference table. This list also contains variation laws of the detector response with altitude, and energy to calculate activities to calculate ground contamination. Data processing of the records produces the following results:

Area n°2: Source file: FIL2.ACQ
Sample time: 2 seconds
Number of measurements: 3100

TABLE II. SYNTHESIS OF NUCLIDES DETECTION OVER AREA No. 2

<i>Nuclides</i>	<i>Energy (keV)</i>	<i>Number of detections</i>	<i>Average activity</i>	<i>Experimental precision (%)</i>	<i>Statistical precision (%)</i>	<i>Average detection threshold</i>
²¹² Pb	238	290		35	19	
²¹⁴ Pb	295	482		34	27	
²²⁸ Ac	338	11		32	29	
²¹⁴ Pb	352	515		36	28	
¹³⁷ Cs	662	3091	64.3 kBq/m ²	38	3	1.6 kBq/m ²
¹³⁴ Cs	795	2210	4.0 kBq/m ²	36	17	0.5 kBq/m ²
²²⁸ Ac	911	2147	12.0 kBq/m ²	37	25	2.7 kBq/m ²
⁴⁰ K	1461	3096	380.1 Bq/kg	37	9	16.3 Bq/kg
²¹⁴ Bi	1764	2826	24.9 Bq/kg	32	22	3.5 Bq/kg
²³² Th	2615	3100	23.1 Bq/kg	33	17	1.4 Bq/kg

Area n°3: Source file: FIL3.ACQ
Sample time: 2 seconds
Number of measurements: 2600

TABLE III. SYNTHESIS OF NUCLIDES DETECTION OVER AREA No. 3

<i>Nuclides</i>	<i>Energy (keV)</i>	<i>Number of detections</i>	<i>Average activity</i>	<i>Experimental precision (%)</i>	<i>Statistical precision (%)</i>	<i>Average detection threshold</i>
²¹² Pb	238	149		47	16	
²¹⁴ Pb	295	461		42	25	
²²⁸ Ac	338	187		42	26	
²¹⁴ Pb	352	441		39	26	
¹³⁷ Cs	662	2562	51.5 kBq/m ²	39	2	1.5 kBq/m ²
¹³⁴ Cs	795	1907	3.4 kBq/m ²	38	14	0.6 kBq/m ²
²²⁸ Ac	911	1956	8.7 kBq/m ²	41	22	2.3 kBq/m ²
⁴⁰ K	1461	2584	365.5 Bq/kg	41	7	19.2 Bq/kg
²¹⁴ Bi	1764	2388	21.3 Bq/kg	34	22	3.7 Bq/kg
²³² Th	2615	2590	25.4 Bq/kg	36	15	1.6 Bq/kg

Only nuclides which have peaks of energies higher than 662 keV are detected in a great proportion of measurements. The high caesium concentration creates an important background at low energies and the detection at these energies is disturbed.

The experimental precision of activities represents:

- Spatial variations of nuclides concentration on the area,
- Statistical fluctuations of counting (which depends on concentration).

The statistical precision represents the incertitude associated with the calculation of peaks area. The detection threshold is computed for each nuclide and depends essentially on the scattering background intensity.

3. CONCLUSION

3.1. Hidden sources

After a detailed processing of measurements, ten sources have been clearly pointed out. The other sources were collimated or their activities were close or lower than the detection threshold of the system because of the high level caesium background.

The trace of four other sources has also been detected with the knowledge of their positions but their contributions are too weak to conclude about their attendance.

3.2. Radioactive fallout

Caesium fallout is always very active today. On area n°2, ^{137}Cs average concentration is about 65 kBq/m², with some forest parts reaching 110 kBq/m². For cultures areas or villages (Auttoinen for example, at south-east of area n°2), ^{137}Cs contamination is between 30 and 40 kBq/m². The activity is approximately twice weaker in villages where the fall-out has been washed or in cultivated areas where the soil has been turned over.

The area n°3 can be divided into two parts of different concentrations. At south-east ^{137}Cs concentration is comparable with area 2 (about 60 kBq/m²) and at north-west the concentration is between 40 and 50 kBq/m².

^{134}Cs concentration on both areas is proportional to ^{137}Cs concentration with a ratio of about thirty, in accordance with today's proportions of Chernobyl fallout. ^{134}Cs maps show great variations because of the great count rate fluctuations at these concentrations (1 à 8 kBq/m²). These fluctuations are not significant.

3.3. Natural activity

The isoactivity maps of ^{40}K , ^{214}Bi et ^{232}Th show activity levels which are comparable with measurements recorded in France. Concentrations are rather homogeneous with some local increasing on villages or cultures probably because there is an important attenuation by trees above forest areas.

In spite of restricting conditions (distance, reduce team, respect of time allowed), HELINUC team have achieved all tasks defined by the organisers. This exercise, very close to an accidental situation, has been a good test for equipment and has shown the ability of the team to operate in this conditions.

The new developments concerning spectral analysis and calibration of airborne measurements were tested during this exercise for mapping caesium fallout and natural activity. Airborne results are in good agreement with in situ measurements and confirms the performances of new airborne data processing methods. For ^{137}Cs fallout, the maximum concentration recorded reaches 100 to 110 kBq/m² on area 2, for both airborne and in-situ measurements.

The detection of a great part of the hidden sources has confirmed the sensibility of our device HELINUC and this exercise has confirmed the ability of airborne gamma spectrometry to evaluate

quickly man-made and natural radioactivity, and to perform lost sources searching. Our results are in good agreement with other teams results but some differences show the necessity of an harmonisation of processing methods.

ACKNOWLEDGEMENT

We want to congratulate and to thank all the organisers for the remarkable arranging and development of this exercise which has been a real evaluation of mobile radiological control means.

REFERENCES

- [1] CORTELLA, J., BOURGEOIS, C., CHASTEL, R., ROSENBERG, A., "Post-accident radiological measurements: contamination map", Recovery Operations in the Event of a Nuclear Accident or Radiological Emergency (Proc. Symp. Vienna, 1989), IAEA, Vienna (1990) 347 (in French).
- [2] BOURGEOIS, C., BRESSON, J., CHIFFOT, Th., GUILLOT, L., RESUME 95, Nordic field test of mobile equipment for nuclear fallout monitoring, CEA/VA/HELINUC Report (January 1996).
- [3] GUILLOT, L., Ph. D. (previous 12/1996).
- [4] WINKELMAN, I., BUCHRÖDER, H., THOMAS, M., Aerial measurements with helicopters to determine accidental releases from nuclear facilities, IRPA9, Vienna, April 14-19/1996.
- [5] IAEA/MEL, A study of radioactivity in and around the lower Danube river, Contract IAEA-FC-2-91, Monaco (1992).

**NEXT PAGE(S)
left BLANK**



QUANTITATIVE Cs-137 DISTRIBUTIONS FROM AIRBORNE GAMMA RAY DATA

G. OBERLERCHER, W. SEIBERL
Geological Survey of Austria,
Vienna, Austria

Abstract

The Chernobyl reactor accident caused in Austria Cs-137 activities up to 180 kBq/m². The following paper explains how airborne NaJ-spectroscopy, originally designed for geological surveys, was used as an accurate method to obtain the ground activity of Cs-137 in certain regions of Austria. To retrieve the net count rate in a Cs-137 window it is necessary to subtract all background contributions from the peak, including the Compton continuum and the contribution of overlapping peaks. Therefore the measurement of Cs-137 with a NaJ detector system must take into account radioactive elements with gamma-ray lines near the peak energy of Cs-137 at 662 keV. In regions with higher concentrations of the natural radioactive elements uranium and thorium a peak near 600 keV is found, containing the 609 keV line of Bi-214 and the 585 keV line of Tl-208. Additionally a Cs-134 line is located at 604 keV. Because of the poor energy resolution of NaJ detectors it is not possible to find a clear separation between these peaks and the Cs-137 peak. The following section describes the method that was used to obtain accurate quantified Cs-137 activity values.

1. CONTRIBUTION OF DIFFERENT PEAKS TO THE CS-137 WINDOW

Table I shows the different radioelements with gamma-ray lines near the Cs-137 peak at 662 keV.

TABLE I. GAMMA-RAY LINES NEAR THE CS-137 WINDOW

Gamma ray energy (keV)	Radioelement	T _{1/2}	Relative intensity %
511	Tl-208		8.1
583	Tl-208		31.0
604	Cs-134	754.2 d	97.6
609	Bi-214		42.8
662	Cs-137	30 a	85.0
666	Bi-214		1.5
727	Bi-212		6.7
768	Bi-214		4.8
795	Cs-134	754.2 d	85.4

The different influences of this gamma-ray lines will be discussed and a new method will be represented to achieve an accurate and quantitative determination of Cs-137. Figures 1 and 2 show sample spectra measured during a calibration procedure with the Austrian calibration pads (IAEA 1989). As additional information the centroid peak energy of Cs-137 at 662 keV is shown in the figures. From this samples it is obvious that the peak regions of Bi-214 and Tl-208 would partially overlap with a Cs-137 peak. Cs-134 has a clear peak at 604 keV that would also overlap with the Cs-137 peak. Fortunately, experience has shown that the ratio of Cs-134 to Cs-137 can be regarded as constant if the duration of measurements is short compared to the half live of Cs-134. The Bi-214 line at 666 keV will usually not lead to a peak because of its small relative intensity of only 1.5%.

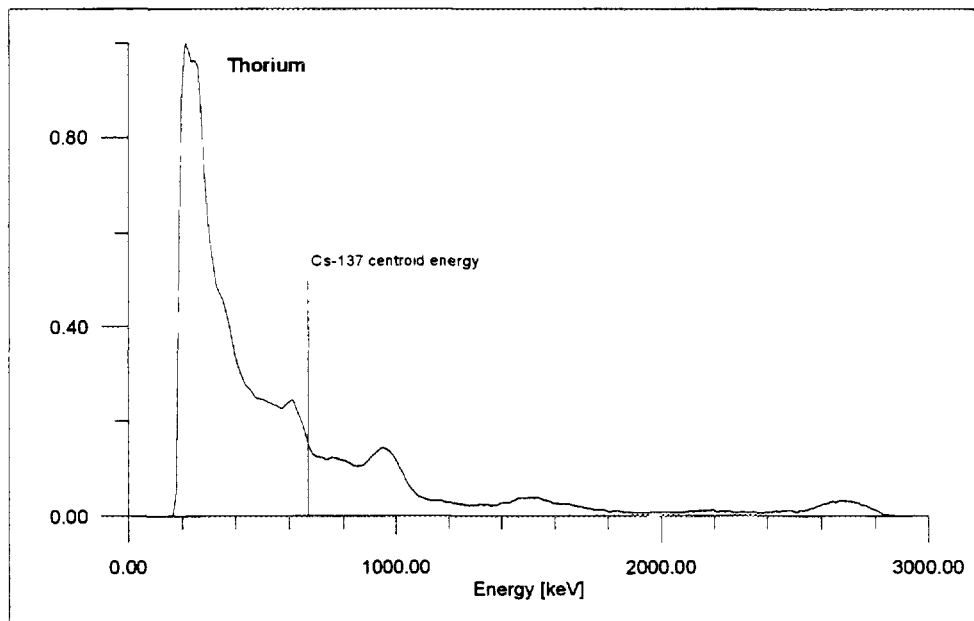


FIG. 1. Thorium spectrum obtained from Austrian airborne system on the thorium calibration pad (normalized count rates); IAEA, 1989.

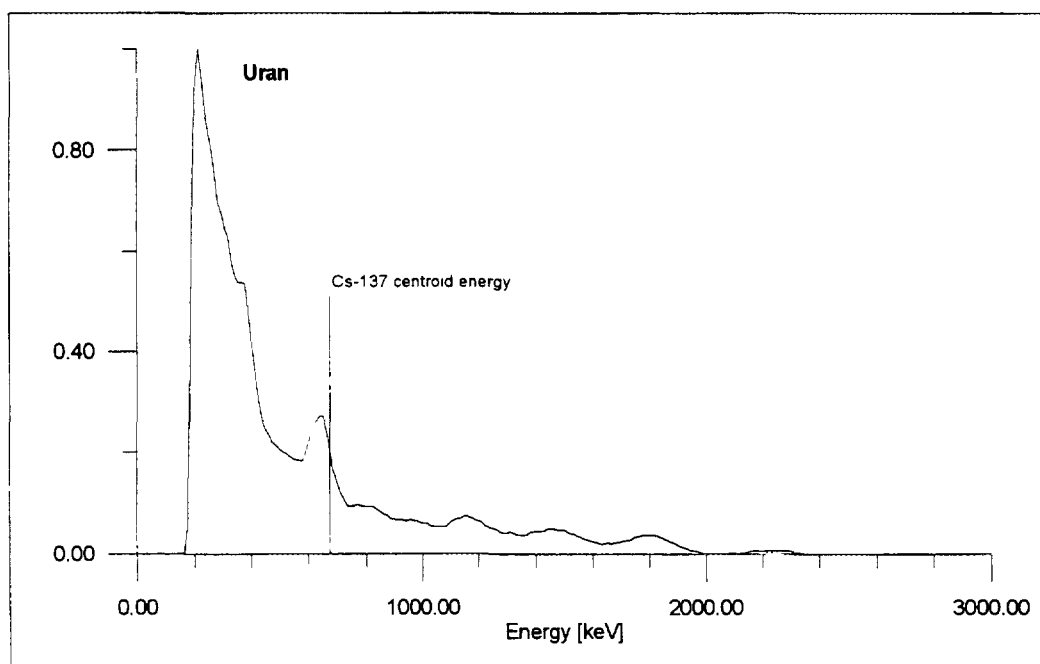


FIG. 2. Uranium spectrum obtained from Austrian airborne system on the uranium calibration pad (normalized count rates); IAEA, 1989.

Radon in air is another source of error in determining the Compton continuum in the Cs-137 window because of the overlapping 609 keV peak of Bi-214 with its high relative intensity of 42.8%. Bi-214 count rates might origin from uranium in subsurface as well as from radon in the air, with a different amount of absorption on the way from their source to the detector. Therefore the relation of 609 keV to 1765 keV count rates varies with the amount of radon in the air and a reliable

calculation of the contribution of the 609 keV peak depends on a reliable radon estimation, using either an upward looking detector or the method suggested by Minty 1992. Unfortunately the procedure suggested by Minty using the 609 keV and the 1765 keV lines of Bi-214 cannot be applied at the presence of Cs-137 and the use of the 1220 keV and 1760 keV Bi-214 peaks is less accurate because the difference of the corresponding attenuation coefficients is too small. The use of upward looking detectors might also lead to errors because they show some sensitiveness to the vertical distribution of radon in the air.

2. DETERMINATION OF THE COMPTON CONTINUUM

To reduce the influence of the natural radioactive elements uranium and thorium on the Cs-137 window a new method had to be developed. For K, U and Th-windows usually stripping factors are used to determine the lower energy windows Compton background originating from higher energy gamma-rays. We did not find this method to yield good results for low energy windows because the stripping factors are rather high. The uncertainty of a measured count rate N is proportional to \sqrt{N} and therefore statistical variations in the high energy windows can lead to large variations in the calculated Compton background.

So, while high count rates for the natural radioactive elements lead to overlapping peaks in the Cs-137 window, low concentrations of natural radioelements would increase the statistical error of a Compton background determined with stripping methods.

An alternative to the use of stripping factors is to determine the shape of the Compton continuum by a least square fit of the entire spectrum or selected areas of the spectrum. Anyhow our experience has shown that, if a small window is used, it is sufficient to describe the Compton continuum with a trapezoid. The situation is shown in Fig. 3.

The start and end channels of the spectrum which determine the shape of the trapezoid were obtained empirically from multiple spectra over different geological formations. It was proven that the location and shape of the minima at the rising and falling flanks of the Cs-137 peak area are not influenced by other peaks. Experience has shown that the chosen areas, shown in Table II, lead to stable results and are therefore well suited to obtain the Compton continuum.

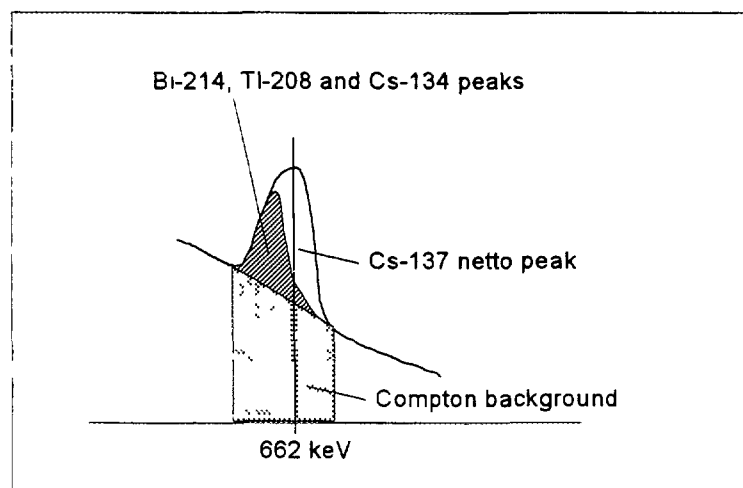


FIG. 3 Different contributions to the background of the Cs-137 window and the Compton continuum modelled by a trapezoid

TABLE II. ENERGY WINDOWS USED

Radionuclide	Start Energy (keV)	End Energy (keV)
Cs-137	648	732
Cs-134	744	864
U	1692	1884
Th	2448	2844
Compton Background	540	732

Because of its relative intensity of 42.8% the dominating disturbing gamma line origins from Bi-214 at 609 keV. The problems due to radon in the air and poor statistics have already been mentioned above.

The only way to reduce the errors made by wrong estimated count rates due to the 609 keV Bi-214 peak is to decrease the influence of this peak with a reasonable setting of the Cs-137 window as far as possible off the 609 keV line. At the same time the influence of the Tl-208 and Cs-134 peaks would be minimized too.

Choosing a Cs-137 window that does not include the peaks around 600 keV would also lead to a lower (and better) limit of detection LLD for Cs-137, because it is proportional to $\sqrt{N+2B}$ where B is the background count rate including all background contributions to the peak (Compton continuum, overlapping peaks, equipment contamination) and N is the net count rate for Cs-137. On the other hand using only a part of the Cs-137 window means a loss of counts and therefore a higher uncertainty of the measured values.

The best compromise seemed to be to use only the high energy part of the Cs-137 peak including of course the central energy line of 662 keV. The influence of unwanted sources of errors is minimized, while on the other hand there is a higher statistical uncertainty in areas with low uranium and thorium concentrations in the subsurface. A comparison in a region with low natural radioactivity and with Cs-137 activities $< 10 \text{ kBq/m}^2$ has shown that the results using a wide and a small peak are almost similar, especially when the measured data are filtered or interpolated onto a grid as it is usually done for the data representation.

Table III. shows the quantitative influence of different peaks onto the chosen Cs-137 window from 648 to 732 keV. The values are valid at ground level and were derived with the Austrian standard calibration pads. At higher altitudes the factors would be smaller, because low energy gamma-rays are more attenuated on their way from the ground to the detector. The very right row in table 3 contains the ratio from the high energy count rate that can be seen in the chosen Cs-137 window. It is obvious that taking only the high energy part of the peak reduces the influence of natural radioactive elements on the Cs-137 count rate drastically. Tl-208 could even be neglected.

TABLE III. CONTRIBUTION OF DIFFERENT RADIOELEMENTS TO CS-137 PEAK

Radionuclide	Low energy peak found at	High energy peak conventionally used	Net count rate ratio Low/High	Net count rate ratio Cs-137/High
Tl-208	583 keV (31.0%)	2615 keV (36.0%)	0.57	0.02
Cs-134	604 keV (97.6%)	796 keV (85.4%)	1.14	0.14
Bi-214	609 keV (42.8%)	1765 keV (15.9%)	1.86	0.23
	666 keV (1.49%)		0.07	0.07

The formula that was finally used for total background reduction includes the differences of absorption in air for high and low energy peaks of the different radioelements. The used attenuation coefficients were derived from calibration flights at low altitudes from 35 m up to 300 m above ground. Fig. 4. shows the results for Cs-137.

At last the helicopter background was estimated by a calibration flight at high altitudes from 2000 m to 4000 m above ground and the conversion factor from cps to kBq/m² was derived from an intercalibration with a portable spectrometer over a homogenous contaminated area.

The formulas used for complete Cs-137 activity calculation are

$$N_{Cs137} = T_{Cs137} - CB - 0.23 U e^{(-0.0018 h)} - 0.02 Th e^{(-0.0039 h)} - Rn$$

and

$$Cs_{137} [kBq/m^2] = 0.48 N_{Cs137} e^{(-0.00967 h)}$$

N_{Cs137}	...	Cs-137 net count rate
T_{Cs137}	...	Cs-137 total peak count rate
CB	...	Compton background with trapezoid
U, Th	...	net window count rates of high energy windows
Rn	...	Radon count rate in Cs-137 window
h	...	detector altitude in metres

The radon count rate is measured with an upward looking detector, the corresponding factors to calculate the influence of the Bi-214 energy peak of the upward looking detector on the Cs-137 window were obtained from a calibration procedure with the uranium pad.

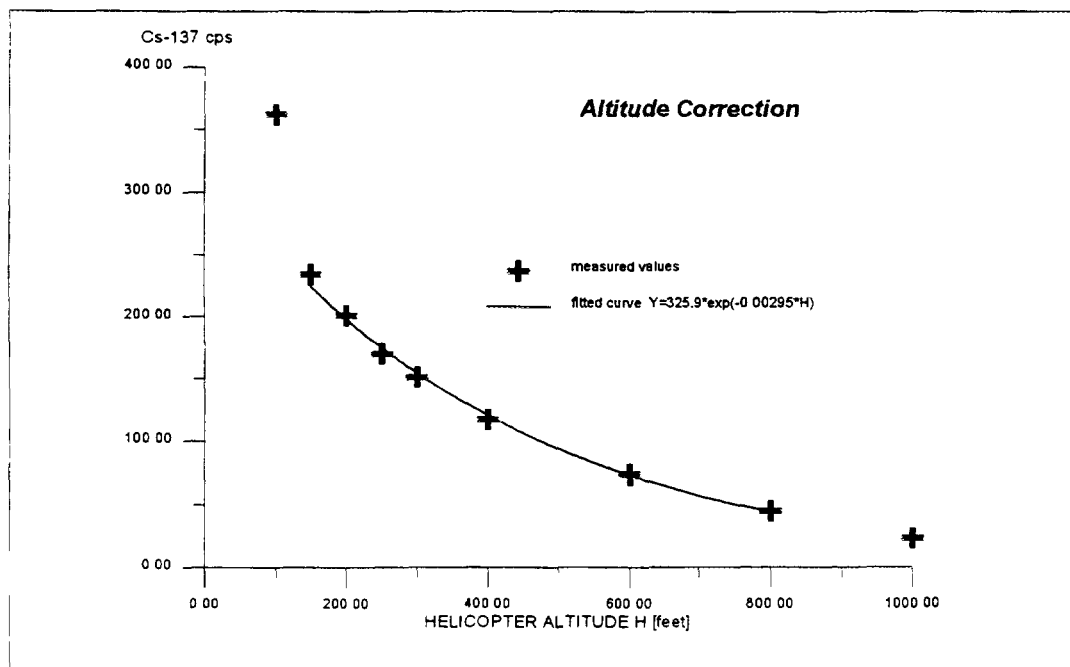


FIG. 4. Cs-137 attenuation coefficients obtained from calibration flight at low altitudes.

Cs-134 correction is not necessary because the peak ratios of Cs-134 to Cs-137 is thought to be constant and therefore included in the sensitivity factor to convert the Cs-137 count rates into activities. This assumption is of course only true if the calibration for the sensitivity factor is repeated within a time that is short compared to the half live of Cs-134.

3. CASE HISTORY OF MEASUREMENTS IN THE HAUSRUCK AREA

To test the described procedure gamma-ray data in the Hausruck area in Northern Austria gamma ray data were made available by the Geological Survey of Austria (SEIBERL & PIRKL, 1991). The area was chosen because it shows a rather great variability in natural radioelement concentrations. The areas of very low natural radioactivity are caused by hills of the so called Hausruck Gravel reaching thicknesses of up to 150 m above the underlying sediments, which show higher activities due to minerals from the Bohemian Massif.

After background reduction the contrast of these geological structures should no longer be visible in the Cs-137 count rates. Additionally ground measurements after the Chernobyl accident have shown Cs-137 activities increasing from north to south (Umweltbundesamt 1996). The reason for the gradient in the Cs-137 distribution is the varying rainfall during the pass of the radioactive clouds. The rain clouds coming from the North were partly stopped by the high mountains of the northern side of the Alps, causing more intensive rain with decreasing distance to the alps.

Figs 5 and 6 show the uranium and thorium plot of the Hausruck area, clearly indicating the hills of Hausruck Gravel.

Fig. 7 shows a plot of the background radiation obtained with the described method. Because of Compton scattering from uranium and thorium into the Cs-137 window the geological structures are visible in this background plot. Finally the Cs-137 activity plot is shown in Fig. 8. The result shows very good agreement with ground measurements (Umweltbundesamt 1996). The rather rough anomaly pattern of the uranium plot cannot be found anymore in the Cs-137 plot. This is an evidence that it was possible to eliminate the influence of the Bi-214 peak from the Cs-137 peak.

4. DISCUSSION

Because the influence of the overlapping peaks is minimized by using just the high energy part of the Cs-137 peak, the described method will lead to reliable results, even if a calibration to obtain the influence of the Tl-208 and Bi-214 peaks or radon measurement is not applied.

In addition it is not necessary to process a calibration to obtain Compton stripping factors if a trapezoid is used to estimate the Compton background in the Cs-137 window. Of course this method will only lead to reliable results if no peaks are influencing the areas of the spectrum that are used to determine the shape of the trapezoid. Although usually a lot of radioelements are found in a spectrum during the first time after a nuclear accident, there influence on the Cs-137 peak can be neglected after several weeks because almost all of them have very short half live time.

The results in certain areas of Austria proof that the described method is easy to apply and represents a reliable procedure to achieve good quantitative results for Cs-137 activity distribution from airborne gamma-ray measurements.

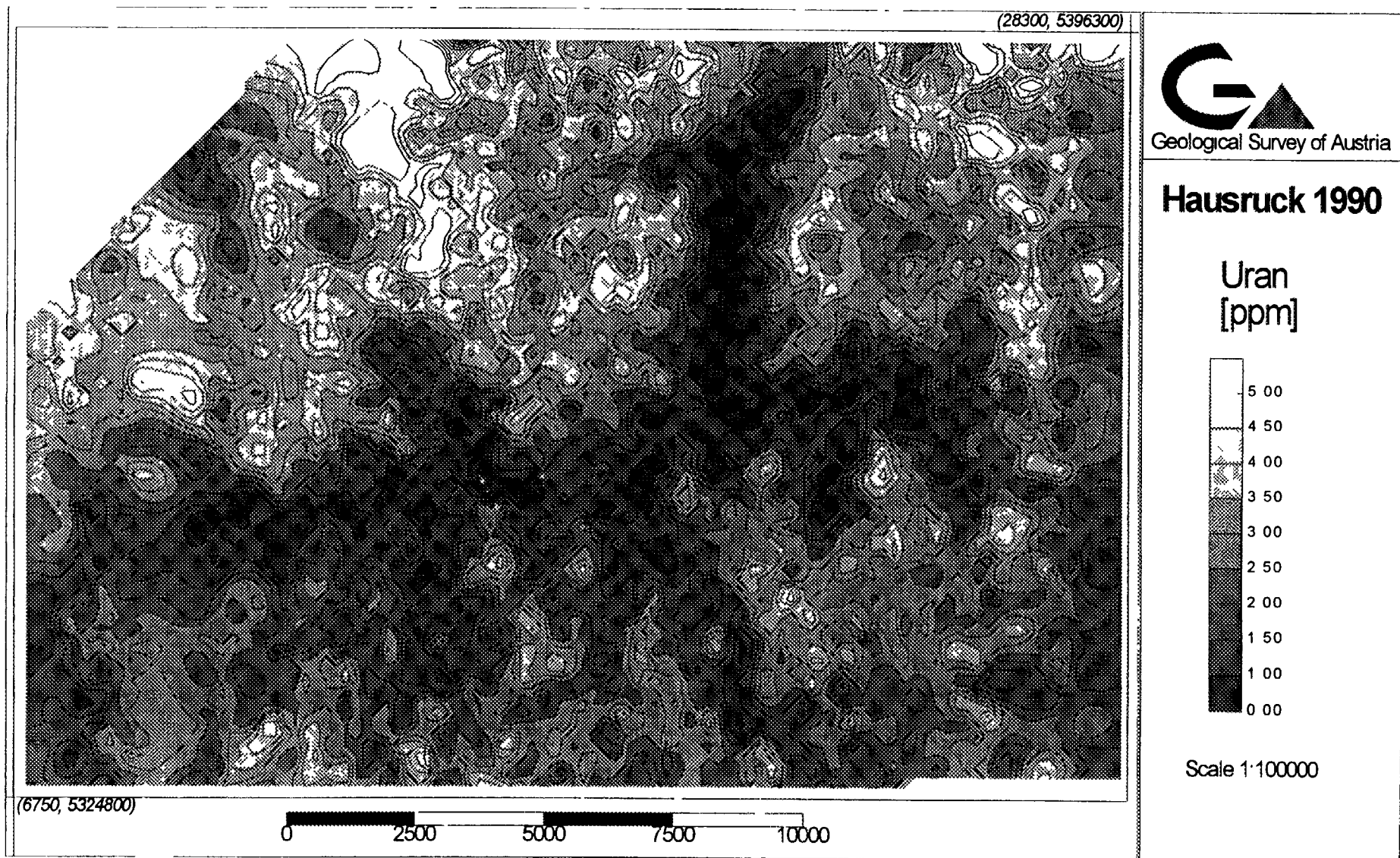


FIG. 5. Uranium plot of the Hausruck area.

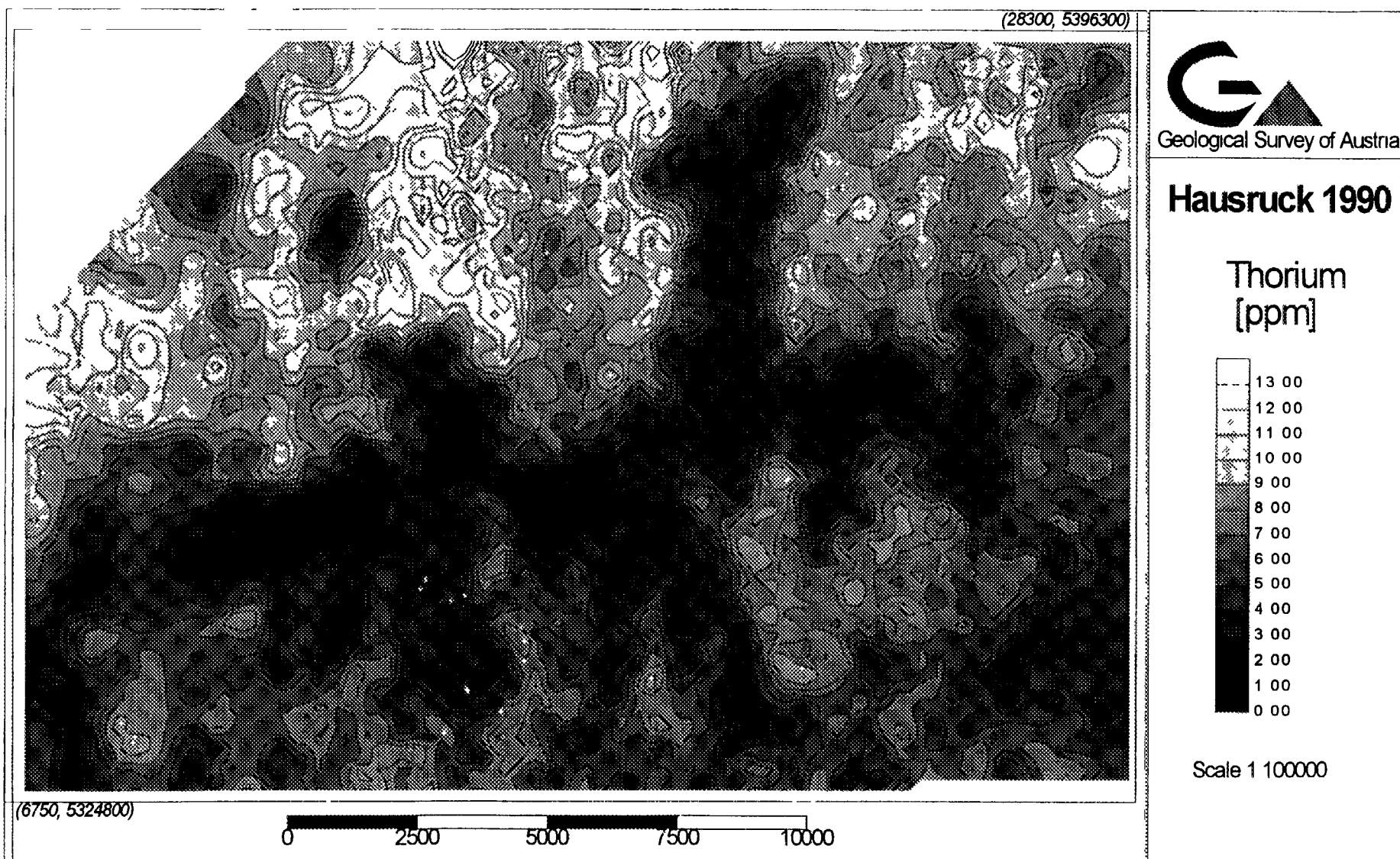


FIG. 6. Thorium plot of the Hausruck area.

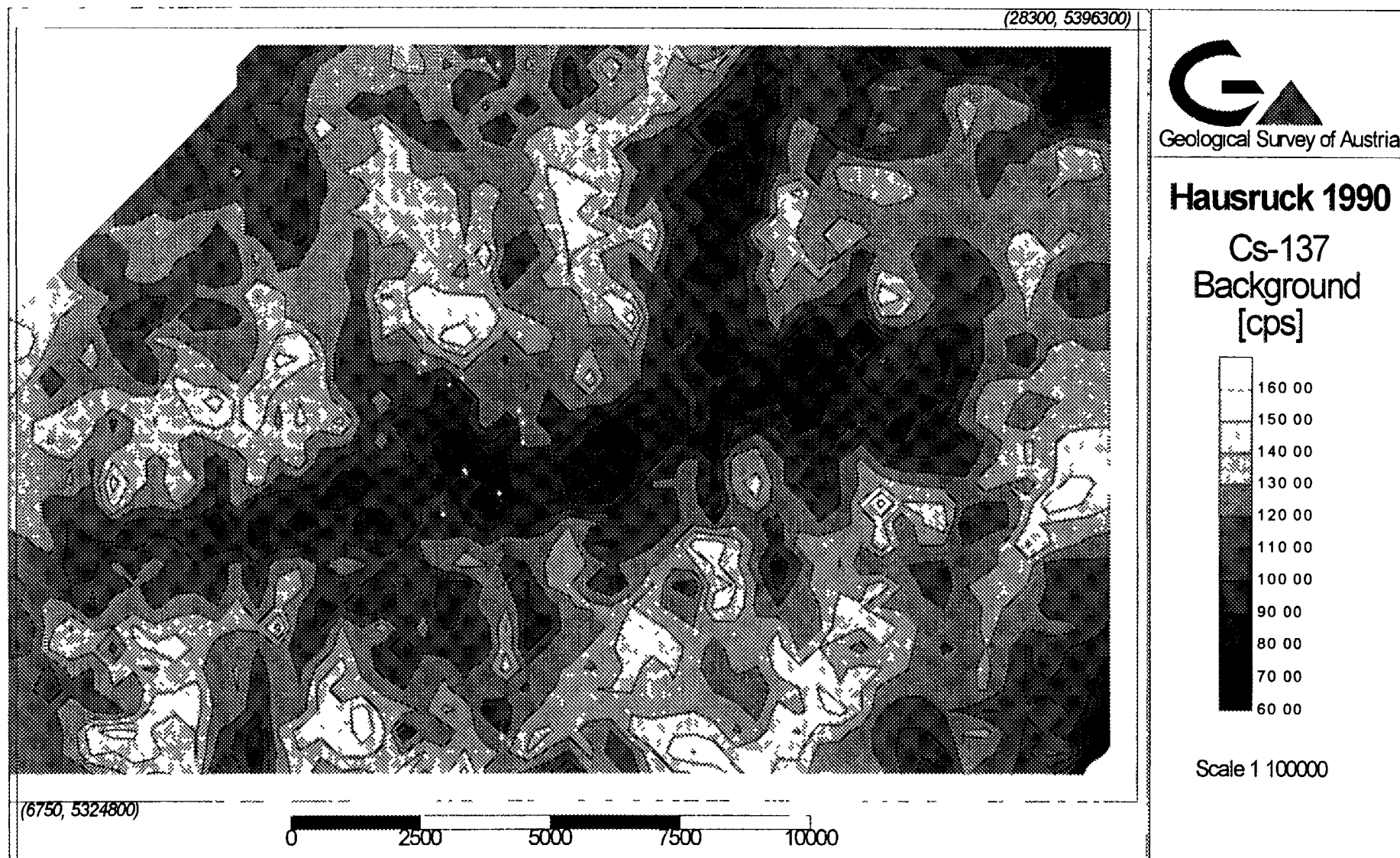


FIG. 7. Plot of the background radiation obtained with the described method.

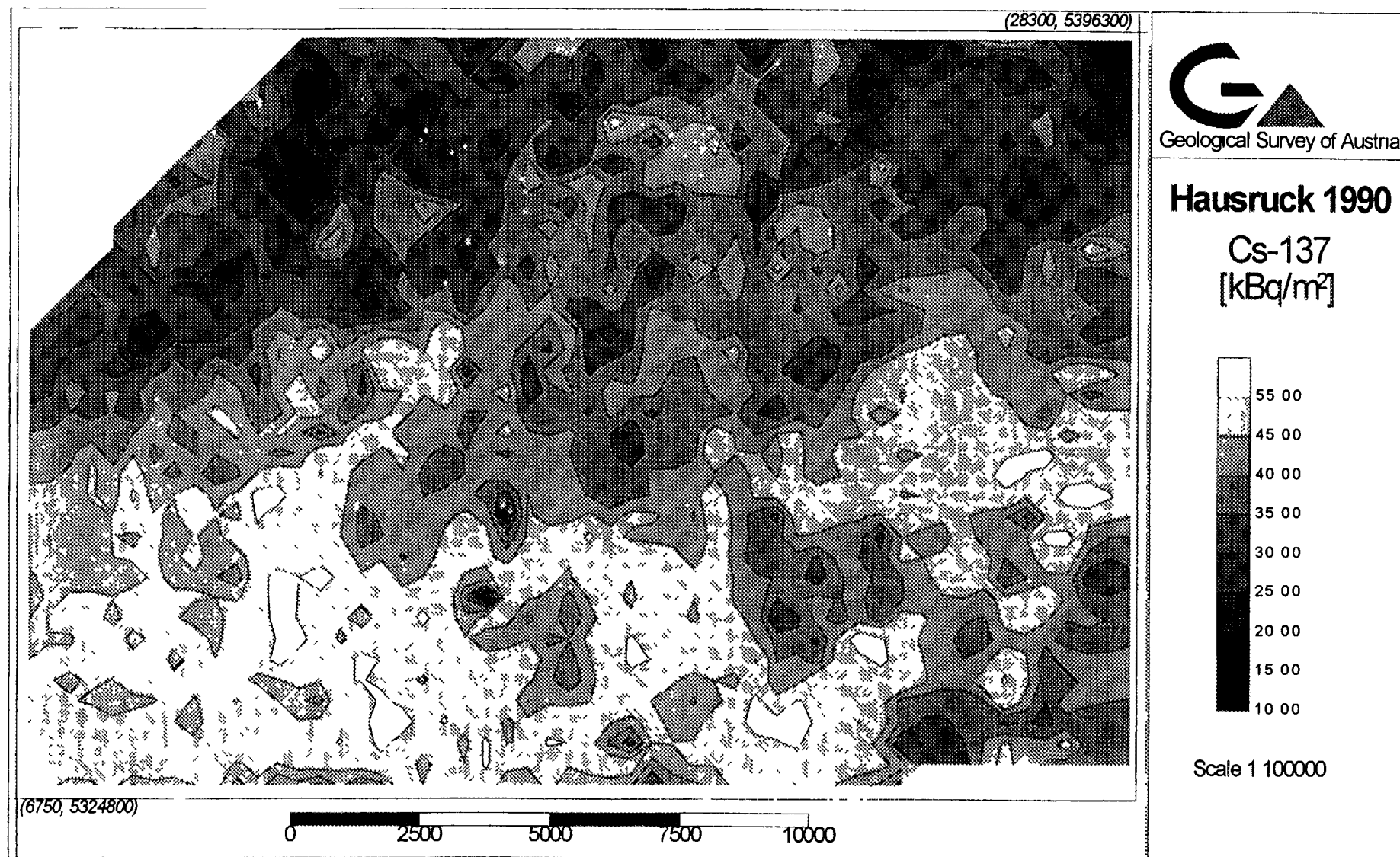


FIG. 8. Cs-137 activity plot.

BIBLIOGRAPHY

INTERNATIONAL ATOMIC ENERGY AGENCY, Construction and Use of Calibration Facilities for Radiometric Field Equipment, Technical Reports Series No. 309, IAEA, Vienna (1989).

MINTY, B.R.S., Airborne Gamma-ray Spectrometric Background Estimation Using Full Spectrum Analysis, Geophysics 57/2, Tulsa (1992) 279–287.

SEIBERL, W., PIRKL, H., Aerogeophysikalische Vermessung im Raum Hausruck, Proj.Ber. UELG-20/90-1, Geol.B.-A., Wien (1991) (in German).

UMWELTBUNDESAMT, Cäsiumbelastung der Böden Österreichs, Monographien Band 60, Wien (1996) (in German).

**NEXT PAGE(S)
left BLANK**



**FIELD GE GAMMA SPECTROMETRY FOR ON SITE
MEASUREMENTS OF SOME PARAMETERS
CHARACTERIZING RADON-222 EXHALATION
RATES FROM SOILS AND COVERS**

P. ZETTWOOG

Office de protection contre les rayonnements ionisants,
Le Vésinet, France

I. KOBAL

Josef Stefan Institute,
Ljubljana, Slovenia

J.F. PINEAU

ALGADE,
Bessines sur Gartempe, France

Abstract

We describe a new method based on differential gamma spectrometry for on site determination of some of the parameters which are relevant for the production of radon 222 in soil gas and its transfer from soil to indoor and outdoor atmospheres. This method is investigated in the context of a 3-year Slovenian-French cooperation programme, the PROTEUS project. We are currently using a germanium detector of 100 cm³. The height of the 20° collimated detector above the soil surface is from 1.5 to 3 m when using a tripod. This arrangement provides results which are representative of soil areas ranging from 1 to 4 square metres. Routine measurements would require larger detector volumes. The main objective is to provide technology and methodology for an efficient mapping of zones with potential for being the source of a high level of indoor radon, eliminating the need for soil sampling followed by laboratory analysis. The feasibility of an airborne mapping laboratory flying at low altitude will be investigated. Another objective is the rapid measurement of radon profiles across covers used to reduce exhalation rates from the surface of a pile of tailings, with characterisation of the influence of humidity content of the top layer. Airborne survey would allow for measuring exhalations from surfaces of slurries not otherwise accessible.

1. INTRODUCTION

We have identified two requirements for the measurement of radon in the environment which appear to us to be poorly covered by current methods.

1.1. Requirements for mapping zones of high radon risk in premises

The *Office de Protection contre les Rayonnements Ionisants* (OPRI: the French Radiological Protection Board) is a technical organisation set up two years ago under the Ministry of Health and the Ministry of Labour. OPRI's sphere of competence includes the exposure of the general population to ionising radiation of natural origin. The increase in these inescapable exposures of natural origin may be caused by industrial practices, lifestyles or the type of dwelling. The management of such humanly created increases in exposure to radiation of natural origin is a matter of paramount importance to OPRI.

With the prospect of new European Union directives on radiological protection coming into force in the near future, OPRI is at the stage of developing a strategy for identifying, monitoring and decontaminating premises used professionally in which workers would be exposed to significant radon levels. The annual effective dose equivalent for a worker exposed for 2000 hours to a radon 222 volume activity of 1500 Bq m⁻³ is of the order of 10 mSv.

The health risks associated with the exposure of the population in premises used as dwellings are certainly not lower than those which will have to be managed within the rules laid down for workers. The annual effective dose equivalent for a person exposed for 7000 hours to a radon 222 volume activity of 600 Bq m^{-3} is of the order of 10 mSv. For the sake of consistency, OPRI thus envisages extending the strategy of radon risk management to all buildings in France. For some very good reasons, the French health authorities have not so far been very active in the management of potential health risks associated with high exposures to radon 222 of domestic origin.

The envisaged strategy is based on a set of laws which have existed in public health regulations since 1971, and which aim at eliminating insalubrious dwellings. A new criterion of insalubrity would be introduced into a list already containing 12 such criteria. The dwelling would be declared insalubrious when the mean concentration of daughter products of radon 222 in living rooms exceeds a statutory limit. The latent defect in such a dwelling would then be brought to light, and it could no longer be sold without prior decontamination.

The value of the statutory limit is planned to be quite high (of the order of 1000 Bq m^{-3}), so that the proportion of buildings concerned is statistically an anomalous fraction of them. The levels of concentration of domestic radon in a given region are generally distributed in a lognormal fashion, the median being of the order of 50 Bq m^{-3} , and the geometrical standard deviation being 2. The fraction with levels above the limit is therefore not part of the general distribution. Maps currently available that show the distribution of exposure levels in the French départements [1] describe only the general distribution and do not allow this anomalous fraction to be geographically located with sufficient precision, since there are not enough measurements. In the proposed strategy, it is envisaged that the mechanism for declaring insalubrity would be initiated only in a limited number of communes: those with the highest probability of finding insalubrious dwellings. From the information provided by France's neighbours and from our own results, this probability could be significantly greater than 1% in some communes with unfavourable geology.

With the proposed statutory limit, the only mechanism that could lead to insalubrity in the legal sense would be an intake of radon through the aspiration of air from the soil due to a reduction of pressure indoors. It is known that this mechanism occurs only for certain combinations of radon 222 concentration in the porous volume and the permeability of the soil under the foundations. Various indices for characterising the soil according to its propensity to release radon have been proposed using these two quantities. The parameters underlying them are those dependent on the geology and the properties of the local soil.

Other mechanisms not related to the soil under dwellings, such as radon from walls or from the water in showers, would not be sufficient to cause the 1000 Bq m^{-3} limit to be exceeded. It is therefore quite possible to produce maps showing the radon potential of the soil. Such maps would be useful for the management of both professional risk and domestic risk. The production of such maps on a regional and then on a cadastral scale is a major feature of the strategy envisaged in France. A map (not generally distributed) of the radon potential on a scale of about 1/1 000 000 and with a $500 \text{ m} \times 500 \text{ m}$ grid, mainly concerning land with crystalline geology, has been produced for the Ministry of the Environment by BRGM [2].

A similar analysis has been carried out for Slovenia by the Josef Stefan Institute in Ljubljana (JSF) [3]. Maps of uranium and thorium concentrations in the soil based on radiometric and geochemical measurements in Slovenia have been drawn up for Slovenia by the Ljubljana Institute for Geological Research [4].

The production of maps showing the "potential radon risk" forms part of the proposals recommended by ICRP Publication no 65. This recommendation is now applied in several countries and many papers have been published on it. We quote here a leaflet intended to inform the general public in the USA [5], which includes a selection of US publications.

1.2. Requirements for evaluating surface emissions of radon 222 from mines

Modelling the atmospheric transfer of the radon 222 emitted by radium-bearing surface deposits is an essential step in evaluating the environmental radiological impact of projected mine workings and that of mines not covered by an appropriate monitoring network. This exercise has been carried out by JSF for the Zirovski mine in Slovenia [6, 7].

The ALGADE company, a service subsidiary of COGEMA, specialises in the radiological monitoring of uranium ore workings, and is developing a numerical 3D program simulating the transfer of radon 222 for complex mountainous terrain. This development has revealed the need for the precise measurement of the global emission of radon from the surface of radium-bearing tailings piles: the sampling procedure and the measuring equipment must lead to an accuracy in the value of the "source" terms matching the sophistication of the numerical simulation.

2. INADEQUACIES IN CURRENT TECHNIQUES FOR MEASURING RADON 222 EXHALATION FROM SOILS AND COVERS

2.1. In maps showing the potential radon risk in dwellings

The production of maps showing the propensity of the soil to release large quantities of radon 222 into houses depends on the procedures used for marking out the grid and on the measurement of a certain number of soil parameters, either on site or on soil samples in the laboratory. In the US Department of Commerce document [8], which we have used as a reference, these parameters are identified and some observational techniques, procedures and methods of measurement are described.

We should point out that the cost of producing these maps is proportional to the fineness of the grid used for them. Moreover, the area of soil covered by each measurement is very much less than a square metre. As soon as the surface geology and the soil characteristics are variable, therefore, it seems to us a risky undertaking to guarantee that the map will be a good representation at an appropriate scale, with not too expensive a grid and with measurements made on relatively small areas of the mapped region.

The geostatistical problems encountered in producing potential radon maps of the soil have been studied in the case of the English Midlands [9]. The variogram drawn up using the method of regionalised variables [10] for measurements of radon concentration of the soil with a 10 m grid over distances from 10 to 10 000 m is one characterised by the "pure nugget" effect. In other words, no spatial dependency occurs for measurements made over distances greater than 10 m.

The result of a measurement is valid for the point at which the measurement is made and for a surrounding region with a diameter significantly less than 10 m. Standard kriging methods could therefore not be applied to such terrain.

Evidently, to have a radon map that is representative and not too expensive to produce is not an easily obtainable objective.

As a result, we considered using on-site gamma spectrometry. With a 20° collimated detector at the top of a mast 3 metres above the soil, the area sampled is 3 m², at 10 m it is 37 m², on a helicopter at 25 m it is 230 m². This is the ground area of a dwelling.

A review of the methodological and practical aspects of on-site high resolution gamma spectrometry was carried out by the Environmental Measurement Laboratory of the US DOE in 1994 [11].

The conclusion of this article supports the expectations of our Franco-Slovene team that on-site gamma spectrometry will overcome the problems of cost and of the statistical representativeness of the ground measurements required to produce a map and isointensity curves for the potential soil radon. The article specifies that, for differential measurements of the intensities of the gamma lines from emitters in the uranium chain for soils with a mean terrestrial background level, a Ge detector of large volume and with an efficiency greater than 75% would produce results in a counting time of less than 30 minutes. A measurement can be made in a few minutes with a relatively small detector if the soil activity is greater than 1 Bq g^{-1} .

2.2. IN THE MEASUREMENT OF RADON FLUX AT THE SURFACE OF RADIUM-BEARING TAILINGS PILES AND THEIR COVERS

This is a matter of calculating the total emission by integrating the results of measurements of the surface radon flux, using a representative grid, made in less than a day or, more precisely, within a period of stable weather conditions.

The current method is based on measurements of diffusive radon flux by plenum chambers covering at most a few tenths of a m^2 over a grid which in practice cannot be smaller than the $20 \text{ m} \times 20 \text{ m}$ grid. The question arises of how statistically representative this is.

In addition, the method does not provide a result with a sufficiently short time constant, bearing in mind the time variations of the flux if the weather is changeable.

Above all, however, it assumes that it is at least possible to go on foot over the surface of the deposit. Now it is impossible to set foot on wet tailings without getting stuck in them. As a result, the method cannot be used in many cases. The need for a method of measurement that could be operated from a helicopter thus becomes evident.

The problems of the cost of the determination of the source term and the statistically representative nature of the measurements here again justify the interest in on-site spectrometry. Moreover, the inaccessibility of the surface of muddy piles of fine tailings necessitates the use of an airborne laboratory, and high resolution gamma spectrometry has been tried and tested for such use. In France, the helicopter method (Hélinuc system) has been developed mainly at the Commissariat à l'Energie Atomique (CEA, Centre d'études de Valduc, 21120 Is/Tille, France) with a view to the recovery of small radioactive sources. An application of this system to post-accident gamma cartography is described in [12].

3. PROGRESS MADE IN THE RESEARCH PROGRAMME

The Franco-Slovene programme (the PROTEUS project on the characterisation of the propensity of soils to produce radon 222 anomalies in dwellings) was planned to last for three years and started at the end of 1994. We now describe the progress made in the work.

3.1. Theoretical aspects

Fig. 1 illustrates the principle of the spectrometric method of measuring the rate at which radon 222 is produced in the porous volume of soils and its diffusive transfer to the atmosphere. The theoretical aspects of the method are dealt with in Annex 1. It is shown that, with an appropriate processing of the line spectrum of gamma emitters in the uranium chain, it is possible to obtain independently the activity of radon 226 per unit of mass (Bq g^{-1}), the emanation coefficient of radon 222 and the product of its diffusional relaxation length (m) in the porous volume and the soil density (g cm^{-3}). The diffusive flux is deduced from this. The theory assumes that the soil properties are

uniform over the volume of soil measured by the detector. The radon diffuses into the porous volume vertically (one-dimensional assumption). Annex 1 also deals with the measurement of the flux emitted by the covers on radium-bearing tailings piles. Theoretical support for the processing of the data provided by the measurements on calibration blocks using 20° collimated detectors and for the laboratory validation of the method is also described.

3.2. Programmes of measurement

3.2.1. Procedures

Some of the measurements were made in France on the crystalline terrain of Limousin and in Slovenia on sedimentary land and on piles of mine tailings¹ or fly ash.

20° collimated detectors of relatively small volume were used (an Ortec HPGe detector with a height of 49.8 mm and a diameter of 53.7 mm with 17% efficiency, and a Canberra HPGe detector with a height of 55.2 mm and a diameter of 54 mm with 36% efficiency). The detector was placed on a mast 3 m above ground level.

Measurements were also made on calibration blocks. Four cylindrical blocks of diameter 48 cm and heights of 7 cm, 22 cm, 35 cm and 63 cm were made from metal drums fitted with a watertight cover and a device for scavenging the porous volume. These heights cover the absorption lengths of the gamma lines used. The height of 63 cm is of the same order of magnitude as the expected value of the radon relaxation length. The drums were filled with finely crushed uranium ore.

When the covers are closed, and after radioactive equilibrium has been established between the radon and its daughter products, intensity measurements on the various gamma lines give the output from the collimated detector as a function of the energy of the chosen lines. The Ra₂₂₆ line at 186.2 keV and that of Pa^m₂₃₄ at 1001 keV serve as references for the other lines, using the known uranium concentration of the ore for verification.

When the covers are withdrawn, and after establishing the profile of the radon diffusion, new measurements lead to the calculation of the emanation coefficient and the relaxation length. The ore in place has quite a low saturation level of less than 30% in the porous volume. The air in the porous volume is then scavenged. The ratio of the gamma lines of the daughter products of radon to those of the radium provides a new measurement of the emanation coefficient.

If necessary, these blocks could be used to produce experimental values of the gamma photon absorption coefficient for samples of soils forming the basis of a gamma spectral mapping.

3.2.2. Results

The ground results are currently being analysed, as are those relating to the calibration blocks.

The method is illustrated using the results obtained on the piles of tailings from the treatment of uranium ore from the Zirovski mine (BORST site) in Slovenia. The results presented in Annex 2 are those provided by the CARTOGER procedure from processing raw spectrometric data in Excel 5.

¹ We should like to thank the management of Rudnik Zirovski Vrh who kindly allowed us access to their installations

4. WORK IN PROGRESS

A great deal of work remains to be done in analysing the ground measurements already made and those now being made. The possibility of taking into account the saturation levels of the water in the porous volume of the soil and its spectrometric determination is still to be studied.

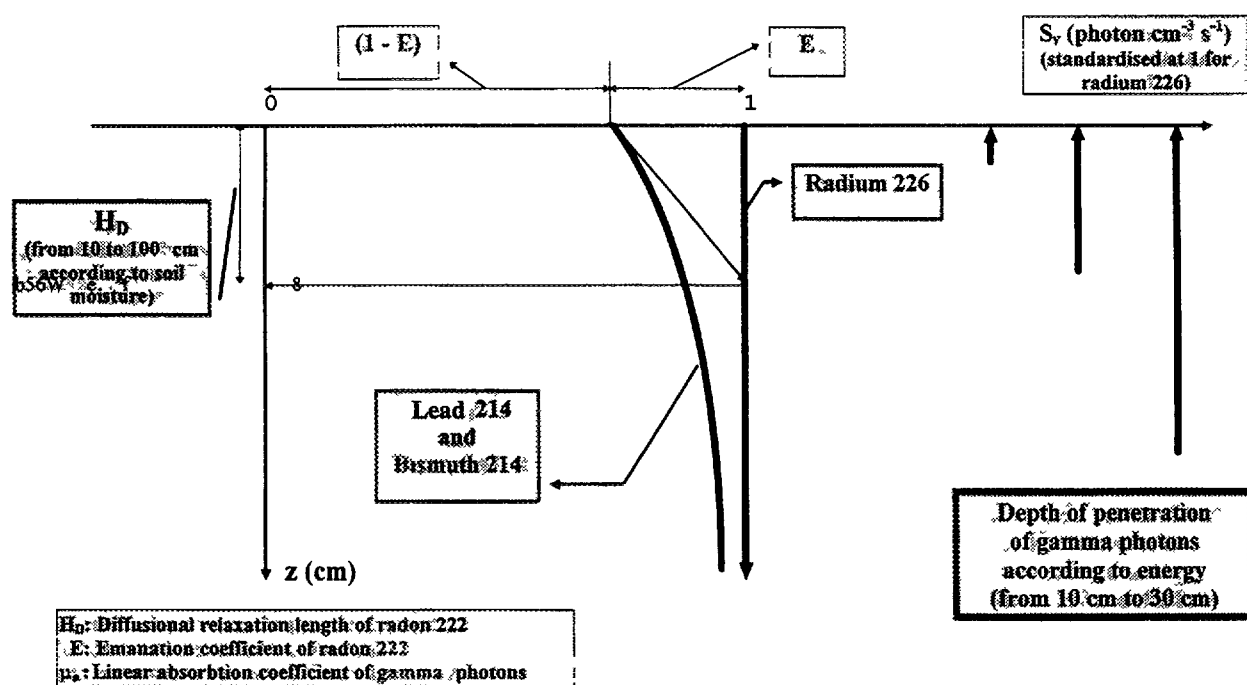


FIG. 1. Strength of emission S_v of γ photons of radium 226, of lead 214 and of bismuth 214 as a function of soil depth z .

5. PROVISIONAL CONCLUSIONS

The proposed method undoubtedly has potential applications, but we still have to define its limitations, the conditions under which it can be used and its cost. As regards characterising the propensity of the soil to produce radon 222 anomalies in premises, the method should be able to provide the intensity of the production of radon in the porous volume and characterise its diffusion to the soil-atmosphere interface. On the other hand, the method does not seem capable of providing a characterisation of the soil permeability, which is the other factor involved in the problem of domestic radon anomalies. As regards the measurement of flux at the surface of covered or uncovered waste dumps, the method should lead to a good characterisation of the exhalation flux, which is of diffusive origin.

REFERENCES

- [1] GAMBARD, J.P., PIRARD, Ph., LACATON, F., National programme for measuring the natural radioactivity in French départements, radon mapping in France, IPSN/SEGR document, (February 1996).
- [2] MINISTRY OF THE ENVIRONMENT, Map showing the potential emanation from radon gas in France, DPPR (1992).
- [3] BRAJNIK, D., MIKLAZIC, U., TOMSIC, J., "Map of natural radioactivity in Slovenia and its correlation to the emanation of radon", Radiation Protection Dosimetry, Vol. 45 No. 1/4 Nuclear Technology Publishing (1992) 273-276.

- [4] ANDJELOV, M., "Results of radiometric and geochemical measurements for the natural map of Slovenia", *Geologia* 36, Ljubljana (1994) 223–248.
- [5] OTTON, J.K. and coworkers, "The Geology of Radon", published U.S. Department of the Interior/U.S. Geological Survey, by J.K. Otton and coworkers (available from USGS, Branch of Distribution, PO Box 25286, Denver, CO 80225 USA).
- [6] KRIZMAN M., STEGNAR, P., "Environmental Impact of the Zirovski Vrh Uranium Mine on the Enhancement of Outdoor Radon Concentrations", *Radiation Protection Dosimetry*, Vol. 45 No. ¼, Nuclear Technology Publishing (1992) 723–28.
- [7] KRIZMAN, M., BYRNE, A.R., BENEDIK, L., "Distribution of Th 230 in Milling Wastes from the Zirovski Vrh Uranium Mine (Slovenia) and its Application", *J. Environmental Radioecology* 26 (1995) 233–235.
- [8] YOKEL, F.Y., TANNER, A.B., "Site Exploration for Radon Source Potential", US Department of Commerce, Housing and Urban Development, NISTIR 5135, Washington DC (Dec. 1992).
- [9] BADR, I., OLIVER, M.A., HENDRY G.L., DURRANT, S.A., "Determining the spatial scale of variation in soil radon values using a nested survey and analysis", *Radiation Protection Dosimetry*, Vol. 49, N04 Nuclear Technology Publishing (1993) 433–442.
- [10] Matheron, G., "The Theory of Regionalized Variables and its Applications", *Cahiers du Centre de Morphologie Mathématique* No. 5 Ecole des Mines de Paris (1971) (in French).
- [11] MILLER, K.M., SHEBELL P., KLEMIC, G.A., "*In situ* Gamma Ray Spectrometry for the Measurement of Uranium in Surface Soils", *Health Physics* (Aug. 1994) Vol. 67, No. 2.
- [12] CORTELLA, J., BOURGEOIS, C., CHASTEL, R., ROSENBERG, A., "Post-accident radiological measurements: contamination map", *Recovery Operations in the Event of a Nuclear Accident or Radiological Emergency* (Proc. Symp. Vienna 1989) IAEA, Vienna (1990) 347.

ANNEX 1

Theoretical Aspects

P. ZETTWOOG

Auffargis, France

DESCRIPTION OF A METHOD OF MEASURING THE FLUX OF RADON 222 EXHALED BY SOILS FOR DIFFUSION

1. SUMMARY

We describe a method of distance measuring the flux of radon 222 at the soil-atmosphere interfaces, based on the use of a high resolution gamma spectograph. This method only functions for diffusive flux. The radon atoms are transported under the effect of a gradient of the concentration of the radon atoms in the pore spaces of the soil in the vicinity of its interface with the atmosphere. The gas which fills the pore spaces is itself at rest, there is no convective flux. The method uses the values of the intensities of the gamma radiation emitted during the radioactive decay of radium 226, parent of radon 222, and of two of its short-lived daughter products, bismuth 214 and lead 214.

According to the energy of the different radiations, the measurement takes into account the varying thicknesses of the soil. Since we know the characteristics of the soil for the absorption of gamma radiation, we can deduce the value of the parameters which come into the calculation of the diffusive exhalation flux, with a hypothesis of the uniformity of the physical properties of the soil.

2. INTRODUCTION

This method is based on the measurement of the intensity of the radiation of the gamma emitters in the U 238 chain of the soil obtained by a high resolution spectrometer. Exploitable gamma emitters are to be found in table I.

We can distinguish the peak Ra 226 + U 238 at 184.08 KeV on the one hand, and all the peaks of the daughter products Pb 214 and Bi 214 of Rn 222 on the other hand. That is γ_0 the photons of the first peak and γ_i those of the daughter products.

The number of photons per second received by a detector in a peak i coming from the layer of soil between z and z + dz is:

$$dCi = \alpha_{air}^i \times A_{Ra} \times Ri \times e^{-\frac{z}{H_{\gamma_i}}} dz \times f_1 \times f(H_D, E, z) \times \Omega$$

H_{γ_i} : Length of attenuation in the soil for γ_i (cm)

$$H_{\gamma_i} = \frac{x^{1/2}}{0.693}$$

If $x^{1/2}$ is the distance where half the photons have interacted ;

A_{Ra} : Soil activity concentration of Ra 226 per unit of volume (Bq.m⁻³)
 f_i : Number of photons per desintegration of emitter i
 Ri : Efficiency of the detector for γ_i

Table 1
List of the exploitable gamma emitters of the uranium 238 chain.

From A. Canet and R. Jacquemin, Methods for measuring radium isotopes : Gamma spectrometry. AIEA - TRS No. 310, The Environmental Behaviour of radium, Vol. 1, Chap. 3 - 4

Emitters	Lines (keV)	Emission f_i (%)	Remarks
Ra 226	186.2	3.3	Interference with the line 185.7 keV of U235, emission of 2.5 % ¹ , try to use the line 1001.03 keV of Pa ^m 234 to calculate the concentration of U238, then of U 235. There is no equilibrium between U 238 and Ra 226 in the soil.
Pb 214	242.0 295.2 351.9	7.4 18.7 35.8	Interference with the line 351.0 keV of Bi 211, its contribution may be calculated from line 270 keV of Ra 223.
Bi 214	609 1120 1764 2448	45 14.9 16.07 1.57	Reference line for the measurement of Ra 226, after placing at equilibrium. Reduction in the effectiveness of the detectors.

¹ The value 2.5 % takes into account the isotopic composition of natural uranium, 99.28 % of U 238 and 0.72 % of U 235.

Ω	:	Solid non-collimated angle
σ	:	Surface of the detector
$f(H_D, E, z)$:	A function which takes into account the disappearance of radon 222 by emanation and diffusion (description of the divergence at the equilibrium between Ran 222 and Ra 226 in the vicinity of the soil)
H_D, E	:	Length of diffusional relaxation of radon in the pore space and emanation factor of radon
α_{air}	:	Attenuation in the air over the soil-detector surface

For the peak of radon 226, we have :

$$dCo = \alpha_{air}^0 \times A_{Ra} \times Ri \times e^{-\frac{z}{H_D^0}} dz \times f_o \times \Omega \times \sigma$$

We suppose that the radium concentration is uniform ;

We have :

$$Ci = \int_0^\infty dCi \text{ for the peak } i$$

$$Co = \int_0^\infty dCi \text{ for the peak readium 226}$$

With the help of measurements carried out on a large enough number of peaks, we can, with a hypothesis on the form of the function $f(H_D, E, z)$, determine the parameters H_D and E , taking into account the lengths of attenuation for the peaks considered.

3. ESTABLISHMENT OF A CALCULATION FORMULA FOR DIFFUSIVE FLUX

A soil includes heterogeneities of a more or less random nature, large stones, roots, tunnels dug by burrowing animals. If we place ourselves on a large enough scale, the three-dimensional aspect introduced by these heterogeneities finishes by disappearing.

We can then consider that the physical properties of the soil depend only on the depth z . Pedologists differentiate in a soil several types of "horizons", or layers parallel to the surface, situated between the surface and the non-modified rock situated at the base of the soil, called "horizon R". These layers, horizons A, B, C, and their subdivisions, are of variable importance depending on the type of soil. Briefly, the A layers, the most superficial, contain a notable proportion of organic matter and are impoverished in clays. The C layers, above the horizon R, correspond to the alteration of the subjacent rock, but the constituents do not derive from the pedogenetic processes which individualise the horizons above. The B layers make the transition between the A layers and the C layers, and are richer in clay. Organic matter and clays are capable of absorbing radon and slowing its migration.

If the physical properties of the soil according to these different horizons are known according to depth, we may establish the equations which describe at each depth z the emanation of radon and its diffusion in the pore space. We may deduce from that the concentration profile $N(z)$ in radon and therefore the flux according to the equation :

$$\phi_{ex} = \epsilon \frac{D}{T} \left(\frac{dN}{dz} \right)_{z=0} \quad (1)$$

with

ϕ	:	exhalation flux, atom.m ² .s ⁻¹
ϵ	:	porosity
D	:	coefficient of diffusion in the pore space, m ² .s ⁻¹
T	:	tortuousness, to take into account the lengthening of the migration lines in relation to the vertical
$N(z)$:	concentration of the atom radon 222 in the pore space

If the soil is an artificial soil placed as a cover over a stock of solid radium-containing residues, we know the physical properties and the thickness of the layers making it up, we know how to calculate $N(z)$ and therefore the flux according to equation (1).

In what follows, we suppose, both as an example and as a first approximation, that the properties of the soil are uniform. In particular, that the activity concentration of radium 226 A_{226} (Bq.m⁻³), porosity ϵ , the coefficient of diffusion D and tortuousness T are constant.

In the pore space, diffusion is described by :

$$\frac{D}{T} \frac{d^2 N}{dz^2} - \lambda N + E A_{Ra} = 0 \quad (2)$$

We calculate that the concentration profile is described by :

$$N(z) = N_{\infty} (1 - e^{-z/H_D}) \quad (3)$$

The flux being equivalent to :

$$\phi_{ex} = A_{226} \times E \times H_D \quad (4)$$

with

$$N_{\infty} = \frac{E \times A_{226}}{\lambda_{222} \epsilon} \text{ atome.m}^{-3} \quad (5)$$

λ_{222} = the decay constant of radon 222, $2,1 \times 10^{-6} \text{ s}^{-1}$

$$H_D = \sqrt{\frac{D}{T \lambda_{222}}}, \text{ length of relaxation (m)}$$

This formula is valid for a stock of non-covered uranium milling wastes.

If the wastes are covered, we may consider that, in the pore space of the covering, atoms of radon 222 coming from the wastes are far more numerous than those emanating from the traces of radium 226 in the materials of the covering.

In the covering, the equation (2) is reduced then to :

$$\frac{D}{T} \frac{d^2 N}{dz^2} - \lambda N = 0 \quad (2bis)$$

The solution is of the form :

$N(z) = N^* h z/H_D$, N^* being a value of the concentration such that the continuity of the real flux of radon be ensured at the interface waste-covering $z = H_c$, that is the continuity of :

$$\frac{\epsilon D}{T} \left(\frac{dN}{dz} \right)_{z=H_c} \quad (\text{equation 1})$$

The indices R and C designating the waste and the covering, we

$$\frac{z-H_c}{H^D}$$

have:

$$N_R(z) = N_\infty - (N_\infty - N^*) e^{\frac{-z \cdot H_c}{F_{DR}}} \quad (\text{from equation 2})$$

$$N_C = N^* Sh \frac{z}{H_{DC}} \quad (\text{from equation 2bis})$$

$$\frac{\epsilon_R D_R}{T_R} \cdot \frac{N_\infty - N^*}{H_{DR}} = \frac{\epsilon_C D_C}{T_C} \frac{N^*}{H_{DC}} Ch \frac{H_C}{H_{DC}}$$

that is:

$$\epsilon_R H_{DR} (N_\infty - N^*) = \epsilon_C H_{DC} N^* Ch \frac{H_C}{H_{DC}}$$

$$N^* = N_\infty \frac{\epsilon_R H_{DR}}{\epsilon_R H_{DR} + \epsilon_C H_{DC} Ch \frac{H_C}{H_{DC}}} \quad (6)$$

4. THE DISTRIBUTION OF GAMMA EMITTERS ACCORDING TO DEPTH

We shall use the following gamma lines:

- the line of Ra 226, at 186.2 keV. In the vicinity, we also find the line of U 235.
- the lines of Pb 214 and Bi 214, those that provide the most easily readable peaks being those of Pb 214 at 242 keV, 295.2 keV, and 351.9 keV, and those of Bi 214 at 609 keV, 1120 keV, 1764 keV and 2448 keV.

According to the hypotheses above, we know that :

- A_{Ra226} not depend on z and is equivalent to zero in a covering ;
- ϵ , H_D , E , are constants specific to the soil ;
- N^* is a constant specific to the respective thickness of the stocks and the covering and of their physical properties.

The emission constants f_0 , f_1 of the gamma lines of the radium 226, bismuth 214 and lead 214 emitters are to be found in Standards (see Table I).

In the case of soils or non-covered stocks, the activity concentrations of radon and its daughter products in the pore space on the one hand, in the mineral space on the other, are at equilibrium. The activity concentration of radon is evaluated in relation to the activity concentration of radium by :

$$A_{222} = A_{226} \times f(z, E, H_D)$$

$$f(z, E, H_D) = (1 - E + \left(1 - e^{-\frac{z}{H_D}}\right))$$

$$A_{222} = A_{226} \times f(z, E, H_D) = \left(1 - E e^{-\frac{z}{H_D}}\right) A_{226} \quad (6)$$

In the case of a covering, the activity concentrations of radon and its descendants are at equilibrium and are given by :

$$A_{222} = \lambda_{222} N(z) = \lambda_{222} N^* Sh \frac{z}{H_d} \quad (6bis)$$

We are in fact neglecting the radium 226 activity of the materials of the covering.

The number of disintegrations per second and per unit of volume of each emitter is, by definition, equal to its activity concentration.

The number of photons per disintegration, according to the different energies, f_1 is provided in Table I.

5. FLUX OF PHOTONS TO THE SITE OF THE DETECTOR OF THE GAMMA SPECTROGRAPH

The flux of gamma photons ϕ (number of photons per cm^2 and per second) received by a target at a point P situated at a distance R from a source S (photon s^{-1}), is such that

$$\phi = \frac{S}{4 \pi R^2} \quad (7)$$

Let us consider a detector situated at P at a distance a from the soil. Either all the emitters of the annulus dV situated at the distance R from P between the depths z and z + dz and of rays between r and $r + dr$, or between $R \sin \theta$ and $R (\sin \theta + d\theta)$ (see Fig 1)

The volume of this element is $(2 \pi R \sin \theta) (R d\theta) dz$, with

$$R = \frac{a + z}{\cos \theta}, \quad dR = \frac{dz}{\cos \theta},$$

$$\text{i.e. } dV = 2 \pi R^2 \frac{\sin \theta}{\cos \theta} d\theta dz$$

That is S'_v , the number of photons of energy i emitted per unit of volume and per second in the plane z

The flux of photons received at P, coming from dV is, according to (7), and neglecting air gamma absorption:

$$d^2 \phi^i = \frac{S'_v}{2} x \frac{\sin \theta}{\cos \theta} e^{-\frac{\mu_s^i z}{\cos \theta}} d\theta dz \quad (8)$$

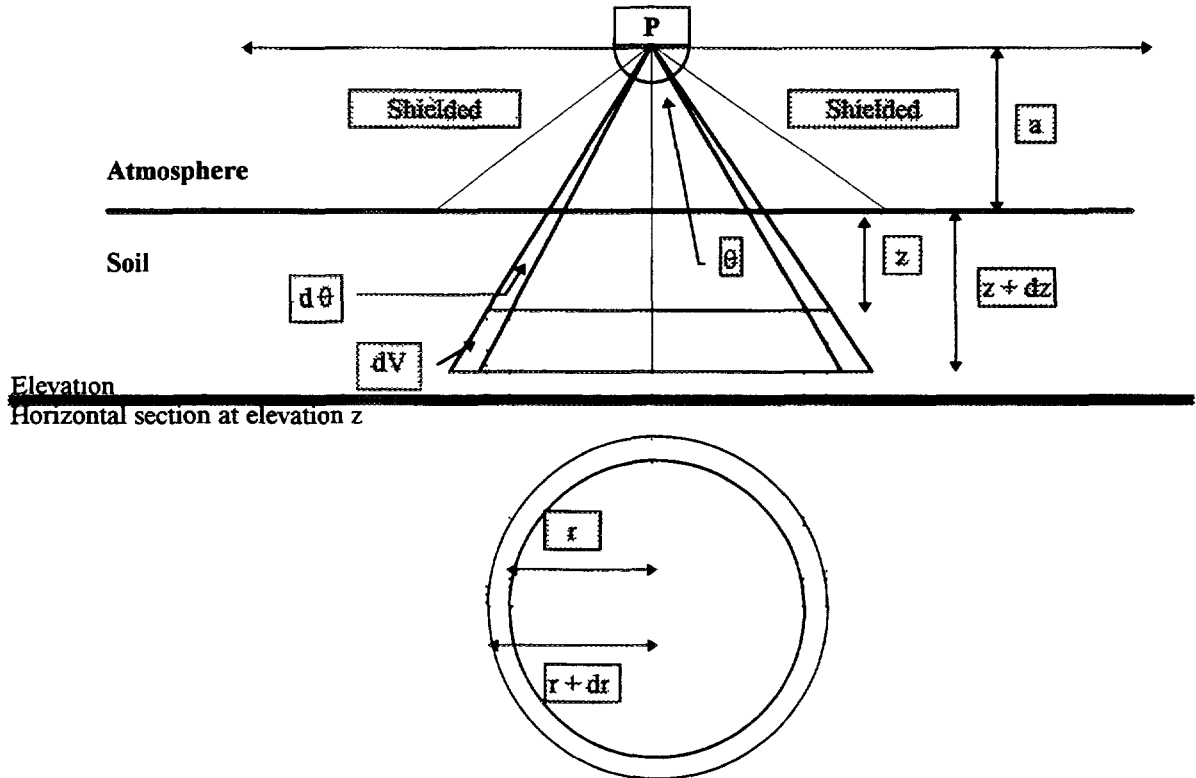


FIG 1 Diagram showing integration of the flux of photons received by the detector

Here we have introduced the term :

$$e^{\frac{-\mu_s^i z}{\cos \theta}}$$

which represents the fraction of photons remaining in the direct flux between dV and P after passing through the thickness:

$$\frac{z}{\cos \theta}$$

in the soil.

μ_s^i , characterises the soil's properties of absorption for the photons of energy and the quantity :

$$\left(1 - e^{\frac{-\mu_s^i z}{\cos \theta}} \right)$$

represents the fraction of photons which have undergone an interaction with the matter and which have left their initial path.

Moreover, is equivalent to $A_{222} f_i$, A_{222} being provided according to z by equations (6) or (6b), f_i emission constant.

As far as radium 226 is concerned, which has only one line which is can be exploited, at 186 keV, it will be given the exponent or the index zero.

We have

$$S_v^i = A_{226} \times f_0$$

A_{226} does not depend on z .

The values of f_0 and of the f_i 's for the most easily exploitable lines of bismuth 214 and lead 214 are given in Table I.

We can write then, according to the problem,

- In the case of soils and non-covered wastes (6)

$$d^2 \phi^i = \frac{A_{226}}{2} \left(1 - E e^{-\frac{z}{H_D}} \right) f_i \times \frac{\sin \theta}{\cos \theta} e^{-\frac{\mu_s^i z}{\cos \theta}} d\theta dz \quad (9)$$

- In the case of a covering (6bis)

$$d^2 \phi^i = \left(\frac{\lambda_{226} N^*}{2} \text{Sh} \frac{z}{H_D} \right) f_i \times \frac{\sin \theta}{\cos \theta} e^{-\frac{\mu_s^i z}{\cos \theta}} d\theta dz \quad (8\text{bis})$$

N^* is given by (5).

For the photons from radium 226, we have :

$$d^2 \phi^i = \frac{A_{226}}{2} f_o \times \frac{\sin \theta}{\cos \theta} e^{-\frac{\mu_s^o z}{\cos \theta}} d\theta dz \quad (8ter)$$

We suppose that the gamma photons coming from wastes are absorbed in the covering if there is one $d^2 \phi^0$ is then of no use.

5.1. Radium 226 gammas

The equation (8ter) is immediately integrated, the limits of integration being, for z, zero and infinite, and for θ , 0 and θ_1 , θ_1 being the collimating angle of the receiver (opening $2 \theta_1$).

Let us integrate $d^2 \phi^0$ at z then at θ .

This gives rise to :

$$\begin{aligned} d\phi^o &= \int_0^\infty d^2 \phi^o = \frac{A_{226} f_o}{2 \mu_s^o} \sin \theta d\theta \\ d\phi^o &= \int_0^{\theta_1} d\phi^o = \frac{A_{226} f_o}{2 \mu_s^o} (1 - \cos \theta_1) \end{aligned} \quad (9)$$

We note that ϕ^o is independant of the distance a. For a small enough θ_1 ,

$$\phi^o \approx \frac{A_{226} f_o}{4 \mu_s^o} \theta_1^2$$

In so far as the distance a is over 10 m (spectograph on board an aircraft), we must however take account of the absorption of the photons by the molecules of the air, characterised by, for the photons of radium 226. We have :

$$\phi^o = \frac{A_{226} f_o}{2 \mu_s^o} \int_0^{\theta_1} e^{-\frac{\mu_a^o a}{\cos \theta}} \sin \theta d\theta$$

If ϕ_1 is small enough, we have, to within the second order in θ :

$$\phi^o = \frac{A_{226} f_o}{4 \mu_s^o} \theta_1^2 e^{-(\mu_a^o a)} \quad (9ter)$$

We can see that half the photons of the line 200 keV is absorbed over 25 metres and half the photons of the line 2,5 MeV is absorbed over 110 metres.

5.2. Bismuth 214 and lead 214 gammas, on a stock of covered waste

We obtain :

$$d^2 \phi' = \frac{A_{226} \hat{f}l}{2} \left[\int_0^\infty \frac{\sin \theta}{\cos \theta} e^{-\frac{\mu_s' z}{\cos \theta}} d\theta dz - E \int_0^\infty \frac{\sin \theta}{\cos \theta} e^{-\left(\frac{\mu_s' z}{\cos \theta} + \frac{z}{H_D}\right)} d\theta dz \right]$$

The first integral is equivalent to

$$\frac{\sin \theta d\theta}{\mu_s'}$$

The second integral is equivalent, putting down :

$$\left(\frac{\mu_s'}{\cos \theta} + \frac{1}{H_D} \right) z = x$$

$$\left[\frac{\frac{\sin \theta d\theta}{\cos \theta}}{\left(\frac{\mu_s'}{\cos \theta} + \frac{1}{H_D} \right)} \right] \int_0^\infty d^{-x} dx = \frac{\sin \theta d\theta}{\mu_s' \left(1 + \frac{\cos \theta}{\mu_s' H_D} \right)}$$

From which, for $d \phi'$:

$$d \phi' = \frac{A_{226} \hat{f}l}{2 \mu_s'} \left(1 - \frac{E}{1 + \frac{\cos \theta}{\mu_s' H_D}} \right) \sin \theta d\theta$$

From which for :

$$\phi' = \int_0^{\theta_1} d \phi'$$

$$\phi' = \frac{A_{226} \hat{f}l}{2 \mu_s'} \left[(1 - \cos \theta_1) - (E \mu_s' H_D) \log \frac{1 + \mu_s' H_D}{\cos \theta_1 + \mu_s' H_D} \right]$$

If θ_1 is small enough, we may write, to within the second order :

$$\phi' = \frac{A_{226} \hat{f}l}{4 \mu_s'} \theta_1^2 \left[1 - E \frac{\mu_s' H_D}{1 + \mu_s' H_D} \right]$$

5.3. Coverings

We suppose that the ground noise due to the radium 226 of the covering is negligible.

Equation (8bis) gives, by integrating only over the thickness of the covering for the ranges of Bi 214 and Pb 214, which correspond to the radon 222 of the wastes which have diffused into the covering :

$$[d \phi^i]_c = \frac{\lambda_{222} N^* f_i \sin \theta}{2 \cos \theta} \int_0^{H_c} Sh \frac{z}{H_{DC}} e^{-\frac{\mu_s^i z}{\cos \theta}} d\theta dz$$

$$\phi_c^i = \frac{\lambda_{222} N^* f_i}{Z} \int_0^{\theta_1} \frac{\sin \theta}{\cos \theta} d\theta \int_0^{H_c} Sh \frac{z}{H_{DC}} e^{-\frac{\mu_s^i z}{\cos \theta}} dz$$

There are no difficulties in the calculation of the two integrals, but the expression obtained for is less concise after integration than after, and we did not carry it out.

6. EXPLOITATION OF THE SPECTROGRAPHIC MEASUREMENTS

6.1. Soils and non-covered wastes

The method leads to the calculation of the exhalation flux of radon 222.

The spectograph gives, after taking into account the Ri and Ro detection efficiency for the energies of index i and zero, the counting rates C' and C/ which are in the ratio :

$$\frac{C'}{C^0} = \frac{f_i Ri H_\gamma^i}{f_0 Ro H_\gamma^0} \left[1 - \frac{E H_D}{H_\gamma^i + H_D} \right]$$

We introduce :

$$H_\gamma^i = \frac{1}{\mu_s^i}, H_\gamma^0 = \frac{1}{\mu_s^0},$$

which are lengths such that after having covered them, the direct flux of photons is divided by $e = 2.718$. By covering $0.693 H_\gamma$, the flux is divided by 2.

We write, supposing that θ_1 is small enough :

$$\frac{C'}{C^0} = \frac{f_i Ri H_\gamma^i}{f_0 Ro H_\gamma^0} \left[1 - \frac{E H_D}{H_\gamma^i + H_D} \right]$$

Let us introduce the soil mass absorbtion coefficient σ_{Ti} ($\text{cm}^2 \text{ g}$). μ_s^i is given by the product $\sigma_{Ti} \times \rho_{\text{soil}}$, ρ_{soil} being the soil mass density (g cm^{-3}). The software associated with the spectrograph allows us to introduce, on lign, the parameters f_i , R_i , f_0 , R_0 so that we obtain directly the ratio :

$$A^i = \frac{C' / f_i Ri}{C^0 / f_0 Ro} = \frac{\sigma_{T0}}{\sigma_{Ti}} \left[1 - \frac{E \rho_{\text{soil}} H_D}{\frac{1}{\sigma_{Ti}} + \rho_{\text{soil}} H_D} \right] \quad (10)$$

In this formula, E and the product ($\rho_{\text{soil}} \times H_D$) are the two unknown quantities to be determined, the σ_T being given by Standards, see for instance British Standards Institution, B. S. 4094 Part 1, 1966.

By exploiting the various peaks i, we obtain i equations of type (10) for the two unknowns which allows us, by using an appropriate process, to improve the precision of their calculations.

Moreover, the spectograph gives, as an absolute value, after taking into account f_0 and the detection efficiency for the peak Ro, the quantity :

$$\Gamma_0 = \frac{A_{226}}{2 \rho_{\text{soil}} \sigma_{T0}} (1 - \cos \theta_1)$$

We deduce A_{226}^m , which is the soil activity concentration per unit of mass (Bq g⁻¹), by:

$$A_{226}^m = \frac{A_{226}}{\rho_{\text{soil}}} = \frac{2 \sigma_{T0} \Gamma_0}{1 - \cos \theta_1}$$

which, associated to $\rho_{\text{soil}} H_D$ and to E, allows us to calculate, according to (4), the flux of radon 222 by

$$\phi_{\text{ex}} = A_{226} \times E \times H_D = A_{226}^m \times E \times (\rho_{\text{soil}} H_d) \quad (11)$$

Construction of a calculation chart to determine E and H_D (assuming $\rho_{\text{soil}} = 1.56 \text{ g cm}^{-3}$)

Let us consider, among all the possible lines, the 2 lines :

$$\begin{aligned} \gamma_1 &: \text{Pb 214} : 242 \text{ keV} \\ \gamma_8 &: \text{Bi 214} : 2448 \text{ keV} \end{aligned}$$

with as a reference γ_0 : Ra 226 : 186 keV.

In Table II we give the mass absorption coefficients for these 3 lines, and we calculated the corresponding $H_{\gamma'}$ values assuming $\rho_{\text{soil}} = 1.56 \text{ g cm}^{-3}$.

With the enclosed calculation graph, Figure 2, we obtain values of H_D and E corresponding to a given couple of A^1 and A^8 , according to equation (10) and the values of Table 2 for the $H_{\gamma'}$.

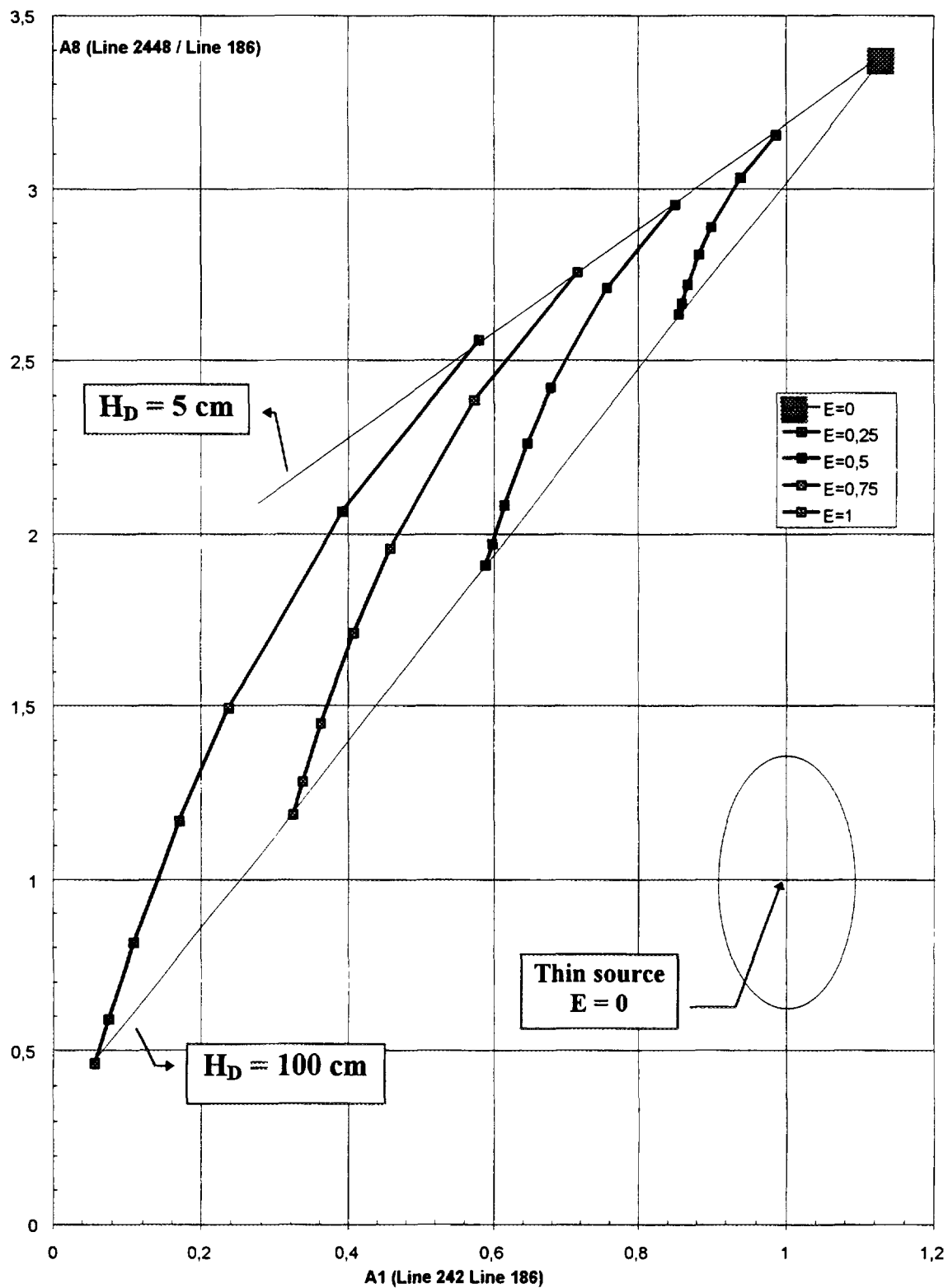
The calculations are made with $\rho_{\text{soil}} = 1.56 \text{ g.cm}^{-3}$, which is obtained in a standard soil with porosity 0.4.

To be noted is that the subsequent calculation of the radon 222 flux is not dependant of the here assumed value for ρ_{soil} , that is $\rho_{\text{soil}} = 1.56 \text{ g.cm}^{-3}$, as indicated by equation (11).

6.2. Coverings

We are dealing with the case of the single layer covering with uniform properties.

What we are looking for here is the value H_{DC} , which characterises the covering. The factor



E_0 : 186 keV

E_1 : 238 keV

E_8 : 2448 keV

The 7 H_D values in this graph are: 5 cm; 10 cm; 20 cm; 30 cm; 50 cm; 75 cm; 100 cm.

FIG. 2. Chart for determination of E and H_D using the 7 most exploitable gamma emitters and assuming $\rho_{\text{soil}} = 1.56 \text{ g.cm}^{-3}$.

of reduction of the flux of radon is approximately equal to $e^{-\frac{H_{DC}}{H_C}}$

Supposing that $\cos \theta_1 \approx 1$ et $\sin \theta_1 \approx \theta_1$, we have from (8bis)

$$[d\phi]_c = \frac{\lambda_{222} N^* f \theta_1^2}{2} \int_0^{H_C} Sh \frac{z}{H_{DC}} e^{-\mu_s' z} dz$$

$$\frac{[d\phi]_c}{[d\phi]_c}$$

The ratios are functions of H_{DC} tabulatable according to H_C, μ_s', μ_s'' . The measurement of anyone of these by the spectograph allows us to calculate H_{DC} , knowing H_C, μ_s', μ_s'' .

We can then calculate N^* . We deduce from that the exhalation flux of radon by

$$\frac{\epsilon_c D_c}{T_C} \left(\frac{dN}{dz} \right)_{z=0} = \epsilon_c H_{DC} N^*.$$

At the same time we have a value close to the coefficient of reduction of the flux due to the covering,

that is $e^{-\frac{H_{DC}}{H_C}}$.

6.3. Calibration pads

These pads are made up of a cylindrical bed of ore in the form of a homogenous powder of thickness H_p with a measured uniform density ρ_{mn} , the length of diffusional relaxation being H_{DP} . The bottom section of the pad is seen under the angle θ_1 by the detector placed in the axis of the cylinder.

The concentration profile of radon 222 is obtained by the resolution of equation (2). We obtain:

$$N_p(z) = N_\infty \left[1 - \frac{Ch \frac{(Z - H_p)}{H_{DP}}}{Ch \frac{H_p}{H_{DP}}} \right]$$

which allows us to respect

$$N_p(0) = 0 \text{ et } \left(\frac{dN_p}{dz} \right)_{z=H_p} = 0$$

We have (see above),

$$A_{222} = A_{226} \left[1 - E \frac{Ch \frac{Z H_p}{H_{Dp}}}{Ch \frac{H_p}{H_{Dp}}} \right]$$

$$S^i = F_i A_{222}$$

$$d^2\phi^i = f_i \frac{A_{222} \sin\theta}{2 \cos\theta} e^{-\frac{\mu_s^i z}{\cos\theta}} d\theta dz$$

$$\phi_i = f_i \frac{A_{226}}{2} \int_0^{\theta_1} \int_0^{H_p} \left[1 - E \frac{Ch \frac{(Z-H_p)}{H_{Dp}}}{Ch \frac{H_p}{H_{Dp}}} \right] \frac{\sin\theta}{\cos\theta} e^{-\frac{\mu_s^i}{\cos\theta}} d\theta dz$$

$$\phi_0 = f_0 \frac{A_{226}}{2} \int_0^{\theta_1} \int_0^{H_p} \frac{\sin\theta}{\cos\theta} e^{-\frac{\mu_s^0}{\cos\theta}} d\theta dz$$

From these countings on the radium line, we obtain (see above) the value of A_{226} (or of A_{226}^m).

$$\frac{\phi_1}{\phi_0} \quad \text{up to} \quad \frac{\phi_8}{\phi_0},$$

From the 7 ratios (see Table II), we may then determine E and H_{Dp} for the ore.

Moreover, the experimental set-up allows :

either the scanning of the pore space of the bed by fresh air, which gives :

$$A_{222} = A_{226}(1 - E)$$

over all the thickness of the bed, and allows for an independant determination of E,

or the putting into place of an airtight lid which gives, when the radioactive equilibrium between radium 226 and radon 222 is obtained,

$$A_{222} = A_{226},$$

which comes down to considering $E = 0$.

We have then :

$$\phi_i = f_i \frac{A_{222}}{2} \int_0^{\theta} \int_0^H \frac{\sin\theta}{\cos\theta} e^{-\frac{\mu_s^i}{\cos\theta}} d\theta dz$$

$$\frac{\phi_i}{\phi_0}$$

The ratios obtained are leading to the experimental determination of the values of μ_s^i and therefore of the products $\sigma_{Ti} \times \rho_{min}$.

Table 2
Values of H_γ for the 7 most easily exploitable gamma emitters, assuming $\rho_{\text{soil}} = 1.56 \text{ g.cm}^{-3}$

N° of line	Emitter	Energy (keV)	$\sigma_T \text{ (g cm}^{-2}\text{)}$	$H_\gamma \text{ (cm)}$
0	Ra 226	186	0,134	4,78
1	Pb 214	242	0,120	5,36
2	Pb 214	295	0,109	5,38
3	Pb 214	352	0,098	6,54
4	Bi 214	609	0,083	7,72
5 ⁽¹⁾	Pa ^m 234	1001	0,067	9,57
6	Bi 214	1120	0,062	10,33
7	Bi 214	1764	0,050	12,82
8	Bi 214	2448	0,040	16,03

⁽¹⁾ This line is not used for E and H_D determination but for checking the U 238 concentration.

ANNEX 2

Programmes of Ground Measurements: Application of the CARTOGER procedure to the Treatment of Results Obtained at the BORST Site in Slovenia

M. ANDJELOV

Geological Survey Ljubljana, Ljubljana, Slovenia.

P. JOVANOVITCH

Institute of Occupational Safety, 61000 LJUBLJANA, Slovenia

J. CLOUTÉ-CAZALAA, M. JANOT

Algade, R & D Dept., Bessines sur Gartempe, France

P. ZETTWOOG

Office de Protection contre les Rayonnements Ionisants, Le Vésinet, France

We illustrate the application of the theory of measuring diffusive radon 222 flux in Annex 1 by presenting the results obtained on the pile of tailings remaining from the treatment of ores at the Zirovski Vrh mine in Slovenia. At the time when the measurements were made, the tailings had not been covered. The specific activity of the radium 226 expected from the tailings was of the order of 10 Bq g⁻¹. This relatively high value for the specific activity compensated for the relatively small volume of the detector. The assumptions that the medium has uniform properties and that the radon diffusion is a one-dimensional process are acceptable for this type of deposit.

The spectral data provided by spectrometry are processed using the CARTOGER procedure, which is an application of the theory given in Annex 1 and which runs in Excel 5 on a portable computer.

The characteristics of the gamma lines involved and of the detector (geometry, efficiency) together with the mass absorption cross-section of the soil σ_{Ti} for the *i*th gamma line are introduced using data from the table in Plate 1.

The calculated values of the specific activity (Bq/g) for the 8 gamma lines used appear in Plate 2.

The specific activities of radium 226 and uranium 238 are derived from measurements on lines of energy 185.7 keV and 1001 keV. We find:

Specific activity of radium 226	$A_{Ra}^m = 12.34 \text{ Bq/g}$
Activity of uranium 238	$A_U^m = 0.41 \text{ Bq/g}$

The efficiency of the plant's extraction treatment calculated from this is 97%.

These results, although optimistic as far as the plant's efficiency is concerned, are not in conflict with the data from the operator.

The values of the apparent specific activity for the different gamma lines emitted by the daughter products of radon 222 are plotted in the graph of Plate 2. These activities show a shortfall in activity compared with that of radium 226. This is explained by the fact that a fraction of the radon 222 has emanated from the solid phase and diffused towards the atmosphere. We introduce the ratio U_i between the activity of line i time σ_{Ti} and the activity of line 0 relative to radium 226 time σ_{T0} . For the line with the lowest energy, the spectrometric examination concerns only a layer of the tailings with a thickness of the order of a few cm. To a first approximation, the ratio U_i for this line is $(1 - E)$. As the energy of the gamma lines used increases, regions at increasing depths are probed. The concentration of radon 222 and therefore that of its daughter products increase in the porous volume.

The concentration profile is characterised by an exponential law whose characteristic length is the diffusional relaxation length for radon 222. This length can be obtained from the rate at which the apparent specific activities increase with energy, knowing the soil density.

More precisely, the theory presented in Annex 1 showed that, with the assumptions made, U_i is given by:

$$U_i = 1 - EX/(1/\sigma_{Ti} + X)$$

where $X = \rho_{\text{soil}} H_D$ (g/cm²), ρ_{soil} (ρ_{waste} in fact for this measurement) is the apparent density of the waste in situ, and H_D is the relaxation length.

Having selected 6 lines relating to the daughter products of radon 222 for this analysis, we have 6 values of U_i for the two unknowns X and E . This overdetermination can be used to improve the accuracy of the results.

In the CARTOGER procedure, we note that the 5 ratios $(1-U_i)/(1-U_1)$ involve only the unknown X . Using tables providing values of σ_{Ti} for the minerals in the tailings in question, we can establish the law governing the variation of these ratios with the photon energy γ_i .

A least squares method is applied to find the value of X that minimises the difference between the theoretical and measured profiles. This is illustrated by Plates 3 and 4. For the measurements made at Borst, this gives $X = 35$ g/cm². If we take $\rho_{\text{waste}} = 1.56$ g/cm³, which corresponds to tailings with a 40% porosity, we deduce that $H_D = 22.4$ cm. This is a very likely value for wet tailings.

Having found the best value for X , we now have to find the best value for E . We have 6 determinations. A least squares method is once again used and gives $E = 0.58$ (see Plate 5). Such values have been measured in the tailings from the processing of ore.

The radon 222 exhalation rate can then be calculated. It is:

$$F_{\text{Rn222}} = A_{\text{Ra}}^m \times E \times (\rho_{\text{waste}} H_D) \quad (\text{atom s}^{-1} \text{ cm}^{-2})$$

We thus have $F_{\text{Rn222}} = 12.34 \times 0.58 \times 35 = 251 \times 10^4$ atoms per sec per m², or a radon 222 activity flux of 5.27 Bq s⁻¹ m⁻².

Figure A.2.1 can be used to compare the measured values of U_i with those obtained theoretically for the above values adopted for X and E .

SUMMARY OF RESULTS

Activity of radium 226	12.34 Bq/g
Activity of uranium 238	0.41 Bq/g
$X = \rho_{\text{waste}} \times H_D$	35 g/cm ²
Relaxation length	22.4 cm (for $\rho_{\text{waste}} = 1.56 \text{ g/cm}^3$)
Emanation coefficient E	0.58
Radon 222 activity flux	5.27 Bq s ⁻¹ m ⁻²

A1:I23

Plate 1

Procedure Cartoger

Treatment of soil measurements

Input data in italics

DETECTOR

Surface of detector (cm ²)	<i>22,65</i>
Angle teta (°)	radian <i>0,349</i>
(1 - cos(teta))	<i>0,0602</i>

Data		Gamma emission		Efficiency	Absorbion	Density (g/cm ³)	
N° of Line	Energy (keV)	f _i	Ri (ajusted)	σ_{π} (g/cm ²)	1/ σ_{π} (cm ² /g)	1,56	Depth H _r (cm)
0	185,7	0,033	<i>0,972</i>	<i>0,134</i>	<i>7,46</i>		<i>4,78</i>
1	238	0,074	<i>0,855</i>	<i>0,120</i>	<i>8,36</i>		<i>5,36</i>
2	295,4	0,19	<i>0,715</i>	<i>0,109</i>	<i>9,17</i>		<i>5,88</i>
3	352	0,3586	<i>0,58</i>	<i>0,098</i>	<i>10,20</i>		<i>6,54</i>
4	609,4	0,45	<i>0,342</i>	<i>0,083</i>	<i>12,04</i>		<i>7,72</i>
5	1001	0,015	<i>0,21</i>	<i>0,067</i>	<i>14,93</i>		<i>9,57</i>
6	1120,4	0,148	<i>0,189</i>	<i>0,062</i>	<i>16,12</i>		<i>10,33</i>
7	1764,7	0,166	<i>0,118</i>	<i>0,050</i>	<i>20,00</i>		<i>12,82</i>
8	2448	0,02	not used	<i>0,040</i>	<i>25,00</i>		<i>16,03</i>

Procedure Cartoger*Counting rates in italics>*

Calculation of specific activities

Site: BORST

Date: june 1995

Identification: 001

$$X = \rho_a H_0 \text{ (g/cm}^2\text{)}$$

$$U_i = 1 - E X / (1/\sigma T_i + X)$$

Measurements			Calculation				
N° of Line	SITE:		Source		Figure 1		
	BORST	Counting	$C_i/(R_i f_i dO)$	$[A_{Ra}^m/(2 \sigma_{Ti})] \times U_i$	$A_{Ra}^m \times U_i$		
	cps	cps/cm²	photon/(s cm²)	Bq/cm²	Bq/g		
0	2,015	0,089	radium 226	46,04	46,04	12,34	(U _i = 1)
1	2,37	0,105		27,45	27,45	6,57	
2	5,677	0,251		30,62	30,62	6,68	
3	9,844	0,435		34,68	34,68	6,80	
4	8,868	0,392		42,23	42,23	7,01	
5	0,013	0,001	uranium 238	3,02	3,02	0,41	(U _i = 1)
6	2,252	0,099		59,00	59,00	7,32	
7	1,995	0,088		74,64	74,64	7,46	

Mass activity of radium 226

 A_{Ra}^{m} (Bq/g) 12,34

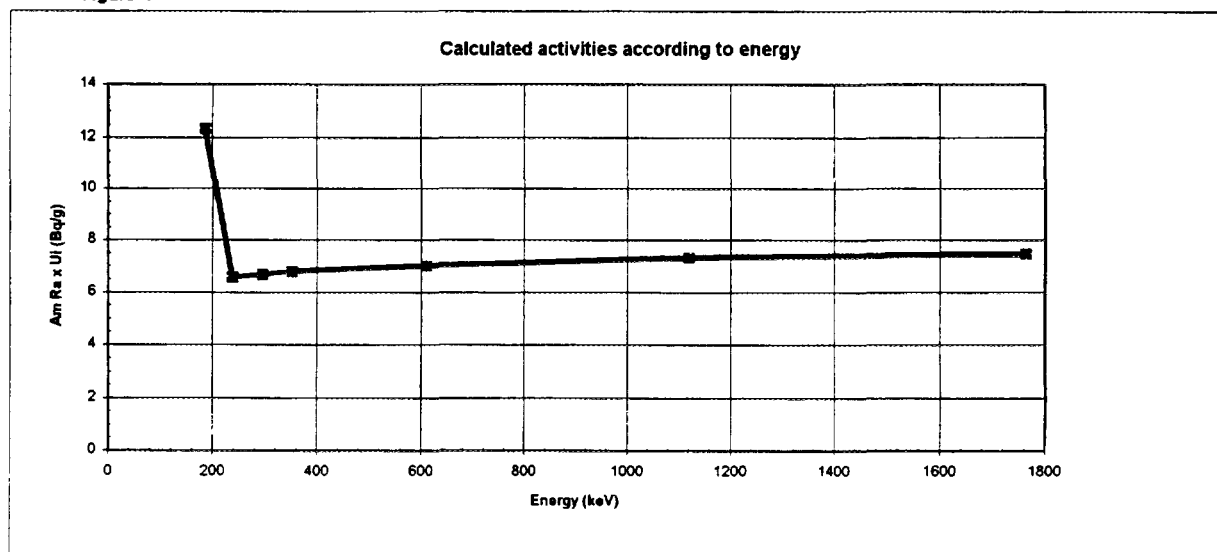
Mass activity of uranium 238

 A_U^{m} (Bq/g) 0,41

Uranium extraction efficiency

% 97

Figure 1



U1:AI31

Plate 3

Procedure Cartoger

Finding X optimal value in view of the 5 values for δ_i/δ_1

$$U_i = 1 - E X / (1/\sigma T_i + X)$$

2 unknowns, \bar{E} and X (g/cm²)

$$\delta_i = (1 - U_i) \quad EX / (1/\sigma T_i + X)$$

Site: BORST

Date: june 1995

Identification: 001

from measures

U_i	$1 - U_i$
1	0
0,532	0,468
0,541	0,459
0,551	0,449
0,569	0,431
1	0
0,593	0,407
0,605	0,395

$$\delta_i = EX / (1/\sigma T_i + X)$$

				Try for X				
				32	33	34	35	36
Mesure	keV	δ_i	δ_i/δ_1	δ_i/δ_1	Calculated with σ_T adjusted			
0	186	0	measured	32	33	34	35	36
1	242	0,46771456	1	1,000	1,000	1,000	1,000	1,000
2	295,4	0,45888932	0,981	0,980	0,981	0,981	0,982	0,982
3	352	0,44876916	0,959	0,956	0,957	0,958	0,959	0,960
4	609,4	0,43146012	0,922	0,916	0,918	0,920	0,922	0,923
6	1120,4	0,407	0,870	0,860	0,863	0,866	0,868	0,871
7	1764,7	0,395	0,845	0,839	0,842	0,845	0,848	0,851

Squares of differences measured and theoretical values

Try for X					
X (g/cm ²)	32	33	34	35	36
2/1	0,00000	0,00000	0,00000	0,00000	0,00000
3/1	0,00001	0,00000	0,00000	0,00000	0,00000
4/1	0,00004	0,00002	0,00001	0,00000	0,00000
6/1	0,00009	0,00004	0,00001	0,00000	0,00000
7/1	0,00003	0,00001	0,00000	0,00001	0,00004
Σ	0,00017	0,00007	0,00002	0,00001	0,00005

Optimal X value

35 g/cm²

Plate 4

Site: **BORST**

Date: june 1995

Identification: 001

Procedure Cartoger

Looking for the optimal E value

X optimal: 35 g/cm²

optimal X according to U_i values

Try for E	0,4	0,5	0,55	0,58	0,6	0,65
X optimal	35	35	35	35	35	35
Calculating: $EX(1+X)$						
Try for E	0,4	0,5	0,55	0,58	0,6	0,65
0						
1	0,324	0,405	0,446	0,470	0,487	0,527
2	0,319	0,398	0,438	0,462	0,478	0,518
3	0,314	0,392	0,431	0,455	0,471	0,510
4	0,297	0,371	0,409	0,431	0,446	0,483
5						
6	0,276	0,346	0,380	0,401	0,415	0,449
7	0,260	0,324	0,357	0,376	0,389	0,422

1-U _i			Calculated values					
Identification	Energy	Measures	Try for E					
			0,4	0,5	0,55	0,58	0,6	0,65
1	238	0,468	0,324	0,405	0,446	0,470	0,487	0,527
2	295,4	0,459	0,319	0,398	0,438	0,462	0,478	0,518
3	352	0,449	0,314	0,392	0,431	0,455	0,471	0,510
4	609,4	0,431	0,297	0,371	0,409	0,431	0,446	0,483
6	1120,4	0,407	0,276	0,346	0,380	0,401	0,415	0,449
7	1764,7	0,395	0,260	0,324	0,357	0,376	0,389	0,422

Squares of differences measured and theoretical values

Identification	Try for E					
	0,4	0,5	0,55	0,58	0,6	0,65
1	0,0206	0,0039	0,0005	0,0000	0,0004	0,0035
2	0,0197	0,0037	0,0004	0,0000	0,0004	0,0035
3	0,0182	0,0032	0,0003	0,0000	0,0005	0,0037
4	0,0180	0,0036	0,0005	0,0000	0,0002	0,0026
6	0,0170	0,0037	0,0007	0,0000	0,0001	0,0018
7	0,0184	0,0050	0,0015	0,0003	0,0000	0,0007
Σ	0,1118	0,0231	0,0039	0,0004	0,0015	0,0159

Optimal E
0,58

AR1:BC47

**NEXT PAGE(S)
left BLANK**



APPLICATION OF SENSITIVE AND SUPERSENSITIVE RADON DETECTORS FOR RADON FLUX DENSITY AND RADON CONCENTRATION IN ENVIRONMENTAL MONITORING

W. ZAHOROWSKI, S. WHITTLESTONE

Australian Nuclear Science and Technology Organisation, Menai, Australia

Abstract

The paper presents a review of principles and operational parameters of the latest instrumental development in sensitive and high sensitive radon detectors at Australian Nuclear Science and Technology Organisation (ANSTO). The focus is on advances in measurement technology of radon concentration in air and radon flux density. Two areas in which ANSTO is actively involved are discussed. The first area concerns radon in air monitoring at Cape Grim Baseline Air Pollution Station. Results recorded at the Station with a supersensitive radon detector characterised by lower limit of detection down to few mBq m^{-3} with time resolution better than 90 minutes are presented to illustrate importance of the technique in global monitoring of airborne pollution. The second area concerns estimates of radon and thoron fluxes from large geographical areas. This is illustrated by results obtained during an Australia-wide survey of radon fluxes and from thoron flux measurements around the Mauna Loa Observatory in Hawaii. The radon flux estimates from Australia come from a coarse net of spot measurements combined with data from aerial gamma surveys. It is argued that as radon global flux and air concentration estimates improve, the data will provide progressively more stringent tests of global air transport models.

1. INTRODUCTION

It is now widely accepted that anthropogenic atmospheric pollution is strongly linked with global climate change. There are limits to the amount of pollution which can be injected into the atmosphere without causing climate change or serious deterioration of the human environment. It is therefore very important to know how much of what gases can be safely injected into the atmosphere. A precise answer to this question is of major economic and political significance. An essential component of the answer comes from air transport modelling. With modern computers one can take any available pressure, temperature, wind speed and direction, and other data to estimate air transport with a horizontal resolution of the order of a hundred kilometres, and vertical resolution better than a thousand meters.

Despite these achievements the problem of the models' accuracy and precision needs to be addressed at each new step in improvement. Inevitably, a question arises of an independent validation of the atmospheric transport models.

One way to monitor polluting gases on the global scale is to establish a set of baseline air monitoring stations. This is done to monitor pollution far away from its source. In such a way background changes in concentration of polluting gases are recorded and the data can be compared with predictions calculated by models. Transport and dispersion components of global models can be verified using suitable tracers. Radon is a naturally available tracer which can be successfully used for verification of transport models. Radon can also be used in establishing the baseline condition. Measurements of radon concentration in baseline air impose very demanding requirements on instrumentation. A description of the latest in the series in radon detectors for baseline research deployed by ANSTO will be given in Section 2.

Section 3 will elaborate on two related problems concerning the mapping of the distant and local radon source. The distant radon source term is a crucial parameter in global transport models.

In this context, it will be demonstrated how one can use radon flux measurements and radiometric data to evaluate average fluxes from large continental areas. A detailed mapping of the local radon and thoron source term is valuable as a quantitative measure in evaluation of both local and distant air analysed at a baseline air monitoring station.

2. RADON CONCENTRATION IN BASELINE AIR MONITORING STATIONS

Figure 1 shows locations where ANSTO radon detectors have been deployed. At the moment ANSTO records radon in three baseline stations. The first one is located at Cape Grim in the north-western Tasmania, the second station is at Macquarie Island, and the third radon detector is installed at the Mauna Loa Observatory (MLO) in Hawaii. The map shows other places where ANSTO supplied radon detectors and run radon projects together with other organizations.

2.1. Validation of global atmospheric transport models based on radon concentration measurement

Imagine a distant continent which is a source of pollution (and also a source of radon) and a small island away from major pollution sources where a baseline pollution station is located (Fig. 2). Once radon is injected to the atmosphere on the continent it might travel over the ocean and be detected on the island. While over the ocean, there will be no further radon injection since the flux from the ocean is about two orders of magnitude smaller than that from land. Because of radon half-life there is no radon build-up in the atmosphere. On the other hand, the half-life is long enough to allow radon to move over large distances. Also, being a noble gas, radon does not interact chemically with other species. These features make radon a very good tracer [1]. In fact, there is no other tracer as good as radon for global transport on a time scale of a week, except for gases released in occasional special events such a volcanic eruption.

Overall characteristics of radon concentrations in baseline air, such as the range and rate of change following the change in meteorological conditions do not differ much in baseline air from station to station. Results will be given of observations at Cape Grim baseline pollution station. The definitions of wind sectors at the station are given in Fig. 3: the baseline sector with westerly winds coming from the Southern Ocean, the Tasmanian Sector covering the island of Tasmania and the Australian Sector where most pollution comes from. Melbourne is about 500 km to the north.

A typical weekly data sheet is shown in Fig. 4. Important meteorological data are at the top. They include wind speed and sector. The sector indicators are given by letters T, A and B, for Tasmanian, Australian (continental) and Tasmanian wind sectors, respectively. Radon concentrations are shown at the bottom. All data points are hourly averages. Such weekly data sheets are used for quality control. Ozone and condensation nuclei (CN) concentrations are usually included since they provide further useful information. There are two observations to be made here. First, the radon range is from few tens of mBq m^{-3} to few Bq m^{-3} . Second, the time scale at which meteorological conditions can cause significant changes in radon concentration is an hour. This is well illustrated in an event at the beginning of day 106, when a relatively brief period of the change in wind direction from Baseline to Tasmanian resulted in about 5 times higher radon concentrations. Both the radon range and expected rate of change impose demanding conditions on radon detection.

2.2. Radon as a baseline criterion

Baseline atmospheric observations aim at monitoring long term trends in concentrations of trace constituents of the atmosphere. It is very important to distinguish between air masses which are

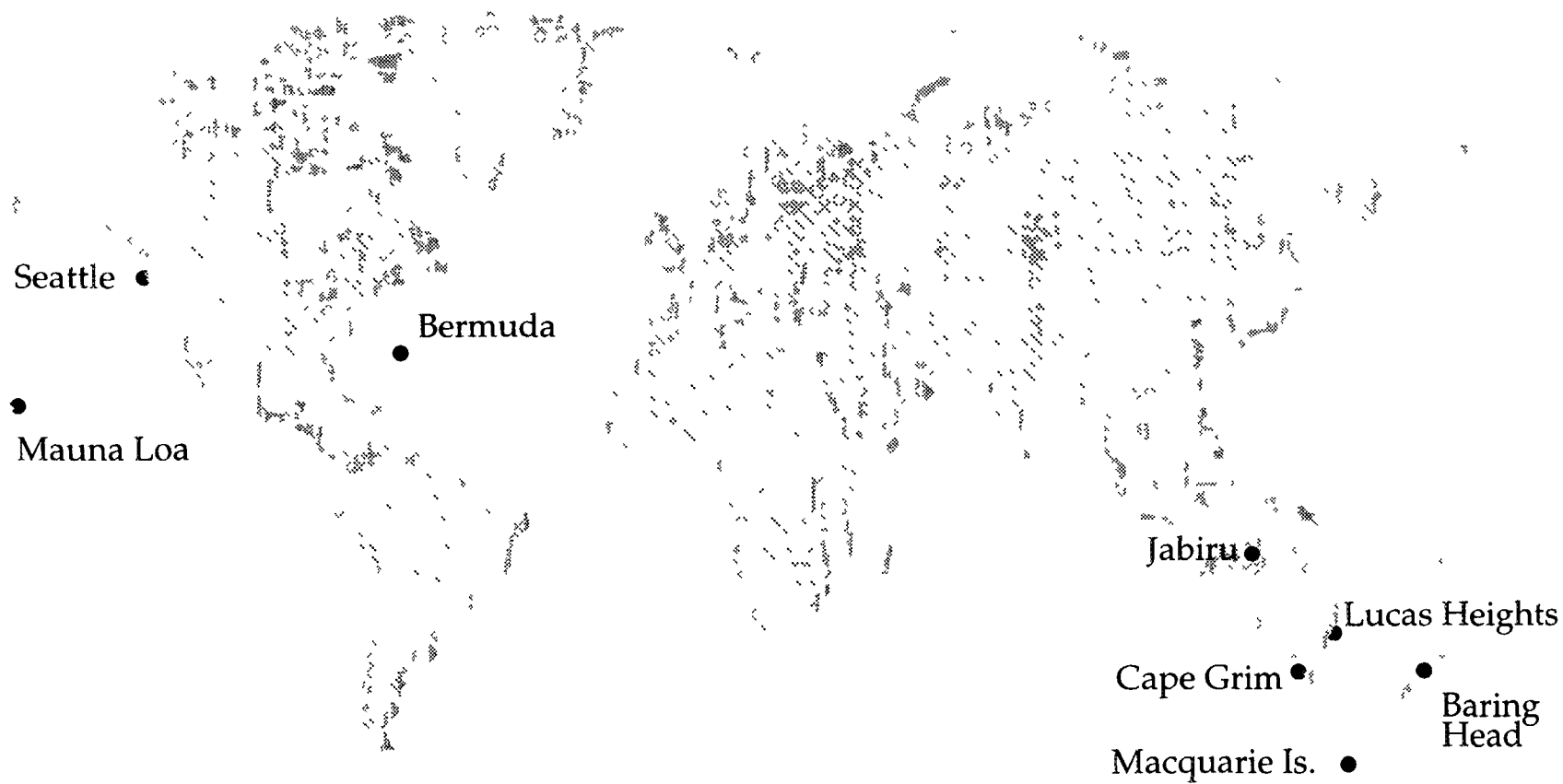


FIG. 1. Deployment of ANSTO's baseline radon detectors.

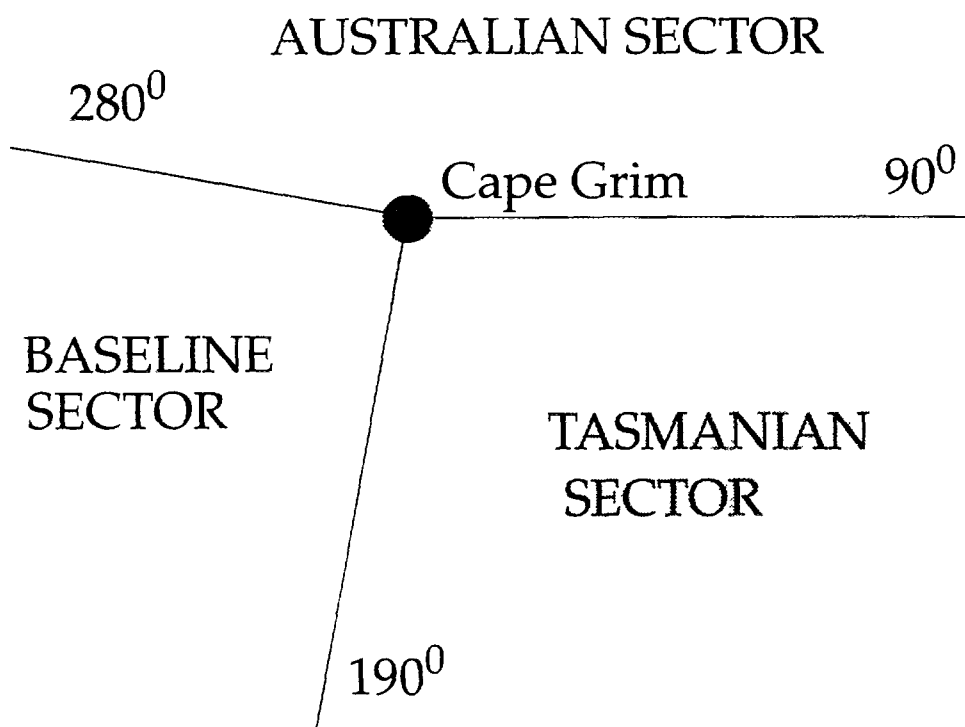


FIG. 2. Radon in boundary layer, sources and sinks.

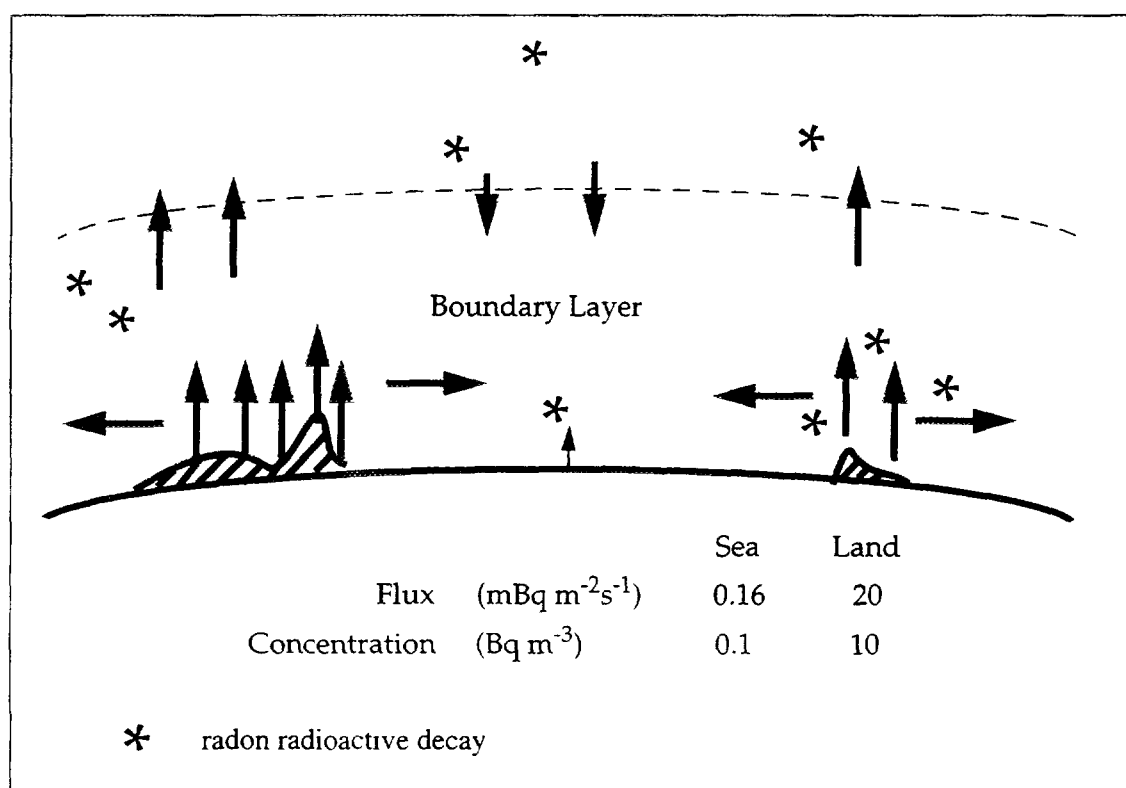


FIG. 3. Sector definition at Cape Grim.

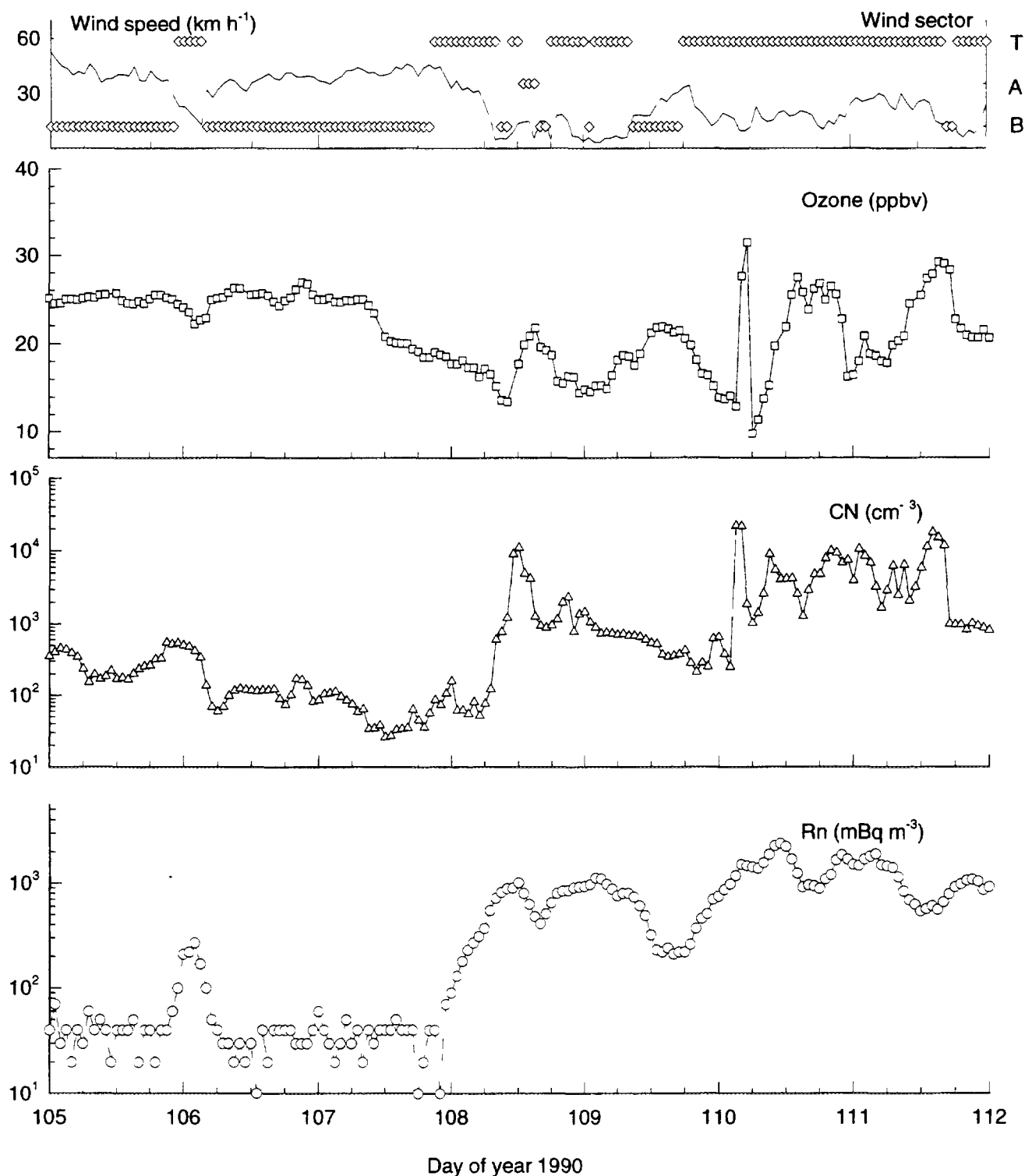


FIG. 4. Typical weekly data recorded at Cape Grim.

baseline from those which have been subject to recent pollution. This requirement is very important, especially for those analytical methods which rely on long sampling periods or when air is collected for archiving purposes.

Table I shows a list of measurable quantities which are the most generally applicable as baseline selection criteria because of the reliability and low cost of the instruments involved and the ease of interpretation of the data.

TABLE I. RANGE OF APPLICABILITY OF DIFFERENT BASELINE SELECTION CRITERIA

Criterion	Distance of pollution source from sampling point (km)			Timing Accuracy
	< 10	10–1000	> 1000	
Wind direction	yes	yes	no	1 minute
Condensation Nuclei (CN)	yes	yes	no	1 minute
Lead-212	yes	yes	no	1 hour
Radon-222	no	yes	yes	1 hour
Air Trajectories	yes	yes	yes	hours–days

Radon concentration is the only practicable baseline criterion for air parcels coming from distances over 1000 km. In fact, because of the negligible radon flux from the ocean and 3.8 days radon half-life, the low radon signal always indicates that the sampled air parcel has not been with a significant contact with land for two-to three weeks. This can correspond to distances far exceeding 1000 km distance which is the limit for other baseline criteria. It might be argued that for distances lower than 1000 km the wind direction can be a universal baseline criterion. Some case studies revealed, though, that it is radon rather than the wind direction which provides a better criterion for the baseline condition at such distances [2]. The radon baseline threshold can be easily established by examining a sufficient amount of hourly observations. In case of Cape Grim it is equal to 100 mBq m^{-3} .

2.3. Principles and practice of radon detection in baseline air

The principle of operation of ANSTO's high-sensitivity radon detector is based on two filter detector: air is drawn continuously through one filter which removes all radon and thoron decay products (daughters), then through a delay chamber in which some daughters are produced [3]. Finally air passes through a second filter which collects the daughters at a rate proportional to the radon and thoron concentration. The larger the delay chamber volume, the more sensitive the detector will be since more daughters are formed in the chamber. Unfortunately, there are some difficulties when one attempts to scale-up the instrument. A major challenge in the design of high sensitive two filter detectors is to prevent the daughters from being plated out on the walls of the delay chamber.

Most two filter detectors use a high flow rate to ensure that the air passes from the inlet to the outlet filters in a time short compared to the mean plate-out time. In a detector with a volume of one or two cubic metres, the plate-out time is a few minutes. This means that flow rates of about a cubic metre per minute are necessary. As a result, pumping power and the second filter are have to be unacceptably large.

One can solve this problem by injecting and maintaining a constant concentration of sub-micron particles in the delay chamber [4]. With particles in the chamber, the daughters become attached to the particles, which have a mean plate-out time of many hours in delay chambers of a volume greater than about 2 m^3 . This solution delivers excellent results as far as lower limit of detection is concerned but it requires a certain level of maintenance and too high a standard of housing to work unattended at remote sites.

A new ANSTO detector design addresses the above problem by introducing a division of the air flow into the low rate external and high rate internal components and the use of the wire screens

as the second filter [5]. The first measure separates the function of supplying filtered air to the detector from that of preventing plate-out of daughters. The former needs only a low flow rate. The latter requires very high flow rate.

The second measure utilizes the high diffusivity of radon or thoron daughters. Inside the delay chamber there are no aerosols, so the daughters remain as either atoms or small clusters of atoms no more than a few nanometers in diameter. Therefore a wire screen is able to remove the daughters with high efficiency and very low flow impedance. Since the major power consumption in these detectors is by the air pump, use of screens makes it possible to dramatically reduce system power requirements.

Figure 5 illustrates schematically the principle of operation of this new dual flow loop two filter radon detector. The low flow loop takes ambient air through a delay volume to remove thoron and a first filter into the delay chamber. The high flow loop circulates air within the chamber forcing the air to go through a wire screen which acts as the second filter. The screen is mounted as close as possible to a scintillator which emits flashes of light when hit by alpha particles from the decay of the trapped daughters. Also indicated in the figure is a diffuser fitted across the chamber at the outlet of the internal blower. The diffuser makes airflow in the chamber close to laminar thus preventing excessive plate-out of daughters. The ratio of the internal to external flow rates is about 6 to 1.

The lower limit of detection of a 750 L detector is about 30 mBq m^{-3} . The detector can be a cost-effective basis for a global network of high sensitivity radon detectors.

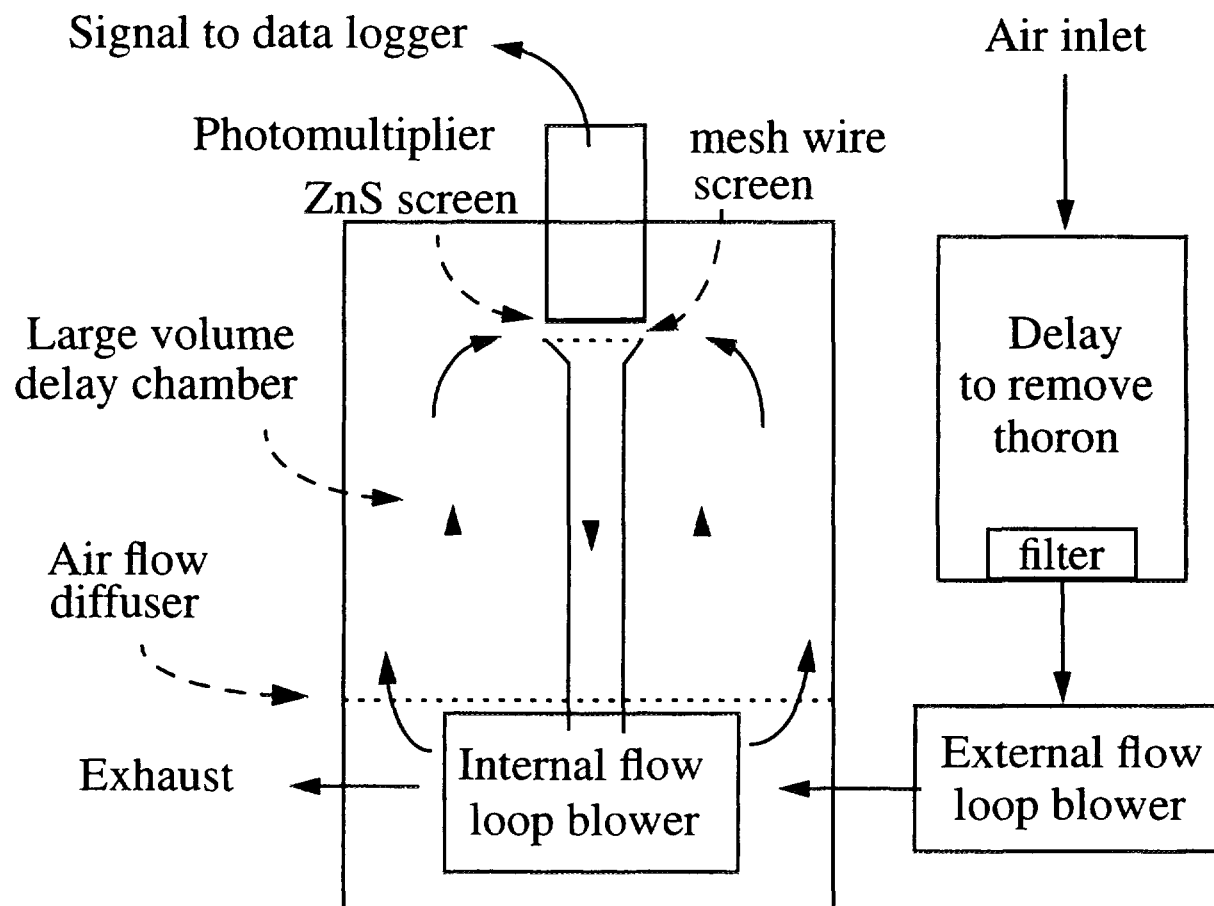


FIG. 5. Diagram of dual loop radon detector.

3. MAPPING OF RADON AND THORON SOURCE

3.1. Radon global source

Figure 6 shows an example of a simulation of radon concentration in air using a global atmospheric transport model. The radon data were in 1990 at Macquarie Island (solid line) using an ANSTO radon detector. The simulation (dashed line), based on a global air transport model, have been performed by Michel Ramonet of CNRS, France.

Although there is a measure of agreement between the experiment and calculations, there is a number of discrepancies, too. One reason for the discrepancies may be uncertainties in the radon source term. In the calculations shown, it has been assumed that all land emanates radon at the rate of $1 \text{ atom cm}^{-2} \text{ s}^{-1}$ (approximately $21 \text{ mBq m}^{-2} \text{ s}^{-1}$). The assumption is an obvious simplification. An improved estimate of radon flux from every $5 \times 40^\circ$ grid has been done for Australia.

Australia has a good regional radon flux survey [6] and an extensive aerial gamma survey. Figure 7 shows a summary of the flux survey. In the figure some arrows are reduced to dots. This is a consequence of the radon scale (0 to $50 \text{ mBq m}^{-2} \text{ s}^{-1}$). Results obtained around uranium mines have not been included in the figure. Rectangular grids indicate areas where airborne gamma data and/or radon flux measurements are available. A simple procedure was adopted to find the average radon flux from spot flux measurements and aerial gamma surveys (Fig. 8). The first step was to select maps covering an area of $100 \times 120 \text{ km}$ for which both radon fluxes and airborne gamma data were available. A relationship was found between the two by selecting six points from each gamma map according to a strict rule, so the selections were unbiased. The six values were averaged to give an estimate of the average gamma count which was converted to a map average radon flux. The maps were then matched as well as possible to the $5 \times 4^\circ$ grid, and grid averages obtained.

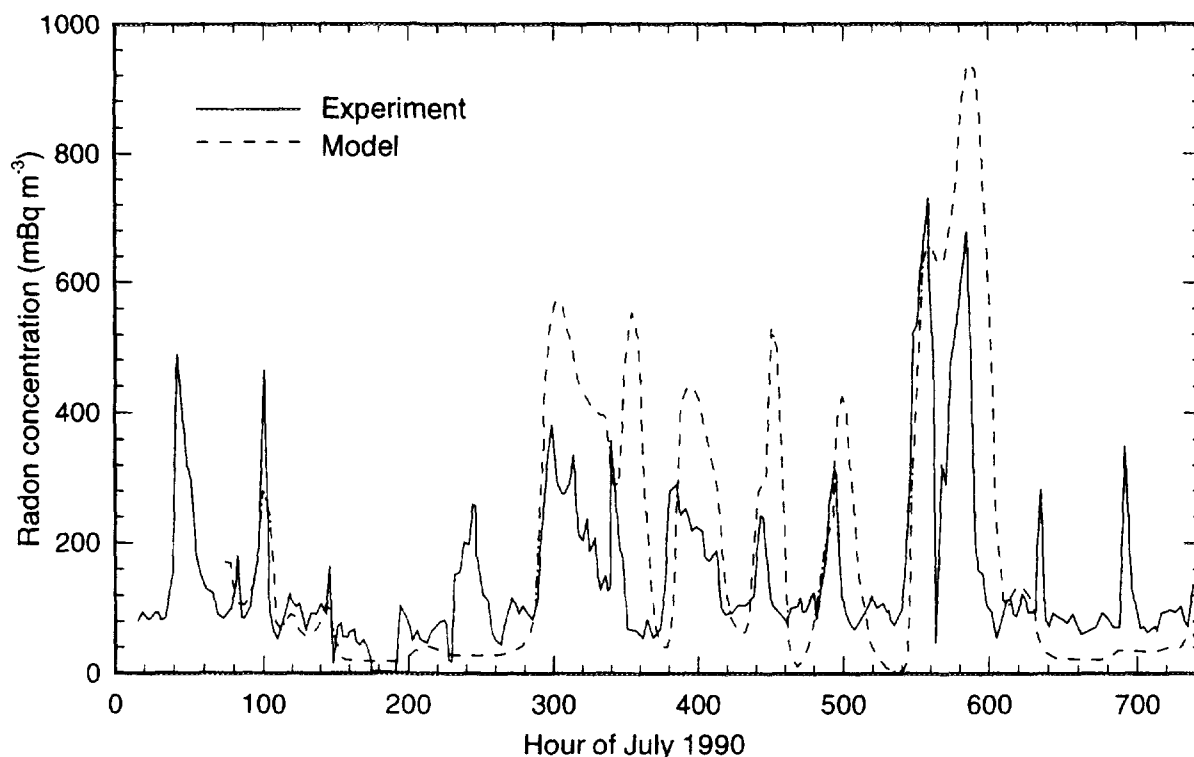


FIG. 6. Radon concentrations at Maquarie Island in July 1990; experiment and model calculations.

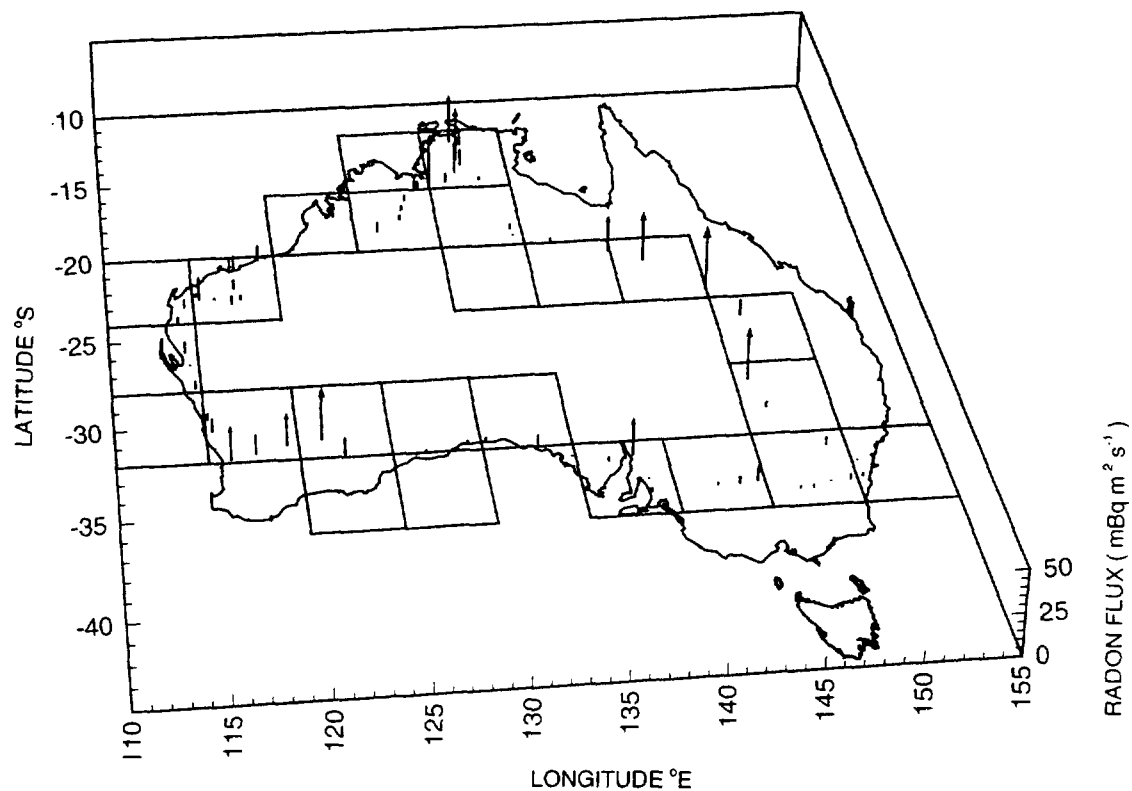


FIG. 7. Radon flux measurements in Australia.

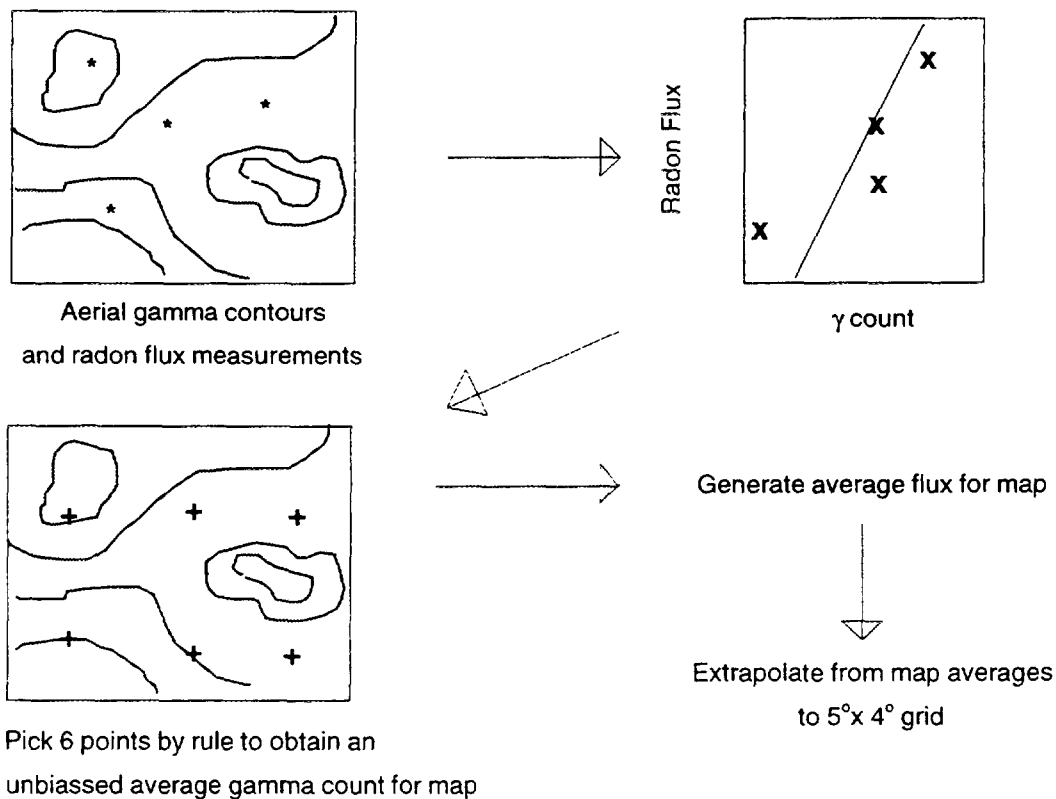


FIG. 8. Procedure for finding map average radon flux from spot flux measurements and airborne gamma survey.

The results of the flux evaluation procedure is shown in Fig. 9. The grids shown are the same as in Fig. 7. The top number in a cell is derived from spot radon measurements and the bottom from airborne gamma data. The two values, when both are available for a cell, agree quite well. It is also clear that the $1 \text{ atom cm}^{-2} \text{ s}^{-1}$ assumption is very inaccurate even on the $5^\circ \times 4^\circ$ grid basis. From the bottom half of Australia, the average is 1.1, but for the upper, northern half it is 1.8. The whole data set gives $1.4 \text{ atom cm}^{-2} \text{ s}^{-1}$. The extrapolation procedure can be improved in many ways starting with the use of more representative averages from digital airborne gamma maps.

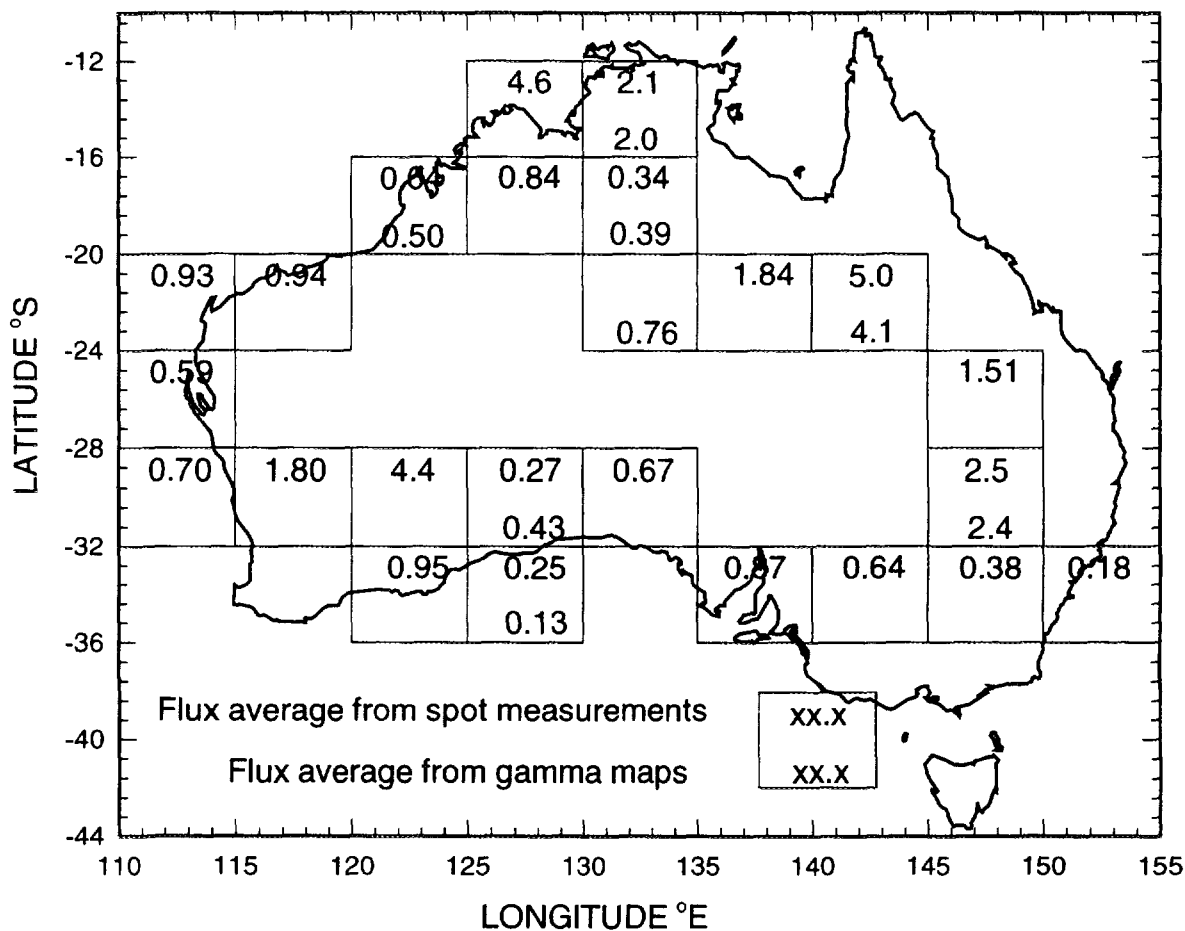


FIG. 9. Average radon fluxes from $5^\circ \times 4^\circ$ grid boxes (one $\text{atom cm}^{-2} \text{ s}^{-1}$ corresponds to about $21 \text{ mBq m}^{-2} \text{ s}^{-1}$).

3.2. Fast measurements of radon environmental fluxes

A radon flux survey aimed at covering large, frequently remote areas needs specific instrumentation. The main requirement, besides the lower limit of detection matching expected flux levels, is an adequate sampling frequency.

Figure 10 shows the essential features of a fast radon and thoron emanometer used in the survey summarized in Fig. 7. The principle of operation of the emanometer is as follows [7]. At the start of the measurement the accumulation chamber (A) is placed over the ground. Air is drawn from the chamber into the first scintillation cell (SC1) which records counts from both radon and thoron. From here, the air passes via a 6 minute delay tube in which 99% of the thoron decays, into the second cell (SC2) which records essentially counts from radon. The computer controlling the device stores the counts and resets the counts each 6 minutes. After 3–4 counting cycles it switches the inlet of the scintillation cells to ambient air. There is a small fan to ensure that thoron is well mixed in the emanometer chamber.

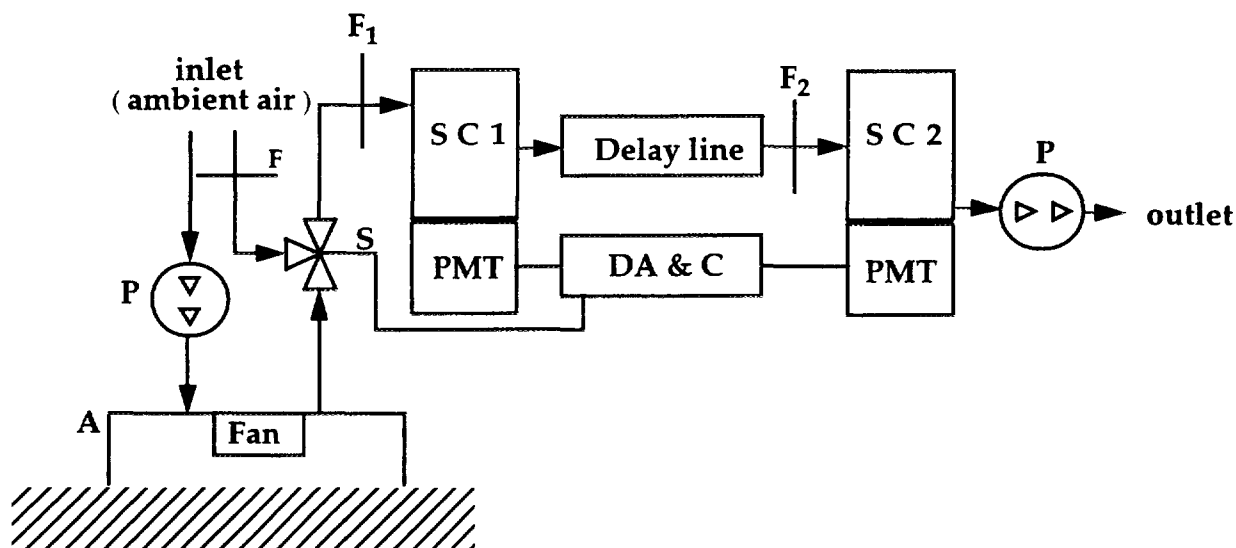


FIG. 10. Diagram of fast radon and thoron emanometer.

In practice, one can perform one measurement per hour providing that the next destination is within 30 minutes drive from the previous one. Table II shows the emanometer's sensitivity and Table III its lower limit of detection. It is clear that the 24 min count is adequate for a fast and precise evaluation of most naturally occurring radon and thoron fluxes. The sampling frequency per day of field work is typically less or equal to 10 sites, depending on site preparation time and distance between adjacent sites.

3.3. Local radon and thoron sources

Pb-212 is a decay product of thoron (Rn-220) which, like Rn-222, emanates from all land surfaces. Thoron is inert, but its very short half life of 55.6 s prevents it from being used as a tracer of air masses over distances more than a kilometre. Pb-212, with a half life of 10.64 h, can become attached to aerosol particles, and remain in air less than about 1000 km away from the thoron's source. The tracer would detect periods when air samples have been influenced by passage close to Hawaiian land. This complements radon measurements which do not distinguish between local and distant land contact.

In baseline air monitoring stations located at island or coastal sites with continental land masses being away more than 1000 km, only air trajectories close to local land will contain lead-212. The baseline air pollution station at the Mauna Loa Observatory in Hawaii is an example of such a station [8].

Meteorological data will indicate that an air parcel has approached local land, but lead-212 may give a quantitative measure of the degree of contact. This can be done providing that a detailed mapping of the local thoron source is available. Two conditions have to be fulfilled. First, thoron fluxes are to be measured over as wide a range of soils as possible. Second, a selection of sites has to take into account all major air trajectories over Hawaiian land to the MLO.

A survey aimed at measuring the thoron source term to evaluate the use of Pb-212 as an atmospheric tracer was done on Hawaii. Figure 11a shows the measurement sites and the height contours. Fig. 11b includes average rainfall isopleths and the measured thoron fluxes which are quantified by a subdivision into values below and above $300 \text{ mBq m}^{-2} \text{ s}^{-1}$. A detailed discussion [9] of the survey reveals that the observed fluxes are strongly dependent on rainfall, soil depth, soil

TABLE II. FAST EMANOMETER SENSITIVITY FOR DIFFERENT COUNTING TIMES

Flux sensitivity (counts/mBq m ⁻² s ⁻¹)					
24 min count		60 min count		180 min count	
Radon	Thoron	Radon	Thoron	Radon	Thoron
8	0.8	39	2.1	188	6.5

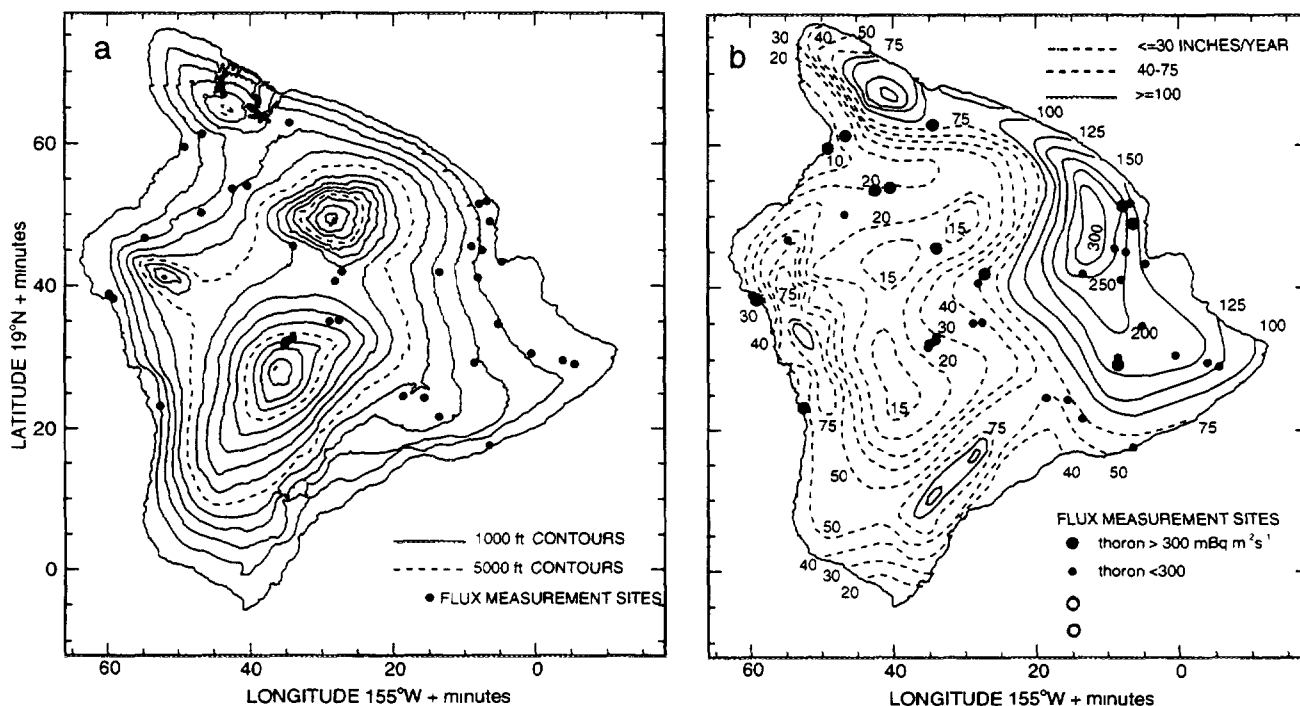


FIG. 11. Map of Hawaii showing thoron flux measurement sites.

particle size and land use. While the soil depth and particle size are not greatly different between the east and west sides of the island, the rainfall is much greater on the east side, resulting in distinctively different average fluxes. The estimated average fluxes from the dry western side of the island were a factor 5 higher than those from the wet eastern side.

3.4 High sensitivity thoron emanometer

Most of the thoron fluxes shown in Fig. 11 were determined by the fast emanometer described above. Fluxes from barren lava, ranging from 5 to 50 mBq m⁻² s⁻¹, located above and immediately below the MLO were measured with a high sensitivity thoron emanometer which was assembled specifically for the survey [5,8]. The principle of operation is shown in Fig. 12. A large sampling area was obtained by taking a 2.7 × 3 m tarpaulin and spacing the central 6 m² a distance of 9 cm from the ground with rows of plastic cups. Air from the centre of the chamber was drawn at 400 L/min through a filter to a 400 L delay chamber where about half of the thoron decayed. The resulting lead-212 was collected on a nylon mesh.

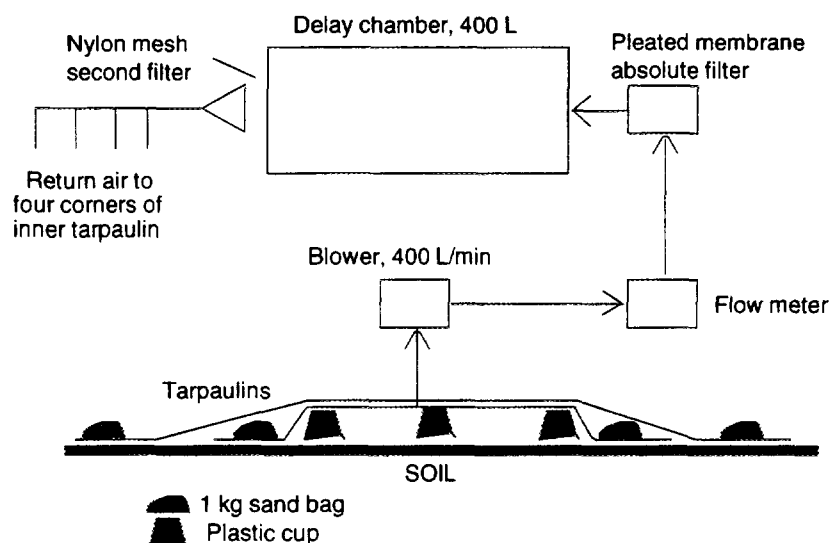


FIG. 12. High sensitivity thoron emanometer.

Air from the delay chamber was recycled to the four corners of the chamber. The concentration of thoron in the volume under the tarpaulin is inversely proportional to the height of the spacers. It is therefore possible to improve the sensitivity of the measurement by lowering the spacing as far as possible. On the other hand, the accuracy of the measurement is dependent on how well the volume is defined. On rough ground, a height greater than the roughness is needed. It is clear that at least some constructional parameters depend strongly on measurement sites.

Calibration of the instrument was performed by making side-by-side measurements with the fast emanometer which resulted in an agreement within 30% of a calculated value. It was estimated that the high sensitivity emanometer was able to detect thoron flux down to $1 \text{ mBq m}^{-2} \text{ s}^{-1}$.

TABLE III. FAST EMANOMETER LOWER LIMIT OF DETECTION FOR DIFFERENT COUNTING TIMES

Lower level of detection ($\text{mBq m}^{-2} \text{ s}^{-1}$)					
24 min count		60 min count		180 min count	
Radon	Thoron	Radon	Thoron	Radon	Thoron
4.0	40	1.0	20	0.35	10

4. CONCLUSIONS

Radon-222 and lead-212 recorded at baseline air monitoring stations are effective indicators of contact of the air with distant and local land, respectively. Radon-222 concentrations measured at baseline stations can be modelled using global atmospheric transport codes. Hence the radon record enables an independent validation of global atmospheric transport models. The validation can be done for the response of the models to radon concentration changes on time scales as short as 1 hour. The use of radon as a tracer requires a better knowledge of the radon global source term if such comparisons are to become more precise.

It is possible to construct a map of radon flux averages from large land masses based on radon flux spot measurements and airborne gamma maps. Unique radon instrumentation had to be developed to measure baseline radon concentrations and radon and thoron fluxes to meet the requirements for the lower limit of detection and response in time.

REFERENCES

- [1] POLIAN, G., LAMBERT, G., ARDOUIN, B., JEGOU, A., Long-range transport of continental radon in subantarctic and antarctic areas, *Tellus* 38B (1986) 178–189.
- [2] ZAHOROWSKI, W., GALBALLY, I.E., WHITTLESTONE, S., MEYER, C.P., Ozone and radon at Cape Grim: A study of their interdependence, in *Baseline Atmospheric Program (Australia) 1992*, eds. Francey, R. J., Chad, A.L, Derek, N., Bureau of Meteorology in cooperation with CSIRO Division of Atmospheric Research, Melbourne (1996) 30–37.
- [3] Thomas, J.W., LeClare, P.C., A study of the two-filter method for radon-222, *Health Physics* 18(1970) 113–122.
- [4] WHITTLESTONE, S., ZAHOROWSKI, W., The Cape Grim huge radon detector, in *Baseline Atmospheric Program (Australia) 1992*, eds. Dick, A.L. and Fraser, P.J., Bureau of Meteorology in cooperation with CSIRO Division of Atmospheric Research, Melbourne (1995) 26–30.
- [5] WHITTLESTONE, S., ZAHOROWSKI, W., WASIOLEK, P., High sensitivity two filter radon/ thoron detectors with a wire or nylon screen as the second filter, *ANSTO/E718* (1994) 1–22.
- [6] SCHERY, S.D., WHITTLESTONE, S., HART, K.P., HILL, S.E., The flux of radon and thoron from Australian soils, *J. Geophys. Res.* 94 (1989) 8567–8576.
- [7] ZAHOROWSKI, W., WHITTLESTONE, S., A fast portable emanometer for field measurement of radon and thoron flux, *Radiation Protection Dosimetry*, 1996, in press.
- [8] Whittlestone, S., Schery, S.D., Li, Y., Thoron and radon fluxes from the island of Hawaii, *J.Geophys.Res-Atmos.* 101 (1996) 14787–14794.
- [9] SCHERY, S.D., WHITTLESTONE, S., LI, Y., Pb-212 as a tracer for local influence on air samples at Mauna Loa Observatory, Hawaii, *J.Geophys.Res-Atmos.* 101 (1996) 14777–14785.



MAPPING OF GROUNDWATER RADON POTENTIAL

G. ÅKERBLOM

Swedish Radiation Protection Institute,
Stockholm

J. LINDGREN

Geological Survey of Sweden,
Uppsala
Sweden

Abstract

The domestic use of water with elevated radon concentration may represent a public health hazard, partly due to the release of radon to the indoor air, but also due to the radiation dose caused by radon and its progeny upon intake. While only a limited number of countries have implemented regulations with respect to radon in water, many more are considering doing so. The compulsory limits proposed by Swedish authorities are 100 Bq/l for public water, while water from private wells is not to exceed 1000 Bq/l. Furthermore, it is recommended that water with a radon content above 500 Bq/l should not be given to children under five years of age. In Sweden, the estimated number of wells with radon levels above 1000 Bq/l exceeds 10 000, with a considerable amount in excess of 10 000 Bq/l. The highest radon concentration in a well supplying drinking water encountered so far is 57 000 Bq/l. Radon levels exceeding 500 Bq/l are almost exclusively found in wells drilled into bedrock and in springs with intramontaneous water. Elevated ground water radon levels require that the water has passed through bedrock with elevated concentration of uranium, or through fractures with coatings of minerals containing enhanced concentrations of radium-226. Intramontaneous water from areas with uranium-bearing rock types (e.g. uranium-rich granites, pegmatites and vulcanites) often manifests elevated radon levels. The implementation of compulsory radon limits has led to a demand from Society regarding regional information on ground water radon risk. Routines for the establishment of risk maps focusing on water are currently under development. The backbone of the process is the access to high spatial resolution radiometric information together with bedrock and soil information on a detailed scale (1:50 000). This information is available from the Geological Survey of Sweden, which is routinely carrying out airborne measurements at an altitude of 30 m and a line spacing of 200 m. While some 60% of Sweden is covered up to now, 75% is expected to be covered within the next ten years. Moreover, an increasing part of Sweden is covered by digital geologic information on an appropriate scale. Other available databases utilized in the risk mapping process include radon measurements in wells, geochemical data from ground- and biogeochemical sampling, ground radiometric measurements on outcrops and soils, and the information gathered during the former Swedish programme for uranium resource evaluation.

1. INTRODUCTION

Radon in water may be a cause of cancer. Given the radon concentrations normally found in ground water, health risks are small. However, the radon dose may be important if ground water containing a high concentration of radon is consumed by infants and young children regularly as drinking water or if radon gas is released into an indoor environment. Elevated radon concentrations in ground water are most common in areas where the crystalline bedrock contains elevated concentrations of uranium. Geological, geophysical and geochemical data from uranium exploration and other surveys of natural radiation are used to indicate and delimit areas of varying risk of elevated radon concentration in ground water in Sweden. This information is utilised by local authorities in an effort to discover which wells may have unsuitably high radon concentrations.

2. RADON IN WATER — A HEALTH RISK

Radon in water may constitute a health risk, partly due to inhalation of the radon gas released from water and partly due to ingestion of the water. When water containing radon is used, 10-90% of the radon is released into the air. The release is greater the more the water is atomised, processed

or heated. For example, showering causes the release of 50–70% of the radon in water [1]. If the release occurs indoors and the water radon concentration is elevated, the radon concentration in the indoor air could be high. How high depends upon the water's radon concentration, how much water is used and how the water is used. In Sweden, a very rough rule of thumb is used to estimate the concentration which a household is subjected to: residential radon concentration is 2×10^{-4} of the water radon concentration (e.g. if the concentration of radon in the water is 1000 Bq/l, then the concentration of radon in the indoor air of the home will be 200 Bq/m³). In air, radon gas decays into its progeny which are inhaled along with air and whose radiation may cause lung cancer.

When water containing radon is ingested, a dose of radiation is imparted to the digestive system by the radon gas and its progeny. The greater portion of the radon is absorbed through the intestinal walls, transported throughout the body and, for the most part, released upon exhalation. The radon which decays in the body and the continued decay of radon's short- and long-lived progeny impart radiation to the various organs of the body. Because radon is quite soluble in fat, the radon progeny may concentrate in organs rich in fat. The greatest risk associated with the ingestion of water containing radon and radon progeny is considered to be that the radiation could cause stomach-colon cancer [2] and other organ cancers. Radon as a cause of leukaemia has also been discussed [3].

Earlier, it was calculated that the greatest radiation dose from radon in water would be derived from the contribution of radon to the air and that the ingestion of water containing radon would give a considerably lower radiation dose. That calculation is still accurate for adults. However, in recent years, it has been shown that young children, especially infants, receive a greater dose of radiation from ingesting water containing radon than do adults [4, 5]. This is because the ingestion of water is great in comparison to body weight and because young children drink more unprocessed water than do adults. Table I shows radiation doses calculated for Swedish adults, children and infants for various radon concentrations in water [6]. The calculation of the radiation dose received from indoor air assumed that an average household used 200 l of water per day. The calculation of the radiation dose due to ingestion of water is based upon the assumption that adults ingest 50 l of unheated or otherwise unprocessed water per year, children 75 l/y and infants 100 l/y [7]. In comparison, consider that the highest radiation dose allowed for persons exposed to radiation in the workplace is 50 millisievert per year (mSv/y) during one year and at most 20 mSv/y as an average for five consecutive years. Individuals within the most exposed group of the general public, but who

TABLE I. TYPICAL VALUES FOR EFFECTIVE RADIATION DOSES VIA INHALATION AND INGESTION OF RADON FROM HOUSEHOLD WATER FOR ADULTS, CHILDREN AND INFANTS CALCULATED FOR THE LIMITS PROPOSED BY THE SWEDISH NATIONAL FOOD ADMINISTRATION FOR RADON CONCENTRATIONS IN PUBLIC AND PRIVATE DRINKING WATER, 100 AND 1000 Bq/l, RESPECTIVELY. INDIVIDUAL DOSES MAY VARY GREATLY [6]

Radon in water (Bq/l)	Inhalation Approximate effective dose (mSv/y)	Ingestion Approximate effective dose (mSv/y)	Rounded Sum Approximate effective dose (mSv/y)
100	0.4	0.05	0.45
		(0.15) ^a	0.55
		(0.7) ^b	1.1
1000	4	0.5	4.5
		(1.5) ^a	5.5
		(7) ^b	11

^a Children aged 10 years

^b Infants aged 1 year

do not work with radiation, must not be exposed to a dose in excess of 5 mSv/y resulting from human activity involving radiation. This is according to the European Union suggestion for Directive on basic safety standards (BSS) for the protection of the health of workers and the general public against the dangers arising from ionising radiation [8].

Radiation doses from radon in water can be very high. In Sweden, households have been discovered in which the children daily ingest water with radon concentrations of 55 000 Bq/l. Every day approximately 60 000 Swedes (population of Sweden 8.8 million) consume water having radon concentrations higher than 1000 Bq/l.

Radon gas released from household water into the indoor air is calculated to cause approximately 50 cases of lung cancer per year. Ingestion of water containing radon is calculated to cause 13–20 cases of cancer per year [9].

After consultation with the Swedish Radiation Protection Institute and the Swedish National Board of Health & Welfare, the Swedish National Food Administration proposed limits for radon in drinking water in 1995 (Table II) [10]. These will be compulsory limits. None of Sweden's large public water works deliver water with radon concentrations above 100 Bq/m³. On the other hand, Sweden has 20 000–30 000 drilled wells in which the water contains radon concentrations above 500 Bq/l, and approximately 10 000 drilled wells with more than 10 000 Bq/l. In total, there are approximately 200 000 drilled wells in Sweden which are utilised year round by permanent residents and 200 000–300 000 drilled wells which are utilised irregularly by non-permanent recreation residents. The latter will not be subject to the proposed limits for radon in water.

TABLE II. PROPOSED SWEDISH LIMITS FOR RADON CONCENTRATIONS IN DRINKING WATER

Concentration	Subject to limits	Comments
100 Bq/l	Public water supply	Compulsory limit. Concerns concentrations in water delivered by public water works.
500 Bq/l	Private water supply	Recommended limit. Concerns the maximum concentration in water given to children under 5 years of age.
1000 Bq/l	All drinking water	Unfit for human consumption.

Finland since 1993 has a compulsory limit of 300 Bq/l for public water supplies [11]; the Czech Republic has a compulsory limit of 50 Bq/l for public water supplies and a compulsory limit of 1000 Bq/l for all water supplied to dwellings [12].

3. RADON IN WATER — WHY AND WHERE

Radon in water is primarily a problem for water supplies which extract water from drill holes in rock or from springs flowing through areas with crystalline rocks, which have somewhat higher uranium concentrations than the average bedrock. Examples of rock types which often have enhanced uranium concentrations, > 5 ppm U (approx. 60 Bq/kg), include the following: granites, syenites, pegmatites, acid volcanic rocks, and acid gneisses. Wells in areas with these rock types commonly contain intramontaneous ground water with radon concentrations of 50–500 Bq/l or considerably higher. Intramontaneous waters from sedimentary rocks such as limestone, sandstone, and shales, as

well as igneous, volcanic intermediate and basic rocks usually have radon concentrations of 5–70 Bq/l, which is to be expected since these rock types generally have low uranium concentrations. Exceptions do exist, however rare. Well waters with elevated radon concentrations from wells in bedrock with low uranium concentrations are known. In such instances, the water has been in contact with uranium mineralizations, e.g. in sandstone and basic rocks, or the ground water has passed through sedimentary layers of bedrock with high uranium concentrations and then travelled long distances, e.g. artesian water in contact with underlying granites. In the latter case, the reason for the high radon concentration in the well water or spring is that uranium and radium have leached from the underlying bedrock, been transported by water and precipitated out along the path of transportation, but relatively near the well or spring.

Ground water in soil layers has considerably lower radon concentrations, as a rule, than does water occurring in cracks in the bedrock. Normal radon concentrations are 5–100 Bq/l in water from dug wells, which receive water from the surrounding soil layers. Factors which determine the radon concentration in the ground water of soil layers are as follows: radon concentration in the soil, the emanation coefficient of the soil (how much of the radon formed is released from the mineral grains into the water in the soil pores), and the soil porosity. Radon concentration in pore water in soil is governed by Formula 1:

$$A_{w \max, \text{ pore}} = A_e = r_a \cdot e \cdot \delta \frac{1-p}{p} \quad (1)$$

where

$A_{w \max, \text{ pore}}$	= radon concentration in the pore space water
A_{ra}	= activity of radium-226 (Bq/kg) ^a
e	= emanation coefficient (emitted radon / formed radon)
δ	= compact density (kg/m ³), normal rock material 2700 kg/m ³
p	= porosity (pore volume/total volume)

^a 1 ppm uranium is equivalent to 12.3 Bq/kg Ra-226 assuming equilibrium in the decay series

Normal emanation, e , for soils is 0.2–0.4, and may for certain clays reach 0.6. Porosity, p , is normally 0.25–0.45. The radium concentration, A_{ra} , is 5–25 Bq/kg for silts, sands and soils with origins in rocks with low uranium concentrations, e.g. limestone. Soils originating from rocks with normal uranium concentrations have radium concentrations of 10–50 Bq/kg. These values correspond to radon concentrations of 5–50 Bq/l for ground water in soils with low uranium concentrations, and 10–100 Bq/l in soils with normal uranium concentrations.

In water from surface water reserves, the radon concentration is low, <2 Bq/l, mainly because the radon has had time to decay during the long holding period in the surface reserve, among other reasons.

Radon concentrations in intramontaneous water are normally considerably higher and often much higher than in ground water in soil layers. Water arising from uranium-rich rocks, e.g. uranium-rich granites and pegmatites, commonly have radon concentrations in excess of 500 Bq/l, with maximum concentrations of 20 000–60 000 Bq/l. This concentration is 2–100 times higher than the radon concentration of the surrounding bedrock, calculated per kg rock. One explanation for the elevated radon concentration in intramontaneous ground water is that 6-valence uranium is relatively easily dissolvable and is leached out of the rocks by the ground water. Dissolved uranium and its decay products precipitate onto the surface of fractures, partly because they react chemically with fracture minerals on the surfaces of the cracks, and partly because the decay products are sparingly soluble, thus precipitating out [13]. Landström and Tullborg [14] found that uranium concentrations in fracture coatings are often 3–20 times higher than in the surrounding rock. Consequently, a coating of radium-rich material builds up on the surfaces of cracks and fissures, from which radon emanates directly into the water in the crack. Figure 1 illustrates the process. Another possible reason for

increased radon in ground water is that in any particular grain of uranium, the radon concentration is many times greater than that of the surrounding rock and water, thus it diffuses from the grain of uranium into the water phase. Since the rock porosity is very low, conditions exist for the water radon concentration to be 10–100 times greater than the rock matrix radon concentration (Formula 1).

4. RADON IN WATER IN SWEDEN

Radon in water is a relatively great problem in Sweden. As discussed earlier, many Swedes drink water containing high concentrations of radon, and approximately 40% of the population obtain their water from drilled wells. The reason for the pervading relatively high radon concentrations is that a major portion of the bedrock in Sweden is made up of Precambrian rocks, which consist mainly of granites, acid gneisses, and acid volcanics. In regions of gneiss, pegmatites and aplites are abundant. Table III presents normal concentration variations for radon, as well as radon concentrations for various types of water reserves and bedrock in Sweden. Figure 2 shows the distribution of water radon concentrations of some 1200 drilled wells in Southern and Central Sweden, and Fig. 3 areas with uranium-rich rock types. The wells were randomly selected for radon analysis during hydrogeological surveys carried out by the Geological Survey of Sweden and a national survey of water radon concentration performed by the Swedish Radiation Protection Institute [15]. It is evident from the map that there is a cluster of wells with enhanced radon concentrations in the central portion of the map, at Bergslagen, where the bedrock consists primarily of acid gneisses, granites, and acid vulcanites containing numerous pegmatites. Another area with numerous radon wells is the northeast coast of Sweden, with geology similar to that of Bergslagen. In Scania, Southern Sweden, where the bedrock mainly consists of non-metamorphic Cambrian-Tertiary sediments, the radon concentration in water is low. These conditions are also applicable to Southwest Sweden which primarily exhibits intermediate and acid gneisses, and intrusives low in uranium.

TABLE III. RADON AND RADIUM IN SWEDISH GROUND WATER. NORMAL AND MAXIMUM CONCENTRATIONS [13]

	Radon-222 (Bq/l)	Radium-226 (Bq/l)
<i>Lake and sea water</i>	< 2	0.005–0.007
<i>Wells dug in soil:</i>		
normal in Sweden	10–300	0.001–0.09
in granite areas	40–400	
<i>Wells bored in sedimentary rocks:</i>		
Eocambrian -Tertiary	10–50	
<i>Wells bored in crystalline Precambrian bedrock:</i>		
normal bedrock	50–500	0.01–0.25
uranium-rich granites	300–4000, max. 57 000	
uranium-rich pegmatites	max. 30 000	max. 2.5
<i>Uranium ores:</i>		
Lilljuthatten, Stenfjällen	2000–100 000	max. 6
Pleutajokk, Arjeplog	18 000–55 000	0.1–0.17

Bohus granite is generally uranium-rich, 5–40 ppm U, and occurs in a large contiguous area along the northwest coast of Sweden, where wells with high radon concentrations are frequent. The Municipality of Sotenäs lies in that region and 60% of the drilled wells have radon concentrations in excess of 500 Bq/l and 30% in excess of 1000 Bq/l. Wells with much higher radon concentrations, > 5000 Bq/l, are primarily located within uranium-rich granite regions. A campaign to measure radon in Sweden's drinking water is currently underway and several wells with more than 20 000 Bq/l have been discovered. So far, the well found with the highest radon concentration, 57 000 Bq/l, was drilled in Blomskogs granite, a uranium-rich granite.

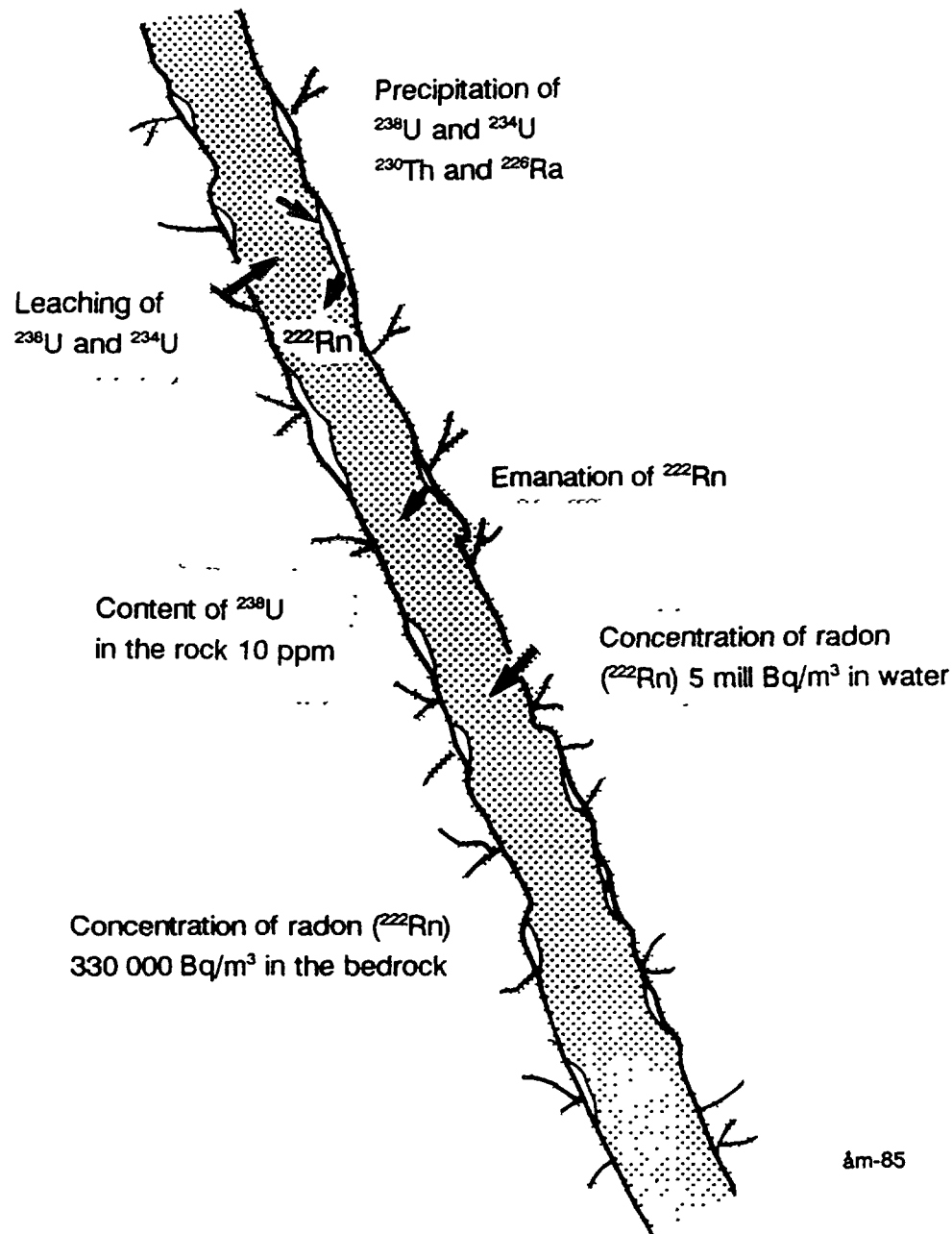


FIG. 1 Formation of radon gas in a water-filled crack [13]

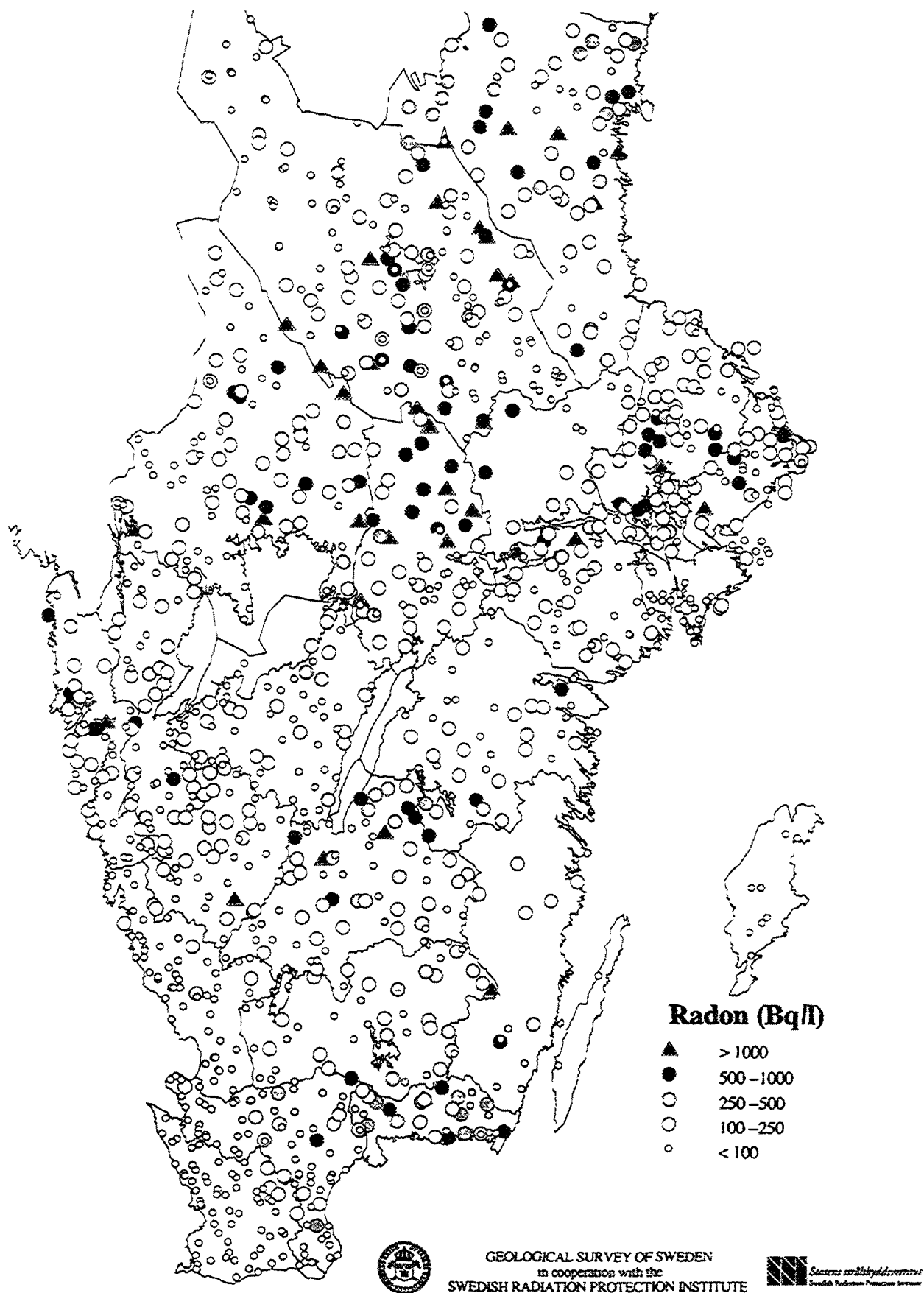


FIG.2. Radon concentrations in randomly selected bedrock wells in Southern Sweden

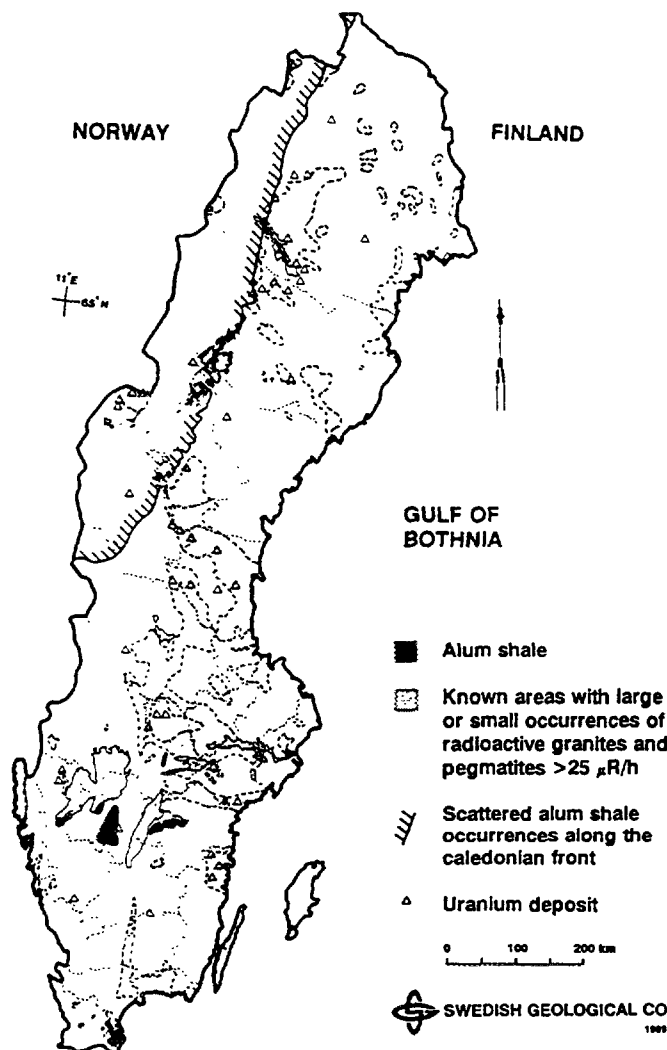


FIG. 3. Distribution of uranium-rich bedrock in Sweden.

5. USE OF DATA FROM GEOLOGICAL AND GEOPHYSICAL SURVEYS

5.1. Airborne radiometry

The Geological Survey of Sweden (SGU) is routinely carrying out airborne gamma spectrometric measurements over the Swedish territory since the late 60's. Details on the airborne equipment can be found in [16]. Today, the measurements are carried out at an altitude of 30–60 m with a line spacing of 200 m and a sampling frequency of 4 Hz, implying a sampling distance of 16 m along the flight line. These measurements are generally reprocessed to generate a 40 m sampling distance along the flight line to achieve sufficient counting statistics. While some 60% of Sweden's 410 934 km² is covered with digital radiometric information up to now, 75% is expected to be covered within the next ten years.

While the only airborne radiometric surveys carried out today are performed by SGU, some other surveys have been conducted by ore prospecting companies over specific regions in Sweden. Until 1984, when the Swedish programme for uranium exploration was brought to an end, most surveys were carried out for the purpose of uranium exploration. Today, the measurements are conducted within the national airborne geophysical mapping programme. The system used today is based upon a 256-channel Exploranium GR-820 with a 1024 cuin downward looking crystal package and a 256 cuin upward looking detector.

Swedish authorities have recognised airborne radiometric mapping as an important tool for the detection of radon prone areas; thus, the Survey has obtained a general permission to fly at an altitude of 50 m over urban areas provided that the information is used for predicting radon risk. After two serious accidents in recent years, it has been decided to increase the altitude to 60 m over rural areas, while the altitude over urban areas is decided upon at the pilot's discretion.

The spatial resolution of the airborne measurements enables the detection of even relatively minor geological objects with elevated levels of radioactivity, such as radioactive springs and pegmatites [17]. Moreover, a number of anomalies of anthropogenic origin are generally seen on the resulting maps. This includes roads and squares paved with material with elevated content of radioactive isotopes, arenas covered with ashes of burnt alum shale and buildings made up of radiating building material. Between the years 1929 and 1975, a type of light-concrete made from uranium-rich alum shale was produced and extensively used as building material. Today, it is estimated that one inhabitant out of ten is living in a dwelling partly made up of this material, something which significantly has increased the radiation exposure to the Swedish population, both through the direct exposure to gamma radiation emitted from the material and from radon being released to the indoor air.

There is evidence that, under favourable circumstances, even single buildings made up of uranium-rich alum shale-based light concrete may be identified from the airborne radiometric measurements.

5.2. Bedrock and quaternary geology

The Geological Survey has continuously been mapping the geology of Sweden since 1858. It is, however, not until recently that the Survey has moved to the production of geological information in digital form. The Swedish territory is covered as a whole with digital bedrock and quaternary geologic information, but only in the scale of 1:1 000 000, which is not sufficient for radon prognostics. Quaternary information in the scale 1:50 000 is rapidly becoming available, while the process of converting bedrock information to digital form is still somewhat in its infancy.

5.3. Geochemistry

Within the framework of the programmes for ground geochemical and biogeochemical mapping, samples are being analysed with respect to uranium among other elements. The former programme samples a silt and clay fraction of till from the undisturbed C-horizon, while the latter samples roots from stream plants. Both programmes provide information on uranium concentrations, the former on till and the latter on bioaccessible uranium in streams.

More research is needed to illuminate to what extent the results from geochemistry may be considered to be representative of the uranium/radium content of the underlying bedrock.

5.4. Ground radiometry

During the national uranium prospecting, extensive work were carried out to identify possible sites of interest for uranium mining. A large number of outcrops were visited and radiometrically investigated, although only to a lesser extent with the help of gamma spectrometry. These results are, however, not readily available in digital form.

Today, ground follow-up of anomalies identified from the airborne radiometry are performed to a limited extent, the principal aim being the detection of possible radon prone areas.

5.5. Hydrogeology

In Sweden there exists no obligation to report analyses of radon in water to the Survey. To get a general overview of the regional trends in the distribution of wells with elevated radon levels, the Survey in co-operation with the Radiation Protection Institute has collected a data set based upon analyses of radon in some 1200 wells drilled into the bedrock, randomly selected in the south and central part of Sweden as described above. Moreover, within the framework of the regional hydrogeological mapping programme, some selected wells are being analysed with respect to radon among other parameters.

5.6. Other sources of information

It is not until recently that local authorities have initiated ground water radon mapping programmes. The major part of analyses of radon in water, however, resides in databases maintained by these authorities. While some municipalities only measure upon request, others have chosen to analyse all known drilled wells within the municipality, thus providing an unbiased material of great value for correlation with geology.

Juridical obstacles have so far hampered the access to this information, since the individual measurements are considered to be the property of the customer and not as information available to the public. It is, however, believed that the measurements in the near future may become accessible to the Survey for the purpose of radon prognostics.

6. GROUND WATER RADON PROGNOSTICS

Following the forthcoming implementation of compulsory limits for radon in water, local authorities, charged with the tracing and identification of possible public health hazards, have manifested an increasing interest in material showing the spatial distribution of ground water radon risk. In analogy with traditional radon risk maps, used in the urban planning process to delimit areas where special building construction protocols should be followed to prevent the occurrence of elevated indoor radon levels originating from the ground, there is a demand for maps where ground water radon prone areas may be identified. To meet this demand, the established Swedish practice for the compilation of radon risk maps must be enlarged to allow for the focusing upon features of relevance for the problem of radon in water, which essentially is a problem related to the bedrock.

6.1. National risk maps

To meet the demand, essentially from the public, when the problem of radon in water first was invoked, the Survey in co-operation with the Radiation Protection Institute decided to compile a map showing the main trends of occurrence of wells with elevated radon content. The first version of this map was presented in August 1994, and was based upon airborne radiometry, the limited data set of direct measurements of radon in drilled wells described above, along with the knowledge gathered during the Swedish programme for uranium exploration. The public debate following the publication of the map, including the possible health hazard that radon in water may represent, put a considerably pressure upon national as well as local authorities to delineate ground water radon prone areas in more detail. A second version of the national map is presented in Fig. 4.

6.2. Regional risk maps

Although of public interest, national overviews as described above are of limited interest to local authorities involved in the detection and prevention of radon hazards. Maps on a regional scale with a correspondingly higher spatial resolution are therefore needed.

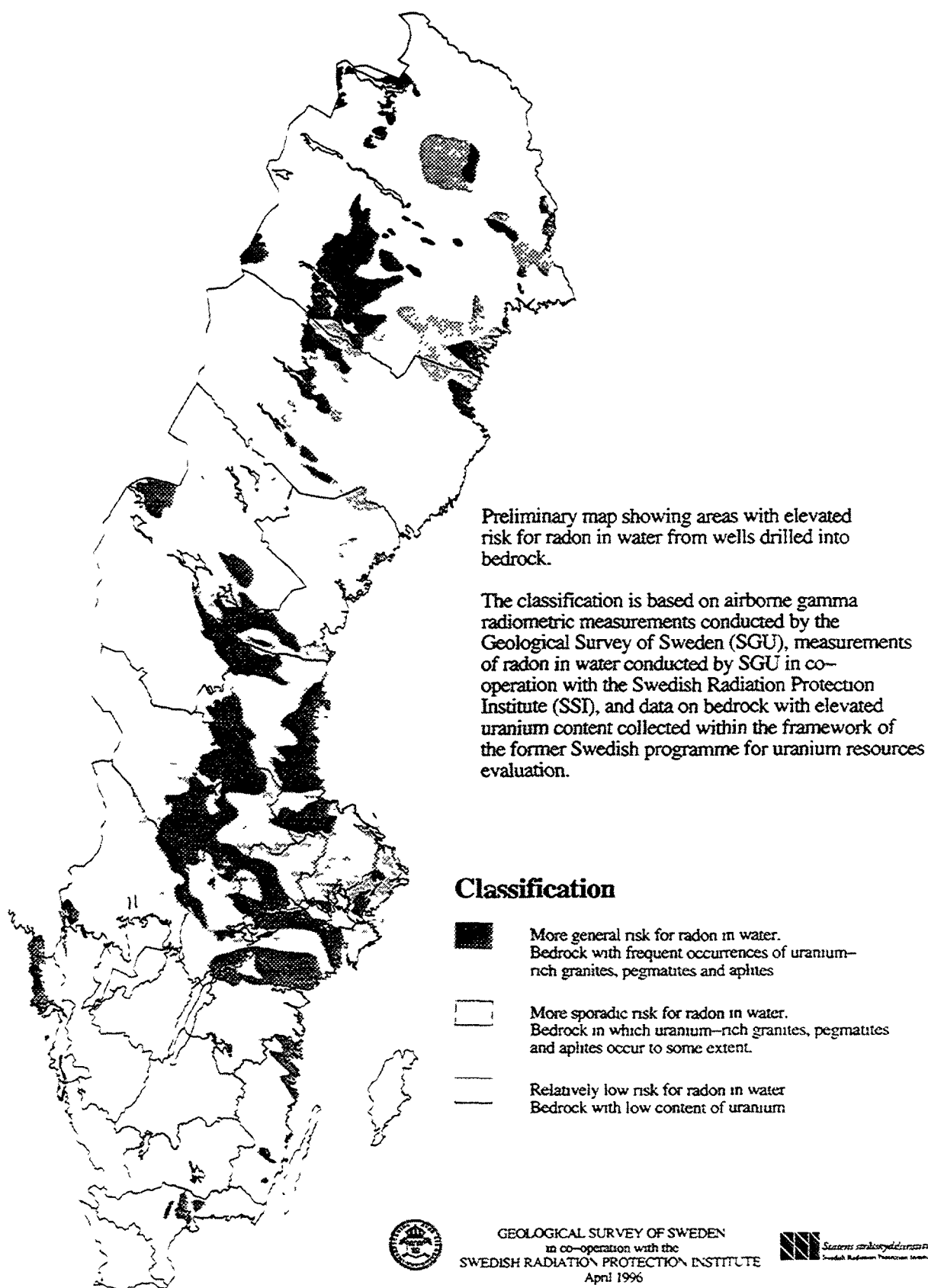


FIG. 4. Preliminary ground water radon risk map of Sweden.

At the Survey, ongoing research are currently addressing the question to what extent existing digital geoscientific information, in particular high spatial resolution airborne data, can be used to delineate risk areas with respect to ground radon. The work is being carried out within the framework of a geographical information system, and aims at the compilation of radon prognosis maps in the scale 1:50 000, suited to meet the demands from local authorities in the urban planning process, and in particular to serve as baseline information for the compilation of radon risk maps. Reflecting the current focusing upon radon in water, the aim of the research has been extended to incorporate the prognostics of ground water radon prone areas.

To develop the methodology, a 25×25 km test area in Central Sweden has been chosen (Fig. 5). The northern part of the area is mainly covered with postglacial clays, slightly enhanced in thorium, while the southern part is dominated by till. As the whole area is situated below the highest shoreline, the till in large areas is wave-washed and especially in the highest parts redeposited as beach sediments. Crossing the area from north to south is the esker¹ Köpingsåsen, which can be clearly identified on the topographic map in Fig. 5.

The bedrock of the area belongs to the Svecofennides of Central Sweden and was developed 1700–2100 millions of years ago. The principal rocks are metamorphosed volcanics and sediments, synorogenic granitoides, most frequently gneissic, migmatites, serorogenic granites and associated pegmatites.

The area is well covered with geoscientific information in digital form, and is known to comprise areas with serious ground and ground water radon problems. In particular, several bedrock units within the area manifest elevated uranium levels.

The quaternary and bedrock maps of the area are shown in Figs. 6 and 7 [18, 19], while the uranium component of the airborne radiometric measurements is shown in Fig. 8. When addressing the problem of radon in ground water, one needs to establish a map showing the uranium (radium) content of the bedrock. This is achieved as follows:

- the quaternary map is reclassified into two classes, the first comprising outcropping bedrock and till, and the second containing all other quaternary units
- the reclassified quaternary map is applied as a logical mask to the uranium component of the airborne radiometric data, retaining measurements over outcrops and till only, thus rejecting all other data
- the remaining radiometric data are processed together with the bedrock data to yield estimates of the mean radiometric signal over the individual bedrock units

In such a way, a uranium map of the bedrock is compiled, bearing information on all units that are exposed, either directly through outcrops or indirectly through overlying tills, assumed to be representative of the underlying bedrock. To yield a smoother map, radiometric means are calculated rather than cell-by-cell values. This approach also allows the information to be extrapolated beneath the quaternary cover.

The resulting radiometric map of the bedrock, presented as a ground water radon risk map, is shown in Fig. 9. Note that features and trends appear which are not readily visible on the raw radiometric map due to signals originating from the quaternary overburden.

Shown also in Fig. 9 are the limited number of wells that have been sampled so far within the study area. As for the wells above 500 Bq/l, they fall into two distinct classes: (1) situated in

¹ glacial ridge formation comprised of gravel and coarse sand

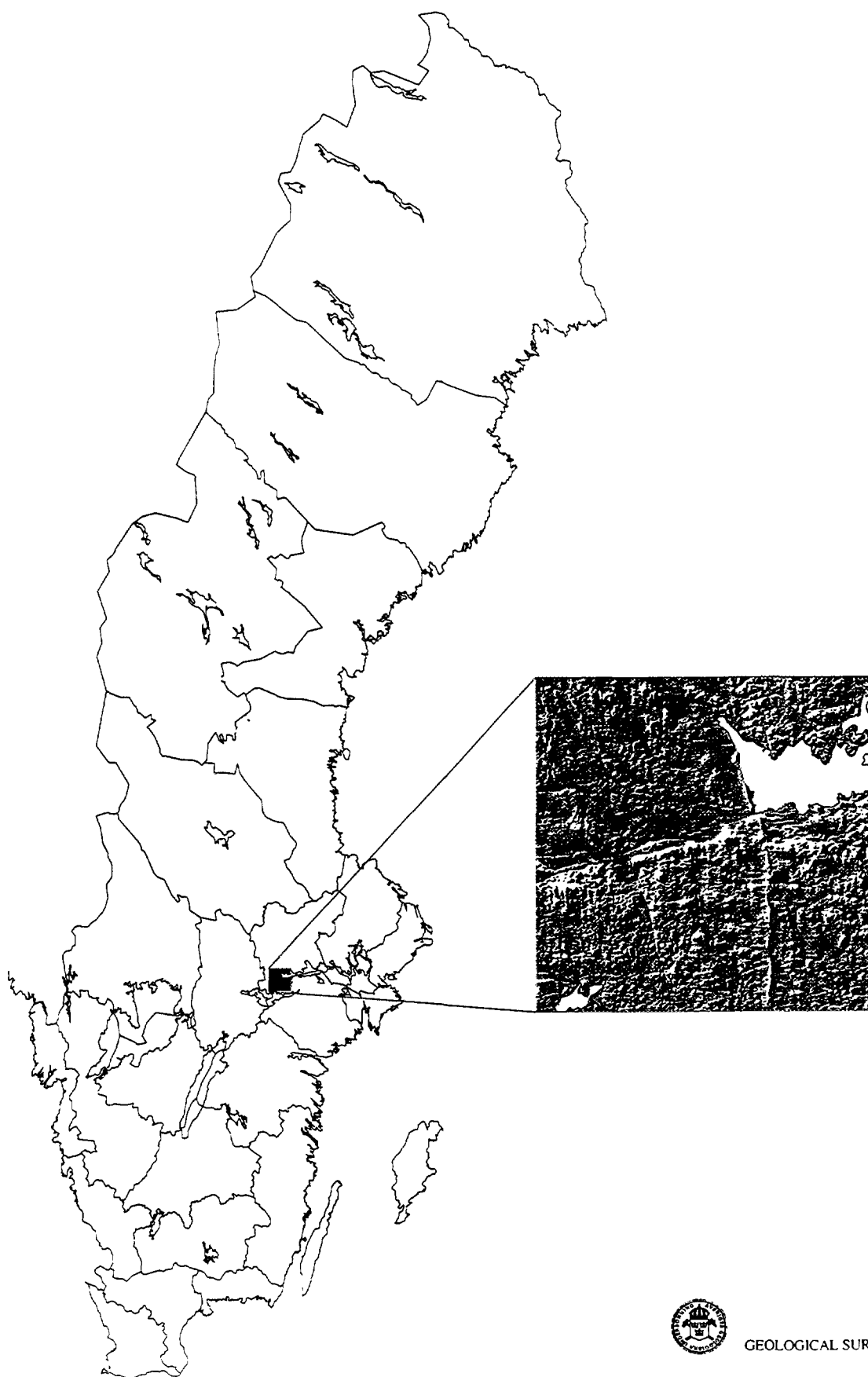


FIG. 5. Study area for regional ground radon prognostics with topographic map.

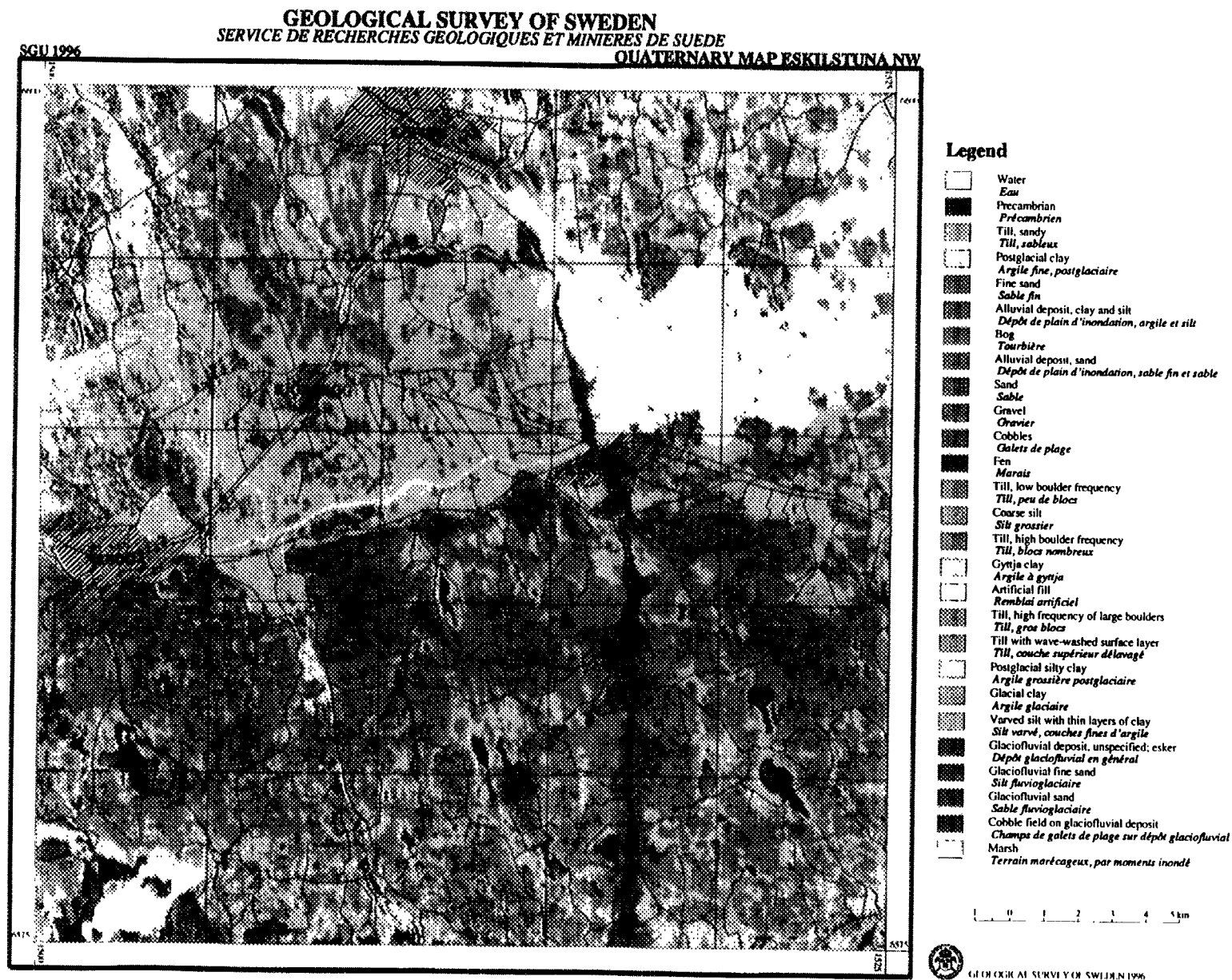
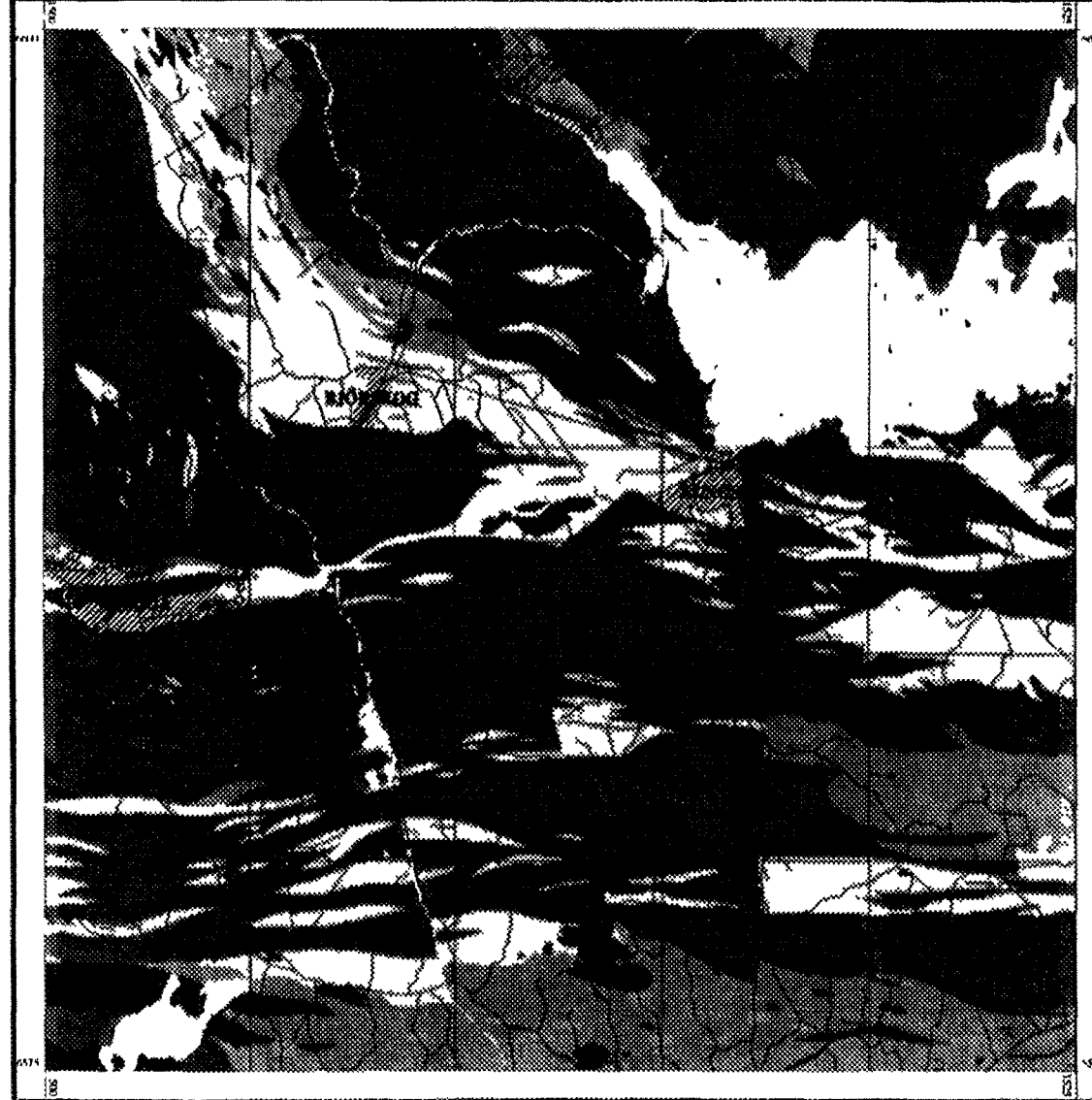


FIG. 6. Quaternary map Eskilstuna 10G NW.



Legend

- Pegmatite
Pegmatite
- Younger granite red
Granite récent rouge
- Younger granite grey
Granite récent gris
- Granodiorite augen structure
Granodiorite, structure ocellée
- Gneissic granite augen structure
Granite, structure ocellée
- Older granite mostly gneissic
Vieux granite gneissic
- Granodiorite mostly gneissic
Granodiorite, en général gneissique
- Quartz-diorite mostly gneissic
Diorite quartzique, en général gneissique
- Metabasite
Métabasite
- Paragneiss
Paragneiss
- Greywacke gneiss transformed
Greywacke, transformée gneissique
- Greywacke, mica schist transformed
Greywacke, transformée mica schist
- Quartzite, quartzitic gneiss
Quartzite, gneiss quartzique
- Carbonate rock, mainly dolomitic marble
Roche carbonatée, en général marbre dolomitique
- Hälleflinta and leptyte, mica schist transformed
Hälleflinta et leptyte, transformée mica schist
- Hälleflinta, leptyte and leptytic gneiss mostly alkali intermediate
Hälleflinta, leptyte et leptyte gneissique en général alkali intermédiaire
- Agglomeratic leptyte
Leptyte agglomératique
- Leptyte and leptytic gneiss with hornblende
Leptyte et gneiss leptytic avec hornblende
- Hälleflinta and leptyte potassium dominant
Hälleflinta et leptyte, potassique
- Hälleflinta and leptyte albite dominant
Hälleflinta et leptyte, albitique
- Water
Eau
- Conglomerate
Conglomérat

1 0 1 2 3 4 5 km



GEOLOGICAL SURVEY OF SWEDEN 1996

FIG. 7. Bedrock map Eskilstuna 10G NW.

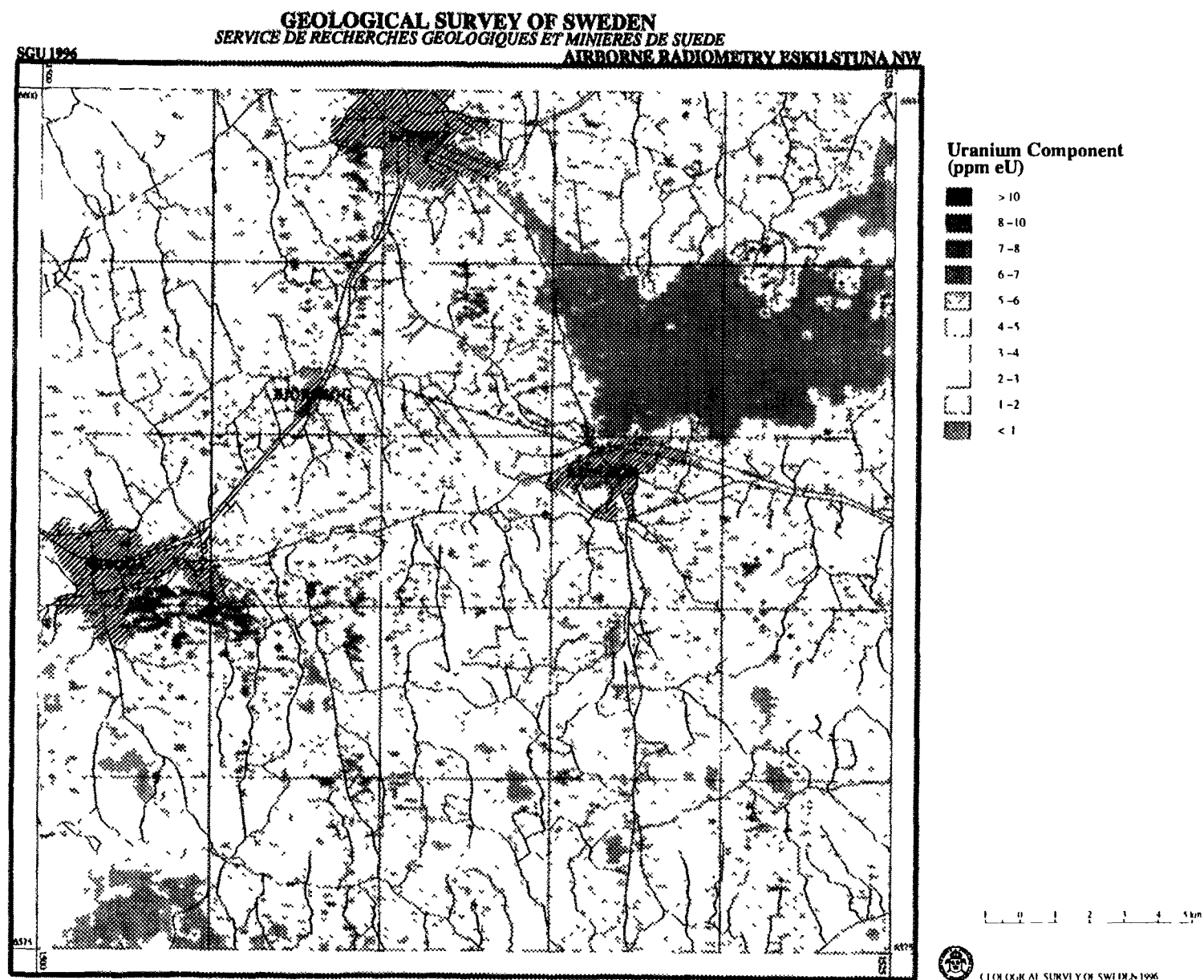


FIG. 8. Airborne radiometric map (uranium component) Eskilstuna 10G NW.

SGU 1996

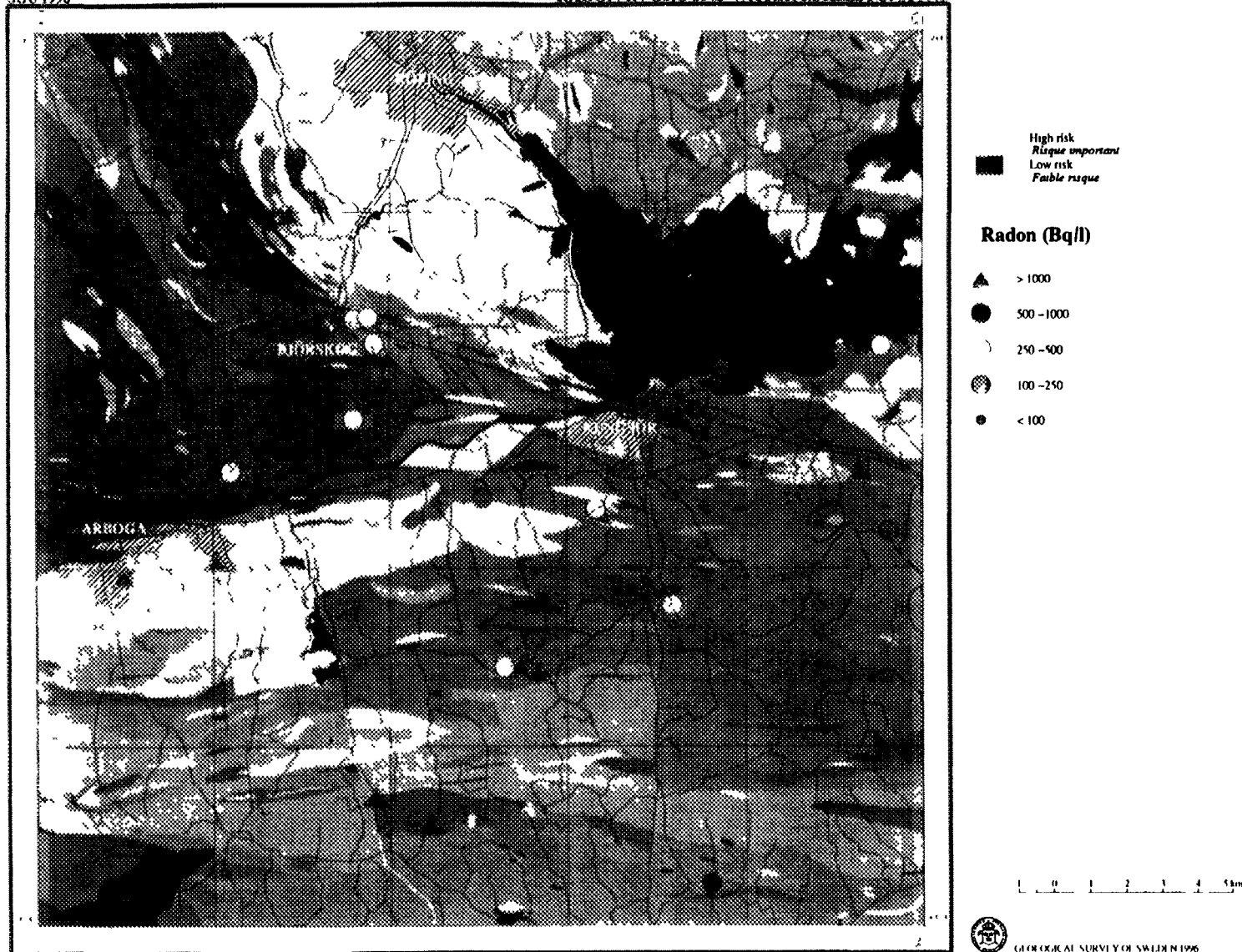


FIG. 9. Ground water radon prognosis map Eskilstuna 10G NW. Shown also on the map are wells drilled in bedrock analysed with respect to radon.

uranium-rich bedrock, or (2) situated in bedrock where the bulk rock manifests no elevated uranium content, but where there is an abundance of pegmatitic intrusions (not seen on the simplified bedrock map shown in Fig. 7). These pegmatites are known often to be fairly radioactive, but they seem not to appear to a sufficient extent to have any major influence on the airborne radiometric measurements and/or not to be enough exposed as outcrops.

The limited control obtained so far regarding the validity of the prognosis thus indicate that it is possible to predict to some extent areas where the relative probability of encountering radon problems is higher. A prognosis based upon airborne information should, however, be modified to include areas where the bedrock information suggest that uranium-rich intrusions may be present, even if they do not have an impact on the airborne radiometric signal.

Future research will incorporate the sampling of outcrops with the help of ground gamma spectrometry as well as the evaluation of the geochemical information over the area.

7. FUTURE ASPECTS

The implementation of compulsory limits for radon in drinking water will probably trigger an avalanche of measurements of public and private water in Sweden, leading to a better understanding of the distribution of wells with elevated levels. The medical implications of the radiation doses caused by radon in water have already drawn a considerable amount of attention from the public, forcing governmental as well as local authorities to put priority to the problem.

The occurrence of drilled wells with elevated radon content is well correlated with geological conditions. Any attempt to identify areas with ground water radon problems should therefore incorporate all available geoscientific information of relevance to the occurrence of radon, and in particular high spatial resolution airborne radiometry.

It is the definite conviction of the authors that ground water radon prognostics, based upon available geological, geophysical and geochemical information in connection with ground water radon mapping programmes will play an increasingly important role in the regional and municipal planning process with respect to radon risk.

REFERENCES

- [1] NAZAROFF, W.W., DOYLE, S.M., NERO, A.V., SEXTO, R.G., Portable water as a source of airborne ^{222}Rn in US dwellings: A review and assessment, *Health Physics*, 52, 3 (1987) 281–296.
- [2] VON DÖBELN, W., LINDELL, B., Some aspects of Rn–222 contamination following ingestion, *Arkiv för fysik*, Band 27 No. 32, Stockholm (1964) 531–572.
- [3] RICHARDSON, R.B., EATOUGH, J.P., HENSSHAW D.L., Dose to red bone marrow from natural radon and thoron exposure, *Br. J. Radiology* Vol. 64, No. 763 (1991) 608–624.
- [4] KENDALL, G.M., FELL, T.P., PHIPPS, A.W., A model for evaluating doses from radon in drinking water, *NRPB Radiological Protection Bulletin*, 1988:97 (1988).
- [5] UNSCEAR 1993, United Nations Scientific Committee on the Effects of Atomic Radiation. Sources and effects of ionizing radiation. Report to the General Assembly, with scientific annexes, New York, United Nations 54, ISBN 92-1-142200-0 (1993).
- [6] SWEDJEMARK, G.A., Radon and radium in water. Baseline information for regulations, Rep. Swedish Radiation Protection Institute 93-34 1-3, ISSN 0282-4434 (1993) (In Swedish).
- [7] ICRP 23, Report on the Task Group on Reference Man, The International Commission on Radiological Protection, ICRP (1974) 1–480.

- [8] EUROPEAN UNION, THE COUNCIL, Proposal for Council Directive 96/ Euratom of laying down basic safety standards (BSS) for the protection of the health of workers and the general public against the dangers arising from ionizing radiation, Doc. 12733/95 Brussels, 28 February (1996) 1–74.
- [9] SWEDISH RADIATION PROTECTION INSTITUTE, Radon - Risk - Dose. Dwellings and places of work, SSI i94-06 (1994) 1–17 (in Swedish).
- [10] SWEDISH NATIONAL FOOD ADMINISTRATION, Proposal for limits for radon in drinking water. Letter to the Swedish Ministry of Agriculture, National Food Administration, Dnr 4049/95 (December 1995) (in Swedish).
- [11] FINNISH CENTER FOR RADIATION AND NUCLEAR SAFETY, Radioactivity of Household Water, ST Guide 12.3, 1–8, ISBN 951-47-8651-3 (9 August 1993).
- [12] THE MINISTRY OF HEALTH OF THE CZECH REPUBLIC, Decree 76 on requirements for limiting radiation exposure due to radon and other natural radionuclides, Acts Collection, Part 16, February 12 (1991) 365–366.
- [13] ÅKERBLOM, G., PETTERSSON, B., ROSÉN, B., Radon from the ground - Handbook on investigation of the radon situation in areas before building, The Swedish Council for Building Research and the Swedish National Board for Housing, Building and Planning. Report R88:(1988), New revised edition (1990) 1–159, ISBN 91-540-4937-7 (in Swedish).
- [14] LANDSTRÖM, O., TULLBORG, E-L., The influence of fracture mineral/groundwater interaction on the mobility of U, Th, REE and other trace elements, Swedish Nuclear Fuel and Waste Management Company, Technical report 90-37 1-71, ISSN 0284-3757 (1990) 1–71.
- [15] KULICH, J., MÖRE, H., SWEDJEMARK, G.A., Radon and radium in household water. Rep. Swedish Radiation Protection Institute 88-11 (1988) 1–74 (in Swedish).
- [16] MELLANDER, H., Airborne gamma spectrometric measurements of the fall-out over Sweden after the nuclear reactor accident at Chernobyl, USSR, IAEA/NENF/NM-89-1 (1989).
- [17] LINDÉN, A., ÅKERBLOM, G., Method of detecting small or indistinct radioactive sources by airborne gamma ray spectrometry, In: Geology, mining and extractive processing of uranium (JONES, M. J., Ed.) (1976) 111–120.
- [18] MAGNUSSON, E., Description to the quaternary map Eskilstuna NV, SGU Ae 18 (1975) (in Swedish with summary in English).
- [19] LUNDEGÅRDH, P. H., Description to the map of solid rocks Eskilstuna NV, SGU Af 111 (1974) (in Swedish with summary in English).

**NEXT PAGE(S)
left BLANK**



THE ROLE OF HOUSE SURVEYS IN GEOLOGICAL RADON POTENTIAL MAPPING

K. BALL

Natural Environment Research Council,
Keyworth, Nottingham,
United Kingdom

Abstract

Because radon levels vary widely between apparently identical buildings on the same geological unit, no map can predict the radon level in an individual building. Maps can, however, give the probability that a building in a particular locality is above a threshold of radon concentration such as a reference or action level. The probability may be calculated for a particular building type or for a mixture of building types. In the latter case the probability is in effect an estimate of the proportion of buildings above the threshold level. Alternatively maps can provide estimates of the mean radon levels in buildings by area. Maps showing the geographical variation in probability that new or existing buildings will exceed a radon reference level are used to prevent excessive exposures to radon. The information may be used in various ways, such as to target information campaigns encouraging measurement of radon levels in homes or to modify regulations for new buildings. The data which are used to provide the estimates of the proportion of buildings above a threshold may be radon measurement results from a sample of buildings, or may be indirect indicators such as ground radium concentrations, emanation coefficients and permeability measurements. Consistency in radon measurement protocols and detailed positional information are prerequisites for mapping radon prone areas based upon house data. Testing the radon in house data indicates that the data is usually lognormally distributed and from such a distribution probabilities may be calculated for small data sets. Probabilities may then be assigned to mapping areas. Geological maps comprise juxtaposed irregular polygons and the data for these are mostly distributed lognormally, with rare exceptions. Grouping building radon measurements by geological formation and superficial cover can produce radon potential maps which are more spatially accurate than grid square maps and more accurate in estimating numbers of homes affected than mapping based only on measuring geological and pedological properties.

1. INTRODUCTION

Radon potential mapping is a means of summarising data so that attention can be drawn to areas with differing radon emanation characteristics. The result usually divides the area into sub-areas each of which is classified according to the probability of typical houses being affected by radon. The probability may be expressed as a percentage of the housing stock that is above a threshold (reference or action level) or as a mean radon level for whichever class is represented. The map ideally shows the potential of the ground to generate a radon problem but whether this potential is realised depends upon the construction and maintenance of the house and the life style of the occupants.

Such maps are particularly useful for directing action to prevent excessive exposures to radon, for example, to target information campaigns encouraging measurement of radon levels in existing homes or for construction control regulations for new buildings.

The data used to provide the estimate of the proportion of buildings above a threshold include measurements from a sample of buildings, or indirect indicators such as the uranium or radium concentrations of rocks and soils, emanation coefficients, permeability, and ground gas radon measurements.

Various different types of boundary are used in the analysis of data and presentation of maps, such as administrative boundaries, geological boundaries or arbitrary divisions such as 5 or 10 km squares. Use of administrative areas has the advantage of simplifying subsequent administrative action, and it is usually easier to determine the administrative area in which a building falls than its map coordinates. However, it has the disadvantages that the areas have shapes and sizes which may obscure the underlying pattern of variation in radon levels. Use of grid squares allows an appropriate

size of area to be chosen and simplifies the analysis, but can make it difficult to apply administrative action. Geological boundaries delineate differences in radon potential much more closely than other types of boundary, but are often complex and, unless well mapped prior to the radon investigations, may be difficult to determine

Generally any radon potential map is multi-sourced. The major controls on labile radon distributions are the uranium or radium content, the mineralogy and the permeability of the ground. A limited number of carefully sited field geochemical measurements can be used to assess an area with good accuracy. However since radon is mostly a problem when it gets into houses this inevitably means that after provisional geologically or geographically based maps have been produced, the emphasis changes and measurements in houses have priority. House measurements are required, in any case, for purposes other than radon potential mapping. The emphasis inevitably given to house measurements means that such data-sets frequently are more abundant and available for many more areas than are relevant geochemical data.

Since the main purpose of maps of radon potential is to indicate high radon levels in buildings, maps based on actual measurements in buildings are preferable to those based on other data. In such cases, the extent of the problem, assuming that the sampling is truly representative of the housing stock, is exactly indicated by the results.

2. METHODOLOGY AND STATISTICAL BASIS

When a parameter depends on the sum of a number of independent factors, the measured values of that parameter will follow the normal distribution. In the case of radon in buildings, there are many independent factors, but they are multiplicative rather than additive. The radon concentration indoors can be represented by the equation of the kind:

$$Rn_i = Rn_o + A \times B \times C \dots \quad (1)$$

where Rn_i is the annual average radon level indoors, Rn_o the annual background level of radon in the atmosphere, A, B, C, \dots are factors such as radium concentration in the ground, permeability of the ground, number and size of entry routes, underpressure in the building and ventilation of the building etc. These factors determine how much of the radon from the source enters the building and how long it remains. This model assumes that these factors are largely independent and are multiplicative. The equation can be rewritten using natural logarithms as:

$$\ln (Rn_i - Rn_o) = \ln(A) + \ln(B) \ln(C) + \dots \quad (2)$$

This equation now conforms to the requirements for normal distributions since it is still a sum of independent terms: hence if there are a number of independent terms, each randomly distributed, then $\ln(Rn_i - Rn_o)$ should be normally distributed or $Rn_i - Rn_o$ is lognormally distributed.

The lognormal distribution has been widely observed in practice in surveys of radon levels in buildings when whole countries are considered [3]. Results grouped by US county also conformed to the lognormal distribution [6]. Miles [4] showed that the same applied to UK radon results grouped by 5 km grid square. Given data which conform in this way, it is simple to estimate the proportion of the distribution above a threshold from the geometric mean (GM) and geometric standard deviation (GSD) for each area by subtracting average outdoor radon concentration, taking natural logarithms and calculating mean and standard deviation.

Statistical testing of the data in terms of geological polygons shows that in the vast majority of cases the data are distributed lognormally [5]. In a small number of cases the situation is more complex but even in those cases, the data can usually be resolved into a small number of lognormally distributed populations. In a very small number of cases the data are not distributed obviously

according to the lognormal rule and sometimes are closer to being normally distributed. These latter cases are most common where houses are built over unconsolidated overburden on top of thicker bed-rock units.

3. SAMPLING NEEDS

The requirements for mapping radon-prone areas using the results of radon measurements in buildings are:

1. accurate and representative radon measurements made using a consistent protocol
2. centralised or easily accessible data holding
3. sufficient data evenly spread
4. precise location of addresses of measurements

The first three requirements depend on financing and organising a survey of radon levels. Making a survey properly representative of the building stock is a point that is often neglected.

It is clear that houses of different design and floor area, have different average susceptibilities for radon ingress. Bungalows are worse than detached houses which in turn are worse than semi-detached and then terrace houses and flats and so on. Terrace houses and flats are more common in towns and detached houses in rural areas. For map sheets with large urban areas it is likely that there will be bias from these sources which may invalidate extrapolation to rural areas of similar geology.

Given sufficient data however correction factors can be determined to reduce the variation from this source. The data can thus be normalised to a convenient standard. In the UK a normal two storey, three bedroomed house with single glazing has been selected as the norm. This is the most common type of dwelling. Correction factors for houses of different basic design can then be applied.

4. CONSTRUCTION OF MAPS

In the UK there have been two basic approaches to the production of radon potential maps. Maps produced by analysis of house radon data gained by sampling the housing stock on a grid square basis enables an accurate prediction of the radon statistics for existing dwellings. However it is clear from some areas that each square may have a number of rock formations within it, each of which may result in different amounts of radon in the ground gas and unless the house sampling takes this into account the areally weighted statistical validity may be compromised.

The geological approach, has been to determine or estimate the amount of radon passing into ground gas and, in conjunction with permeability considerations, to map areas according to broad classes. Calibration was by house radon data and divisions between the classes were based upon existing legislation, which relates to the proportion of homes exceeding the Action Level of 200Bq/m³. The groups used to date are of the form: High (over 10% of houses affected), Moderate (3–10% of houses affected), Low/Moderate (1–3%) and Low (<1%). Further classes have been introduced according to the local geological conditions [1]. Although the spatial accuracy was good, there were uncertainties in the class limits necessitating the choice of broad categories.

A combination of both approaches enables the merging of the best features: the spatial accuracy of the geologically based information with the numerical/statistical accuracy of the house data [5]. The application of house radon measurements to the production of radon potential maps at many scales is described, from the country wide to the use of the data for the production of detailed maps at scales of about 1:10 000.

4.1. Small scale maps

The relationship between the house information and geology on a small scale is illustrated for England and Wales (Figs 1 and 2). Especially high levels for the geometric mean radon concentration in houses are observed over the intrusive Hercynian granitic rocks and over their metamorphic aureoles in Cornwall and Devon and for the Caledonian Cheviot Granite on the Scottish Border. The lower Paleozoic rocks have moderate levels of affected houses, especially the shelf facies rocks from the Silurian period.

Carboniferous limestones form large massifs in Somerset, Derbyshire, southern and North Wales and northern England and have high levels of radon in houses. The major Carboniferous coalfields have variable levels ranging from high in North Wales, moderate in the East Midlands of England to low in South Wales and Northern England. Permian dolomitic limestones in northern England have moderate levels of radon in houses.

A broad sinuous band of high values extends from the south coast across Somerset through Northamptonshire and on to the NE coast, and is a zone underlain by the Lower Jurassic. The high radon emanating lithologies are dominated by limestones and associated calcareous sedimentary ironstones.

The Cretaceous beds in England are mostly Chalk, a soft homogenous limestone, and are characterised by an irregular but nevertheless perceptible incidence of houses exceeding the action level. With the exception of minor areas the red beds of the Permo-Trias (the New Red Sandstone) and the Tertiary rocks have a low incidence of affected houses.

The effect of overburden can be great. The major source of superficial deposits is from the glaciations which were common in the Pleistocene. Ice sheets extended as far south as north Somerset (Fig. 1). The deposits are thickest over low ground in the north, the upland areas were usually glacially eroded. The main till deposit was Boulder Clay, usually a stiff tenacious clay containing sub-angular blocks of various sizes. It forms a mantle of centimetres to several metres thick. The deposit is usually locally derived and, not unexpectedly because of its high clay content, it reduces the flow of gas which is reflected in the marked reduction in the numbers of affected houses compared with bed-rock. Glacial Lake Deposits are usually clay rich and similarly reduce the radon levels. The effect of Fluvio-glacial Sands and Gravels is dependent upon the nature of the substrate, enhancing the radon levels over permeable rocks and rocks which weather in a brittle manner, whilst reducing the radon levels over relatively impermeable rocks. Coastal estuarine and marine alluvium generally reduce the radon fluxes. The combined properties of drift and bed-rock should always be assessed because of the complex interplay of permeabilities and radiochemistry.

4.2. Medium scale maps

Small scale maps may show different geological features to those on a larger scale. They are usually based upon stratigraphical limits whereas on the larger scale both stratigraphic and lithological properties are recorded. Maps such as those based upon the 1:50 000 scale are particularly useful. It is at this or larger scale that the modifying effect of the superficial deposits can best be assessed.

The relationship between the geological map and the assessment of house data for each geological unit for Derbyshire is shown in Fig. 3. Examples of such relationship on log-probability plots are given in Fig. 4. The oldest rocks are the heavily karstified Carboniferous Limestones. These generally have low uranium levels (commonly 1–2ppm) but the uranium bearing minerals are often widely disseminated or are in low density components of the rocks. The specific surface area of the uranium bearing phases is often large and radon can be released from the mineral host with great efficiency. Some of the marginal reef limestones, are uranium mineralised [1]).

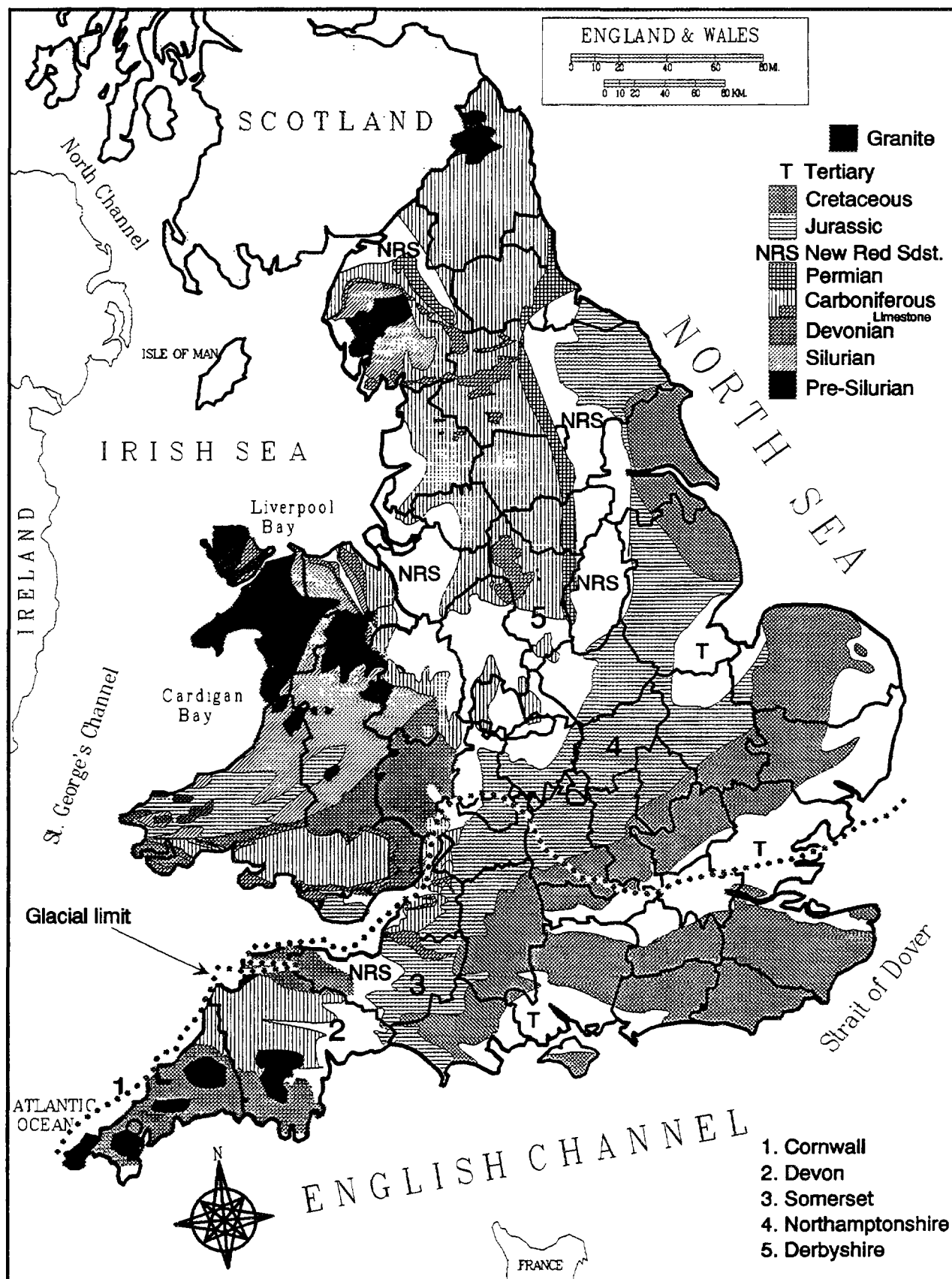


FIG. 1. Simplified geological map of England and Wales showing the location of the major stratigraphical systems. The approximate southerly limit of Pleistocene glaciation is also denoted.

Estimated geometric mean radon level
in each 5 km grid square of England and Wales.

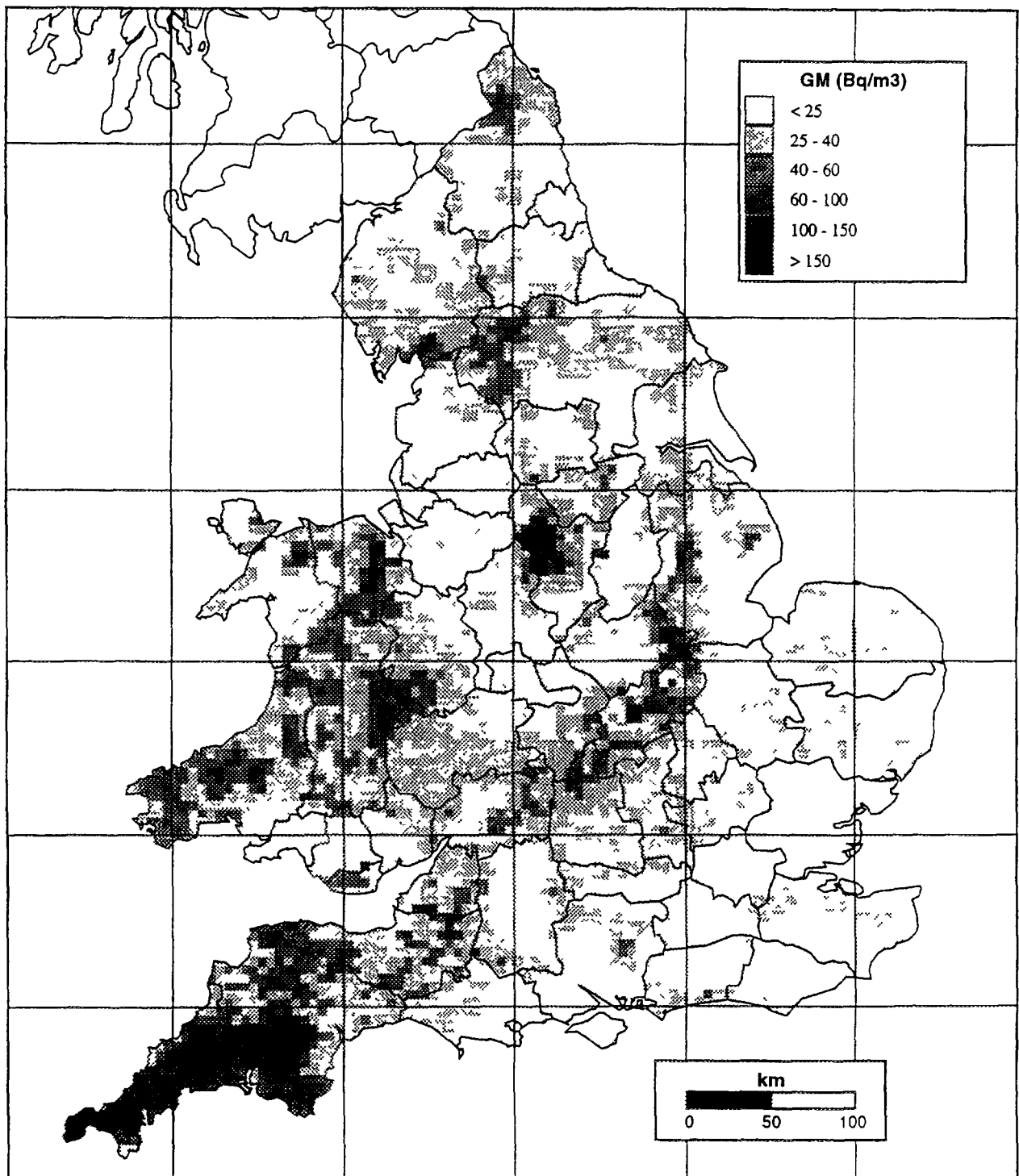


FIG. 2. Estimated geometric mean radon levels in each 5 km grid square of England and Wales, based on lognormal modelling of radon measurements in houses.

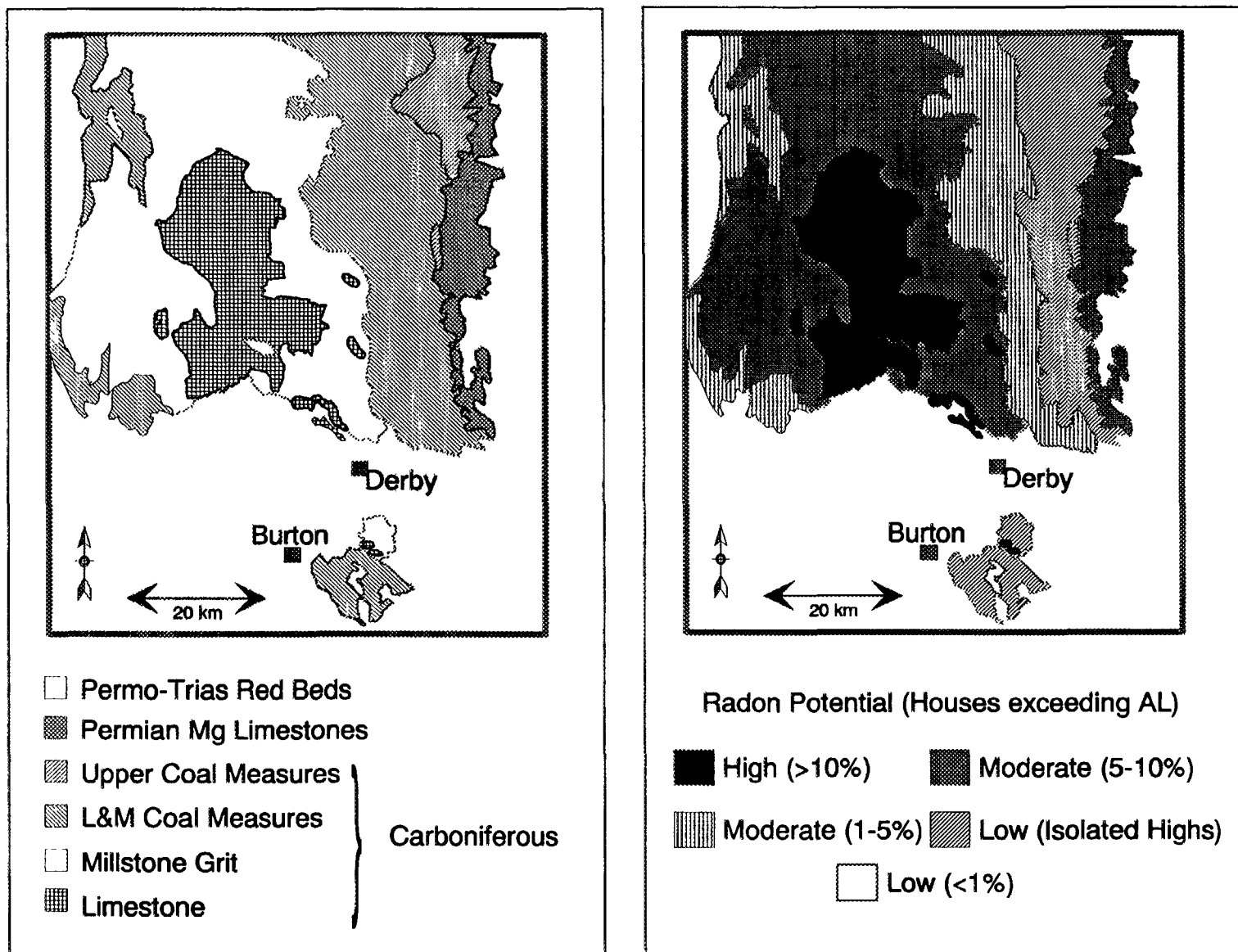
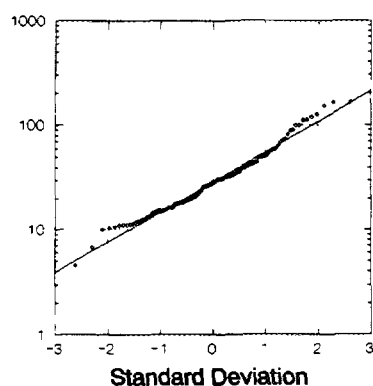
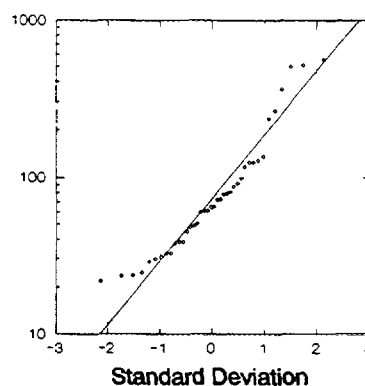


FIG.3. Simplified geological map of Derbyshire and the surrounding area used as a basis for the Radon Potential Map.

Sherwood Sandstone Group

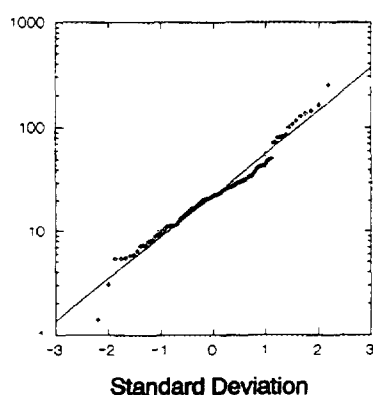


Millers Dale Limestone

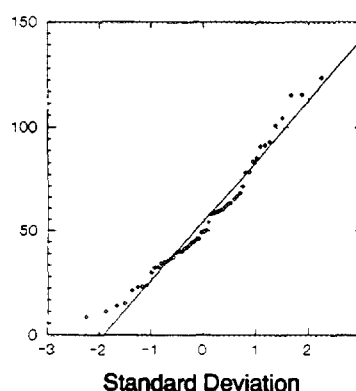


House survey
data, Bq/cum.

Upper Namurian Shale



Boulder Clay on Edale Shale



House survey
data, Bq/cum.

FIG. 4. Log-probability plots for house data underlain by the Triassic Sherwood Sandstone Group arenaceous red-beds (199 houses), Millers Dale Limestone (40 houses) and Upper Namurian shales (136 houses) from the Carboniferous. House survey data for Boulder Clay on the uraniferous Edale Shales (Lower Namurian, 53 houses) is shown as a normal probability plot.

The limestones are overlain by Namurian rocks, the basal members of which are highly radioactive black shales. The main part of the succession however comprises a sequence of thick shales and sandstones with average uranium concentrations. These are overlain in turn by the Coal Measures (= Westphalian): a cyclothem sequence of sandstones, shales, seat-earth and coals. In places, especially in the Lower Coal Measures, the sandstone units are thick and abundant. Highly radioactive "Marine Bands" occur sparsely within the Namurian and Westphalian Strata.

The rocks were folded uplifted and eroded prior to the deposition of Permo-Triassic rocks. In the east the first representative of these periods is a dolomitic limestone. Elsewhere the lower beds belong to the Sherwood Sandstone Group (= Bunter Sandstones) and are overlain by marls of the Mercia Mudstone Group (= Keuper Marl).

The whole region was glaciated during the Pleistocene. Since the area is largely upland the main part underwent glacial erosion, with deposition on the lower ground, which is mostly underlain by the Permo-Triassic rocks. In the high ground glacial deposits are mostly valley-confined and fluvio-glacial, comprising sands, gravels and terrace deposits.

Limestones are the most important radon generators in the region. The Permian limestone, which is karstified but to a smaller extent than the Carboniferous, shows lower levels of radon emanation, and this is also reflected in houses. The clay rich rocks in the south of the area have little radon potential except for small-area sub-environments.

The sandstones in the Namurian and Westphalian are fractured rock aquifers and despite having low levels of uranium, much of this is disseminated in the cement surrounding the individual sand-grains. They are consistent moderate generators of radon.

Radon from the shales of the Namurian and Westphalian correlates with their uranium concentrations. The highest levels occur over uraniferous black shales (Edale Shales) in the lowermost part of the Namurian and over marine incursion horizons higher in the Namurian and the Westphalian.

4.3. Large scale maps

Whereas the smaller scale maps are most useful in focussing attention on areas where further investigation is required, they are of limited value where controls on new building may be necessary. A larger scale map is often required for this.

Several thousands of house surveys were available for the Northampton area and as a result very fine details of the house radon surveys can be related to various combinations of drift and solid geology. Relatively low values are found over clay rich rocks, either bed-rock or combinations of bed-rock and glacial drift, mostly boulder clay and glacial sands and gravels. The broad zone of high values (8% > Action Level) corresponds with higher ground and is underlain by the Northampton Sand Formation, a sedimentary calcareous and phosphatic iron ore, at one time extensively mined. It is laterally variable and in the Northampton area the upper part is well indurated with lower radon generation and transmission characteristics. Elsewhere this feature is not so apparent and the percentage of affected houses increases. Near the lower contact the formation becomes more uraniferous, and more permeable.

The nature of the ground and the presence of soft plastic clays underlying the Northampton Sand Formation, has resulted in slumping of disaggregated, and hence highly permeable, uraniferous material from the lower part of the Northampton Sand Formation onto the underlying Upper Lias Clay. The result is that there is a zone of higher house values which overlaps the contact between the Northampton Sand Formation and the Upper Lias Clays (Figs 5 and 6).

5. CONCLUSIONS

Basing radon potential maps on geological boundaries in which information on bed-rock and drift geology is combined, and in conjunction with house data, provides an useful tool for the environmental geochemist. Analysis of this type is possible only where there are sufficient results of measurements in homes for each combination of geological formation and superficial cover. In areas where there are insufficient house surveys (either because the population density is too low or because the geological variation is too great) other information such as radon in soil gas assists in estimating radon potential. This data requires careful interpretation and may only provide a provisional estimate.

By grouping building radon surveys by geological formation and superficial cover, radon potential maps can be produced that are more detailed than grid square maps and more accurate in estimating numbers of homes affected than mapping based only on geological/geochemical measurements. However, lateral facies variations in some geological formations mean that conclusions drawn for one area cannot necessarily be extrapolated to adjoining areas. Furthermore the mapped stratigraphical boundaries may not accord with the radio-geochemical stratigraphy. Where large data sets are available these more subtle variations in response can be mapped with great precision.

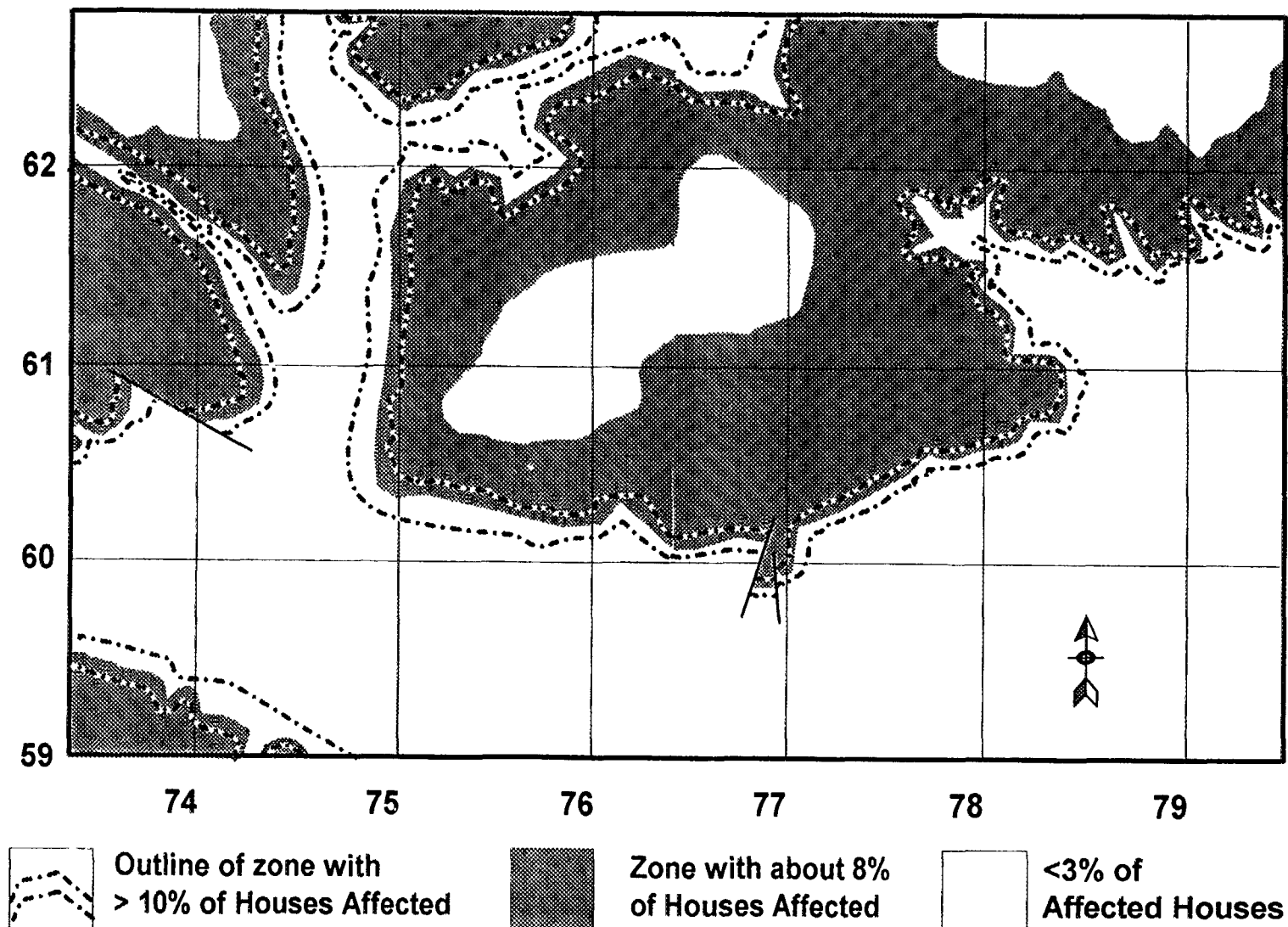


FIG. 5. Estimated percentage of houses above 200 Bq/m^3 in Northampton, United Kingdom, based on lognormal modelling of radon measurements in homes grouped by geological formation. Each square shown is 1 km^2 .

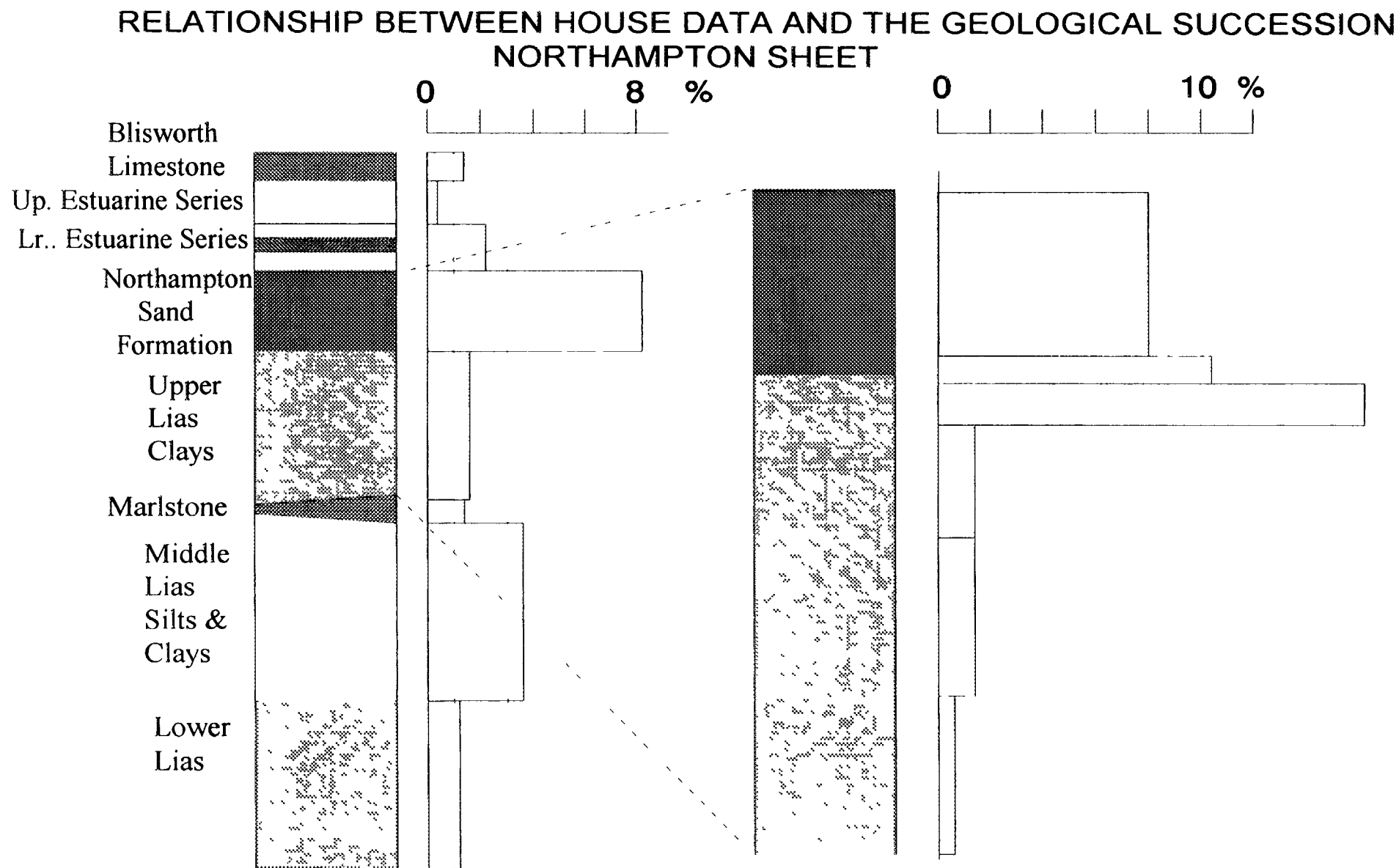


FIG. 6. Estimated percentage of houses exceeding 200 Bq/m³ for the stratigraphical column in the Northampton area. The Upper Lias Clay is about 50m thick.

REFERENCES

- [1] BALL T.K., CAMERON D.G., COLMAN T.B. ROBERTS P.D., "The use of uranium exploration data for mapping radon potential in the UK — Advantages and Pitfalls, Application of uranium exploration data and techniques in environmental studies, TECDOC-827, IAEA, Vienna (1995).
- [2] BALL, T.K., MILES, J.C.H., Geological and geochemical factors affecting the radon concentration in homes in Cornwall and Devon, UK, *Environmental Geochemistry and Health* 15 (1993) 27–36.
- [3] GUNBY, J.A., DARBY, S.C., MILES, J.C.H., GREEN, B.M.R., COX, D.R., Factors affecting indoor radon concentrations in the United Kingdom. *Health Physics* 64 (1993) 2–12.
- [4] MILES, J.C.H., Mapping the proportion of the housing stock exceeding a radon reference level. *Radiation Protection Dosimetry* 56 (1994) 207–210.
- [5] MILES, J.C.H., BALL, T.K., Mapping radon-prone areas using house radon data and geological boundaries. Presented at the Sixth International Symposium on the Natural Radiation Environment, Montreal, 1995 June 5–9 (1995).
- [6] NERO, A.V., LEIDEN, S.M., NOLAN, D.A., PRICE, P.N., REIN, K.L., REVZAN, H.R., WOLLENBERG, H.R., GADGIL, A.J., Statistically based methodologies for mapping of radon "actual" concentrations: the case of Minnesota. *Radiation Protection Dosimetry* 56 (1994) 215–219.



AIRBORNE AND TRUCK-BORNE "RADIATION FOOTPRINTS" OF AREAS PRODUCING, STORING, USING OR BEING EXPOSED TO NUCLEAR MATERIALS

B. PAVLIK, F. BOTTOS

Picodas Group Inc.,
Richmond Hill, Ontario,
Canada

P.J. CUNEEN

World Geoscience Corporation Limited,
Perth, Australia

P. JURZA, V. HOESCHL

Picodas Prague s.r.o.,
Prague, Czech Republic

Abstract

The paper discusses the use of advanced Airborne Gamma Ray Spectrometer for environmental assessment of nuclear radiation in areas exposed to radioactive materials. The use of high capacity real time processors operating in parallel mode packaged into one mechanical enclosure together with navigation, allows implementation of highly sophisticated proprietary algorithms to produce results in absolute physical units. Airborne footprinting provides rapid, well defined spatial images of natural and manmade radioactive contamination. Integrated GPS guidance systems provides instant position information related to the internal geographical data base. Short time span of data acquisition provides consistent data. Airborne acquisition of data guarantees good spatial resolution. Airborne measurements are calculated via special algorithms in absolute units and related to the individual radioactive nuclei on the ground in real time. Full raw and calculated data recording is provided including the position coordinates. More precise results may be achieved via post flight processing. Principles of ground contamination estimates measured from the air and the sensitivities for different radioactive nuclei are also discussed. Results from an Ontario Hydro (Canada) test over a nuclear power plant, an Atom bomb blast measurements in Maralinga (Australia), after 40 years, and a Nuclear power plant in Slovakia and Uranium mining area in Germany are presented and discussed.

1. GAMMA RADIATION SURVEY — A NECESSITY

The general lack of natural sensors to detect and monitor radioactive hazards, particularly in this technologically advanced society has necessitated the development of new instrumentation and processing techniques that can rapidly produce visual images of areas exposed to radiation. Protecting the health of the population in case of a nuclear accident is essential and a social priority.

Monitoring of existing levels of natural and manmade radioactive sources, in and around nuclear installations and nuclear materials handling facilities becomes a valuable reference data source "footprint" that quickly determines the current levels of contamination and can assist in directing future emergency planning.

Fast deployment of airborne radiation monitoring systems in the case of nuclear accidents is essential. The portability of the new range of instrumentation with accurate navigation, data acquisition and real time processing can provide fast and low cost surveys that produce almost instant maps indicating the radiation distribution over the surveyed area.

Repeated surveys, once or twice per year, over nuclear facilities, including active and non-active uranium mines provide a history of the radioactive background and contamination of these areas. This information will become a part of the ISO14000 environmental documentation. At the same time it provides important information for public education and information that can address early remedies and avoid potentially serious problems. Also the proper documentation of the long term radiation levels may reduce liability risks to companies handling nuclear materials.

2. TYPES OF RADIATION SURVEYS — GROUND AND AIRBORNE

There are two techniques on how to produce radiation images over nuclear handling facilities and surrounding areas.

Ground survey

Data can be collected on foot or by a survey vehicle.

Advantages:

- Very detailed image depending only on the selected grid size or speed of the vehicle.
- Different measurements such as Alpha, Beta and Gamma can be obtained.

Disadvantages:

- Limited or restricted access (buildings, terrain).
- Time consuming, takes long time to cover suitable area.
- Geographically non consistent data.
- Dangerous in case of high radiation levels.

Airborne survey

Advantages:

- Fast, with no access limitation.
- Almost instant classification of the area.
- Efficient and large coverage per time unit.
- Integral view of the area, with resolution of the measurements related to the altitude and speed of the aircraft.
- Low cost per surveyed line km.
- Geographically consistent data.
- With proper safety procedures, limited potential to dangerous exposure.

Disadvantages:

- Initial cost of renting/using aircraft or helicopter.
- Somewhat limited spatial resolution.
- Only Gamma measurements can be recorded.

When comparing the total cost and time required to collect and process the data to obtain a global image and assessment of the surveyed area, it is apparent that an airborne survey is the practical answer. With the new technology, particularly with the advanced navigation system, it is possible to collect adequate information flying at the altitude of 50 to 80 metres with the flight line separation as close as 50 metres or less. To survey an area of 10 by 10 kilometres at an altitude of 70 metres with a line separation of 70 m, the total line kilometres flown is approximately 1 400 km. While taking into consideration the necessary turns and the average speed of the airplane (helicopter) at about 120 km/hr, the required time to fly this area is about 16 flight hours or approximately 3 working days. Preliminary maps can be processed within hours after the flight and final images of the area can be ready in a couple of days. To acquire similar volume of data on the ground would take a considerably longer time at a much greater cost.

3. AIRBORNE TO GROUND DATA CONVERSION

In order to be able to interpret airborne survey data properly, the data must be recalculated into absolute (physical) units. This can be achieved in two ways. In real time and in postflight processing. In case of emergency response the real time processing is a must. Health authorities need processed information as soon as possible (in real time) in order to activate emergency procedures. Picodas Group Inc. together with the Technical University of Prague, Faculty of Nuclear Engineering, developed modeling techniques to provide the required results.

A complex mathematical model of air to ground data conversion was developed. There are two models, both based on an infinite ground plane of radioactive contamination. A surface model

for deposits of manmade radioactive materials and a spatial, homogenous, model for natural elements. Both models are theoretical and in most cases depending upon time, the distribution of manmade contamination is somewhere in between. The time factor in determining a homogenous environment is weather dependent. Longer in dry areas, shorter under wet conditions.

Surface contamination produces a hemisphere distribution of the Gamma flux above the ground and is measured in activity per area (square metre). The homogenous (isotropic) contamination produces the Lambertian (cosine) distribution and is measured in activity per volume (kg, cubic metre etc.). Activity of radiation is measured in Bq. One Bq is a unit for one disintegration.

Airborne equipment flown at altitudes over 10 metres can only measure the Gamma content of disintegrations. Any disintegration of a radioactive element is characterized in relation to the Gamma radiation by the "Peak Energy Intensity" expressed in percent of Gamma particles emitted by one disintegration.

Altitude of the aircraft is the next variable in the process relating airborne data to the ground level (see Fig. 1). The attenuation of the Gamma particles going through the air layer is dependent upon the energy of the particle and thickness of the air layer.

Detector size and shape are other factors of the model. A Gamma particle on its way from its origin to the detector faces many obstacles and only a small number of the particles are detected with its original energy by the airborne detector. The number of these particles is further reduced by the inadequate stopping efficiency of the detector.

To properly detect the lower energy emitting elements, the deconvolution of the higher energy elements from collected spectra, called stripping, must be applied. To be able to classify the elements, the "Net peaks" (e.g. peaks stripped of the attenuated content from higher energies and not properly detected particles) in the collected spectrum must be properly determined.

Speed of the aircraft only defines the spatial resolution of the detection.

The air to ground model can be expressed as a function:

Model = Function(Distribution of contamination, Detector shape and size, Detector efficiency, Altitude of the aircraft, Energy of the radioactive element, Peak energy intensity, Stripping).

4. INSTRUMENTATION SENSITIVITIES

To define the system sensitivity for individual radioactive elements we have to consider the Spectral Energy Resolution of the system and statistical character of the Gamma detection process. Since the sensitivity of the detector is directly proportional to the detection area of the detector, for non emergency airborne footprinting, a larger size of detectors is desirable. The NaITl crystal ($10 \times 10 \times 40$ cm) is a generally accepted detector size. An array of these detectors (usually 4) are mounted in a single detector package forming a detection surface area of 40×40 cm.

Statistical character of the measurement limits the sensitivity related to the unit of time (usually 1 second). Resolution of the detector limits the detectability of the neighboring energy peaks. Even though the model of air to ground is quite complex and the statistical nature of the detection process further complicates the issue, a relatively simple sensitivity formula for each element can be drawn.

For instance for **K-40** (1.4612 MeV) with a detector size of $40 \times 40 \times 10$ cm the estimated number of detected Gamma particles for one Bq of homogeneously saturated layer with the density of 1.66 g/cm^3 in relation to the altitude of the detector are:

Altitude	Distribution (model)	Gamma/Bq	Bq/Gamma
30 m	lambertian	0.4121	2.430
60 m	lambertian	0.3221	3.104
90 m	lambertian	0.2333	4.286
120 m	lambertian	0.1621	6.169
150 m	lambertian	0.0965	10.36

Statistically the results vary within ± 3 standard deviations. In other words **ten** detected Gamma particles in the **K-40 Net peak** energy window in a time unit will give $\pm 90\%$ reliability of the measurement.

At the altitude of 90 metres the described detector can theoretically detect 1 647 Bq for isotropic and 1 250 Bq for lambertian distribution with the reliability of $\pm 30\%$. The reality is not as good since the stripping is introducing additional statistical noise. For Potassium we should consider the lambertian model only. The Gamma events detected in the Net K-40 window are related to the emanation from one metre square. Should we assume that the K-40 is dispersed homogeneously in a saturated layer (density of 1.6 g/cm³) then the detectable contamination of K-40 is 16.5 Bq/kg. This level is well below the normal natural radiation level (approx 250 Bq) and therefore this method provides reliable measuring results.

Element	Cs-137 Bq/m ²	Co-60 Bq/m ²	K-40 Bq/kg	Bi-214 Bq/kg	Tl-208 Bq/kg
Normal (area related) Background	7000	1000	250	30	40
Detection $\pm 50\%$ @90 m	6200	3320	214	112	50

We conclude that the above discussed detector package can, with the exception of Co-60, and Bi-214 quite reliably measure levels of the background radiation and anomalies exceeding twice the background levels. Since a secondary peak of Bi-214 may be measured, the reliability of Bi-214 increases to the level of the other elements. It is to be noted that the higher measured radiation levels provide better statistics and therefore better reliability of the measurements.

5. PROCESSING TECHNIQUES AND INSTRUMENTATION

Picodas Group Inc., Picodas Prague s.r.o., both part of the World Geoscience Corporation Limited, together with the Faculty of Nuclear Engineering of the Technical University of Prague developed the above mentioned models for use in practical applications. Picodas Group Inc. has developed the portable, fully integrated instrumentation ENMOS 2001 for this application comprising of a fully digital Gamma Spectrometer, Data Acquisition, Differential GPS Navigation, Pilot Guidance system and Geographical Data Base with flight and ground support software, as well as having developed a processing model to be used on board of the aircraft in real time. A complete data set (raw and processed) are recorded in the aircraft and may be reprocessed on the ground to higher resolutions. An integrated data processing package, including modelling and map making software has been developed to provide preliminary and final dosage and contamination maps soon after survey flights.

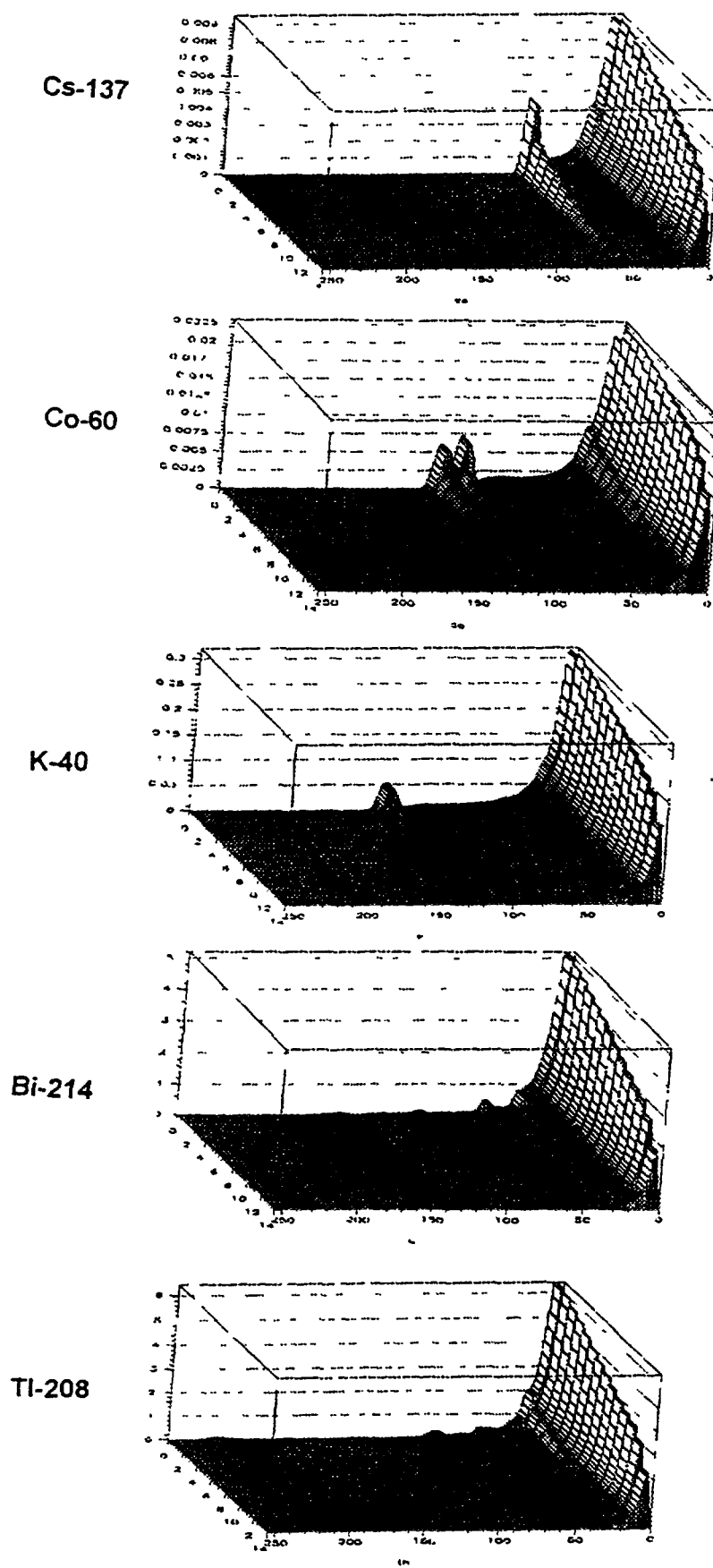


FIG 1 Altitude attenuation and energy distribution for Cs-137, Co-60, K-40, Bi-214, TL-208

6. CASE HISTORY

6.1. Ontario Hydro BRUCE Nuclear Power Plant

The Bruce NPP is a large complex with eight nuclear reactors, each in the range of 900 MW capacity. The site is located on the shore of Lake Huron, 150 km northeast of Toronto. In October 1995 Ontario Hydro and Picodas Group Inc. conducted a joint test to overfly and document the Bruce NPP and surrounding area.

Equipment:	ENMOS 2001 (256 channel spectrometer) GPS real time differential navigation system Radar Altimeter TRA 3000
Measured Energy range:	200 keV to 3 MeV in 256 channels above 3 MeV one channel
Altitude:	80 m above ground
Ground speed:	35 m/second
Aircraft:	Hydro Bell 206 Jet Ranger Helicopter
Line spacing:	inside NPP perimeter 75 m outside perimeter 150 m

Survey Procedures and Methodology

Due to bad weather conditions the survey was carried out in two time periods requiring two separate equipment installations. Each installation took approximately 1 to 2 hours and 30 minutes to remove the equipment.

The total survey time was about three working days with 16 hours of helicopter flight time to cover an area approximately 10×20 km or 200 km² with 1800 km of survey lines.

The survey area may be divided into three main parts.

- a) Inside perimeter of the NPP.
- b) Swampy belt approximately 1 to 2 km wide close to the lake shore.
- c) Agricultural inland area outside of the perimeter of the NPP.

Observations

- a) The inside perimeter of the Bruce NPP shows relatively low natural radiation. However there are small localities showing distinctive anomalies of man made radionuclides such as Cs-137 and Co-60. Some of those localities are exhibiting anomalies of natural radionuclides of U-238 (Ra-226) and Th-232.
- b) Because of the water content, the swampy belt shows substantially suppressed radiation levels and no anomalies are detected in this area.
- c) The agricultural (inland) area does not indicate any radiation generated from man made products. Natural radiation is affected mostly by the surface of the ground (plowed), vegetation and humidity. The highest "natural contamination" seen is the K-40. Observed variations of the K-40 contamination are caused by changes of ground moisture, vegetation and by fertilization of the fields.

Low energy (up to 3 MeV) radiation exposure (dosage rate) reaches maximum of 250 nSv/hr in the locality of the strongest anomaly inside the perimeter of the NPP. Most of the inside perimeter and all of the outside perimeter indicate the low levels of radiation reaching only approximately 40 nSv/hr.

The highest anomalies within the inside perimeter are composed approximately of:

Cs-137	29%
Co-60	26%
K-40	4%
U-238	30%
Th-232	11%

Collected data sets indicate that there is an increase of the high energy radiation (above 3 MeV) over the active nuclear reactors. This is caused by the N16 in the energy range of 4 and 6 MeV. It is estimated that the dosage rate related to the normal cosmic radiation is approximately 30–40 nSv/hr. Estimation of the additional dosage due to the high energy radiation above the reactors is the ratio of measured "cosmic rays" over normal terrain and the reactors. Additional dosage produced by the high energy radiation is in the order of 250 nSv/hr.

Relation of units

Absorbed dose 1 Gy = 1 Sv (dose equivalent) for quality factor Q = 1

Quality factor Q characterizes specific radiation. Further we assume the Q = 1.

Dose equivalent

1 Sv = 100 rem

1 uR/hr = 2.4139 pG/s

1 pG/s = 31.536 uG/year

1 pG/s = 3.6 nG/hr

1 uR/hr = 8.7 nG/hr = 0.0087 uG/hr

Natural exposure measured in dose equivalent is 3 to 10 μ R/hr (25 to 87 nSv/hr or 2.5 to 8.7 urem/hr), therefore all of the areas except for the anomalous locations are well within the normal natural radiation levels of less than 5 μ R/hr (45 nSv/hr or 4.5 urem/hr).

Normal limitation of absorbed dosage for humans is about 273 nSv/hr (2.4 mSv/year or 240 mrem/year).

List of anomalous locations

There are six detected locations with noticeable elevated Dose Rates:

three small locations (A-south, B, C-north) on south west shore of the N.P.D., one larger one (D) on the north shore of the N.P.D., one in the middle of the N.P.D. (E) and one in the south central location (F).

Notes: L.E.D. low energy dosage — up to 3 MeV

H.E.D. high energy dosage — above 3 MeV

backg = background

Location	L.E.D. nSv/hr	H.E.D. nSv/hr	Cs-137 Bq/m ²	Co-60 Bq/m ²	K-40 Bq/kg	U214 Bq/kg	Tl-208 Bq/kg
approximate (area specific)							
background	35	35	7000	1000	300	30	40
A	< 40	> 200	backg	< 2000		backg	backg
B	45	> 200	backg	> 2300		backg	> 30
C	54	backg	< 6000	> 1000		backg	> 40
D	72	> 200	> 10000	> 4500		backg	> 50
E	250	backg	> 22000	> 8000	backg	> 150	> 80
F	105	backg	> 31000	> 2400	backg	backg	backg

Relatively large contributions of H.E.D. to the total dosage *may not* be noticed at the ground level since the immediate dosage levels depend upon the heavy shielding of the reactor. Upwards shielding above the reactors is considerably less. The contribution to the ground dosage from the H.E.D. would be mostly through radiation scattering.

The Co-60 map exhibits substantial level of noise in the area of the outside perimeter. This corresponds to the model sensitivities calculated for Co-60. This could be considered an indirect verification of the air to ground model assumptions. All images of the data were overlaid on the aerial WGS84 calibrated photography.

6.2. Atom bomb blast measurements in Maralinga - Australia

World Geoscience Corporation Limited has recently flown the nuclear bomb test site last used in the 1950s. From images collected over this area it is obvious that the levels of radioactive contamination are still very high. It indicates that after forty years the isotropic model is becoming lambertian with a relaxation depth to about 15 cm. All data was overlaid on Spot satellite imagery.

6.3. Nuclear power plant in Slovakia

In 1992 a series of tests flights over a Slovakian Nuclear Power Plant were carried out. One area of the power plant shows substantial increased levels of radiation. To better delineate areas of interest the data was overlaid on Spot satellite imagery.

6.4. Uranium mining area in Germany

In 1994 a pilot project was conducted over an old uranium mining area near Gera in Germany. Increased Uranium contamination was detected and it is directly related to previously known mining activities.

7. CONCLUSIONS

- Detection sensitivities of the demonstrated system are adequate for the altitudes of operation under 90 m. Portability allows for rapid engagement and disengagement of the system. It is possible that the system may be used not only for new measurements, but also for calibration of older, regionally collected data by other airborne multichannel instruments to recalculate the pulses per second or ppms to absolute physical units.
- As is evident from the observed results, a reliable dosage based map (footprint) over any nuclear facility can now be produced rapidly and at a reasonable cost.
- There is a considerable value in having a comprehensive regional background radiation footprint, which provides the basis for environmental assessment and can assist in directing future emergency planning.

ACKNOWLEDGEMENT

Picodas Group would like to express thanks to Ontario Hydro for the support and help to test this new monitoring technology in North America. At the same time we would like to express our thanks and appreciation to all government agencies and private companies who helped and allowed us to acquire extremely valuable data sets worldwide.

BIBLIOGRAPHY

CECHAK, T., KLUSON, J., MALUSEK, A., Spectra Processing in Airborne Gamma-Ray Spectrometry Using the ENMOS Detection System, Technical University of Prague, Faculty of nuclear Engineering, Department of Dosimetry (May 1994).

DEPT. OF PRIMARY INDUSTRIES AND ENERGY, Rehabilitation of Former Nuclear Test Sites in Australia, IRAP-M Report, REF 0-4399-M-15

KLUSON, J., Calculation of the field spectrometer response and calibration for the operational and accidental monitoring of nuclear power plant neighbourhood, Progress in Nuclear Energy, Vol.24 (1990).

KRTEN, O.J., Relating Airborne Detector Response to Ground Gamma Activity, Report for Picodas Group 9 (1993).

KRTEN, O.J., Relating Airborne Detector to Ground Gamma Activity, Report for Picodas Group 2 (1996).

PAVLIK, B., New Instrumentation for Airborne or Truckborne nuclear pollution surveillance

**NEXT PAGE(S)
left BLANK**



ENVIRONMENTAL MONITORING SYSTEM BASED ON AIRBORNE GAMMA RAY SPECTROMETRY DEVELOPED AT GEOINSTITUT BEOGRAD

M. MILOJEVIĆ, V. ŠTRUMBERGER
Geoinstitut, Beograd.
Belgrade, Yugoslavia

Abstract

The continuous hazard of nuclear reactor failures, which may exceed in consequences that of the Chernobyl accident on 26 April 1986, makes it imperative for us to develop and introduce soil, water and air contamination control systems to protect the environment. A most efficient means of the contamination control at the artificial radioactive radiation sources is the complex MONITORING SYSTEM controlled from a centre by competent and recognised experts. Such systems have been used for years now many western world countries (USA, Canada, Sweden, etc.). The modest purpose of this paper is at least to leave a trace of the efforts, both individual and of the institute, made in developing a component of the monitoring system — airborne gamma-ray contamination control, which in western systems is a principal technique of remote detection.

1. INTRODUCTION

For the control and protection of a state against the artificial fission products, three equally important control systems should be established.

First, the system is based on the operation of automatic radioactivity level recorders. This system includes a number of instruments installed in the expected directions of radiodebris cloud approach. The information is radiotransmitted automatically to the main control centre.

Second, the control system is operated on analytical airborne survey data of soil radioactivity, during or immediately after contamination of large areas of the national territory. The purpose of the survey is to establish soonest possible the regional, provincial or national contamination data. At this stage of monitoring, the use of a multichannel gamma spectrometer is necessary which analyses the gamma-ray energy within the interval from 0 to 3000 KeV.

Third, the control system is organised on ground with the direction clearly defined on the former two system results. The direction is always to be the highest-hazard region with the greatest human, animal and vegetative populations.

In order to test the airborne survey techniques, a survey to determine the level of soil contamination, size, type, nature and amount of decay radionuclides was carried out. The results will be presented in this paper. The pilot area was 200 km² in size,. Surveying was carried out on a parallel grid with a total length of 1000 km of flight lines. The aircraft used was an AN-2. The flight altitude was 100–150 m above the ground.

The specific area was selected for the announced possible fallout of artificial fission isotopes, not only of Chernobyl origin. The expected "surface" contamination in the area was by cesium-137 and -134. The only expected point sources were europium 152/154 and cobalt 60, which are incorporated in radioactive lightning conductors.

2. A CONCEPT OF THE ARTIFICIAL RADIOACTIVE ISOTOPE DETECTION ON GROUND SURFACE

The possible detection of artificial radioactive isotopes on the surface is based, for the explorers, on suitable characteristics of their energy gamma radiation. Almost all radionuclides

produced in fission reactions are characterised by emissions of gamma photon energies up to 1000 KeV. In a registered 256-channel spectrum they are in the group of "low" energies. On this fact are based many methodological techniques for detecting the presence of artificial gamma-ray emitters. The physical aspect will be explained through the analysis of Fig. 1.

If an aircraft, equipped with an airborne gamma-ray spectrometer, flies the path ABC (Fig. 1a), and if the gamma radiation emitted from the ground is measured each second from a height of 150 m, a spectrum would be recorded in points A, B and C. Let points A and C be granitic rocks, which naturally possess an increased concentration of naturally radioactive potassium, uranium and thorium or their decay products, and let point B contain artificial radioactive isotopes produced by fission in a nuclear reactor. The radiation spectrum measurement results, already on the analog record (Fig. 1b), will show the presence of three anomalies, or increased intensities of gamma radiation, in points A, B and C.

The nature of an increased radiation emitter can be determined in general terms by analysis of the digital record of the gamma-ray energy spectrum and design of the spectrum (Fig. 1d). A natural source of gamma radiation will give a spectrum as those shown for points A and C. The spectrum for point B is distorted by the presence of an artificial gamma-ray emitter of "low" energies between 0 and 1000 KeV.

This step of the data analysis alone allows, by drawing each spectrum, to pinpoint qualitatively the discrete points where sources of artificial gamma radiation are manifested. This, however, is a time-consuming technique for the computer. Therefore a more elegant data analysis was used, reduced to the calculation of ratio of "low" and "high" energy sums for each singly recorded gamma-ray spectrum.

The idea is essentially the following: Both theoretically and empirically it was determined that for natural gamma-ray spectra without the effect of artificial isotopes, the ration "low" (300–900 KeV) and "high" (900–1500 KeV) energy sums is a value between 3 and 3.3. Any added artificial source of fission gamma radiation disturbs the ratio, causes its anomaly from the increased gamma radiation intensity within the "low" energy domain (Fig. 1e). The described technique was one of the departing points for construction algorithm "Ecology".

3. ALGORITHM ECOLOGY

The algorithm named Ecology (Fig. 2) served as a guide to develop all procedures under The Project of Developing AGS Application Methods in Environmental Control. It is designed on the basis of the available theoretical knowledge, data from the available literature on identical systems in the United States [2], Canada [1] and Sweden [5] and represents the approach in this country to the problem.

The algorithm clearly defines each information to be registered in AGS for the set goal, which is the nonambiguous answers to the following questions:

- Is there any artificial radioactive source?
- How large an area has been contaminated?
- What is the contamination level?

An one-second digital record was designed that contained a series of relevant data. The record of 751 bytes included information on time, date, flight line number, fiducial number, ordinal number of the record, aircraft altitude, gamma radiation from the ground, and from the air, etc. Additional data planned for use included analog records, photographs, topographic and geological maps.

It has been established, and algorithm designed, that the minimum required data could be fitted into a record of 512 bytes, which formed the initial GAMMASPEC file, now on a large computer disk (VAX-9000).

GAMMASPEC is a data file for analysis of nature, type and intensity of gamma radiation. From it two files are formed. One, comprising data on intensity of gamma radiation from natural elements (potassium, uranium and thorium), is named NATURAL GAMMA RADIATION (NGR), composed of records, each of 51 bytes. This file will not be considered here as it does not involve the selected subject of the study. Another file, named ARTIFICIAL GAMMA RADIATION (AGR), contains information on artificial radioactive isotope gamma radiation intensities. The length of the AGR record is 108 bytes

3.1 Artificial Gamma Radiation File Analysis

Environmental studies of contamination from artificial radioactive sources require a reliable definition of two kinds of information. One information is the clearly identified parameters indicating the presence of point, or individual, sources of artificial gamma radiation. The other will serve to determine the surface distribution of artificial radioactive sources

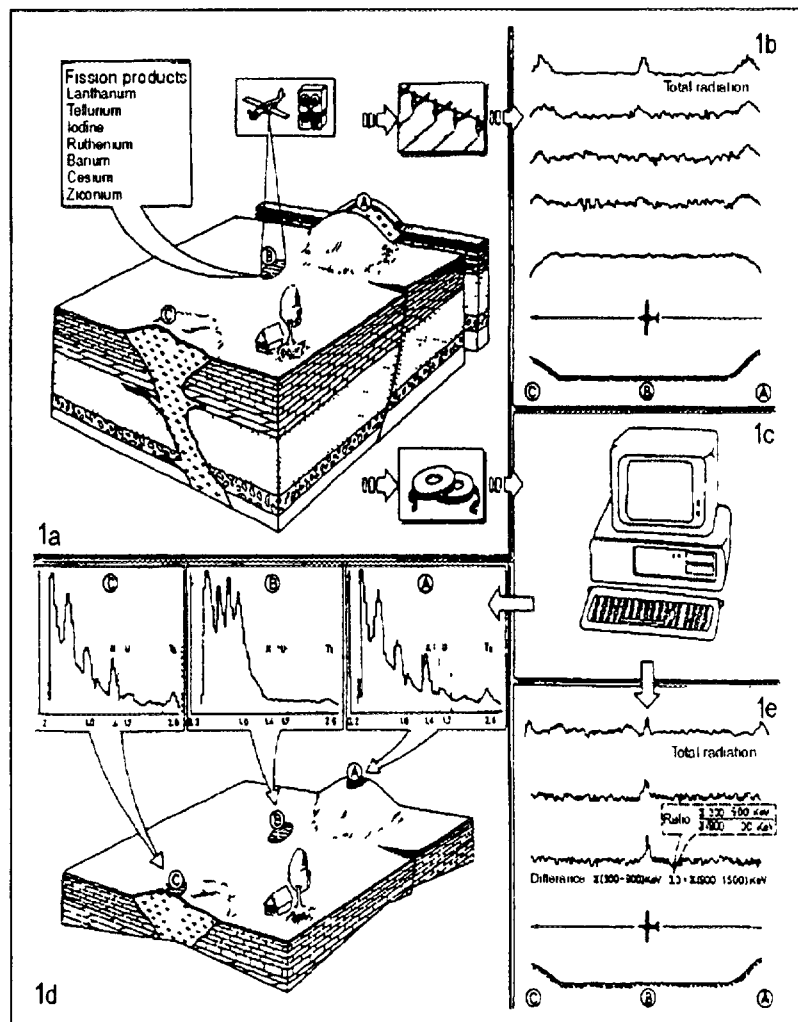


FIG. 1 Airborne detection of artificial gamma ray emitter.

ALGORITHM "ECOLOGY"

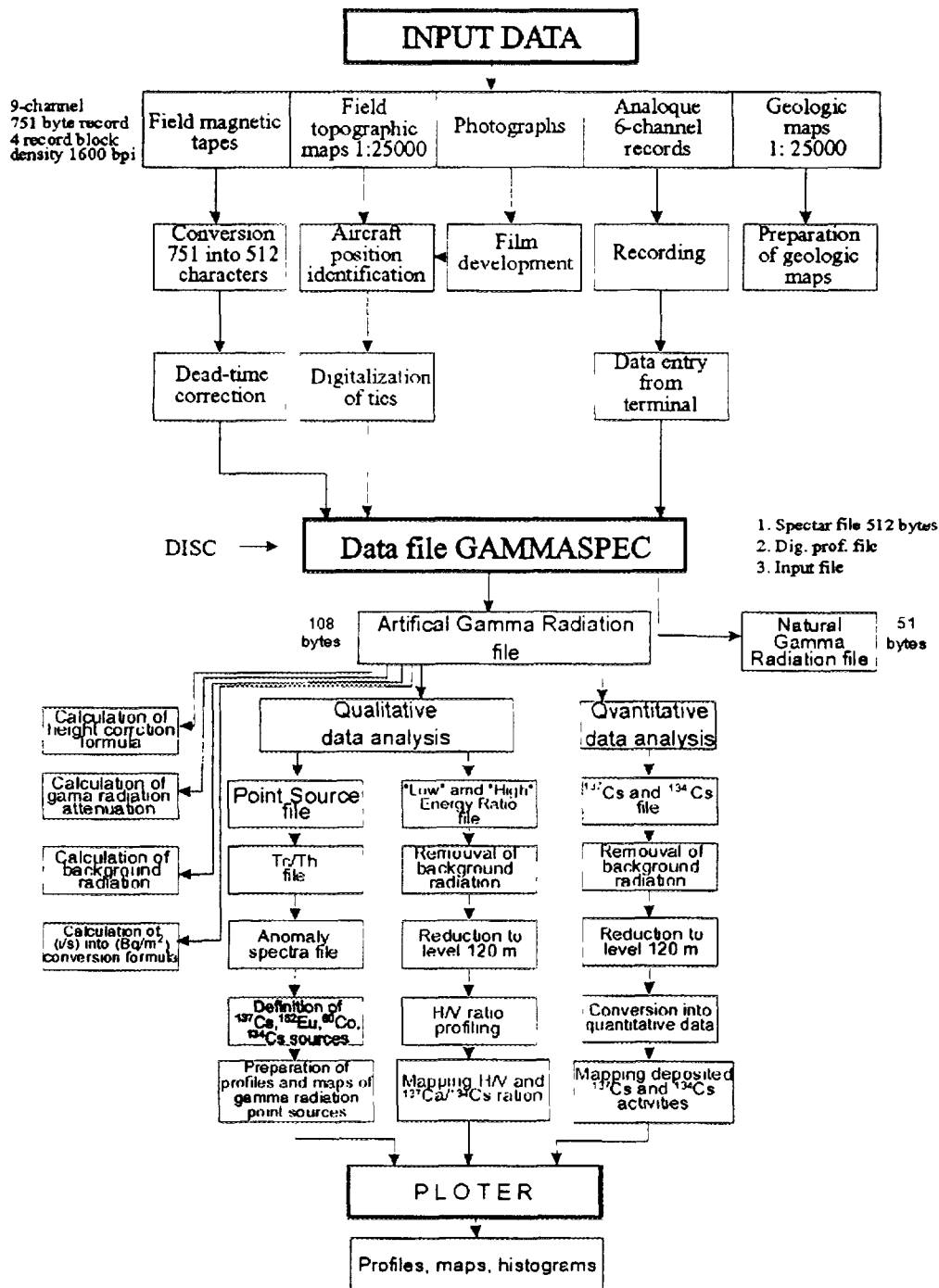


FIG. 2. Algorithm "Ecology".

From the above information, two more types of analytical data can be derived. One is **qualitative** analysis which gives answer to the question: Is there any artificial source of radioactivity? The other is **quantitative** which answers the questions: How large is the contaminated area? and What is the activity of deposited radioactive sources that contaminated the areas?

For the purpose of both analyses, the algorithm anticipates three separate data files: POINT sources, RATIO, and CESIUM 137 and 134. The former two are used to identify the presence of POINT artificial radiation sources.

Point or individual sources have been known to occur by specific accidents which have not resulted in large-scale contamination. An example is the fall of the Soviet nuclear-powered satellite KOSMOS 954 [1]. This required development of specific detection techniques for numerous artificial point radiation sources, as has been earlier explained.

Figure 3 shows all windows for calculation of (L/H) ratios of "low" and "high" energy sums necessary for location of discrete gamma radiation anomalies caused by the artificial sources. The "L/H" ratio is not appreciable for urban centres in Serbia because of the high presence of europium 152, incorporated in lightning conductors.

Any presence of artificial radioactive sources is always recorded in the energy range 200–3000 KeV and never in the energy range 2400–3000 KeV. For this reason, the Algorithm anticipated calculation of TC (200–3000 KeV) and Th (2400–2000 KeV) energy sum ratio (TC/Th).

The following step in the Algorithm development was identification of gamma energy spectra for each anomalous TC/Th ratio. The cause of the anomaly was found visually on the monitor or drawn on the plotter, as in Figs. 4, 5 and 6; The identified causes were Eu-152, Co-60, Cs-137 and Cs-134.

In the described way, on a qualitative level, the presence was identified of discrete artificial gamma radiation anomalies, their causes and, additionally, coordinates of their position on the ground were determined. Qualitative information may suffice to attain some of the goals, This particularly refers to detection of a single artificial point radioactive source, its location and identification in the field.

For environmental control and protection of the population, the data must be quantitatively analysed. The Algorithm Ecology includes a data file of records from Cs-137 and Cs-134 energy windows (Fig. 3). The most delicate step in this stage of AGS data analysis is the conversion of

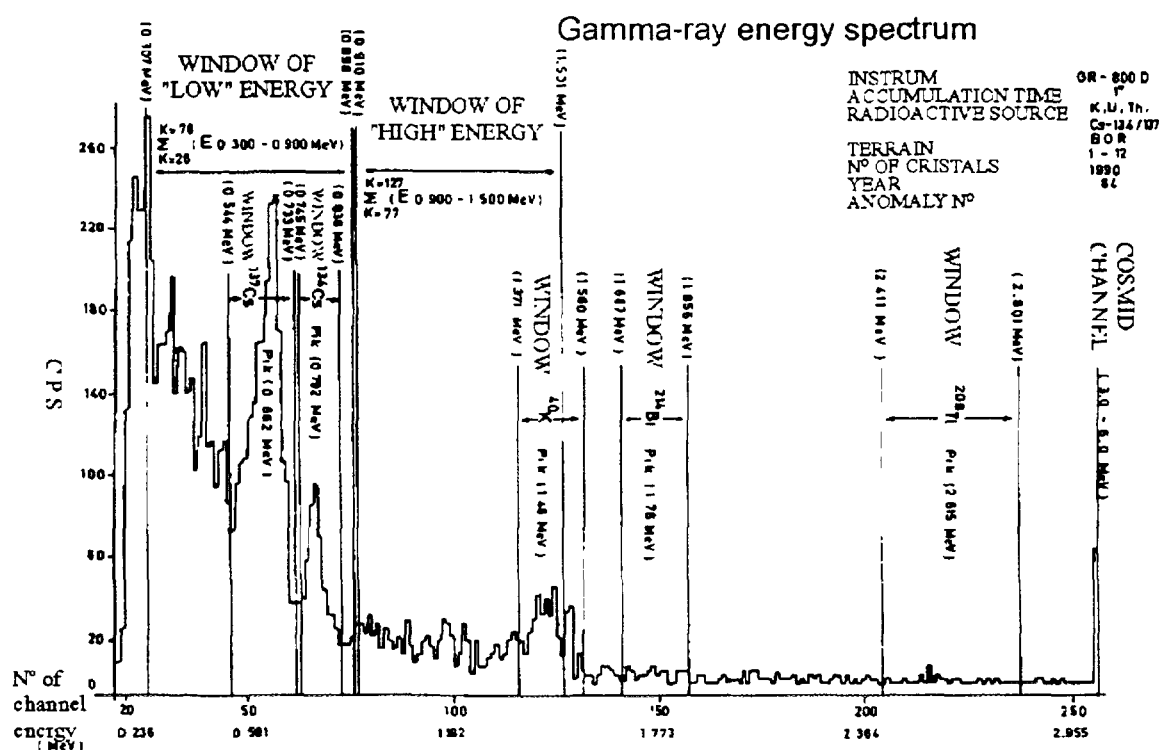


FIG. 3. Gamma ray energy spectrum.

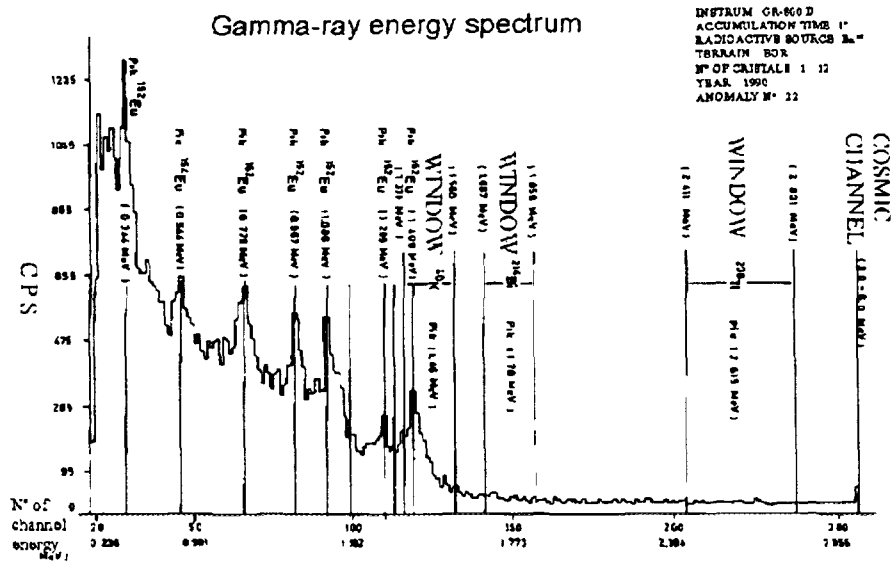


FIG. 4. Gamma ray energy spectrum, Eu-152.

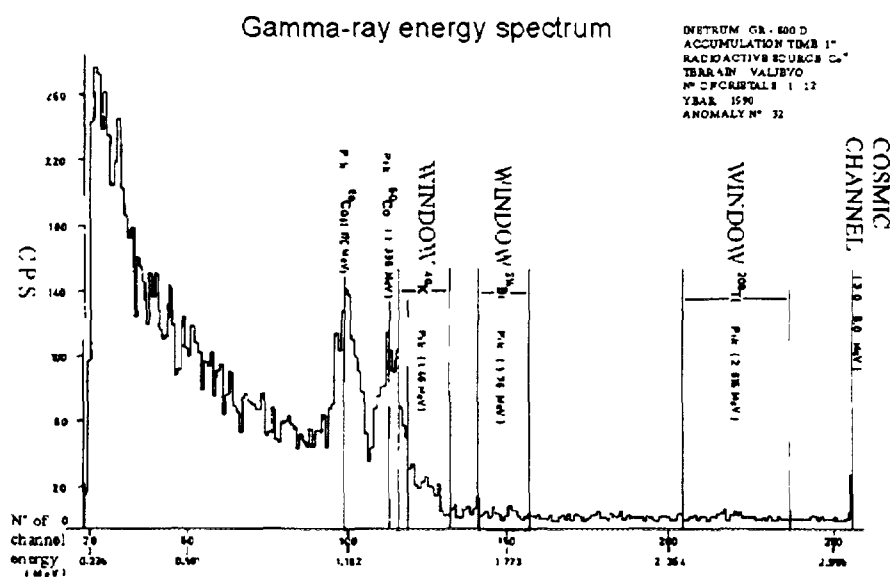


FIG. 5. Gamma ray energy spectrum, Co-60.

corrected gamma radiation recorded in Cs-137 and Cs-134 energy windows, expressed in the number of counts measured per second (cps), into deposited Cs-137 and Cs-134 activities, expressed in becquerel per square metre (Bq/m²).

Conversion factors are determined on diagrams of AGS data conversion (Fig. 7), with the abscissas showing plotted values of recorded Cs-137 and Cs-134 gamma-ray intensities reduced to the level of 120 m above the control profile surfaces, and the ordinates values of deposited Cs-137 and Cs-134 activities in soil samples from the same control profiles.

The relation between the deposited Cs-137 and Cs-134 activities and the number of recorded counts is linear and it is not difficult to develop analytical relation of the line expressing the

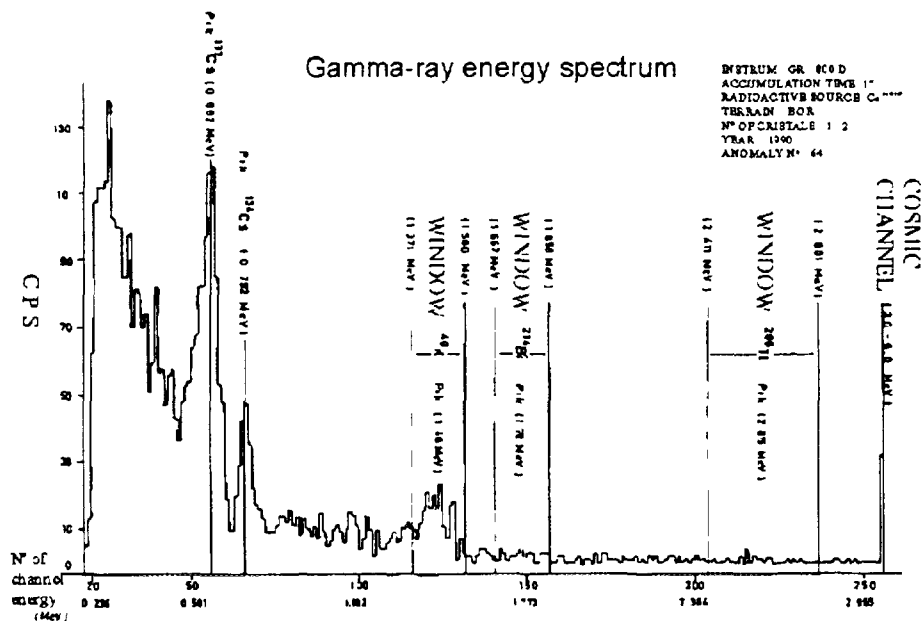


FIG. 6. Gamma ray energy spectrum, Cs-137 and Cs-134.

correlation of gamma radiation activity and intensity in a point. Constants for Cs-137 and Cs-134 allow the conversion of data into the deposited activity and the preparation of maps showing qualitative analytical results.

The concept of Algorithm Ecology and the package of computer was tested over an area of the Bor District. The test results will be presented in the following text section.

4. DETERMINING NATURAL K, U AND Th CONTRIBUTIONS IN THE "LOW" ENERGY SPECTRAL COMPONENT

A problem in routine procedure of using airborne gamma spectrometry results to detect ground contamination by radioactive isotopes — artificial gamma-ray emitters — is separating the components of man-made and natural gamma-ray spectrum. Two mathematical procedures have been developed. One is named the **correlation technique** and the other **factor analysis**. Both techniques are based on experimental results obtained on concrete slabs at Grand Junction in 1981 [4 and 6].

Experimental studies, in laboratory, and field surveys, from airplane or helicopter, have shown that a natural gamma-ray spectrum, recorded by NaI (TI) detectors, varies in shape with altitude from which it was recorded. The spectral variations were determined in the function of the amount of absorbing material (air) between the gamma-ray emitter and the detector. Practically, the variations were established by flying at different altitudes over three different areas with the prevailing concentration of uranium or thorium or potassium. Identical results, even representative ones, were acquired using concrete calibration slabs.

Because calibration slabs eliminate many effects normally present in the field, such as from artificial gamma-ray emitters, inaccurate attitude of aircraft, airborne radioactive gas around the aircraft, etc., specialists decided to develop a technique of separating natural and man-made spectral components using calibration slabs for spectral measurements. The material used in the experiment were 2.4×2.4 m plywood sheets each an inch (2.54 cm) thick to simulate by their number the air density (from 0 to 112 m) between the flying aircraft and ground surface. It is worth mentioning to

the reader that the author of this article, while specializing in Canada, was a part of the team which conducted a similar experiment where a helicopter (Hudson Bay Oil and Gas) AGS system was used at the Calgary University Center.

Radioactivity rates of a terrain contaminated by artificial isotopes recorded in Cs-137 and Cs-134 energy windows are burdened by the effects of natural gamma-ray emitters. If measurement results are to be used in the control of the entire human, vegetative and animal environment, accurate information is required separately on the natural and the artificial radioactivity components.

This was the purpose of the mentioned experiment which resulted in nine gamma-ray spectra for altitudes from 0 to 112 m for each calibration pad, with altitude increments of 14 m (Fig. 8). The fourth calibration pad was used for the background radiation.

AGS data conversion into deposited Cs-137 and Cs-134

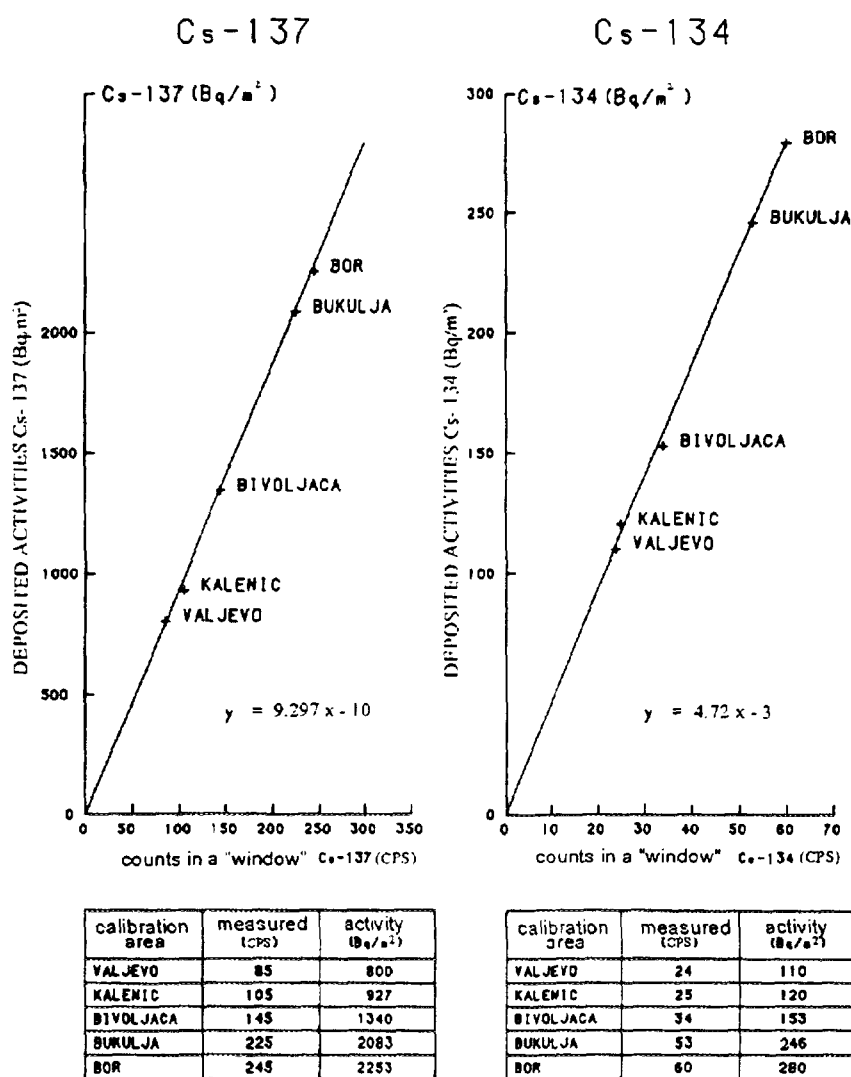


FIG. 7. AGS data conversion for Cs-137 and Cs-134.

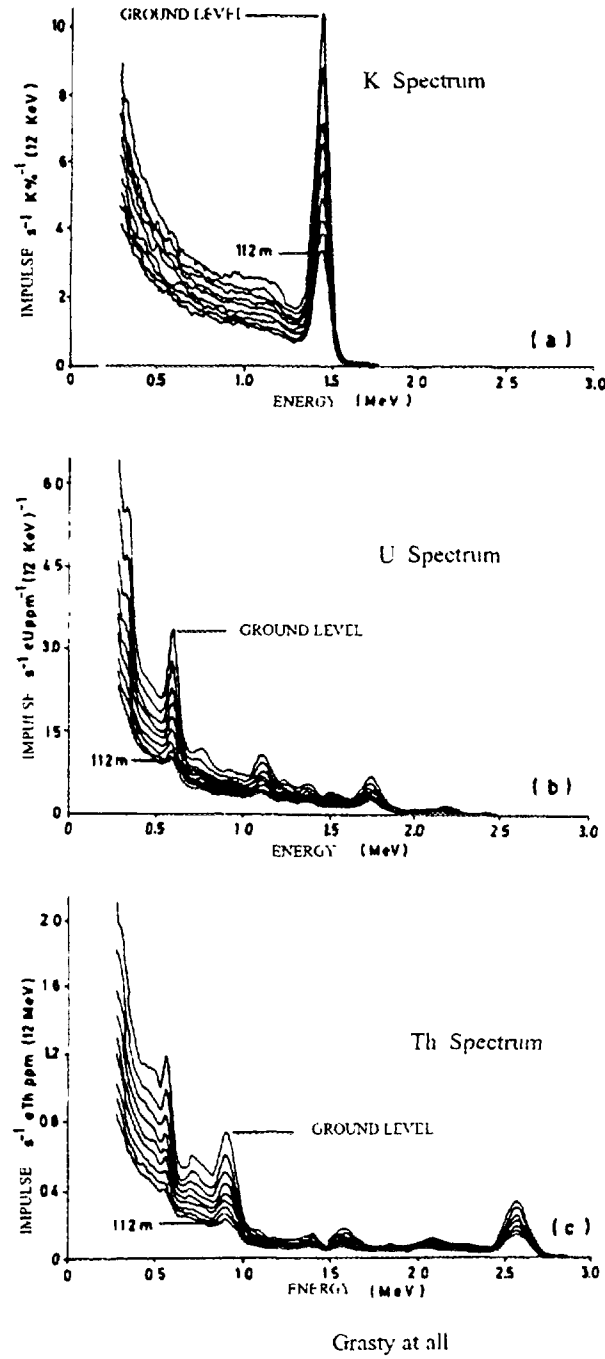


FIG. 8. Gama ray spectra for deposited K, U, Th.

Digital record of counts provided for calculation of the factor of natural gamma-ray contribution in each spectral channel (a_1 ; a_2 ; a_3) by correlation or linear regression procedure, based on a matrix for a system of three linear equations with three unknowns. Assume that records from Cs-137 and Cs-134 windows, with the detector on potassium, uranium or thorium pad, are designated (RCs_k , RCs_u , RCs_t) respectively, and records from potassium, uranium and thorium windows (K_k , U_k , T_k), (K_u , U_u , T_u) and (K_t , U_t , T_t), the relations can be written as:

$$RCs_k = a_1 K_k + a_2 U_k + a_3 T_k + BR \quad (1)$$

$$RCs_u = a_1 K_u + a_2 U_u + a_3 T_u + BR \quad (2)$$

$$RCs_t = a_1 K_t + a_2 U_t + a_3 T_t + BR \quad (3)$$

where BR is background radiation subtracted from each spectral channel data.

The presented relation can be written as a matrix, assuming preliminary elimination of background radiation (BR):

$$\begin{vmatrix} RCs_k \\ RCs_u \\ RCs_t \end{vmatrix} = \begin{vmatrix} K_k & U_k & T_k \\ K_u & U_u & T_u \\ K_t & U_t & T_t \end{vmatrix} * \begin{vmatrix} a_1 \\ a_2 \\ a_3 \end{vmatrix} \quad (4)$$

The general form of the matrix is the following:

$$| A | = | B | * | X | \quad (5)$$

where from follows:

$$| X | = | B |^{-1} * | A | \quad (6)$$

Developing matrix from equation (6) it follows:

$$\begin{vmatrix} a_1 \\ a_2 \\ a_3 \end{vmatrix} = \begin{vmatrix} K_k & U_k & T_k \\ K_u & U_u & T_u \\ K_t & U_t & T_t \end{vmatrix}^{-1} * \begin{vmatrix} RCs_k \\ RCs_u \\ RCs_t \end{vmatrix} \quad (7)$$

because the inverse matrix $(B)^{-1}$ reads:

$$| B |^{-1} = \begin{vmatrix} A_{11} & A_{21} & A_{31} \\ A_{12} & A_{22} & A_{32} \\ A_{13} & A_{23} & A_{33} \end{vmatrix} \quad (8)$$

and matrix , or from:

$$| A | = \begin{vmatrix} b_{11} & 0 \\ 0 & b_{21} & 0 \\ 0 & b_{31} & 0 \\ 0 & 0 & 0 \end{vmatrix} ; \text{ and } | X | = \begin{vmatrix} a_{11} & 0 & 0 \\ a_{21} & 0 & 0 \\ 0 & 0 & 0 \\ a_{31} & 0 & 0 \end{vmatrix}$$

Terms b_{12} , b_{13} , b_{22} , b_{23} , b_{32} , b_{33} , a_{12} , a_{13} , a_{22} , a_{23} , a_{32} , and a_{33} are equal to zero, and the solutions are reduced to the general formulas:

$$a_{ij} = A_{i1}b_{1j} + A_{i2}b_{2j} + A_{i3}b_{3j} \quad (9)$$

where from follows the problem solutions:

$$a_1 = A_{11}RCs_k + A_{12}RCs_u + A_{13}RCs_t \quad (10)$$

$$a_2 = A_{21}RCs_k + A_{22}RCs_u + A_{23}RCs_t \quad (11)$$

$$a_3 = A_{31}RCs_k + A_{32}RCs_u + A_{33}RCs_t \quad (12)$$

Relations (10, 11, 12) give final solutions for factors (a_1 , a_2 , a_3) which provide for assessment of natural radioactive emitter contributions (K, U, Th) in CS-137 and Cs-134 energy windows.

Since there are no concrete calibration pads in Yugoslavia, and because the described experiment was performed with gamma radiation detectors and a spectrometer of identical characteristics as those used in all surveys in Yugoslavia, the experimentally obtained spectra were used to calculate constants of the type (a_1 , a_2 , a_3) applied in the survey of a part of Timok magmatic

complex (TMC). The technique was tested first on one spectrum — anomaly A-64, and then on all recorded spectra.

The procedure to determine coefficients expressing the natural gamma-ray emitter contributions recorded in potassium, uranium and thorium energy windows to the "low" energy (250–1000 KeV) spectral components, has been developed in Geoinstitut on the ALGORITHM named EFFECT.

The algorithm was based on preceding digitalization of nine spectral diagrams of gamma radiation recorded on potassium, uranium and thorium pads [4 and 6]. Spectra were recorded for simulated altitudes, on the principle described in the preceding section, of 0 m, 14 m, 28 m, 42 m, 56 m, 70 m, 84 m, 98 m, and 112 m. Only summarized K-40, U-238, and Th-232 gamma-ray window records from these spectra's are presented in Fig. 9. The data, however, were used to graphically relate sums of gamma radiation records in the mentioned windows to simulated altitudes. Gamma radiation values were read from the graphs, for selected altitude, and used to develop the matrix by equations (1–12).

In the analysis of anomaly A-64 (Fig. 6), mathematical operations were preceded by subtraction of the background radiation (BR) recorded during a flight over the river Danube at an altitude of 20 m. In this case we handled data representing the sum of natural and artificial gamma radiation for the selected altitude. As mentioned, it was decided to take altitude 112 m for the measuring data reduction level because it was closest to the actual aircraft altitude during the experiment in TMS, that is an area of the Bor District.

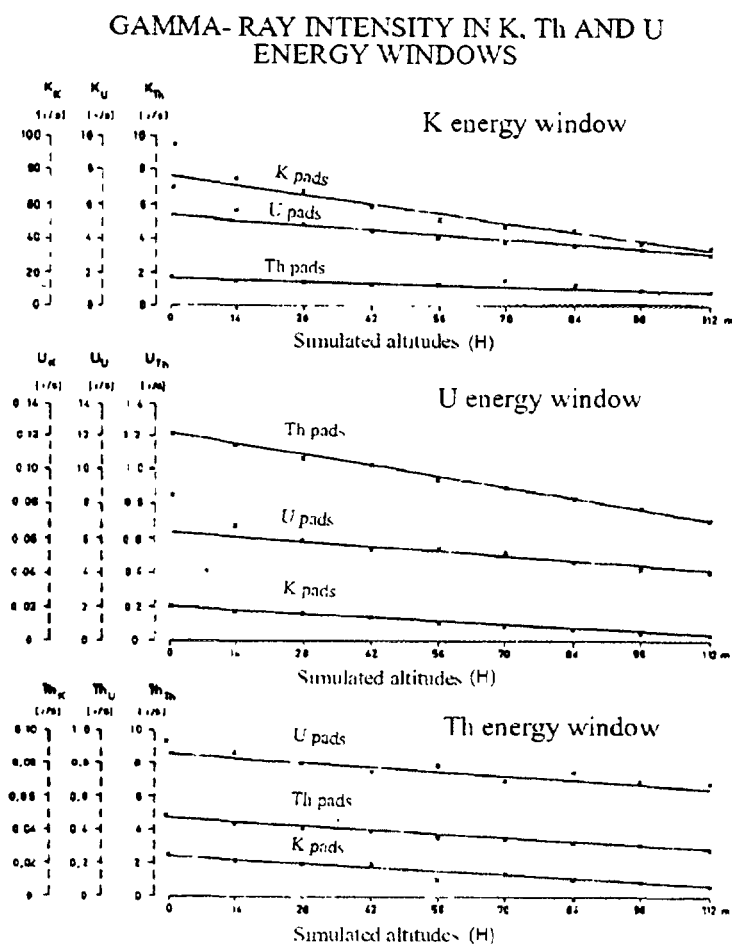


FIG. 9. Gamma ray intensity in K, Th and U energy windows.

The procedure is presented in this paper for estimation of the artificial gamma radiation contribution by the correlation technique is based on separation of two gamma ray spectral components, one natural recorded in AGS survey and the other caused by artificial radioactive isotope produced by fission. The described correlation technique, on the principle of natural radioactive sources of gamma rays (potassium, uranium, thorium) determined in each channel of the measured gamma-ray spectra in low-energy region (0–1000 KeV), gives the component, or spectrum, of natural emitters which is subtracted from the measured spectral values. Thus, the subtraction difference is the component caused by artificial isotopes, of fission derivation, which primarily originate from the Chernobyl accident.

5. EXPERIMENTAL SURVEY RESULTS

The background knowledge for the experiment were international experiences, the Chernobyl accident, and AGS geological exploration results from 1982–1988 for the Timok magmatic rock complex. It was presumed that all radioactive lightning conductors, with europium-152, were a good example of point artificial gamma radiation sources.

For analysis of the recorded gamma energy spectra a VAX-9000 computer was used. Single anomaly points which indicated the presence of gamma radiation from artificial emitters were located from TC/Th ratios. A total of 412 anomalous points were identified in the survey area, all artificial (Fig. 11).

Graphical presentation of all 412 spectra revealed two types of emitters, one europium-152 (Fig. 4) and the other cesium-137 and cesium-134 (Fig. 6). Particularly important for development of the methodological procedure of AGS application in environmental control and protection was the recorded spectrum 64 (Fig. 6).

Size of the area contaminated from artificial sources was determined from a map of ratios of "low" and "high" energies of gamma radiation (Fig. 12).

Mapping Cs-137 and Cs-134 activities (Figs. 13 and 14) indicated surface contamination spreading from Bor westward, on which the magnitude and direction of contamination were identified. The map of Cs-134 contamination (Fig. 14) clearly shows locations of lightning conductors with Eu-152/154, where the 779 KeV peak falls within the Cs-134 energy window.

The time of contamination and the origin of the gamma radiation source could be deduced from the map of Cs-137/Cs-134 ratios of gamma radiation intensity sums (Fig. 15) using also Fig. 16. From the calculated values, given in Fig. 16, and values $\text{Cs-137/Cs-134} = 7$ to 9 we have concluded that the identified contamination Northwest of Bor, 100 km² in size, occurred four years earlier, at the time of the Chernobyl accident.

Our analyses led to two likely explanations on the origin of the radioactive material that contaminated the area. The first possibility is contamination by radioactive material from Kozlodui, which occurred two or three years before the survey of 1990, and not more than one year after the Chernobyl accident. In this case, the radioactive material must have had the initial Cs-137/Cs-134 ratio equal to 1.7 to 2, and the area Southeast of Bor was not preliminary contaminated.

The other explanation is an almost synchronous contamination with that related to Chernobyl reactor failure. It affected the entire survey area, and was emitted by artificial radioactive isotopes from a nuclear-fuel which was used full time in nuclear reactors; the Cs-137/Cs-134 ratio was 1 at the end of the firing cycle in those reactors. In this case, four years after the likely contamination by such a fuel, the ratio would reach a value of about 4 (Fig. 16). The explanation is obviously non-unique. The available information only suggests new questions which can be answered through accurate analysis of samples from the contaminated ground, but this is beyond the scope of the

objective of developing the airborne environmental control of contamination from artificial fission gamma-ray emitters.

The following stage of data processing was selection of quantitative data necessary for final estimates of the contamination hazard of a threatened area. Laboratory assays were used in drawing

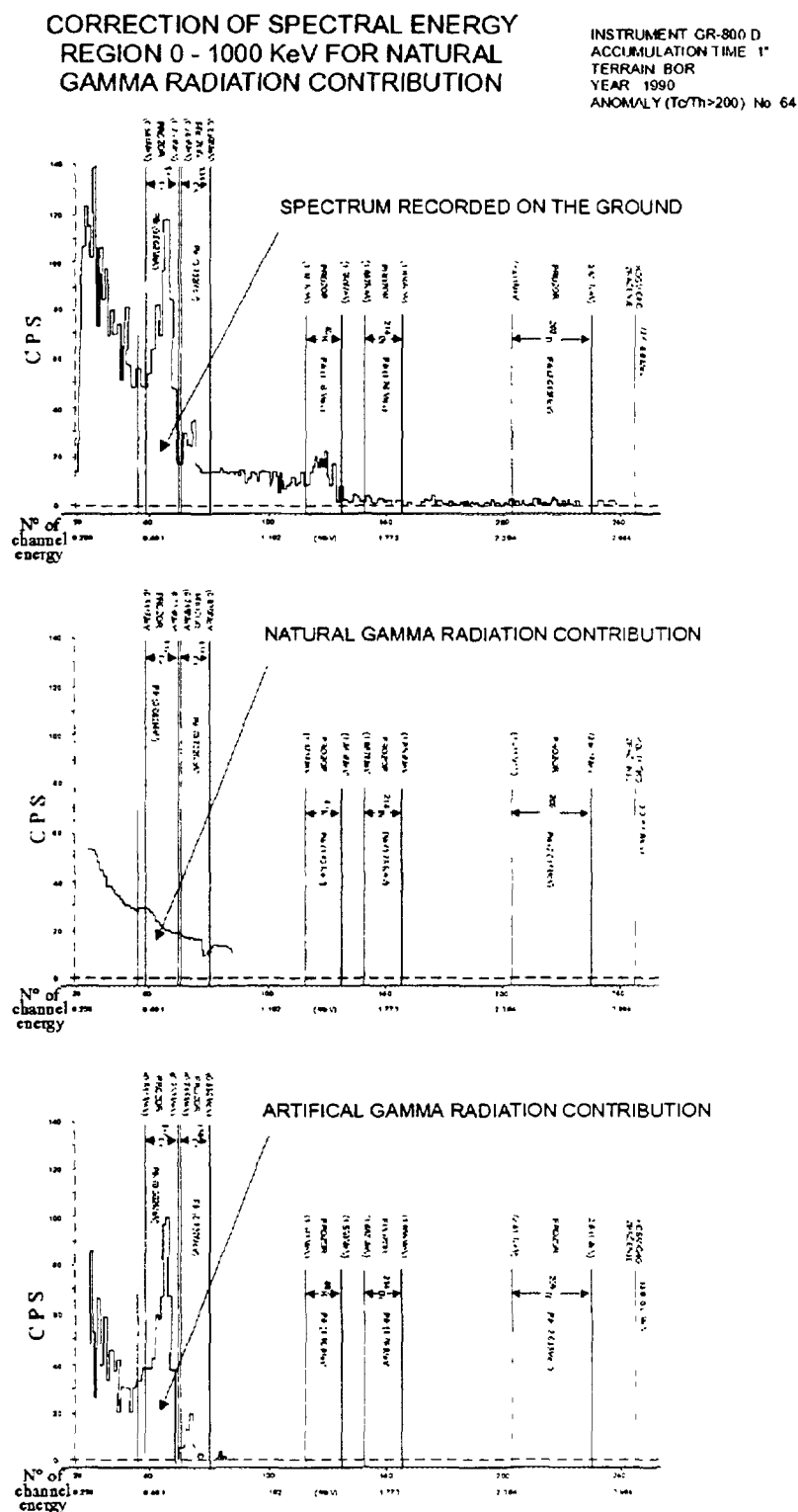


FIG. 10. Correction for spectral energy region 0-1000 KeV for natural gamma radiation contribution.

dependence diagrams of recorded, or corrected and processed, data on the content of natural and artificial radioactive elements in the ground. It was assumed that the dependence could be analytically expressed by a linear equation.

The map of deposited Cs-137 activity (Fig. 13) reflects the fact that a large part (about 100 km²) of the survey area is contaminated mainly with cesium-137. The quantity of the amounts deposited varies from 1500 Bq/m² to 3000 Bq/m². The contaminated area is a part of the surveyed surface located NW of the town of Bor and extending to Crni Vrh hill in the same direction. It is clearly separated by the Brestovačka Banja-Bor-Krivelj limit from the south-eastern part of the explored area where the deposited activity level is lower, below 500 Bq/m².

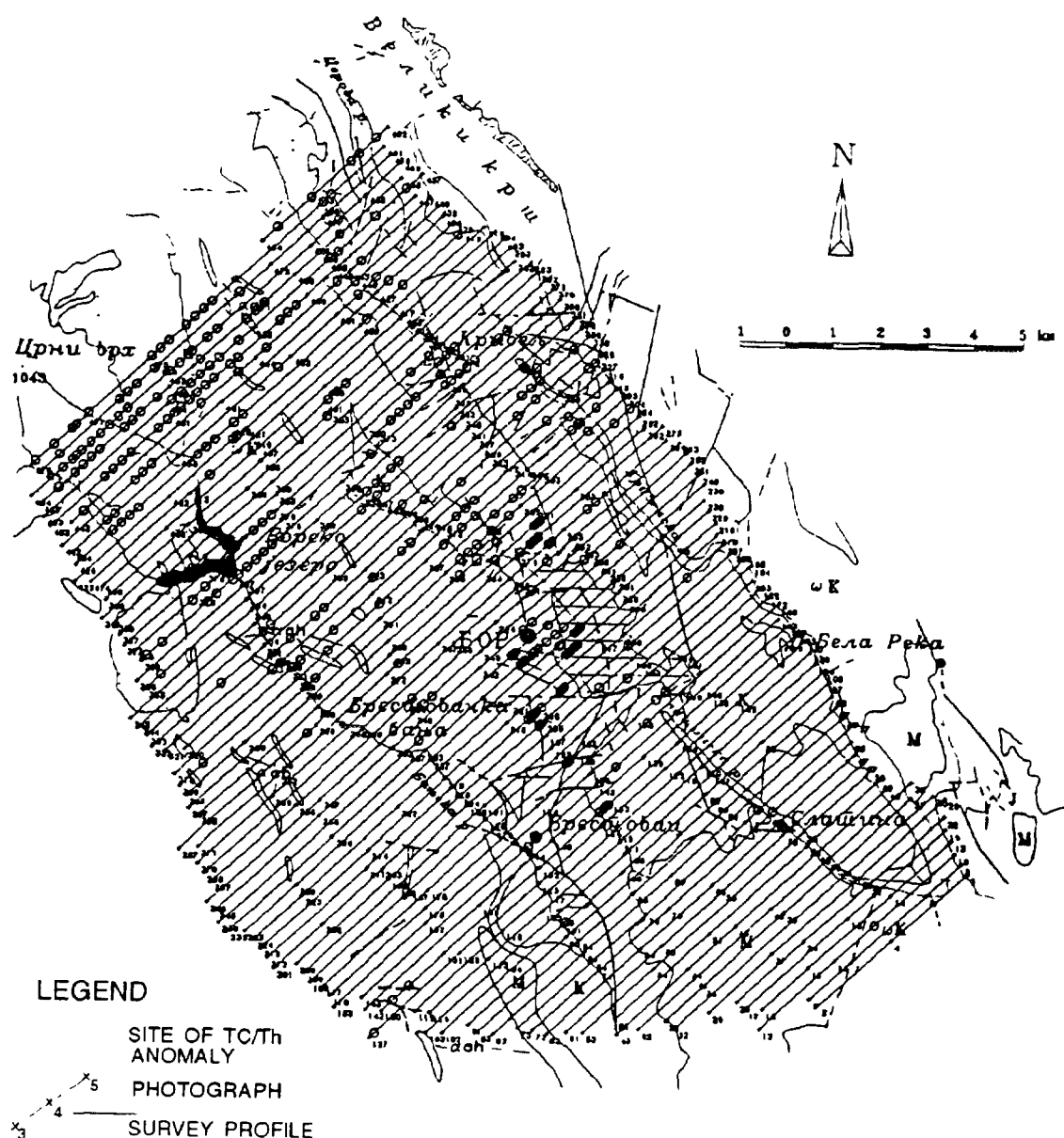


FIG. 11. Map showing locations of artificial point radioactive emitters — TC/Th > 100 anomalies.

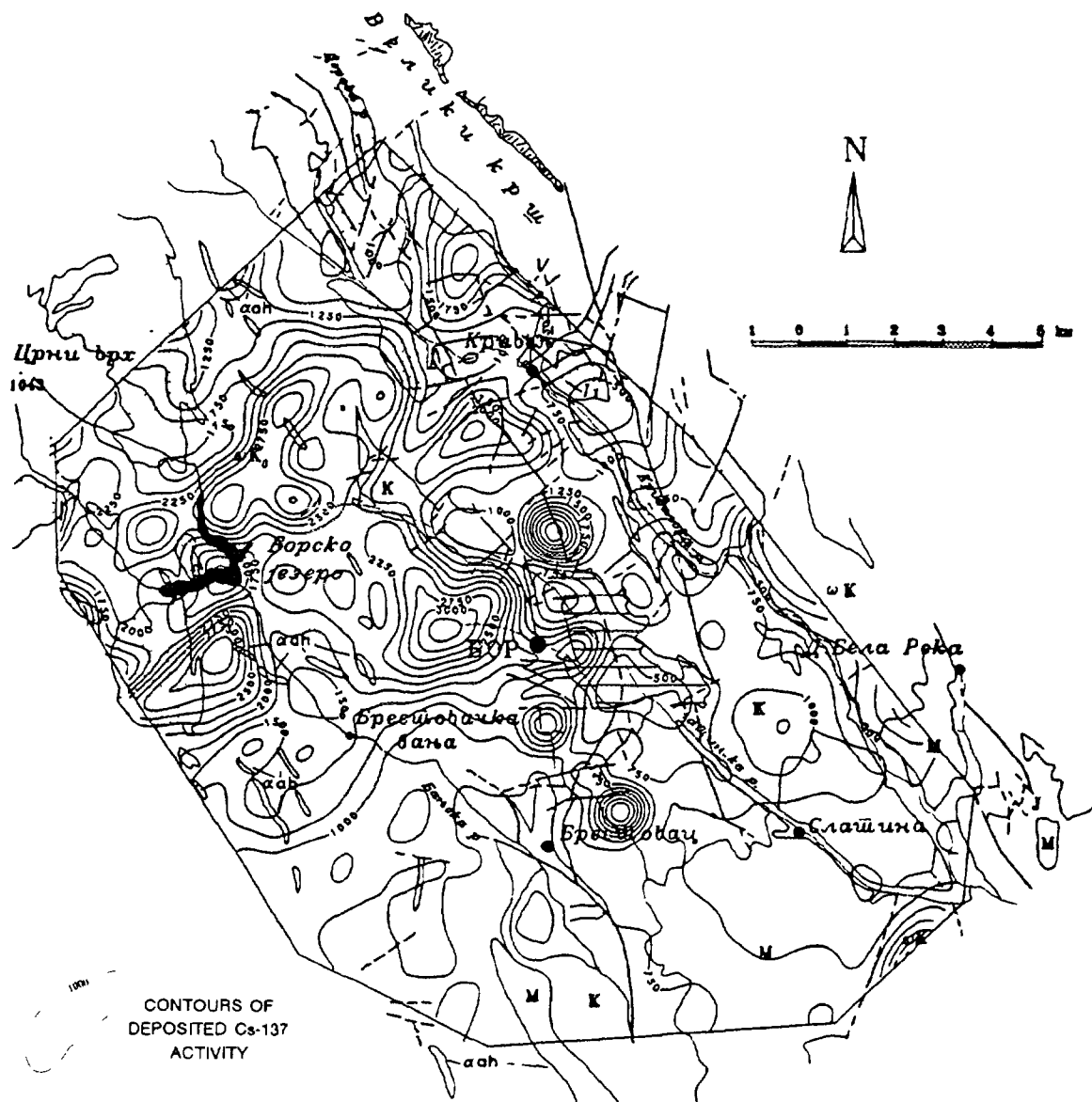


FIG. 13. Map showing deposited Cs-137 (Bq/m^2).

In some cases of ground contamination it is easy to detect the increased radioactivity in air by a system of fixed points. There are cases, however, in which the increased radiation has not been generally established, only registered on ground surface. In such a case, ratios of Cs-137 and Cs-134 sums recorded in energy windows are used.

These ratios indicate some important facts. One is the degree of nuclear fuel utilisation in the reactor, and the other is the length of time since the fuel was removed from the reactor. Both facts are important in finding the truth when there are some indications of various contamination sources.

6. ASSESSMENT OF METHOD AND EXPERIMENTAL RESULTS

The development of the method has three critical stages, each liable to errors which may significantly affect the interpretation of results and the conclusions.

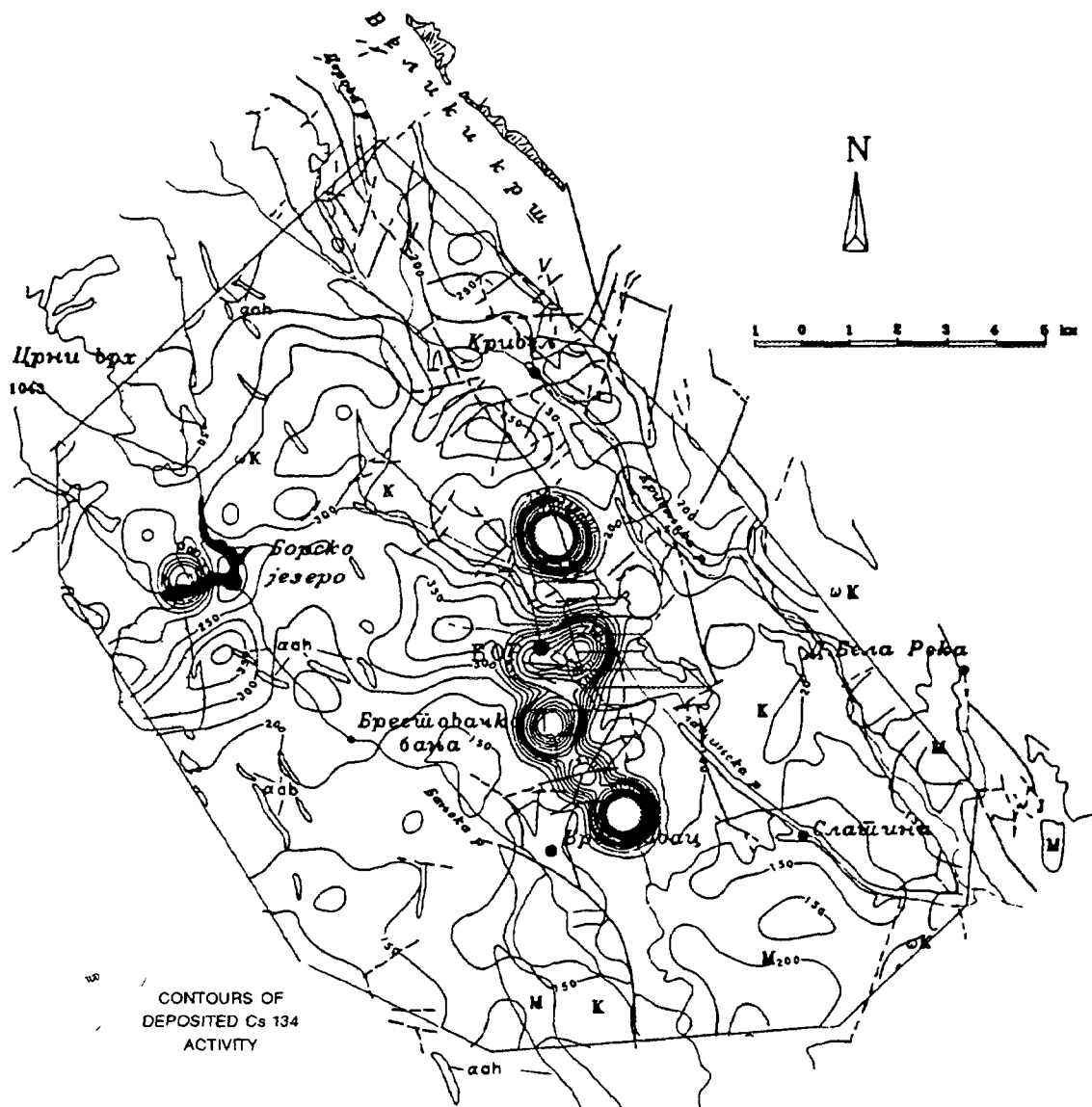


FIG. 14. Map showing deposited Cs-134 (Bq/m^2).

The first of the three stages includes development and planning of AGS exploration. The difficulties of this stage are believed to have been overcome, and that both theoretical and practical requirements were satisfied.

The second stage of AGS use in environmental examinations is the organisation of experimental surveys after the designed algorithm. It is more open to errors. One possible error is the selection of aircraft. It has been learned from experience that a fixed wing aircraft is satisfactory for surveys of flat and large areas. Another possible error concerned calibration of instruments and sampling for conversion of measurements into concentration or activity of natural or artificial radioactive isotopes. The conversion of the measured qualitative into a quantitative information is particularly important and very sensitive, as it is liable to errors that may lead to significant even contrary conclusions on the field situation. The use of a helicopter would have resulted in a far higher consistency of the gamma radiation measurements and the laboratory radiometric analyses. A most important addition to the design will certainly be the definition of the relationship, in the form of a mathematical relation, between radioactive elements of artificial origin and gamma radiation intensity caused by them.

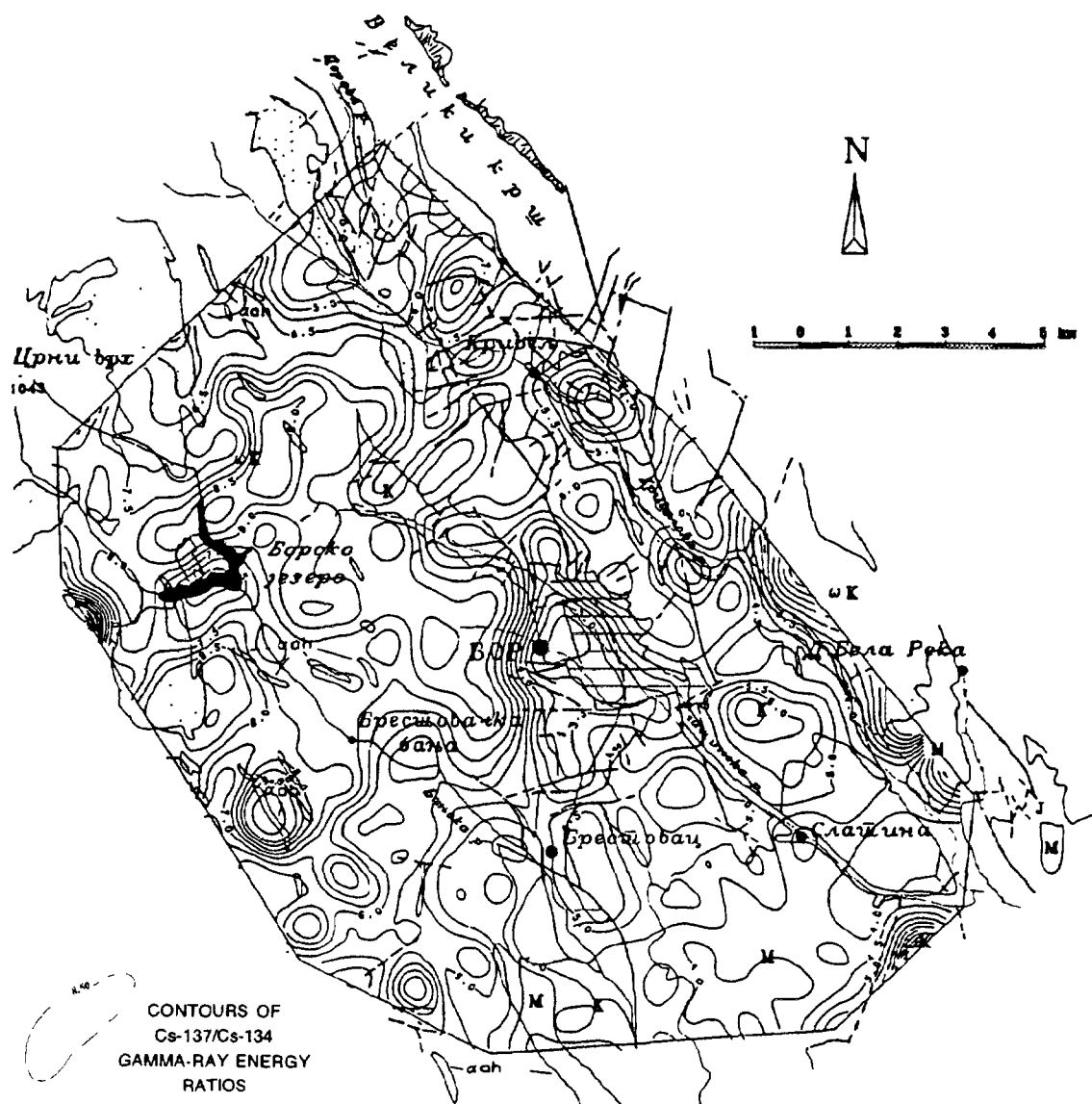


FIG. 15. Map showing deposited Cs-137/Cs-134 gamma ray energy ratios.

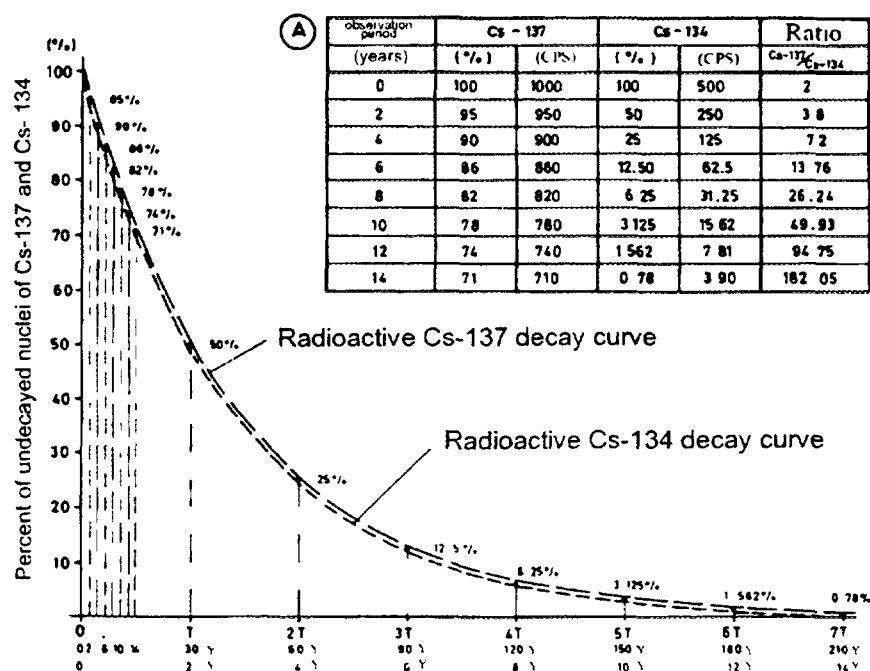
The third stage in the development of AGS application in the environmental control refers to the organisation of data processing procedures. It also involves corrections for the background radiation, for effects of aircraft and of cosmic radiation. Of some importance for the data quality is also correction for the effect of Compton scattering. We believe that the computer programme package supporting the Algorithm Ecology has largely satisfied the method requirements and that its complementation and extension are desirable.

7. CONCLUSIONS

The results of the developed procedures for airborne control of ground contamination from artificial gamma radiation sources have confirmed the thesis that an area contaminated from radioactive sources, type, nature and size of the contamination can be defined with gamma radiation measurements from the air. It has also been shown that the presented procedure of the airborne gamma-ray spectrometry must be included in any complex gamma radiation monitoring system on a national scale.

The constructed Algorithm, named ECOLOGY, defines the form of data presentation, modes of processing, analysis and presentation of results. The main algorithm test, over an area of the Bor District, 200 km² in size, detected a significant contamination, Northwest of Bor, by cesium 137 and 134, in the deposited activity of over 3000 Bq/m². The south-eastern part of the study area had 4-5 times lower deposited Cs-137 activity.

The conclusion based on all the available data and experimental results is that the airborne control of ground contamination by artificial radioactive isotopes should be used as one of the methods within complex monitoring systems of any country.



Samples analysed in Swedish Radioactivity Protection Institute

(B)

observation period (years)	Cs - 137		Cs - 134		Ratio $\frac{Cs-137}{Cs-134}$
	(%)	(CPN)	(%)	(CPN)	
0	100	1000	100	588	1.7
2	95	950	50	294	3.24
4	90	900	25	147	6.12
6	86	860	12.5	73.5	11.70
8	82	820	6.25	36.25	22.31
10	78	780	3.125	18.125	42.43
12	74	740	1.562	9.062	80.52
14	71	710	0.78	4.59	154.68

Completely exhausted nuclear reactor fuel

(C)

observation period (years)	Cs - 137		Cs - 134		Ratio $\frac{Cs-137}{Cs-134}$
	(%)	(CPN)	(%)	(CPN)	
0	100	1000	100	1000	1
2	95	950	50	500	1.9
4	90	900	25	250	3.6
6	86	860	12.5	125	6.88
8	82	820	6.25	62.5	13.12
10	78	780	3.125	31.25	24.96
12	74	740	1.562	15.62	48.59
14	71	710	0.78	7.80	91.02

FIG. 16. Analyses of samples carried out at Institute "Dr. Dragomir Karajović" and Swedish Radioactivity Protection Institute.

REFERENCES

- [1] BRISTOW, Q., The application of airborne gamma-ray spectrometry in the search for radioactive debris from the Russian satellite "Cosmos-954" operation "MORNING LIGHT" GSC, Ottawa (1987) p 78-1b.
- [2] JOBST, E.J., The Aerial Measuring Systems Program, Nuclear Safety vol 2 N° 2 March-April 1979.
- [3] DICKSON, B.H., Analytic methods for multichannel airborne radiometrics M. Sc thesis University of Toronto, Canada (1980).
- [4] DICKSON, B.H. & BAILEY C.R., GRASTY, R.L., Utilising multichannel airborne gamma-ray spectra, Canadian Journal of earth science vol. 18. (1981) p 1793-1801.
- [5] LINDEN, A & MELLANDER, H, 1986: Airborne measurement in Sweden of the radioactive fall out after the nuclear reactor accident in Chernobyl, USSR (1986) preliminary report.
- [6] GRASTY, R.L. & MULTALA, J., A correlation technique for separating natural and man-made airborne gamma-ray spectra, GSC paper 901D (1991).
- [7] MILOJEVIĆ, M.M., Report on the results of the project "Development of the monitoring system for environmental protection", Geoinstitut, Belgrade (1990) file 39-90.
- [8] MILOJEVIĆ, M.M., Airborne gamma-ray spectrometry exploration natural and artificial gamma radioactivity and ecogeological aspect of application, Ph D thesis University of Belgrade, Yugoslavia (1992).
- [9] MILOJEVIĆ, M.M., Airborne environmental control of contamination by artificial gamma-ray emitters, Proceedings of Geoinstitute vol 29. (1994) p 36-54.



**AIRBORNE GAMMA RAY SPECTROMETRY —
AN EFFICIENT METHOD FOR FINDING AND MAPPING
POLLUTION WITH RADIOACTIVE ELEMENTS FROM
URANIUM EXTRACTION AND ORE MINING**

L.M. KERBELOV, R. RANGELOV
Airborne Geophysical Surveys Limited,
Sofia, Bulgaria

Abstract

The concentration of uranium (by radium), thorium and potassium (by the isotope K-40) in the 50 cm surface layer can be defined with relative high precision by the airborne gamma spectrometric surveys. It is well known that certain ore mining and extraction of non-radioactive ores create polluted areas. Pollution can generate from geochemical migration of uranium (radium) and its transport by surface or underground waters. Considerable pollution can be obtained with the so-called "geochemical barriers", generated from the change of physical-chemical properties in the surface layer. Accumulations of uranium are formed close to such barriers. There are, of course, other mechanism of radioactive pollution, from mechanical carriage of rock masses, with uranium concentration, to settling of uranium from radioactive waters in the flooded plains. Bulgaria is rich in geological formations of various uranium concentrations, sometimes very high, and we should accept it as variations of the natural radioactive background. This paper explains one of the methods used for eliminating the natural radioactive background when mapping the pollution from the ore mining industry. The example is the Buhovo area and the method described is the airborne gamma ray spectrometry. Information is also provided on the spectrometer KS 16, developed with Bulgarian and Canadian expertise.

Modern airborne gamma ray spectrometry determines with relatively high precision the concentration of uranium (Bi-214), Thorium (Th-208) and Potassium (K-40) in the 50–80 cm. layer. It is known that in the mining of some uranium ore and some non radioactive ore with relatively increased concentrations of uranium, radioactive pollution can form, with an undefined configuration and an area that is difficult to predict. The genesis of the pollution can be different. There is the geochemical migration of uranium (radium), transformed to a geochemical mobile form, due to taking the uranium (radium) out of its natural environment as an undestroyed ore body. The transportation of uranium (radium) can also happen through surface waters. In both cases more significant pollution occurs in the areas, where in the change of the physical and chemical properties in the subsurface area "geochemical barriers" exist in the vicinity of which, uranium is accumulated. The other mechanisms of radioactive pollution are from mechanical transportation of rock masses, enriched in uranium, to sedimentation of the uranium from radioactive waters in the flooded terraces of rivers and streams. Together with the above, Bulgaria is abundant with geological formations with different concentrations of uranium, sometimes very high, which have to be accepted as variations in the natural radioactive background.

Airborne gamma ray spectrometry surveys have been carried out in Bulgaria since 1963. The surveys have been flown systematically until 1989 as an aid to geological mapping and as an aid to the exploration for oil, gas, rare earth elements, gold, silver, lanthanum, lead, tungsten, copper, zinc, boxites, and others.

Through the years different equipment has been used — from 6 channel crystals with a volume of 4 litres with analogue registration of the data to 256 channel differential analyzers with a crystal volume up to 52 litres and digital registration of the data. Light airplanes and light to heavy helicopters have been used with a line spacing of 250 m to 500 m. In the above mentioned years airborne gamma ray spectrometry has been used twice for the detection and control of radioactive pollution — in 1972 for the finding of a powerful point Iridium source from a gamma ray tester and in 1986 for the control of fallout from Chernobyl. (256-channel spectrometer with about 52 litres.)

Since 1967 the compilation and interpretation of the airborne gamma ray spectrometry data is being done by computers. Since 1990, airborne gamma ray spectrometry in Bulgaria, is used for detection and mapping of pollution with natural and artificial radionuclides and determining the background level of specific areas — the area of the nuclear power station “Kozludoi”, and N-E Bulgaria, which is closest to the new Romanian nuclear power station.

Since 1993 the airborne gamma ray spectrometry surveys in Bulgaria are carried out by the Bulgarian-Canadian joint venture Airborne Geophysical Surveys Ltd. with a 50% Bulgarian government participation and 50% Canadian participation of the company UDL using a spectrometer with 256 channels and different combinations of crystals — from 16 litres to 52 litres.

We established through mathematical modeling and experimental flights that the detection and mapping of artificial radioactive elements depends largely on the quality of the crystals, the number of channels in the spectrometer and the respective software. For the pollution of natural radioactive elements there are other basic problems and the success depends largely on considering a series of geological factors in the interpretation of the data, and naturally on the sensitivity of the equipment.

The uranium mines and the respective technogenic pollution from the mines in the area of Buhovo are located in a non-homogeneous, relatively complicated, geological, radio geochemical environment. Most of the mines, the ore dumps and areas with possible technogenic pollution are found in granites with high radioactivity. The radioactivity is determined from the high concentrations of U, Th and K. Judging by the map of U, there are signs of pollution as well, of the quaternary sediments in the Sofia field, which are characterized with relatively low background content of U, Th and K. The problem is to establish the contours of the areas with a technogenic accumulation of U from these background concentrations. For this purpose an airborne gamma ray survey was carried out in 1990. A MADACS gamma ray spectrometry system with 256-channels spectrometer, and total volume of crystals 52 litres was mounted on a helicopter MI-8.

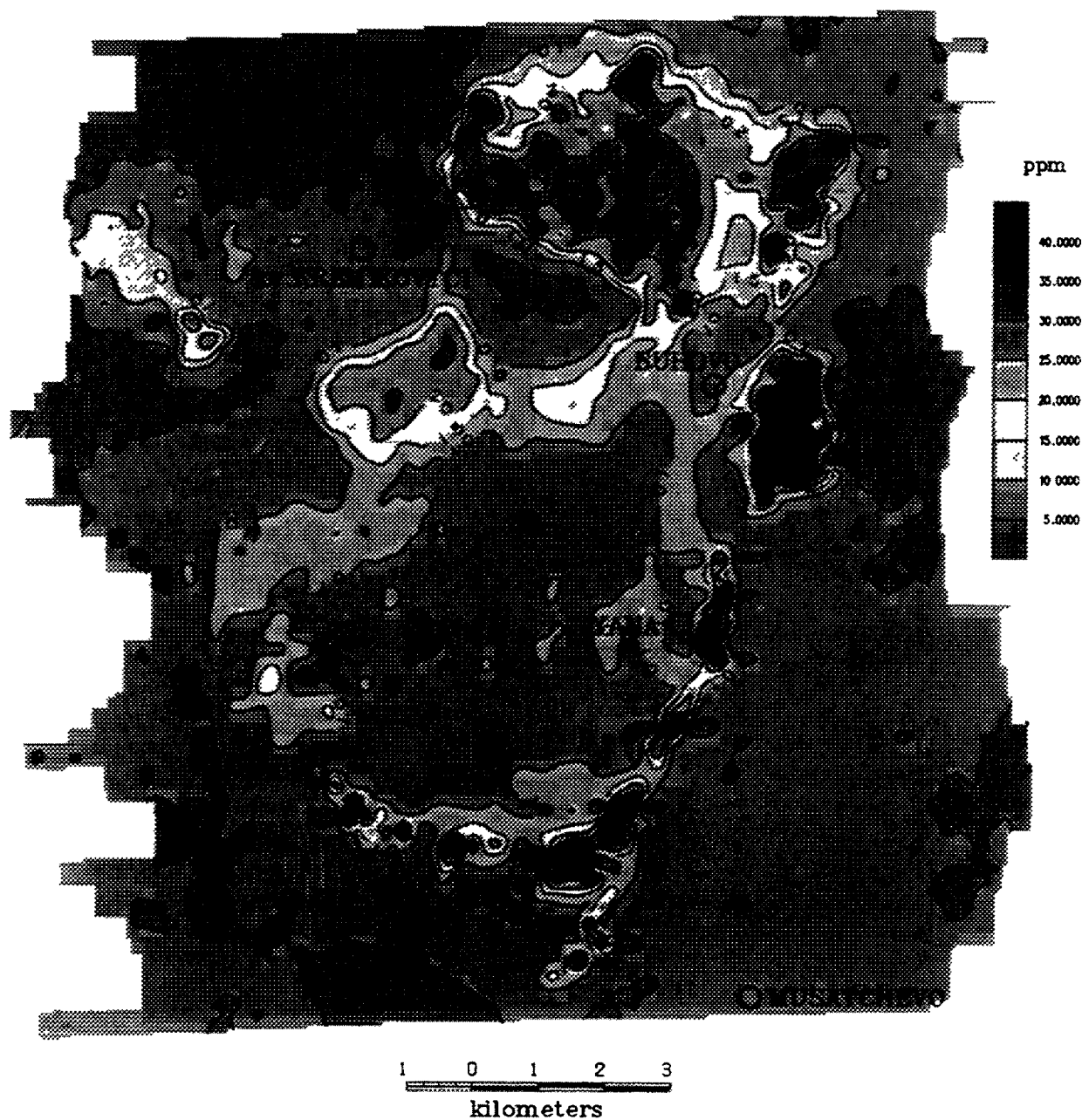
The flying was made at parallel routes with line spacing 250 m, with 80 m altitude and speed of about 80 km/h. In this way an almost complete coverage of the area was achieved according to the zone of effective detection of the crystals, which is about 3 times the height of the flight.

From the airborne gamma ray spectrometry data maps were built and Figure 1 and 2 show the maps of U (Bi-214) and potassium (K-40) distribution. On them the contours of the highly radioactive granites are clear, as well as a linear zone with increased content of uranium and a patch with an increased concentration of uranium, which by area coincides with the tailing of the ore-dressing factory (Fig. 1). From this map, viewed independently, the following conclusions can be made: possibly there is a technogenic pollution, coinciding with the tailing and the viewed linear zone. It is not clear, however, if and where, there is pollution with U in the of the borders of the highly radioactive granites.

The analysis of these maps (Figs 1 and 2), as well as samples from the soil and granites, have shown, that in the background systems of both the granites and the low radioactive soil of the Sofia field, the ratio U/K remains almost unchanged. Therefore a map of U/K will contour the technogenic pollution with uranium.

On this map (Fig. 3) the above described areas with technogenic pollution are clearly contoured, and a series of new polluted areas, are established, both in the borders of the granite massif (where the ore dumps are seen), as well as in other places.

All these areas have undergone ground verification and the existence of technogenic pollution is proved. For example, the “newly” polluted patch in the S-W part of the area is a result of the ashes from the burned coal in “Kremikovzi”, which are stored there.



AGS Airborne Geophysical Surveys Ltd.

FIG. 1. Uranium (Bi-214) map of the Buhovo area.

A similar methodology, with small variations, is used successfully in other areas of the country as well, for example in a part of the UpperTrackia crest. There, however, variations of the trend analysis had to be applied.

The main conclusion is that, in the surveying of pollution with natural radioactive elements for every concrete case in the geological structure and radio geochemical characteristics of different type of rocks the methodology for interpretation of the data has to be chosen carefully.

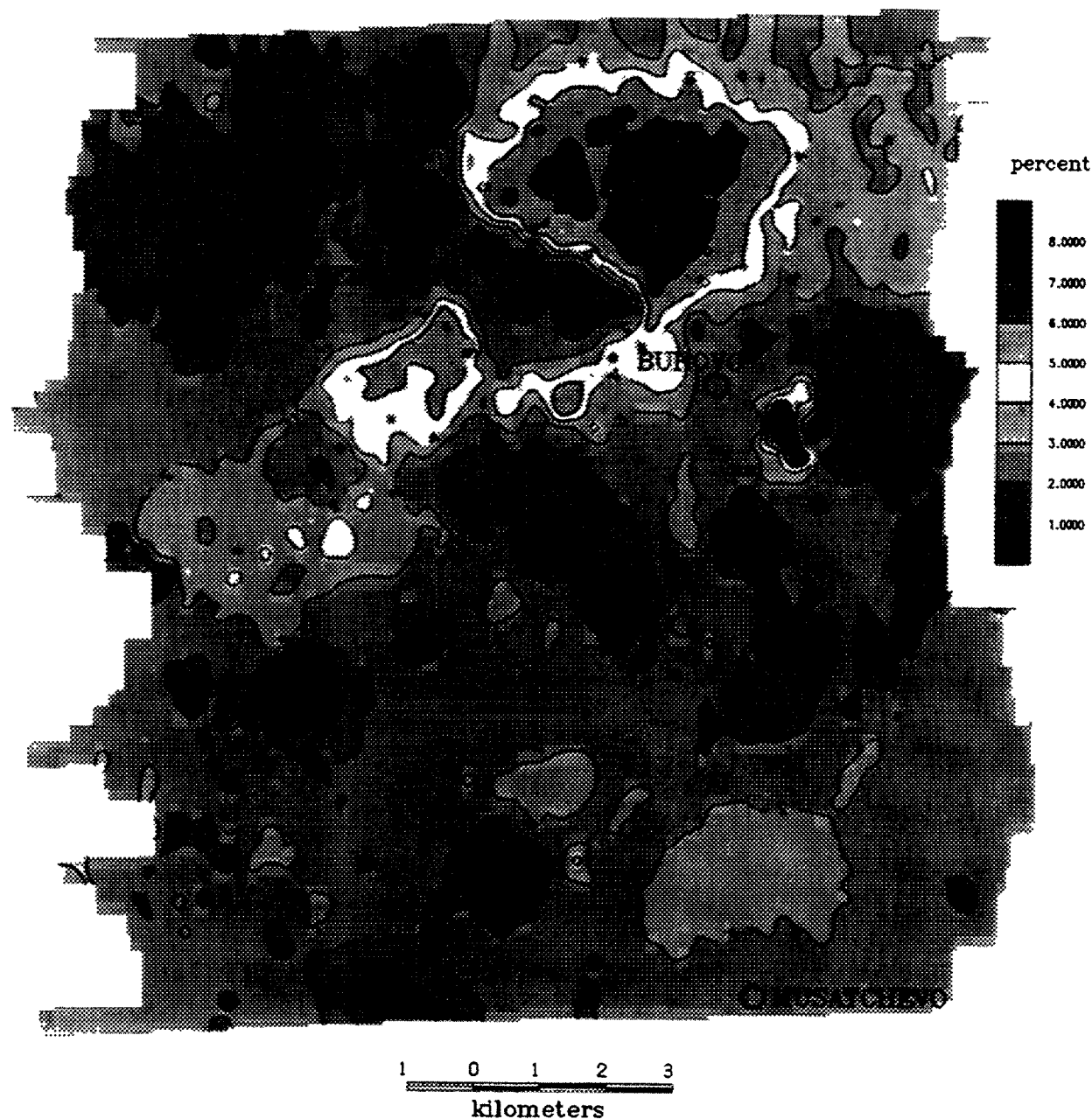
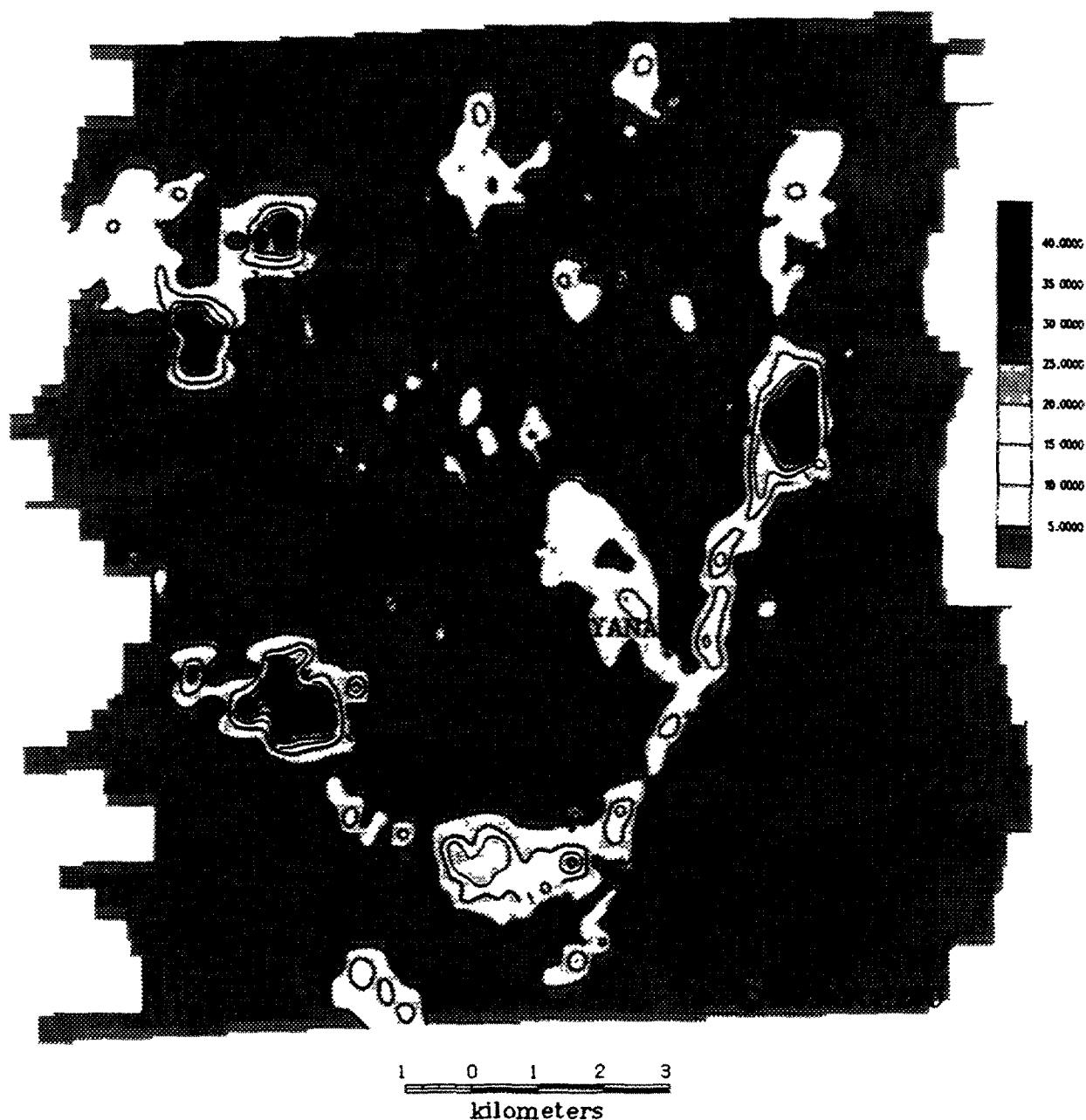


FIG. 2. Potassium (K-40) map of the Buhovo area.

For the development of the methodology for mapping of pollution with natural and artificial radionuclides, in respect to the new capacity of the PC equipment and experience gained, Airborne Geophysical Surveys Ltd. together with the Canadian partner High-Sense Geophysics Ltd. has completed the development of a principally new universal airborne gamma ray spectrometry system with a code name KS16 together with the respective software for survey of all radioactive pollution and for purely geological purposes.

The software for graduation, applying of corrections and computer compilation has been developed according to the standard set by the International Atomic Agency [1].



AGS Airborne Geophysical Surveys Ltd.

FIG. 3. Map of the ratio U/K of the Buho area.

The main original parameters of the KS-16 and the data acquisition system are:

- 2048 channels analyzer. Through the analyzer the concentrations of up to 16 radioactive elements can be measured simultaneously with a synchronized applying of all corrections. This is due to the circumstance that the energy resolution in this number of channels drastically increases the possibility for using fully the energy resolution of the NaI(Tl) crystals especially in the area of the high and low energies. For example in the standard 256-512 channels spectrometers, in the existence of intense pollution with Cs-137 it is practically impossible to measure the photopeak of Rn with energy 609 KeV and respective corrections for Rn.

On the contrary, in the case of an intense pollution with U, the determination of Cs-137 is a problem. There is a similar situation with the photopeaks of K-40 and Ba-140.

- KS 16 can control simultaneously up to 16 photocystals.
- With the software the system makes a linear energy scale of every separate crystal, so that at the exit a linear energy spectrum is received. Again with the software, during the flying period a possible energy drift of every separate crystal and of the system as a whole is eliminated with chosen by the specialists bench-mark photopeaks.
- The system is designed, so that after a preflight semiautomatic calibration the system works automatically, and on board of the aircraft an operator is not needed.

At the moment several systems are working for geological purposes. A specialized software for artificial radioactive elements is being tested.

BIBLIOGRAPHY

- [1] INTERNATIONAL ATOMIC ENERGY AGENCY, Airborne Gamma Ray Spectrometry Surveying, Technical Reports Series No. 323, Vienna (1991) (out of print).
- [2] KOGAN, NAZAROV, FRIDMAN, Fundamentals of gamma spectrometry of Natural Media, Atomizdat, Moscow (1976) (in Russian).



AIRBORNE GAMMA ANOMALIES IN THE ELBE VALLEY NEAR KÖNIGSTEIN, GERMANY — ORIGIN AND VARIATION WITH TIME

G. RUHRMANN, B. SCHMELING

Uranerzbergbau GmbH,
Wesseling

M. SCHAUER, R. GATZWEILER

Wismut GmbH, Chemnitz

Germany

Abstract

In 1982, an airborne gamma spectrometer survey was undertaken by SDAG WISMUT which was directed at the detection of further uranium mineralization in Saxony and Thuringia. Anomalies outlined along the Elbe river near the existing Königstein uranium mine were attributed to one or a combination of the following causes: radioactive residues from uranium processing facilities located upstream, temporary accumulation of Rn-decay products attached to dust particles in the atmosphere at the time of the survey, and radioactive waters emerging from uraniferous rocks along tectonic structures. In 1994, WISMUT GmbH re-evaluated the survey to determine the need for implementing cleanup measures. Subsequent to the verification of the original airborne data, ground surveys were undertaken that included gamma spectrometry, percussion probing and river sediment sampling. The new results did not confirm the magnitude of most of the 1982 airborne anomalies. The general decline of the radioactivity pointed out by the 1994 ground measurements is interpreted to be a result of the partial erosion and dilution of radionuclides in fluvial sediments as well as burial by additional river sediments since. Additional anomalous copper and zinc concentrations are attributed to sources other than mining. The ground follow-up delineated a new anomalous zone that is caused by radionuclides discharged with treated process and mine water. It is the only area, which may require further investigations and possible remedial action.

1. INTRODUCTION

In Saxony and Thuringia, exploration for uranium started under the supervision of the Soviet military in 1945 and was initially focused on the historic mining districts in Saxony. Successful exploration lead to production of uranium ore in 1946. In 1947, all mining activities in the Soviet occupation zone were transferred into Soviet ownership as part of the reparation payments after World War II. Uranium exploration and mining was carried by the company SAG Wismut until 1954. Then, the hitherto purely Soviet company was converted into the bi-national Soviet-German Aktiengesellschaft (SDAG) Wismut with the East German and the Soviet government holding 50% each. SDAG Wismut continued mining under a Soviet-German agreement renewed in 1962 and 1975. Production ceased by the end of 1990 as result of an agreement between Germany and the Soviet Union dated October 9, 1990. The produced uranium ore and the yellowcake were shipped to the Soviet Union for further processing.

By the end of 1990, Wismut had produced a total of 216 000 tonnes of uranium. Most of this production originated from the black schists-type ore in the Ronneburg district and the world largest uranium vein deposit Schlema-Alberoda in the Aue district. Minor contributions to the total production came from sediment-type ores of Permian and Cretaceous age at Culmitzsch, Gittersee and Königstein (Fig. 1). This puts Germany after USA. and Canada in third place with regard to total post-war world uranium production [1a, 1b].

In 1991, the Soviet-held shares were absorbed by the German government. At the end of 1991, Wismut-GmbH was created as a company wholly owned by the German government. The business objective of Wismut-GmbH is to close down all mining and to rehabilitate the uranium mining and milling facilities in Saxony and Thuringia, which had not been abandoned by 1962.

The rehabilitation of the areas affected by the mining activities encompasses a wide variety of measures including assessing the present site conditions and establishing the need for rehabilitation activities, cleaning up the underground workings, i.e. removal of hazardous and toxic materials and backfilling as required by the hydrological or geomechanical conditions, flooding of the mines and treatment of contaminated waters that discharge into surface waters, demolition of contaminated surface structures and disposal of contaminated materials, stabilization of tailings ponds including the removal of supernatant and pore water as well as the construction of covers, rehabilitation of waste rock piles entailing the contouring of slopes where required and installation of covers, environmental monitoring of radiological and chemical parameters in order to take corrective measures during the rehabilitation activities and to document the success of the restoration efforts.

In order to support the environmental assessment of the Königstein mine site, a portion of a regional airborne gamma spectrometer survey originally directed at the expansion of uranium ore reserves during the mining phase was re-evaluated.

The present account deals with the results of the original survey and its re-evaluation. It is based on the compilation of Wismut data and investigations undertaken by Geophysik GGD, Leipzig [2] commissioned by Wismut-GmbH in 1994. Similar investigations were carried out by the Bundesamt für Strahlenschutz [3] within a regional assessment program.

2. GEOGRAPHICAL AND GEOLOGICAL SETTING OF THE KÖNIGSTEIN AREA

The survey area is located near the Königstein mine where the Elbe river valley cuts into the "Elbsandsteingebirge" — plateau to a depth of approximately 150 m. The valley is 300 to 500 m wide. The river itself has a width of about 100 m. The river banks are used mostly as pastures. A number of towns and settlements are located on both sides of the river. A road and railway track pass along the river connecting Dresden in the west with Prague, the capital of the Czech Republic, in the southeast (Fig. 2).

The uranium ore at Königstein had been discovered in 1961 and exploited from 1966 to 1990. The orebody extends over an area of 10 km by 4 km. The underground mine covers an area of up to 5 km by 3 km. Average grades were in order of 0.08% U. A total of 19 500 tonnes of uranium was produced initially by conventional methods and from 1984 onward exclusively by underground leaching [4].

The structural geology of the Königstein area is characterized by the presence of the tectonically controlled northwest — southeast trending Elbe River Valley trough. Accordingly, the major structures trend northwesterly. A conjugate system of structures strikes in northeasterly direction. In addition, east-west as well as north-south trending joints have developed of which the "Nordstörung" is of major significance for the Königstein mine (Fig. 2).

The oldest rock units are Paleozoic granites and granodiorites. Within the Elbe trough, Upper Cretaceous sediments with a thickness of up to 800 meters overlie the partially eroded paleoweathered crystalline rocks (Fig. 3). The sedimentary sequence consists from bottom to top of a Cenomanian series of basal terrestrial sandstones passing into younger marine silt and mudstones, which in turn, are overlain by Turonian marlstone and sandstone. The series is discontinuously developed due to synsedimentary tectonic activity. It dips northeast at one to three degrees. The youngest rock units are Tertiary basalt dykes and sills cutting through the Cretaceous sedimentary sequence.

The Königstein deposit belongs to the peneconcordant, stacked [5] or "tabular/peneconcordant sandstone" uranium deposit type [6]. Mineralization is present in two horizons of the terrestrial basal Cenomanian sediments and in one horizon of the transitional terrestrial/marine sediments. The principal ore mineral is pitchblende. The ore is spatially associated with clay stone and organic material and often paragenetically combined with iron sulfides. Elevated concentrations

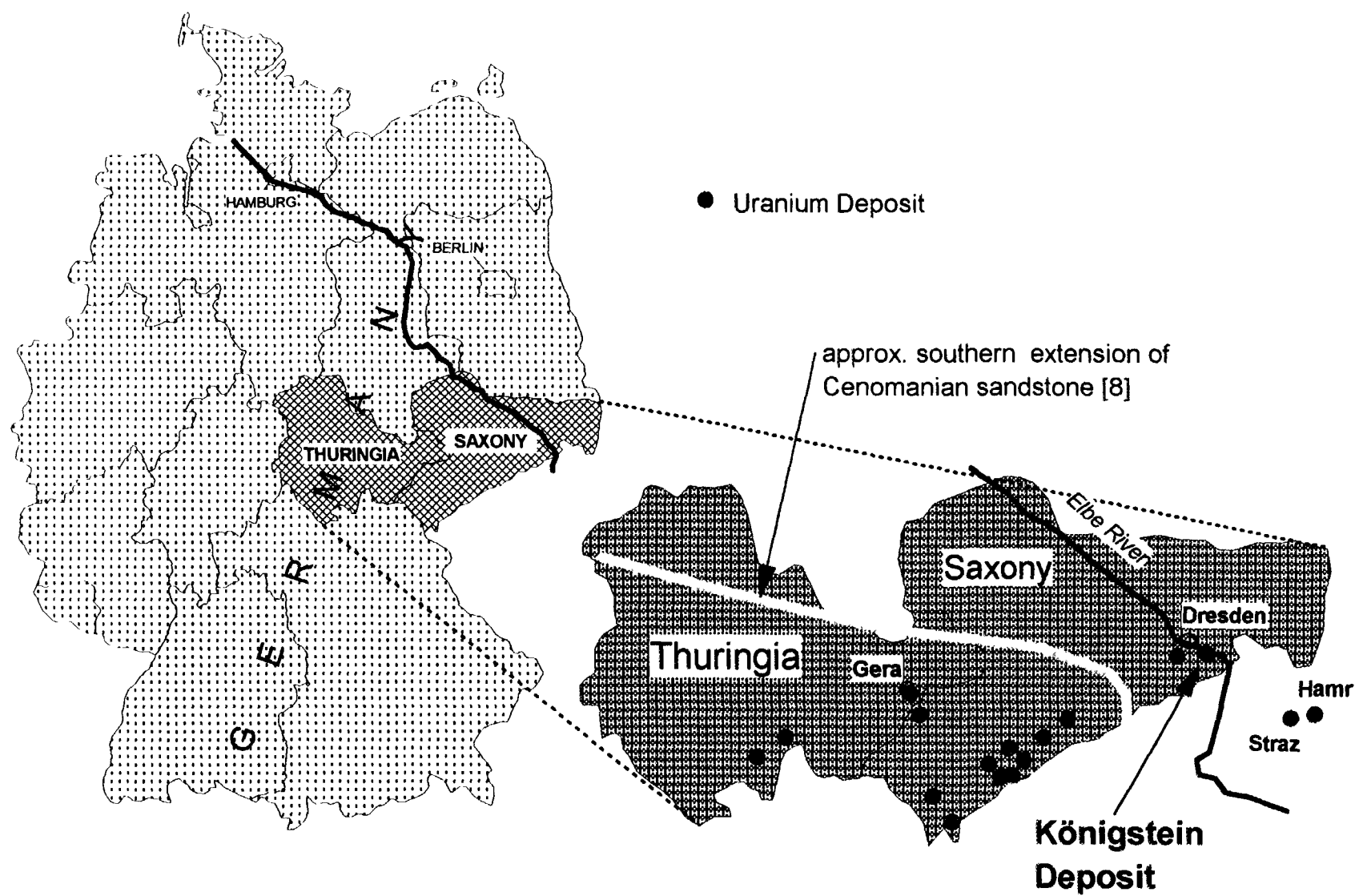


Fig. 1. Uranium deposits in Thuringia and Saxony.

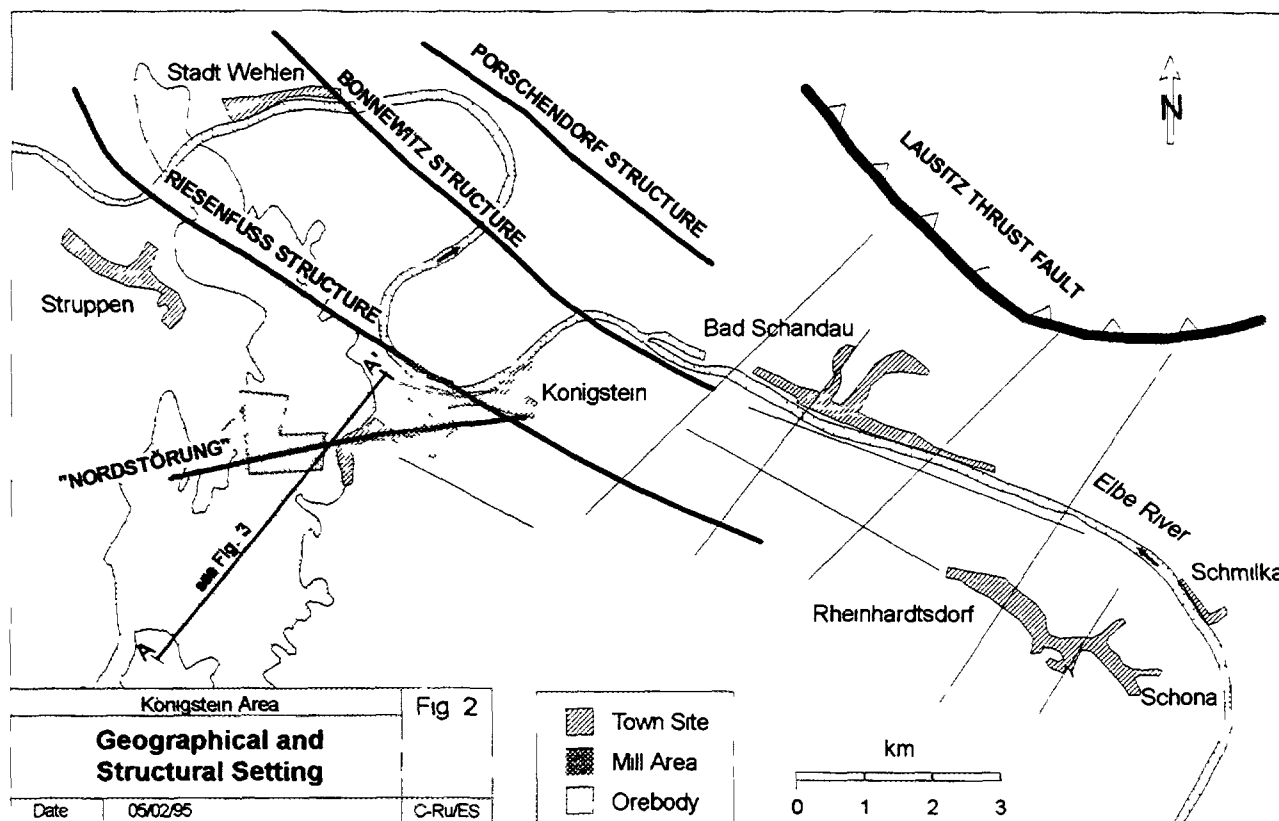


Fig. 2. Geographical and structural setting.

of lead and zinc are commonly associated with the ore. Fractures filled with pitchblende are also present. In that case, the ore is associated with sulfides, hematite and barite [2]. The structural and stratigraphic setting is similar to that of the North Bohemian ore bodies of Hamr-Strá in the Czech Republic [7].

3. AIRBORNE GAMMA SPECTROMETER SURVEY (1982)

The helicopter-borne survey had been flown during the time period from September 16 to 19, 1982 after calibration over test pads with known eU concentrations. The flight lines were oriented in north-south direction at a spacing of approximately 250 m. The flight altitude was 100 m (Fig. 4).

The results showed that most anomalies are located in the Elbe valley (Fig. 5). They form part of a broad anomalous zone straddling the Elbe river and side valleys. The geographic situation, which is characterized by the pronounced relief, gave rise to the assumption that atmospheric conditions were causing at times higher radioactivity in the deep valley. It was speculated that the anomalies had been partially the result either of a wash-out of radon decay products, particularly ^{214}Bi , or of decay product particles adhering to suspended water droplets shortly before the survey had been flown.

The strongest anomaly was detected in some distance from the Elbe river valley. This anomaly is in the order of 10 times background ($10 \times \text{BG}$) and is located over the mill facilities at Königstein including a portion of the cable conveyor that transported ore to a railway terminal. The airborne data indicated otherwise eU-anomalies in the order of $2 \times \text{BG}$ mostly confined to the Elbe river valley. Some anomalies could be allocated to certain geographic features. For instance, the anomaly located close to the center of Bad Schandau is caused by the pavement at the market square.

SSW

NNE

A

A'

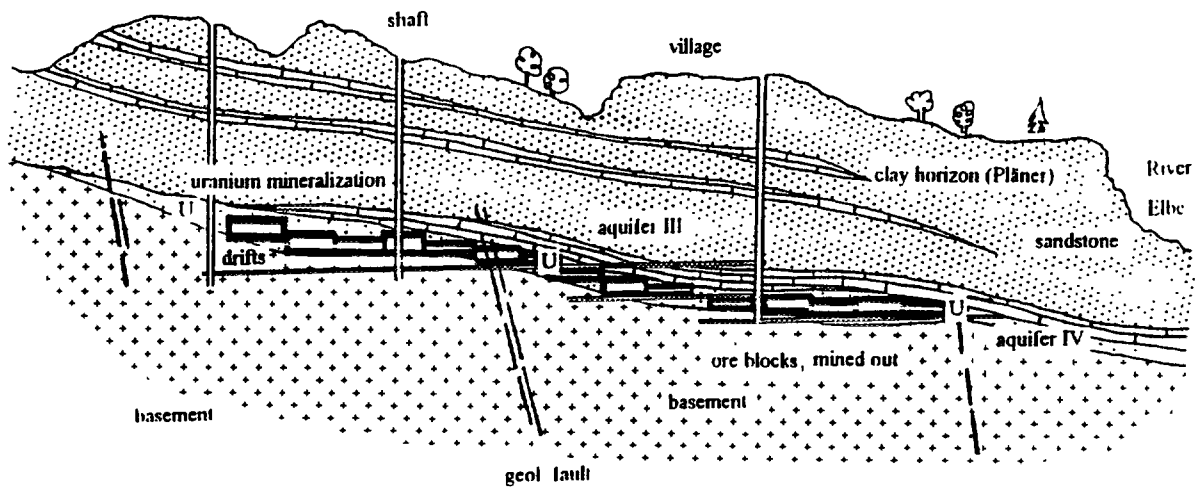


Fig. 3. Schematic cross section of the Königstein Mine.

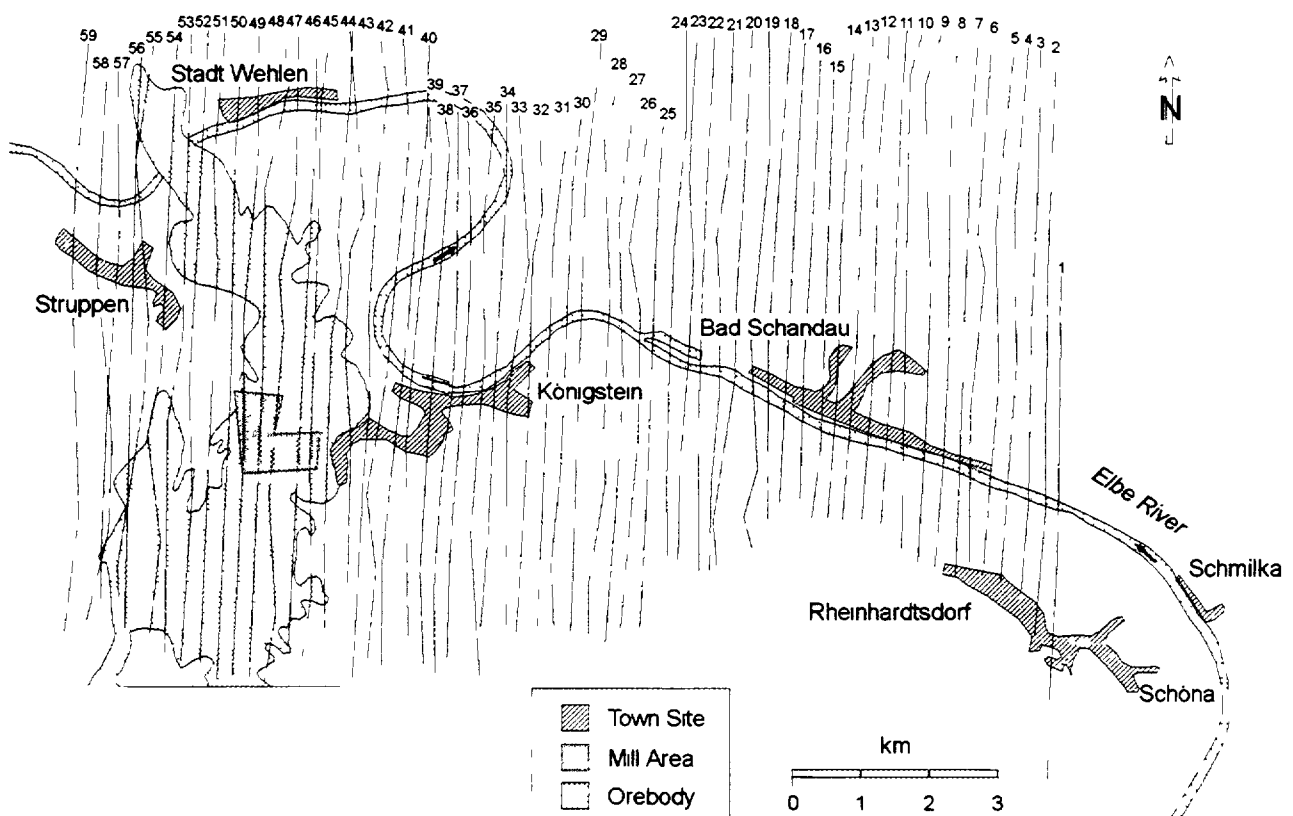


Fig. 4. Survey area - flight lines.

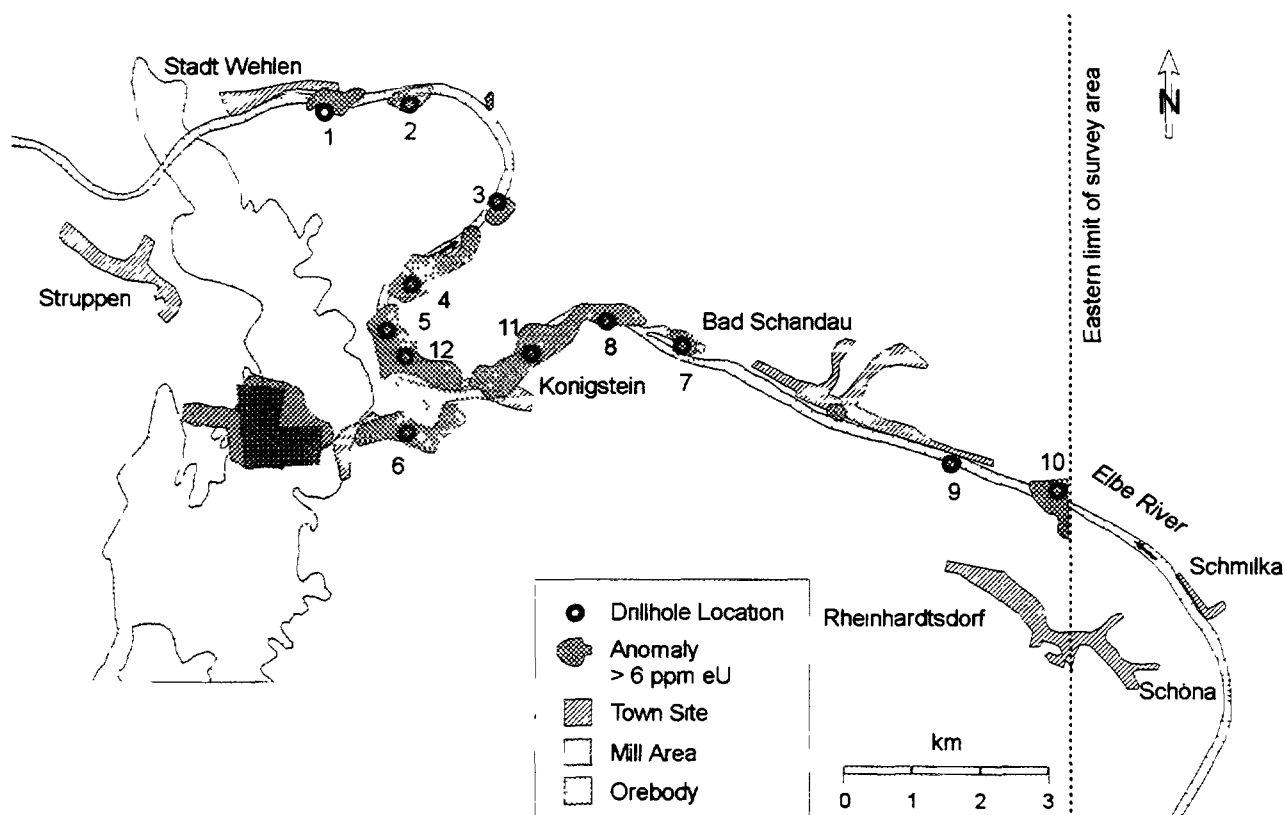


Fig. 5. Major airborne anomalies.

Here, slag from the smelters that processed uraniferous copper ore from the Mansfeld area in Saxony-Anhalt was used as construction material. The anomaly over the protruding table mountain of Lilienstein is most likely caused by reduced flying altitude (mass effect). Similarly, the valley geometry may have contributed to a mass effect resulting in the broad anomaly along the river. Then, atmospheric processes need not be invoked for its explanation.

The better defined anomalies along the river were attributed to contamination from ore processing facilities. Upstream from the Königstein mine, contamination of the fluvial sediments could have been related to the uranium ore processing facilities at Hamr-Strá in the former Czech-Slovak Federal Republic. These facilities are located within the catchment area of the Elbe river. Ore processing residues may have been released some time before the survey had been flown.

Alternatively, anomalies were thought to be caused by radioactive waters and their precipitates emerging from mineralized rock along tectonic structures. A definite relationship between airborne anomalies and tectonic structures could, however, not be established.

Ground follow-up investigations were undertaken on several anomalies as part of the WISMUT site assessment in 1991–1992. The ground measurements yielded puzzling results since the airborne anomalies could not be reproduced. It was speculated that the radioactive material in the alluvial beach sediments had been either diluted, covered by younger non-radioactive river sediments or altogether eroded. In order to explain the disappearance of the anomalies, an investigation on all anomalies delineated by the 1982 survey was initiated in 1994.

4. FOLLOW-UP WORK IN 1994

On the basis of a regional background of 4 to 5 ppm eU, a total of 12 anomalous areas exceeding two times background were identified for ground follow-up. In these areas, gamma spectrometric measurements were centered on the airborne anomalies. A hand-held Scintrex GAD-6 with a 20 cubic inch sodium iodide crystal was used. Data from four channels (potassium %, eU ppm, eTh ppm and total count - 0.8 to 2.77 MeV) were recorded on a grid with 50 m spaced stations. Atmospheric background was established daily by taking three control readings (integrating over 1000 seconds) in the middle of the Elbe river.

The ground data confirmed the lack of correlation between airborne anomalies and follow-up measurements as already indicated by the initial radiometric test survey undertaken by WISMUT in 1991/92. Exceptions were the market place of Bad Schandau and the area of the Königstein mine that both could be clearly confirmed by the ground follow-up measurements.

As the airborne survey had been successful in detecting obvious anomalies like the mine site and the market square of Bad Schandau, it remained unclear why the other anomalies did not have a ground spectrometer expression.

In order to identify the source of the airborne gamma anomalies, soil samples were collected from 11 locations centered on the original anomalies and one anomalous location identified by the recent ground spectrometric survey. Percussion probing was employed to recover sub-surface material from a depth of between 10 cm and 1.7 m (39 samples). In addition, 11 surface and river sediment samples were taken from near-shore zones, ox-bow lakes and river harbors using a rubber dinghy. All 50 samples were analyzed for radionuclides, lead, zinc, copper, nickel, arsenic and aluminum. The radionuclide analyses included ^{40}K (4 Bq/kg - detection limit), ^{226}Ra (1 Bq/kg), ^{228}Ra (3 Bq/kg), ^{210}Pb (8 Bq/kg), ^{238}U (8 Bq/kg), ^{228}Th (1 Bq/kg) and ^{137}Cs (1 Bq/kg). These were determined by spectrometry of gamma radiation emitting nuclides or their long-lived daughter products. For instance, uranium concentrations were determined by the activity of ^{234}Th (half-life of 24.1 days) which produces values comparable to chemical assays.

The soil samples collected from the upper zone (0.1 to 0.3 m) and the river sediment samples display equivalent uranium concentrations in the range of 27 Bq/kg (2.2 ppm) to 260 Bq/kg (21 ppm). The highest concentrations are located close to the discharge point of the "Elbe-Leitung" in agreement with the ground spectrometer anomaly discovered by the latest survey (Fig. 6). Similarly, the ^{226}Ra activity concentrations in sub-surface soil range from 58 Bq/kg to 230 Bq/kg. The highest value of 1800 Bq/kg is also related to the discharge point of the "Elbe-Leitung" (Fig. 7). Since the accumulation of radionuclides near the discharge point of the "Elbe-Leitung" must have occurred mostly after the survey was flown (1982), the values from this location are not considered in the following attempt to correlate the soil anomalies with the airborne anomalies.

The concentrations of up to 9.6 ppm eU encountered in the 0.1 to 0.3 m layer in the centers of the airborne anomalies indicate that radionuclides are still present. Hence, a complete erosion of the radioactive material has not occurred but the material is rather shielded by soil of background radioactivity. This soil was deposited most likely from flood waters of the Elbe river.

In order to test whether the eU concentration in the 0.1–0.3 m layer would produce an airborne anomaly if it was at the surface, the respective eU concentrations were calculated taking into account any disequilibrium. Fig. 8 shows that the adjusted eU concentrations in the 0.1–0.3 m depth zone match the airborne data fairly well. It shows also that the majority of the samples produces a lower eU concentration than was measured 12 years before. This points to a partial removal of the radioactive particles since then.

The activity concentrations of the radionuclides show that in addition to erosional and sedimentary processes uranium was mobilized chemically. The profile of activity concentrations shows

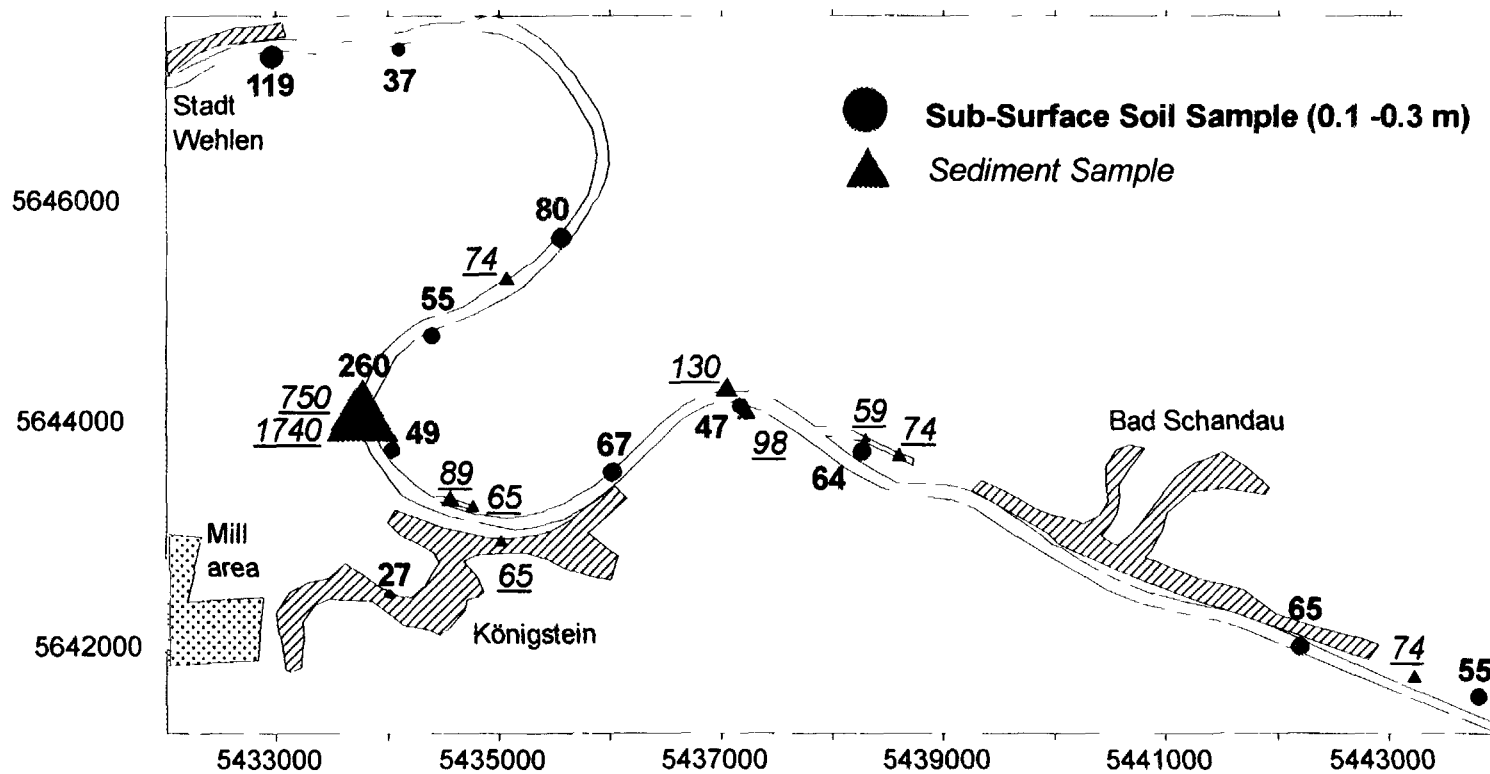


Fig. 6. Uranium in soil and sediment samples (Bq/kg).

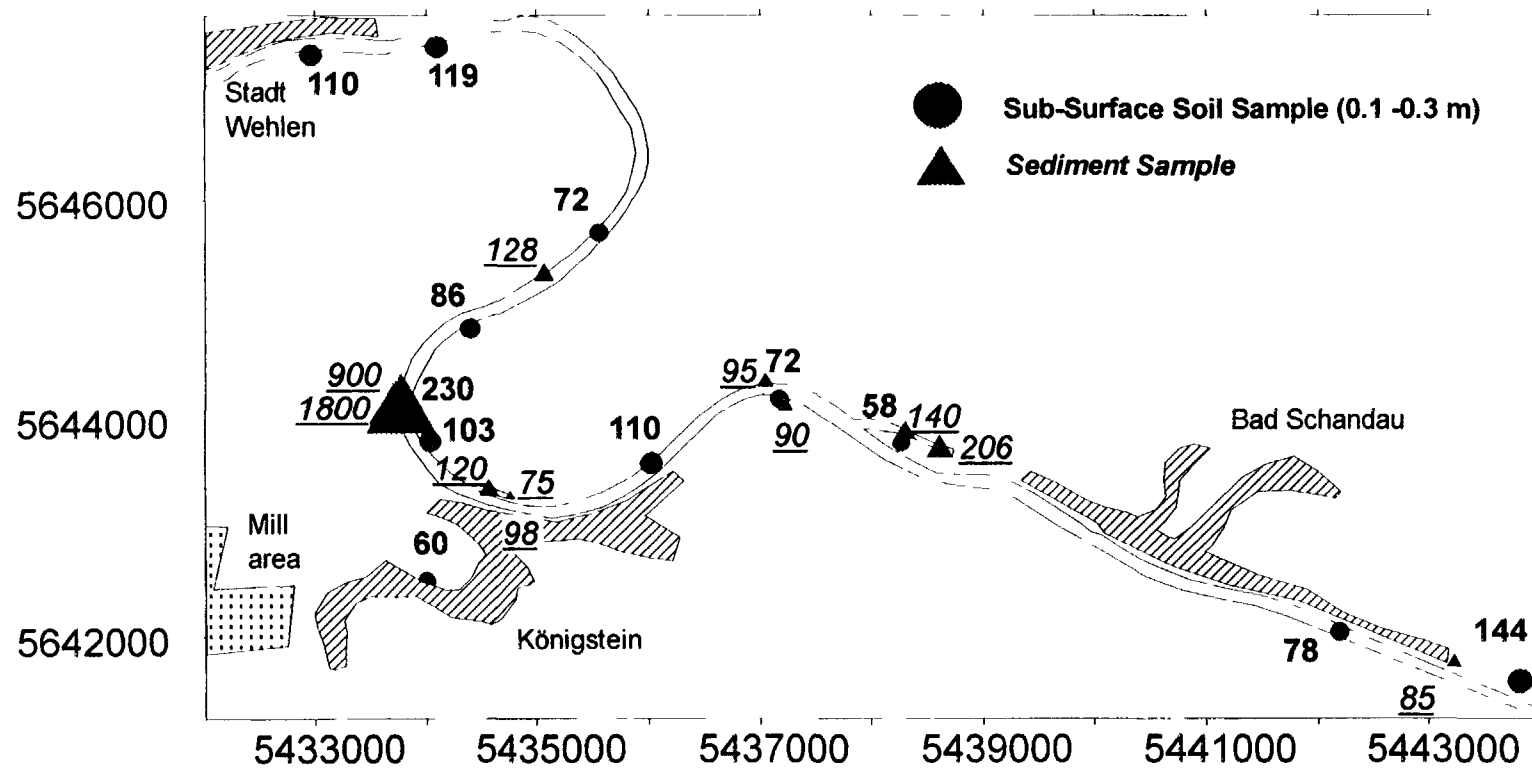


Fig. 7. Radium in soil and sediment samples (Bq/kg).

that radium is relatively enriched near the surface and uranium at depth (Fig. 9). This points to a mobilization of uranium from the oxidizing near surface zone to a more reducing environment at greater depth by percolating rain or meltwater. It is therefore unlikely that radium was mobilized upward.

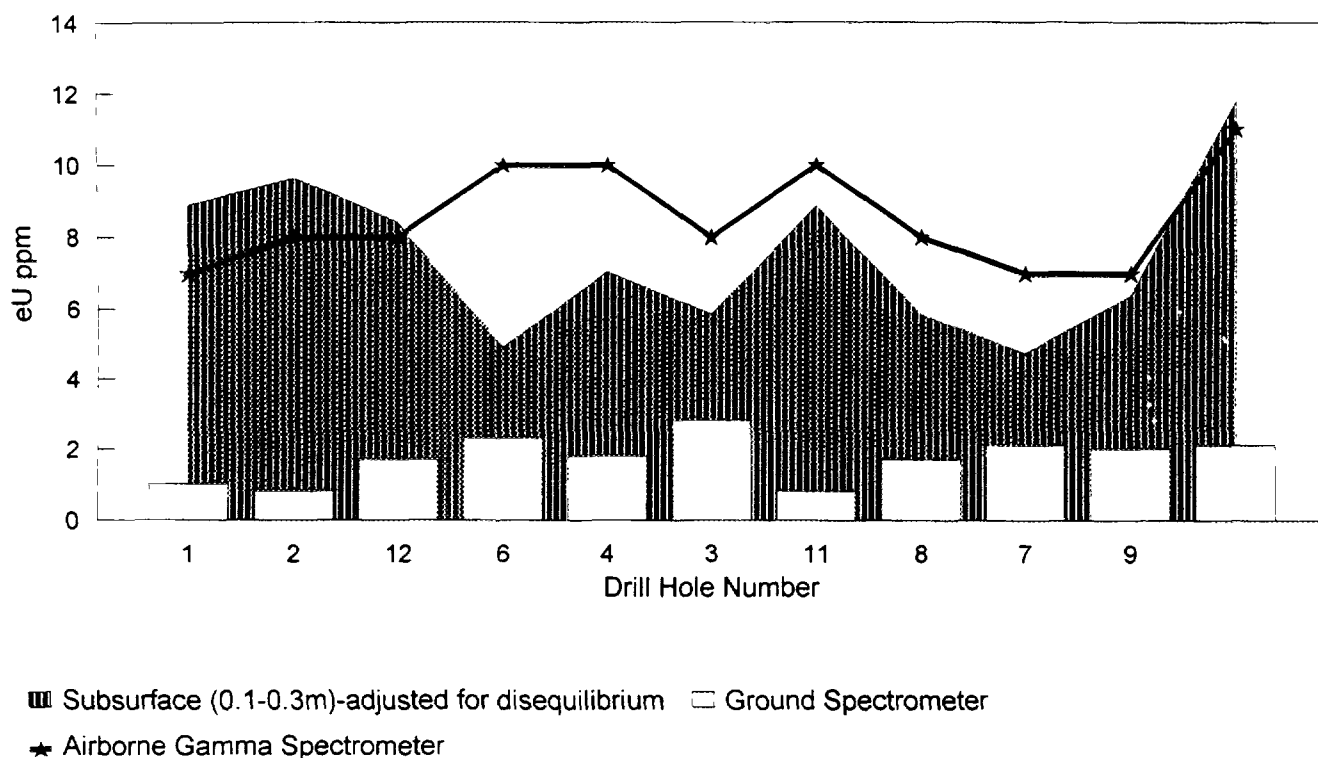


Fig. 8. Comparison of airborne spectrometer with ground spectrometer and soil measurements.

The overall near-equilibrium state of the radionuclides (Fig. 10) in combination with the systematic change of disequilibrium with depth suggests that the radioactive material represents natural mineralization introduced into the river sediments by mine water rather than by uranium-depleted tailings. Accordingly, the widely varying U/Ra ratios along the Elbe river (Fig. 11) suggest that a fractionation of the radionuclides occurred locally subject to the respective chemical conditions.

The concentrations of both radionuclides and base metals decrease toward depth. The ratios of the concentration at the upper level (0.1 to 0.3 m) and at greater depth (1.0 to 1.2 m) range from 1.5 for uranium to 9.5 for Zn (Table I). This could be explained by either increasing load with time or segregation of finer mineralized particles from coarser unmineralized sand grains during the deposition process. The second explanation is supported by the presence of silty material in the upper portion of the soil profiles versus predominant sandy material at depth.

While the maximum concentrations of uranium, radium and arsenic are present in the soil at shallow depth, nickel, lead, zinc and copper attain even higher concentrations in surface sediment samples, particularly in harbor sediments (Fig. 12). The increased concentration of nickel, lead, zinc and copper, which is not accompanied by corresponding radionuclide activities points to another source of contamination than mining residues. It is assumed that the use of the Elbe river as shipping route contributes significantly to the base metal pollution.

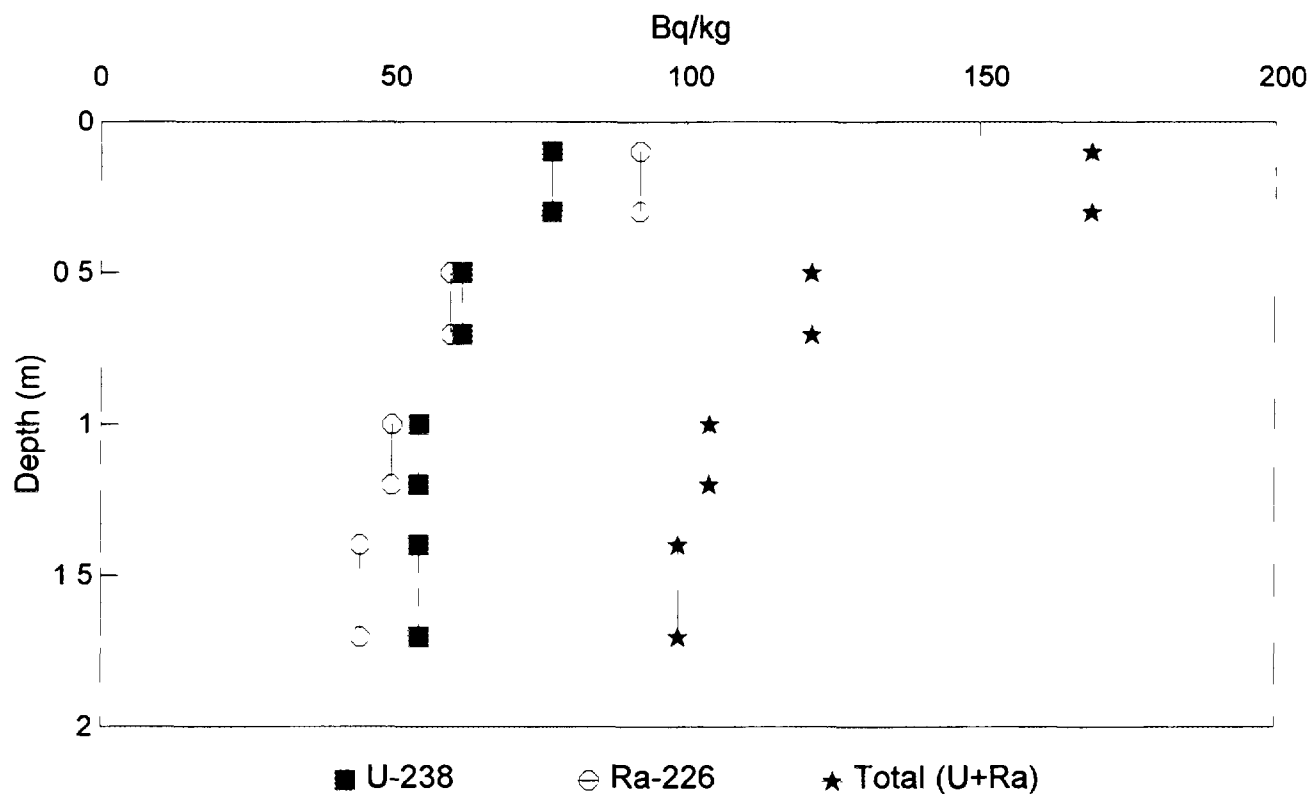


Fig. 9. Average activity versus depth.

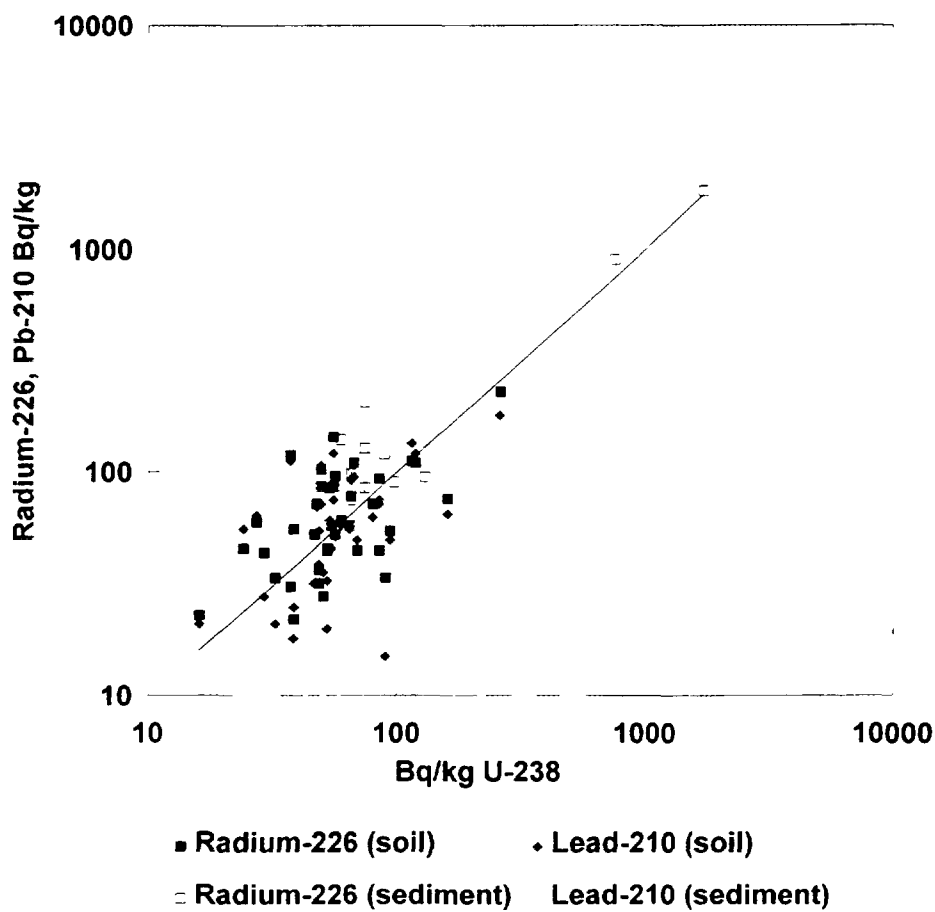


Fig. 10 Ra-226 and Pb-210 versus U-238.

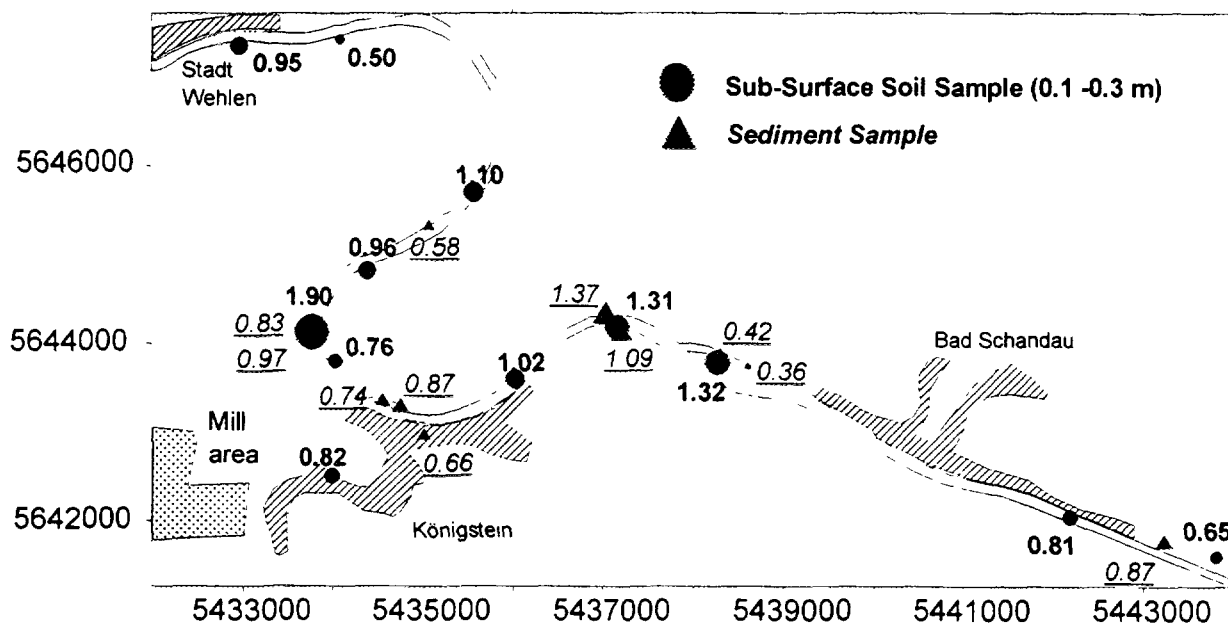


Fig. 11. U-238/Ra-226 ratios in soil (0.1-0.3 m) and sediment samples.

TABLE I. DISTRIBUTION OF ACTIVITIES/CONCENTRATIONS IN SUB-SURFACE SAMPLES

	PARAMETER						
	²³⁸ U	²²⁶ Ra	A	Ni	Pb	Cu	Zn
	Bq/kg	Bq/kg	ppm	ppm	ppm	ppm	ppm
minimum at 0.1–0.3 m depth	27	58	12	31	57	28	97
maximum at 0.1–0.3 m depth	260	230	54	63	148	119	696
average at 0.1–0.3 m depth	77	103.5	31	44	96	75	411
minimum at 1.0–1.2 m depth	24	31	8	5	14	3	10
maximum at 1.0–1.2 m depth	160	85	17	27	57	29	150
average at 1.0–1.2 m depth	54	50	12	18	30	16	66
average of concentration ratios avg(conc.@0.1–0.3m/conc.@1.0–1.2m)	1.5	2.1	2.5	3.1	3.7	6.0	9.5
harbor sediment maximum	130	206	75	134	216	244	1347

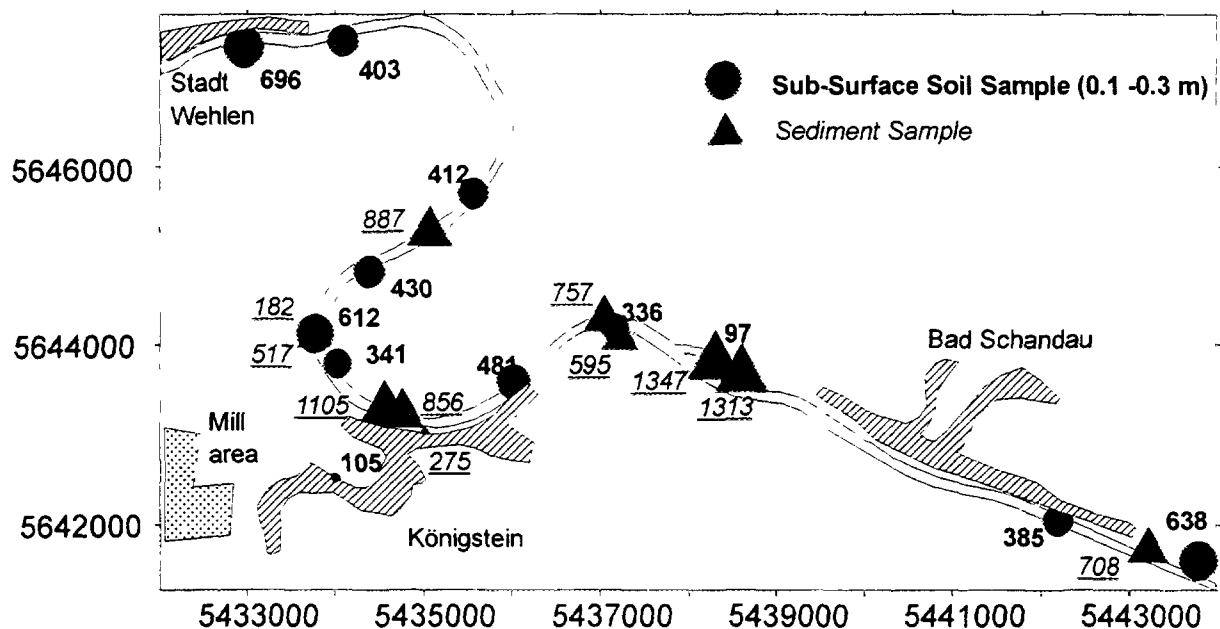


Fig. 12. Zinc in soil (0.1-0.3 m) and sediment samples (ppm).

5. CONCLUSION

Historical exploration data represent a source of valuable information for the environmental assessment of sites near former uranium mine and mill facilities. The value of airborne spectrometric data in connection with mine and mill remediation is, thereby, mainly in outlining large areas with potentially contaminated sites. The characterization and definition of such sites requires detailed ground investigation. Although the anomalies detected by the airborne survey in the Königstein area did not delineate locations requiring remediation, the data resulting from ground follow-up investigations provided an explanation for the change of radionuclide concentrations in river bank soils. In particular, the following results were obtained:

- flooding events resulted in dispersion, dilution and burial of radionuclides,
- as far as anomalies upstream of the Königstein mine are concerned, a source in the Czech republic must be considered, and
- the ground follow-up delineated a new anomalous zone that is caused by radionuclides discharged with treated process and mine water. It is the only area, which may require further investigations and possible remedial action.

In addition, the follow-up data show that the radionuclide source causing the airborne radiometric anomalies was related to mine water discharge rather than the release of residue from uranium ore processing, after deposition, uranium has been chemically mobilized, and additional base metal contamination is possibly related to the use of the Elbe river as shipping route.

ACKNOWLEDGEMENTS

The authors thank Wismut-GmbH for permission to publish the data on the airborne and ground surveys. Dr. H. Schubert of Geophysik GGD is thanked for helpful discussion of radiometric data and their interpretation.

REFERENCES

- [1a] BMWi, Wismut — State of Decommissioning and Remediation, BUNDESMINISTERIUM FÜR WIRTSCHAFT, Federal Ministry of Economics; Documentation No. 335.
- [1b] BMWi, Wismut — Fortschritte der Stilllegung und Sanierung, BUNDESMINISTERIUM FÜR WIRTSCHAFT, Federal Ministry of Economics; Documentation No. 370.
- [2] SCHUBERT, H. HESSE, R., Studie zur Untersuchung der durch Aerogammaspektrometrie markierten Gammaanomalien in der Elbtalaue zwischen Pirna und Schmilka, Geophysik GGD Leipzig (1994).
- [3] UHLENBRUCK, H., HOLZHAUER, U., BACHNER, D., BIESOLD, H., "Radiologische Erfassung, Untersuchung und Bewertung bergbaulicher Altlasten in den neuen Bundesländern", Altlastensanierung '93, (ARENDT, F., ANNOKKEE, G.J., BOSMAN, R., VAN DEN BRINK, Eds.), Kluwer Academic Publishers (1993) 807–814.
- [4] BARTHEL, F. H., Die Urangewinnung auf dem Gebiet der ehemaligen DDR von 1945 bis 1990, Geol. Jb., A142, 335–346, 1993.
- [5] LANGE, G., MÜHLSTEDT, P., FREYHOFF, G., SCHRÖDER, B., Der Uranerz- Bergbau in Thüringen und Sachsen — ein geologisch-bergmännischer Überblick, Erzmetall 44 Nr. 3 (1991) 162–171.
- [6] DAHLKAMP, F. J., Uranium Ore Deposits, Springer Verlag Berlin Heidelberg (1993).
- [7] LANGE, G., "Technical rehabilitation options for former mining and milling facilities of Wismut GmbH", Planning and Management of Uranium Mine and Mill Closures, TECDOC-824, IAEA, Vienna (1995).
- [8] ZIEGLER, P.A., Geological Atlas of Western and Central Europe, Shell Internationale Petroleum Maatschappij B.V., Elsevier Scientific Publishing Company, Amsterdam (1982).
- [9] MAGER, D. VELS, B., Wismut: An example for the uranium industry in Eastern Europe? (Proc. Seventh Int. Symp. Uranium Institute, London, 9-11 September 1992).



THE DISTRIBUTION OF RADIONUCLIDES IN THE UPPER SOIL HORIZONS IN LOWER SAXONY, SAXONY AND THURINGIA, GERMANY

F. BARTHEL, V. THOSTE

Federation Institute for Geoscience and Natural Resources,
Hannover

K.H. BORSDORF

Federal Institute for Radiation Protection,
Berlin

Germany

Abstract

After the Chernobyl accident the Federal Institute for Geoscience and Natural Resources carried out a scintillometer and soil sampling survey to monitor the terrestrial gamma radiation in the states of Lower Saxony (1987–1988), Thuringia (1991) and Saxony (1992). The results of the single surveys in Lower Saxony, Thuringia and Saxony have been described in former reports (BECKMANN, FAAS, 1992; BORSDORF, MALINOWSKI, 1995; BARTHEL, BORSDORF, MALINOWSKI, THOSTE, 1996). Within the scope of terrestrial radiation assessment the main interest was to differentiate gamma radiation caused by geogene radionuclides from that caused by fallout nuclides or contamination from uranium mining and milling. The field readings of the scintillometers were correlated against readings of calibrated instruments and the values were corrected for cosmic radiation and background radiation from the instruments. The final data were expressed as exposure rate to terrestrial gamma radiation (nGy/h) and ambient energy dose rate (nSv/h). The calibration work was done by the Federal Institute for Radiological Protection, Berlin. To demonstrate the distribution of terrestrial gamma radiation in Lower Saxony, Thuringia and Saxony, the field data (3487 measurements, 4 by 4 km grid) were processed by UNIRAS software and printed as isoline maps. Additionally at 334 sites soil samples were collected and analysed with a pure Ge-detector. The isoline maps show anomalous exposure rates of 100 to <140 nGy/h over the southeastern part of the Harz Mountains, the Thuringian Mountains, the western part of the Erzgebirge and the Vogtland. Within the low land regions of Lower Saxony, the Thuringian basin and regions in Saxony north of the Erzgebirge moderate values of 50 to 90 nGy/h dominate. The high regional exposure rates correlated with high concentrations of K-40, Ac-228 (Th-232 decay chain) and Ra-226 (U-238 decay chain) in the soils. In the same areas Cs-137 reaches the highest concentrations of 40 to >60 Bq/kg in soil samples. In Thuringia and Saxony it is difficult to detect eight years after the Chernobyl accident any correlation of the regional distribution pattern of Cs-137 fallout with heavy rainfalls in May 1986. Only one anomaly in the western Erzgebirge shows the well known NNW trend, which was recognized from fallout measurements directly after the accident in Lower Saxony. No anomalous contaminations were detected around the uranium mining areas of the former WISMUT SDAG in the Ronneburger and Aue districts. The environmental exposure rates fall in the range of <200 nGy/h. The general results indicate, that today there is no large scale contamination existent, either from fallout or from uranium mining, which could cause radiological health hazards to the population.

1. INTRODUCTION

The external radioactivity of the human environment exists of radiation of cosmic and terrestrial origin. The cosmic component originates from the reaction of cosmic radiation with the atoms of the upper atmosphere. It varies with elevation above the ground. The sources of terrestrial radiation are concentrations of geogene radionuclides in the rocks, the soil, the water and the atmosphere near the ground. Near the ground some gaseous radionuclides such as radon are very important.

Since the introduction of nuclear energy, artificial radionuclides too contribute to the external radiation. The sources of artificial radionuclides are nuclear explosions, escape from nuclear reactors or from their use as tracers or radiation sources in medicine. By far the most radioactive contamination of the environment originates from nuclear bomb tests in the atmosphere (1945–1991) and accidents in nuclear power stations.

After the Chernobyl reactor accident, the environmental radioactivity in several areas in Europe rose by a factor of ten, depending on the rate and direction of radionuclide transport under atmospheric conditions. The degree of contamination was closely connected to the intensity of fallout and washout during rainfalls in the period 1 to 4 May 1986. Especially the southern part of Germany was contaminated with the radionuclides Iodine-131, Ruthenium-103, Cesium-137 and Cesium 134. In Fig. 1 the readings of a NaI-scintillometer uranium prospecting survey show how much the fallout sources contributed to the total terrestrial radioactivity in the days directly after the fallout.

In 1986 the Federal Institute for Geosciences and Natural Resources, Hannover (Germany) started detailed investigations in Lower Saxony to prove how much the radiation from the artificial radionuclides contributed to the terrestrial radiation. After German reunification, the survey was extended to the states of Thuringia and Saxony. An important problem which these investigations were designed to resolve was whether additional contamination from uranium mining and milling was present. In Thuringia and Saxony uranium mining and milling was carried out between 1946 and 1990 by the former WISMUT SDAG. After reunification, uranium production was stopped because it was uneconomic under international market conditions. Over the years, mining and milling produced large amounts of waste, much of it as fine grained residues, of which the tailings of the Ronneburger and Aue mining districts produce the largest environmental impact. Much of the waste from underground mining and open pits was used for road making and other purposes. Because of this, it was expected that much contamination could exist in the area surrounding the mines and mills. To detect and analyse the type of contamination, the Federal Institute for Radioprotection is carrying out an extensive project entitled "Radiological survey to investigate and evaluate abandoned mining sites in Saxony and Thuringia". An initial evaluation yielded 5000 contamination points in an area of about 1500 km². In the second phase of the project a contaminated area of 250 km² was selected for rehabilitation.

2. ENVIRONMENTAL GAMMA RADIATION

2.1. Measurement of Terrestrial Gamma Radiation

To monitor environmental radioactivity levels after the Chernobyl accident, the BGR carried out scintillometer surveys during 1991 and 1992 on grassland in Thuringia and Saxony.

The density of the grid was six to eight points/100 km², thus allowing washout areas, which are normally about 4 km wide and several tens of kilometres long, to be detected. Each measuring point is representative of one ha (100 × 100 m = 10 000 m²). When counts rates clearly over the normal background were obtained, the grid was narrowed in order to detect the source. The program excluded active mining areas, industrial centres and residential areas. A total of 2164 measurements were taken (see Fig. 2), of which 1138 are located in Thuringia and 1026 in Saxony.

Two types of portable NaI scintillometer were used to measure the gamma radiation in the field; one NaI scintillometer (Type SPP 2 Saphymo Stel) to record the gamma rays with energies > 30 keV and a 3-channel scintillometer to record the count rates in channel A > 300 keV, channel B > 900 keV and channel C > 1400 keV. The gamma radioactivity with these instruments is expressed in counts per second (cps). The detectors were put on the ground. In view of the fact that clayey soil absorbs gamma rays from geogene radionuclides (maximum energy Tl-208 = 2.62 MeV, half-thickness $X_{1/2} = 7.82$ cm), it was calculated that nearly all gamma rays detected originated from a spherical volume with a radius of 108 cm (DURRANCE 1986).

The count rates of the SPP 2 scintillometer were correlated against a calibrated dose-meter using the following formula:

$$x = y \cdot 0.814 + 22.7 \quad (x = \text{reading in nGy/h, } y = \text{reading in cps}).$$

Fig 1. Radiometric effects of Chernobyl Fallout to terrestrial gamma radiation
Anomaly 6/1 Ruppertsgrün

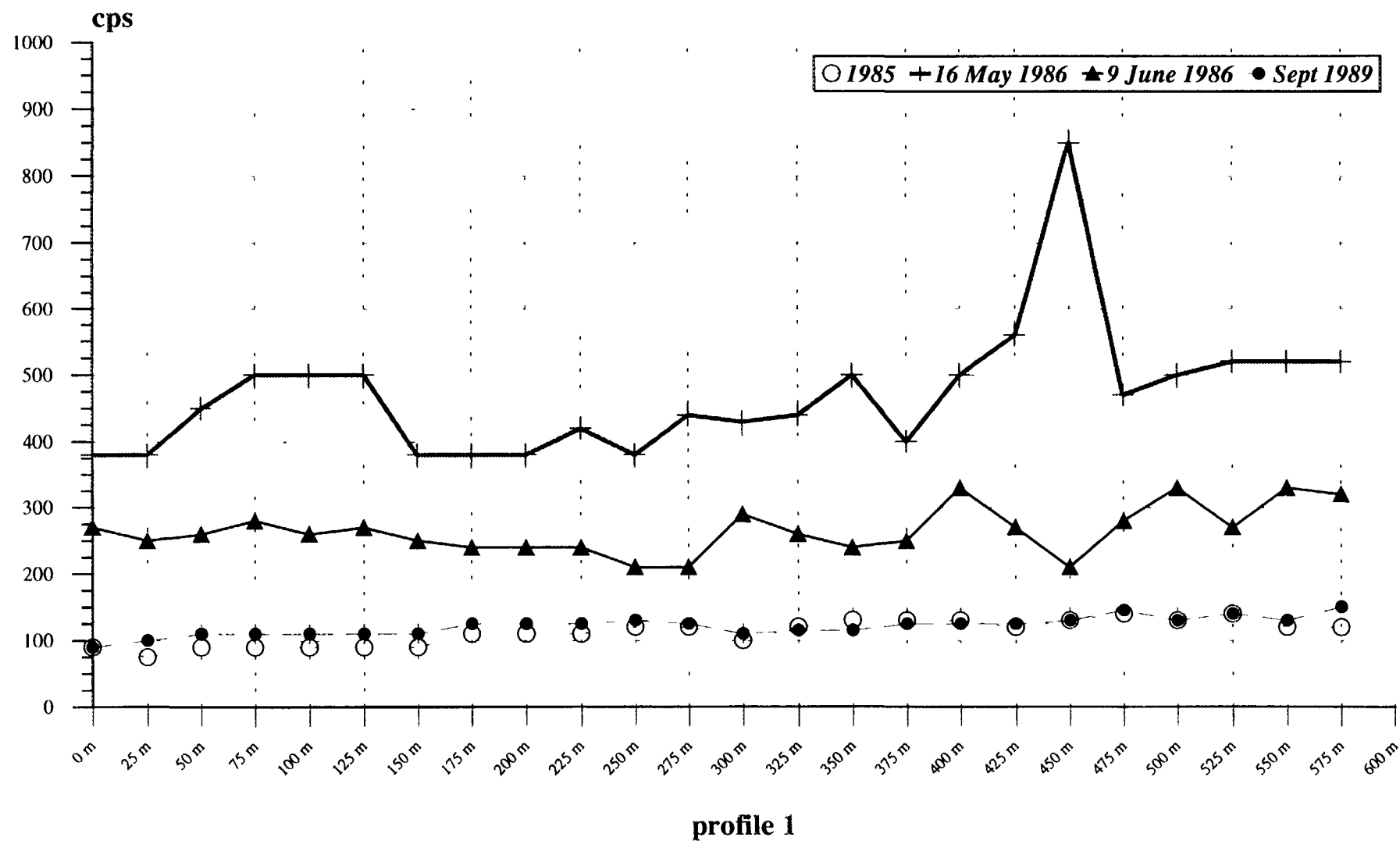


Fig. 1. Radiometric effects of Chernobyl fallout to terrestrial gamma radiation.

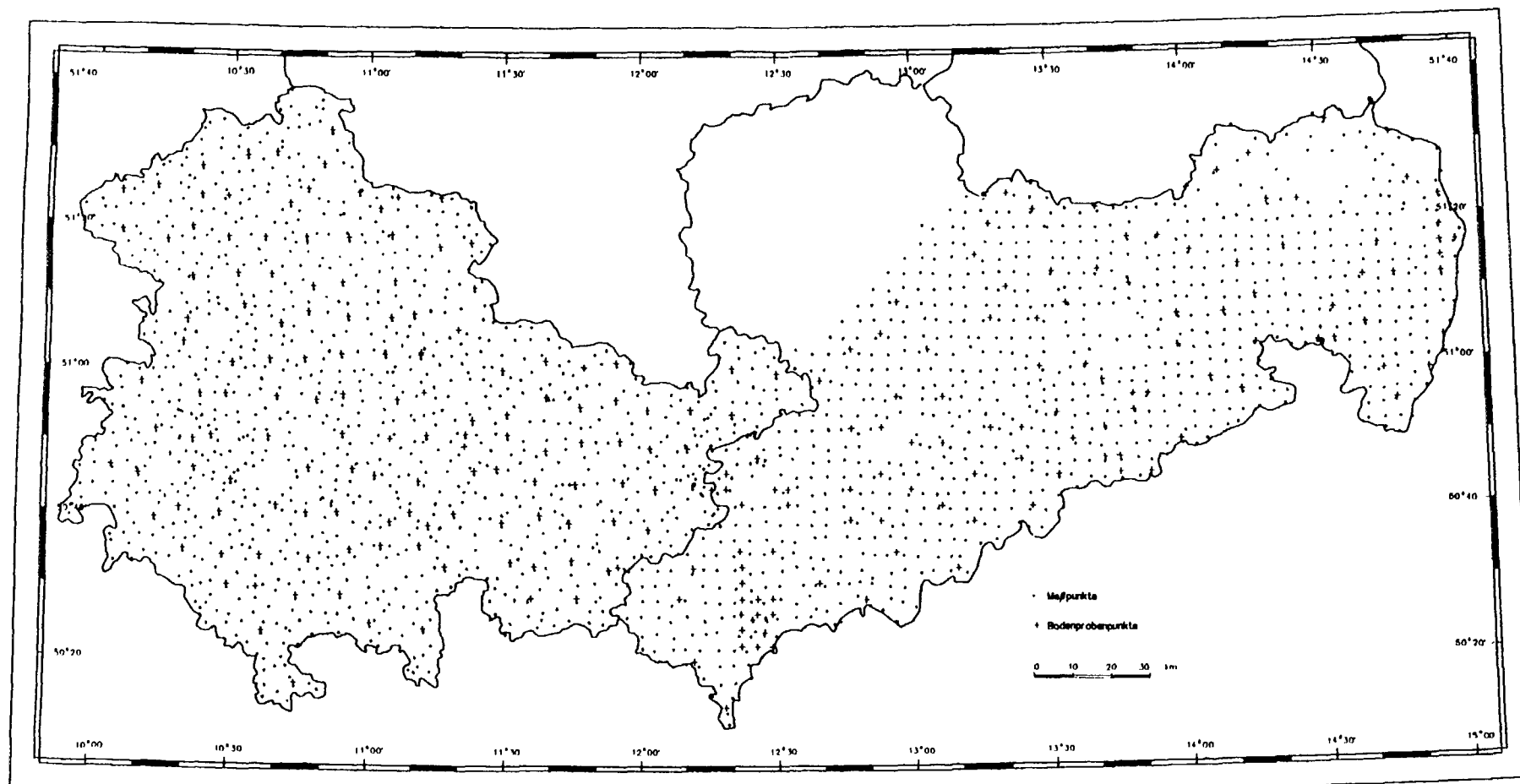


Fig. 2. Regional distribution of gamma ray measurement and soil sampling localities.

The correlation diagram is shown in Fig. 3 a. Then the regional distribution of energy dose rates was calculated using a contour program and plotted on maps at a scale of 1: 100 000. At the

Fig. 3 a Correlation cps / nSv/h (SPP2/ BfS Ref.)

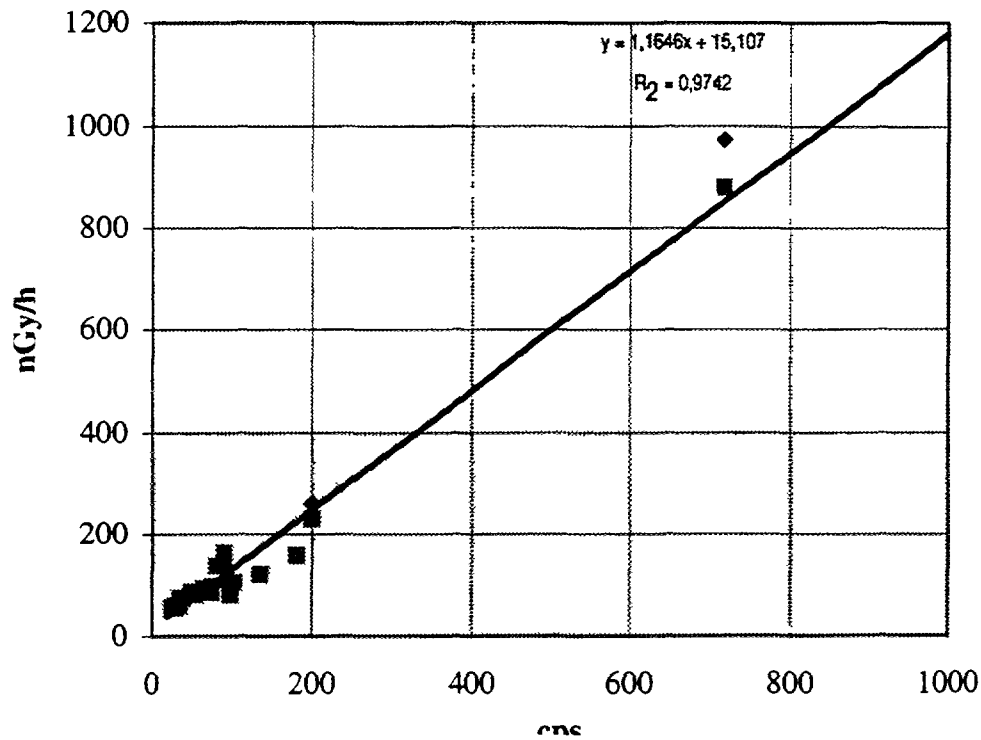


Fig. 3a Correlation of scintillometer (cps) and dose meter units (nGy/h).

Fig. 3 b Correlation (A-B) / (B)

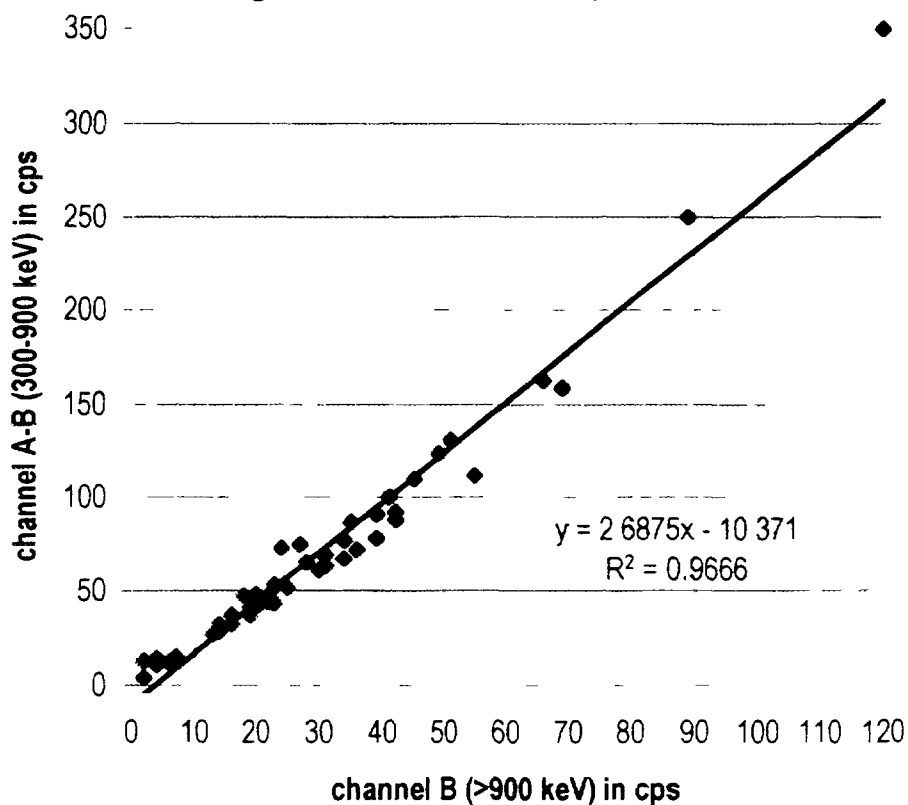


Fig. 3b Correlation of count rates in channel A-B (300–900 keV) and count rates in channel B (900–3000keV).

basis of the contour maps it was possible to eliminate areas with anomalous gamma energy dose rates and to calculate exposure rates (of the population) with respect to natural gamma radiation.

2.2. Conversion to External Gamma Ray Dose Rates (nSv/h)

The Federal Institute for Radiation Protection (BfS), Berlin-Karlshorst, is conducting measurements of the ambient gamma dose rate on a 4×4 km grid in eastern Germany. The program should be completed by the end of 1996. The field measurements are carried out with a portable calibrated gamma ray dose-meter. The field measurements are corrected for internal radiation and cosmic radiation. The instruments were calibrated for terrestrial gamma rays at the calibration facilities of the BfS in Berlin-Friedrichshagen, for cosmic radiation on a lake near Berlin and for internal radiation in a laboratory in the Asse salt mine (WILL, MIELCAREK & SARENIO, 1994).

The results of the BGR investigations from Saxony and Thuringia are incorporated in the background radiation measuring programme of the BfS. Correlation factors were established for the readings of the BGR scintillometers using special field calibration pads. After correction of the BGR records, it was possible to introduce the 2164 scintillometer readings into the new ODL programme (regional distribution of ambient gamma energy dose rate), in which terrestrial exposure is expressed in Nsv/h.

2.3. Regional Distribution of Gamma Ray Dose Rates

The dose rates vary in Saxony and Thuringia between 10.4 and 226.8 nSv/h (0.09–2 mSv/a, exposure time 365 days). The mean is 62 nSv/h with a standard deviation of 19.7. All readings are under the national recommended intervention value of 300 nSv/h. Only eight readings are higher than 160 nSv/h.

Fig. 4 displays the regional distribution of the ambient dose rate, which in some areas reflects the different geological units. Remarkable is the local occurrence of the main anomalies, which coincide with the highest elevations of the Thuringian Forest, the Vogtland and the Ore Mountains. The lowlands of eastern Saxony are characterized by values of 40–60 nSv/h. The radioactivity of the uranium- and thorium-rich granitic rocks of the Görlitz massif and that of the monzonites, syenodiorites and biotite granites of the Meissen intrusive complex is masked by the local soil. The soils consist mainly of clay and are often over 10 m thick. Clear elevated values of > 100 nSv/h occur over the of Kirchberg and Eibenstock intrusions, in the contact zone with Paleozoic rocks, in the Teplitz quarz porphyry and over acid and intermediate dyke rocks.

The uranium deposits of the Aue mining district, the Poehla-Globenstein district and the Freital area are inside these anomalies. The mining districts of Ronneburg, the middle part of the Ore Mountains and of Königstein do not display elevated dose rates. North of Zwickau, elevated values show up contamination derived from the mill at Crossen and contamination in the river valley of the Zwickau basin from uranium mining

2.4. Gamma Radiation from Chernobyl Fallout and Washout

In the context of the assessment of exposure to external radiation, it is important to investigate the degree of contamination of the soil in view of the fact that, during the first year after the Chernobyl accident, external soil radiation accounted for approximately 29% of the total dose for adults in Germany. A three-channel scintillometer was used to obtain an initial estimate of the artificial portion of the terrestrial radiation. This instrument divides the count rates into three channels: channel A > 300 keV, channel B > 900 keV, and channel C > 1400 keV. By subtracting the count rates of channel B from channel A, the counts in the energy range 300–900 keV are

obtained. In this channel the counts originating from the decay of Cs-137 (specific energy 661.6 keV, half-life 30.17 years) and Cs-134 (specific energy 795.8 keV, half-life 2.06 years) are collected. One problem is that, in the channel 300–600 keV, the Compton electrons generated by high energy decay of Bi-214, Tl-208 and K-40 are also counted. This fact is regarded of relatively little importance because the Compton-electron decay rate shows a fixed ratio to the photo-electrons and for the estimate of the artificial decay rate only the additional decay rate from the artificial nuclides in the channel 300–900 keV is important. This means that the higher the ratio of channel A-B/B is, the higher the count rate in the range 300–900 keV. The method was first successfully tested by the Geological Survey of Canada to search for debris from the Russian satellite cosmos (BRISTOW Q., 1978). BGR tested the same method directly after the Chernobyl accident in Lower Saxony. A combined soil sampling program proved that even concentrations of 40 Bq Cs-137 + Cs-134/kg soil are detectable. This was the reason for using the same method six years after the deposition of the nuclides in Saxony and Thuringia.

For the investigation of the count rates from geogene sources, measurements were carried out in open pits on fresh rocks with different radioactivity. The results show a good correlation of the ratio A-B/B (see Fig. 3b). The mean of the ratio of 34 measurements in Thuringia was 2.25 with a standard deviation of 0.36, in Saxony 55 measurements gave a mean of 2.19 with standard deviation of 0.27. The regional distribution of the ratio of count rates in channel A-B versus channel B is shown in Fig. 3b.

In Thuringia 1146 soil measurements gave a mean of the ratio of 2.29 (standard deviation 0.27) and in Saxony 905 soil measurements 2.27 (standard deviation 0.33). In comparison to Thuringia, the total count rate in Saxony is generally higher because of the elevated natural radioactivity of the granitic rocks.

In Saxony and Thuringia the regional distribution of the ratio (contour maps) does not show clear anomalies. Weak anomalies ($A-B/B > 2.9$) are visible over the highest elevations of the mountains. In the east of Saxony one anomaly near the border to Poland is clearly visible. This anomaly proves the sensitiveness of the method, because scintillometer readings are only 35 to 60 cps and the specific radioactivity of Cs-137 is 31–40 Bq/kg. The high ratio contains almost no rock radioactivity component although small concentrations of the fallout nuclide Cs-137 are present.

Based on the results of the radiometric survey of Lower Saxony directly after the Chernobyl fallout (BECKMANN C. & FAAS C., 1992), it can be stated that in 1991/92 only relics of fallout anomalies are existent in Saxony and Thuringia. The relics are the remainder from the washout from rainfalls in May 1986. The washout was concentrated to three rainfall areas that strike NNW-SSE and are still present on the highest elevations of the Thuringian Forest, the Vogtland and western Ore Mountains. A small anomaly at the border to Poland is part of another fallout region.

3. SOURCES OF TERRESTRIAL GAMMA RADIOACTIVITY

3.1. Soil Sampling and Measurement of Activity Concentrations

Soil samples were taken at 259 different localities (138 in Thuringia and 121 in Saxony) to determine their specific radioactivity. In Thuringia soil sampling was carried out at the intersections of grid lines with a spacing of 10×10 km. At each grid point four samples were taken on flat ground from undisturbed grassland along one diagonal of a 100×100 m square. In Saxony the same method was applied; however, the sampling density was increased in areas of elevated radioactivity. Plant material, roots and rock fragments > 1 cm were removed from the individual samples. Then the samples were mixed to obtain a composite sample representative of a sampling area of $10\,000$ m². To calculate the bulk density, the mass of the soil with a given volume was determined in both wet and dry condition. Each composite sample was dried at 106°C for 24 h and then crushed in a mortar. After sieving, the < 2 mm fraction was stored in a gas-proof container for 20 days before gamma

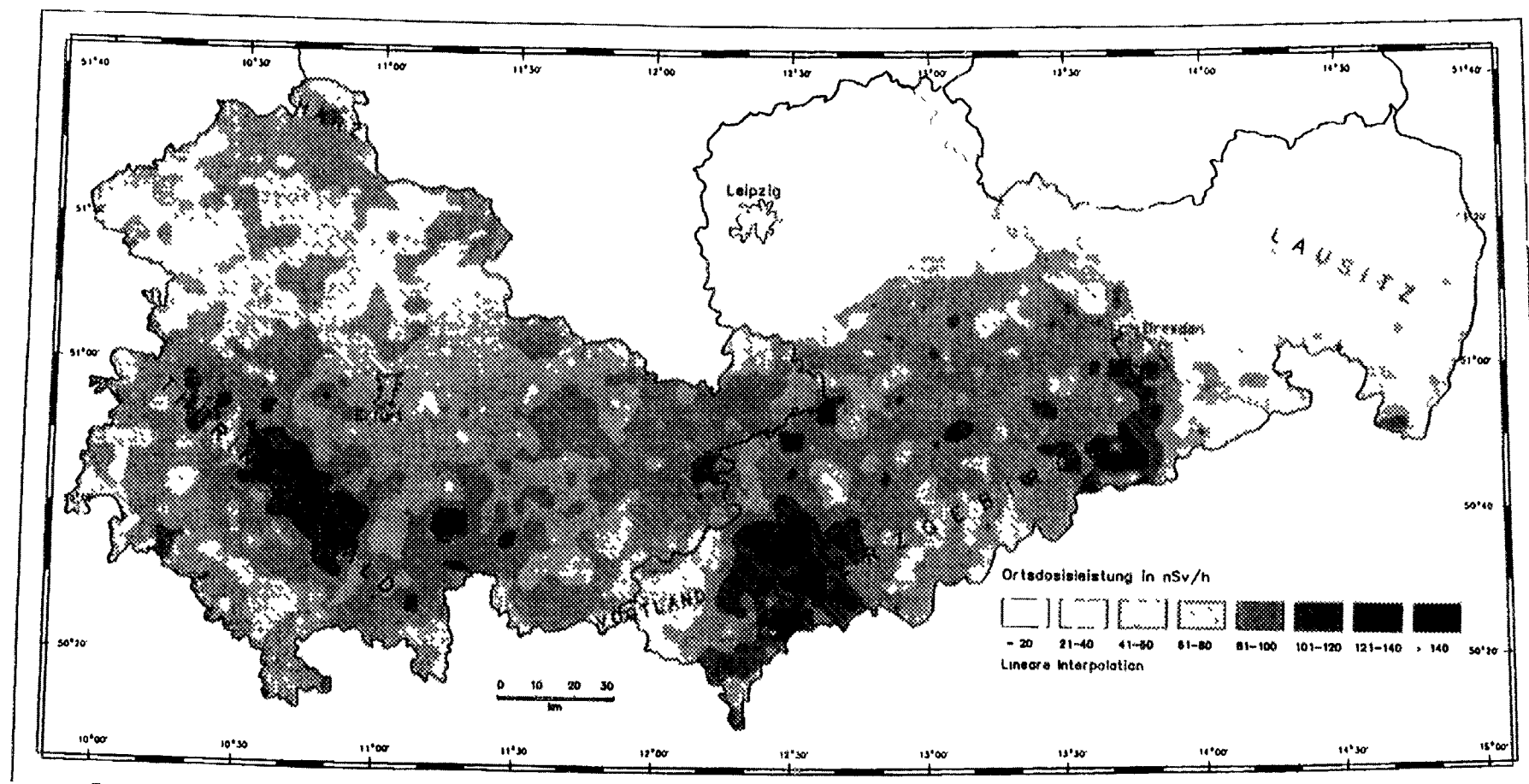


Fig. 4. Regional distribution of ambient energy dose rates.

spectrometry measurements were carried out (Ge detector, volume 126 cm³). The detection time for each sample was 1000 to 2000 seconds, depending on their relative radioactivity. The total error of the gamma activity measurements, comprising the sampling error and the experimental error, was about 25%. The specific activities were expressed in concentration of nuclides Bq per kg dry mass of soil. Table I shows the radionuclides and the specific energies at which they were determined.

Tab. I. EXAMINED RADIONUCLIDES IN SOIL SAMPLES

Radionuclide	Energy in keV	Land
K-40	1460.8	Saxony, Thuringia
Ac-228	911.0	Saxony, Thuringia
Th-232 via Ac-228, Pb-212, Tl-208		Saxony
Th-234 (U-238)	63.3	Thuringia
Ra-226 (U-235) via Pb-214, Bi-214	186	Saxony
Pb-210	46.5	Saxony
U-235	185.7	Saxony
Cs-137	661.6	Saxony, Thuringia
Cs-134	795.8, 605	Saxony, Thuringia

The concentrations of Th-234 (U-238 decay chain), Ac-228 (Th-232 decay chain) and K-40 were used as reference nuclides for the concentrations of natural radioelements in Thuringia, whereas Ra-226 was determined in addition in the samples from Saxony (BORSODORF et al. 1995). For reference purposes the activities of the artificial nuclides from the Chernobyl fallout were recalculated to the 1 July 1991.

3.2. Concentrations and Regional Distribution of Naturally Occurring Nuclides

Potassium-40 (Fig. 6)

Natural potassium contains 0.012% K-40. K-40 decays with the emission of gamma and beta radiation and has an extremely long half-life of 1280 million years. The specific radioactivity of K_{nat} is 30.9 Bq/kg K. Therefore it is possible to determine the natural potassium content from the concentrations of the specific radioactivity of K-40.

The soil samples investigated in our study show a range of specific radioactivities of K-40 between 114 and 1480 Bq/kg, mean 645 Bq/kg. In 75% of the samples investigated, the specific radioactivity varies between 400 and 800 Bq/kg. Of all the naturally occurring nuclides, K-40 contributes the highest amount of gamma radiation to the terrestrial radioactivity. The regional distribution of K-40 concentrations shows some relationship to the petrography of the underlying rocks, especially to porphyritic K-feldspar granites and contact rocks. Anthropogenic input due to fertilizers may influence the pattern to a minor degree.

The regional distribution of K-40 concentrations is shown in Fig. 6. The lowest concentrations were obtained in the sandy regions of the lowlands in NE Saxony and northern Thuringia. The mountainous regions of the Ore Mountains (Erzgebirge) and the Thuringian Forest generally show enhanced concentrations. Anomalous concentrations with > 1000 Bq K-40/kg were observed in soils over the granites of the Western Ore Mountains and on granites and porphyries of the Eastern Ore Mountains. In the Thuringian Forest enhanced K-40 concentrations are due to soils on acidic volcanic rocks of Permian age. In the lowlands of Saxony and Thuringia, only those regions show elevated concentrations, where the Permian rocks are covered by loess and brown podsol soils.

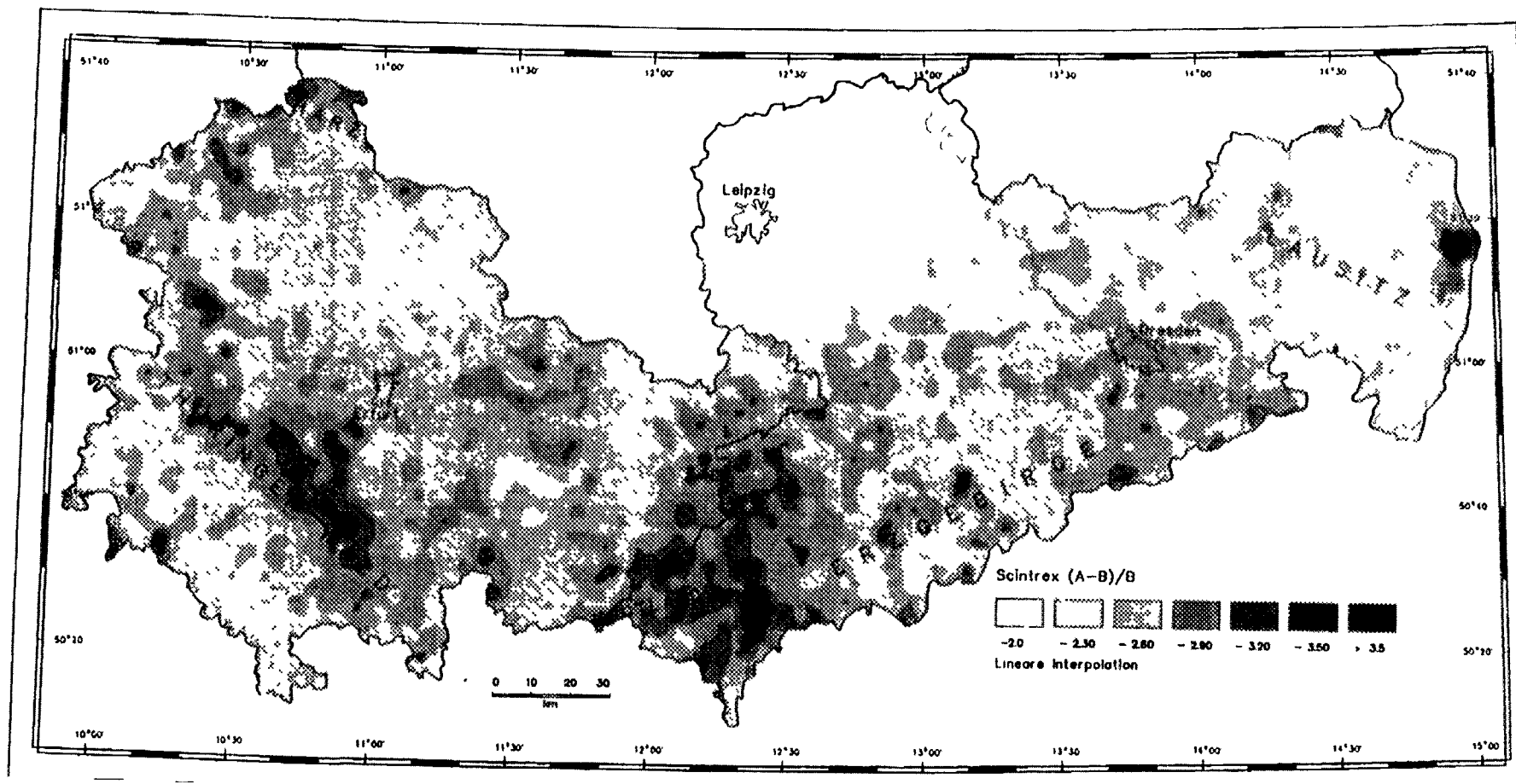


Fig. 5. Regional distribution of ratio of count rates in channel A-B (300-900 keV) and channel B (> 900 keV).

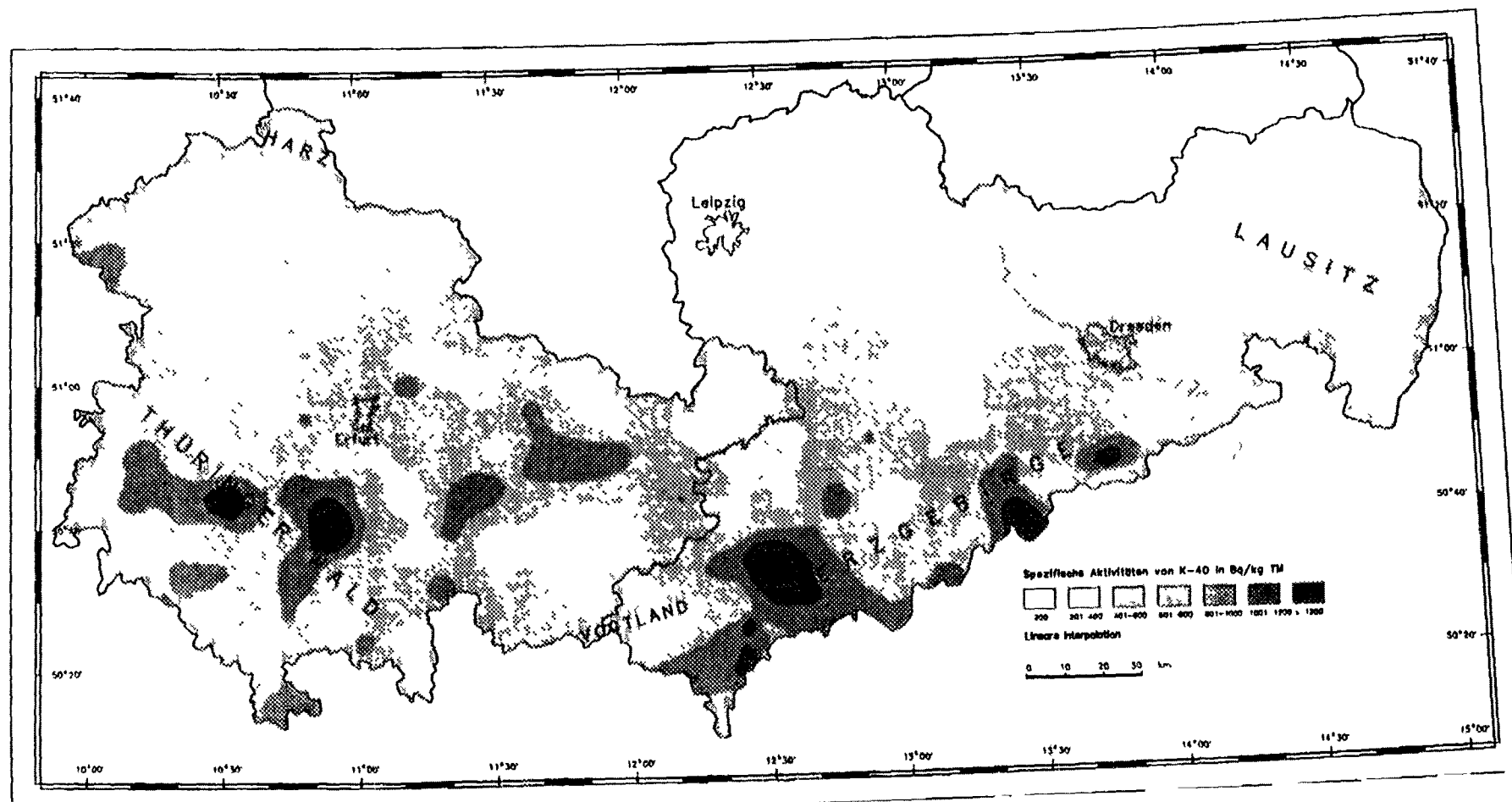


Fig. 6. Regional distribution of K-40 concentrations in the upper soil horizons of Thuringia and Saxony.

Actinium-228, Thorium-232 decay chain (fig. 7)

Ac-228 is the second daughter of the Th-232 decay chain. Its half-life is 6.13 h and it is easily recognizable from several energy peaks. The 911 keV peak was used for measurement of the specific radioactivity of the soil samples. Under normal natural conditions, thorium and its immediate decay products are generally immobile.

The distribution of Ac-228 concentrations are shown in Fig. 7. The average of all samples is 40.3 Bq/kg (standard deviation 15.8). Enhanced concentrations of Ac-228 (> 100 Bq/kg) are strictly related to the Kirchberg Granite in the western Ore Mountains and to rhyolites in the Zinnwald area in Saxony. In Thuringia, enhanced values of Ac-228 (> 60 Bq/kg) occur in soils over Permian rhyolites of the Zella-Mehlis and Ilmenau areas. The thoriferous minerals in the underlying rocks seems to be the source of the specific radioactivity.

Radium-226 and Thorium-234, U-238 decay chain (fig. 8)

Ra-226 (alpha and beta decay) has a half-life of 1600 years. Its geochemical behaviour is different from the behaviour of its parent U-238. This is the reason why it can be separated from U-238 during weathering or hydrothermal processes. Both enrichment and depletion of Ra-226 in relationship to U-238 was observed. As Ra-226 is followed in the decay chain by radon-222 its concentration is important for the calculation of the radon exhalation rate of a soil. The distribution of Ra-226 concentrations were investigated in Saxony to detect the impact of previous uranium or silver/cobalt mining activities.

In Saxony the concentration of Ra-226 varies between 30 and 70 Bq/kg (mean 46 Bq Ra-226/kg, standard deviation 25 Bq/kg). The lowest value measured was 5, and the highest 151 Bq Ra-226/kg. From the regional distribution, it can be concluded that the Ra-226 content is mainly due to its natural occurrence in the rocks; however, enhanced values along the crest of the Ore Mountains could indicate some artificial input due to fallout from combustion of lignite in northern Bohemia. The anomalies over the Eibenstock and Kirchberg Granites (HHM granites) in the Ore Mountains are clear indicators of geogenic sources.

For Thuringia the analysis of Th-234 was chosen to determine the concentration of uranium-238 in the soil. The main concentrations vary from 80 to 400 Bq Th-234/kg, some anomalous values above 700 Bq/kg were obtained from samples of soils (brown podsolc soil) over rhyolites of Carboniferous age from the Thuringian Forest. Loess and brown podsolc soil samples from the Triassic of the Thuringian basin show the lowest activities (< 200 Bq Th-234/kg).

3.3. Concentration and Regional Distribution of Fallout and Washout Radionuclides

Cesium-137, Cesium-134 (Fig. 9)

The artificial radionuclides Cs-137 and Cs-134 were transported by clouds from the Chernobyl reactor site to Saxony and Thuringia at the beginning of May 1986. The radionuclides were deposited by washout on to the surface of the vegetation and soils. On account of the short half-life of most of the radionuclides, only cesium-137 and cesium-134 are detectable 10 years after the deposition. Besides Chernobyl cesium, a small concentration of cesium from nuclear weapon tests carried out in the 1960s is also present in the soil samples.

In 1994 only cesium-137 was detectable in measurable quantities in the soil samples from Saxony and Thuringia. Owing to its short half-life of 2.06 years, Cs-134 was only detectable in few samples. In most of the samples the concentrations were below the detection limit.

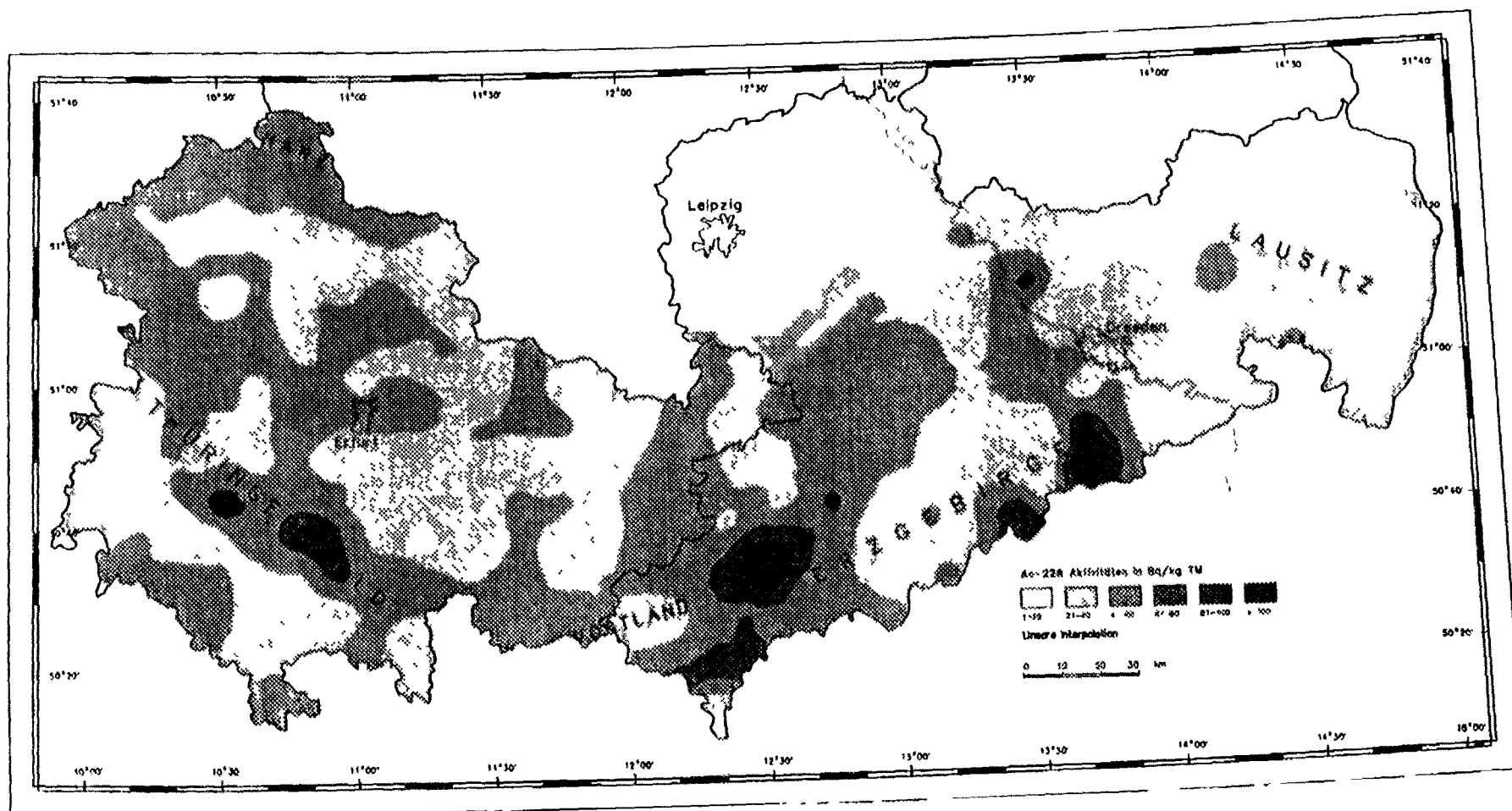


Fig. 7 Regional distribution of Ac-228 concentrations in the upper soil horizons of Thuringia and Saxony.

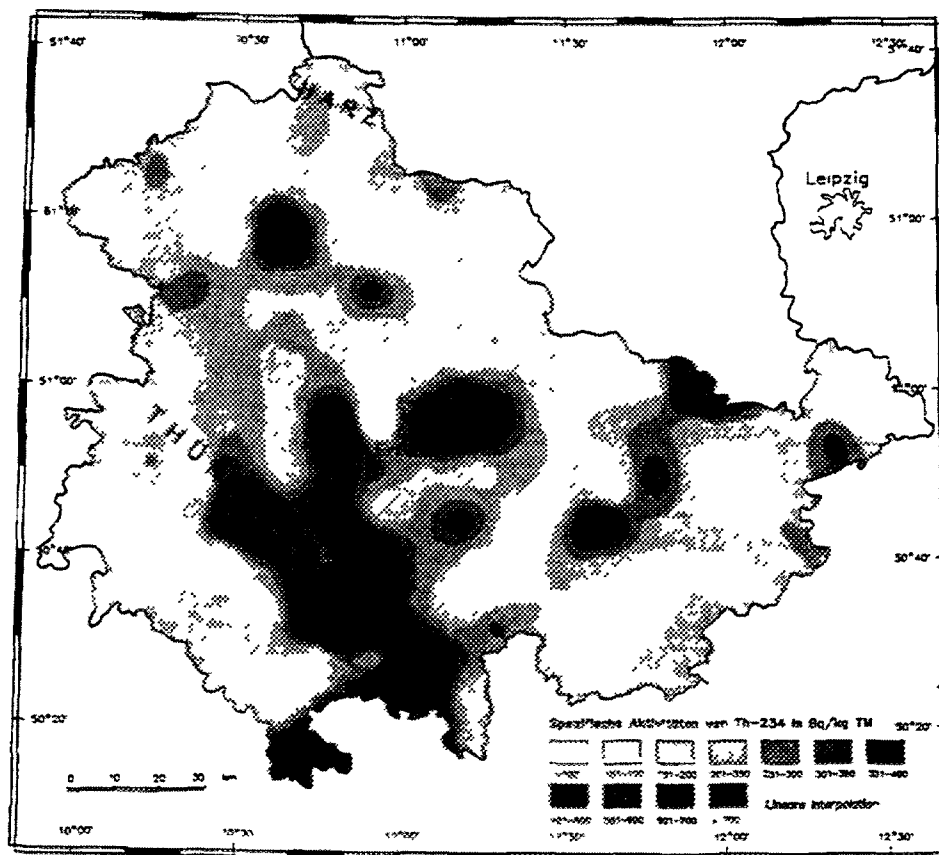


Fig. 8a Regional distribution of Th-234 concentrations in Thuringia.

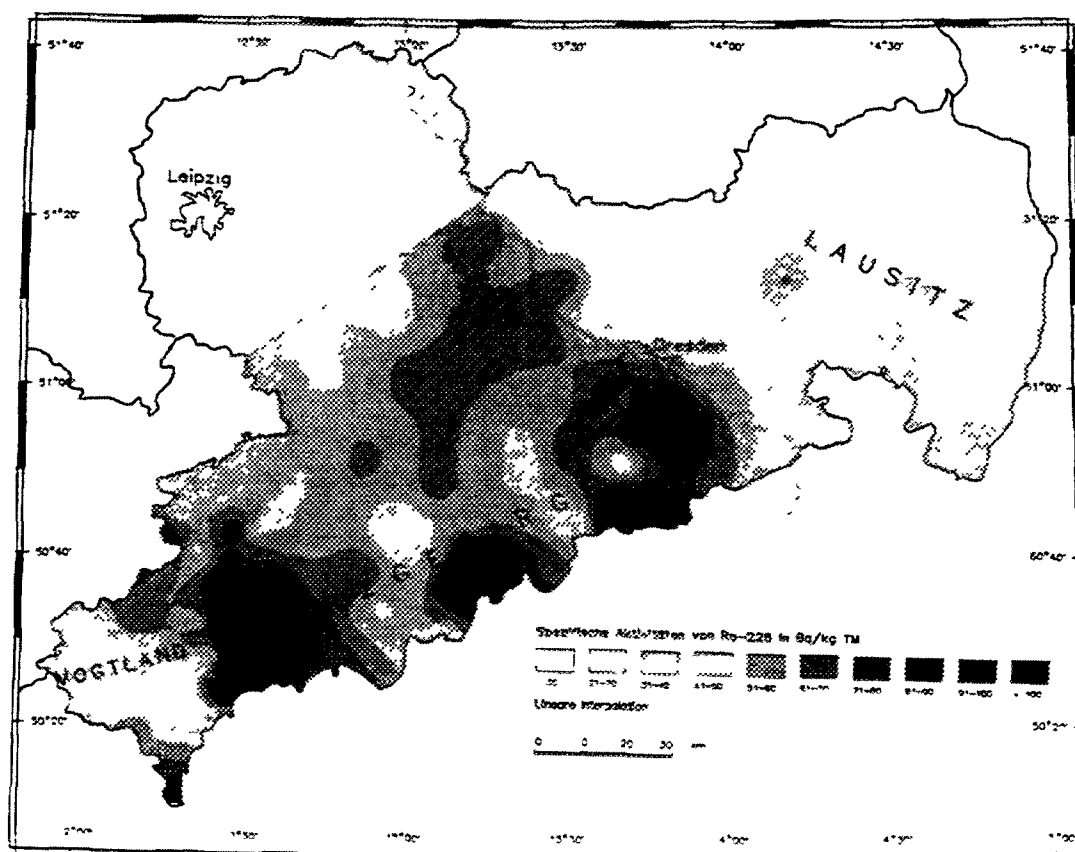


Fig. 8b Regional distribution of Ra-226 concentrations in the upper soil horizons of Saxony.

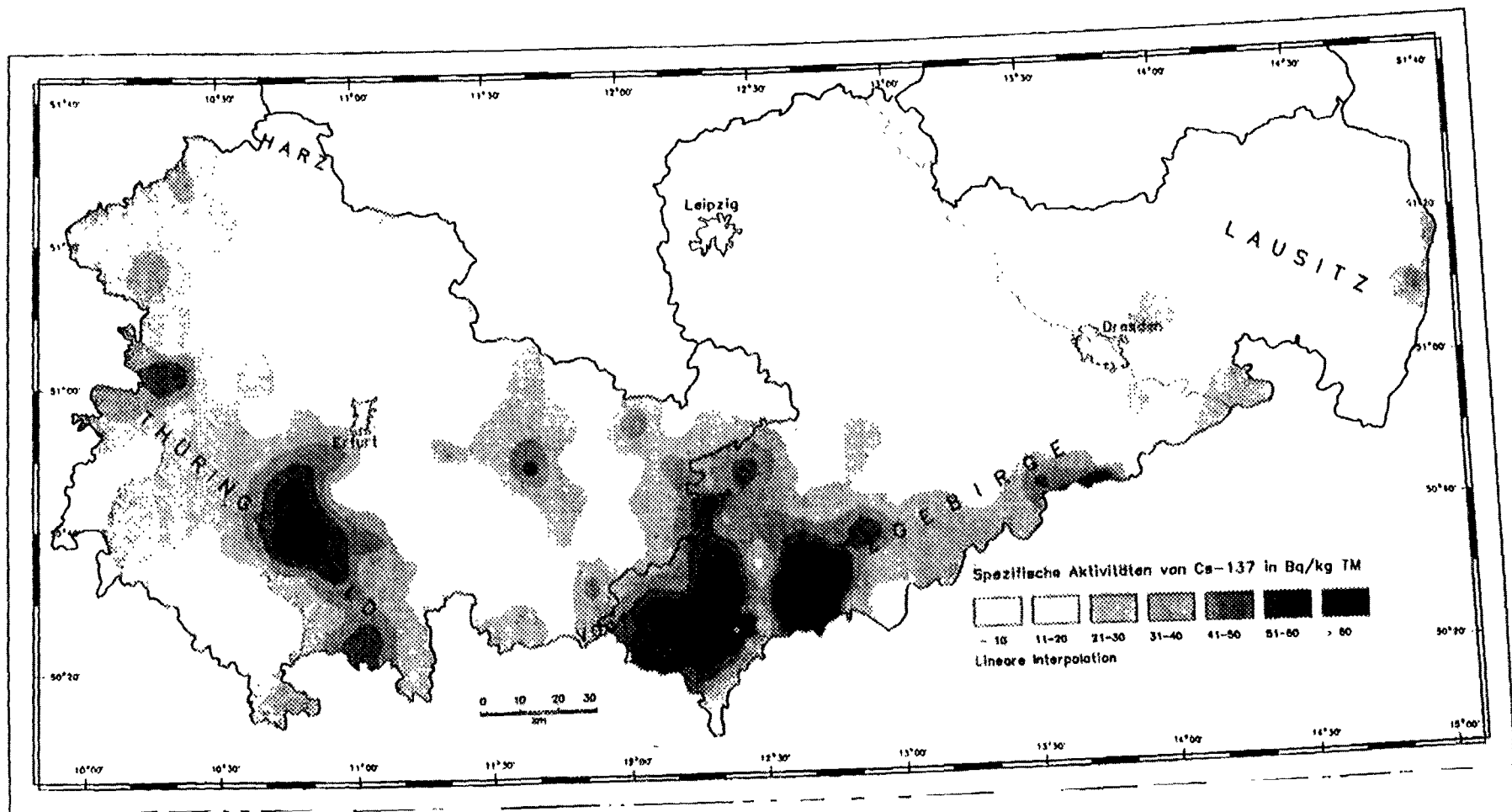


Fig. 9. Regional distribution of Cs-137 concentrations in the upper soil horizons of Thuringia and Saxony.

The majority of the samples have cesium-137 concentrations between 10 and 30 Bq/kg (mean Thuringia 20.3 Bq/kg, standard deviation 11 Bq/kg). Maximum values of > 50 Bq/kg have been measured in soil samples from sampling localities in the upper part (600–1000 m above m.s.l.) of the Thuringian Forest, the Vogtland and the Ore Mountains. The northern Thuringian Basin and the lowlands of Saxony (150–250 m above m.s.l.) are characterized by low concentrations (< 10 Bq/kg).

Fig. 8 shows the regional distribution of the concentrations of Cs-137 in the upper soil horizons in Thuringia and Saxony.

3.4. Interpretation of Regional Radionuclide Distribution

According to DURRANCE (1986) and SARENIO (1994), the concentration of radionuclides in the upper 30 cm of the soil are responsible for most of the gamma rays reaching the detector. The measurements of the ambient dose rate are therefore closely related to radionuclide concentrations in this part of the soil profile. As the spectrometric results show, nearly all fallout and washout radionuclides are enriched in the upper soil horizons. Generally the soil is a open geochemical system, where the decay series of U-238 and Th-232 may not be in equilibrium. As shown in the study, the method which was applied — measurement of terrestrial radioactivity at energies between 30 and 3000 keV and dividing the energy range into three channels A, B and C — can be used for detection of natural and artificial radionuclides in the upper soil horizons. Also the NaI scintillometer can be converted by calibration with dose meters to obtain dose rates.

One striking result is that the highest concentrations of natural radionuclides and artificial radionuclides are limited to the same areas. These areas are the highest elevations of the Ore Mountains, the Vogtland and the Thuringian Forest. In these areas rocks with elevated enrichment of natural radioactivity (granites and rhyolites) also show enhanced Cs-137 concentrations. It can be assumed that the Cs-137 accumulation from washout was best preserved in these undisturbed regions by natural processes such as absorption.

4. CONTAMINATION FROM URANIUM MINING AND PROCESSING

No concentrations above the radiological safety limit have been observed. The study area excluded areas of ongoing rehabilitation of uranium mining. Although uranium mining was undertaken in the study area from the late 1940s to the late 1960s, no significant impact could be found during the measurements of the ambient dose rate nor in the soil samples. Only few samples of low grade ore were found along roads used for transport or in road gravel. The reason for not detecting a significant number of these pieces of ore may be due to use of the 10 × 10 km grid, however our results are in good agreement with the results of investigations carried out by the Federal Institute for Radiation Protection and other organizations. In general the exposure rate in the areas outside the uranium mining facilities does not exceed 200 nGy/h.

5. CONCLUSIONS

Regions with the highest terrestrial radioactivity (exposure rates 100–140 nSv/h) are located on the most elevated parts of the Thuringian Forest, the Vogtland and the Ore Mountains. The basins in the forelands of the mountains show moderate to low values (40–80 nSv/h). The lowest rates were measured over sand of Holocene age in the Niederlausitz, eastern Saxony.

Remarkable is the spatial correlation of anomalous concentrations of artificial radionuclides with high concentrations of geogenic radionuclides (K-40, Ac-228, Ra-226) in the mountainous regions. In these regions, concentrations of 40– > 60 Bq Cs-137/kg soil are typical. The isoline plot interpretation of the soil sample measurements correlates very well with the NaI-radiometric field

measurements (three-channel method). Eight years after the Chernobyl accident, there is not a very close correlation of the fallout anomalies with rainfall areas from May 1986, although directly after the fallout there was a strong correlation in Lower Saxony. Only one anomaly trending NNW from the Eibenstätter Massif to the Kirchberger Granite Massif remains. Fallout concentrations appear to be preferentially preserved in undisturbed grassland or forests, where minimal erosion takes place.

Terrestrial radioactivity can be measured with NaI scintillometers as used in uranium prospecting. The scintillometers have to be calibrated against a dose meter. It is very important that the dose meters are calibrated in the range from around 30 to >3000 keV, not only to 1300 keV as is normal in the nuclear industry. Field measurements with scintillometers with energy discrimination (channel A = >300 keV, channel B = >900 keV, channel C = >1400 keV) and calculation of count ratios give very good indications of fallout concentrations.

BIBLIOGRAPHY

BACHHUBER, H., BUNZL, K., SCHIMMACK, W., Spatial variability of fallout ¹³⁷-Cs in the soil of a cultivated field. in: Env. Monitoring and Assessment 8 (1987) 93–101.

BARTHEL, F.H., MAGER, D., Uranium Mining and Rehabilitation: International Aspects and Examples from Germany, Technical Committee Meeting on Recent Changes and Events in Uranium Deposit Development, Exploration, Resources, Production and the World Supply/Demand Relationship, IAEA, Kiev, Ukraine (in press).

BARTHEL, F.H., BORSDORF, K.H., MALINOWSKI, D., THOSTE, V., Die Verteilung von Radionukliden in den oberflächennahen Böden in Sachsen und Thüringen, Ztsch. Geol. Wiss., Berlin (in press).

BECKMANN, CHR., FAAS, CHR., Radioactive contamination of soils in Lower Saxony, Germany, after the Chernobyl Accident.- Analyst, 117 (1992) 525–527.

BORSDORF, K.H., MALINOWSKI, D., NAUMANN, M., Radiologische Belastung von Böden in Sachsen.- Z. angew. Geol., 41(2) (1995) 111–117.

BMWi (1993), Dokumentation Nr. 335, 370: WISMUT, BMWi, Bonn, August 1993, Mai 1995

BRISTOW, Q., The application of airborne gamma-ray spectrometry in the search for radioactive debris from the Russian satellite Cosmos 954 (Operation "Morning Light"), Current Research, Part B, Geol. Survey Can., Paper 78-1B, p. 151-162, Ottawa (1978).

DURRANCE, E. M., Radioactivity in geology, Chichester (1986).

SARENIO, O., Meßanleitung Ortsdosisleistungsmeßung für natürliche Gammastrahlung, Radiologische Erfassung, Untersuchung und Bewertung bergbaulicher Altlasten, BfS (1993).

THOMPSON, I.M.G., BOTTER-JENSEN L., LAUTERBACH, U., PESSARA, W. et al., The assessment of external photon dose rate in the vicinity of nuclear power stations; an intercomparison of different monitoring systems, EG Brüssel, Dec. 1992

WILL, W., MIELCAREK, J., SARENIO, O., Flächendeckende Messung der natürlichen Gamma-Ortsdosisleistung in den neuen Bundesländern — Meßmethoden, BfS-Jahresbericht für 1995, Salzgitter (1996).

**NEXT PAGE(S)
left BLANK**



USE OF ISOTOPIC SIGNATURE OF RADIONUCLIDES RELEASED FROM URANIUM MINES AND MILLS TO DISCRIMINATE LOW LEVELS OF ENVIRONMENTAL IMPACT AGAINST NATURAL BACKGROUND LEVELS

P. ZETTWOOG, N. LEMAITRE

Office de protection contre les rayonnements Ionisants,
Le Vésinet

S. BERNHARD, Y. VAUZELLE

ALGADE,
Bessines sur Gartempe

France

Abstract

In France, uranium ores have been exploited in rural areas with a low population density. The critical population group which is identified for radiological impact studies lives close to the uranium facilities, at distances from a few hundred metres to 1 kilometre. Within this range, the radioactivity of the environment is still detectable amongst the natural background. Mining companies manage surveillance networks according to strict specifications laid down by the government authorities. For active mining operations it is the exposure to daughter products of radon 222 that forms the bulk of the total effective dose. After closure of a mine and rehabilitation of the site, products such as uranium 238 and radium 226 in the water can become the major components of the total effective dose. Surveillance networks are built to allow direct measurement of the radon daughter products critical to the alpha energy and measurements of the water activities for uranium 238 and radium 226. Annual limits for the effective individual doses are given and determined by the authorities. The industry must manage effective annual doses of the order of 1 mSv. The natural exposure which is not part of the regulation is of the same order (1 mSv) as the exposure created by the industry. The results given are therefore lacking in clarity for the public. The *Office de Protection contre les Rayonnements Ionisants* (OPRI) and ALGADE are developing methods which allow differentiation between natural phenomena and man-made phenomena. It has been recognised that for a region where mining activities have taken place, the isotopic signature of uranium, radium and radon can clearly be recognised from the same product of natural origin. In the case of radon, for example, the industry produces only radon 222 while natural emanations are composed of radon 220 and radon 222.

1. FRENCH REGULATIONS RELATING TO ENVIRONMENTAL PROTECTION AT URANIUM MINES

1.1. Historical background

In France, the legal document specifically covering environmental protection around uranium mines, ore treatment plants, storage plants for mining waste and solid waste from treatment is Decree no 90-222 of 9 March 1990. The decree was published in the Official Journal of the French Republic of 13 March 1990, and was introduced into the general regulations governing the extractive industries brought into force by Decree no 80-331 of 7 May 1980.

Arrangements for monitoring waste disposal and measuring the exposure of the general population to ionising radiation were progressively put into place by the producers from the beginning of the 1970s under their own initiative, the design of these arrangements being based on the recommendations of international organisations in force at the time. For the most part, the above document ratifies these arrangements.

Among the documents used as reference material by those drafting Decree no 90-222 were AIEA SS no 43 of 1975 [1] (which laid down the objectives of surveillance networks) and ICRP Publication no 43 [2] of 1984. The latter publication confirmed that the objectives of document SS

no 43 were sound, clarified a few important concepts, among them that of "critical population groups" already introduced in ICRP Publication no 26 [3], and endorsed two types of monitoring strategy: those aimed at qualifying environmental impact via a determination of sources and transfers, and those aimed at direct estimates of the exposure of populations.

1.2 The key points in Decree no 90-222

Decree no 90-222 is based on the concept of "critical population groups". Its objective is to limit the fraction of their annual exposure attributable to the "industrial" discharges of mining companies and plants that depend on them.

The "critical population groups" are identified during the radiological study of the site carried out prior to the establishment of the surveillance network, taking into account the sources and critical transfer routes of the radionuclides significant for radiological protection. Specific Prefectorial Orders specify the frequency and siting of the sampling points in the environment and the methods of measurement to be used.

As regards the radioactivity contained in drainage water discharged from mines and in liquid effluent from industrial plants, the decree introduces the principle of optimising radiological protection. The limits for discharge are fairly severe as regards both the dilution provided by the waterway receiving it and the possible transfer routes. If there is a demand that a radium or uranium purification station is necessary, the operator must use the best available technology leading to the smallest possible discharge.

1.3. Annual dose limits introduced in the *circulaire d'application* (memorandum of application)

A *circulaire d'application* lays down the limits to be complied with as regards the effective dose equivalent added by industry to that of natural origin for the same radionuclides and the same exposure routes. Except for special cases, the effective dose is determined by taking into account the exposure to gamma radiation, the inhalation of short-lived daughter products of radon isotopes and of long-lived alpha emitters in radioactive dust, the consumption of water at the site and the local food produced.

At present (May 1996), the annual limit for the effective dose equivalent for people belonging to the critical population group is 5 mSv. It is assumed in the calculation that 5 mSv corresponds to the inhalation of a potential alpha energy (PAE) of 2 mJ due to the daughter products of radon 222, 6 mJ due to those of radon 220, 170 Bq due to ore dust, and to the ingestion of 7000 Bq of radium 226 and 2 g of natural uranium.

In the near future, the *circulaire d'application* will in all probability have to legalise a limit on the effective dose equivalent of 1 mSv per year averaged over 5 years, a limit that the EU is preparing to introduce officially into its directives. The value of 1 mSv will correspond in particular to the ingestion of a PAE of 0.73 mJ from radon 222 daughter products. This quantity is inhaled by a person exposed for a year to an equilibrium radon 222 concentration of 18 Bq m⁻³, the concentration expressed as a PAE being about 100 nJ m⁻³.

2. PROBLEMS ENCOUNTERED BY THE OPERATORS IN APPLYING DECREE NO 90-222

2.1. Current situation

After discussion, operators have accepted and implemented the arrangements included in the Prefectorial Orders for the monitoring of discharges and the surveillance networks. It turns out that the value of the effective dose equivalent corresponding to the combination of "industrial" and "natural" exposures is in general less than the annual limit of 5 mSv. Everything is thus fine, and there are no problems still to be solved.

In order to recover the contribution of "industrial" origin, the operator subtracts a fixed value for the "natural background" from the total. Since even the total dose falls within the legal limit, the operator is not very particular about the way in which this natural background is determined. To ease matters, he adopts values measured relatively distant from the industrial sources, which are more representative of the regional background than of the local background at the mine workings being monitored and thus possibly too low. This could lead to an overestimate of the industrial component.

2.2. The current annual limit of 1 mSv

The total exposure at mines leads in general to an effective dose for populations of more than 1 mSv per year. With the present arrangements for monitoring discharges and the release of solid waste by containment facilities, it might be impossible at some sites to comply with a limit on the industry-related annual effective dose equivalent of 1 mSv (with the above-mentioned corresponding value for radon 222) for all critical groups.

The operator should clearly improve his containment facilities, and he is in fact quite prepared to do this provided, however, he is convinced that in his case the limit is not complied with. The operator sees that the natural background is of the same order as the statutory limit and is often greater than the legal industrial contribution. He will have to produce sound arguments for the natural background values that, at the moment, he will have calculated at most just before subtracting them from the total values.

The introduction of a stricter limit reveals a problem which has not existed so far: that of discriminating between contributions from natural sources and those from industrial sources in the total effective doses. In the case of mines, using the regional background is not in general adequate. This is because the radioactive atmospheric load of radon 222 due to its exhalation from local soils varies considerably on a local scale, depending as it does on the ventilation capacity and the weather conditions. High values obtained at a station do not necessarily indicate that it is marked by radon of industrial origin. It could simply be a case of a station installed in a poorly ventilated location.

Similarly, the radioactive load of natural origin in underground and surface waters, observed in the catchment area of the mine, corresponds to a geological formation which contained an anomalously high uranium concentration. Such a radioactive load of natural origin may be very different from that observed in another catchment area nearby having the same geology but never having contained a uranium deposit. It is therefore essential to find a method of discriminating between the two contributions which is based on measurements made on the scale of the site being monitored and not on any measurements made elsewhere.

3. DISCRIMINATION BASED ON THE DIFFERENCE BETWEEN ISOTOPIC SIGNATURES

The *Office de Protection contre les Rayonnements Ionisants* (OPRI) is a technical organisation under the Ministry of Health and one whose main task is the measurement of exposures of populations

whether of natural, industrial or medical origin. It is currently concerned, in collaboration with the ALGADE company, a service subsidiary of COGEMA specialising in the monitoring of mines, with the development of a method for making a rigorous measurement of each of these two components.

3.1. Principle of the method of isotopic signatures

We examine the possibility of discriminating between the environmental load due to radionuclides of natural origin and those of industrial origin from their isotopic signature. The principle of the method is simple. Assume that, on the scale of the area being monitored and in the various physical compartments covered by the measurement network (atmosphere, surface water, underground water, soils and sediments), the isotopic signature of naturally occurring radionuclides in the relevant medium is always the same. This means that the atomic concentrations of the different isotopes may vary from one point to another over the area but that the ratios of these concentrations remain constant. It will be appreciated that this situation can occur if the uranium and thorium concentrations in the local soil and geological formations on the one hand, and the processes leading to the release and transport of radionuclides in the receiving media on the other hand, vary little on the scale of the area being monitored.

If the area being monitored is large enough for there to be some zones where it is certain that no industry-related contamination exists, then the isotopic signature of the natural radioactivity may be established there for all the media sampled. It is then assumed that this signature is the same in those zones of the area which are marked by industrial waste. The industrial component can then legitimately be constructed from the measurement of the distortion it has produced in the signature of the natural component.

3.2. Progress made in validating the method

Our intention is to examine to what extent the isotopic signature method can solve the problem raised, and to investigate the conditions under which the associated assumptions are valid, for the case of French mines. Where the terrain is uncomplicated, as in the sandy clay and calcareous clay plains of the Paris basin, the method works. However, the concentrations of radionuclides of natural origin are almost constant over the whole area, and simply subtracting the uniform background recovers the industrial component quite easily. In fact, in most French mines, the situation as regards natural radioactivity is less simple, the background varying at least in absolute value from one end of the area to the other. It is our objective to identify those sites for which the method of recovering the industrial component from isotopic signatures is valid.

We describe the research in progress and the results obtained. As regards the impact of atmospheric discharges of radon 222, the method appears to us to be valid for at least three sites characterised by very pronounced relief (differences in height above sea level of a few hundred metres, existence of several waterways, variable soil roughness). As regards the impact of the discharges and releases of radium and uranium into aquifers, our research has only just started.

4. RESULTS OF THE METHOD FOR RECOVERING THE RADIOLOGICAL IMPACT OF INDUSTRIAL RADON 222

The networks used by ALGADE for measuring the radiological impact of atmospheric radon 222 have the special feature that they measure not only the atomic concentrations of radon 222 and its daughter products but also those of lead 212, a daughter product of radon 220. It is thus possible, for each station in the network, to calculate the ratio A between the concentrations of radon 222 and lead 212 of natural origin. Lead 212 atoms replace equal numbers of radon 220 atoms exhaled by the soil a few minutes earlier. The ratio A is therefore interpreted below as giving the ratio of exhalations

of radon 222 and radon 220, such exhalations having been weighted on the regional or continental scale according to the case.

Reference [4] examines the theoretical conditions under which we might hope to obtain a constant value for A, the ratio of the atomic concentrations of radon 222 and lead 212¹ in the air sampled by all the stations in the surveillance network.

In practice, our confidence that it is valid to apply the method was based on the small dispersion in the values of A measured for a sufficient number of background stations covering the monitored area adequately, including both poorly ventilated stations with high radon loads and well ventilated stations with low radon loads.

Table I shows the values of the ratio $\langle A \rangle$ we have obtained over several sites in France and in a few African countries. For the sedimentary areas in the table, it can be seen that values of $\langle A \rangle$ lie in the range 280 - 300 except for Languedoc, which is outside the range with $\langle A \rangle = 860$. For crystalline terrain, the values of $\langle A \rangle$ extend from 500 to 5200. The ratio of the atomic flux of radon 222 to that of radon 220, in a simplified scheme, is given by:

$$[\text{Ra}_{226}] E_{222} H_{D222} / [\text{Ra}_{226}] E_{220} H_{D220}$$

H_{D222} , H_{D220} are the diffusional relaxation lengths of the radon isotopes.

The central value of the ratio of relaxation lengths is of the order of 80 for a profile showing a uniform saturation of the porous volume, but higher and lower values are to be expected according to whether the soil is dry or wet. The ratio of the emanation coefficients is of the order of 1, except for special mineralogical features. On the average over the whole earth's crust (but not necessarily in soils), the activities of the radium in the two radioactive series are of the same order. The mean expected terrestrial value is thus of the order of 100. The values of $\langle A \rangle$ in Table 1, which are for sites where uranium ore is extracted, are 3 to 50 times as great.

4.1. Results for the Limousin network

COGEMA has been mining uranium ores in the Nord-Limousin region for 45 years and treating them on site. There are several radon 222 sources, including heaps of mining waste and residues from treatment. The radiological impact of radon 222 emissions is monitored by a network of 44 operational stations equipped with the exposimeters described in the Introduction.

The region covered by the Nord-Limousin "radon" surveillance network (50 km²) has a relief consisting of small rounded tree-covered hills, with fairly deep valleys and many lakes. Stations along hill tops have low exposures because of the large atmospheric dispersion at such sites. Stations in valleys or protected by an obstacle have high exposures because of the poor air circulation.

The region is characterised geologically by granitic formations (binary granites and biotite granites) with metamorphic series at the boundaries (mica schists and paragneiss). A geological survey of Nord-Limousin showed that the uranium content of the soils associated with the granites in the region covered by the network was significantly higher than that observed on the average for more distant formations. A programme of airborne gamma-spectrometry enabled a map to be drawn up of

¹ More precisely, the sum of the atomic concentrations of lead 212 and bismuth 212 in view of the decay chain of radon 220. A is therefore the ratio of the sum of the atomic concentrations of the radon 222 series to the sum of those of the radon 220 series as measured by the surveillance network stations at mines.

TABLE I. RATIOS $\langle A \rangle$ OBTAINED OVER SOME NETWORKS EQUIPPED WITH THE ALGADE ALPHA SPECTRAL DOSIMETER

Network	Geology	Radon 222 volume activity Bq m ⁻³	Atomic concentration for members of the radon 222 series 10 ³ atom m ⁻³	Atomic concentration for members of the radon 220 series 10 ³ atom m ⁻³	Ratio $\langle A \rangle$
(1)	(2)	(3)	(4)	(5)	(6) = (4)/(5)
Paris Basin, France 1990- 1995	calcareous clay or sandy clay soil	11.2	5340	16.5	324
Limousin, France 1993	granites	20	9520	6.8	1400
Charentes, France 1992- 1993	limestone, marine sediments	6.5	3100	9.2	285
Vendée, France 1993	metamorphic and granitic series	13	6200	12	5170
Forez, France 1993	granites	11	5240	10.4	504
Morvan, France 1993	granites	17.5	8330	14.4	578
Languedoc, France 1991	sedimentary and volcanic permian sandstone	15	7140	8.3	860
Mounana, Haut Ogooué, Gabon	sandstone and products of weathering	14	6670	18.4	363
Arlit, Southern Sahara, Niger	sands, sandstone	33	15700	41	383
Kanyemba, Zimbabwe 1991	sands, sandstone	8.5	4050	13.6	298

If such a small dispersion demonstrates that the method is valid, a mean ratio $\langle A \rangle$ is calculated by averaging the values of A obtained over the unmarked stations in the area. Since lead 212 concentrations are also measured in stations marked by industrial radon 222, the concentrations of radon 222 of natural origin can be recovered from this by applying the factor $\langle A \rangle$ to it.

the surface concentrations of uranium and thorium in the soil, concentrations which appear to be roughly proportional to each other.

Programmes involving local measurements of radon 222 flux have enabled a map of radon 222 fluxes to be produced from the map of uranium concentrations. These programmes showed that the local fluxes are about 5 times higher than those obtained for soils associated with more distant sedimentary formations. These conditions favour the introduction of values for the ratio A that are relatively constant over the area.

Table II contains the results obtained over the Limousin (France) network in 1993. Thirteen stations were identified as representative of the background. The table gives for each station the annual mean value of the atomic concentration of radon 222 and lead 212, the ratio A of these two values, the potential alpha energy (PAE) and the mean volume activity A_v of the radon 222 and its equilibrium factor F. The means are calculated from the 12 monthly values measured in 1993 by alpha spectral active dosimeters installed by ALGADE in the stations monitoring mine workings.

TABLE II. ANNUAL MEAN VALUES OBTAINED IN 1993 AT THE "BACKGROUND" STATIONS OF THE NORD-LIMOUSIN NETWORK

Station No	Rn 222 10^6 atom/m ³	Pb 212 10^3 atom/m ³	A 10^3	PAE222 nJ/m ³	A_v 222 Bq/m ³	F
8	8.5	6	1.42	50	17.85	0.50
9	8.8	6.5	1.35	54	18.48	0.52
16	7.1	6.8	1.04	41	14.91	0.49
19	8.3	6.2	1.34	56	17.43	0.57
20	5.7	4.4	1.30	43	11.97	0.64
23	12	10	1.20	57	25.2	0.40
27	6	4.6	1.30	33	12.6	0.47
30	6.1	4.9	1.24	38	12.81	0.53
31	11	8.1	1.36	61	23.1	0.47
35	15	9.9	1.52	94	31.5	0.53
40	6.2	3.5	1.77	34	13.02	0.46
42	13	7.8	1.67	68	27.3	0.44
43	15	9.4	1.60	92	31.5	0.52
	< Rn 222 >	< Pb 212 >	< A >	< PAE 222 >	< A_v 222 >	< F >
"Network" mean over background stations	9.4	6.8	1.39	55.5	19.8	0.5

It can be seen that the *mean annual* values of the background volume activities of radon 222 measured by the 13 stations vary considerably, by a factor of 2.6 between the highest value (31.5 Bq m⁻³ at station 35) and the lowest value (12 Bq m⁻³ at station 20). *The method of recovering industrial exposures by subtraction of a uniform background exposure would be inadequate here.*

As regards the *monthly means* of the activities obtained in 1993 by each "background" station, the variation is still greater. See reference [4] for more information. The mean value of A over all the background stations is $1.39 \cdot 10^3$, the highest value being $1.77 \cdot 10^3$ and the lowest $1.04 \cdot 10^3$. The standard deviation for the distribution of A values is 0.14.

**The isotopic dilution method is validated for the Nord-Limousin network
by the fact that the ratio A is relatively constant over all the
background stations of the network**

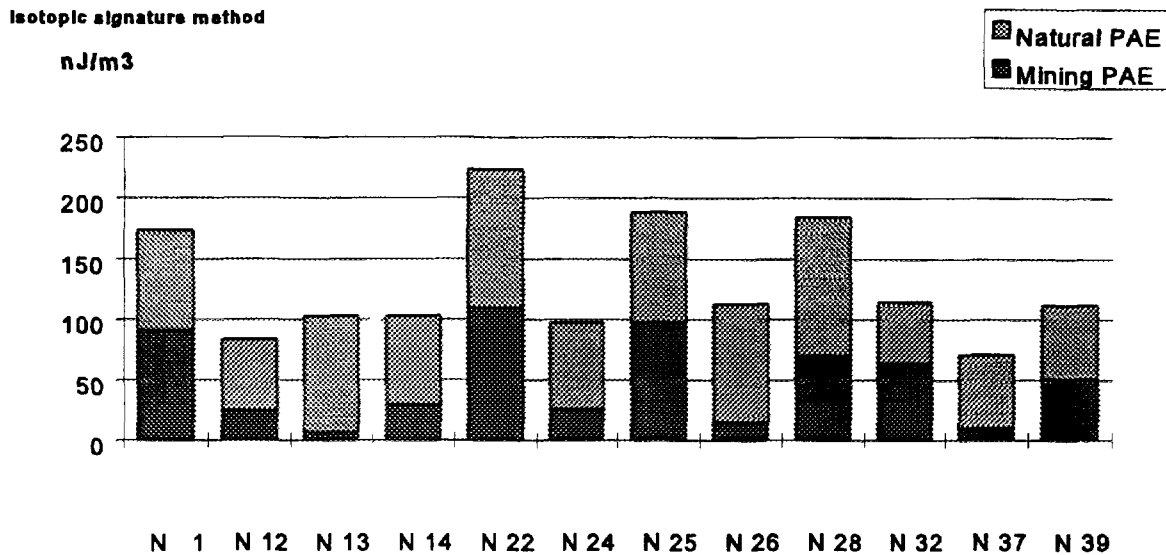


FIG. 1. Recovery of the PAEs of industrial radon 222 by the isotopic signature method. The Nord-Limousin network: 12 stations marked by industrial radon 222. Mean values for 1993.

Since these results are for land showing only a small variation in A, it was assumed that the criterion for the applicability of the procedure is satisfied. We therefore continued to use the technique in processing the data for the network.

The Pb 212 concentrations for stations subjected to the effect of COGEMA radon 222 sources were used to calculate the Rn 222 concentrations of natural origin for these stations by multiplying by the factor $\langle A \rangle$, i.e. $1.39 \cdot 10^3$.

The industry-related radon 222 concentrations could be obtained by subtraction. Supplementary processing enabled the PAE 222 of its daughter products to be recovered. Here, the mean value of the equilibrium factor for the "background" stations, 0.5, is used (see Table II).

Figure 1 summarises the results of the recovery procedure by giving the annual mean values of PAE 222 concentrations of industrial and natural origin for stations located outside the perimeter of COGEMA plants. Some of these stations are located near critical population groups. It can be seen that almost all the industry-related values remain lower than the derived limit of 100 nJ m^{-3} , which over a year corresponds to an effective dose of 1 mSv.

Figure 2 shows the results of a recovery procedure based on the subtraction of a uniform background over the whole area. It can be seen here that this method falsely identifies 4 stations where the mean annual industry-related exposure exceeds the derived limit of 100 nJ m^{-3} .

4.2. Selection of stations representative of the regional background of natural origin

It is clear that, in the case of a recovery procedure based on the subtraction of a uniform background over the whole area, the mean PAE concentrations in the Nord-Limousin network are underestimated for poorly ventilated stations and overestimated for well ventilated stations. This may

The variability in the PAE concentrations measured over the background stations invalidates the method using subtraction of a uniform background in the case of the Nord-Limousin network

Method using the subtraction of a uniform background value

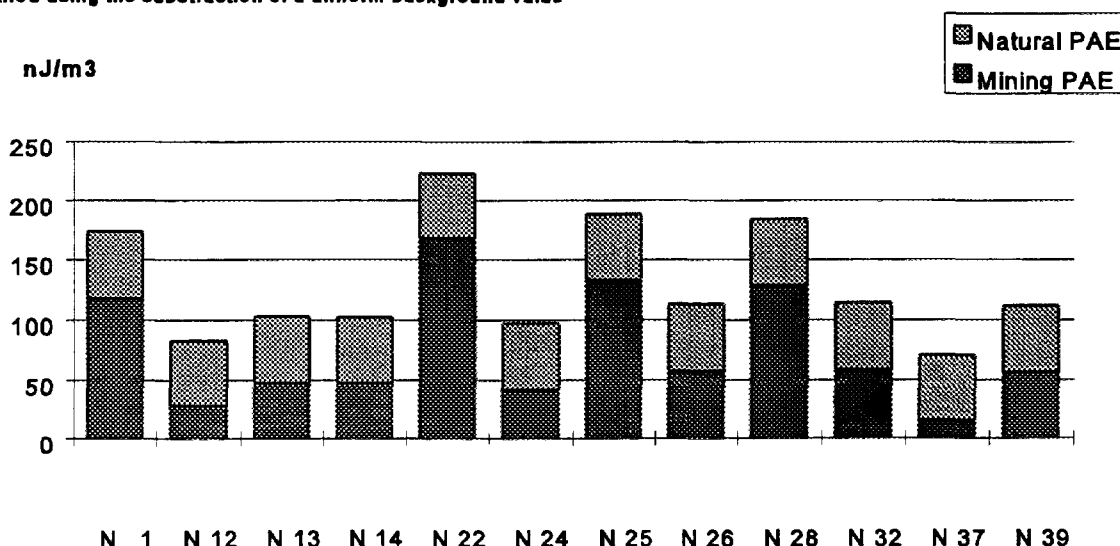


FIG. 2. Recovery of the PAEs of industrial radon 222 by the uniform background method. The Nord-Limousin network: 12 stations marked by industrial radon 222. Mean values for 1993.

result in disputes between the operator, the authorities and the local environmental associations, a situation that is all the more likely in that some background values will exceed the derived limit if the basis for this is a value of 100 nJ m^{-3} . There is no satisfactory scientific solution in the context of this method if the background is variable.

The isotopic signature method may provide the solution to the problem of the correct recovery of industrial values if the ratio A remains constant over the background stations of the network. It should be pointed out, however, that the operation of selecting a subset of stations to be taken as background stations of the network is a crucial and delicate operation. Such a subset on the one hand should be selected to represent all the ventilation conditions in the area and on the other hand should include only those stations truly unmarked by industrial sources or by local anomalies in radon 220 or radon 222 exhalations.

We select the background stations over a network assumed to be dense enough in comparison with the orographic and geological complexity of the area, using two indicators: *the ventilation index* and *the isotopic signature of short-lived polonium, a daughter product of radon 222*.

For each background station, the relative ventilation index is defined as the ratio of the local atomic concentration of lead 212 to the mean atomic concentration of lead 212 over the network. In the case of Nord-Limousin, for example, we ended up with the set of ventilation indexes shown in Figure 3, which seemed representative of the orographic variability of the area.

We then use the fact that the alpha spectral dosimeter separately measures the potential alpha energies emitted during the decay of polonium 218 atoms (energy of 6 MeV) and polonium 214 atoms (energy of 7.7 MeV) trapped or formed on the sampling filter. The ratio R of the number of alpha tracks recorded in the channels for these two energies is then calculated, i.e. the isotopic signature of the short-lived polonium resulting from the decay of radon 222.

When the radon 222 load of the air masses passing over the network originates only from exhalations from soils that the same air masses have previously scavenged, the isotopic signature of the short-lived polonium from the decay of radon 222 is that of the natural background and is well characterised. An elementary simulation (see [4]) shows that the ratio R varies with the age of the first load of the air mass according to the law shown graphically in Figure 4. Apart from air masses of recent oceanic origin, continental air masses have been over the region for more than 2 hours, and we expect the ratio R to be less than 0.12, the equilibrium factor F being greater than 0.4.

On the other hand, if the air mass has just been loaded by exhalations from a waste heap, the later evolution of the ratio R to be associated with this radon 222 of industrial origin varies with time according to the law shown in Figure 5. The air mass reaches the critical groups quite quickly, a time of less than 40 minutes being a realistic assessment. We should expect R values greater than 0.2 with F less than 0.2.

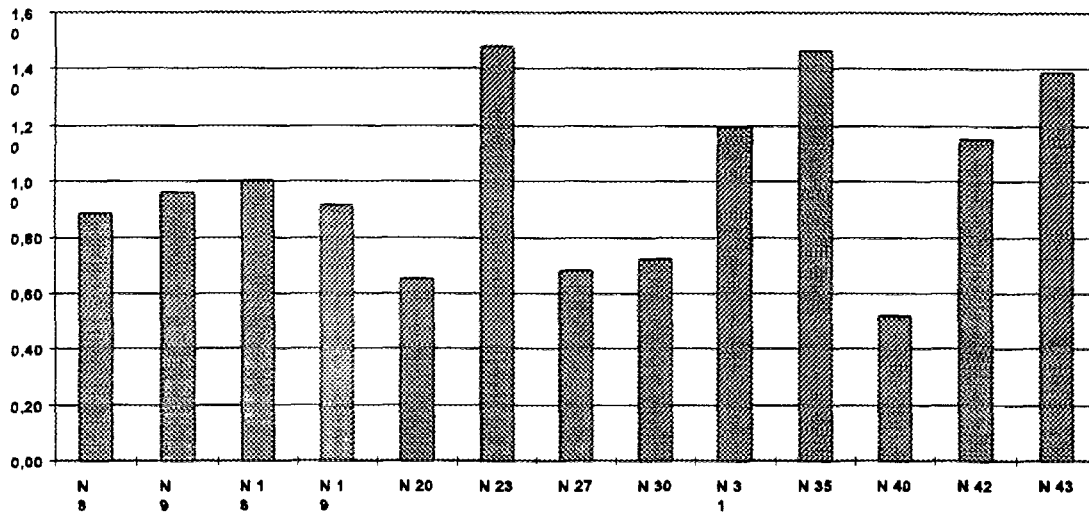


FIG. 3. Ventilation index of the 13 background stations in the Nord-Limousin network.

Variation in R et F with the age of the first exhalation

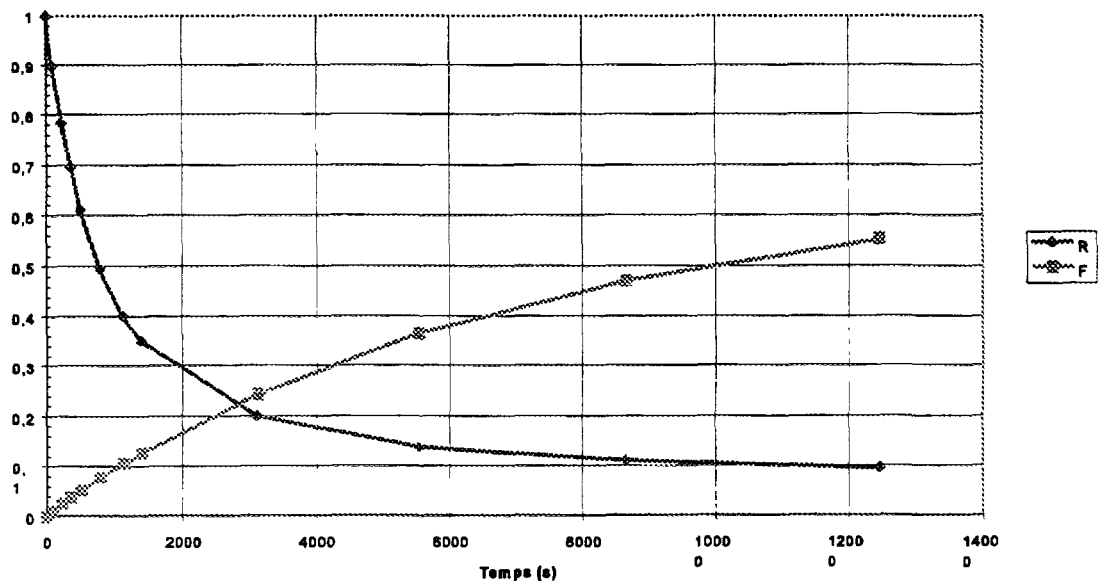


FIG. 4. Evolution of the isotopic signature of polonium R and of the equilibrium factor F for the radon 222 load of natural origin.

In practice, the stations for which the value of R is on average less than 0.12 are kept as candidates for selection as background stations; those for which the value of R is on average greater than 0.2 are identified as stations marked by a local radon 222 anomaly. This may be due either to an industrial source or an as yet unmined uranium-bearing outcrop.

4.3. Application of the isotopic signature method to other networks

The method works only if there are sufficient stations and if their locations satisfy the requirements listed above. In the light of this, some networks need to have a higher density.

The mine surveillance networks with a high density of stations will be incorporated into networks which are less dense but representative on a regional scale and which will be equipped with the same active alpha spectral dosimetry equipment.

As an example, Figure 6 shows the recovery of the industry-related radon 222 PAE for the surveillance network of the mine workings run by COGEMA at Lodève⁵ (Languedoc network). In 1991, this network comprised 14 environmental stations, eight of which were adopted as background stations with $\langle A \rangle = 860$, the relative standard deviation of the A values being 22%.

5. THE ISOTOPIC SIGNATURE METHOD IN THE CASE OF URANIUM AND RADIUM INGESTION THROUGH THE FOOD CHAIN

As part of its general task of protecting the population against ionising radiation, OPRI has long been concerned with the radioactivity of mineral waters. The results of systematic programmes for analysing the radioactivity of French mineral waters were published in 1968 [6]. A new collection

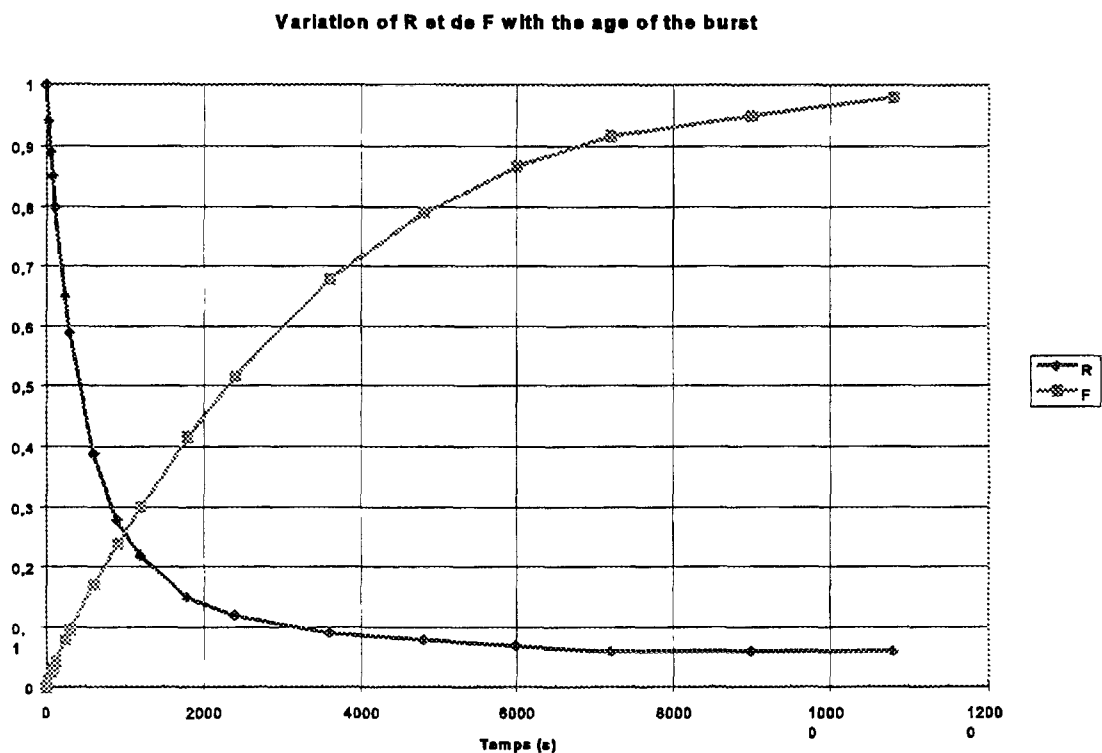


FIG. 5. Evolution of the isotopic signature of polonium R and of the equilibrium factor F for a burst of radon 22 of industrial origin.

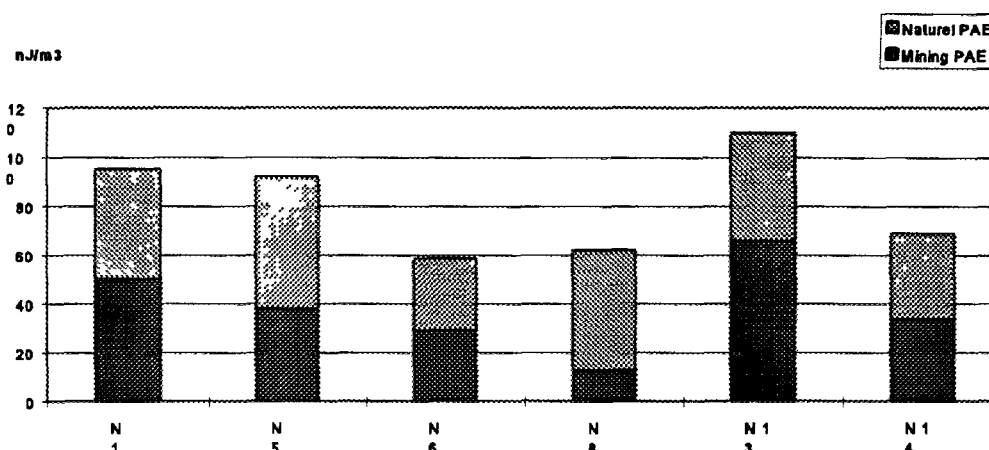


FIG. 6. Recovery of the PAEs of industrial radon 222 by the uniform background method. Languedoc network: 6 stations marked by industrial radon 222. Mean values for 1991. Isotopic signature method.

of results, mainly concerning the relative abundance of the radium isotopes ^{228}Ra and ^{226}Ra and the disequilibrium of the uranium isotopes, together with a description of OPRI's physical and radiochemical methods of analysis, was published in 1990 [7]. The physico-chemical and geochemical processes capable of explaining the relative abundances and the radioactive disequilibria of the isotopes of the radionuclides in the uranium and thorium chains dissolved in mineral waters were the subject of publication [8], while note [9] concerned the disequilibrium states of ^{234}U and ^{238}U .

Between 1950 and 1980, in the granite massif of Forez in France, COGEMA extracted and treated uranium ores with uranium concentrations of a few kg per tonne, providing about 15000 tonnes of metal. The waste from the treatment is stored at the surface under water upstream from a retaining dam, the most granular fractions sometimes being used as pack for the mining works. A considerable rehabilitation of this deposit is under consideration. A prior study of the radiological impact of the rehabilitation is planned. If the isotopic signature method is applicable to the case of environmental transfers of industrial uranium and radium by underground and surface waters, it will render great service to this complex site from the radiological and ecological points of view, because the ingestion of uranium and radium through the local food chain will then be taken into account for certain critical groups around this site.

5.1. Disequilibrium states of ^{234}U and ^{238}U

Since the publications of Cherdyntsev et al [10,11], we know that the activities of the ^{234}U and ^{238}U uranium isotopes dissolved in underground waters are rarely in equilibrium. Results published in the literature [12,13] show that the ratio of the activities $\text{AR} = ^{234}\text{U}/^{238}\text{U}$ is in general greater than 1 and can reach values of 4 or 5, in Vichy water for example (see [7] and [8]).

Several mechanisms are suggested in the literature to explain this disequilibrium. The difference in mass does not explain the fractionation. A theoretical model of the variation in the ratio AR with the time of contact between the water and the rock is proposed in [14]. This is repeated for Stripa granites in [15]. The model takes two mechanisms into account:

- the difference in the leaching rate of the two isotopes, due to their different radioactive, mineralogical and physico-chemical histories,
- the ability of ^{234}Th atoms to escape from the crystalline matrices of the host rock. These atoms descend from ^{238}U by alpha decay and have a recoil energy sufficient to travel a few tens of nanometres in the crystal lattice¹⁶. They are therefore able to pass into the aqueous phase if they are close enough to the surface of the uranium-bearing grain

The reference time for the period of contact is the radioactive half-life of ^{234}U : 2.45×10^5 years. For short times, AR is equal to the ratio of the leaching rates. It is only for long times and for uranium-rich mineralisation in veins that the escape mechanism of the ^{234}Th atoms through their recoil energy can predominate. A survey of the published attempts of groundwater dating by uranium isotopes is made in [17].

The aim of note [9] was to explain the disequilibrium of the ^{234}U and ^{238}U isotopes by the fact that U can change from a valency of 4 to one of 6 by radiochemical processes during the radioactive decay which convert the uranium ion of mass 238 into one of mass 234 in three stages (1 alpha emission, 2 beta emissions). Uranium with a valency of 6 is more soluble than uranium with a valency of 4. This note was based on the results of measurements made on underground water in granitic terrain in the Forez region of France. The ratio of the dissolved activities $\text{AR} = ^{234}\text{U}/^{238}\text{U}$ was 2.09 with a relative error of 5%, the water-bearing granite being in equilibrium.

It is known that waste from the mining of uranium ores may contain pyrites which, in an oxygenated medium, leads to the possibility of acid drainage from waste heaps and the in situ dissolving of traces of uranium. This process can also take place in the residues from treatment stored in wet conditions, and very often at the surface in lixiviation plants using low-grade ores, which might well leak in the long term.

An increase in soluble uranium is sometimes observed in the water from boreholes or rivers located downstream from these deposits, but it is difficult to distinguish between that generated by natural leaching from undisturbed geological formations already in place and any that may be due to leakage from industrial plants.

Attempting to discriminate between the industrial and natural components of the radiological impact on the ingestion of uranium implies that we can measure the marking of an underground aquifer by any leaks that may occur from the bedrock of a surface deposit containing uranium in solution.

We make the following two points in favour of using the isotopic signature method for the marking of underground water by industrial uranium:

- (a) The water of underground aquifers has an activity ratio $\text{AR} = ^{234}\text{U}/^{238}\text{U}$ generally greater than 1, which can be measured very accurately in a specialist laboratory.
- (b) The isotopes of uranium are in equilibrium in the ores and in the liquid effluent from industrial plants.

This may be a difficult undertaking, because the water which has percolated from the surface installations of the mine or plant is also loaded with mineral salts, such as chlorides and sulphates, with extraordinary pH values. Complex geochemical processes can make the quantitative interpretation of changes in the isotopic signatures of natural waters very difficult. The chemical load of underground drainage waters from surface deposits may itself lead to an increase in the natural leaching of uranium from the water-bearing rocks. One of the key points in our research programme is to assess the importance of this difficulty.

5.2. Relative abundance of the radium isotopes

The mineralogical, radiochemical, geochemical and adsorption processes accounting for the relative abundance of radium isotopes in underground and surface waters have been satisfactorily identified by uranium prospectors and specialists in isotopic dating methods. The effects of the anion content of the water (chlorides, carbonates, sulphates) and the redox potential are brought out in [8].

We make the following two points in favour of using the isotopic signature method for the marking of underground water by industrial radium:

- On the scale of a catchment area, the underground and surface waters each have a radium isotopic signature (^{228}Ra , ^{226}Ra and ^{224}Ra) which can be accurately identified with the analytical resources at the disposal of OPRI.
- Liquid effluent from mines and industrial plants, and the water percolating from radium-bearing surface deposits discharge only ^{226}Ra into the environment.

REFERENCES

- [1] INTERNATIONAL ATOMIC ENERGY AGENCY, Objectives and Design of Environmental Monitoring Programmes for Radioactive Contaminants, Safety Series No. 41, IAEA, Vienna (out of print).
- [2] ICRP, Principles of Monitoring for the Radiation Protection of the Population, ICRP Publication No.43, Pergamon Press, Oxford, New York, Frankfurt (1984).
- [3] ICRP, Recommendations of the ICRP, ICRP Publication No. 26, Pergamon Press, Oxford, New York, Frankfurt (1977).
- [4] BERNHARD, S., VAUZELLE, Y., ZETTWOOG., P., "Measurement of the Radiological Impact of Environmental Radon 222 Releases from Heaps of Solid Wastes from the Mining Industry", IRPA endorsed Int. Conf. on Radioprotection and Radioactive Waste Management in the Mining and Mineral Industries, Johannesburg, South Africa, 20-24 February 1995.
- [5] BERNHARD, S., GOUX, M., ZETTWOOG., P., "Dosimetric Monitoring of the Radon Risk to Populations Near Mines", Int. Conf. on Radiation Protection in Uranium Mines, Saskatoon, Saskatchewan, Canada, 25-68 May 1992.
- [6] REMY, M.L., PELLERIN, Pr.P., "Radioactivité naturelle de 250 sources hydrominérales françaises" (Natural radioactivity of 250 sources of mineral water in France), SCPRI Report No. 117, Bull. INSERM, 23 No.1 (1990) 23-62.
- [7] REMY, M.L., LEMAITRE, N., "Eaux minérales et radioactivité", (Mineral waters and radioactivity), Hydrogéologie No. 4 (1990) 267-278.
- [8] MAISONNEUVE, J., REMY, M.L., "Les éléments radioactifs naturels et les eaux thermo-minérales" (Natural radioactive elements and thermal mineral waters), Conference on current data on natural radioactivity, SFRP, Monte Carlo, 5 - 7 November (1984).
- [9] CLANET, F., LECLERC, J., REMY, M.L., MORONI, J.P., "Mise en évidence expérimentale du rôle de l'absorption différentielle du thorium et de l'uranium sur les roches silicatées dans l'état d'équilibre entre les activités ^{234}U et ^{238}U dans la nature" (Experimental observation of the part played by the differential absorption of thorium and uranium by silicate rocks in the state of equilibrium between the ^{234}U and ^{238}U activities in nature).
- [10] CHERDYNTSEV, V.V., CHALOV, P.J., KHAIDAROV, G.Z., Izv. Akad. Nauk, USSR (1955) p 175.
- [11] CHERDYNTSEV, V.V., ORLOV, D.P., ISABAEV E.A., IVANOV, V.I., Geokhimia 1961, p 840.
- [12] ASIKAINEN, M., "State of disequilibrium between ^{238}U , ^{234}U , ^{226}Ra and ^{222}Rn in groundwater from bedrock", Geochimica et Cosmochimica Acta, Vol. 45, Pergamon Press Ltd. (1981)201-206.
- [13] COTHERN C.R., LAPPENBUSCH, W.L., "Occurrence of uranium in drinking water in the US", Health Physics, Vol. 45, no 1 (July), (1983) 89-99.
- [14] ANDREWS J.N., KAY, R.L.F., "The evolution of enhanced $^{234}\text{U}/^{238}\text{U}$ ratio for dissolved uranium and groundwater dating", Fourth Int. Conf. Geochronology and Isotope Geology, Denver, USA, US Geol. Surv. Open File Report (1978) 78-701, p 11.

- [15] ANDREWS, J.N., GILES, I.S., KAY R.L.F., LEE, D.J., "Radioelements, radiogenic helium and age relationship for groundwaters from the granites at Stripa, Sweden", *Geochimica et Cosmochimica Acta*, Vol 46, Pergamon Press Ltd, USA (1982) 1513-1543.
- [16] HONGBIN SUN, "Monte Carlo Simulation of Radon Emanation from dry building Materials", *Health Physics*, April 1995, Vol 68, no 4.
- [17] FRÖHLICH K., GELLERMAN, R., "On the potential use of uranium isotopes for groundwater dating", *Chemical Geology (Isotope Geoscience section)*, Elsevier Science Publishers B. V. (1987) 65-77.

**NEXT PAGE(S)
left BLANK**



THE DISPERSION OF RADON IN THE STRÁŽ-HAMR AREA OF THE CZECH REPUBLIC AS AN EFFECT OF URANIUM MINING AND RELATED ACTIVITIES

R. SMETANA, J. NOVÁK
DIAMO s.p.,
Stráž pod Ralskem,
Czech Republic

Abstract

Uranium is exploited in the deposit Stráž pod Ralskem-Hamr since 1968. During all the time two mining methods have existed side by side — the deep mining and the "in situ leaching" technology using the sulphuric acid. The uranium mining culminated in the second half of 1980s in the deposit. Higher concentrations of radon is expected in the uranium mining area. It is caused for one thing by higher content of the mother elements in the crust of the earth, for another by the various mining and reprocessing processes. To evaluate a radon exposure in the Stráž-Hamr area an analysis of radon distribution was worked out. The analysis was prepared in 1986 in the mining company Uranové doly Hamr (now DIAMO s.p.) and it described dispersion of radon emitted to the air in connection with the mining activities. The sources of radon could be divided into two groups — area sources (leaching fields, ore depots, water basins) and point sources (stacks, ventilation boreholes, ventilators). This paper describes the methodology of the radon dispersion calculation, based on the stationary Gaussian model of dispersion of the gaseous contaminants from the point source. Modification of the methodology for the area sources and extension for the radioactive decay are also presented. Results of the calculations are represented graphically in the contour maps of the ground-level concentrations of radon and an assessment of the doses for the critical group is presented.

1. INTRODUCTION

Relating to the development of the uranium mining in the North Bohemia (Fig.1) and to the construction of necessary technological facilities the demand for an evaluation of radon emission in Stráž-Hamr mining area was formed in the half of the 80s. At that time there were neither sufficient measurement devices for measurement of radon emission from surface unit of the area sources nor the methodology of calculation of radon dispersion from the different types of sources.

For evaluation of radon emission a methodology was developed. The methodology with small changes, resulting from greater performance of the used computers and high precision of the measurement, is still used. This methodology was used in our company for the first time in 1986. The results showed, that in the area the limits for population are not exceeded. An evaluation of the individual sources influence gave the possibility to improve a situation and the possibilities were realized in sequence. During the next period a radiation impact on population was slightly decreasing, even though the area of the leaching fields was still enlarging and the volume of cleaned mining water was increasing. Presented situation is the state of maximum impact on the atmosphere in the region by radon emission from the uranium mining.

2. THE SOURCES OF RADON IN THE AREA HAMR-STRÁŽ

An intensity of radon emission from technological sources is usually many times higher than natural emanation from soil or water. High number of the sources was in the uranium mining area Hamr-Stráž in time of the most intensive mining activity, i.e. in the second half of the 80's. Calculation of the radon distribution using measured values in the sources seemed to be an optimum possibility how to get information on impact of radon and daughters in the area.

From the point of view of distribution calculations it is possible to split these sources into two classes — point sources and area sources. In the first class there were ventilating stations of the deep

mines, individual ventilating boreholes, the chemical recovery plant ventilation and ventilating flue of the central decontamination station (CDS). In the class of the area sources there were the uranium ore depots, the tailing dumps, the sedimentation reservoirs of the mining water cleaning system and the waste pond of the chemical recovery plant. System of the production wells of the chemical leaching plant was considered as an area source — about 2400 of wells were replaced by system of the area sources (Fig.2). The point sources were the elevated sources with forced flow of the air only, the area sources were on the one hand the elevated sources on the other hand the sources with zero height (water reservoirs).

The chemical leaching mine has specific position among the radon sources. In 1986, when the radon distribution was evaluated, the chemical mine had an area of 3.63 km² and very broken shape. The area was covered with circular sources so that the shape would be respect as much as possible. It means to cover it completely, with minimum duplicity and with uniform density of measured wells. Result values of radon emission from these sources were calculated from several hundreds of measured wells.

A complete list of radon emission in the Hamr-Stráž area is shown in Table I and in map (Fig.3). In calculation there were used 7 point sources, 10 real area sources and 9 circular area sources, which represented the production wells of chemical leaching mine. A region of interest had an area of 240 km², about 40 km² was lying above the uranium deposits. Table I shows, that radon emission from technological sources was more then two times higher then from natural sources. Total emission of radon in the region was 12.9.10⁶ Bq/s, i.e. 4.1.10¹⁴ Bq/year.

There are two towns in the area of interest — Stráž pod Ralskem, where the head office of the mining company is located and where in the second half of the 80s lived about 4 thousands. of inhabitants and almost 2.5 thousands. of uranium workers, and Mimoň with 7.5 thousands. of inhabitants. Several small villages are situated in the centre of the uranium mining area (Hamr na Jezerce).

3. THE DISPERSION FUNCTION

The dispersion of radon from the point and area sources is solved by different way, although the basic dispersion function is the same in both cases.

For calculation of radon dispersion from technological sources the well-known Sutton's method was used. This method is used in Czech republic officially by the Czech hydrometeorological institute [1]. This method comes from the diffusion equation based on application of the statistical theory of the turbulent diffusion, describing dispersion of a pollutant from a continual source in homogenous stationary atmosphere. The equation for pollutant dispersion is based on the Gaussian normal distribution, where in the downwind direction a transport predominates a diffusion. The methodology is relevant for computing of air pollution with gaseous exhalations from the continual elevated point sources.

For the receptor with coordinates (x,y,x) and for the source with coordinates (x',y',z') the dispersion function R is

$$R(x-x', y-y', z-z') = \frac{1}{2 \pi \sigma_y \sigma_z} \cdot \exp \left[-\frac{1}{2} \left(\frac{(y-y')^2}{\sigma_y^2} + \frac{(z-z')^2}{\sigma_z^2} \right) \right] \quad (1)$$

where u is wind speed (m.s⁻¹), σ_y , σ_z are dispersion coefficients dependent on the distance from the source and on the atmosphere stability. Regarding to the relatively flat surface, comparing with



DIAMO s.p. Stráž pod Ralskem
Czech republic

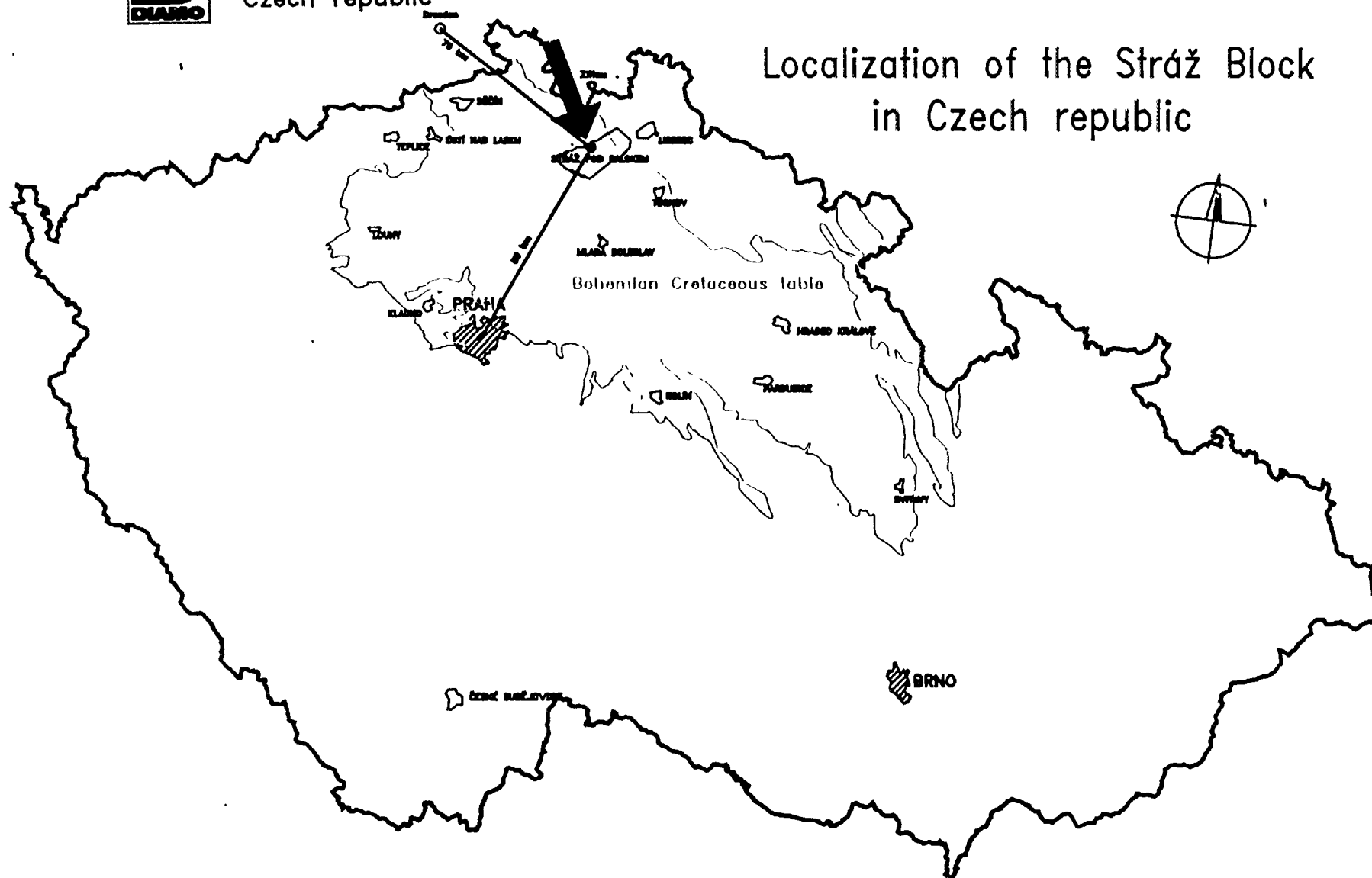


FIG. 1. Localization of the Stráž Block in the Czech Republic.

distances of the sources and the settlements in the area, the flat terrain was used in calculation. The z' coordinate was replaced by the effective height of the source, the ground-level activity was calculated ($z = 0$) and the term describing a reflect was added to the dispersion function.

The dispersion function is then given by

$$R(x-x', y-y', z-z') = \frac{1}{u\pi\sigma_y\sigma_z} \cdot \exp\left(-\frac{(y-y')^2}{\sigma_y^2}\right) \cdot \exp\left(-\frac{h^2}{\sigma_z^2}\right) \quad (2)$$

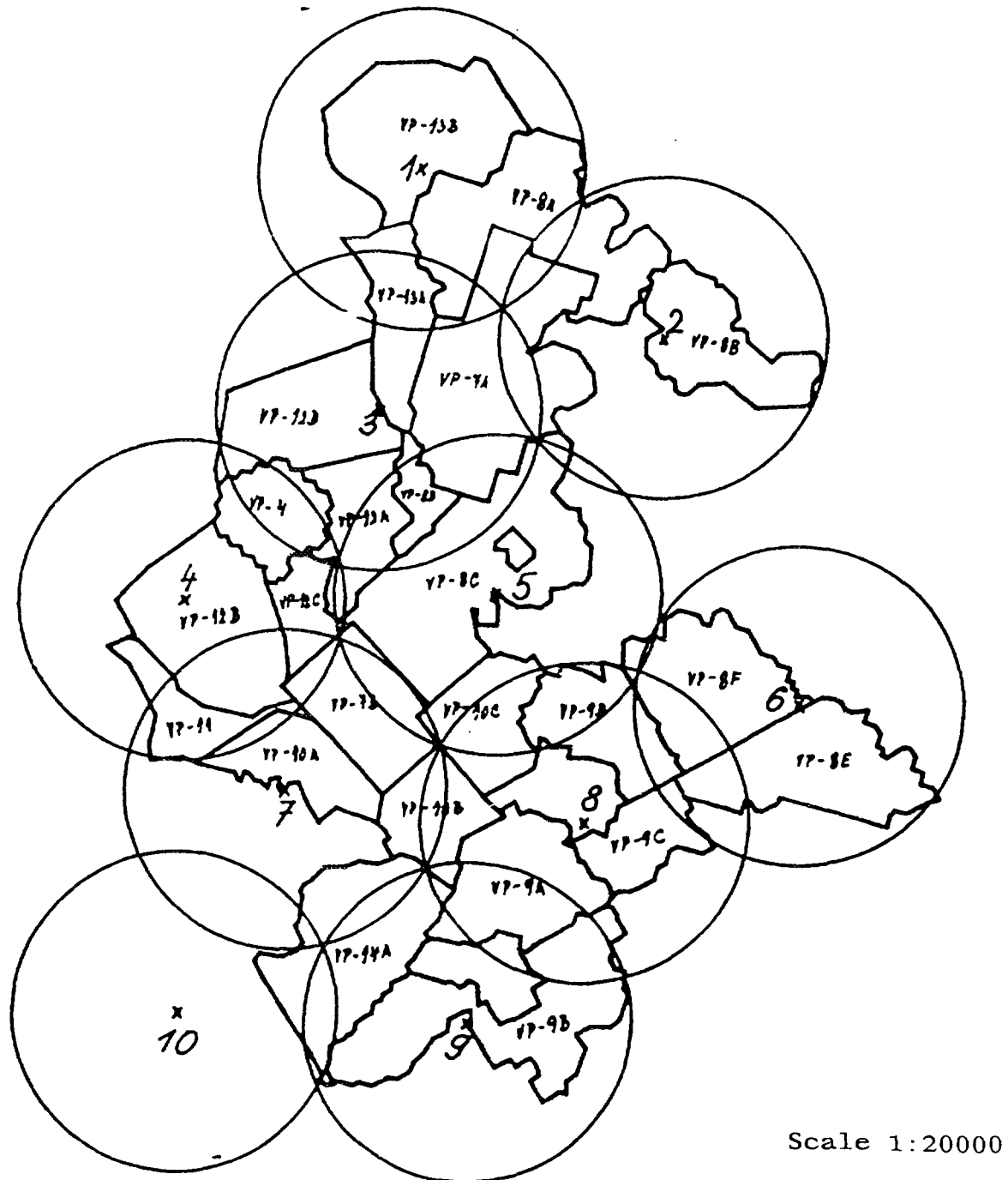


FIG. 2. Substitution of the chemical leaching mine wells system with 9 circular area sources of a radius of 500m.

For calculation of the radon dispersion the decay term $f_R(t) = e^{(-\lambda t)}$ with the decay constant $\lambda = 2.006 \cdot 10^{-6} \text{ s}^{-1}$ was added to the general function.

TABLE I. LIST OF THE RADON SOURCES IN THE HAMR-STRÁŽ AREA

Source	Emission of radon	
	immediate 10^6 Bq/s	total 10^{14} Bq/y
1. ventilation of the mine DH1	2,184	
2. ventilation of the mine DK	0,406	
3. ventilating well VV-2	0,189	
4. ventilating well VV-8	0,320	
5. ventilating well VV-13	0,015	
6. ventilating system of CHRP	1,875	
7. Central Decontamin. Station	1,319	
sum of the point sources	6,308	1,989
8. ore depot DH1	0,559	
9. ore depot DK1	0.333	
10. ore depot CHRP	0.266	
11. tail dump DH1/1	0,004	
12. tail dump DH1/3	0,007	
13. tail dump DK1	0,005	
14. waste pond CHP	0,109	
15. reservoir Pustý	0,042	
16. reservoir DK1	0,002	
17. reservoir Ještědka	0,010	
18.-26. chemical mine	1,162	
sum of the area sources	2,99	0,788
sum of the technocal sources	8,807	2,77
background above the deposit	1,120	0,353
background the Stráž block	2,960	0,933
sum of the natural sources	4,080	1,286
T O T A L	12,887	4,063

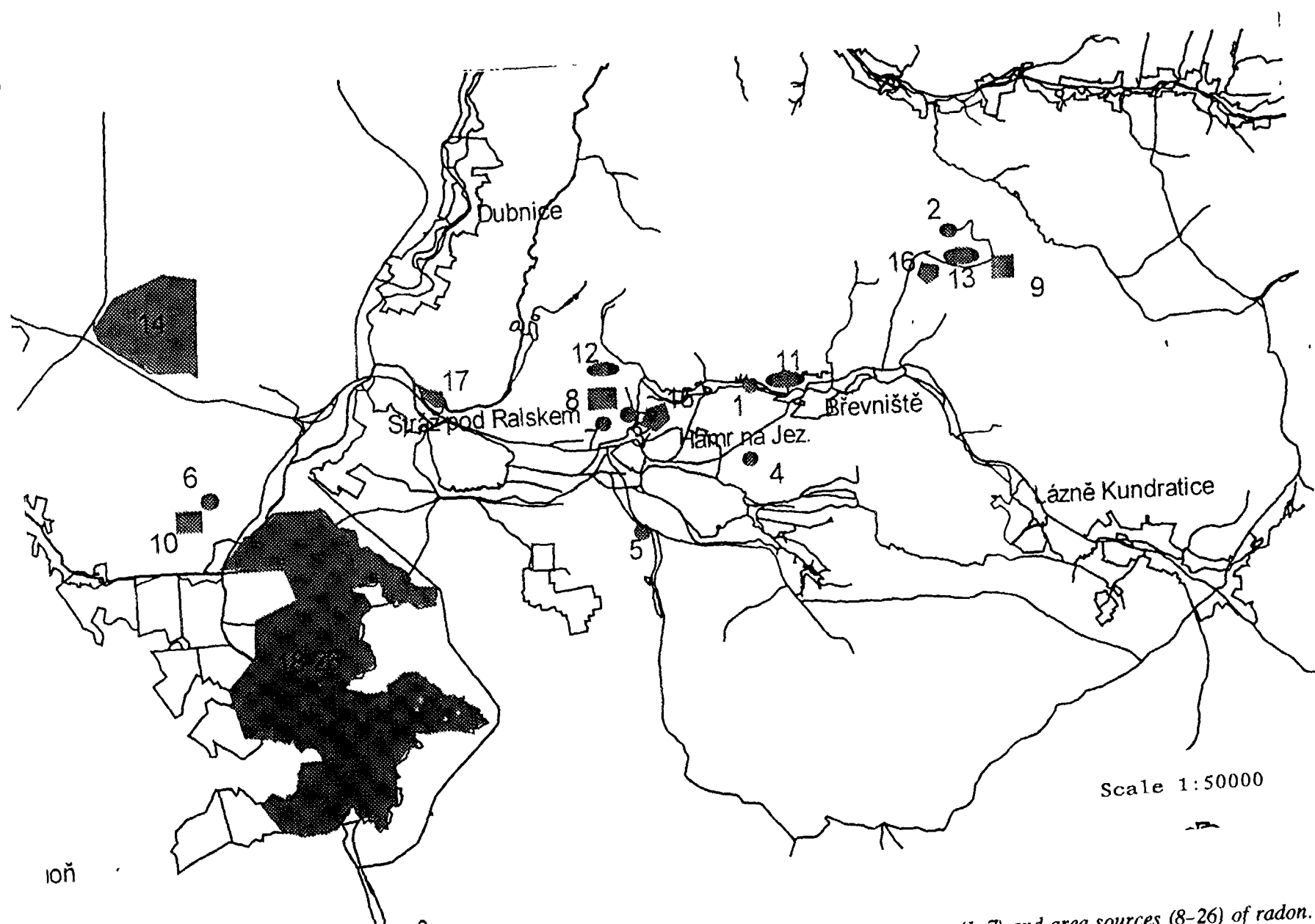


FIG. 3. Model area — situation, point sources (1–7) and area sources (8–26) of radon.

4. AN AREA SOURCE

In general the volume activity of radon at point (x,y,z) is given by

$$a_v(x, y, z) = \iiint V(x', y', z') R(x-x', y-y', z-z') f_R dx' dy' dz' \quad (3)$$

where V is emission rate at the point (x', y', z') of the source (Bq/m²/s), R is dispersion function and f_R is decay function.

For circular source with radius r , with constant area intensity of emission V , with the dispersion function (2) and with the origin of the coordinate system at the centre of the source the volume activity is given by

$$a_v = \frac{2V}{u\pi k_x k_y} \int_{-r}^r \int_{-\sqrt{r^2-x'^2}}^{\sqrt{r^2-x'^2}} \frac{1}{(x-x')^{2-n+m_y+m_z}} \cdot \exp\left(-\frac{y-y'^2}{k_y^2(x-x')^{2-n+2m_y}}\right) \cdot \exp\left(-\frac{h^2}{k_z^2(x-x')^{2-n+2m_z}}\right) f_R dy' dx' \quad (4)$$

where σ_y, σ_z were replaced by $k_i \cdot 2^{1/2} \cdot (x-x')^{1-n/2+m_i}$ for $i = y, z$. The constants k_i, n, m_i are dependent on atmosphere stability.

If the substitution $a = 1-n/2+m_y, b = 1-n/2+m_z$ is used, then

$$a_v(x, y) = \frac{V}{\sqrt{\pi} u k_z} \cdot F(x, y), \quad (5)$$

where
and

$$\Phi(u) = \frac{2}{\sqrt{\pi}} \int_0^u \exp(-t^2) dt \quad (7)$$

is probability function.

$$F(x, y) = \int_{-r}^r \frac{\Phi\left(y + \frac{\sqrt{r^2-x'^2}}{k_y(x-x')^a}\right) - \Phi\left(y - \frac{\sqrt{r^2-x'^2}}{k_y(x-x')^a}\right)}{(x-x')^b} \exp\left(-\left(\frac{h}{k_x(x-x')^b}\right)^2\right) \cdot f_R dx' \quad (6)$$

The integral $F(x,y)$ is possible to solve only numerically and for the computer calculation the algorithm for numerical integration have been prepared.

5. Results of calculations

As a receptors for calculation of expected volume activities were chosen both the nearest residences where greater emission of radon could be expected, and the nearest larger residential zones (Mimoň). These points were chosen with consideration of locations of the radon sources in the area and of the character of the settlement of the area. Greater attention was then given to villages Hamr n.J. and Stráž p.R., which are situated in the centre of the observed area. The background value was not included into calculation and therefore all calculated values represent an increase of volume activity of radon from technological sources.

There is a brief list of the results shown in Table II. It is only a summary of the most important results of the large set of output files. Seeming clash between columns 1 and 4 in Table II is caused by different meaning of both values - the maximum value a_{\max} is the most unfavourable situation, which could happen in the given place regardless of its probability. Number of hours of exceeding of certain value is calculated from real wind rose for given area and therefore it corresponds with relative frequency of the direction and the speed of wind during the different atmospheric situations.

Watching results, we can see that the highest values were reached in Hamr n.J. whose population can be therefore considered as a critical group of population. In 1986 there lived 110 inhabitants in Hamr n.J., 26 children and 84 adults.

The average volume activity from technological sources in Hamr n.J. (5.73 Bq/m^3) was of the same order as presupposed values of the background level — average worldwide ground-level volume activity of radon on surface is 7.4 Bq/m^3 [2], in Czech Republic it is 5.5 Bq/m^3 [3] — and it was here influenced by the fact, that Hamr n.J. is situated right above the deposit. Total exposure per year of the population of Hamr n.J. is calculated from this average volume activity. The value $1.45 \times 10^9 \text{ MeV}$ represents 18 per cent of the year limit of inhalation per individual. This outcome is actually slightly lower, because except the case of the atmospherical inversion there is never reached the balance of radon and its decay products in the location of inhalation because of short transport distance between the source and the receptor.

TABLE II. RESULTS OF CALCULATIONS

The maximum and average volume activity of radon per year, the numbers of the sources with maximum addition to the maximum activity and numbers of hours per year with activity in the different classes.

Town/ village	1 max. a Bq/m^3	2 avr. a Bq/m^3	3 no. of source	4 hours > 29 Bq/m^3	5 hours < 1 Bq/m^3
Hamr n.J.	111.7	5.73	8	401	4963
Útěchovice	71.7	2.78	8	141	5529
Břevniště	82.9	3.62	8	278	6183
Dubnice	83.2	1.89	8	55	6409
Žibřidice	54.8	1.11	1	18	7158
Stráž p. R.	52.4	3.25	10	95	5353
L. Kundratice	50.0	1.05	1	0	6995
Mimoň	26.0	0.56	6	0	7805

The value of cca 29 Bq/m³ would correspond with the limit income per year (according to the regulations of former CSSR). Although maximum reachable value was 111.7 Bq/m³ in Hamr, value 29 Bq/m³ would be exceeded only during 401 hours per year. In the other hand, volume activity during 4960 hours would be lower than 1 Bq/m³.

Despite the fact that point sources with high emission values (ventilation stations, ventilation system of CDS, ventilating wells) were to be found in close range of Hamr, from the emission point of view the influence of ore depot DH1 was the greatest. The most decisive factor against the point sources was low elevation of this area source over terrain.

The area sources (especially ore depot DH1) were the most decisive within the area. The point sources with higher emission values and greater height were manifested more on the boundary (Zibřidice, Mimoň, L. Kunderatice). Result volume activities of radon were much lower in these cases than presupposed background and were so low that calculations of dispersion for larger and more distant (more than 30 km) residential areas as Liberec or C.Lipa proved as useless.

Figures 4 and 5 show the isolines maps of average and of maximum volume activity of emitted radon from the technological sources.

6. NEXT PROGRESS IN THE AREA

The supply of exploited and non-processed ore was gradually decreased to unnecessary technological minimum because of the results of these calculations. Area of the leaching fields was increasing at the same time until it reached final 6.2 km². This happened with the low increase of circulated volume of solutions. The cleaning station of acid mining waters was also built. This plant is as well the source of radon. Total emissions of radon therefore stayed on the same level in years 1986–1991, but impact on population was decreased as a result of the reduction of the most risk sources.

The radical decrease of the uranium mining in the area was started in 1992. The deep mine Krizany is already liquidated and technological emissions of radon (except the unimportant addition of tail dump) are completely over. There is only a cementation of the shaft and corridors in the deep mine Hamr. As a result of the reduction of the ventilated area of the mining field the emissions from the mine were decreased. Emissions from the cleaning of the mining waters are still without changes. Supply of the exploited ore were processed and the chemical recovery plant finished its work. The number of the active wells and the amount of the circulated solutions and therefore amount of the emissions was lessened in the chemical mining. The total level of the technological emissions of radon till year 1995 was decreased by 50%.

The next important change will take place around year 2000 when liquidation and flooding of the mine Hamr stop. Only remediation works will be done in the area — covering of the waste pond of the chemical recovery plant and liquidation of the remaining technological solutions in the Stráž deposit. Remediation of the Stráž deposit will last around 30 years. The solutions will be pumped out onto surface, where contaminants would be separated. It is important to count with emissions of radon in the range from 0.5 to 1.5×10^6 Bq/s in dependence on changing volume of pumped out solutions during all this time.

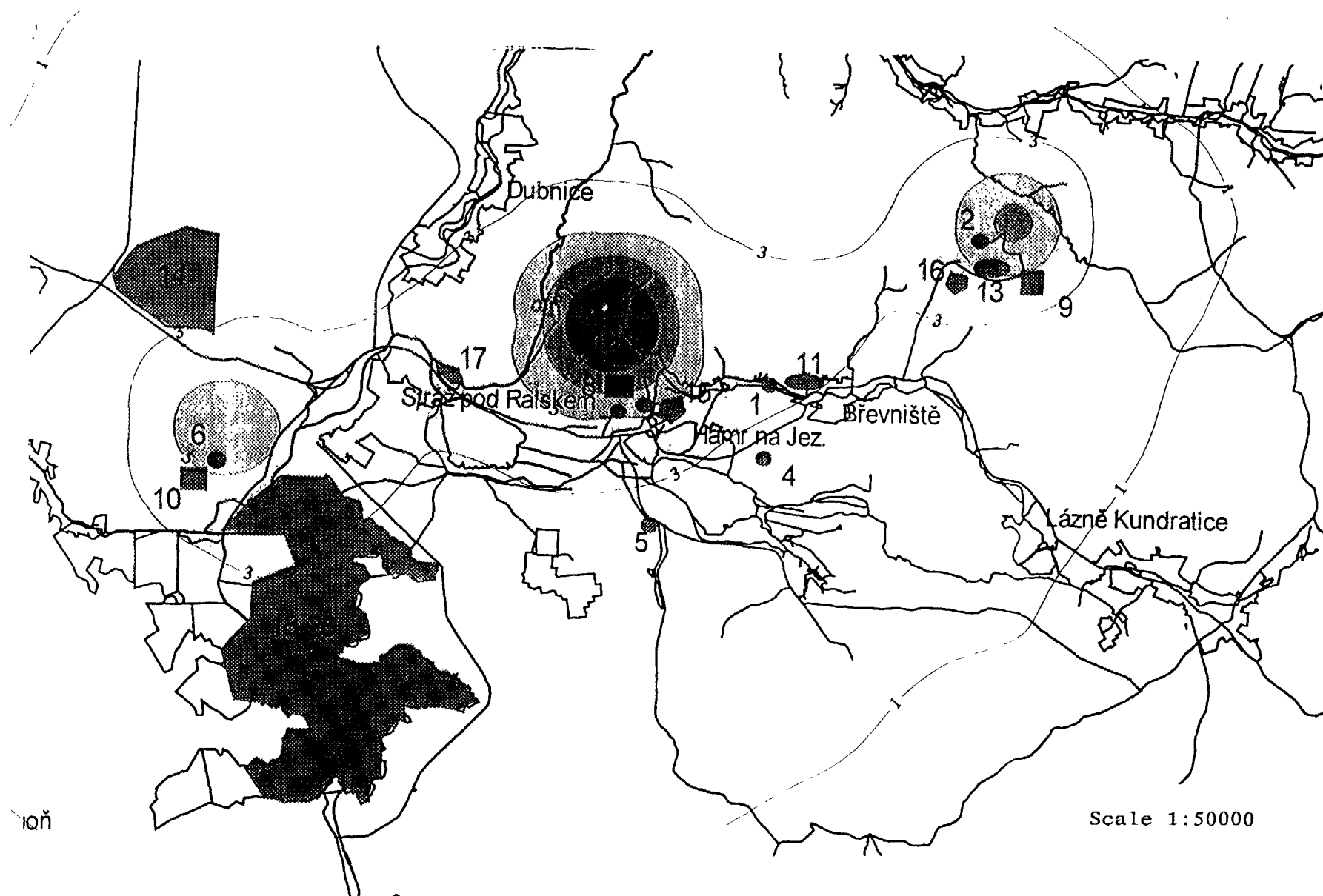


FIG. 4. Isolines of average (per year) volume activity of emitted radon from the technological sources in Bq/m^3 .

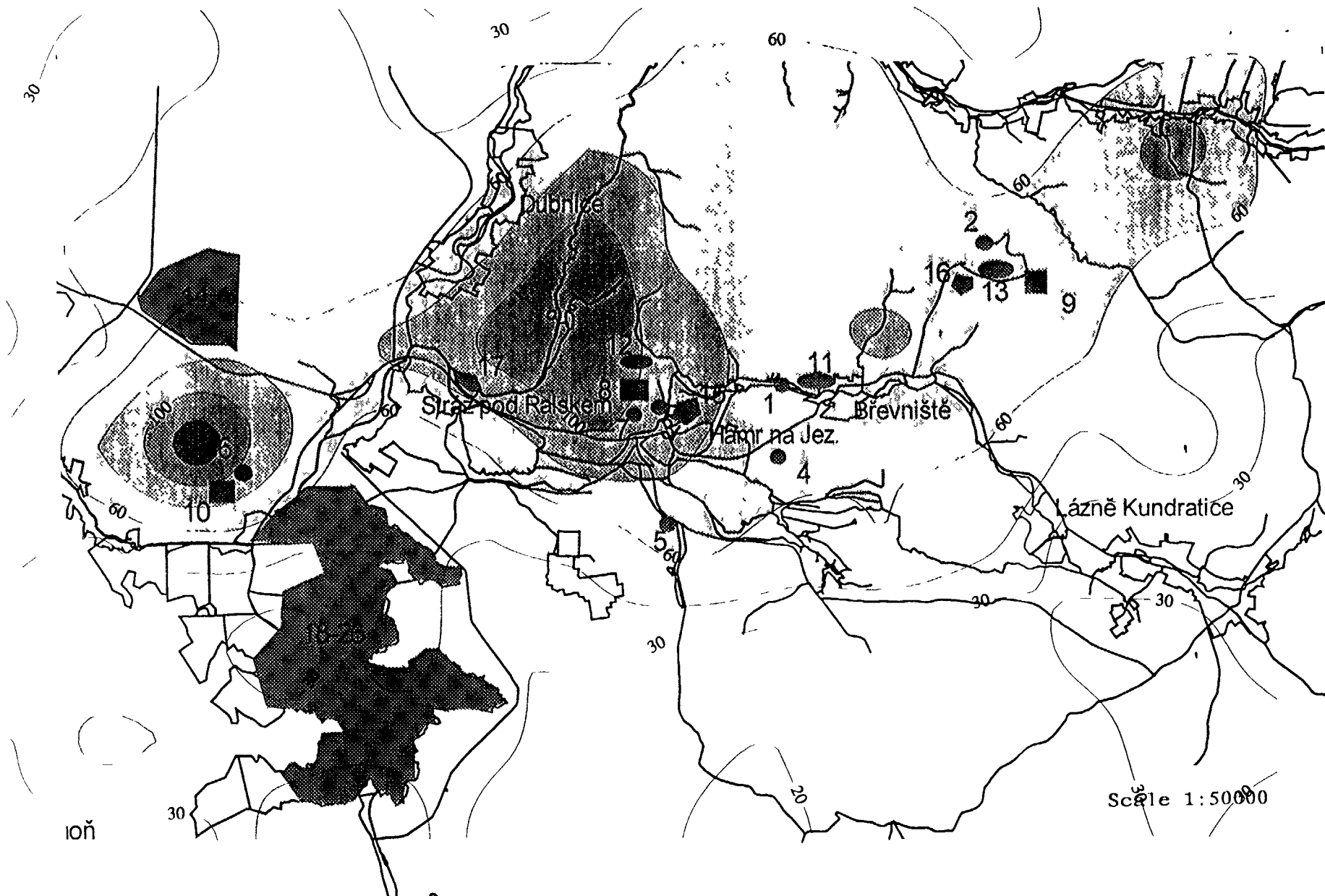


FIG 5 Isolines of maximum volume activity of emitted radon from the technological sources in Bq/m^3

7. CONCLUSIONS

1. The technological emissions of radon were cca 8 times greater than the natural background above the area of the deposit in the period of the maximum progress of the uranium mining in the area of Stráž and Hamr.
2. The limits of the allowed impact on the population were not exceeded in the area. The impact on the critical group of the population of Hamr n.J. reached 30% of the limit.
3. Emissions of radon from the chemical mining represented only 20% of the emissions from the deep mining with the comparable production of uranium.
4. In these days the liquidation of the mining takes place. Emissions of radon are roughly the half of the presented maximum state and are still decreasing.
5. Technical emissions will be lessened to the level of the background above the deposit after the liquidation of the deep mine in the period of remediation of the chemical mine (years 2000–2030) is finished.

REFERENCES

- [1] BUBNIK J., The calculation of the air pollution from the point sources (in Czech), MLVH Praha (1979).
- [2] COHEN B.L., Radon: Characteristic, Natural Occurrence, Technological Enhancement and Health Effects, Progress in Nuclear Energy, Vol.4, Pergamon Press (1979) 1–24.
- [3] Ionising Radiation in the Environment (in Czech), SNTL Praha (1988).



NEW APPROACH TO AIRBORNE MONITORING OF RADIOACTIVE POLLUTION

V. HÖSCHL, P. JURZA
Picodas Prague Ltd,
Prague, Czech Republic

B. PAVLIK
Picodas Group Inc.,
Toronto, Canada

Abstract

The use of remote sensing methods in the monitoring of an environment is increasing. The best results are obtained when various types of exploration methods are available. This paper presents the use of airborne gamma ray methods, which can be included in a wide scope of works related to environmental problems. It may concern uranium mining areas, areas surrounding various nuclear facilities or areas of Chernobyl fallout. Gamma ray spectrometry data can be combined with airborne magnetic, surface gravity and satellite imagery data to obtain maximum information in data output. Airborne geophysics is able to detect and delineate radioactive contamination and to find important geological trends defining the geological structure of the monitored area. Our company PICODAS Prague Ltd. introduces new sophisticated airborne instrumentation as well as up-to-date data processing and data presentation techniques. In the Czech Cretaceous, a long term project, "The Structurally-tectonic Survey of the South-West Foreland of the Stráž Deposit" has been undertaken, concerning the ecological load on the environment, especially the pollution of the underground water level horizons due to uranium mining in that area. The major interest is the complicated tectonic structure which interferes heavily with the hydrogeological situation of the region. The paper presents the results of airborne surveys and the interpretation of other geophysical data from the surroundings of Stráž pod Ralskem and from Karlovy Vary.

1. INTRODUCTION

The paper refers to airborne gamma ray spectrometry as a useful tool that can be included in the scope of remote sensing methods while monitoring an environment. In the past this method was developed for the purpose of geological survey, today it finds numerous applications in monitoring of radioactive pollution associated with uranium mining, radioactive waste disposal sites, nuclear processing plants, nuclear power plants and heavy industry. Collected data are used as a special layer for GIS applications.

For the data acquisition we use new sophisticated instrumentation ENMOS (Environmental Monitoring System). This system was manufactured by PICODAS Group Inc. and was specially developed with the intention to speed up survey mobilisation. In the case of emergency the response is available in the aircraft with the use of real time processing and smart data output. The in house developed software that controls data acquisition system utilizes GPS navigation and GIS or satellite image data as a geographical data base for collected data.

The data presented at this conference was processed by PICODAS Prague and World Geoscience Corporation in Perth. For graphic representation of results we use the software Geosoft and ER-Mapper. In the next text we will present some part of the data that was collected in Czech Republic in the years 1992–1996 by Picodas Prague.

2. SURROUNDING AREA OF THE SPA KARLOVY VARY (W BOHEMIA)

This year we performed measurements in the surroundings of the spa Karlovy Vary and we found that the sediments of the river Rolava are polluted (exposure rate is higher then 15 mR/h) with radioactive nuclei. This can also be seen in Fig. 1 (illustrating the distribution of ^{238}U). This pollution must be caused by man made activities.

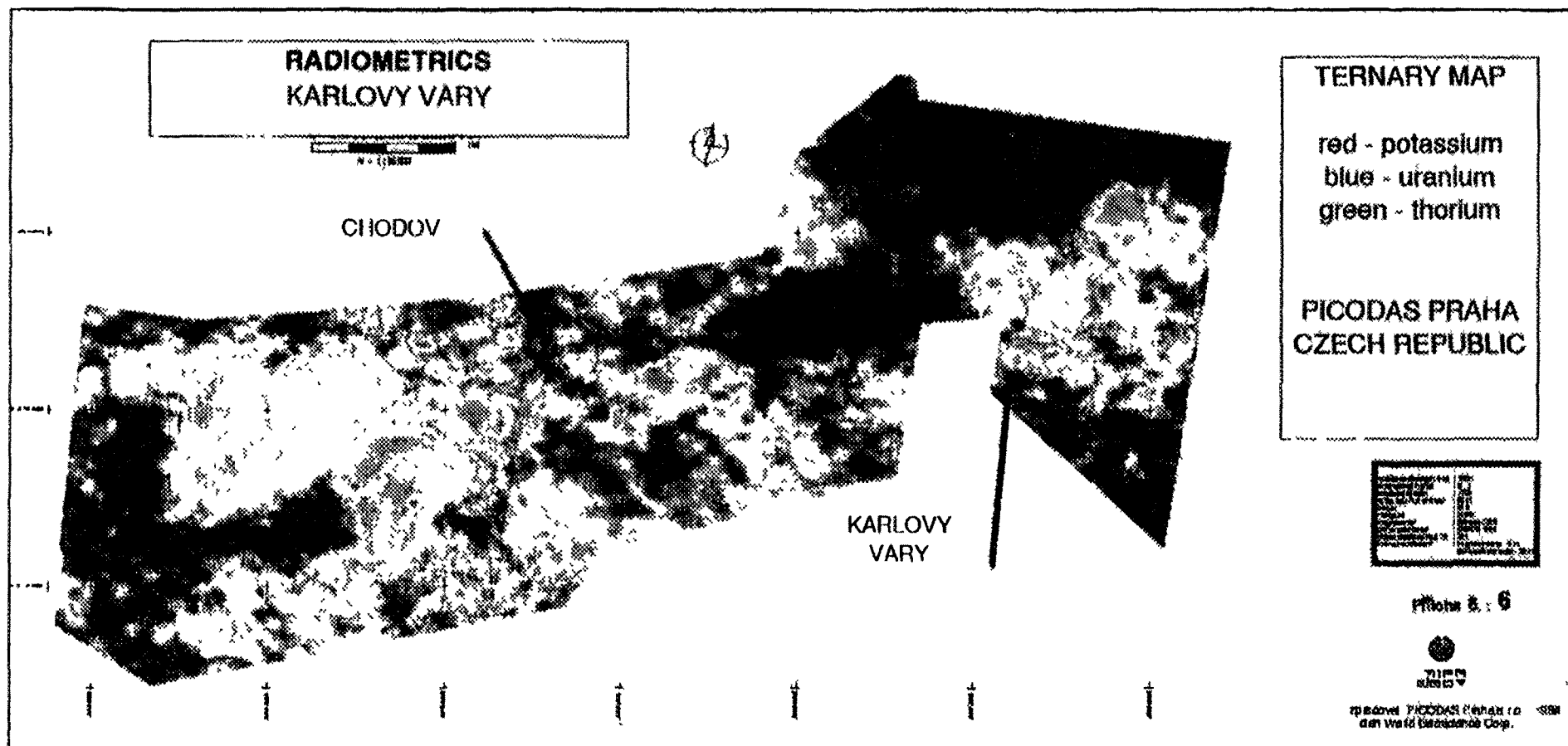


FIG. 1. Ternary map. Surrounding area of the spa Karlovy Vary.

Very interesting is also the distribution of U, Th and K (ternary map) of this area (Fig. 2). This indicates the geology and can help us to understand the relatively complicated tectonic structure of this area. These structures are typical not only for uranium mineralisation but also for wells of mineral water.

3. THE AREA OF URANIUM MINE STRÁŽ (N BOHEMIA)

The results of airborne magnetic and radiometrics in combination with airborne thermometry and surface gravity prospecting allowed the construction of the structural and tectonic scheme of the area. The second result was the map of risk zones (Fig. 3). We interpreted three kinds of zones [1]:

- type indicates surface pollution of soils caused by uranium mining activity,
- type indicates areas of possible communication of polluted water along the tectonic structures,
- type is interpreted in the area of relatively deep structures that can involve the communication of underground polluted water.

The artificial pollution (river Plouènice, mine Hamr, setting pit) is very clear in the ^{238}U distribution map and in the map of exposure rate (Fig. 4). The thorium anomalies are natural and are caused by neovolcanic bodies. Combination of residual gravity anomalies together with the first vertical derivatives of the magnetic field show the third dimension of geological structures.

4. CONCLUSIONS

The above mentioned examples show the capability of ENMOS system for monitoring the environment. The methodology for the calculation of exposure rate, developed by Picodas and the Technical university in Prague [2], helps to present the data in the units useful for hygienic review. The combination of magnetics and radiometrics measurements with additional geophysical methods allows us to determine both: the risk assessment of the area and to complete the knowledge of the geological structures.

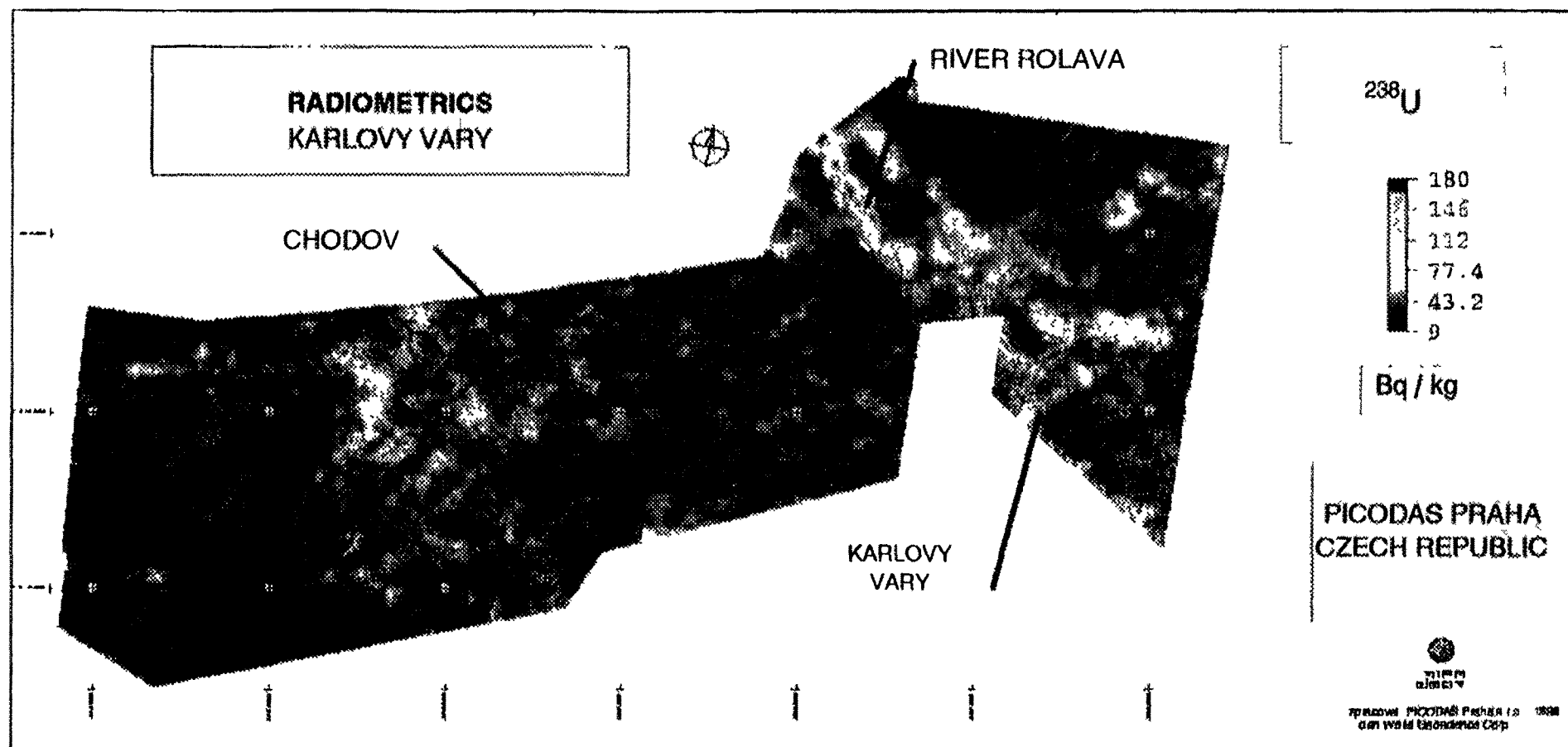


FIG. 2. Distribution map of ^{238}U . The anomaly around the river Rolava was caused by uranium industry.

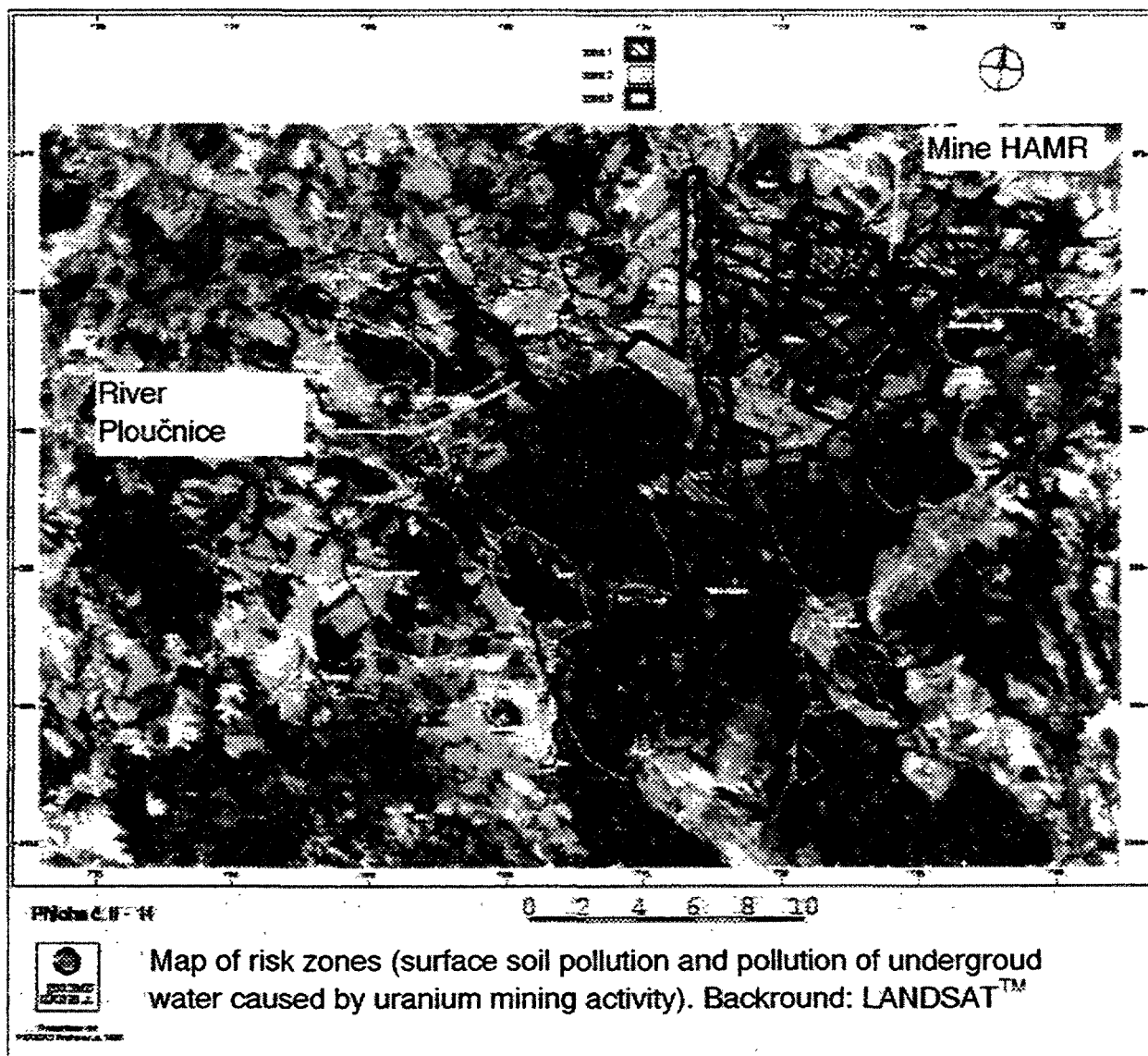


FIG. 3. Map of risk zones: 1 (red) — surface pollution; 2 (magenta) — possible communication of polluted water along the tectonic structures; 3 (blue) — the area of relatively deep structures can involve the communication of underground polluted water.

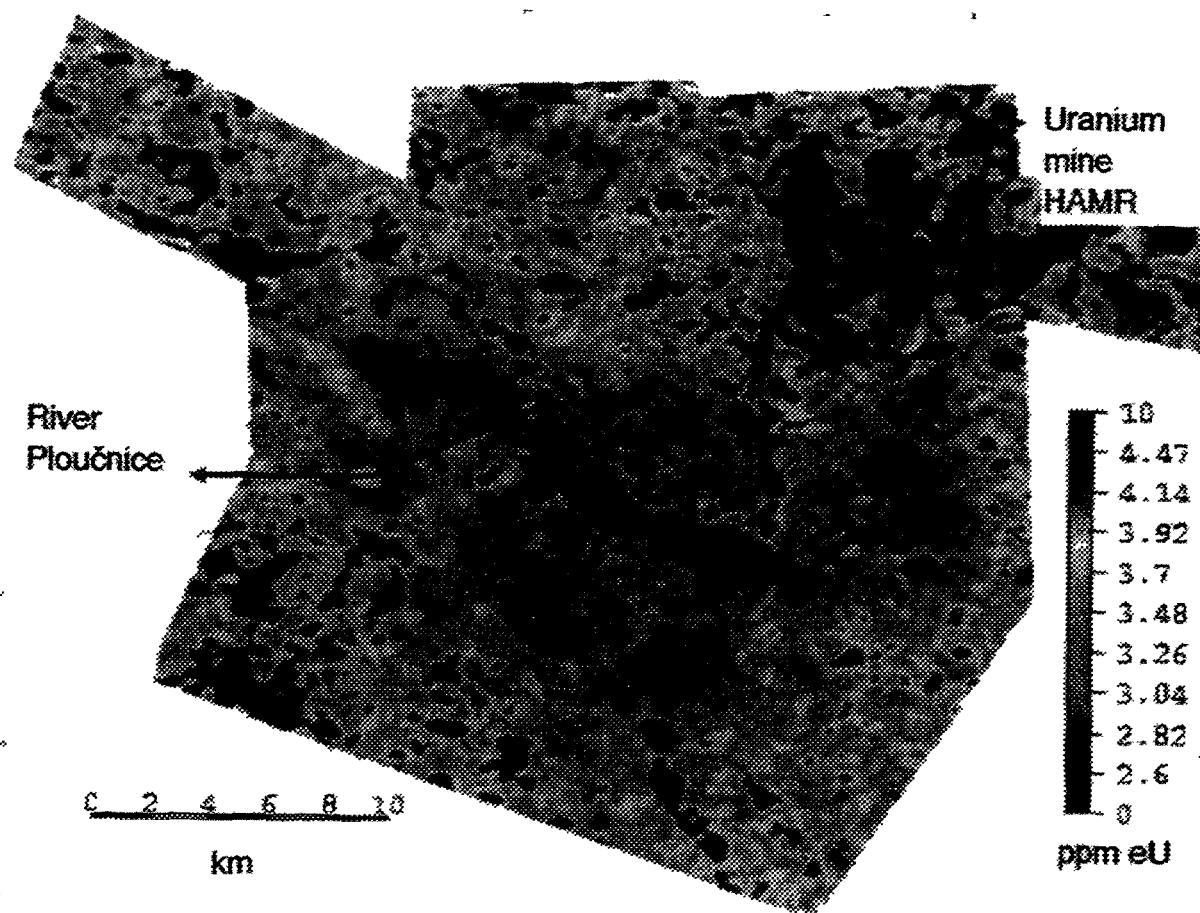


FIG. 4. Distribution map of U. Stráž pod Ralskem — area of uranium mine; Czech Republic.

TABLE I. COMPARISON OF AREAS (EXAMPLE OF THE MONITORING OF RADIOACTIVE POLLUTION IN THE CZECH REPUBLIC)

Area	Karlovy Vary	Stráž
project objectives	tectonic mapping	environmental monitoring
key methods	magnetics	radiometrics
associated methods	radiometrics gravity	magnetics gravity
deposits	BRAWN coal kaolin	uranium building stone
resources	mineral water	water
geology	sedimentary basins crystalline complex	sedimentary basin neovolcanic bodies
industrial noise	high	low
results	tectonic scheme	interpretation of risk zones
pollution caused by	mining activity, industry	uranium mining activity

TABLE II. AIRBORNE SURVEY DETAILS

Area	Karlovy Vary	Stráž
Line spacing	100 M	250 m
Tie lines	500 M	1000 M
Line direction	N-S	N-S
Ground speed	30 m/s	
Sampling interval	radiometrics (30 M), MAG (3 M)	
Data acquisition system	ENMOS 2001	
Radiometric sensor	Na I (Tl) crystal box, volume 20 l	
Magnetometer	Caesium sensor, Scintrex CS-2	
Sensor height	80–100 M	80–100 M
Navigation	differential GPS	
When flown	1996	1992, 1993
Aircraft	MI - 8	MI - 17, Shirke Commander
Data processing	Picodas Prague	

ACKNOWLEDGEMENTS

We would like to acknowledge the authorization for publication of the Stráž data by Diamo s.p. and the Karlovy Vary data by Geokonzult. The geological interpretation of geophysical data of deposit Stráž was done in close co-operation with the geologists from DIAMO s.p. and BGC a.s.

REFERENCES

- [1] HÖSCHL V., JURZA P., Interpretation of remote sensing method (final report in Czech), DIAMO s.p., Stráž pod Ralskem (1996) 40 p.
- [2] ĚECHÁK J., KLUSOŮ P., MALUŠEK I., Spectra Processing in Airborne Gamma-Ray Spectrometry Using the ENMOS Detection System. Technical Report, Faculty of Nuclear Science and Physical Engineering, Prague (1994).

**NEXT PAGE(S)
left BLANK**



ESTIMATE OF THE RADIOLOGICAL STATE OF THE ELESHNITZA URANIUM DEPOSIT, BULGARIA

I. BOJKOV, T. TZENOV
Committee of Energy,
Sofia, Bulgaria

Abstract

The uranium deposit "Eleshnitza", located within the palaeogenic sandstones, was discovered 40 years ago when an airborne X ray picture at 1:100 000 was taken. The deposit is located in the south west of Bulgaria, around 150 km south of Sofia. Around 20% of the total amount of uranium originates from that deposit. A processing plant has been in operation for 30 years on the territory of the deposit. Production has been developed with shafts and galleries on an area of 153 decares, and 43 dumps with a mining capacity of 1 750 00 m³ (around 3 million tonnes). The processing plant along with the tailings pond cover an area of 900 000 m² with 8.5 million tonnes of waste. The radioactive estimate conducted on the territory of the deposit, after production phase-out in 1992, demonstrates quite a contrasting picture of proliferation (exceeding the radioactive background values) of natural radionuclides. The high value of radon, "soil" gas, and airborne gas (60–65 Bq/m³) is due to the increased emanation potential of the uranium ore left in the deposit. The natural (geogenic) and technogenic radioactive pollution were defined. The average night value of the potential energy in the summer months measured in the area of the settlement is 350 nJ/m³ (at morning's level 710 nJ/m³). These values characterize the region as a radiological phenomenon. The geophysical methods applied in studying and operating the uranium ores — emanation picture, gamma spectrometry, radiometry were successfully applied in making a radioactive assessment of the whole area of the deposit after the production phase-out.

THE DEPOSIT

The uranium deposit "Eleshnitza" is located in the south-west part of Bulgaria, around 150 km to Sofia. The deposit was discovered during the parallel conduction of ground radiometric works and the taking of an airborne X ray picture in 1954–1956. The intensive explorative and geological works on an area of 16 km² drilling and horizon and upward mining led to finding a surface uranium ore deposit at a depth of 600–650 m.

The area of the "Eleshnitza" deposit is located in the north-east part of the Razlog valley at 700 to 900 m above sea level. The deposit region itself represents a local fold basin surrounded by heights. The climate within the region is moderately continental with an average annual temperature of the air 9°C, average annual minimal temperature 3.6°C and average annual maximal temperature 14.8°C. The studies that have been carried out on the wind potential (windrose) show that annually 77% of the time the weather is quiet and the winds are mainly western (66%) and north-western (22.3%). The average annual rainfalls fluctuate from 658 to 747 mm, as the maximal rainfalls occur in December and the minimal in August. The river Mesta is the main river in the region. The river Zlataritsa is the main river draining the entire area. The village of Zlataritsa is located on the territory of the uranium deposit along the Zlataritsa river.

LITHOSTRATIGRAPHIC AND TECTONIC CHARACTERISTICS

The uranium deposit "Eleshnitza" is located in the Northern part of the Mesta Tertiary volcanic-tectonic depression. The foundation and the surrounding heights are made up of pre-Cambrian metamorphites and later granitoides. The depression is filled up with sand-conglomerated molasses of the Oligocene period. During the time of its packing an acid, effusive and volcanic, activity occurred.

During the time of the sedimentation and the volcanic activity as well as later in the Neogene period, as a result of an intensive elevation of the neighboring blocks the depression took on a clearly

defined graben aspect. This aspect is most clearly defined in the Mesta and Osenovo-Ribново north-west fault-lines. The subsequent movements have caused the development of north-east and east-north tectonic zones. In the deposit region these zones represent clearly defined fissures along which the subsequent distribution of the uranium ore has occurred.

The "Eleshnitsa" deposit is a sandstone type and of average scale. The uranium ore is located among monowedge-like pointing north-east sandstones, alevrolites and conglomerates. The ore is predominantly made up of seam-lens-shaped particles and is located within the perimeter of the fissures and the transversal "vein" bodies. The more cohesive ore is tied into sandstones and alevrolites and has the following measures: length: 20–30 to 200 m, width: 20–100 and capacity: 1.0 to 3–5 m. The average content of uranium therein is around 0.05%.

The uranium mineralization is made up of — nasturanium, coffinite and uranium mica — autunite, torbernite, uranophane and zippeit. As a matter of fact these are ore combined with iron sulfides — pyrite and marcasite and non-ore minerals represented by zeolites, (heylandite, desmin and limontite) and calcites. The uranium ore is most often accompanied by carbonaceous substances. There are no other accompanying elements. The uranium ore dates back to the Oligocene period.

During the operation period (1956–1992) 66 adits were driven, 6 shafts and 4 large quarries. Since 1965 a processing plant has been in operation on the mine's territory (its southern part). The operation activity with 43 tailing ponds covered 153 000 m² representing some 1 750 000 m³. The sanitary protection zone of the processing plant together with the tailings pond is located on a 900 000 m² with 8.5 million tonnes of waste.

RADIOACTIVE STATUS OF THE FIELD

The good outcropping of the rocks in the area of the uranium deposit "Eleshnitsa" represents an extremely favourable factor for the finding and exploration of both surface and aerogeophysical works. As a result of the aerogeophysical gamma-picture one of Bulgaria's largest (about 16 km²) aerogamma anomaly was discovered with a radioactive dose amounting to 350 nGy/h in sandstones and in 70 nGy/h conglomerates.

The radioactive anomalies are associated mainly with the layers of sandstones and conglomerates and range from 700 to 7100 nGy/h. In alevrolites and tuffaceous sandstones the dose reaches 13 300 nGy/h. The exploration and working of the deposit has indicated the tabular character of the ore-mineralization along stratigraphic levels.

The gamma and emanation maps of the area show development of ore-bearing horizons and the orebodies in the immediate vicinity of the village Zlataritsa.

The sudden closure of the production and processing activities greatly disrupted the planning of preparatory estimation activities in the region with vertical and horizontal uranium ore-bodies, refuse dumps, ore mass for heap surface extraction, etc.

The radiological estimate of the soils and air performed by means of geophysical methods used so far for exploration and production includes: radiometry, gamma-ray spectrometry, track method with solid body detectors, thermoluminescent detectors, aerosol measuring and laboratory analyses.

RESULTS OF THE PERFORMED EXPLORATIONS

Explorations and conditions of the soils

The radioactive pollution of the surface is caused mainly by the uranium ores extracted during mining operations. Measures of the flow of α and β particles and γ emission taken along profiles over the mine area indicated several polluted zones. The most serious radioactive pollution has been registered over the dumps of the adits and the quarries, the heap leaching complexes and around the roads leading to them. The measurements were carried out with a radiometer CPI 68-07 and dosimeter MKC-01 P-01. The values over the polluted areas range from 500 to 1000 nGy/h.

At specific points the absorbed dose of γ -emissions reaches 2600 nGy/h, and the surface α and β -pollution 2 and 350 $\text{cm}^{-2} \cdot \text{min}^{-1}$, respectively.

For the purposes of radiation control and reclamation of the mine co-relational dependence between specific activity of Ra^{226} and the γ -emissions was calculated in samples. It has the following expression:

$$\Delta X_{\gamma} / \Delta A(\text{Ra}^{226}) = 0.0016 \mu\text{Sv/h}^{-1} / \text{Bq} \cdot \text{kg}^{-1}$$

with co-relation co-efficient $\nu = 0.83$.

The equation allows to differentiate the material which needs to be treated for reclamation.

The average specific activities established in the substratum of the dumps in front of the mine workings for U^{238} , Ra^{226} , Th^{232} and K^{40} are 540 Bq/kg, 750 Bq/kg, 55 Bq/kg and 850 Bq/kg, respectively. In the gardens, in the vicinity of the dumps, these activities are: for U^{238} 344 Bq/kg and for Ra^{226} 178 Bq/kg. The established reverse dependence in the distribution of the activities of the two radionuclides is due to the bigger migration capability of U^{238} . It is even more clearly expressed in the samples from the bottom sediments of the gullies and small rivers.

Explorations and conditions of the air

The Ra^{222} content in the air depends both on the availability of significant sources and the location of the site and the conditions of the atmosphere. This applies particularly to closed valleys like the one in which the mining area is located where temperature inversions appear.

Periodical studies on the air condition have been carried out after 1990 and point out a high radon concentration threatening the village [1]. Several measurements have been made regarding the above — with an aerosoloscope type PB-4 of the derivatives of Rn^{222} in two sectors of the village; cumulative measurements of Rn^{222} in the air (at a height of 1–2 m, in 13 sectors of the village and 14 outside its perimeter by means of track detectors LR — 115 (Kodak Pathe type); cumulative measurements in 54 sectors around the village of Rn^{222} in "soil" gas by means of thin dosimetrical thermoluminescent detectors Ca SO_4 ; Dy + B4C.

The average night value of the potential energy is 368 nJ/m^3 . The observations during 24 hours of the fluctuation of the concentrations show that the increase of Rn^{222} and its decomposed matter down to 716 nJ/m^3 starts immediately upon abatement of the air flows in the valley, i.e. after 20–22 p.m.

Thus, the average balance time factor for the period 10 a.m. to 22 p.m. is $F = 0.84$, whereas for the period 22 p.m. to 10 a.m. it is $F = 1.03$. The latter is basically a total balance between the Radon and its derivatives and is due precisely to a considerable abatement of air flows and probably to temperature inversions too. Thus, we define an area of 15–25 km^2 with a high concentration of

The tailings pond of the processing plant located on one side of the village covering an area of 4.2 ha is a substantial local source of Rn^{222} in the region. The average density of the exhalation flow of the surface is around $1 \text{ Bq. m}^{-2}, \text{ S}^{-1}$. For the whole area the flow changes from 210 to 2100 or an average of 420 kBq. S^{-1} .

The problem of accumulation and transportation of Radon in the Eleshnitsa valley appears as a complex task, which will require further efforts. The population in the region is exposed to a serious radiological risk resulting from inhaling derivatives of Rn^{222} .

The periodical measurements and studies using the mentioned geophysical methods and equipment and especially after completion of the technical liquidation and land reclamation, would be most useful. This is especially relevant to a more detailed study of the atmospheric conditions and the natural radioactivity within the region.

BIBLIOGRAPHY

- [1] DIMITROV, M., TOSEV, I., PRESSYANOV, D., Оценка на радиоактивното замърсяване на въздуха с радон и разпадни продукти в някои райони на страната. Свितък доклади XV конференция "Физиката и опазването на човека и околната му среда", Sofia (1990) p. 135 (in Bulgarian).
- [2] GEORGIA, K., Урановые месторождения Елешнишкогo басейна в ЮЗ Болгария. Дисертация за КГМН, (1974), p. 284 (in Bulgarian).
- [3] ICRP, Publications 50 (1988).
- [4] PRESSYANOV, D. Radiation, Protection Dosimetry, 38 (1991) p.315.
- [5] PRESSYANOV, D., GUELEV M., KVITIDIS P., Integrated measurement of Rn^{222} in soil-gas by combination of SSNTD and TLD, Environment International (1996), (in press).



THE USE OF URANIUM EXPLOITATION TECHNIQUES IN THE SELECTION OF A CANDIDATE SITE FOR CS-137 RADIOACTIVE WASTES FROM THE GOIANIA ACCIDENT

S. SAAD

Comissão Nacional de Energia Nuclear CNEN/COMAP,
Rio de Janeiro, Brazil

Abstract

The selection of a candidate site for the disposal of wastes containing Cesium-137 originated by the Goiania accident followed a sequence of studies where specific exploratory techniques in the field of geoscience were applied through geophysical, geochemical, hydrological, hydrogeological and pedological investigations and subsurface drillings. This programme has been aimed at characterizing in detail the selected site, in order to obtain parameters for the conceptual engineering design and also to elaborate the Environmental Impact Report. Among the different options encountered, the site which presented the best characteristics to store those wastes is located about 300 m west of the provisional repository.

INTRODUCTION

To identify sites with favorable characteristics for the choice of a final repository to the disposal of radioactive wastes arising from the accident occurred in Goiania, a site selection study was carried out beginning in 1988 and ending with the selection of three candidate sites.

The selected area is located in the district of Abadia de Goiás (Fig.1), about 20 km southwest of the city of Goiania. The selection of the site and determination of its characteristics are considered important factors for the analysis and evaluation of the engineering design. Through the construction of an engineering barrier system, the repository should allow a long term and safe confinement.

Taking into account the basic requirements for the site selection, it should present natural barriers to maintain the radionuclides isolated in order to avoid effects which should be harmful to the environment. Therefore, the choice of the site was mainly conditioned to the minimization of a feasible groundwater radionuclide migration.

SITE SELECTION CRITERIA

In the evaluation of sites intended for the settlement of repositories at surface of low and mean radiation level wastes, it is important to consider the basic requirements for the site selection, aiming the choice of sites with natural barriers capable of maintaining the release of radionuclides to the environment as low as reasonably achievable. Natural barriers play an important role to minimize the harmful effects of future generations.

For final surface repositories of low and mean radiation level wastes the site selection process considers the criteria of a sequential and selected technical analysis consisting of several levels, in detail, of data and information. Therefore, during each phase of investigation, fundamental criteria of site selection such as: geology, socio-economy, ecology and photography should be taken into account.

The consideration of these criteria aims to determine restraint factors which should restrain or avoid the use of a specific site. Consequently, the site selection of the repository and the determination of its characteristics are considered important factors for the analysis, evaluation and design of the disposal system.

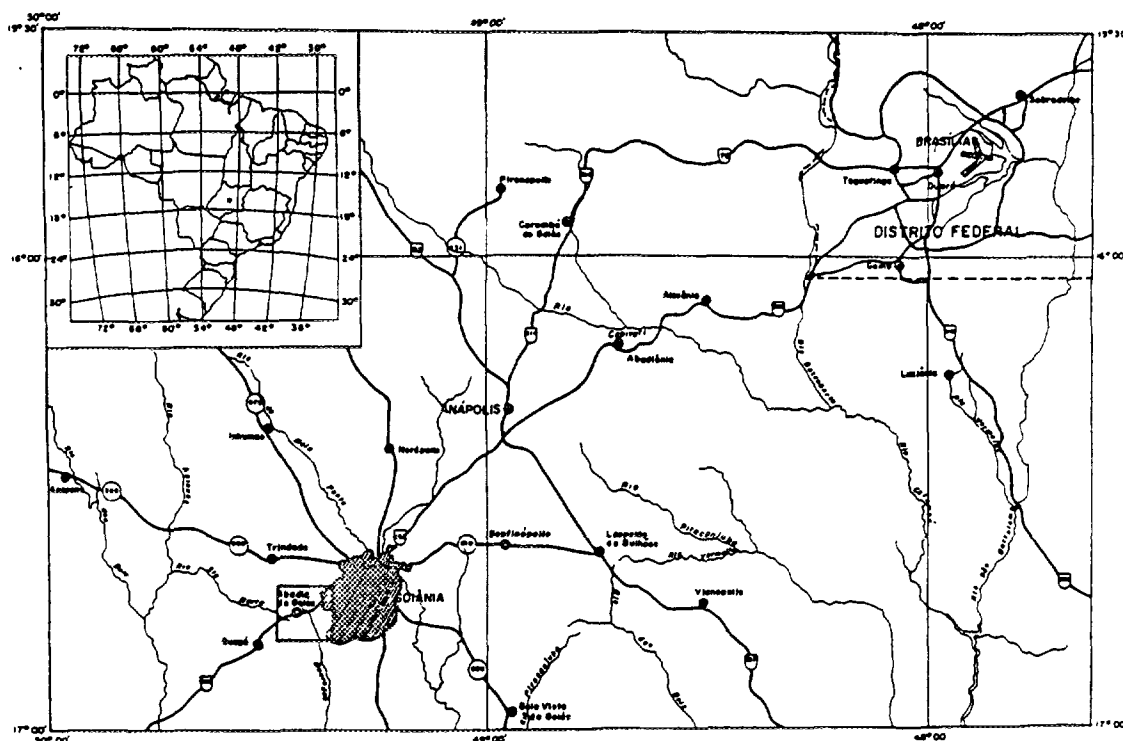


FIG. 1. Situation area.

METHODOLOGY

The studies were carried out considering a sequence of works involving several stages in accordance to the scale under investigation. Therefore, in the beginning, a Region of Interest was defined, in which technical restraint criteria were applied without using details, aiming to define Preliminary Areas was performed by means of restraint factors, using a semi-detailed scale and also the analysis of aerial photographs. For the selection of candidate sites, field reconnaissance of all Potential Areas defined in the previous step has been made, showing their specific characteristics recorded in field registers. Based on this information and using classification and consideration of their characteristics, the Potential Areas were chosen resulting in the selection of three candidate sites.

For the selection of Preliminary Areas, Goiás State was divided in four regions, using a basic cartography on a scale of 1:1 000 000. Afterwards, a series of restraint factors was applied considering the following selection criteria:

- 1) Socio-Economical Criteria
Restraint Factors: Demography, Mineralized Areas.
- 2) Physiographic Criteria
Restraint Factors: Relief, Hydrology.
- 3) Ecological Criteria
Restraint Factors: Areas of Protection to the Ecosystem, Indian Areas, Biological Reserves, National and State Parks.

In this scale of observation, the Geology was not considered as a restraint factor. In addition, a complete seismological survey of the State of Goiás was made.

In a second step, using a basic cartography on a scale of 1:250 000 and 1:100 000 and through the analysis of aerial photographs and applying restraint factors in the field of Geology (lithology, tectonics, hydroecology and geomorphology) was possible to restrain the area to 18 potential areas.

In a third step, candidate sites were selected due the verification "in loco" of potential areas through a detail reconnaissance and using technical restraint criteria.

Then, a methodology of candidate sites selection was established, making possible the comparison of 18 Potential Areas using the punctuation methodology. For the use of punctuation methodology, the following aspects were selected: geology, use of the land, waterground depth, soil thickness, access and distance of means of transport. For each of these aspects, weighing and classification factors were applied. The sum of the product of the weighing factor by the classification factor for each selected aspect results in a punctuation for each area considered.

EXPLORATORY WORKS FOR THE CHARACTERIZATION OF THE SELECTED CANDIDATE SITE

For the selected candidate site, a program of geological studies was set up to define the stratigraphic and structural framework in order to obtain the parameters necessary for the engineering conceptual design. The studies were carried out in several phases according to a pre-established programming.

Phase I (1989)

- Planialtimetric survey of 100 ha, according to NS direction baseline, using the tracing of level curve from meter to meter.
- Geological detailed mapping on a scale of 1:1000, of an area of 100 ha, using geological profiles.

Geophysical Studies

- Scintillometric survey of an area of 100 ha, in a grid of 20 m × 20 m, using a scintillometer SRAT-SPP-2.
- Survey of water table depth of nine water-tanks distributed in the area.
- 18 electric drillings with 15 m to 50 m in depth.
- Electromagnetic survey (VLF-EM) of 9 km of lines along EW profiles.

Phase II (1991)

Geochemical survey of 100 ha, through the collection of soil samples at each 100 m for analysis and characterization of U, Th, K contents and determination of the activities in 230 samples (fractions <2mm and >2mm).

Phase III (1991/1993)

Geological Studies

- Photogeological survey comprising an area of 172 km², on a scale of 1:20 000.
- Geological drillings of 300 m.
- Geological description of seven survey pits.
- Assay of 20 petrographic flakes.

Pedological Survey comprising an area of 100 ha and the description of soil profiles; collection of 20 samples for the analysis of the fertility content; collection of 33 samples for determining chemical, physical and mineralogical characteristics.

Geotechnical Studies

- 15 Percussion drillings.
- 7 survey pits.
- Collection of 181 samples for geotechnical laboratory assays.

Hydrogeological Studies

- Drilling of 4 production wells pits for pumping tests.
- Drilling of 16 piezometers nearby the pumping wells.
- Drilling of 18 piezometers for monitoring water level variation.
- Determination of "in situ" permeability in boreholes for geotechnical studies.

Hydrological Studies

- Excavation of creeks at Quati and Dourado's rivers.
- Setting of level rods (rulers) at Quati's river bank.
- Construction of a meteorological station with pluviometers, lisimeters and two evaporation tanks.

Radiometric Survey

- Gamma spectrometric survey of an area of 4000 m of profiles following EW direction.
- Gamma and Gamma spectrometric profile of 45 boreholes.
- Gamma spectrometric survey of 7 geotechnical survey pits.

RESULTS AND DISCUSSION

Geomorphologically speaking, the area of concern is located in a morpho-structure designated as "Goiana's Peripheric Depression", comprising a sequence of metasedimentary rocks belonging to the Medium Pre/Cambrian Araxa Group.

The area was following a structural-tectonic single scattering regime and presenting NE and NW fractures strikes and NE foliation strikes and a 20° NW dip (Fig. 2).

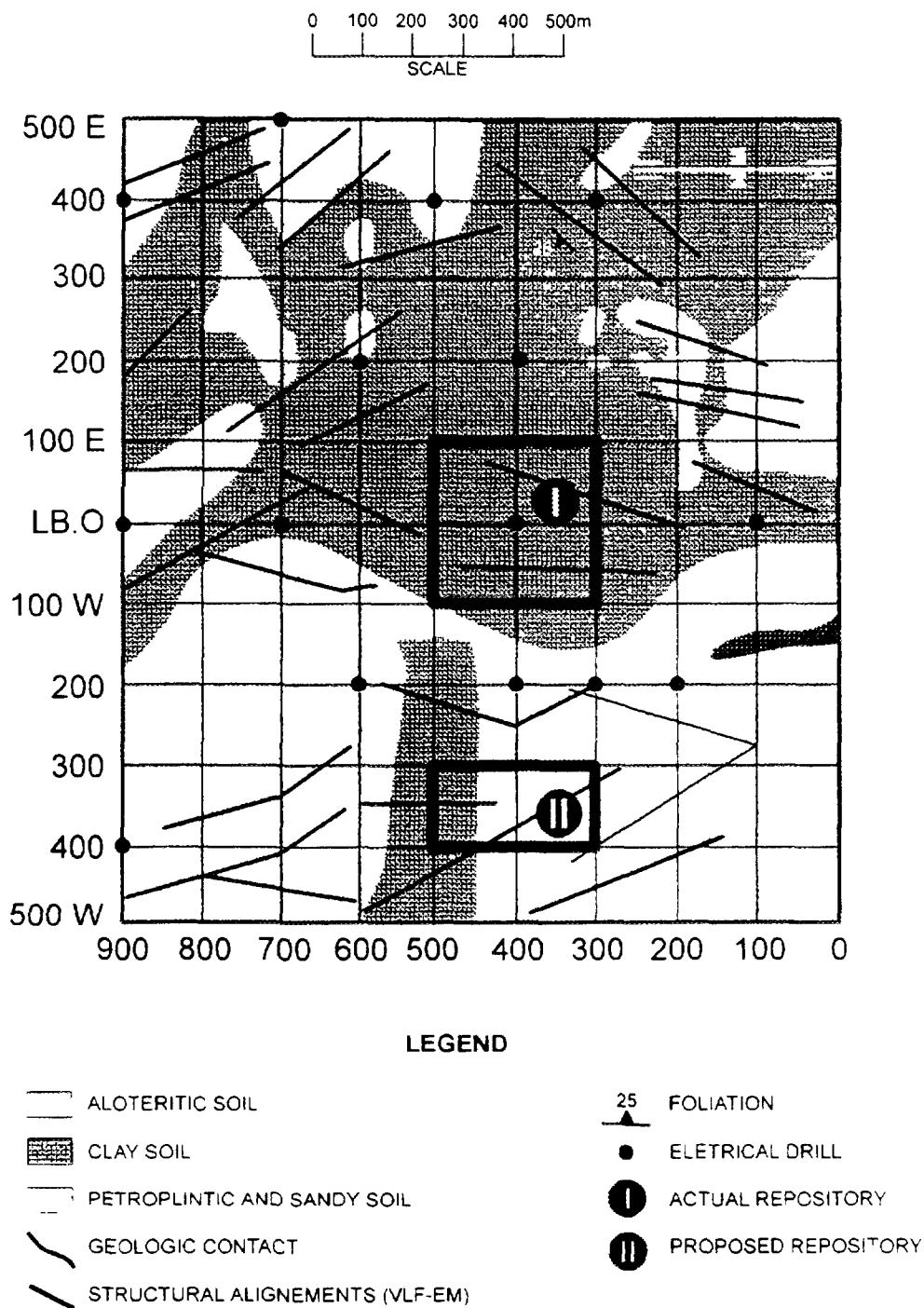


FIG. 2. Area of Abadia de Goiás; geological sketch.

The fresh rock is located nearly 28 m underground. The soil of the area has the following formation:

- yellow-red lathosoils;
- petroplintic soils;
- petroplintic soils;
- areas degraded by men.

The quantities of uranium, thorium and potassium reflect concentrations associated with the existing residual soils, particularly with the potassium concentration which reflects higher concentrations of clay soils of potassium nature. The anomalous quantities of uranium and thorium reflect concentration in more laterised and clay areas.

The geochemical maps and the graphical sections show the dispersions of the analyzed dispersed elements, where it is concluded a much more reasonable correlation between the activities variations and the contents of uranium, thorium and potassium and the corresponding geological context. This identity, between the obtained values and the soil geological nature, show the existence of a contribution of radionuclides of uranium, thorium and potassium families existing in the rocks of the area, which interfere in the Cs-137 channel (Fig. 3).

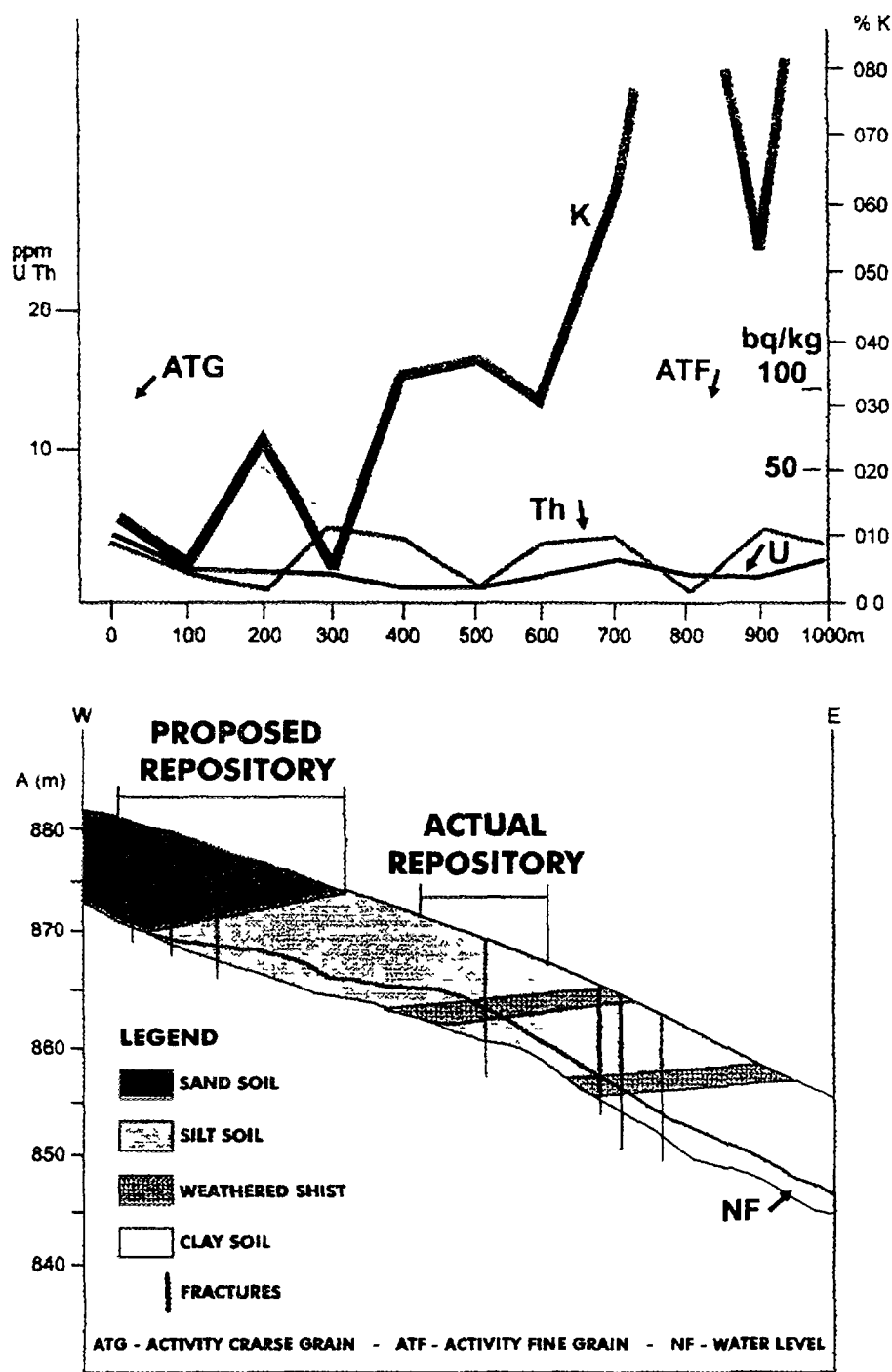


FIG 3 Area of Abadia de Goiás, geochemical cross section. Profile L 300.

The 18 electrical drillings have revealed several resistivity levels whose levels decrease with the depth under consideration, reflecting the subsurface rocks behavior.

The geophysical sections show from three to four resistivity levels, with an upper level of great resistance ($> 10\,000\text{ Ohm/m}$) represented by a petroplintic soil cover, rich in iron and aluminum oxides: an intermediate zone represented by rocks formed by residual soils of schist rocks, with resistivity values from 500 to 5000 Ohm/m and a lower zone constituted by unaltered schist rocks, belonging to the Medium Pre-Cambrian Araxa Group, with a mineralogical composition formed by quartz-feldspar-garnet-sericite schists, and a resistivity varying from 50 to 200 Ohm/m (Fig.4).

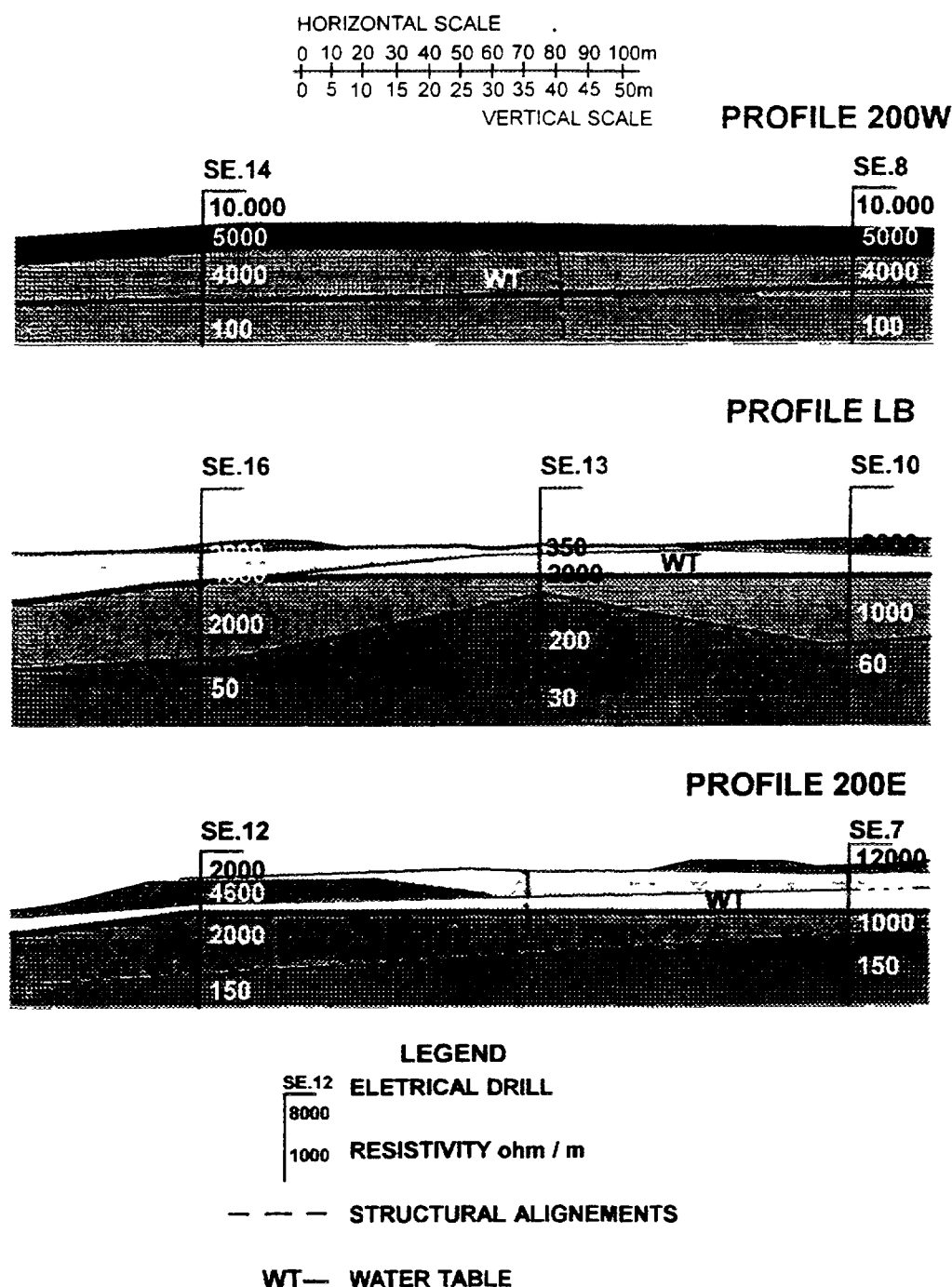


FIG. 4. Area of Abadia de Goiás; geophysical cross section

The 18 electrical drillings have allowed to determinate watertable levels from which the preliminary piezometric map has been elaborated.

The electromagnetic survey (VLF-EM) has allowed to characterize a tectonic framework with a single scattering system and alignments following NW and NE directions, presenting mainly vertical dips and secondarily dips of 50° to NE and NW. The alignments defined through VLF-EM survey can be associated to a low conductivity fracture system with values from 5 to 15 khz.

The scintillometric survey in the grid of 20 m × 20 m has shown, a radioactive zoning, arising from a nucleus where landing-places (platforms) containing radioactive wastes are located with radiometric values up to 80 000 cps, decreasing to the surrounding until achieving normal radiation levels of 100 cps (Fig. 5).

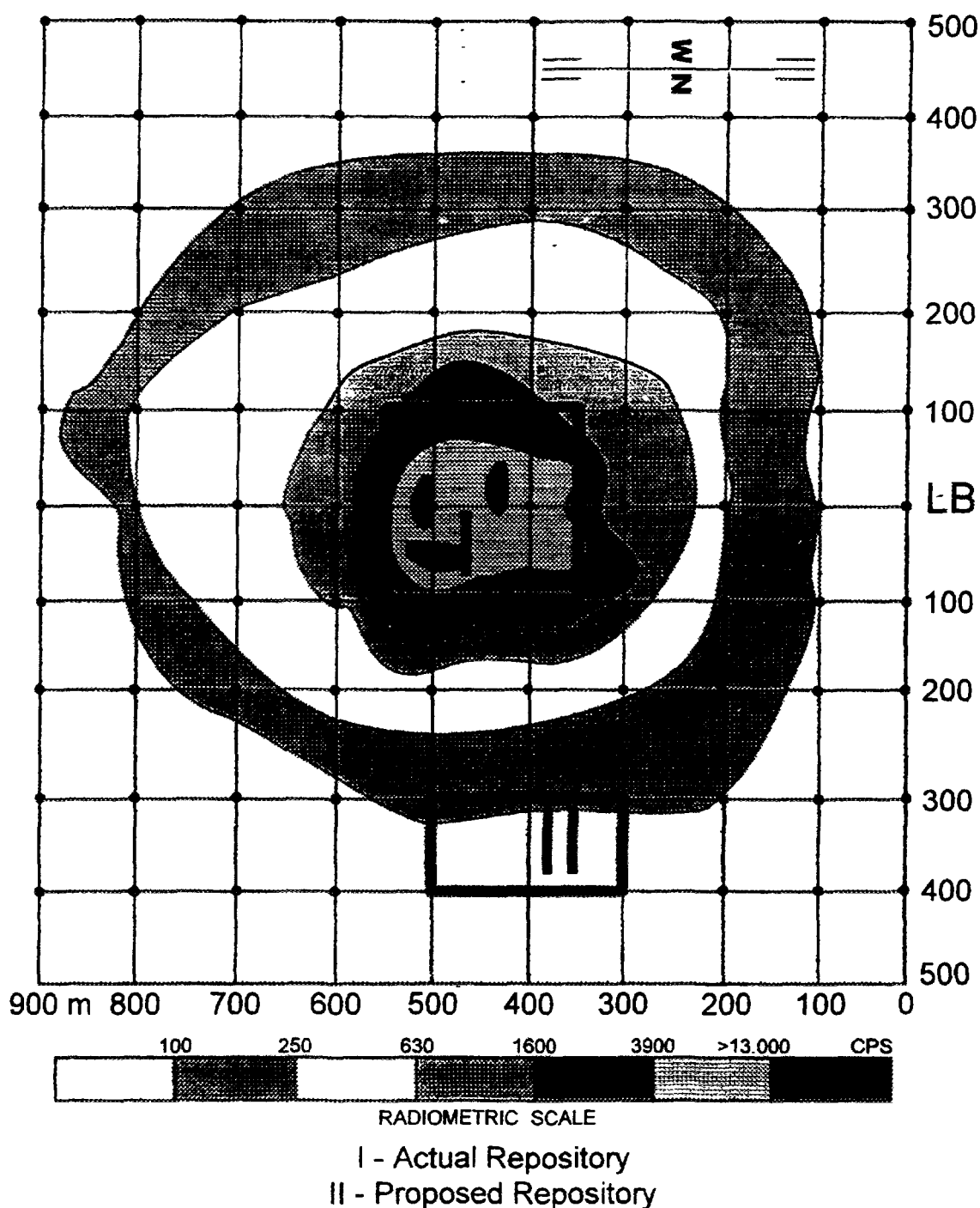


FIG. 5. Area of Abadia de Goiás; radiometric map.

The Gamma spectrometric survey conducted in three profiles following EW direction, crossing the temporary repository, shows a gradual increasing of the radiation levels, as the site where the wastes are stored comes near

The radiometric profiles conducted in boreholes show normal radiation levels related with the nature of the perforated rocks: gamma profiles show values of 25 cps (Fig. 6), while the boreholes gamma spectrometry shows values between 22 and 45 cps for the total counting channel. from 1 to 9 cps for K channel, from 1 to 6 cps for U channel and from 1 to 3 cps for thorium channel (Table I).

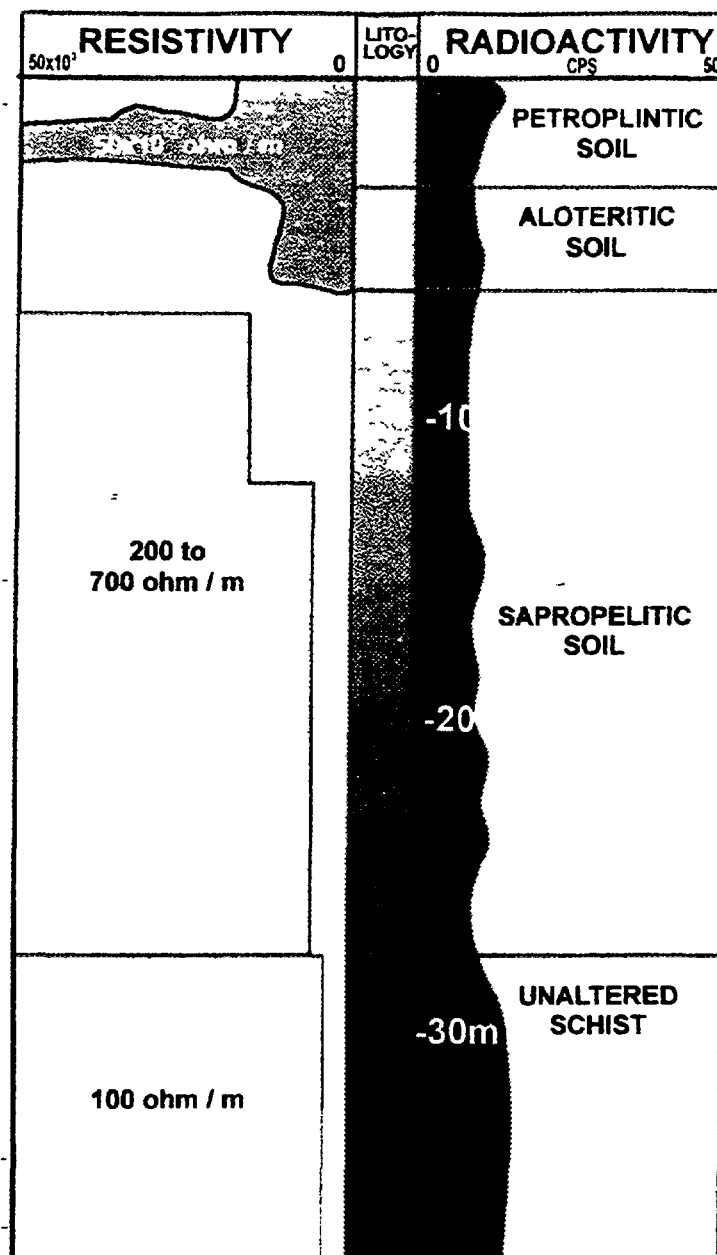


FIG 6 Area of Abadia de Goiás; composed profile; drill F-1.

TABLE I. AREA OF ABADIA DE GOIÁ; GAMMA-LOGIN-BOREHOLE PB-1.

Depth		GAD-6 (TIME 10")			-M.SOPRIS- 1000
metres	T.C.	K	U	Th	CPS
13.00	223	2	4	1	24
14.00	297	1	1	1	24
15.00	327	2	6	1	25
16.00	379	4	5	1	29
17.00	374	4	5	1	25
18.00	357	4	5	1	29
19.00	396	6	2	1	29
20.00	441	7	2	2	27
21.00	347	5	4	1	27
22.00	306	3	1	1	26
23.00	319	2	4	1	23
24.00	291	1	1	1	23
25.00	347	5	8	1	23
26.00	313	4	2	1	25

The geotechnical studies show that:

- The superficial horizon presents SPT values greater than 40 strokes.
- SPT values increase with depth.
- The permeabilities obtained up to 4 m in depth are between 2.2×10^{-4} cm/s and lower than 4 meters are of 7.7×10^{-6} cm/s.

The studies performed in laboratories show:

- Prevailing of siltic-clay fraction.
- Prevailing of clays with low and mean plasticity.
- Materials resistant to low compressibility.
- Moisture of the investigated material between 10 to 20%.
- Specific weight of the dry material varies between 1.6 to 2.0 t/m³.

CONCLUSIONS

The activities measured in the soil samples from the Candidate Site and from the external area (2.5 kilometres) show values compatible with the local rocks. These measured activities include the participation of energy due to the Compton Effect related to other radionuclides (Bi-214, Tl-208 and K-40), as it could be seen in the presented graphs and maps.

The average concentration of uranium in the soils in the area is around 3.5 ppm, which is equivalent to 28 Bq/kg of activity, due to the Bi-214 produced energy. The average potassium concentration in the soils of the investigated area is about 0.52% and 150 ppm of K-40, which participate with energy in the final obtained spectrum. The potassium content in the soil presents one direct relationship with the clay concentration of these soils and with the measured activities. The activity values should consider an error tolerance, of 20%, due to the analytical method.

The absence of anomalies in the drill holes gamma profiles of the area confirms that there is no contamination of cesium in the soil, originated from the radioactive waste disposal. The obtained results using geophysical techniques are considered satisfactory concerning low costs involved and the quick answer obtained. The electric drillings have allowed to characterize three main lithological unities, confirmed lately, through mechanical drillings.

The scintillometric survey has demonstrated several radiation levels, with a more active nucleus, located in the center of the repository, and decreasing levels to the surroundings. The defined pattern is directly associated with the distribution of the radioactive sources stored.

The radiometric map will be used as the basis for future area monitorings and for environmental control. The subsurface investigations show a constant pattern related with the "background" of the investigated rocks not indicating any contamination through the underground water table.

The pre-operational radiometric monitoring was considered very important to show that there is any possible contamination as consequence of radionuclide migration from the stored wastes. VLF EM geophysical survey has shown tectonic system of single scattering, of low conductivity reflecting a Medium Pre-Cambrian tectonics of low intensity level. The obtained benefits using exploratory techniques were very significant, considering the low costs involved and the fast answers achieved.

The subsurface mechanical drillings have confirmed the levels detected by electric drillings and have shown the tectonic stability of the area, as previously demonstrated through the VLF-EM electromagnetic survey.

The geological survey has shown the main geomorphological, structural and lithological features, with the leveling rocks presenting low scattering degree, foliation with low angle and smooth folding. There is no evidence of neotectonic movements showing that the selected area is located in a zone of structural stability and a descending slope between 0 and 5%.

Regionally speaking, Abadia's area is located in a morpho-structural range denominated "Goiania's Peripheric Depression", constituted by rocks belonging to Araxa's Group and presenting a dry morphogenesis formed in semi-aridity climatic conditions.

The hydrogeological studies considered as being of fundamental importance for design approval have shown the behaviour of the "aquifer" based on the underground flow and its directions indicating low permeability values.

The future surface and subsurface monitoring should be based on the geochemical and radiometric pattern obtained by the studies carried out during the pre-operational phase. The exploratory investigations performed by means of geotechnical, hydrogeological and geological works permit to choose the selected area as the most suitable site to store Cs-137 radioactive wastes. The studies carried out in several fields of action should be used as support to the elaboration of the Environmental Impact Report.

BIBLIOGRAPHY

FRASER,D.C., Contouring of VLF-EM data,Geophysics 34.6 (1969) 958-957.

INTERNATIONAL ATOMIC ENERGY AGENCY, Site Investigations for Repositories for Solid Radioactive Wastes in Shallow Ground, Technical Reports Series No. 216, IAEA, Vienna (1982).

KOEFOED,O., Resistivity sounding on an earth model containing transition layers with linear change of resistivity with depth. Geophys Prospect (1979).

SAAD, S. et al., Relatório Técnico Avaliação de Local Candidato, Abadia de Goiás-Estudos Preliminares-CNEN (1989).



ENVIRONMENTAL IMPLICATIONS OF THE LABORATORY GAMMA RAY SPECTROMETRIC MEASUREMENTS MADE ON THE BLACK SAND BEACH DEPOSIT OF THE ABU KHASHABA RADIOACTIVE PROSPECT, ROSETTA, EGYPT

A.M. ELSIRAFE, H.A. HUSSEIN, R.A. ELSAYED
Nuclear Materials Authority of Egypt,
El Maadi, Cairo

A.M. SABRI
Geophysics Department, Faculty of Science,
Ain Shams University,
Cairo

Egypt

Abstract

Laboratory gamma-ray spectrometric measurements carried out on the surficial black sand beach deposits of Abu Khashaba radioactive prospect located 5km east of Rosetta, north Nile Delta, as a part of the comprehensive exploration and assessment program of these radioactive placer deposits has generated a vast amount of radiometric data. These data, initially used for radioelement exploration, provided valuable baseline information necessary for environmental studies and monitoring the impact of any potential environmental radioactive pollution that might occur as a result of nuclear activities in the surrounding regions. Analysis of the acquired spectrometric measurements indicated that both thorium and uranium are the two radioelements that significantly contributed to the measured total natural gamma-ray flux, rather than potassium. This is mainly attributed to the nature of the mineralogical composition of these beach deposits. On the other hand, qualitative interpretation of the produced maps of the three radioelements: potassium, uranium and thorium, supplemented by the examination of their frequency distributions and application of the homogeneity statistical chi-squared test has shown pronounced uranium and thorium comparable zonal distribution patterns that are consistent with the spatial distribution of the heavy mineral concentrations in the studied black-sand deposits. In contrary, these deposits showed uniformly distributed potassium concentrations all over the studied area of Abu Khashaba beach. The two identified radiometric zones displayed a normally distributed uranium and thorium concentration distributions and a contrasting mean background concentration values for these two elements. Concentrations of natural radioelements: potassium, uranium and thorium in the investigated radioactive black-sand deposits were used in producing the environmental total gamma radiation exposure rate map of the studied Abu Khashaba beach and estimation of the mean background levels of the total gamma radiation dose rates. Two zones of contrasting average gamma exposure rates were outlined over the studied Abu Khashaba beach. The first zone displayed an average exposure rate of 13.9 $\mu\text{R/h}$ (average dose rate 115.6 millirem/year) whereas, the second zone displayed a relatively lower average exposure rate of 3.9 $\mu\text{R/h}$ (average dose rate 32.1 millirem/year). The estimated average total gamma dose rates remain in the safe side and within the maximum permissible safe radiation dose without harm to the individual. However in order to have better information about the actual levels of radiations, the contributions from other radionuclides that have not been taken into account should be considered.

1. INTRODUCTION

1.1. Genesis, Mineralogy and Distribution of the Egyptian Black-Sand Deposits

The Egyptian black-sands are beach placer deposits formed by the mechanical concentration of resistant minerals released by weathering of the Precambrian igneous and metamorphic source rocks of the upper reaches of the River Nile. These erosional products have been carried down through the course of the Nile, and were subjected to natural physical and chemical separation and sorting during transportation. By normal surface processes, mainly the combined effect of waves and wind, these transported weathering products were accumulated to form huge deposits, intermittently and in variable proportions, occupying the beach of the Mediterranean Sea of Egypt along a stretch of about 350 km long, extend from El Arish eastwards to Abu Qir westwards. The geology of these

deposits along the Mediterranean coast is directly related to the development of the Nile Delta and the past configuration of the Nile branches [1]. The Egyptian black-sands has drawn an increasing interest since they contain different concentrations of potentially economic heavy minerals that are considered as nuclear raw materials as well as their importance in many of the metallurgical industries.

The Egyptian black-sand deposits are loose fine sands consisting a complex mineral associations of light and heavy fractions. The light mineral fraction is mainly consists of quartz which is the principal constituent (average 95 %) and feldspars which constitute about 5 % of this fraction. The percentage of the heavy mineral fraction varies from 8 % up to 97 % of the total mineral constituents of the black sands. This fraction is mainly formed of a complex association of minerals characterized by their dark color and high specific gravity. The most abundant of these minerals are: ilmenite, magnetite, zircon, garnet, rutile and monazite. Other minerals are also present, but in trace amount such as chromite, cassiterite, wolframite, corundum, beryle, uranothorite and gold [1 and 2].

1.2. Location and General Topography of Abu Khashaba Beach

Abu Khashaba beach occurs in the extreme northwestern corner of the Nile Delta, on the Mediterranean Sea coast (Fig 1). It is situated 5 km to the north of Rosetta (Rashid) City and lies on the eastern side of Rosetta branch of the River Nile, about 7.5 km from the estuary. This area represents the most wider coastal plain, extends for about 2.5 km in the back beach. The present

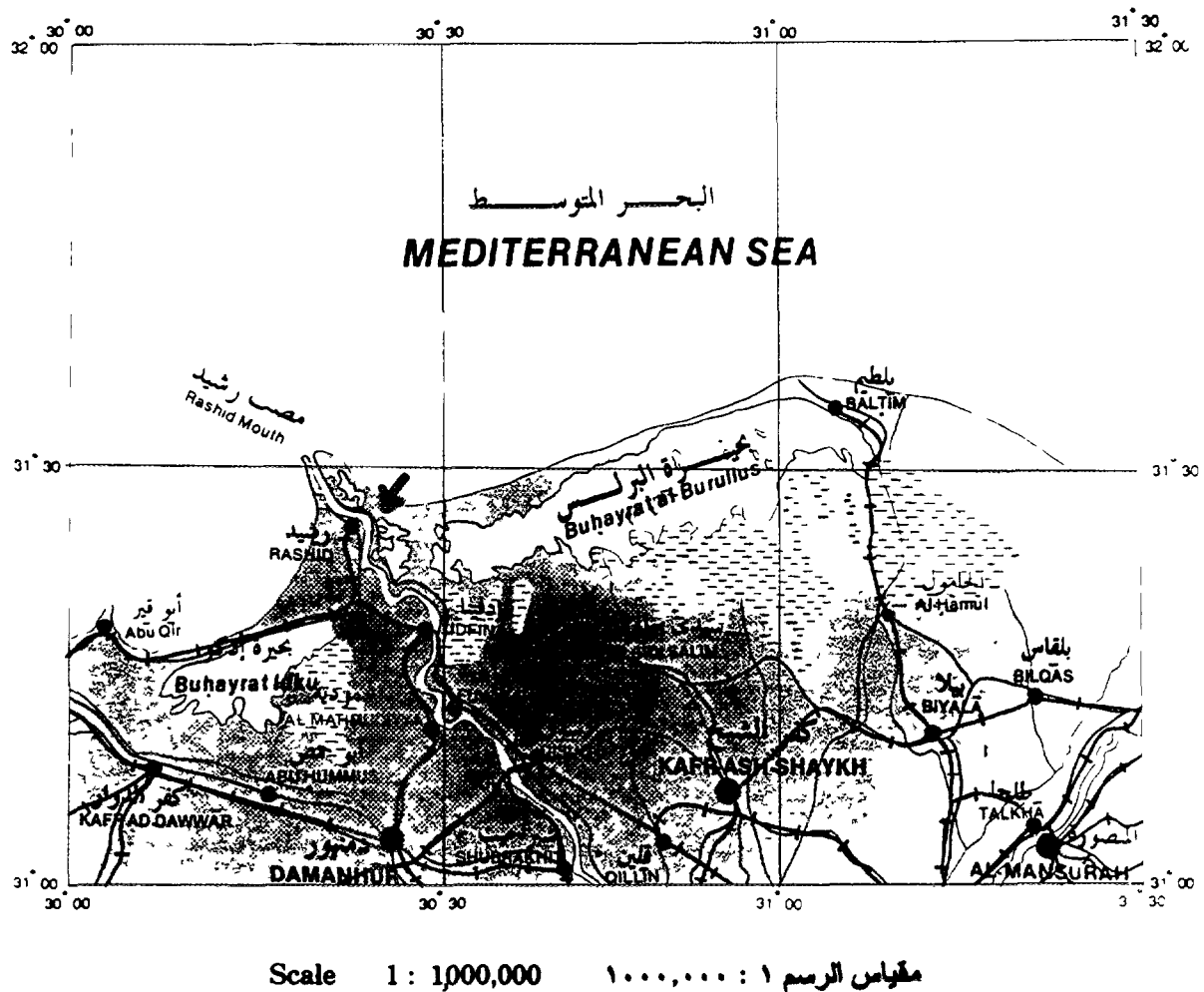


FIG. 1. Map of north Nile Delta, Egypt. The arrow points to location of the studied part of Abu Khashaba beach, east of Rosetta (Rashid) city.

study is only restricted to the western part of Abu Khashaba beach (Fig. 1) and covers a total surface area of 2.4 km². The altitude of Abu Khashaba area is slightly higher than the sea level, and the topography is almost flat where the coastal plain occupies most of the surface except the southern part where accumulations from eolian sands occur as small dune belts and sand bars. The highest concentration of the heavy minerals along the Mediterranean coast of Egypt is found along Abu Khashaba beach where these extend eastward for a distance of about 40 km along the coast (Fig. 2). These conditions favour the area of Abu Khashaba beach as a good prospect for radioactive raw materials.

1.3. Scope and Objectives of the Study

Environmental monitoring and meaningful interpretation of man-made radioactive pollution is impossible without knowledge about the natural abundance of the radioelements and the natural background radioactivity levels in the environment [3]. In that regard comprehensive assessment program of the mineral potentials of the radioactive black sand deposits of Abu Khashaba prospect, carried out by the Egyptian Nuclear Materials Authority, provided a vast amount of potassium, uranium and thorium concentration measurements acquired from the systematic aerial, ground and laboratory gamma-ray spectrometric measurements conducted over these beach placer deposits. The present research work aims essentially to make use of the laboratory spectral gamma-ray measurements, in establishing the environmental natural gamma radiation levels along the surveyed Abu Khashaba beach. This will provide baseline information necessary for the detection and determination the amount and extent of potential environmental changes in the terrestrial background radiation that might result from nuclear testing or accidents involving release of nuclear radiations and accompanied radioactive contamination of the ground.

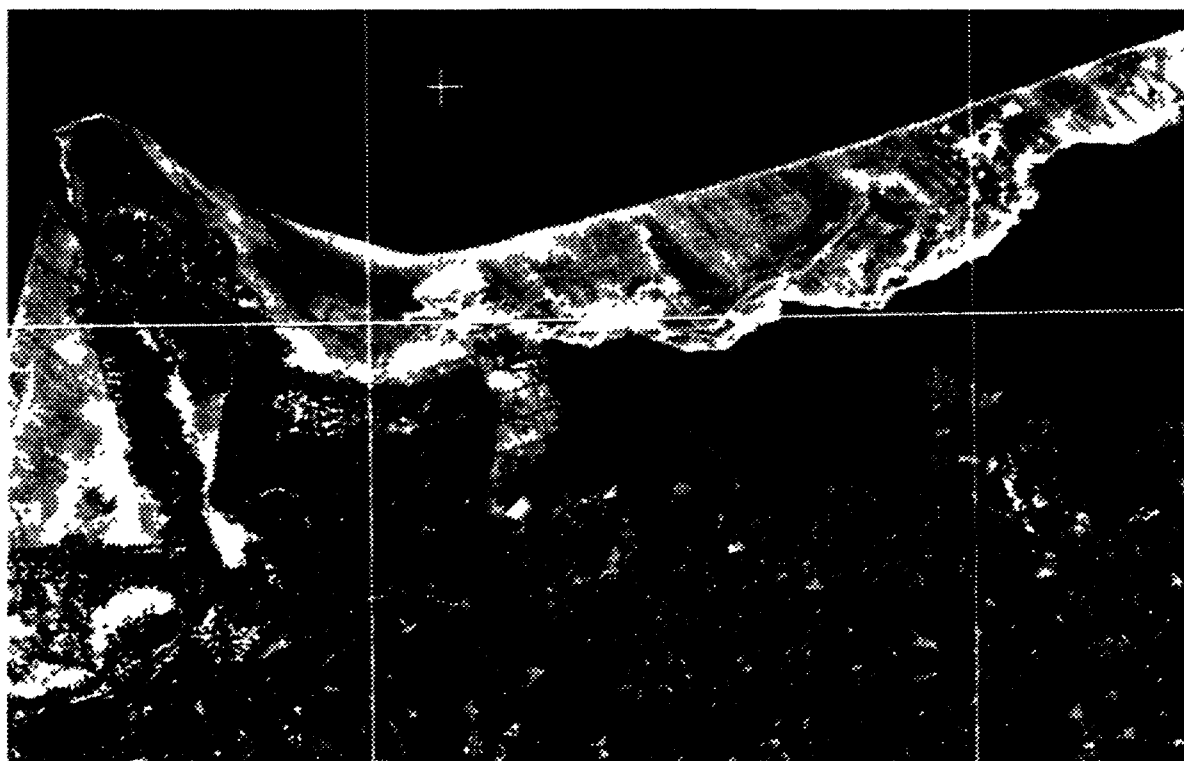


FIG. 2. Photomap of north Nile Delta, Egypt produced by the processing of the digital data acquired with the Landsat Satellite Multispectral Scanner (MSS) of resolution 82×57 m, restored to 50×50 m. This map has been produced by the Egyptian Remote Sensing Center, Cairo. Black-sand deposits (white to light blue colored zones) extend along and parallel to the Mediterranean shoreline, east of Rosetta (Rashid).

2. FIELD WORK (SAMPLING PROCEDURE)

A total of 272 samples, representing the upper 50 cm of the black-sand depoists at the eastern part of Abu Khashaba beach (2.4 km²), were collected on a quadrate grid pattern using 100 m sampling interval. The regular grid pattern of sampling was designed to overcome the variability in the heavy mineral content of these black-sand deposits. These samples were taken by forcing a cylindrical rigid plastic tubes, 50 cm length and 2.5 cm diameter, vertically into the ground at the sampled location. In this way continuous core samples from the sampled locations were obtained. Tubes were then sealed and labeled.

3. LABORATORY GAMMA-RAY SPECTROMETRIC MEASUREMENTS

3.1. Sample Preparation

Preparatory processes were carried out on the collected black-sand samples as a necessary step prior to the execution of the laboratory spectral radiometric measurements. In that regard each sample was thoroughly rubbed and mixed well in order to avoid the non-homogeneity in the distribution of its mineral constituents. Then a proper weight (300–350 gm) of each sample was placed in standard-size cylindrical plastic container 9.5 cm in diameter and 3 cm height. These containers were carefully sealed to prevent contamination. Samples in the sealed containers were stored for three weeks where the radon buildup is back to the normal state and attains radioactive equilibrium.

3.2. Instrument and Methodology

Laboratory determination of the total gamma-ray activity (TC) and absolute concentration of the naturally occurring three radioelements thorium (Th), uranium (U) and potassium (K) in the investigated black-sand samples have been performed with a Bicron multichannel analyzer of a calibrated gamma-ray spectrometer with 285 cm³ NaI (TI) crysta. Thorium and uranium were measured from the gamma-ray photons emitted by Pb-212 (at 238.6 keV) and Pb-214 (at 52 keV) respectively in their decay chain, whereas, potassium was measured directly from the gamma-ray photons emitted by K-40 at 1460.8 keV. The utilized energy regions (windows) for eTh, eU and K were determined on indicated energy lines of the spectra, generated by means of laboratory thorium, uranium and potassium reference standard samples provided by the IAEA [4]. Assaying of the black-sand samples was carried out using long period counts, 1000 second for each, in a shielded environment to determine the gross counts for the total gamma-ray activity and the gross counts of the three radioelements Th, U, and K.

3.2. Data Processing and Presentation

The measured spectrometric data for the analysed 272 black sand samples were processed by computer program "ANALYSIS" [5]. Background corrected and stripped count rates were converted to ground concentrations of potassium (K in percent), uranium and thorium (U and Th in ppm), in addition to the integral gamma-ray activity expressed in units of counts/second/gram, using the sensitivity constants of the used spectrometer determined from the calibration procedure. Estimated absolute concentrations of the three radioelements K, U and Th, as well as the integral gamma-ray activity were finally displayed in the form of colored contour maps (Figs 3-6) using the the Geosoft Graphics System.

4. DATA ANALYSIS

Laboratory spectral gamma-ray measurements have been subjected to conventional statistical methods of analysis, in order to facilitate the manipulation of the large volume of the data and to

reach valid conclusions and reasonable predictions concerning the nature of concentration distributions of the naturally occurring radioelements potassium, uranium and thorium. Hereafter is the procedure steps followed throughout this statistical treatment:

1. Data sets for the individual laboratory spectrometric variables that were monitored over the investigated black-sand deposits were displayed in the form of frequency histograms in order to recognize potential natural grouping within each data set, that consequently might assist the delineation of the spatial distribution of the heavy mineral concentrations in the investigated black sand deposits.

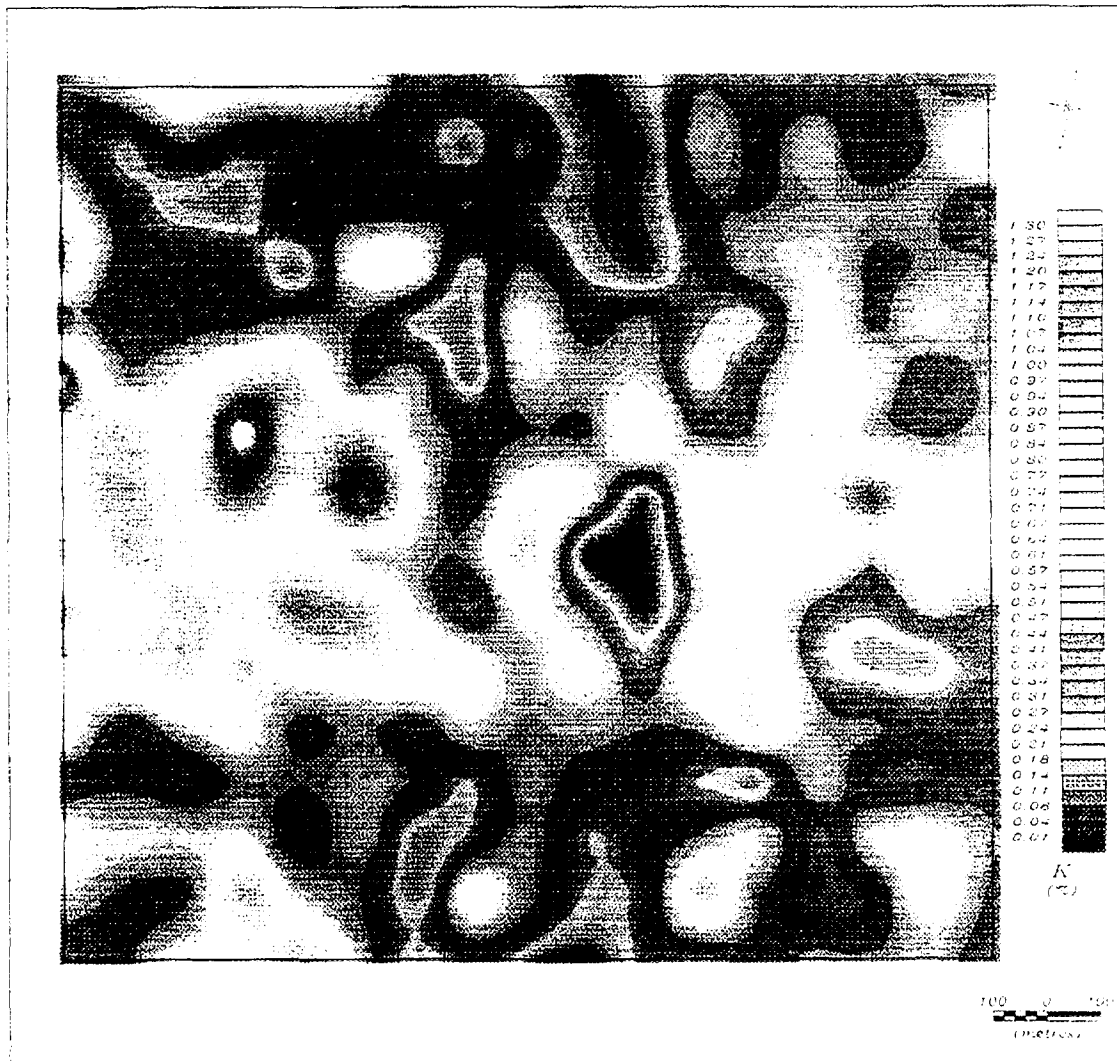


FIG. 3. Map showing spatial distribution of Potassium concentration (K in %) in the black-sand deposits of Abu Khashaba beach, east of Rosetta.

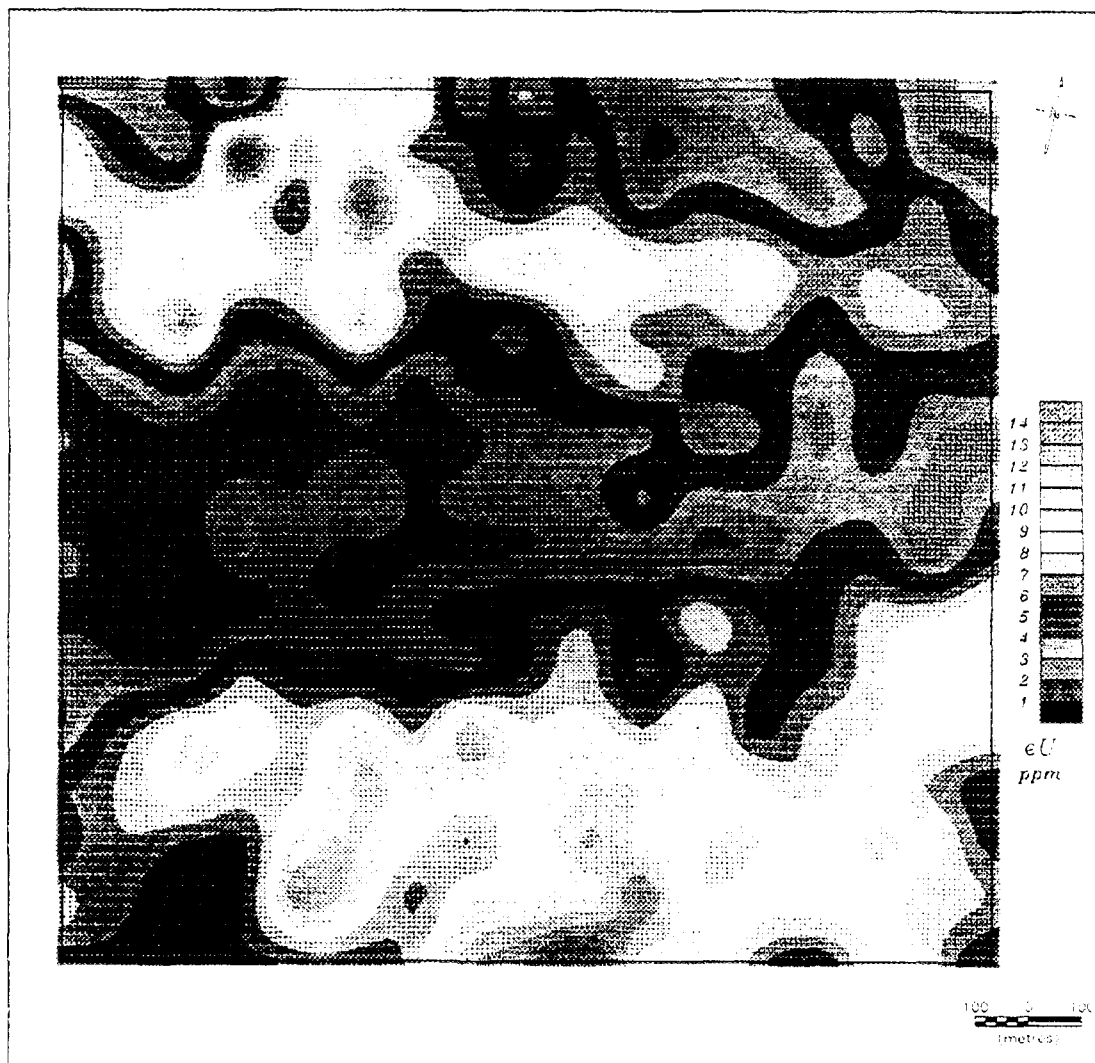


FIG. 4. Map showing spatial distribution of uranium concentration (U in ppm) in the black-sand deposits of Abu Khashaba beach, east of Rosetta.

2. State of homogeneity of the data distribution of the individual four measured spectral radiometric variables has been mathematically tested through the application of the statistical chi-squared Test (Tables I and II).
3. Correlation analysis has been applied, as a bivariate statistical analysis, in order to explore the mutual relations and strength of association between each pair of the four measured radiometric variables, through calculation of the linear Person product moment correlation coefficient (Table III).
4. Calculation of simple statistics that describe the characteristics of the distributions of the data acquired for the four spectral radiometric variables. These included the range (maximum-minimum), the mean (\bar{x}), standard deviation (Sd) and coefficient of variability (CV). These computed statistics are listed in Tables I and II.

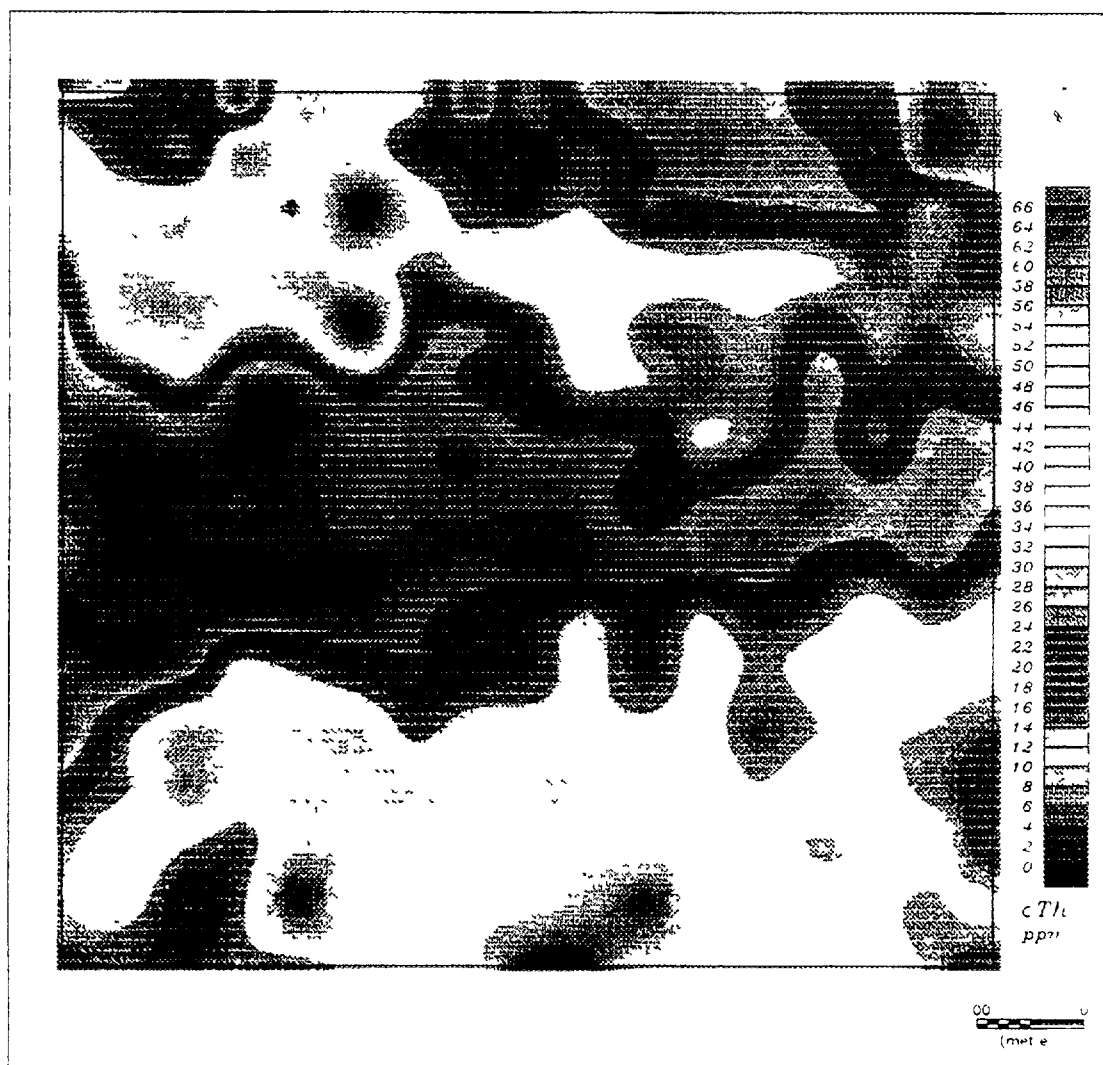


FIG 5. Map showing spatial distribution of thorium concentration (Th in ppm) in the black-sand deposits of Abu Khashaba beach, east of Rosetta.

5 DISCUSSION AND INTERPRETATION

5.1. Qualitative interpretation

Visual examination of the three colored contour maps namely: TC, Th and U (Figs. 3–6) revealed a remarkable consistency in the spatial distribution features of the concentration of these variables over the studied black sand deposits at Abu Khashaba beach. The most striking gross feature of these spatial distributions is the pattern of repetitional zones of high and low concentration levels, striking approximately in the east-west direction more or less parallel to the present shore line. The well-defined sharp boundaries between these zones reflect an abrupt change in the magnitude of the spectrometric responses and imply that there is an abrupt lateral mineralogical variations between these zones in the area under consideration. This distinct zonation pattern is in good agreement with the know sedimentary history of these deposits [1, 6 and 7] and can be observed in the field as alternating dark and light coloured bands that reflect heavy and light mineral concentrations. On the

other hand, the radioactive potassium contour map (Fig.3) revealed independent features with respect to its distribution pattern. It does not display much variations with respect to the whole area. Zonation is less obvious and trends are difficult to define. However the central area of the map, show a remarkable local elevation in the potassium content. Field observation revealed that this is spatially restricted to a zone of high clay and evaporite contents.

The measured spectrometric responses of the studied black-sands are considered as operative physical properties that reflect valuable information about the main causative to such properties. Accordingly, these responses can be interpreted on the basis of general geological considerations, particularly the mineralogical composition of these placer beach deposits.

As inferred from the spectral gamma-radiation response of the investigated black-sand deposits, both thorium and uranium are the two elements that significantly contributed to the observed total gamma-radiation response, as indicated from their highly comparable spatial distribution pattern, rather than potassium. The three heavy minerals zircon, monazite and uranothorite are the major

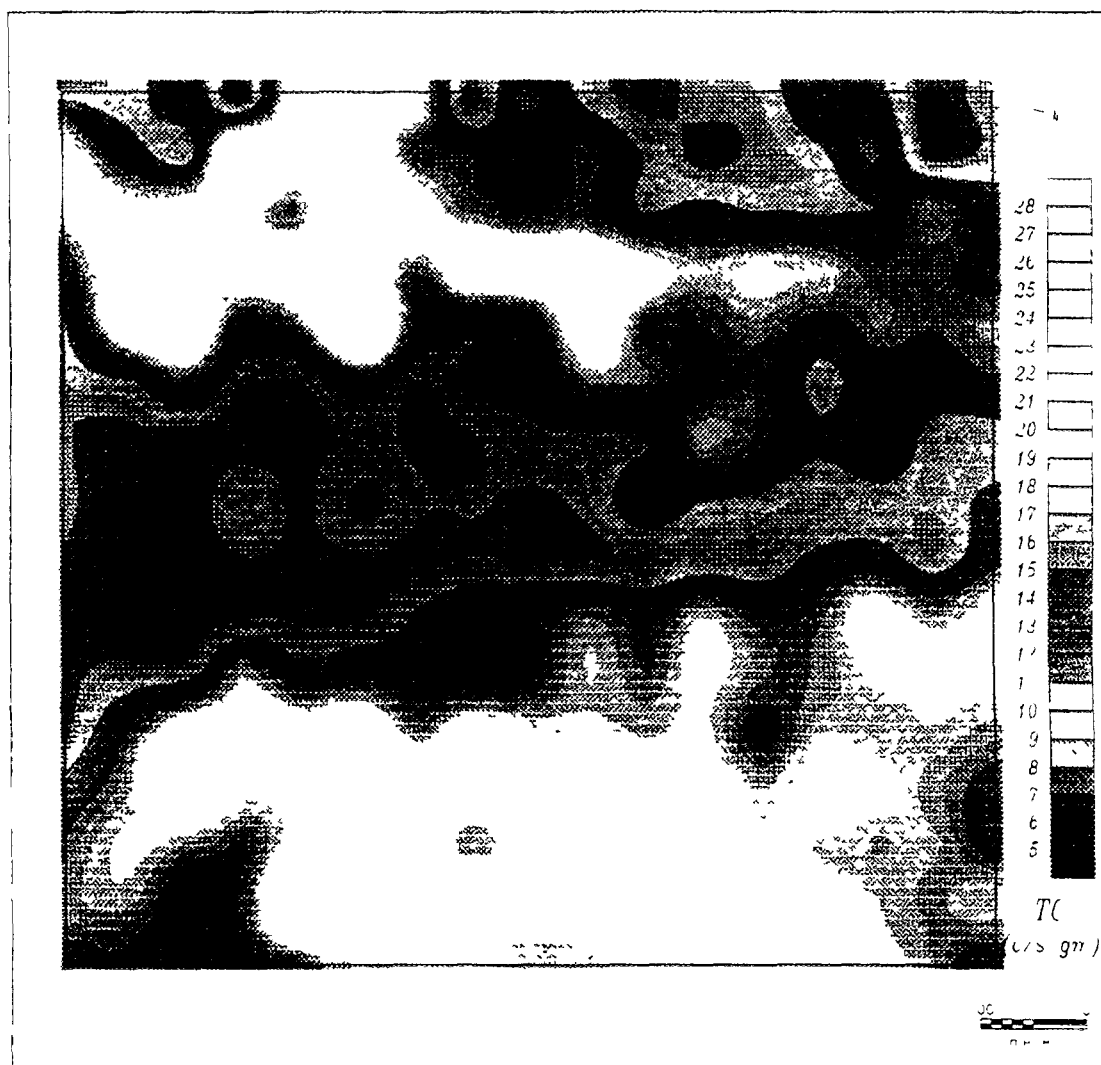


FIG. 6. Map showing spatial distribution of the natural total gamma radiation (TC in c/s/gm) of the black sand deposits at Abu Khashaba beach, east of Rosetta

TABLE I. COMPUTED SIMPLE STATISTICS OF THE DISTRIBUTIONS OF THE LABORATORY SPECTRAL MEASUREMENTS OF THE TOTAL GAMMA RADIATION (TC IN c/s/gm), THORIUM (Th in ppm), URANIUM (U in ppm) AND POTASSIUM (K) CONCENTRATIONS IN THE 272 BLACK SAND SAMPLES COLLECTED FROM THE STUDIED ABU KHASHABA BEACH AND RESULTS OF APPLICATION OF THE HOMOGENEITY CHI-SQUARED TEST

Variable	N	Range		X	Sd	CV (%)	χ^2 -test values		Type of distribution
		Min.	Max.				obs.	crit.	
TC	272	5.10	29.9	14	7.5	54	63	18	Not normal
Th	272	1.10	72.5	24	13.9	58	55	22	Not normal
U	272	0.61	15.0	5.2	3.1	60	52	24	Not normal
K	272	0.01	1.43	0.49	0.25	51	22	27	Normal

TABLE II. COMPUTED SIMPLE STATISTICS OF THE DISTRIBUTIONS OF THE LABORATORY SPECTRAL MEASUREMENTS OF THE TOTAL GAMMA RADIATION (TC IN c/s/gm), THORIUM (Th in ppm), URANIUM (U in ppm) AND POTASSIUM (K) CONCENTRATIONS IN THE IN THE TWO INTERPRETED RADIOMETRIC UNITS OUTLINED OVER THE BLACK SAND DEPOSIT OF ABU KHASHABA BEACH (FIG. 8), AND RESULTS OF APPLICATION OF THE HOMOGENEITY CHI-SQUARED TEST

Unit	Variable	N	Range		X	Sd	CV (%)	χ^2 -test values		Type of distribution
			Min.	Max.				obs.	crit.	
I	TC	204	9.5	29.9	16.4	3.7	22.2	19.5	27.6	Normal
	eTh	190	10.1	72.5	29	10.1	33.7	12.5	21	Normal
	eU	208	2.5	15.0	6.6	2.3	33.3	8.6	22.4	Normal
II	TC	75	5.1	10.8	7.8	1.4	17.9	7.3	12.6	Normal
	eTh	70	1.1	12.6	6.6	2.9	44	3	11.1	Normal
	eU	61	0.61	3.1	1.7	0.68	40	2.9	7.8	Normal

N.B. Units I and II are the high and low radiation units shown in black and grey on Fig. 9.

TABLE III. COMPUTED CORRELATION MATRIX, IN DIAGONAL FORM, OF THE FOUR SPECTRAL RADIOMETRIC VARIABLES MEASURED IN THE 272 BLACK SAND SAMPLES COLLECTED FROM ABU KHASHABA BEACH, EAST ROSETTA, EGYPT

Rad. Variable	Total gamma	Thorium	Uranium	Potassium
Total gamma	1.000			
Thorium	0.975	1.000		
Uranium	0.962	0.915	1.000	
Potassium	-0.401	-0.399	-0.451	1.000

contributors to thorium and uranium in the Egyptian black-sands [8]. Zircon and monazite minerals showed strongly direct correlation with each other at Rosetta area [9]. Accordingly, both uranium, thorium and the total gamma radiation colored maps (Figs. 4–6) discriminate and outline alternating zones that contrast in their content of the radioactive heavy minerals especially zircon and monazite in the investigated Abu Khashaba area. On the other hand, potassium did not display any response that could be related to the heavy mineral concentrations. [10] attributed the main occurrence of radioactive potassium in the Egyptian beach deposits to the light fraction, mainly represented by the clay minerals and feldspars.

5.2. Quantitative interpretation

The area of Abu Khashaba beach consists mainly of black-sand sediments. The whole area under study, therefor, can be considered to comprise a single lithological unit. With this approximation, data sets for the individual laboratory spectrometric variables that were monitored over the investigated black-sand deposits were displayed in the form of frequency histograms. This step aimed to recognize the potential natural grouping within each data set, that consequently might assist the delineation of the spatial distribution of the heavy mineral concentrations within the studied area.

Examination of the frequency distribution histograms of the variables namely; TC, Th and U revealed a bimodal distributions and consequently two levels of responses with respect to these variables. This means that these radiometric variables possess heterogeneous distributions all over the investigated area. This has been confirmed quantitatively through application of the numerical χ^2 -test, [11] as shown on Table I. On the bases of these information, supplemented by the aforementioned qualitative interpretation of the maps, the whole investigated area has been statistically treated and discussed in terms of two geographical areas or zones (Fig. 8) of different radiometric responses. These zones are approximately outlined on the interpreted zonation map (Fig.8). Table II summarizes the computed statistics of the distributions of the four spectral radiometric in these interpreted zones.

Analysis of the frequency distributions and application of the χ -test, (Table II) revealed that the TC, Th, and U are normally distributed within the two outlined low radiation and high radiation zones of the black sand deposits of Abu Khashaba beach (Fig. 8). This consequently reflects the homogeneity of the distribution of the radioactive heavy minerals, monazite zircon and uranotorite within these zones.

The frequency histogram of potassium measurements, revealed a unimodal distribution. This implies that there is no much variations in the radioactive potassium content within the whole area. This result has been quantified through application of the χ^2 -test (Table I) which revealed that the radioactive potassium concentration is normally distributed all over the studied area, with mean background (X) of 0.49%. Consequently, the entire black-sand deposits in the area can be considered to represent a uniform radiometric unit with respect to its radioactive potassium content.

6. ENVIRONMENTAL IMPLICATIONS OF THE SPECTRAL GAMMA RADIATION MEASUREMENTS

6.1. Conversion of Radioelement Concentration Measurements to Total Gamma Exposure and Dose Rates

Concentrations of natural radioelements: potassium, uranium and thorium in the investigated radioactive black-sand deposits were used in producing the environmental total gamma radiation exposure rate map of the studied Abu Khashaba beach (Fig. 8) and estimation of the mean background levels of the total gamma radiation dose rates (Table IV). Conversion factors recommended by Grasty [12] were used. Two zones of contrasting average gamma exposure rates were outlined over the studied

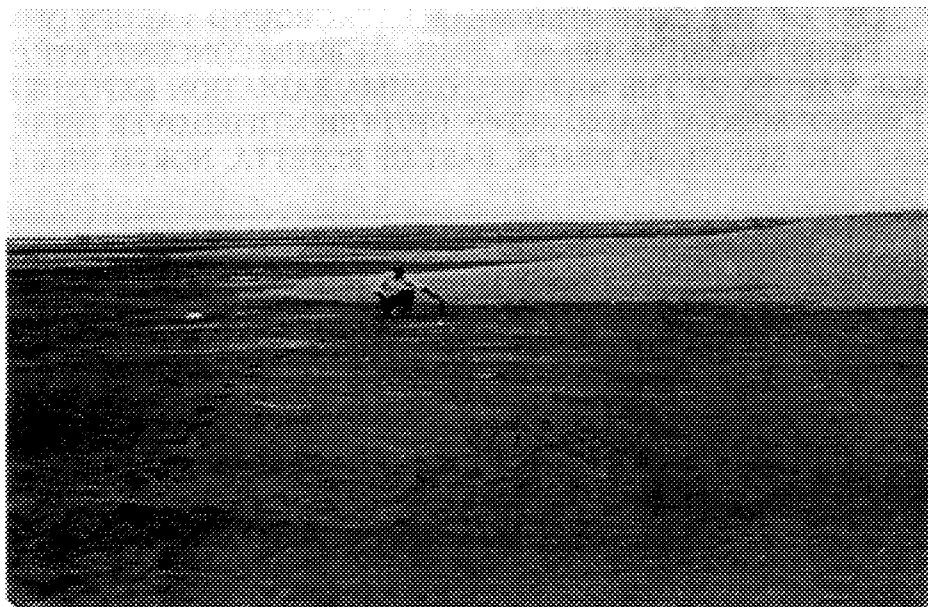


FIG. 7. Photograph, facing south, showing zonal distribution of the heavy mineral concentrations in the black sand deposits of Abu Khashaba beach. Dark colour in this photo indicates zones of high concentration while light colour indicates low concentration zones.

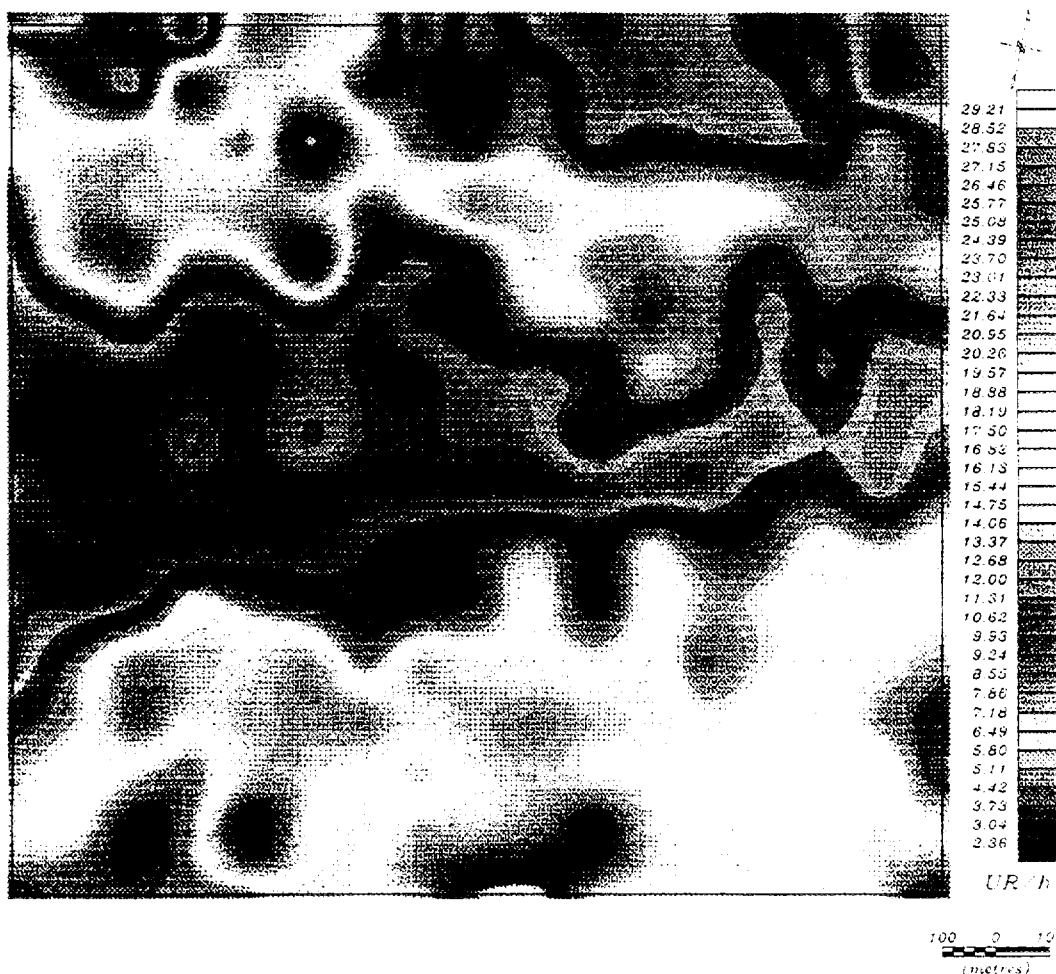


FIG. 8. Map showing spatial distribution of the terrestrial total gamma radiation exposure rate (in $\mu\text{R/h}$) over the black sand deposits of Abu Khashaba beach.

TABLE IV. LIST OF THE COMPUTED MEAN BACKGROUND VALUES OF THE THREE RADIOELEMENTS POTASSIUM, URANIUM AND THORIUM CONCENTRATIONS AS WELL AS AVERAGE VALUES OF THE NATURAL GAMMA RADIATION EXPOSURE RATES OF THE TWO ENVIRONMENTAL RADIOMETRIC UNITS IDENTIFIED OVER THE BLACK-SAND DEPOSITS AT ABU KHASHABA BEACH, EAST OF ROSETTA, NORTH NILE DELTA

Rad. Unit	Potassium (%)	Uranium (ppm)	Thorium (ppm)	Exposure rate ($\mu\text{R/h}$)	Dose rate (millirem/y)
High	0.49	6.6	29	13.9	115.6
Low	0.49	1.7	6.6	3.9	32.1

$$\begin{aligned} \text{Exposure rate (in } \mu\text{R/h)} &= \%K \times 1.505 + \text{ppmU} \times 0.625 + \text{ppmTh} \times 0.310 \\ \text{Dose rate (in millirem/y)} &= \text{Exposure rate} \times 8.33 \end{aligned}$$

Abu Khashaba beach. The first zone (shown in black) displayed an average exposure rate of 13.9 $\mu\text{R/h}$ (average dose rate 115.6 millirem/year) whereas, the second zone (shown in grey) displayed a relatively lower average exposure rate of 3.9 $\mu\text{R/h}$ (average dose rate 32.1 millirem/year).

The radiation doses received by people are frequently measured in "rems". For gamma-radiation, the conversion from exposure rate to dose rate is: 1 $\mu\text{R/h} = 8.33$ millirems/year. The International Commission of Radiological Protection (ICRP) has recommended that no individual should receive more than 5000 millirems/year from all natural and artificial radiation sources in his or her environment [13].

Concerning the studied Abu Khashaba area, the mean natural dose rates from the terrestrial gamma-radiation, to which individuals are exposed in the two outlined natural radiation zones (Fig. 8), was computed as 115.6 and 32.1 millirems/year. These values remain in the safe side and within the maximum permissible safe radiation dose without harm to the individual, with continuous external irradiation of the whole body. But, on the other hand, people in the area of Abu Khashaba beach are exposed to other irradiation sources. These include other potential terrestrial man-made radionuclides that have not been taken into account (e.g Cs-137), radiation in the atmosphere and cosmic radiation. Hence, in order to reach more precise estimation for the total gamma dose rate levels in the study area, contributions of the aforementioned radiation sources should be considered. In that regard in-door radon survey in the populated areas in the surroundings of Abu Khashaba beach is highly recommended, since it was noticed from the field observations that the people in this area frequently use the beach black sands as a building material.

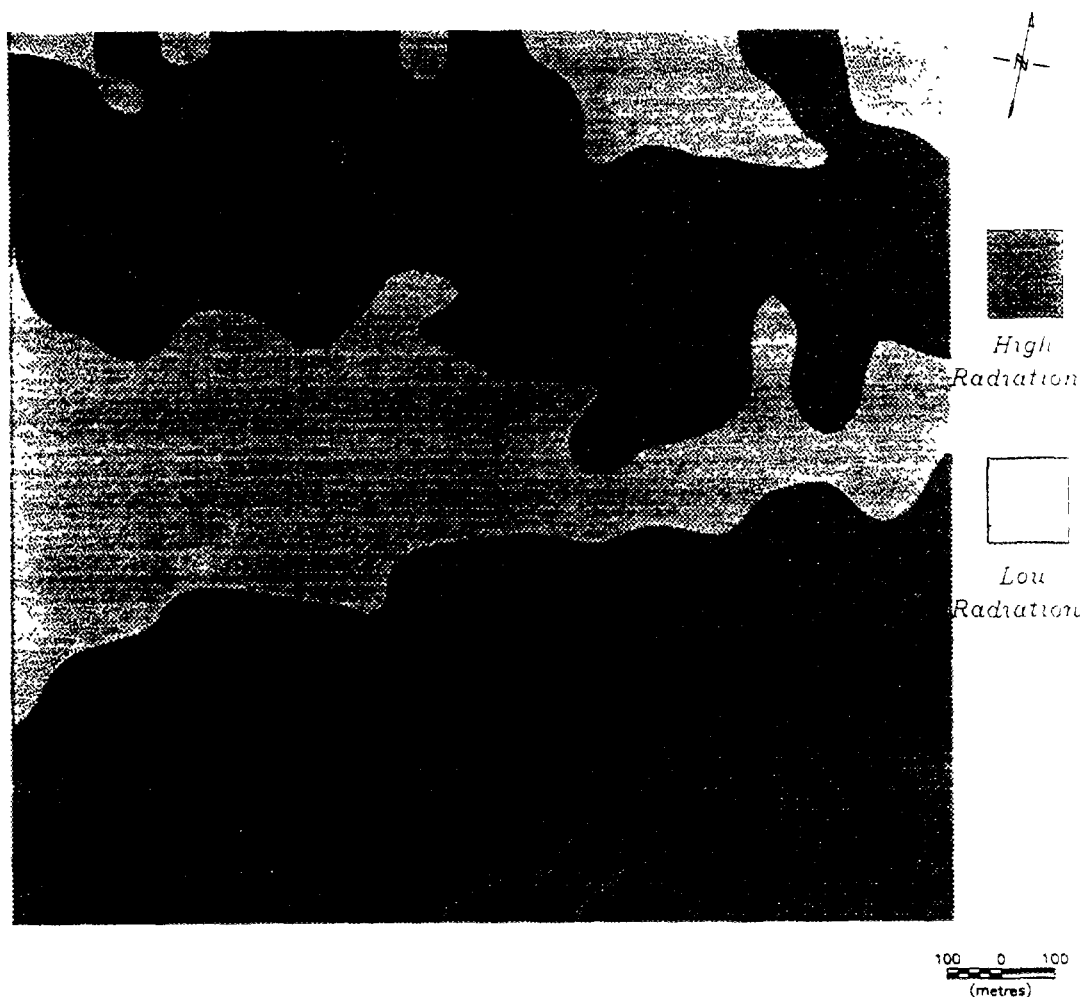


FIG. 9. Environmental natural total gamma radiation unit map of the studied Abu Khashaba beach, as inferred from the qualitative interpretation of the exposure rate map (Fig. 7) supplemented by quantitative statistical analysis of the measured concentrations of the three radioelements: potassium, uranium and thorium.

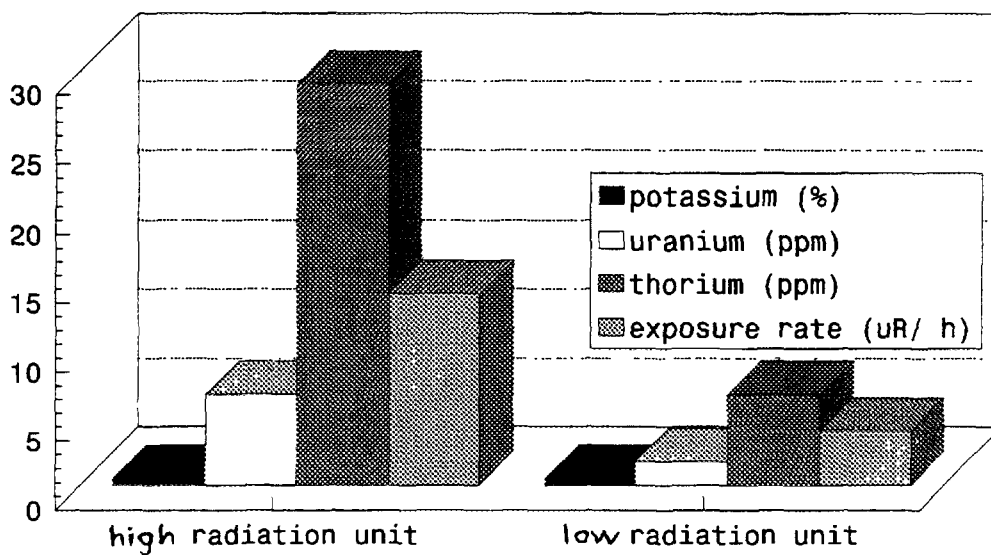


FIG. 10. Bar chart showing mean background concentration of the three radioelements potassium, uranium and thorium as well as average natural gamma radiation exposure rates of the two radiometric units identified over the black-sand deposits at Abu Khashaba beach.

REFERENCES

- [1] HAMMOUD, N. S., Concentration of monazite from Egyptian black sands, employing industrial techniques, M.Sc.Thesis, Faculty of Science, Cairo University (1966).
- [2] EL GIMMIZI, M. A., Note on the occurrence of gold and cassiterite in the Egyptian beach placer deposits, Internal Report, Nuclear Materials Authority, Cairo, Egypt (1984).
- [3] INTERNATIONAL ATOMIC ENERGY AGENCY, Application of uranium exploration data and techniques in environmental studies, IAEA-TECDOC-827, Vienna (1995).
- [4] MATOLIN, M., Construction and use of spectrometric calibration pads for laboratory gamma-ray spectrometry, Nuclear Materials Authority (NMA) of Egypt, Report to the Government of the Arab Republic of Egypt, Project EGY/4/030-03, IAEA (1990).
- [5] SRP, P., MATOLIN, M., Computer program "ANALYSIS" for calibration of the laboratory gamma-ray spectrometer and analysis of the radioactive elements in rock samples, Charles University, Prague, Czechoslovakia (1990).
- [6] HAMMOUD, N. S., Physical and chemical properties of some Egyptian beach economic minerals in relation to their concentration problems, Ph.D Thesis, Faculty of Science, Cairo University (1973).
- [7] DABBOUR, G. A., Geological and mineralogical studies on rutile in the black sand deposits from the Egyptian Mediterranean coast, Ph.D Thesis, Faculty of Science, Cairo University (1980).
- [8] ZAGHLOUL, Z.M., Note on the occurrence of uranothorite and radioactive zircon in the black sands of Rosetta. Egyptian J. Geology, V.4 (1960) 89-91.
- [9] AMMAR, A.A., WASSEF, S.N., MELEIK, M. L., FOUAD, K. M., DABBOUR, G. A., Remote, surface and laboratory detection of radioactive minerals of Rosetta black sand beach deposits, Egypt, INT. J. Remote Sensing, V. 4, No. 4, P. 739-754 (1983).
- [10] ALY, M. M., WASSEF, S. N., YANNI, N. N., HATHOUT, M. H., Natural field radioactivity correlated with thorium, uranium and radioactive potassium in beach sands of east Rosetta, Egypt, Egyptian Desert Institute Bull., No.1-2, P.1-12 (1982).
- [11] CLARK, G. M., COOKE, D., A basic course in statistics, English Language Society/Edward Arnold (Publishers) Ltd., London (1983).
- [12] GRASTY, R. L., GARSON, J.M., CHARBONNEAU, B. W., HOLMAN, P. B., Natural background radiation in Canada, Bulletin 360, Geological Survey of Canada, Ottawa (1984).
- [13] INTERNATIONAL ATOMIC ENERGY AGENCY, Gamma-ray surveys in uranium exploration, Technical Reports Series No.186, IAEA, Vienna (1979).



SPECTROMETRIC AERIAL SURVEY AS A NEW TOOL FOR GEOLOGICAL SURVEY AND MINING PROSPECTING

R. CAMBON
GME,
Creteil, France

Abstract

Airborne survey for radioactive minerals started around 1945. The limited sensitivity of the tools used, the difficulties found for the topographic and training effect corrections, made difficult the evaluation of the results. The technical progresses realized in the recent past years in electronic and computer sciences allowed to overcome these difficulties and gave to the method all its potentialities. With the aerial spectrometric survey, a new step was made, because this method can be used for other topics than radioactive prospection such as geological survey and mining prospection for metallic and industrial minerals. The spectrometric method is based on the possibility to measure photopeak energies (gamma radiation) emitted by radioactive minerals and discriminate between them those emitted by U238, Th232 and K40 respectively daughter products of uranium, thorium and potassium. For airborne survey, one consider that measuring instruments will allow to pick-up 80% of the radioactive emission concerning the first 15 to 30 centimetres of ground (1 metre maximum). The use of this method for geological and mineral exploration is based on the assumption that different rock types or ore bearing rock types are composed of certain amounts of rock forming minerals which comprise specific quantities of radioactive elements such as potassium, uranium and thorium (cf: Gabelman 77). To be able to evaluate the results of the spectrometric survey it will be necessary to know roughly the behaviour of the different radioactive elements through a complete geological cycle.

1. BEHAVIOUR OF THE RADIOACTIVE ELEMENTS

1.1. Igneous rocks

Igneous rocks are relatively rich in uranium therefore both plutonic and effusive rocks have been considered many times as a uranium source for most of the deposits in an igneous and volcano-sedimentary environment and some sedimentary one.

During the set-up of granitic rocks, uranium, thorium, REE, because of their hygromagmaphile characters, will separate very early from the magma and according to its chemical composition (calcium content, SiO₂ activity), physical parameters as pressure, temperature and fO₂ and the importance of the deuteric phase, will give several types of accessory minerals paragenesis.

To illustrate the former remarks, concerning the logic crystallization of accessory minerals, we will consider the three common types of U and Th enriched granitic rocks:

- Low calcium peraluminous granites
- High calcium metaluminous granites
- Peralkaline granites

1.1.1. Low calcium peraluminous granites

During the set-up of this type of granite, monazite which has a low solubility in peraluminous melt will fractionate very early. Most of the REE and Thorium content of the rock is incorporated in monazite. Uranium does not fractionate significantly in the main granitic forming minerals and rarely exceeds 1 wt% in monazite. Thus a major proportion of uranium will crystallize as low Th uraninite which should be able to allow concentration of uranium.

1.1.2. High calcium metaluminous granites

This granitic type of rock contains calcic minerals (amphibole, sphene, pyroxene) which incorporate significant amounts of REE. Exceeding REE are incorporated in allanite because monazite is not stable. Allanite does not accept important Th and U substitutions. Exceeding Th in granitic rocks with high Th/REE ratios forms thorite which is able to incorporate up to 40 mole % uranium in its structure. Therefore uraninite crystallization is limited and only occurs for high U/Th ratios. Uranium will be locked-up in thorite and will not be able to concentrate.

1.1.3. Peralkaline granites

In peralkaline magmas Zr, REE, Th, P possess a very high solubility and therefore have the same strong hygromagmaphile behaviour as U, F, Nb, Ta. Thus large amounts of a wide variety of accessory minerals crystallize more or less simultaneously in the most differentiated and frequently apical part of such granitic complexes. Uranium will be distributed in abundant accessory minerals and cannot crystallize in significant amounts as uraninite.

This type of granite will be characterized by a very abundant and very complex accessory mineral paragenesis in the most differentiated facies. U is not easily leached and remains strongly bounded to the structure of these minerals. However several processes may alter sometimes the structure of these minerals and lead to the release of uranium:

- Metamictization
- Tectonic crushing
- Hydrothermal alteration
 - Ca rich fluids
 - High temperature sodium metasomatism.

Therefore, depending of the type of granitic rock, the spectrometric responses will be different.

1.2. Volcanic rocks

In the volcanic equivalents of the three types of uranium rich granites described above, such as peraluminous rhyolites, metaluminous and peralkaline tuffs, uranium is mostly located in the glassy or finely crystallized matrix. To release the uranium from glassy or finely crystallized matrix, the volcanic rocks must undergo an alteration process which can be subdivided in two ways:

- High temperature process
- Low temperature process

Therefore, all these rocks represent excellent sources for uranium concentration during supergene, diagenetic, hydrothermal or metamorphic events.

The spectrometric survey will allow very often, through the dispersion of the radioactive elements, to study these rocks and differentiate granitic intrusive rocks from the acid volcanic ones. The problem which remains concern the basic volcanic rocks because they do not have or have a very weak radiometric expression. Magnetic airborne survey will allow to overpass this difficulty.

1.3. Sedimentary rocks

Sedimentary rocks resulting of a long geological cycle with rocks weathering, transport,

deposition and diagenesis do not have the same normal ability than igneous rocks to content radioactive minerals. The radioactive expression will depend of the nature of the source rock and the amount of stages these sediments went through before to be deposited.

Conglomerate, sandstone, have some chance to be radioactive if the source was an igneous rock. Clays and marls have some radioactivity because the high potassium content. Limestones have sometimes a very low radiometric expression due to the presence of clay or volcanic clasts but normally are completely depleted.

1.4. Metamorphic rocks

The radioactivity of metamorphic rocks usually increases with their degree of metamorphism and will depend of the original petrographic composition. Schists are less radioactive than gneiss. Marble will have a very low radioactivity.

2. WEATHERING

The impact of the weathering have to be considered for the evaluation of the airborne spectrometric survey. More important than forest covering in tropical areas for the influence on uranium reading, is the strong alteration process of rocks. Primary minerals are destroyed with neoformation of clay and ferralytisation. In acidic environment and important water movement a strong leaching of the uranium could be expected. The thorium don't follows the same leaching process and don't seems to accumulate in organic matter as uranium does.

Therefore, these few remarks concerning the behaviour of the radioactive elements through different geological cycle show the difficulties to evaluate properly the spectrometric results. The person doing the interpretation must be aware about these facts and should be a geologist.

3. AIRBORNE SURVEY EVALUATION METHOD

The first step will be to delineate on the airborne map all the different geological environments :

- Sedimentary formations
- Volcanic rocks or volcano-sedimentary formations
- Crystalline rocks
- Metamorphic rocks

A geological map will give that type of information but the spectrometric survey will permit to confirm the different units, to correct the limits of the major petrographic formations and complete the mapping.

The methodology to be used is as follows:

3.1. Geology

3.1.1. Limits of acid intrusives and volcanic formations

As the thorium content is characteristic of each intrusives and is not very sensitive to hydrothermal or meteoric alteration, the eTh airborne gamma-ray spectrometric survey map will be used first. The contour of the thorium content who seems to fit the best with the geological contour

could be considered with confidence as the limit of the granite or volcanic formation. One way to differentiate between granitic and acid volcanic rocks will be the shape of the contour. Elongate contour seems more appropriate with volcanic formations, especially when they are associated with sedimentary formations.

Inside the limits of the intrusives formations, some detailed mapping could be carried out using different methods. The use of eTh contours could be one way. The second way will be to consider the eTh/K ratios. The potassium variation could give significant differences in the chemical composition of the granite. The third way will be to consider the repartition of the magnetite, using the magnetic airborne survey.

All these methods will allowed to differentiate multi-intrusives inside the limit of the granite. The same methodology could be used with acid volcanic rocks.

3.1.3. Limits of the sedimentary formations

The way to work out the limits of the sedimentary basin, is to use a ternary map, showing eU, eTh and K contents.

Limestones will be represented by the lack of radioactive activity except for areas with karst formation which can show in some places weak U anomaly. Quartzite, sandstone or other detritic formations will show sometimes eTh concentration. U is not frequent in that type of environment. K concentration will depend of the petrographic composition of the rock but also of the presence of clays. The K repartition will show the most argillaceous places.

3.1.3 Limits of basic rocks

The limits of intrusive or effusive basic rocks are more difficult to delineate. The use of the airborne magnetic survey could give some answers. Magnetic anomalies showing a low potassium and sometimes a low eU and eTh could be the expression of igneous basic rocks.

3.1.4. Tectonic

Consideration of any other map like eTh, eU, K, ratio K/eTh will give most of the structural controls.

3.2. Selection of potential areas for mining exploration

The spectrometric data which have been used essentially for uranium exploration could also be used for the research of other mineral concentrations. The selection of areas for mining exploration will depend of the mineral searched for, the type of deposit, the geological environment and the different controls of the mineralization.

3.2.1. Minerals associated with igneous rocks

Selection of potential areas for the prospection of minerals associated with igneous rocks will be easy to do because the radiometric variations will permit to choose between different types of intrusive rocks the one which seems to fit the best with the mineral searched for. The structural controls which are always very important for the position of the mineralization will be also found on

the spectrometric results. Hydrothermalism and potassic alteration will show up on the potassium map results.

So most of the information necessary to select areas of interest for mining prospection will be available through the evaluation of the spectrometric data.

3.2.2. *Minerals associated with sedimentary rocks*

Except for placer type deposits which presents sometimes spectrometric anomalies, the determination of potential areas for sedimentary type deposits is difficult to do. However the airborne radiometric survey could be used by defining the radioactive characters of the known mineralization and searching for the areas of the same radiometric characters. Priority will be given to the areas according to the similarity of radiometric and geological characters.

4. CONCLUSIONS

The knowledge of the behaviour of the radioactive minerals (eU, eTh, K) through different geological cycles allows to use the natural repartition of these elements for geological mapping but also for mineral prospection.

BIBLIOGRAPHY

The ideas concerning the behaviour of the radioactive elements presented in this paper are coming from several papers published by the CREGU (Centre de Recherche Geologique sur l'Uranium, BP 23, F-54501 Vandoeuvre-les-Nancy Cedex, France).

**NEXT PAGE(S)
left BLANK**



DEFINITION OF PROSPECTIVE TERRAINS FOR INDUSTRIAL POLYMINERALIC PLACERS IN THE MISSISSIPPI EMBAYMENT REGION BY USE OF URANIUM EXPLORATION DATA

A.E. GROSZ, W.J. GREENWOOD,
P.G. SCHRUBEN, J.N. GROSSMAN
United States Geological Survey,
Reston, Virginia,
United States of America

Abstract

Titanium, Zr, Hf, rare-earth element (REE), Th, and U data from the Hydrogeochemical Stream Sediment Reconnaissance (HSSR) database, and Th and U from the airborne spectral gamma-ray radiation data base of the National Uranium Resource Evaluation (NURE) program are diagnostic of, and may predict the presence of, commercially important concentrations of industrial heavy minerals. An analysis of these data from the Mississippi embayment region shows that regionally anomalous concentrations of these elements in sediment samples and intensities in airborne radiation surveys can indicate the presence and relative abundance of important industrial heavy minerals such as ilmenite, rutile, zircon, and monazite. Plots of samples with statistically anomalous concentrations of these elements coincide with known placer deposits of industrial heavy minerals. Cretaceous and younger sediments are indicated as likely hosts to undiscovered economic deposits. Volcanic, plutonic, and metamorphic rocks are the sources of the minerals found in these sediments, and thus valley-fill sediments within the crystalline terranes may also host concentrations of placer minerals. Fe/Ti ratios ≤ 1.17 in sediment samples are shown to be sensitive indicators of weathered ilmenite (> 52.7 wt% TiO_2); locations of such samples are coincident with Cretaceous and younger sediments in the study area. The data outline large areas suitable for Ti-Hf-REE-bearing placer exploration. Evidence for potential Ti-Hf-REE placer deposits is given for unconsolidated sediments in the floodplain of the Mississippi River. Good correlations between the abundances of Ce and La, Ce and Th, and Th and U in the sediment samples show how the geographically more extensive NURE airborne spectral gamma-ray data base can be used to outline areas favorable for monazite-bearing placer exploration.

1. INTRODUCTION

Deposits of heavy minerals in modern and ancient beach-complex sediments are important sources for a number of Ti-bearing minerals and are presently the almost exclusive sources for the industrial minerals ilmenite (52.7 wt% TiO_2), weathered ilmenite (containing up to 90 wt% TiO_2), rutile (93–100 wt% TiO_2), zircon (zirconium-hafnium silicate), and monazite (a thorium-rich rare-earth phosphate mineral). Other industrial heavy minerals such as staurolite, garnet, and tourmaline, which are used as abrasives, are common byproducts of such placer mining operations.

The principal variables needed for placer formation are (1) one or more source areas for heavy minerals in particular types of igneous and (or) metamorphic highland terranes [1, 2], (2) a fluvial drainage system that captures, transports, and hydraulically sorts the heavy minerals [for example, 3, 4], (3) a concentrating mechanism consisting of wave, tidal, and eolian action [for example, 5], and (4) the heavy-mineral budget within the depositional environment itself. These variables, coupled with ambient climatic conditions [6], influence the location, quality, grade, and size of the heavy-mineral concentrations.

An economic beach-complex titanium placer may be up to tens of kilometers in length, up to 2 km in width, and 10 m or more in thickness [7]. Grades of ores are highly variable, averaging 3–6 wt% total heavy-minerals, of which typically about 50 percent is economically valuable. The TiO_2 content of ilmenite (including altered ilmenite) in economic deposits ranges from about 50 to 55 wt% in slightly weathered assemblages to about 90 wt% in strongly altered assemblages. Stoichiometric ilmenite contains 52.66 wt% TiO_2 . The weathering processes that remove labile components of heavy-mineral assemblages (for example, pyroxenes, amphiboles, garnet, and sulfides) also remove iron from ilmenite, and as a result the TiO_2 is concentrated.

Modern placer mining methods favor deposits that can be recovered using simple processes. Any large accumulation of sand can be of interest when seeking ilmenite deposits. Loose sands that can be dredged are preferable because dredging is the most economical method of delivering sand to large gravity concentrating units.

Exploration for industrial polymineralic placers traditionally has relied upon geomorphologic and geologic methods. Exploration commonly consists of preliminary field sampling of surficial sediments followed by drill sampling of geomorphologically defined targets. Most commonly these targets are Quaternary beach ridges and associated foredunes or their older equivalents in coastal plain sediments.

Airborne gamma-ray and high-resolution magnetic surveys are also useful in outlining targets for sampling [8, 9, 10, 11]. Induced polarization has been shown to be a promising technique for onshore and offshore placer exploration [12] as well. More recently, Grosz [13, 14, 15] and Grosz and Schruben [16] documented the use of NURE HSSR and spectral airborne radiation data in selecting prospective terranes for placer exploration in the United States.

This report demonstrates the use of national-scale uranium exploration data for delimiting prospective placer areas in the Mississippi embayment region (Fig. 1). The Mississippi embayment is the broad lobe of the Gulf Coastal Plain that extends northward up the Mississippi Valley as far as southern Illinois. Twenty-six areas (encompassing 35 740 km²) having anomalous concentrations of rare-earth elements (REE), 65 areas (encompassing 20 538 km²) having anomalous concentrations of Ti, and 60 areas (encompassing 49 143 km²) having anomalous concentrations of Hf or Zr are delineated. Twenty-five areas (encompassing 5781 km²) having anomalous concentrations of REE, Ti, and Hf and (or) Zr are also delineated. Of these 25 areas, those associated with Cretaceous and younger unconsolidated sediments are most favorable for polymineralic placer exploration. An additional 51 areas (encompassing 80 124 km²) exhibiting anomalous Th aeroradioactivity are delineated and are also permissive for placer exploration.

These areas are delineated by use of NURE HSSR geochemical data and adjunct airborne spectral gamma-ray radiation data. In conjunction with regional geologic information and mineral occurrence data from the Mineral Resource Data System [17] these data are shown to be powerful predictors of industrial placer mineral resource potential.

2. THE NURE PROGRAM

The NURE program gathered data to evaluate uranium resources for the United States and to identify areas favorable for uranium deposits [18]. Between 1975 and 1983, this U.S. Department of Energy program acquired geochemical and airborne spectral gamma-ray data for the conterminous 48 States and Alaska.

The HSSR, one component of the NURE program, entailed collection and analysis of samples of sediment (stream, soil, talus, playa, and others), ground water, surface water, and vegetation to determine concentrations of uranium and other selected elements [19]. These data helped to outline geochemical provinces and to show favorable areas for more detailed investigation.

Another component of the NURE program was aerial gamma-ray surveying. These NURE data compose the only nationwide data set on natural radiation in the environment. The U.S. Geological Survey has reprocessed the aerial gamma-ray data to produce maps showing surface concentrations of K, U, and Th for the conterminous United States [20, 21, 22].

HSSR data reports were issued for 330 of the 468 1° × 2° quadrangles in the 48 conterminous States and for 104 of the 153 quadrangles in Alaska. Thus, about 70% of the Nation has such geochemical coverage. Almost all samples were analysed for uranium, and most were

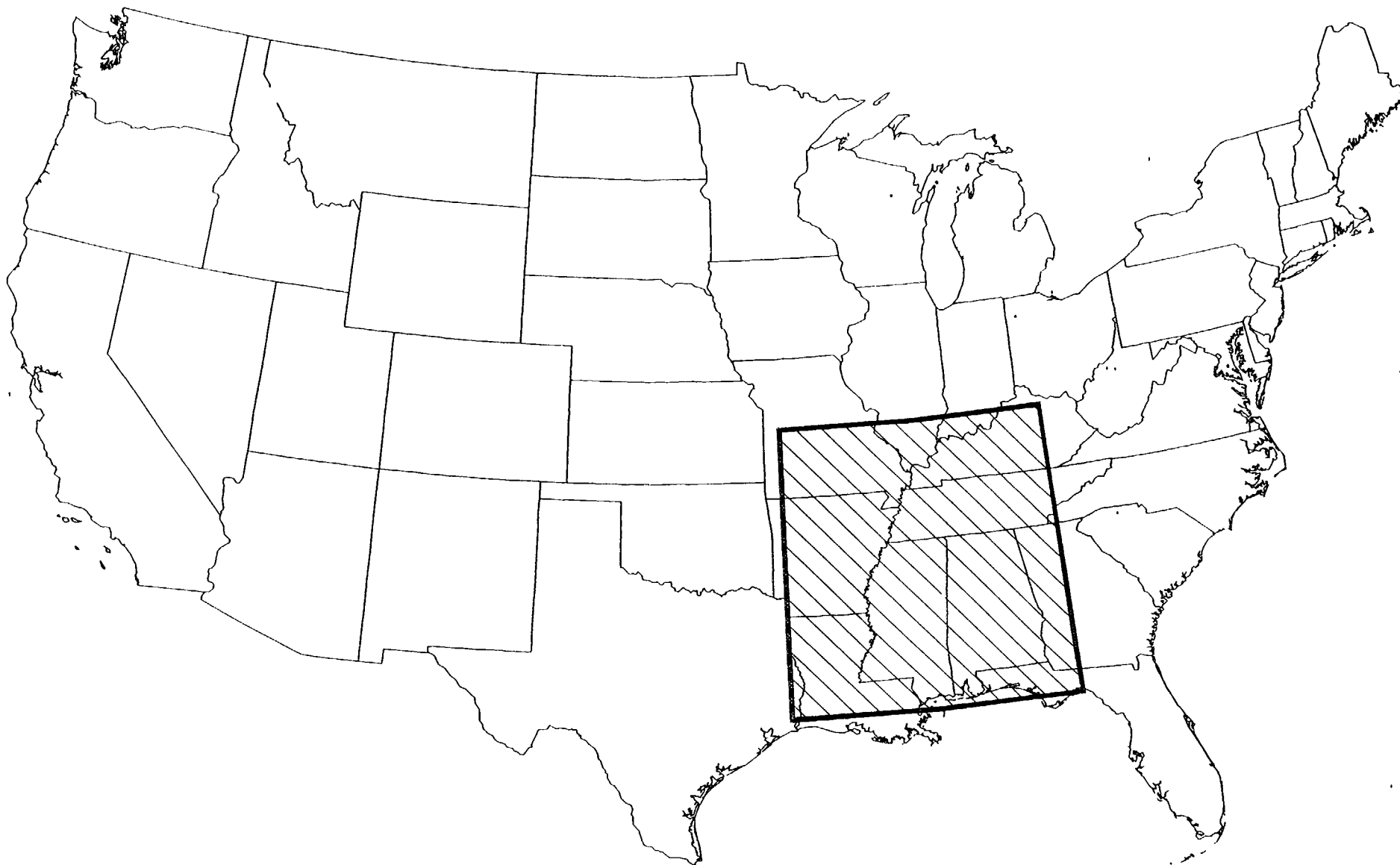


FIG. 1. Map showing the location of the study area.

analysed also for as many as 59 elements [18]. Data used for this study were measured primarily by instrumental neutron activation analysis, and the precision for all elements except U and Th was $\pm 25\%$.

The HSSR data base for each quadrangle contains information on sample types, location coordinates, various descriptive fields, and analytical data. For this study, we did not evaluate the quality of the data or normalize it. We searched the data in the $42\ 1^\circ \times 2^\circ$ quadrangles in the study area for stream-sediment samples (149-micrometer sieve fraction) analysed for Ce, Dy (dysprosium), Eu (europium), Hf, La, Lu (lutetium), Sm (samarium), Th, Ti, Fe, U, Y (yttrium), or Yb (ytterbium); Zr and (or) Hf data are not available for all samples in these quadrangles.

For the area of this study, 57 046 samples (from 19 396 sample sites; most samples were split and analysed for various suites of elements separately) met the search criteria. For each sample, elemental data were originally reported as (1) a positive number (expressed as parts per billion, ppb), (2) zero, or no value (meaning "not analysed"), or (3) a negative number (below the detection limit of the analytical method; that is, $-2000\text{ ppb} = <2000\text{ ppb}$). For this study only positive numbers were used; data are discussed in percent format. Ti values were reported for all samples; however, not all the REE's were analysed in every sample. For most samples, Hf but not Zr was analysed; for the rest of the samples, Zr but not Hf was analysed. Thus, locations of samples with either Hf or Zr anomalies were plotted.

Sample density for the study area varied. As shown on Fig. 2, large segments of central and western Tennessee, Missouri, northern and eastern Arkansas, northern and southern Louisiana, southern Alabama and Georgia, and all of Mississippi were not sampled for stream sediments. Airborne radiation surveys, however, provide coverage for Th, U, and K for regions not sampled for stream sediments.

3. PREVIOUS STUDIES

Russell [23], Olson and Adams [24], Overstreet [25], Sullivan and Browning [26], Mertie [27], Force [4], and Flohr [28], among numerous others, have shown that titanium minerals, monazite, and zircon are present in the Mississippi embayment region. Further, they showed that some sediments and rocks have undergone extensive weathering and (or) other low-temperature alteration that removed much of the labile mineral component (amphiboles and pyroxenes, for example), a process that also concentrates TiO_2 as ilmenite and other Ti-bearing oxide minerals are altered. Recently, Force and others [9], Grosz and others [11], and Owens and others [29] have also documented that radioactive monazite and, to a lesser extent, zircon control the gamma-ray aeroradiometric signature of surficially exposed industrial placer heavy-mineral concentrations.

Olson and Adams [24] show locations of Th and REE deposits in the conterminous United States. Their map shows some of the districts and locations defined as geochemically and (or) aeroradiometrically anomalous by this study. Guild [30, 31] gives additional data on the locations of known deposits and districts in the Mississippi embayment region. Rogers and Jaster [32] and Tooker and Force [33] show locations of Ti deposits and occurrences in the conterminous United States. Their maps also show some of the districts and locations defined as geochemically anomalous by this study.

4. METHODOLOGY AND DATA

The method utilized in this study is given by Grosz [13, 14] and Grosz and Schruben [16] where it is demonstrated to give reliable results. A brief description of the method is given here for clarity. The method is based on the hypothesis that elements such as Ti, and Hf or Zr, in stream-sediment samples indicate the presence of industrial heavy minerals such as ilmenite and rutile, in the

case of Ti, and zircon, in the case of Hf and Zr [34]. The REE are generally assumed to be associated with Y, Th, and U in heavy minerals such as monazite, xenotime, and allanite. Although other commonly occurring heavy and light mineral species can carry these elements as well (for example, Ti, Hf, and Zr in amphiboles and pyroxenes, and REE, U, and Th in apatite), they typically contain only trace-to-minor abundances of these elements.

We attempted to identify anomalous samples by using several statistical methods. Initial attempts to analyse the whole data set (42 1° x 2° quadrangles) resulted in cutoff thresholds that were too high to generate meaningful distribution patterns. This result occurred because high elemental values associated with crystalline terranes produced cutoff thresholds that masked significant variations on the sediment terranes that have generally lower overall abundances. To overcome the controlling effect of the underlying geology, the statistical analysis of data was done on a 1° x 2° quadrangle basis. This approach eliminated some, but not all, of the problems related to changes in thresholds.

Three different methods of defining anomalous values all produced similar geographic distribution patterns. These methods were (1) using two standard deviations above the mean, (2) using curve inflections in cumulative frequency plots to define high-value subpopulations, and (3) isolating the upper 5th, 7th, and 10th percentile values. Although producing similar geographic distribution patterns, the three methods result in different frequencies of anomalous points (that is, the size of the cluster) in a given geographic area. For this study, the upper 10th percentile for each element was found as the most effective for defining anomalies.

For the 42 1° x 2° quadrangles in the study area the upper 10th percentile for individual elements resulted in 1929 samples with REE ranging from 0.001 to 1.43 wt%, 1791 samples having Ti ranging from 0.049 to 9.92 wt%, 1855 samples having Hf ranging from 0.0002 to 0.4806 wt%, and 497 samples with Zr ranging from 0.0072 to 0.0539 wt% as anomalous. These data sets locally define source rocks for possible placer deposits rather than anomalous concentrations of industrial heavy minerals in sediments that may indicate potentially commercial deposits.

Figure 3 displays the relation between Ce and La concentrations for 1,854 samples from the study area having anomalous REE. The r^2 (correlation coefficient) is 0.92. Excluding 6 samples with Ce/La ratios in excess of 85, the average Ce/La ratio of this population is about 2.2 in a range from 0.1 to 14.1. Overstreet [25] states that the monazite in the southeastern United States has a Ce/La ratio of about 2.1. These data suggest that monazite is the dominant carrier of REE in the study area. The minor scatter shown on the diagram may be a function of compositional variability in monazite [25], the presence of apatite (known to occur in the area), and the presence of low-Th, REE-bearing phosphorite in the Cason Shale of northern Arkansas [35].

The relation between Ce and Th for the 1854 samples having anomalous REE is shown in figure 4. The r^2 is 0.96 and indicates that the distribution of Th is very closely associated with that of Ce; Th is also most likely contained in monazite. Figure 5 displays the relation between Th and U for these samples. An r^2 of 0.81 suggests that monazite may also be an important contributor of U. Monazite, therefore, is an important contributor to the radioactivity of the sediments in the study area. Supporting evidence for this interpretation is given by NURE spectral aeroradiometric data [20, 21, 22], which show anomalous REE areas identified in this study to be anomalous in Th and U radioactivity.

5. RESULTS AND DISCUSSION

A generalized lithologic map (shown on Fig. 6) provides the backdrop for the geochemical and aeroradiometric data. Compiled from King and Beikman [36,37], the map shows the general distribution of: 1) crystalline (volcanic, plutonic and intrusive, and metamorphic) and indurated sedimentary (mostly marine) rocks, 2) sediments of Cretaceous age, and 3) sediments of Tertiary and younger age.

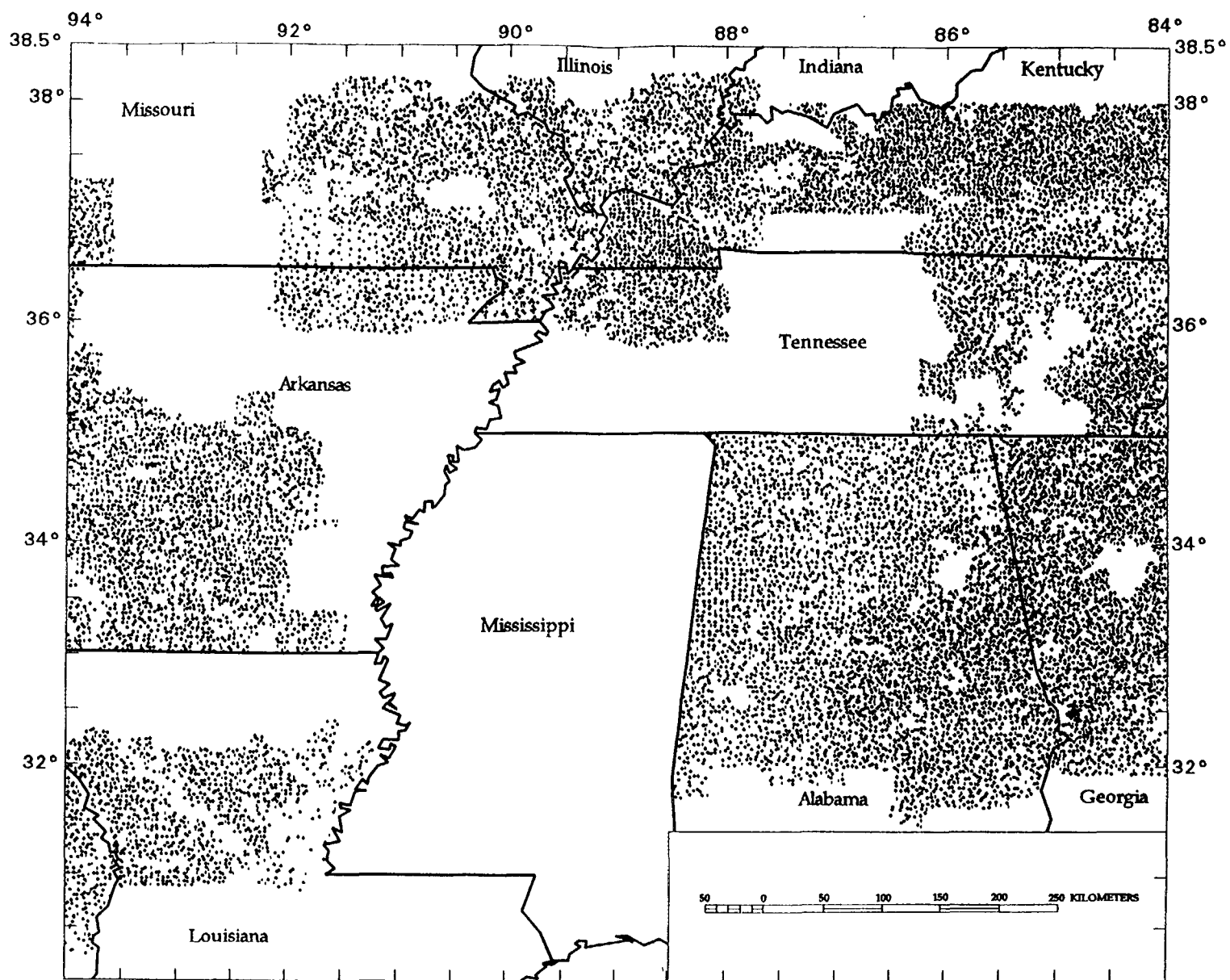


FIG. 2. Map showing stream-sediment sample density in the study area.

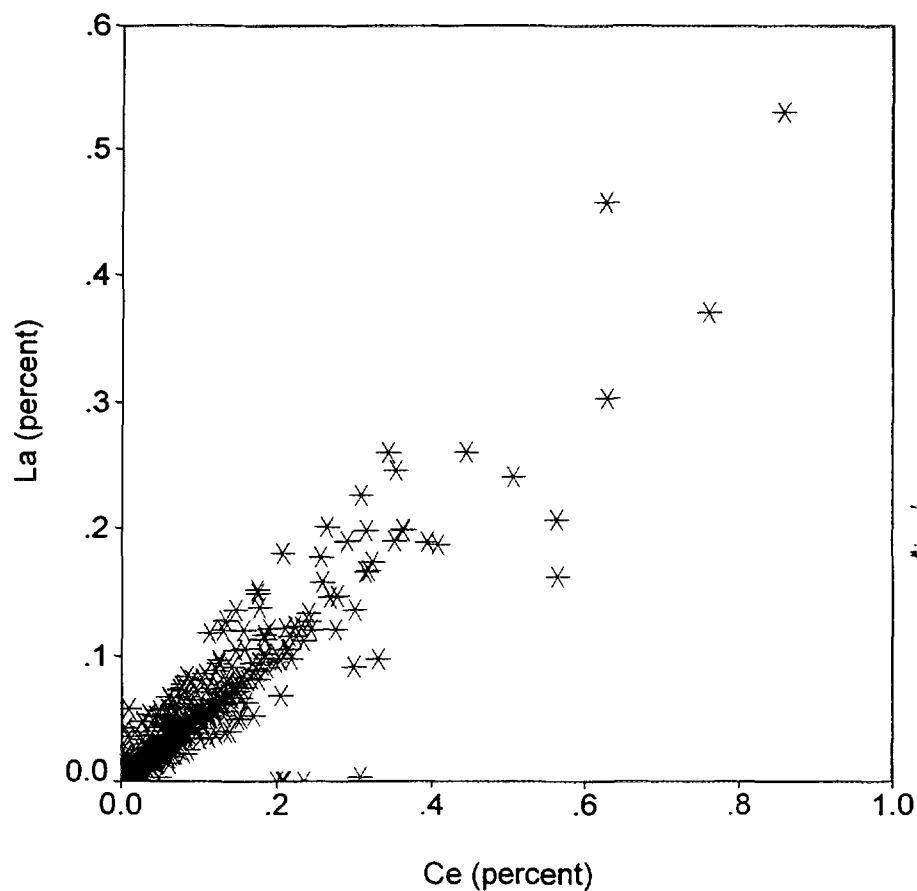


FIG. 3. Relationship between cerium and lanthanum in samples having greater than 0.001% REE.

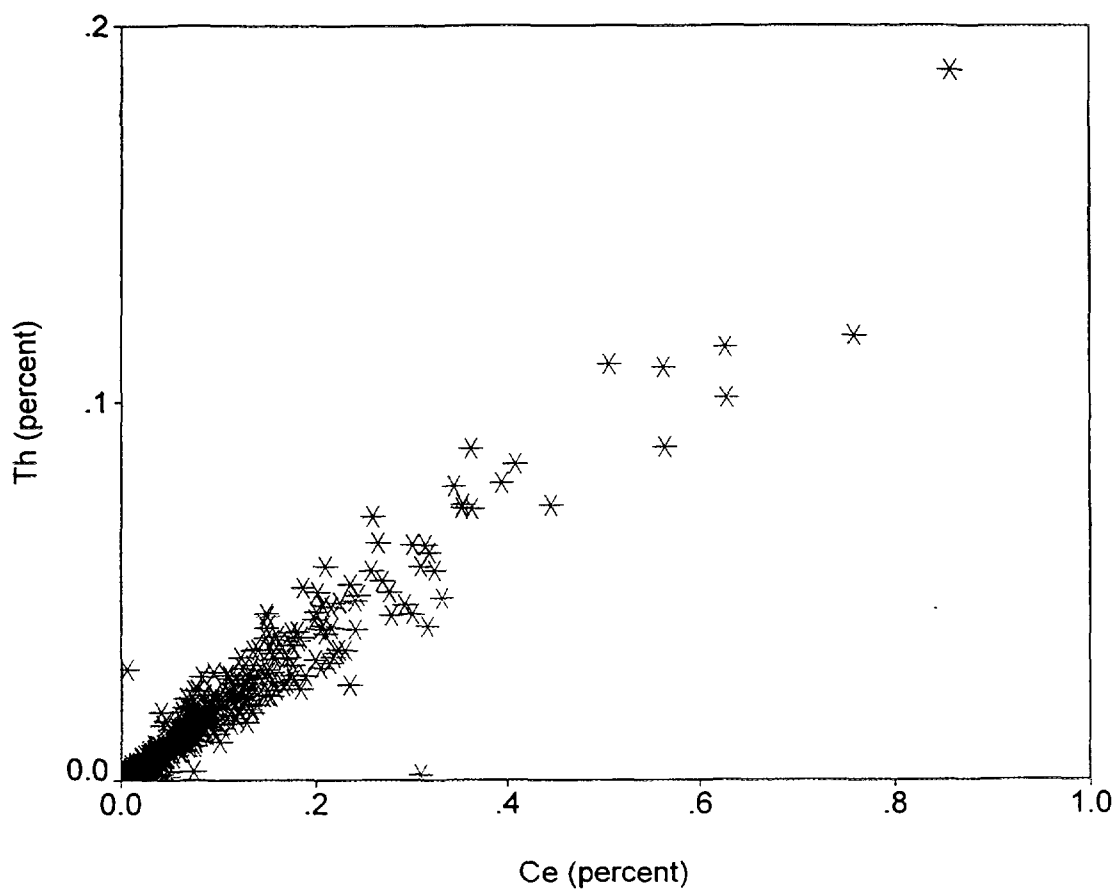


FIG. 4. Relationship between cerium and thorium in samples having greater than 0.001% REE.

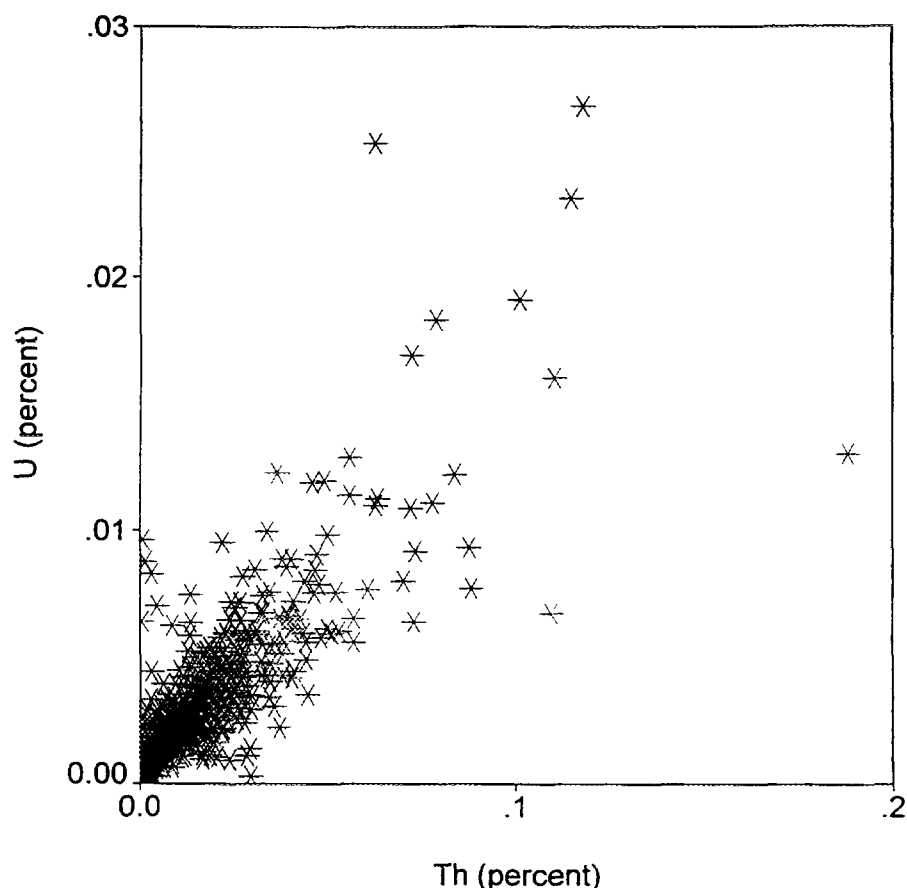


FIG. 5. Relationship between thorium and uranium in samples having greater than 0.001% REE.

Locations of HSSR samples having anomalous Ti, Hf or Zr, and REE concentrations are also shown on Fig. 6. Geochemical anomalies to the east of the Mississippi River are more sharply defined by clustering of samples and have larger absolute values than anomalies to the west. The lower levels of concentration in HSSR anomalies to the west of the Mississippi River are probably a function of source terrane types and distances of sediment transport in samples from these terranes. The lower elemental concentrations in anomalies probably reflect smaller concentrations of industrial placer heavy minerals in these sediments.

Prominent Ti anomalies are associated with crystalline and indurated rocks (henceforth, rocks) as well as with sediments of primary interest in this study. Fe/Ti ratios (discussed in a later section) suggest that most of the Ti anomalies associated with rocks are related to magnetite and titanomagnetite rather than ilmenite, altered ilmenite, or rutile. In western Tennessee, some Ti anomalies (see Fig. 7) are associated with known titaniferous placer deposits of Cretaceous age [32]. Additional known placer deposits in Cretaceous sediments are not shown by the HSSR data because of lack of sample coverage; however, NURE airborne gamma-ray radioactivity data (discussed in a later section) show these areas to be anomalously radioactive in Th because of monazite.

Prominent clusters of anomalous Hf or Zr are associated primarily with crystalline rocks. This association shows these rock types to be important sources of zircon in the study area. Unconsolidated Cretaceous and younger sediments in the Mississippi embayment region have significant and areally extensive clusters of Hf and Zr anomalies.

Most of the large concentrations of REE (≥ 0.1 wt%) are associated with metamorphic, plutonic, and intrusive rocks. Many of the anomalous locations associated with rocks in the eastern portion of the study area are approximately coincident with Mertie's [27] monazite belts.

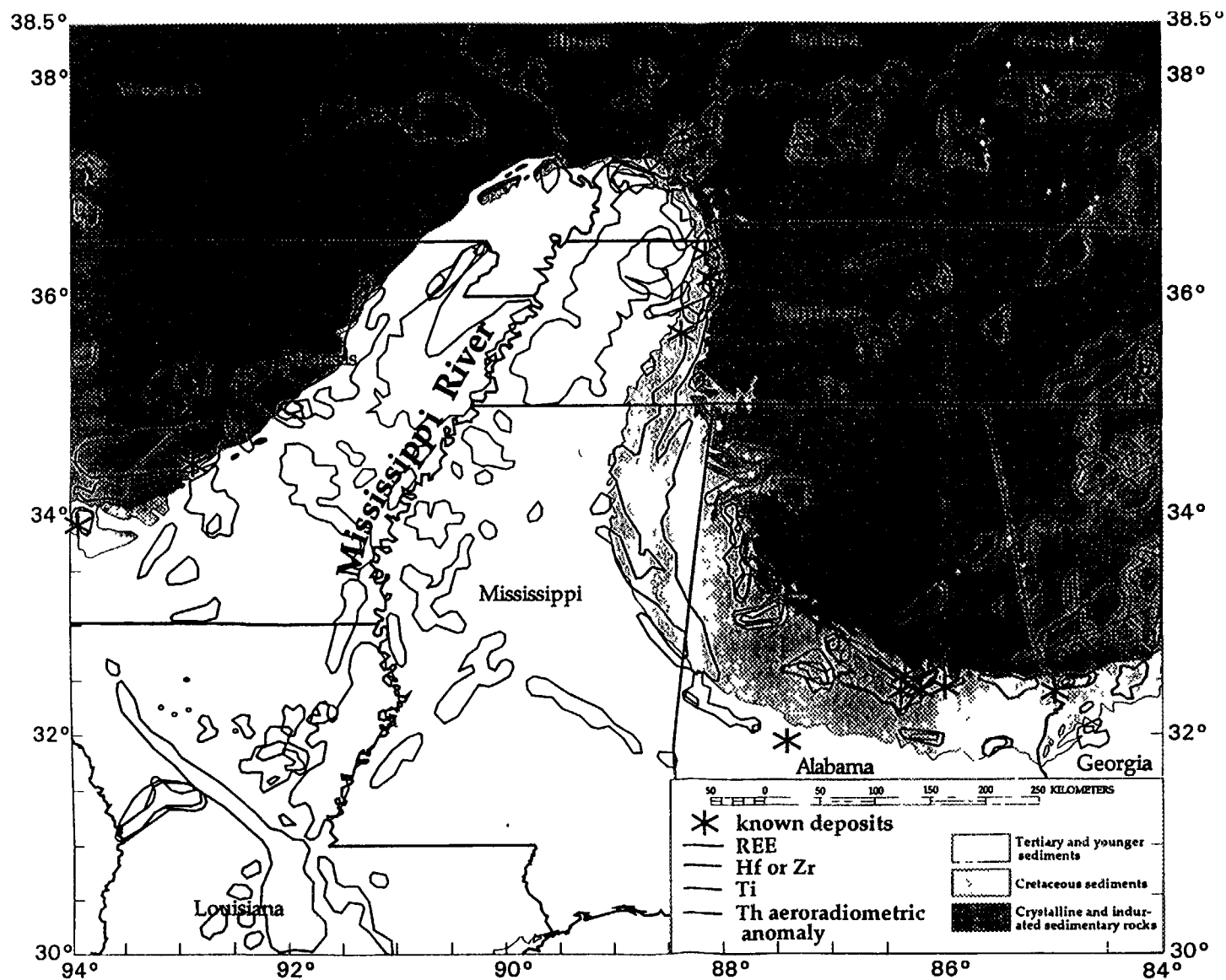


FIG. 6. Map showing the general distribution of rocks and sediments, and locations of samples having anomalous Ti, Hf or Zr, and REE concentrations in the study area.

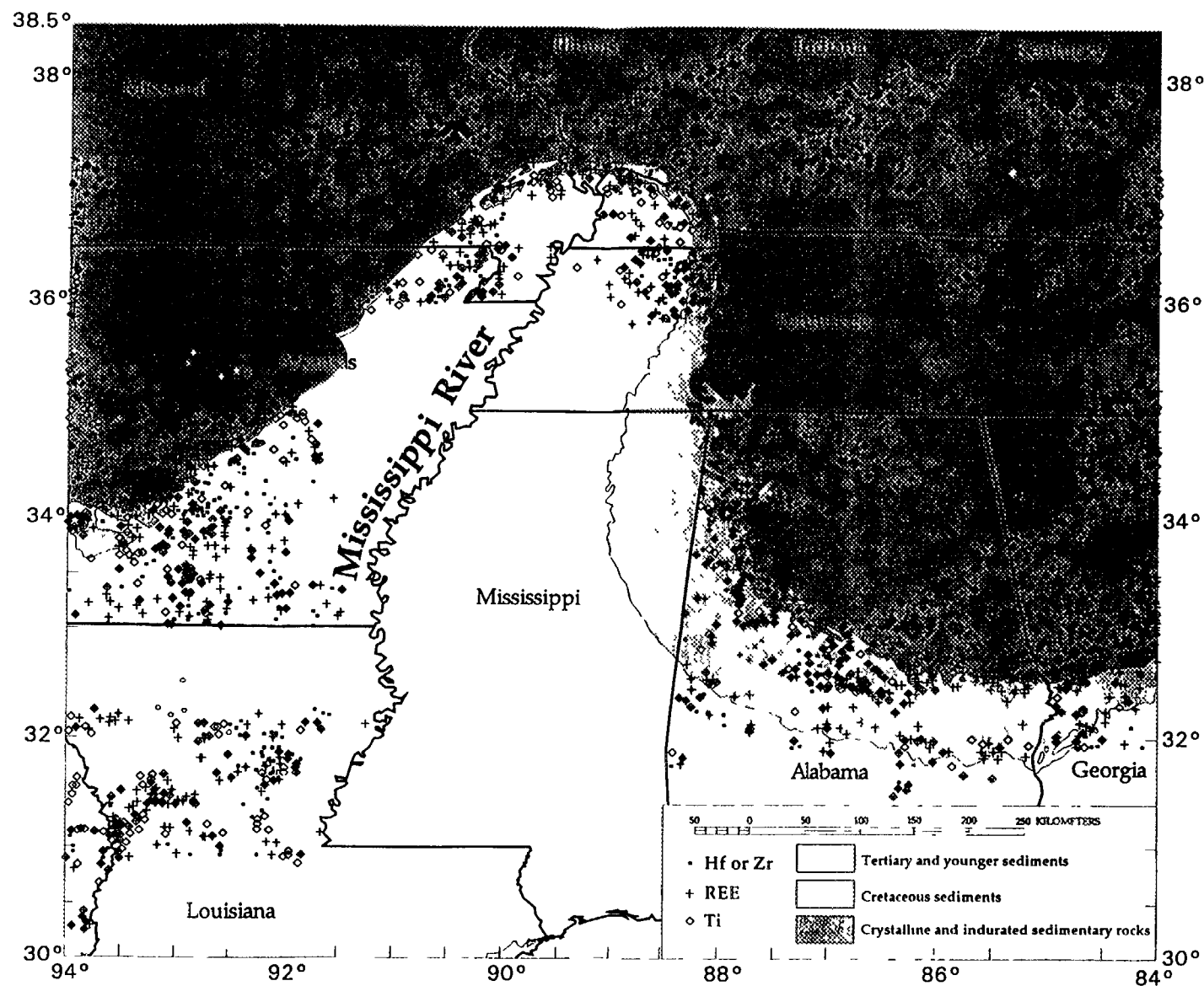


FIG. 7. Map showing locations of Ti, Hf and/or Zr, REE anomalous areas, known prospects, occurrences, and deposits of placer- and rock-hosted industrial minerals [17], and anomalous Th aeroradioactivity in areas not sampled by HSSR.

Unconsolidated Cretaceous sediments host tightly clustered anomalies of varying levels of REE concentration, including some of the largest values in the study area. Some of these anomalies are associated with known deposits of industrial placer minerals.

The principal anomalous clusters and trends of Ti, Hf and (or) Zr, and REE in the Mississippi embayment region are shown on Fig. 7. The clusters (comprising of 5 or more individual HSSR anomalies) encompass surface areas ranging from about 15 km² to over 2500 km². Anomalies for the different elements occur individually, paired, or all together in overlapping element clusters. There are large numbers of individual HSSR anomalies and combinations of anomalies that are not portrayed on Fig. 7; these may indicate areas prospective for industrial polymineralic placer deposits as well.

The best prospects for important concentrations of industrial polymineralic placers are in areas where the three element groups overlap. Such overlap indicates that titanium minerals, zircon, and monazite are probably present. Anomalies associated with rocks have a lower potential for large-volume deposits of industrial mineral placers than anomalies associated with unconsolidated sediments. It is likely, however, that workable fluvial placers of primarily monazite and zircon exist in valley fills within the crystalline terranes, particularly where tightly clustered large-value geochemical anomalies are suggestive of heavy-mineral-rich source rocks.

Although a large number of areally extensive individual and overlapping anomalous clusters are associated with rocks, the best prospects for industrial polymineralic placers are where the clusters are coincident with sediments of Cretaceous and younger age. Evidence for this interpretation is given by the association of Ti, REE, and Hf or Zr anomalous clusters with locations of known deposits, prospects, and occurrences of industrial polymineralic placers (Fig. 7). In Cretaceous sediments of western Tennessee, HSSR anomalies correspond to known deposits of industrial heavy minerals [32, 33, 38, 39]. This association occurs locally over Cretaceous and younger sediments elsewhere in the area of this study.

Aeroradioactivity data [20, 21, 22] show anomalous U and Th signatures over many areas outlined as geochemically anomalous in the study area, because of Th in monazite, and provide guides for locating prospective targets for sampling in Mississippi and in other areas lacking HSSR coverage. Aeroradioactivity anomalies in regions not covered by HSSR are also shown on Figure 7. Numerous analyses of sediment samples from the Mississippi River and from adjacent sediments show the presence of monazite, ilmenite, rutile, and zircon [for example, 23, 25, 40, 41]. Their presence is consistent with the occurrence of aeroradioactivity anomalies as well as with Cretaceous sediments sequences being, at least in part, sources for these sediments. As there are few geomorphic and geologic indicators for selecting placer exploration targets in this region, the combination of geochemical and geophysical data can be used as an alternate tool for exploration.

An important and particularly useful criterion for selecting areas prospective for high-Ti minerals (altered ilmenite and rutile) is the Fe/Ti ratio. This ratio is about 1.17 for stoichiometric ilmenite [42; Fe=36.8 wt%, Ti=31.6 wt%, O=31.6 wt%], and is lower for weathered ilmenite that has had Fe removed.

Of the 1791 HSSR samples with Ti >0.049 wt%, 1740 samples have data for both Fe and Ti. The Fe/Ti ratio for these samples ranges from 0.16 to 28.6. Clusters of samples with anomalous Ti that also have Fe/Ti ratios ≤ 1.17 (297 samples) are closely associated with Cretaceous and younger sediments (Fig. 8). The implication is that Cretaceous sediments have undergone extensive weathering, a process that removes Fe and thereby concentrates TiO₂ during alteration of ilmenite. Fe/Ti ratios smaller than 1.17 could be used to highlight terranes with rutile enrichment, the TiO₂ mineral preferred by mineral producers. It is important to note, however, that sphene can also impart Fe/Ti ratios ≤ 1.17 to sediment samples. Locations of samples having Fe/Ti ratios >1.17 (1443 samples) are typically associated with rocks, suggesting that magnetite and titanomagnetite, rather than ilmenite, altered ilmenite, rutile, or sphene, are the principal Ti-bearing minerals.

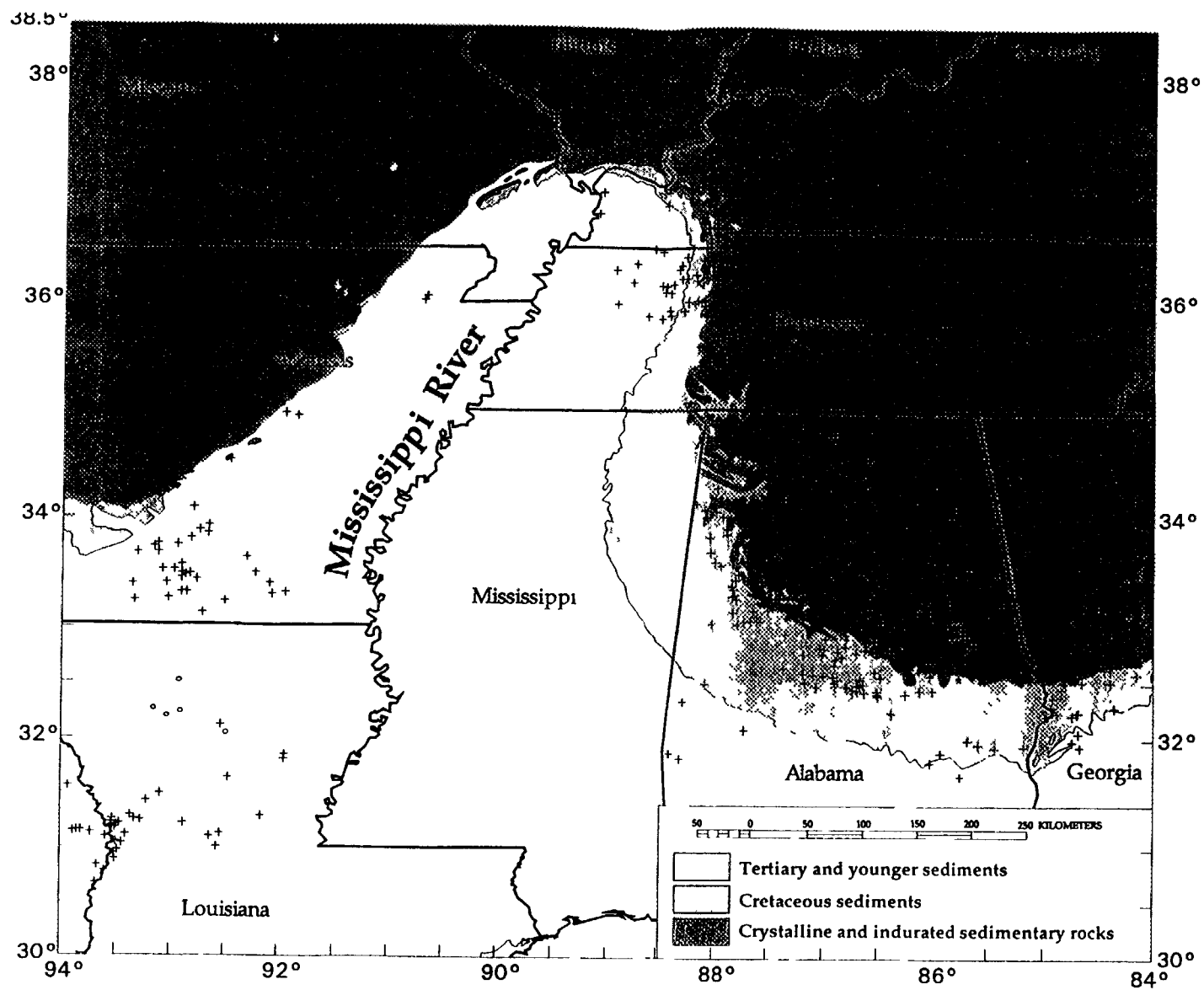


FIG. 8 Map showing locations of samples having Fe/Ti ratios ≤ 1.7

6. CONCLUSIONS

NURE HSSR geochemical and spectral airborne gamma-ray radiometric data for the Mississippi embayment region are well suited for outlining prospective areas for industrial polyminerale placer deposits. In combination with regional geologic and mineral-resource occurrence information, these data are powerful predictive tools for mineral-resource assessment and exploration activities. Data for Ti, Zr or Hf, and REE in the NURE HSSR data base for the United States, are reliable indicators of ilmenite (and other Ti-bearing oxides), zircon, and monazite (and other REE-bearing minerals) in rocks and in unconsolidated sediments.

Ti, Hf, Zr, and REE anomalies occur in a broad spectrum of geologic settings. Unusually high and areally extensive concentrations of Ti, REE, and Hf or Zr are associated with Cretaceous and younger sediments. Rocks in the area of this study also host Ti, Zr, and REE concentrations. Valley fills next to these anomalous rocks could contain commercial accumulations of industrial heavy minerals.

The geochemical data clearly outline areas of known Ti-Zr-REE-bearing industrial polyminerale placer deposits in the Mississippi embayment region; spectral gamma-ray surveys provide supporting evidence for the presence of monazite and associated Th in these deposits. The use of low (≤ 1.17) Fe/Ti ratios enables the selection of areas where weathered ilmenite and (or) rutile are likely the principal Ti minerals present.

Examination of anomalous samples for any given element, as done in this study, excludes much valuable information on potential large-volume, low-grade deposits of industrial mineral placer deposits, particularly in sediments in which geochemical expression is comparatively subdued. However, results of this study suggest that the potential for Ti-Hf-REE-U-Th-bearing industrial polyminerale placer deposits in sediments and sedimentary rocks of the Mississippi embayment region may be much greater than previously recognized.

Regional geochemical and geophysical data bases collected by other nations may also lend themselves to similar interpretation and application to industrial placer mineral resource exploration.

REFERENCES

- [1] FORCE, E.R., Metamorphic source rocks of titanium placer deposits, A geochemical cycle, *in* Geology and resources of titanium: U.S. Geological Survey Professional Paper 959-A (1976) p. A1-A10.
- [2] HERZ, NORMAN, Titanium deposits in alkalic igneous rocks, *in* Geology and resources of titanium: U.S. Geological Survey Professional Paper 959-E (1976) p. E1-E6.
- [3] SLINGERLAND, RUDY, Role of hydraulic sorting in the origin of fluvial placers: *Journal of Sedimentary Petrology*, v. 54 (1984) p. 137-150.
- [4] FORCE, E.R., *Geology of titanium-mineral deposits*: GSA Special Paper 259 (1991) 112 p.
- [5] MACDONALD, E.H., *Alluvial mining*: New York, Chapman and Hall Limited (1983) 508 p.
- [6] FORCE, E.R., and LARSEN, C.E., A paleoclimate-source terrane model for shoreline placer deposits of titanium minerals, and implications for offshore deposits [abs.]: 12th International Sedimentological Congress, August 1986, Canberra, Australia (1986) p. 109.
- [7] COX, D.P., and SINGER, D.A., Mineral deposit models: U.S. Geological Survey Bulletin 1693 (1986) 379 p.
- [8] ROBSON, D.F., and SAMPATH, N., Geophysical response of heavy-mineral sand deposits at Jerusalem Creek, New South Wales: *Bureau Mineral Resources Journal of Australian Geology and Geophysics* (1977) v. 2, p. 149-154.

- [9] FORCE, E.R., GROSZ, A.E., LOFERSKI, P.J., and MAYBIN, A.H., Aeroradioactivity maps in heavy-mineral exploration, Charleston, South Carolina, area: U.S. Geological Survey Professional Paper 1218 (1982) 19 p.
- [10] GROSZ, A.E., Application of total-count aeroradiometric maps to the exploration for heavy-mineral deposits in the Coastal Plain of Virginia, *with a section on* Field-spectrometer-data reduction, by K.L. Kosanke: U.S. Geological Survey Professional Paper 1263 (1983) 20 p.
- [11] GROSZ, A.E., CATHCART, J.B., MACKE, D.L., KNAPP, M.S., SCHMIDT, WALTER, and SCOTT, T.M., Geologic interpretation of the gamma-ray aeroradiometric maps of central and northern Florida: U.S. Geological Survey Professional Paper 1461 (1989) 48 p.
- [12] WYNN, J.C., GROSZ, A.E., and CARLSON-FOSCH, V.L., Induced polarization response of some titanium-bearing placer deposits in the southeastern United States, *in* Fink, J.B., ed., Induced polarization--application and case histories: Tulsa, Society of Exploration Geophysicists, Investigations in geophysics v.4 (1990) p. 280-303.
- [13] GROSZ, A.E., Mineralogy and heavy-mineral resource potential of surficial sediments on the Atlantic Continental Shelf offshore of Georgia: Georgia Geologic Survey Project Report 19 (1993) 31 p.
- [14] GROSZ, A.E., NURE stream sediment geochemical data indicative of prospective terranes for Ti-Zr-REE placer exploration in selected regions of the United States: U.S. Geological Survey Open-File Report 93-240-A (1993) 158 p. (paper copy).
- [15] GROSZ, A.E., NURE stream sediment geochemical data indicative of prospective terranes for Ti-Zr-REE placer exploration in selected regions of the United States: U.S. Geological Survey Open-File Report 93-240-B (1993) (diskette, includes manuscript text and data).
- [16] GROSZ, A.E., and SCHRUBEN, P.G., NURE geochemical and geophysical surveys--Defining prospective terranes for United States placer exploration: U.S. Geological Survey Bulletin 2097 (1994) 9 p.
- [17] MINERAL RESOURCES DATA SYSTEM (MRDS), A data base compiled by the Branch of Resource Analysis, U.S. Geological Survey. [Available from USGS, EMRST, MS 954, 12201 Sunrise Valley Drive, Reston, VA 22092].
- [18] AVERETT, W.R., National uranium resource evaluation guide to data reports of the hydrogeochemical and stream sediment reconnaissance: U.S. Department of Energy, GJBX-5(84) (1984) 119 p.
- [19] ARENDT, J.W., BUTZ, T.R., CAGLE, G.W., KANE, V.E., and NICHOLS, C.E., Hydrogeochemical and stream sediment reconnaissance procedures of the uranium resource evaluation project: U.S. Department of Energy, GJBX-32(80) (1980) 53 p.
- [20] DUVAL, J.S., JONES, W.J., RIGGLE, F.R., and PITKIN, J.A., Equivalent uranium map of the conterminous United States: U.S. Geological Survey Open-File Report of 89-478, (1989) 10 p., scale 1:2 500 000.
- [21] DUVAL, J.S., JONES, W.J., RIGGLE, F.R., and PITKIN, J.A., Potassium and thorium maps of the conterminous United States: U.S. Geological Survey Open-File Report 90-338, (1990) 16 p., scale 1:2 500 000.
- [22] PHILLIPS, J.D., DUVAL, J.S., and AMBROSIAK, R.A., National Geophysical Data Grids: Gamma-ray, gravity, magnetic, and topographic data for the conterminous United States: U.S. Geological Survey Digital Data Series DDS-9 (1993) 1 CD-ROM.
- [23] RUSSELL, R.D., Mineral composition of Mississippi river sands: Geological Society of America Bulletin (1937) v. 48, no. 9, p. 1307-1348.
- [24] OLSON, J.C., and ADAMS, J.W., Thorium and rare earths in the United States, exclusive of Alaska and Hawaii: U.S. Geological Survey Mineral Investigations Resource Map MR-28, with explanatory pamphlet (1962) scale 1:3 168 000.
- [25] OVERSTREET, W.C., The geologic occurrence of monazite: U.S. Geological Survey Professional Paper 530 (1967) 327 p.
- [26] SULLIVAN, G.V., and BROWNING, J.S., Recovery of heavy minerals from Alabama sand and gravel operations: U.S. Bureau of Mines Technical Progress Report 22 (1970) 14 p.
- [27] MERTIE, J.B., Jr., Monazite placers in the southeastern Atlantic States: U.S. Geological Survey Bulletin 1390 (1975) 41 p.

- [28] FLOHR, M.J.K., Titanium, vanadium, and niobium mineralization and alkali metasomatism from the Magnet Cove Complex, Arkansas: *Economic Geology* (1994) v.89. p. 105–130.
- [29] OWENS, J.P., GROSZ, A.E., and FISHER, J.C., Aeroradiometric map and geologic interpretation of part of the Florence and Georgetown 1° × 2° quadrangle, South Carolina: U.S. Geological Survey Miscellaneous Investigations Series Map I-1948-B (1990) scale 1:250 000.
- [30] GUILD, P.W., Preliminary metallogenic map of North America--A numerical listing of deposits: U.S. Geological Survey Circular 858-A (1981) 93 p.
- [31] GUILD, P.W., Preliminary metallogenic map of North America--An alphabetical listing of deposits: U.S. Geological Survey Circular 858-B (1981) 72 p.
- [32] ROGERS, C.L., and JASTER, M.C., Titanium in the United States (exclusive of Alaska and Hawaii): U.S. Geological Survey Mineral Investigations Resource Map MR-29 (1962) scale 1:3 168 000.
- [33] TOOKER, E.W., and FORCE, E.R., Preliminary map of titanium provinces in the conterminous United States, U.S. Geological Survey Open-File Report 79-576-K (1980) scale 1:5 000 000.
- [34] VLASOV, K.A., ed., *Geochemistry and mineralogy of rare elements and genetic types of their deposits* [translated from Russian by Z. Lerman and Y. Brenner, Israel Program for Scientific Translations]: Jerusalem, Israel (1966) 1633 p.
- [35] GROSZ, A.E., MEIER, A.L., and CLARDY, B.F., Rare earth elements in the Cason Shale of northern Arkansas: a geochemical reconnaissance: Arkansas Geological Commission Information Circular 33 (1995) 13 p.
- [36] KING, P.B., and BEIKMAN, H.M., Geologic map of the United States, exclusive of Alaska and Hawaii: U.S. Geological Survey Special Geologic Map (1974) 3 sheets, scale 1:2 500 000.
- [37] KING, P.B., and BEIKMAN, H.M., Explanatory text to accompany the geologic map of the United States: U.S. Geological Survey Professional Paper 901 (1974) 39 p.
- [38] HERSHEY, R.E., Mineral resources summary of the Chesterfield quadrangle, Tennessee: Tennessee Division of Geology (1968).
- [39] WILCOX, J.T., Preliminary investigations of heavy minerals in the McNairy Sand of west Tennessee: Tennessee Division of Geology, Report of Investigation 31 (1971) 11 p.
- [40] BORNHAUSER, MAX, Heavy mineral associations in Quaternary and late Tertiary sediments of the Gulf Coast of Louisiana and Texas: *Journal of Sedimentary Petrology* (1940) v. 10, no. 3, p. 125–135.
- [41] ROSEN, N.C., Heavy minerals and size analysis of the Citronelle Formation of the Gulf Coastal Plain: *Journal of Sedimentary Petrology* (1969) v. 39, no. 4., p. 1552–1565.
- [42] HURLBUT, C.S., Jr., *Dana's manual of mineralogy*, 18th ed.: New York, John Wiley and Sons, Inc. (1971) 579 p.

**NEXT PAGE(S)
left BLANK**

ADVANTAGES OF INTEGRATION OF URANIUM EXPLORATION DATA IN GIS AND MODELS AS TOOLS FOR DECISION SUPPORT

M.C.L. TUSVELD

IWACO Consultants for Water and Environment,
Rotterdam, Netherlands



XA9745965

Abstract

In many areas where uranium has been or is explored, an enormous amount of data on geology and hydrogeology is available. When these uranium exploration data are stored in a structured way, they can be made useful for other purposes than uranium exploration only. For instance, in case of environmental pollution, which is often a side-effect of uranium activities such as mining and leaching, the data can be used to develop a computer model of the environment. With such a model impacts can be calculated of different scenarios for cleaning up or isolation of the pollution. A GIS can be used to store the data, to visualize the data (map production) and to analyse the data, but also to calculate input for the models. The advantages of using GIS and models as tools for decision support are explained with the Contaminant Transport Information System (CTIS) as a case study. The CTIS has been developed for remediation operations in the uranium mining area Stráž pod Ralskem and Hamr in the Czech Republic. The CTIS consists of a GIS database, a regional groundwater flow model and a local contaminant transport model as well as interfaces for data transfer between the components of the information system. The power of the CTIS lies in the fact that the modelling necessary for the design of a remediation operation can be carried out efficiently by using one of the two models, depending on the specific question. Thus alternative remediation scenarios can be judged easily and fairly on their consequences and effectiveness.

1. URANIUM EXPLORATION DATA: SHIFT TO ENVIRONMENTAL DATA

In many areas where uranium has been or is explored, an enormous amount of data is available. Initially the data concentrated on the existence and distribution of uranium as well as the uranium contents of layers. However environmental pollution caused by uranium exploration and exploitation requires more and more attention. Therefore data are coming available on the quality of the air, soil, groundwater and surface water.

Environmental pollution due to uranium activities can be caused in several ways:

- mining and milling;
- leaching: chemical leaching, underground leaching or heap leaching;
- tailing ponds and waste dumps of ore or waste rock.

Due to these uranium activities the air, soil, groundwater and surface water will be contaminated to a certain extent. To determine the amount of environmental pollution all kind of data are measured and collected. In some cases a monitoring system is set up to be able to monitor the environmental pollution.

The available data can be very diverse, such as:

- geological data: depth, thickness and contents of geological layers, including uranium content;
- hydrogeological data: depth and thickness of aquifers and aquitards, groundwater levels, groundwater quality data;
- surface water data: surface water levels, discharge and quality;
- meteorological data: precipitation and evaporation;
- air data: wind directions and velocity, air quality.

2. ADVANTAGES OF USING GIS

When these data are stored in a structured way, they can be made useful for other purposes than uranium exploration only. For instance in case of environmental pollution the data can be used to determine the hazards for public health and to develop strategies for cleaning up the environment or prevent distribution of the pollution.

A Geographical Information System (GIS) can be used to store the data in a structured way. Setting up the structure of the GIS database and filling the database is often a labour-intensive job, but the use of the GIS database has a lot of advantages. The main advantages are that maps can be produced in a quick and cheap way, maps can be easily updated, geometrical data are automatically calculated by the GIS (lengths, areas, volumes), statistical data can be generated from the data (minimum, maximum, average, standard deviation), new data can be derived of existing data without changing the original data and selections or generalisations of maps can be explicitly defined. Moreover maps of different scales can be easily overlain and compared in a GIS and it is easy to experiment with different layouts of maps.

The main functions of a GIS can be characterized as follows (Fig. 1):

- data input: a GIS has many tools to enter data into the digital database, eg. by digitizer, scanner, mouse or keyboard;
- data storage and database management: the data can be stored in a structured way in the GIS by means of the (relational) database management system (DBMS);
- data output and presentation: the GIS can be used to visualize the data in maps, tables, charts or 3D-surfaces. All kind of data layers can be combined into one map, such as measured data (boreholes) and interpreted data (eg. distribution of a parameter);
- data transformation: data transformation can be divided into three different functions:
 - maintenance: tools for updating the data or remove errors;
 - interpolation: data can be interpreted or new data layers can be generated by calculating contour lines, 3D surfaces, Thiessen polygons or by kriging the data;
 - analysis: maps can be analyzed by using overlay techniques. The result of the overlay becomes available as a map. In case a map with the distribution of the environmental pollution is overlain with a land use map, the resulting map will show for instance which agricultural areas are located within the polluted area.

3. ADVANTAGES OF USING COMPUTER MODELS

Computer models are a simulation of the reality. Models are set up with a certain purpose, namely to calculate an existing or future situation. In case of environmental pollution possible computer calculations can be:

- existing situation: to calculate an existing situation is necessary to calibrate the model as well as to generate a reference situation in case of scenario calculations. Models are usually calibrated by comparing measured data with calculated data;
- zero scenario: to calculate a future situation in case no measures are taken to improve the pollution situation;
- stabilize scenarios: to calculate the impact of scenarios to prevent the distribution of pollution;
- cleanup scenarios: to calculate the impact of scenarios to clean-up the pollution.

4. DECISION SUPPORT SYSTEM

The data that are stored in the GIS can be used as input parameters for the modelling of the environment. By coupling the GIS with one or more models a powerful tool becomes available for

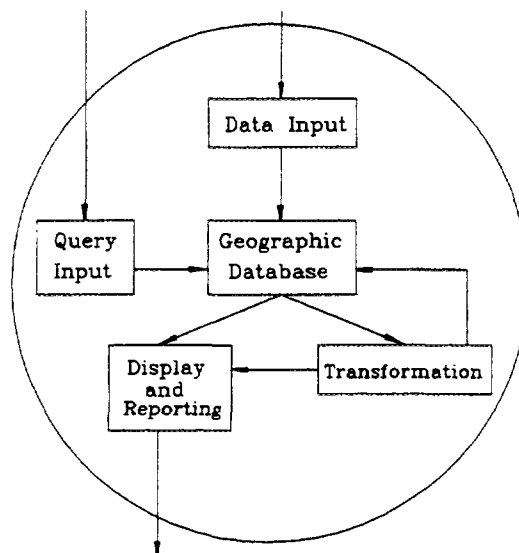


FIG. 1. The main functions of a GIS [1].

environmental management. The GIS can be used for the data management and the presentation of data into maps, while the models can be applied to calculate the impact of scenarios. A decision support system (DSS) is one step ahead of the coupling of GIS and models. In a decision support system the user (decision maker) can develop strategies for improvement of the environment. The data necessary to calculate the impact are retrieved by the DSS from the GIS and the models calculate the impact, the output of the models is redirected to the GIS and displayed to the user. The user has the possibility to compare several scenarios, which will lead to a better understanding of the impacts of potential measures to improve the environment. Therefore the DSS will help to generate useful scenarios as well as facilitates the process of making a decision.

5. CASE STUDY: CONTAMINANT TRANSPORT INFORMATION SYSTEM

The advantages of using GIS and models as tools for decision support are explained with the Contaminant Transport Information System (CTIS) as a case study. The CTIS has been developed for remediation operations in the uranium mining area Stráž pod Ralskem - Hamr (see fig. 2) in the Czech Republic [2]. The Contaminant Transport Information System has been set up for the Czech uranium mining company Diamo s.p. in the frame work of the bilateral Programme for Cooperation with Eastern Europe (PSO) of the government of The Netherlands.

The CTIS consists of a GIS database, a regional groundwater flow model and a local contaminant transport model as well as interfaces for data transfer between the components of the information system. The power of the CTIS lies in the fact that the modelling necessary for the design of a remediation operation can be carried out efficiently, based on a GIS database coupled with two models. Thus alternative remediation scenarios can be judged easily and fairly on their consequences and effectiveness.

5.1. Background

A large uranium deposit is found in the northern part of the Czech Republic near Stráž pod Ralskem (see fig. 2). The uranium is present approximately 200 meters below the ground surface. The exploitation started in 1967 with the excavation of conventional underground mines. Later in-situ hydrochemical leaching was introduced. A large number of injection and extraction wells has been

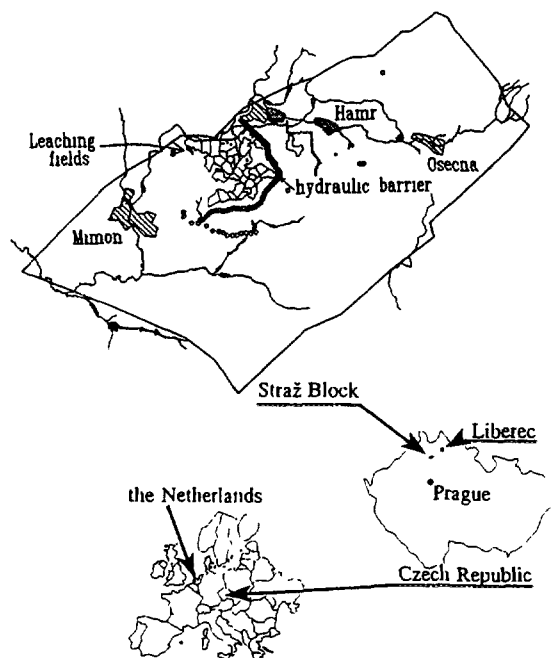


FIG. 2. Location of area of interest.

implemented in some 30 so-called 'leaching fields'. An hydraulic barrier has been installed in between the mines and the leaching fields. The barrier consists of about 200 wells that inject water and prevents the migration of the leaching fluid away from the leaching fields towards the mines. The hydrogeological scheme is shown in fig. 3 and described in more detail in [2, 3].

The leaching of the uranium ore has caused a major groundwater contamination extending over $\pm 20 \text{ km}^2$. Huge quantities of the strongly oxidizing and acidic leaching fluid have been injected and a large volume of this fluid is still present. Near the surface the groundwater has been contaminated by spills and leakage from processing plants and transport pipe lines as well as defective casings of the injection and abstraction wells of the leaching fields. The major constituents of the contamination, both near the surface and at depth, are heavy metals (mainly aluminum) and sulphate. The average density of the leaching fluid is about 1050 kg/m^3 , so that density differences have a significant influence on the groundwater flow. The deep contamination poses a long term threat to the groundwater in a large part of the Czech Republic. The shallow contamination is of immediate concern for the local drinking water supply.

5.2. Why developing an Information System?

Remediation of the aquifers is considered necessary, but it will be a very large, expensive and time consuming operation. A detailed investigation of the present situation and of possible remediation scenarios is of paramount importance. The costs invested in the investigation will save expenses in the actual remediation. For this investigation a Contaminant Transport Information System has been built (CTIS).

The extend and severity of the contamination in the Stráž pod Ralskem area require a thorough investigation prior to the design of any remediation operation. Numerical modelling of the groundwater flow provides a powerful tool in predicting the effectiveness of various remediation scenarios. The modelling has been based on the large amount of data that is available and on new data that have been collected. The data have been stored in a database that is easily accessible and that also allows new data to be added.

5.3. The Contaminant Transport Information System (CTIS)

The entire Stráž Block (180 km²) had to be covered by a numerical model because of the large influence of the uranium exploitation operations on the groundwater flow and the lack of natural boundaries within the block. On the other hand, the density differences in the area of the leaching fields and the intricate geology required a large amount of detail and hence a large model resolution. These conflicting demands can not be met by one single numerical model. Therefore, the various aspects of the contamination and possible remediation scenarios have been investigated using different models (regional and local).

Consequently a large amount of information had to be transferred between the database and the models and mutually between the models. To ensure efficient data transfer and to avoid the introduction of errors, the Contaminant Transport Information System (CTIS) was constructed, combining the models and the database.

The information system consists of the following components (fig. 4):

- a database, set up in the Geographical Information System ARC/INFO;
- a regional groundwater flow model using TRIWACO;
- a local groundwater flow and contaminant transport model using METROPOL;
- a GIS-model interface between ARC/INFO, TRIWACO and METROPOL.

To get an idea of the density of information and the accuracy of the calculations, some characteristics are given here:

ARC/INFO	15.000 boreholes	1.000 observation wells		
TRIWACO	quasi-3D	2537 nodes	4925 elements	3 layers
METROPOL	fully 3D	6944 nodes	5670 elements	8 layers

In figure 5 an example is given of piezometric heads calculated by TRIWACO for the upper Turonian aquifer and for the lower Cenomanian aquifer.

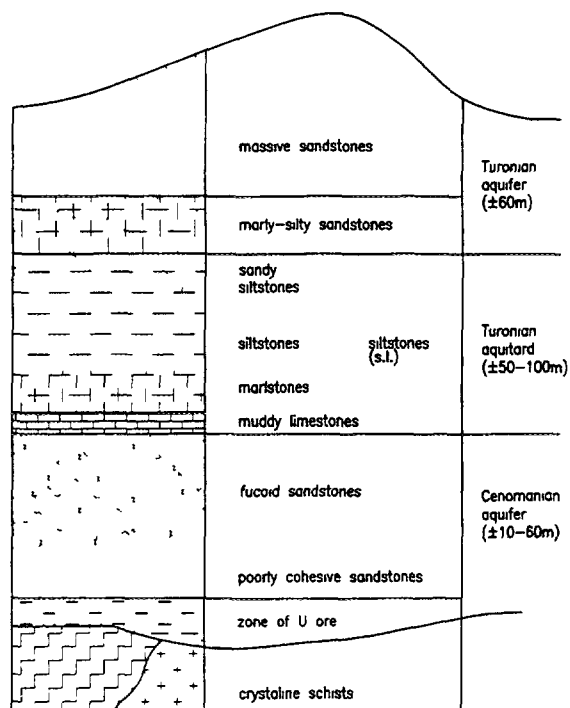


FIG. 3. (Hydro)geology of Stráž Block.

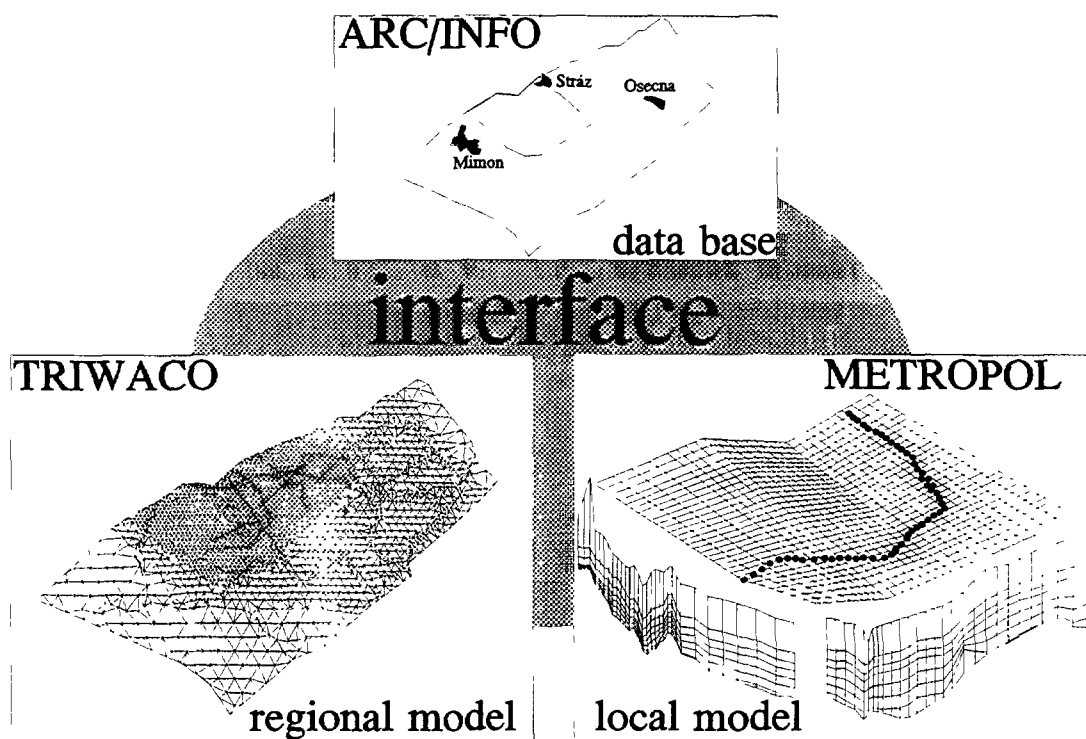


FIG. 4. Contaminant Transport Information System (CTIS).

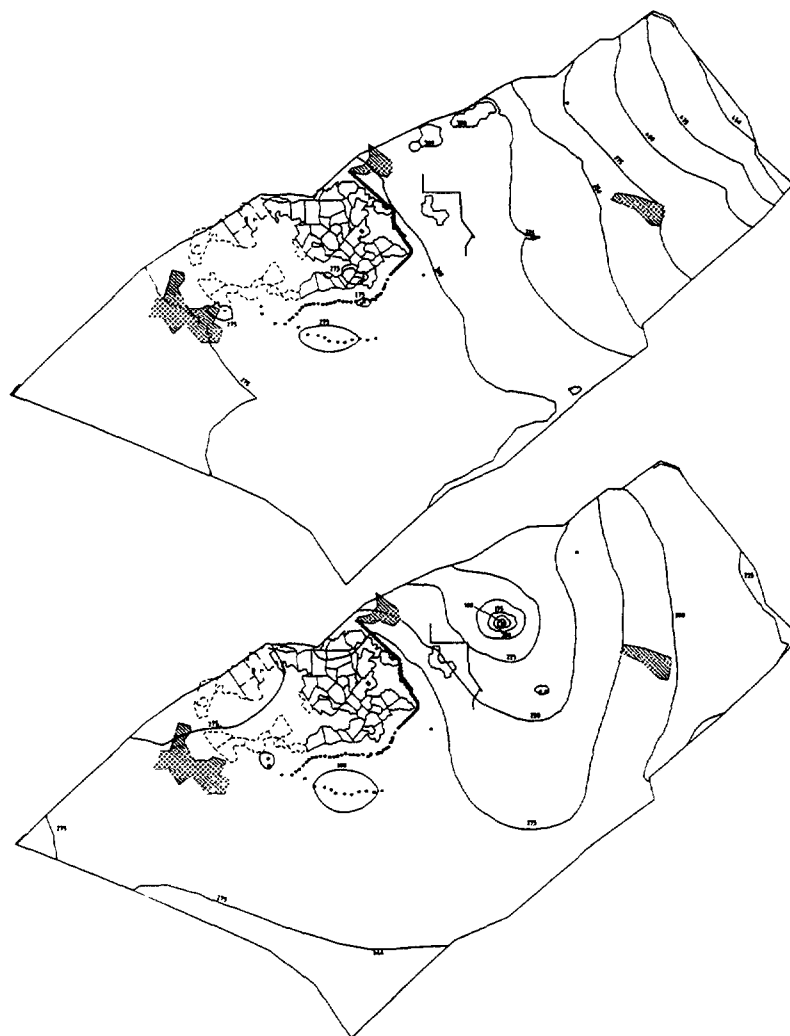


FIG. 5. Calculated piezometric heads (TRIWACO) of the upper Turonian aquifer (top) and lower Cenomanian aquifer (bottom).

6. CONCLUSIONS AND EVALUATION

The case study shows that the Contamination Transport Information System ensures a solid base for risk analysis of remediation strategies that will have to be carried out for the Stráž pod Ralskem uranium mining area. Combination of model results with other data in the GIS database allows one to judge alternative remediation scenarios easily and fairly on their consequences and effectiveness. Thus intercomparison of such scenarios has become possible.

The necessity of environmental management in uranium mining and milling areas is also clear from the EC financed project 'Remediation concepts for the uranium mining operations in CEEC' [4]. Involved are nine countries in Central and Eastern Europe that carry out (or have carried out) mining and/or milling activities. The project is carried by URANERZ, C&E and IWACO. In the first year of the project an inventory of the existing situation will be carried out, the data will be stored in a GIS.

Conclusion: The integration of uranium exploration data in GIS and models creates a powerful tool for facilitating the decision support process, not only for uranium exploration purposes, but also for environmental management.

REFERENCES

- [1] BURROUGH, P.A., Principles of Geographical Information Systems for Land Resources Assessment. Clarendon press, Oxford (1986).
- [2] IWACO B.V., Development of a validated computer-based information system for aquifer rehabilitation at the uranium mining area "Stráž pod Ralskem-Hamr", North-East Bohemia, Czech Republic. Final report. Rotterdam, The Netherlands (October, 1994).
- [3] ZAADNOORDIJK, W.Z., TUSVELD, M.C.L., SLOT, A.F.M., FIEDLER, J., Combined regional and local modelling for aquifer remediation at an uranium mining site in the Czech Republic. Groundwater Quality: Remediation and Protection (Proceedings of the Prague conference, May 1995), pp 391-400. IAH Publications No. 225 (May, 1995).
- [4] EC-PHARE. Remediation Concepts for the Uranium Mining Operations in CEEC, Terms of Reference, PA12, Revision 3 (December 1995).

**NEXT PAGE(S)
left BLANK**



SOME PRACTICAL ASPECTS OF COMPUTER PROCESSING OF URANIUM EXPLORATION DATA FOR ENVIRONMENTAL PURPOSES

V. ŠTRUMBERGER, M. MILOJEVIĆ
Geoinstitut

A. ŠTRUMBERGER
Faculty of Mining and Geology
Belgrade, Yugoslavia

Abstract

During a period of over 40 years an enormous amount of U exploration data has been accumulated. If specific requirements are met, this data can be reprocessed and used very efficiently for environmental purposes. Many IAEA Member States, where U exploration was carried out, are interested in using the data they possess for such purposes. The major difference is that the data is now intended for institutions that are engaged in environmental studies and not in uranium exploration. Moreover, the general interest of the public cannot be neglected. Therefore the data has to be presented with great care where different types of maps are probably one of the most significant forms. An important segment of the whole process is certainly computer data processing. Many countries have already carried out this process with the use of specialized software and modern hardware. Unfortunately many IAEA Member States — government institutions engaged in uranium exploration — are not equipped with the adequate (expensive) hardware and software and very often do not have the funds for this. The presented paper deals with some practical aspects of computer data processing from the initial data input (database) phase to the production of maps but with "general purpose" software that can be acquired with a minimum of expenses. It is worth mentioning that the IAEA has supplied many Member States with software and hardware that can be used immediately for this purpose. Preliminary processing and presentation of uranium exploration data for environmental purposes, with the available hardware and software, would certainly be of great benefit to the corresponding institutions and the whole country.

1. INTRODUCTION

Some activities of IAEA in the last few years have been focused on the application of the existing uranium exploration data in environmental studies [1]. Papers published from the Technical Committee Meeting held in Vienna [2] presented many cases of how uranium exploration data can be successfully reprocessed and used for environmental purposes. Among other things, several papers [3,4,5,6,7] include very sophisticated colour maps. All these maps were produced with the use of specialized software. This paper deals with the possibilities of computer processing of data with "general" purpose software which is less expensive. Emphasis is on the production of maps. The main intention is to present different possibilities and not advertise commercial software/hardware. Therefore no producers or brands are cited. The only exemptions are DOS and Windows, operating systems and some software that can be obtained for the price of a diskette.

2. PHILOSOPHY

Many countries throughout the world where uranium exploration was carried out are interested in reprocessing the data and using it for environmental purposes. Beside selection and reprocessing of the data for environmental purposes, each country in the end will be faced with the problem of computer processing. If it possesses the adequate hardware and software then this is a relatively easy process. However, if it does not have these possibilities it will face a problem that can be solved in several ways:

- Purchase all the necessary hardware and software and train the staff to use it. Unfortunately many countries or government organizations and institutions do not have the adequate funds

for such purposes. This is, beside being expensive in the short run, a process that can last several years.

- Give the data to some other country or institution to process it for them. It should be pointed out that many countries or institutions will be unwilling to give the data to some other party to process. There are two basic reasons:
 - a) In some countries the data is still considered as confidential;
 - b) financial reasons.
- Request assistance from the IAEA; which is not always successful.
- Do nothing ! The worst solution.
- Process the data with the available software and hardware and eventual minimal purchase of both.

During the last decade IAEA has equipped many Member States with hardware (PC computers, printers, plotters, digitizers, etc.) and software (database, mapping, digitizing, etc.) for computer processing of uranium exploration data. What is more essential it has trained the local staff to use it efficiently. The hardware, software and very valuable knowledge can be used for the (initial) reprocessing of the uranium exploration data for environmental purposes. It can be presumed that once these results are presented it would be much easier to obtain funds for further work in the field of environmental protection.

In general, the necessary steps for the use of uranium exploration data for environmental purposes can be divided into two phases:

1st phase: preparation of the data, which includes:

- selection of the data suitable for further processing
- standardization, back-calibration, e.g. carry out all the necessary steps to make the radiometric data suitable for environmental purposes

2nd phase: computer data processing:

- database management
- statistical data analysis
- production of different "environmental" maps with or without a base map.

3. DATABASE MANAGEMENT

The corner stone of any serious computer data processing is a well organized database. Beside coordinates, radiometric and geochemical data, other relevant information (such as Rn in soil, geology, soil type, etc.) should be included.

In general the following steps are required:

- formation of a new database, or
- upgrading of the existing database to meet the current demands
- input of the data, very often accompanied with digitizing of the coordinates,
- import of data from other sources (data files on diskettes, tapes, etc.)

A large variety of database software for mini — mainframe and PC computers is available on the market. The prices for the two former are many magnitudes higher than for the PCs. The complexity of database software for large computers will not be elaborated here. Today's database software for Windows is much more powerful than the DOS versions from just a few years ago. One of the main advantages is the enormous difference in speed. This means that much larger sets (with the adequate hard disk capacity) of data can be processed, such as airborne survey data. Beside being faster, Windows software is much more flexible and "user-friendly", enabling relatively easy formation of a complex database. One additional advantage is that the data can be transferred directly to other software (spreadsheet, statistical, mapping, etc.) for further processing. This software can also be used to perform all the necessary mathematical transformation to convert the radiometric data (cps, ppm, etc.) into the adequate radiation units.

4. DIGITIZING SOFTWARE

One of the crucial steps in the formation of a database is the measurement and input of coordinate data. Digitizing of the coordinates is important in cases of random sampling — measurements, like regional gamma-ray spectrometry, etc. Software that can be used for digitizing the coordinates is numerous and in most cases inexpensive. Prices range from the price of a diskette¹ to several hundred dollars for commercial software. Several techniques of digitizing — data input can be used. This will depend on whether the data is to be transferred to a database or used directly for further processing. If the resulting ASCII data file is well organized the data can be converted — (imported) into a database file and linked with the main database that contains the rest of the (analytical, geological, etc.) data.

5. STATISTICAL DATA PROCESSING

This phase represents an important segment of the whole process. Software for statistical data analysis is numerous and ranges from share-ware to commercial software costing up to approximately US \$1000. However, one very important fact has to be emphasized. Some of the very "sophisticated" commercial software can process only a limited amount of data (approximately in the range of several thousand rows). If matrix operations are needed (for correlation matrices, etc.) the situation is even worse. This automatically excludes processing larger data sets such as car-borne and airborne. As a substitute, database software can be used to determine the basic statistical parameters such as the mean, standard deviation, etc.

6. PRODUCTION OF MAPS

Maps containing information on the radioactivity levels, content-distribution of (toxic) elements, etc. in certain regions are probably the ultimate goal in this whole procedure. Uranium exploration geologists have been engaged in studying the behavior, distribution and migration of uranium, thorium and other elements in nature and representing these phenomena in the form of maps. It is not to pretentious to claim that geologists are the most qualified in this field. Physicist, chemists and other scientists generally engaged in laboratory work (or better to say constricted to a laboratory environment) simply lack the experience for this.

It should be made clear that now these maps and data in general are not intended (only) for geologists. The major difference is that the data will also be used by institutions that are engaged in environmental studies and not uranium (geological) exploration. Also, these maps are now of general public interest and if not prepared and interpreted adequately they can cause considerable

¹ The USGS program GSDXY [8] can be obtained very easily for the price of a diskette and is quite sufficient for this purpose.

misunderstandings or even problems. The impact (social, economical, etc.) of these maps has to be taken into account. This is not directly the problem of the geologist, it is more an obligation that the maps are correct in all aspects and understandable even to the layman..

Most of the software for drawing maps uses a gridding technique. Gridding produces a regularly spaced array of Z values from (in most cases) irregularly spaced XYZ data. Contour map plots require the regular distribution of data points in grid files. The term "irregularly spaced" implies that the points are randomly distributed over the extent of the map area meaning that the distance between data points is not consistent over the map. When the XYZ data is randomly spaced over the map area, there are many "holes" in the distribution of data points. Gridding fills in the holes by extrapolating or interpolating Z values in those locations where no data exists. Large areas without data can be excluded with the use of blanking files. These files can be prepared with a digitizer.

The filling of holes can create considerable problems. Special care has to be taken for large scale maps covering areas where the geology, contents of U, Th, K and other elements vary considerably. A hypothetical case is presented on figures 1 and 2. The area is represented with two different rock units that have a considerable difference in the U, Th and K content, resulting in a significant difference in the total radioactivity. This fact is well known to all geologist, but is this clear to other scientists and to the public? A map created without the intervention of a geologist is shown in Fig. 1

Because of the random and insufficient sampling density the high level contours "protrude" into the area with low radioactivity. This phenomenon of poor "resolution" of the computer techniques is something normal to the geologists. Rarely did he bother to carry out further surveying in the (contour) zones over a rock unit for which he knows that is not uranium bearing. However in the case of environmental maps this problem is important. The map in Fig. 2 is based on the same data but with the intervention of a geologist. The data was processes two times: once for the high radioactivity rock and the second time for the low one. The maps were then joined and printed or plotted as one. Clearly the map in Fig. 2 is a much more realistic presentation of the radioactivity of the region.

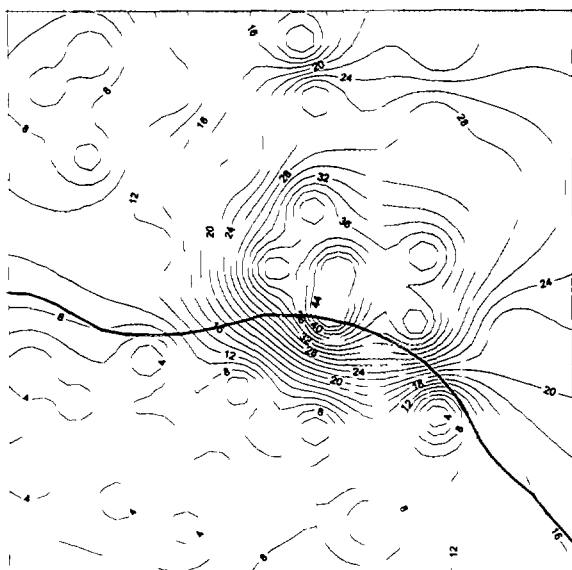


Figure 1. Map created without the intervention of a geologist Units arbitrary

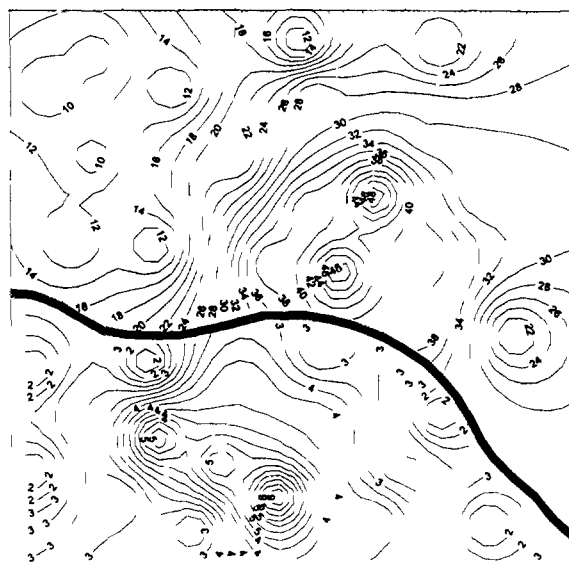


Figure 2. Map created with the intervention of a geologist. Units arbitrary

A very important detail of all "ecological" maps is a base map with different geographical details such as roads, rivers, buildings, etc. A base map can be prepared with a digitizer and CAD software. The price of commercial software ranges from several hundred to several thousand dollars. The less expensive ones are quite sufficient. A base map can also be prepared with the use of a scanner. In general this will be limited to size A4 because of the high price of larger scanners.

Once the contour and base map have been prepared they can be exported and combined together with graphical processing software. The price of this software is in the range of several hundred dollars. In this phase different details can be added, such as text, symbols, etc. Depending on the mode of output (printer or plotter) the whole preparation procedure will be somewhat different.

The final process — a hard copy of the map — can be produced in two ways: printing (with a B/W or colour printer) or plotting (single to multi pen plotter). When using a B/W printer the contour zones can be "coloured" in different shades of gray. Tests have shown that gray shading with a dot matrix printer is not very applicable because of the small number of shades (zones) that can be distinguished by the human eye. Additionally, a large part of the base map details can be lost (overprinted). Also this type of map is not very pleasing to the observer. The use of a B/W ink-jet, bubble-jet or laser printers somewhat increases the quality of the map and the possible number of gray tones. Best results are achieved with a (fairly inexpensive) colour ink-jet printer. The contours can be coloured without a loss of the base map information. When using a printer the maximum size that can be printed is A3. If larger maps are needed it is possible to print the map in segments and join them together.

Beside printing the maps can be plotted. In case of multi pen plotters the contour lines can be in different colours. Filling of the contours is possible but an enormous amount of plotting time and pens is needed. The size of the plotted maps will depend on the size (and price) of the plotter which varies from A4 to A0. If the (combined) map is prepared for plotting then the base map of the area can be included by plotting in two phases: first the contour map and then, without removing the paper, the base map (or vice versa). The shift of the plotter is so small (generally less than 0.5 mm) that it is not noticeable.

8. PRACTICAL EXAMPLE

A volcanic massif in Serbia was covered with a regional gamma ray spectrometric and geochemical survey. The surveyed area was approximately 200 km². A total of 110 gamma-ray spectrometric measurements were made. For the geochemical survey 390 stream sediment samples and 380 heavy mineral samples were collected and spectrochemically analyzed for 30 elements. All the data was already available in ASCII format but without coordinates. This data was chosen as suitable for further processing.

The procedures for all three maps were practically the same:

- Database software was used to prepare the database which consisted of tables for the coordinate data, gamma-ray spectrometry measurements, analytical data for the stream sediments and a table for the heavy mineral analyses. All the analytical data was imported into the database files. The eU, eTh and K content were converted into exposure rate [1].
- The coordinates of the sampling points were digitized. The resulting ASCII file was imported into the database file for coordinates and linked with the adequate table(s) in the database. The sample number was used as the key field for linking.
- The base map (major streams and roads) was digitized with the use of a CAD program. The USGS program GSDRAW [9] could also have been used for this purpose.

- The borders of the area were digitized with GSDXY [8] and prepared as a "blanking file".
- The selected data (with a query) was transferred from the database to an ASCII file.
- With mapping software three different versions (files) were prepared:
 - a. contour (B/W) map for a dot matrix printer
 - b. colour contour map for plotting
 - c. filled contour map for a colour ink-jet printer.
- Statistical data analysis was carried out and a distribution histogram was prepared.
- All three maps and the histogram file were exported into a graphical program and combined with the base map.
- Adjustments of the colour scale were carried out on the colour contour map and histogram.
- The maps were printed — plotted.

Three versions of the resulting maps are presented in Figs 3, 4 and 5. All maps were produced with the same PC computer and software, only the hard copy device was changed.

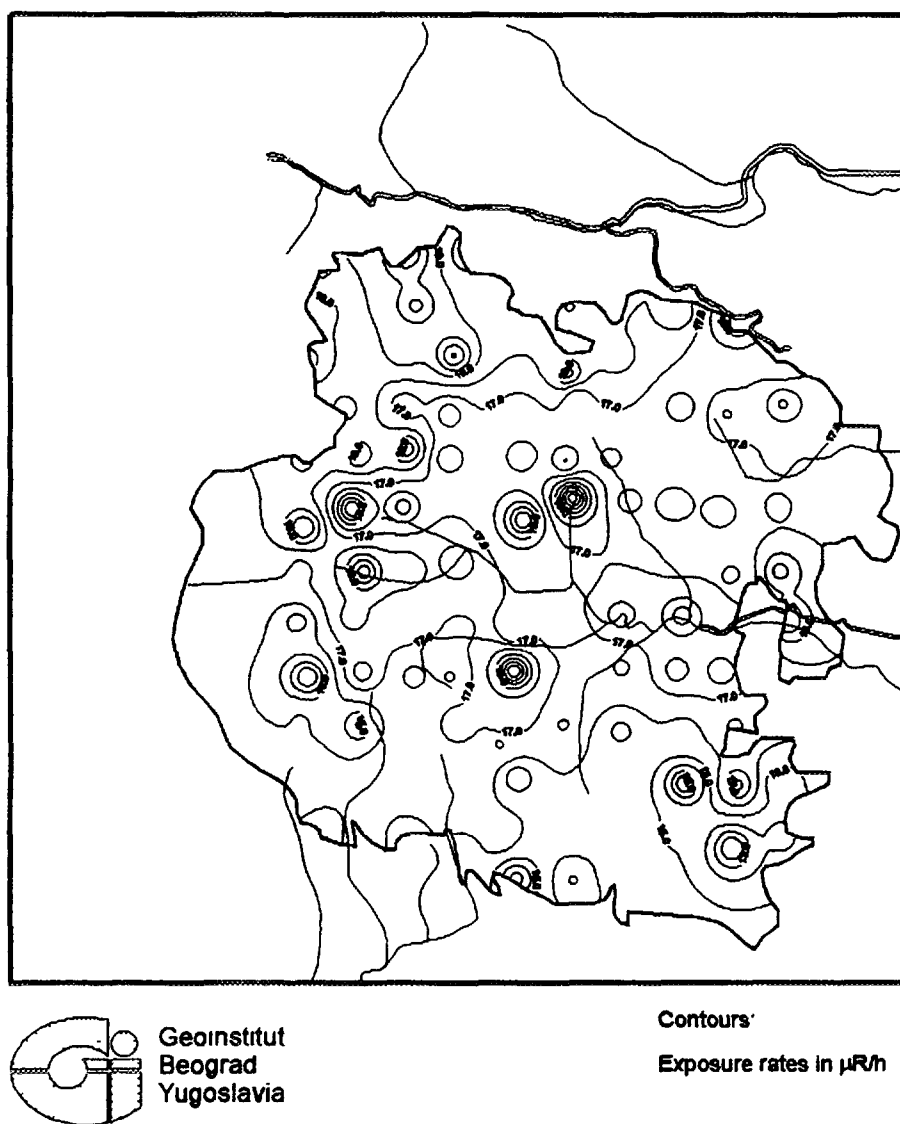
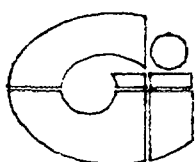
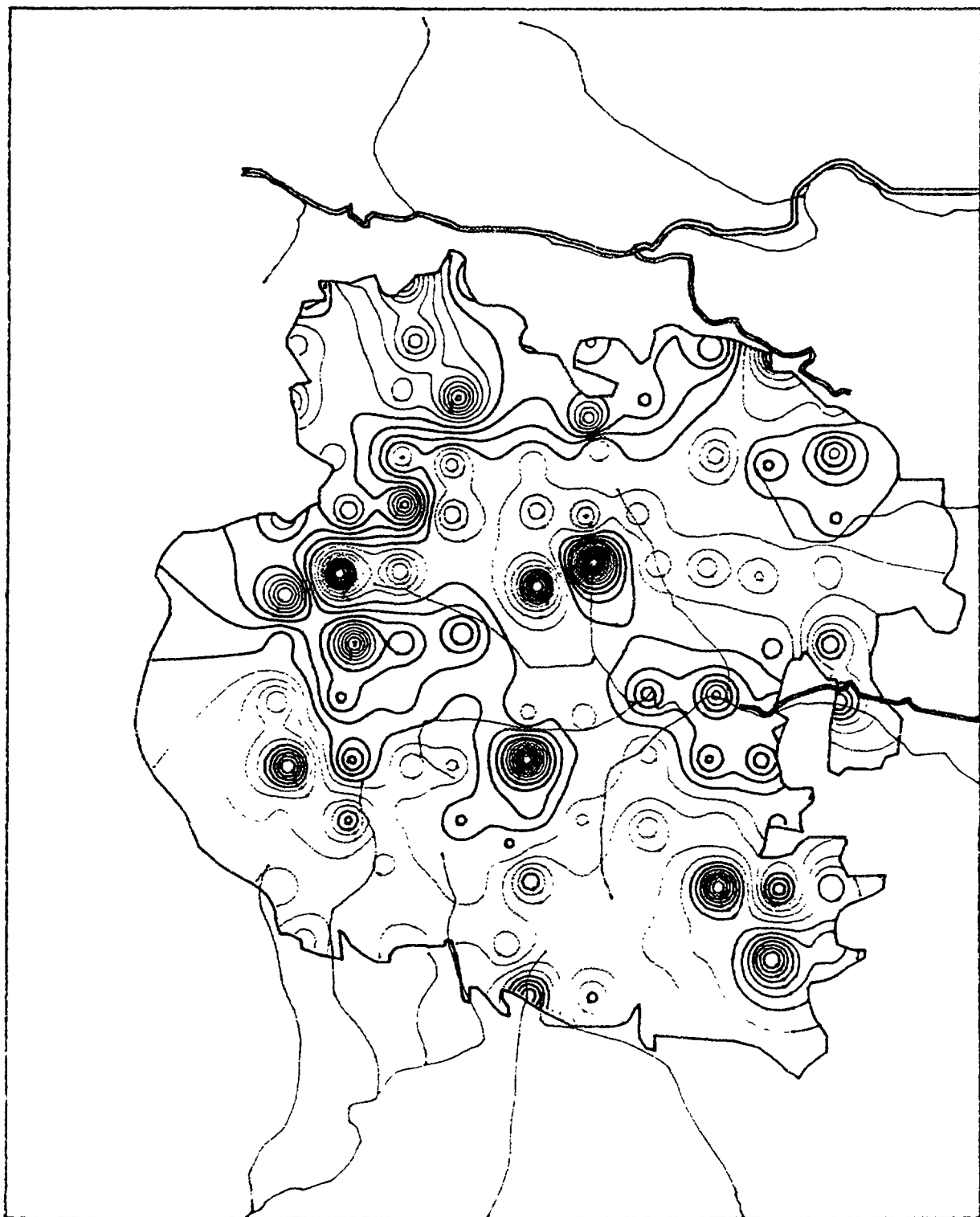


FIG 3. Map printed with a nine pin dot matrix printer.

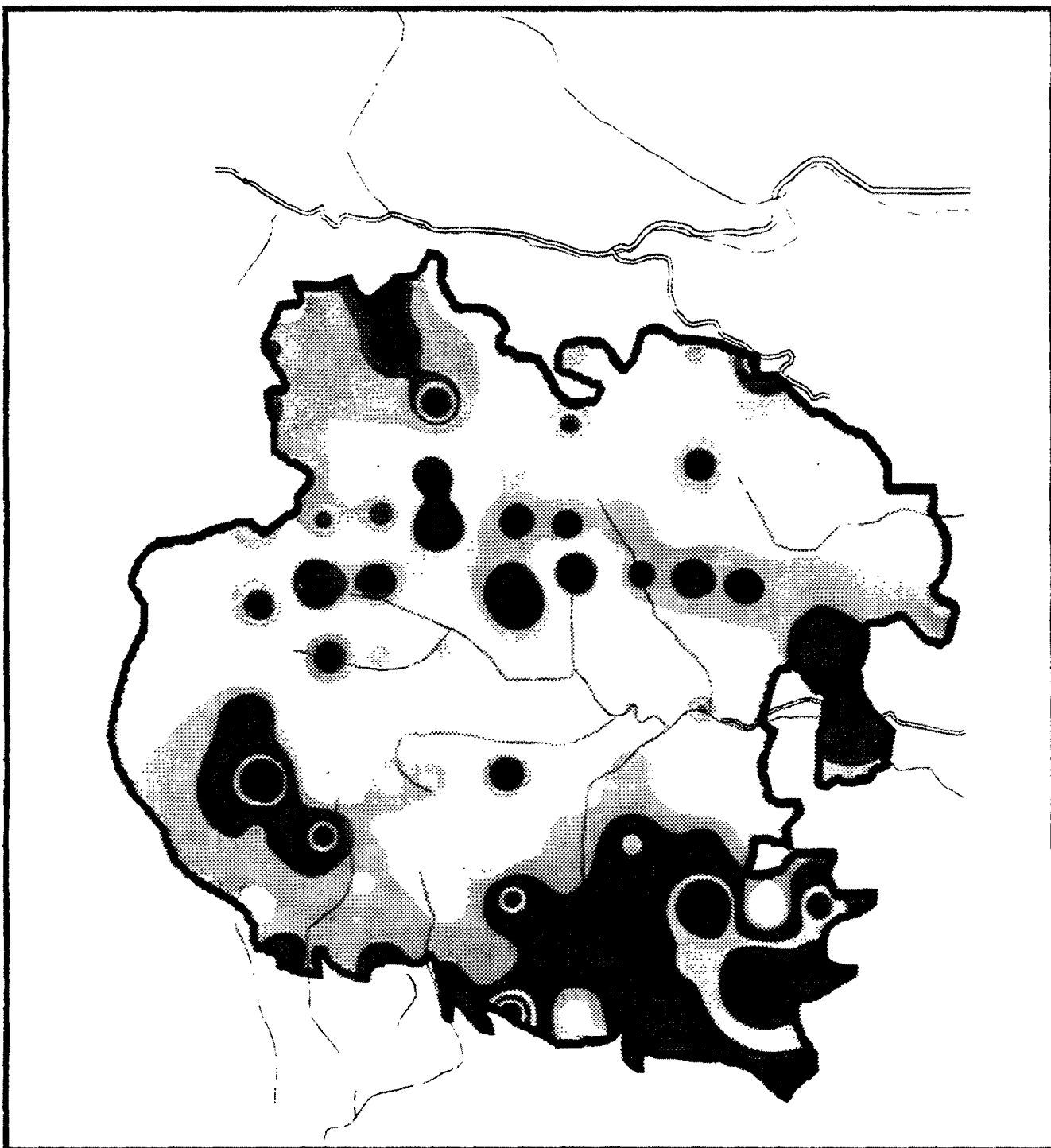


**Geoinstitut
Beograd**

Exposure rates in $\mu R/h$

11 - 13	—
13 - 15	—
15 - 17	—
17 - 19	—
> 19	—

FIG. 4. Map plotted with a multi pen plotter.



Geoinstitut
Beograd
Yugoslavia

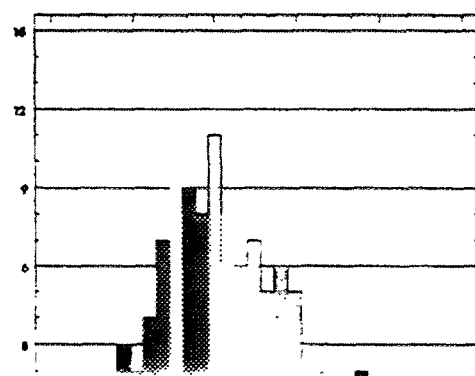


FIG. 5. Map printed with an ink jet colour printer.

For the map in Fig. 3 a nine pin dot matrix printer was used to produce a contour map. It is obvious that the map is of poor quality. For the geologist this is often more than sufficient, but certainly not for public presentation.

The map in Fig. 4 was plotted with a multi pen plotter. It is obvious that the quality of the map is much better for public and other purposes.

Finally, the map in Fig. 5 was produced with a colour ink-jet printer. Evidently this map is, considering the quality, esthetics impact and clearness, very close to the maps produced with much more expensive software and hardware².

9. CONCLUSIONS

As demonstrated, it is possible to process uranium exploration data for environmental purposes with software and hardware that is relatively inexpensive and easy to use. What is more important many IAEA Member States already possess most of the necessary hardware and software. The speed of processing will depend on the hardware, the complexity of data processing and map drawing on the software, but the final quality of the maps will depend on the type (price) of the printer or plotter. It should be pointed out that in most cases the only additional investment for producing colour maps is a relatively inexpensive ink-jet colour printer.

This is why the IAEA should encourage Member States — government organizations — who are not sufficiently equipped with “modern” computer data processing to start this process with the available hardware and software. Preliminary processing and presentation of uranium exploration data for environmental purposes would certainly be of great benefit for the corresponding institutions and the whole country.

REFERENCES

- [1] INTERNATIONAL ATOMIC ENERGY AGENCY, The use of gamma ray data to define the natural radiation environment, IAEA-TECDOC-566, IAEA, Vienna (1990).
- [2] INTERNATIONAL ATOMIC ENERGY AGENCY, Application of uranium exploration data and techniques in environmental studies, IAEA-TECDOC-827, IAEA, Vienna, (1995).
- [3] DARNLEY A.G., Uranium exploration data, International Geochemical Mapping and the Environment, Application of uranium exploration data and techniques in environmental studies, IAEA-TECDOC-827, IAEA, Vienna (1995).
- [4] GRASTY R.L. Environmental monitoring by airborne gamma ray spectrometry, experience at the Geological Survey of Canada, Application of uranium exploration data and techniques in environmental studies, IAEA-TECDOC-827, IAEA, Vienna (1995).
- [5] TORRES L.M., GRASTY R.L., The natural radioactivity map of Portugal, Application of uranium exploration data and techniques in environmental studies, IAEA-TECDOC-827, IAEA, Vienna (1995).

² Note: the exposure rate map and the corresponding scale in [5] is from 1 to 25, at the same time the map and colour scale in [6] is from 0.4 to 14.8 $\mu\text{R/h}$. The problem here is that the colour scale in these two maps do not correspond to the same exposure rate values. As an example in the first map the yellow tones represent exposure rates from 11 to 14 and in the second map from 6 to 7.2 $\mu\text{R/h}$. This makes comparison of different maps difficult and could be misleading if the observer does not pay attention to the colour scale. A basic recommendation here is that IAEA should consider introduction of a standard colour scale for exposure rates (and other measurements, units) which would be used by all member states.

- [6] ANDJELOV, M., TOMSIC, J., PEČNIK, M., Natural background radioactivities and geochemical map of Slovenia, Application of uranium exploration data and techniques in environmental studies, IAEA-TECDOC-827, IAEA, Vienna (1995).
- [7] STRZELECKI, R., WOLKOWICZ, S., SZEWCZYK, J., LEWANDOWSKI, P., Use of gamma ray spectrometric survey for radioecological mapping in Poland, Application of uranium exploration data and techniques in environmental studies, IAEA-TECDOC-827, IAEA, Vienna (1995).
- [8] SELNER, G.I., SMITH, C.L., TAYOR, R.B., GSDIG Version 2.0, a program to determine latitude/longitude coordinates, and GSDXY version 1.0, a computer program to determine X, Y coordinates using a microcomputer (IBM PC or compatible) and digitizer, United States Department of the Interior, Geological Survey, Open file report 88-0428-A and 88-0428-B.
- [9] SELNER, G.I., TAYOR, R.B., GSDRAW and GSMAP system version 6.0-Graphics programs and utility programs for the IBM PC and compatible microcomputers to assist in compilation and publication of geological maps and illustrations. United States Department of the Interior, Geological Survey, Open file report 89-0307-A and 89-0373-B.



URANIUM CONCENTRATION IN BUILDING MATERIALS USED IN THE CENTRAL REGION OF EGYPT

R.H. HIGGY, M.S. EL-TAHAWY

National Centre for Nuclear Safety and Radiation Control,
Atomic Energy Authority,
Nasr City, Cairo,
Egypt

A. GHODS

Chemistry Unit,
IAEA Laboratories,
Seibersdorf

Abstract

Within a radiological survey of the building materials used in the urban dwellings in the central region of Egypt, the uranium concentration in 80 representative samples of raw and fabricated building materials are determined using laser fluorimetry technique. For 40 samples from the studied raw building materials of sand, gravel, gypsum, lime-stone, granite and marble the determined uranium concentration values range between 0.3 and 3.6 ppm for all these samples except for one type of granite having the corresponding value of 7.8 ppm. For 37 samples from studied fabricated building materials of normal cement, clay brick, sand brick, tiles and ceramic plates the determined uranium concentration values range from 0.5 to 3.4 ppm. The corresponding values for three types of iron cement are 3.1, 6.1 and 9.3 ppm. The radium-226 content (of the uranium-238 series) in the same samples was determined using high resolution gamma-ray spectrometers based on HP Ge-detectors. The data obtained by the two techniques are in good agreement for the majority of the studied samples.

INTRODUCTION

A significant part of the total dose rate exposure of the public is due to the indoor exposure which is mainly originated from the radioactive nuclides of the building materials. The radiation exposure of the public can be noticeably increased by using building materials with above normal levels of specific radioactivity. 84% of the annual effective dose to the world population is due to natural radiation and 57% of this exposure is due to ^{238}U series [1].

For the Central Cairo region, where there are more than 20 millions of habitants corresponding to about 33% of the whole population of Egypt, a detailed study of building materials used in the urban dwellings is carried out in the Central Laboratory for Environmental Radiation Measurements, Intercomparison and Training (CLERMIT) of the National Centre of Nuclear Safety and Radiation Control (NCNSRC), Atomic Energy Authority (AEA). 177 of raw and fabricated building materials used in the central region of Egypt were prepared and analysed using γ -spectroscopy technique [2]. The map of this region is given in Fig. 1, where the symbols in frames correspond to the sampling locations of raw building materials (for coding legend see Tables I and II).

In this work, the uranium concentration in some of the same samples were determined using laser fluorimetry (LF). For uranium concentration measurements, laser fluorimetry is quick, simple, reliable and accurate. Under ultraviolet excitation uranyl salts emit a green luminescence. The emission spectrum is quiet characteristic with three peaks at 414, 516 and 540 nm. The luminescence can be measured quantitatively by a suitable photodetector. A more complete description of the principles of LF technique and its applications is given [3-5].

Eighty samples of the above mentioned 177 samples covering all types of raw and fabricated building materials were analysed using LF technique for direct determination of the total uranium concentrations in these samples.

EXPERIMENTAL WORK

Sample Collection

Fourty samples of raw building materials were collected from different quarries in the Cairo region (Fig. 1) and commercial companies. Also, 40 samples of building products were collected from the largest Egyptian factories. The classification of these raw materials and industrial building products are given in Tables I and II.

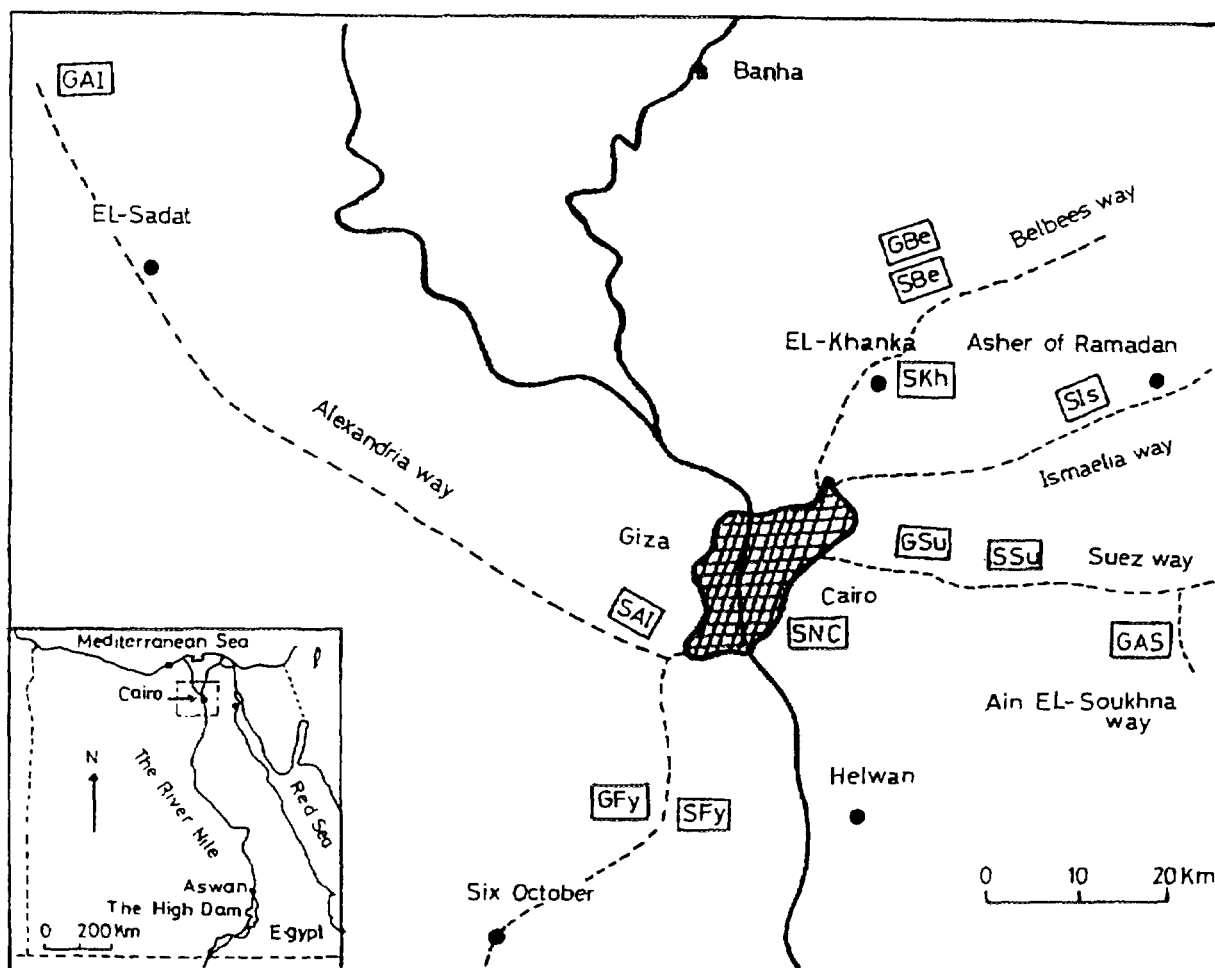


FIG. 1. Map of central region of Egypt.

Sample preparation for laser fluorimetry

Samples of 200–250 mg were ashed in a computerized oven in which the temperature is adjusted to rise from 24°C (room temp.) in 120 min. to 350°C then in 90 min. to 600°C. The residue, after fuming with hydrofluoric acid and nitric acid were taken up in $\text{Ca}(\text{NO}_3)_2$ salting solution, and the uranium was extracted with methyl-isobutyl-ketone (MIBK). After the stripping of uranium from MIBK solution into 0.001 M HNO_3 , it is ready for analysis. This chemical procedure is done according to that developed by Ghods [3–5] and shown in Fig. 2.

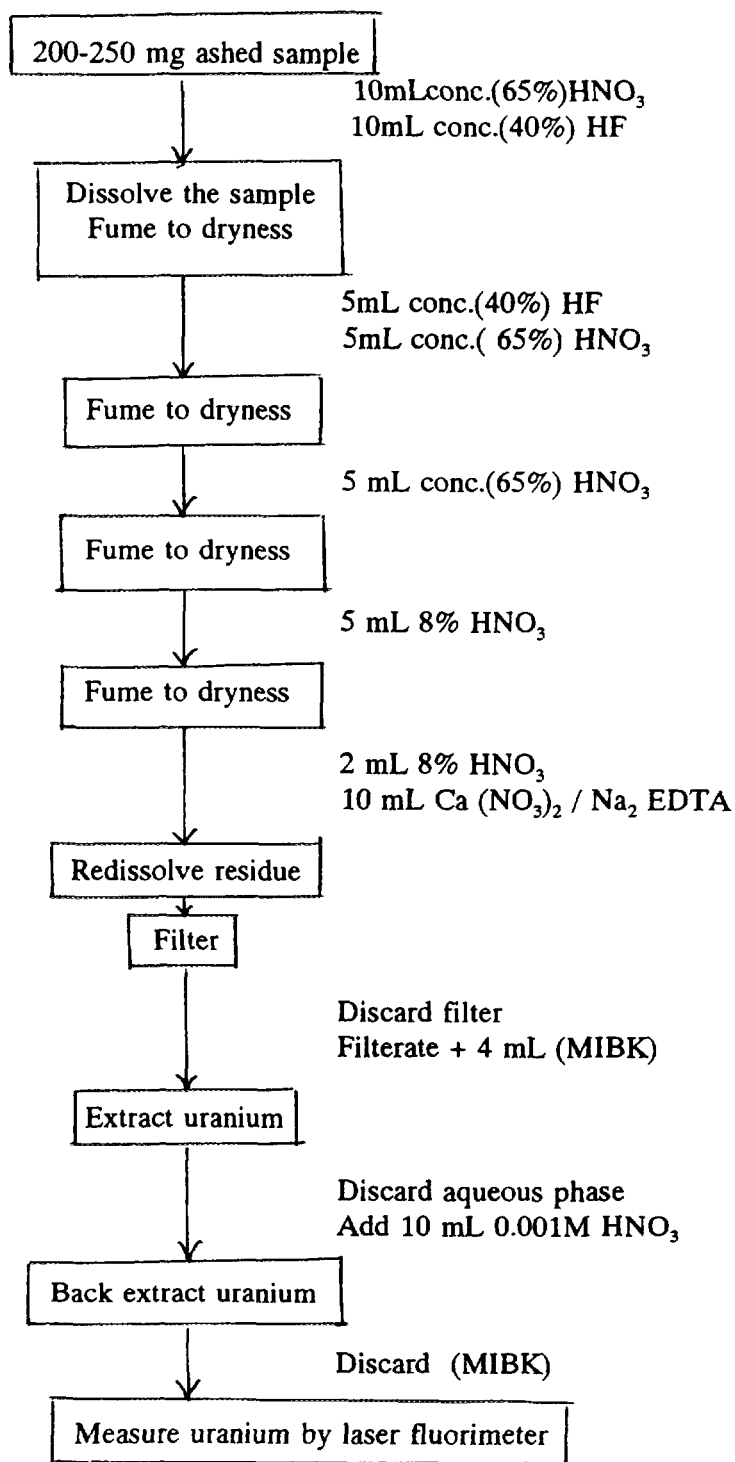


FIG. 2. Chemical procedure for uranium separation.

Laser fluorimetry measurement

The Scintrex UA-3 uranium analyser was used to measure the uranium concentration in the samples. It has a lower detection limit of 0.05 ppb uranium, measurement accuracy +15% at 1 ppb. The UA-3 procedure involves the addition of a buffered agent called Fluran (sodium pyrophosphate, sodium dihydrogen phosphate).

The instrument is calibrated using 0.01mL of uranium standard (1 mg/mL) combining it with 4.99 mL of 0.001 M HNO₃ in the vial. The sample size was 5 to 6 ml of aqueous solution per determination.

The uranium content is determined by measuring the fluorescent yield from the standard D_{st} and the sample D; and the uranium concentration in the sample U is obtained as:

$$U = U_{st} \frac{D}{D_{st}}$$

where U_{st} is the uranium concentration in the standard.

RESULTS AND DISCUSSION

In Tables III–XIV the uranium concentration, obtained by Laser Fluorimetry technique, LF, (in ppm and Bq.kg⁻¹) compared with those obtained by Gamma Spectroscopy technique, GS, (in Bq.kg⁻¹), for the building material samples are given. The maximum and minimum values of concentrations are printed in bold type. The average values for the samples are given. The difference between the two techniques indicates an overall average of 1.2 expressed in terms of the discrepancy of GS analysis from LF analysis.

The uranium concentrations for raw building materials range between 0.1–0.8 ppm (1.7–21.7 Bq.kg⁻¹ dry weight) except in granite samples; it ranges between 0.4–7.8 ppm (4.4–96.3 Bq.kg⁻¹ dry weight); while for industrial building products, the uranium concentrations range between 0.53.4 ppm (5.6–42.1 Bq.kg⁻¹ dry weight).

The data obtained by the two techniques are in good agreement within the experimental error for most of the samples except for ceramic. This agreement satisfies the assumption of secular equilibrium between ²³⁸U, ²²⁶Ra and their further progenies. For the case of ceramic the difference in uranium concentration values obtained by the two techniques may be related to the disequilibrium between ²³⁸U and ²²⁶Ra appeared during the thermal and chemical treatment of the technological processes of ceramic fabrication. This aspect has to be subject of further investigations.

The obtained, in this work, values of uranium concentration are all in the range of typical world values adapted for building materials [1] which is 50 Bq.kg⁻¹ (about 4 ppm) for the uranium concentrations. The exceptions are one type of granite (with uranium concentration 7.8 ppm), two types of iron cement (6.1 and 9.3 ppm) and one type of brick (4.2 ppm).

TABLE I. CLASSIFICATION AND CODING LEGEND OF RAW BUILDING MATERIAL SAMPLES

Sample Code	Description
SSu1-4,11	Sand samples collected from different quarries around the Suez way at distances up to 30 km from Cairo.
SNC2	Sand sample from a quarry in the north-east region of Nasr-City.
SBe3	Sand sample from a quarry 25-35 km from Cairo around Belbees way.
SIs1	Sand sample from a quarry near the 50 km mark of the Ismaelia way.
SFy1	Sand sample from a quarry in Abu-Dahshoor at 20 km on Fayoom way.
SA11	Sand from a quarry on desert Alexandria way near the Pyramids.
GAS6,8	Gravel samples collected from different quarries around Ain-El-Soukhna way 37-120 km from Cairo.
GSu2	Gravel sample from a quarry around Suez way at distances up to 30 km from Cairo.
GBe1	Gravel from a quarry around Belbees way 25-35 km from Cairo.
GFy3,4	Gravel samples from different quarries 35-45 km from Cairo around Fayoom way.
GA11	Gravel sample from a quarry on Alexandria way 100 km from Giza.
GM1	Samples of Normal gypsum from Misr-Kwait company (Jepsa).
GD2,3	Samples of Balah and Star of Sinai gypsum respectively, from the "Distribution Centre of Gypsum" company.
GJ	Sample of gypsum packed in Jamco factory.
LS2,4,5,6	Samples of lime-stone collected from different workshops from distribution centre of lime-stone in Gayara at the south-east of Cairo.
Gr1-8	Samples of granite (from quarries located at the south and north-east regions of Egypt) collected from different companies of granite in Cairo.
Ma2,3,5,8,9,13,14	Samples of marble (from quarries located at the south and north-east regions of Egypt) collected from different companies of marble in Cairo.

TABLE II. CLASSIFICATION AND CODING LEGEND OF INDUSTRIAL BUILDING MATERIAL SAMPLES

Sample Code	Description
CH1-3	Samples of Ordinary, Karnak and White cement respectively, from Helwan factory.
CT1	Sample of Ordinary cement from Torah factory.
CS1	Sample of Ordinary cement from Suez factory.
CKO	Sample of Ordinary cement from Kawmia factory.
CKt	Sample of Ordinary cement from Katamia factory.
CHI,CTI,CKI	Samples of Iron cement from Helwan, Torah and Kawmia factories.
CIB1,5,8,10,11,16	Samples of clay bricks samples from different factories in Cairo, Helwan, Giza, Banha, Asher of Ramadan, Six October and El-Sadat.
CIB20	Sample of a special kind of clay brick for decoration called Sornaga brick fabricated from soil transfered from Aswan region, collected from El-Haram factory in Giza.
CIB21	Sample of a special kind of clay brick called LECA fabricated from light weight expanded clay aggregates.
CeB1,2,7	Samples of cement bricks from different factories in Cairo, Helwan, Giza, Asher of Ramadan, Six October and El-Sadat.
SB1	Sample of sand brick collected from Nasr City factory.
SB4	Sample of sand brick from Six October factory (Senohy).
SB6	Sample of sand brick from Arabia factory.
SB8	Sample of sand brick from Asher of Ramadan factory.
TH5,TH6	Samples of tiles from Hassan Alaam factory under the names: Breshia and Asmanty (cement) respectively.
TS4,TS5	Samples of tiles from El-Shark El-Awsat factory under the names: White Alaay and Asmanty (cement) respectively.
TNC1,TNC2	Samples of tiles from Nasr-City factory under the names: Petchinoand Alabaster1 respectively.
TR5	Sample of tile from Asher of Ramadan factory under the name Zaafran.
THG	Sample of tile from Hassan Alaam factory prepared from waste granite.
CrG,CrC,CrL,CrA,CrM,CrAh and CrF	Samples of ceramic tiles from factories of: El-Gawhra, Cleopatra, Lecico, Aracemco, Misr, El-Ahlya and El-Faraana respectively.

TABLE III. URANIUM CONCENTRATION OBTAINED BY LF COMPARED WITH GS FOR SOME SAND SAMPLES

Sample Code	U-conc in ppm(mg/g) ^c using LF ^b technique	U-conc.in Bq.kg ⁻¹ using LF ^b technique	U-activity in Bq.kg ⁻¹ using GS ^c technique	U_{GS} / U_{LF}
SSu1	0.3 ± 0.03	3.7 ± 0.4	4.3 ± 0.2	1.2
SSu3	0.4 ± 0.08	5.0 ± 1.0	6.3 ± 0.3	1.3
SSu4	0.5 ± 0.08	6.2 ± 1.0	6.7 ± 0.3	1.7
SSu11	0.5 ± 0.09	6.2 ± 1.1	9.4 ± 0.4	1.5
SNC2	0.7 ± 0.1	8.7 ± 1.3	6.5 ± 0.3	0.8
SBe3	0.4 ± 0.08	5.0 ± 1.0	4.4 ± 0.3	0.9
SIs1	0.3 ± 0.06	3.7 ± 0.8	4.8 ± 0.2	1.3
SFy1	0.3 ± 0.06	3.7 ± 0.8	8.3 ± 0.4	2.2
SA11	0.4 ± 0.08	5.0 ± 1.0	8.0 ± 0.3	1.6
Average	0.4	5.0	5.8	1.3

^a Laser Fluorimetry ^b Gamma Spectrometry ^c 1ppm = 12.4 Bq.kg⁻¹

TABLE IV. URANIUM CONCENTRATION OBTAINED BY LF COMPARED WITH GS FOR SOME GRAVEL SAMPLES

Sample Code	U-conc.in ppm (mg/g) using LF technique	U-conc.in Bq.kg ⁻¹ using LF technique	U-activity in Bq.kg using GS technique	U_{GS} / U_{LF}
GAS6	0.8 ± 0.2	9.9 ± 2.1	13.5 ± 0.5	1.4
GAS8	0.8 ± 0.1	9.9 ± 1.4	13.3 ± 0.5	1.3
GSu2	0.4 ± 0.1	5.0 ± 1.0	12.4 ± 0.4	2.5
GBe1	0.1 ± 0.04	1.2 ± 0.5	2.6 ± 0.2	2.2
GFy3	0.7 ± 0.1	8.7 ± 1.3	10.4 ± 0.4	1.2
GFy4	0.8 ± 0.1	9.9 ± 1.5	9.9 ± 0.4	
GA11	0.3 ± 0.06	3.7 ± 0.7	4.9 ± 0.3	1.3
Average	0.6	7.4	9.6	1.3

TABLE V. URANIUM CONCENTRATION OBTAINED BY LF COMPARED WITH GS FOR SOME GYPSUM SAMPLES

Sample Code	U-conc.in ppm (mg/g) using LF technique	U-conc.in Bq.kg ⁻¹ using LF technique	U-activity in Bq.kg ⁻¹ using GS technique	U_{GS} / U_{LF}
GD2	0.2 ± 0.03	2.5 ± 0.4	2.0 ± 0.2	0.8
GD3	0.3 ± 0.1	3.7 ± 1.8	3.5 ± 0.2	1.0
GM1	0.1 ± 0.05	1.2 ± 0.6	3.0 ± 0.2	2.5
GJ	0.3 ± 0.07	3.7 ± 0.9	4.3 ± 0.3	1.2
Average	0.2	2.5	3.2	1.3
GK2	1.1 ± 0.2	13.6 ± 2.5	12.8 ± 0.4	0.9

TABLE VI. URANIUM CONCENTRATION OBTAINED BY LF COMPARED WITH GS FOR SOME LIME-STONE SAMPLE

Sample Code	U-conc.in ppm (mg/g) using LF technique	U-conc.in Bq.kg ⁻¹ using LF technique	U-activity in Bq.kg ⁻¹ using GS technique	U_{GS} / U_{LF}
LS2	1.5 ± 0.2	18.6 ± 2.9	13.3 ± 0.5	0.7
LS4	1.2 ± 0.2	14.9 ± 2.5	18.5 ± 0.6	1.2
LS5	1.8 ± 0.3	22.3 ± 3.0	17.3 ± 0.7	0.8
LS6	0.6 ± 0.2	7.4 ± 1.8	9.5 ± 0.4	1.3
Average	18.3	16.1	14.7	0.9

TABLE VII. URANIUM CONCENTRATION OBTAINED BY LF COMPARED WITH GS FOR SOME GRANITE SAMPLES

sample	U-conc.in ppm (mg/g) using LF technique	U-conc.in Bq.kg ⁻¹ using LF technique	U-activity in Bq.kg ⁻¹ using GS technique	U_{GS} / U_{LF}
CIB1	1.3 ± 0.2	16.1 ± 2.5	17.5 ± 0.8	1.1
CIB5	1.7 ± 0.2	21.1 ± 3.0	23.0 ± 0.9	1.1
CIB8	1.9 ± 0.3	23.6 ± 3.6	21.3 ± 0.9	0.9
CIB10	1.3 ± 0.2	16.1 ± 2.7	23.7 ± 0.9	1.5
CIB11	1.4 ± 0.2	17.4 ± 2.7	23.4 ± 0.8	1.3
CIB16	2.1 ± 0.3	26.0 ± 3.3	30.7 ± 1.0	1.2
Average	1.6	19.8	23.3	1.2
CIB20	1.6 ± 0.3	19.8 ± 3.2	19.8 ± 1.1	1.0
CIB21	4.2 ± 0.6	52.1 ± 7.4	54.8 ± 1.6	1.1

TABLE VIII. URANIUM CONCENTRATION OBTAINED BY LF COMPARED WITH GS FOR SOME MARBLE SAMPLES

Samples Code	U-conc.in ppm (mg/g) using LF technique	U-conc.in Bq.kg ⁻¹ using LF technique	U-activity in Bq.kg ⁻¹ using GS technique	U _{GS} / U _{LF}
Ma2	0.4 ± 0.1	5.0 ± 0.9	3.5 ± 0.1	0.7
Ma3	0.3 ± 0.1	3.7 ± 0.8	3.0 ± 0.1	0.8
Ma5	0.1 ± 0.04	1.2 ± 0.6	2.9 ± 0.2	2.4
Ma8	0.9 ± 0.1	11.2 ± 1.5	10.5 ± 0.3	0.9
Ma9	1.2 ± 0.1	14.9 ± 1.8	7.3 ± 0.3	0.5
Average	0.6	7.4	5.4	0.7
Mal3	2.4 ± 0.3	29.8 ± 3.2	29.2 ± 0.8	1.0
Mal4	2.6 ± 0.3	32.2 ± 4.0	37.0 ± 1.1	1.2

TABLE IX. URANIUM CONCENTRATION OBTAINED BY LF COMPARED WITH GS FOR SOME CEMENT SAMPLES

Sample Code	U-conc.in ppm (mg/g) using LF technique	U-conc.in Bq.kg ⁻¹ using LF technique	U-activity in Bq.kg ⁻¹ using GS technique	U _{GS} / U _{LF}
CH1	1.4 ± 0.3	17.4 ± 4.2	15.3 ± 0.5	0.9
CH2	2.1 ± 0.4	26.0 ± 4.9	24.3 ± 0.8	0.9
CH3	1.8 ± 0.4	22.3 ± 4.4	25.1 ± 0.8	1.1
CT1	2.1 ± 0.4	26.0 ± 4.8	29.9 ± 1.0	1.2
CS1	1.3 ± 0.3	16.1 ± 3.7	22.3 ± 0.7	1.4
CKO	1.7 ± 0.3	21.1 ± 4.1	25.0 ± 0.8	1.2
CKt	2.2 ± 0.4	27.3 ± 4.8	33.2 ± 1.0	1.2
Average	1.8	22.3	25.0	1.1
CKI	3.1 ± 0.5	38.4 ± 5.7	42.7 ± 1.3	1.1
CTI	6.1 ± 0.9	75.6 ± 10.9	103 ± 2.8	1.4
CHI	9.3 ± 1.1	115 ± 13.2	150 ± 4.0	1.3

TABLE X. URANIUM CONCENTRATION OBTAINED BY LF COMPARED WITH GS FOR SOME CLAY BRICK SAMPLES

sample	U-conc.in ppm (mg/g) using LF technique	U-conc.in Bq.kg ⁻¹ using LF technique	U-activity in Bq.kg ⁻¹ using GS technique	U_{GS} / U_{LF}
CIB1	1.3 ± 0.2	16.1 ± 2.5	17.5 ± 0.8	1.1
CIB5	1.7 ± 0.2	21.1 ± 3.0	23.0 ± 0.9	1.1
CIB8	1.9 ± 0.3	23.6 ± 3.6	21.3 ± 0.9	0.9
CIB10	1.3 ± 0.2	16.1 ± 2.7	23.7 ± 0.9	1.5
CIB11	1.4 ± 0.2	17.4 ± 2.7	23.4 ± 0.8	1.3
CIB16	2.1 ± 0.3	26.0 ± 3.3	30.7 ± 1.0	1.2
Average	1.6	19.8	23.3	1.2
CIB20	1.6 ± 0.3	19.8 ± 3.2	19.8 ± 1.1	1.0
CIB21	4.2 ± 0.6	52.1 ± 7.4	54.8 ± 1.6	1.1

TABLE XI. URANIUM CONCENTRATION OBTAINED BY LF COMPARED WITH GS FOR SOME CEMENT BRICK SAMPLES

Sample Code	U-conc.in ppm (mg/g) using LF technique	U-conc.in Bq.kg ⁻¹ using LF technique	U-activity in Bq.kg ⁻¹ using GS technique	U_{GS} / U_{LF}
CeB1	1.2 ± 0.2	14.9 ± 2.8	15.0 ± 0.5	1.0
CeB2	0.5 ± 0.1	6.2 ± 1.5	9.6 ± 0.5	1.6
CeB7	0.8 ± 0.2	9.9 ± 2.0	10.2 ± 0.4	1.0
Average	0.8	9.9	11.6	1.2

TABLE XII. URANIUM CONCENTRATION OBTAINED BY LF COMPARED WITH GS FOR SOME SAND BRICK SAMPLES

Name of factory	U-conc.in ppm (mg/g) using LF technique	U-conc.in Bq.kg ⁻¹ using LF technique	U-activity in Bq.kg ⁻¹ using GS technique	U_{GS} / U_{LF}
SB1	0.7 ± 0.1	8.7 ± 1.2	10.1 ± 0.4	1.2
SB4	0.5 ± 0.1	6.2 ± 1.1	6.8 ± 0.4	1.1
SB6	0.6 ± 0.1	7.4 ± 1.3	7.8 ± 0.4	1.1
SB8	0.6 ± 0.1	7.4 ± 1.1	9.4 ± 0.5	1.3
Average	0.6	7.4	8.5	1.2

TABLE XIII. URANIUM CONCENTRATION OBTAINED BY LF COMPARED WITH GS FOR SOME TILE SAMPLES

Sample Code	U-conc.in ppm (mg/g) using LF technique	U-conc.in Bq.kg ⁻¹ using LF technique	U-activity in Bq.kg ⁻¹ using GS technique	U _{GS} / U _{LF}
TNC1	0.7 ± 0.1	8.7 ± 1.5	7.8 ± 0.3	0.9
TNC2	0.7 ± 0.1	8.7 ± 1.4	8.0 ± 0.4	0.9
TR5	0.9 ± 0.1	11.2 ± 1.6	10.1 ± 0.4	0.9
TS4	0.8 ± 0.1	9.9 ± 1.5	10.2 ± 0.5	1.0
TS5	0.5 ± 0.1	6.2 ± 1.1	7.7 ± 0.4	1.2
TH5	1.0 ± 0.1	12.4 ± 1.7	10.8 ± 0.4	0.9
TH6	1.3 ± 0.2	16.1 ± 1.9	15.3 ± 0.6	1.0
THG	1.1 ± 0.1	13.6 ± 1.7	12.0 ± 0.6	0.9
Average	0.9	11.2	10.2	0.9

TABLE XIV. URANIUM CONCENTRATION OBTAINED BY LF COMPARED WITH GS FOR SOME CERAMIC SAMPLES

Name of ceramic sample	U-conc.in ppm (mg/g) using LF technique	U-conc.in Bq.kg ⁻¹ using LF technique	U-activity in Bq.kg ⁻¹ using GS technique	U _{GS} / U _{LF}
CrG	2.3 ± 0.4	28.5 ± 5.1	44.0 ± 1.6	1.5
CrC	2.2 ± 0.3	27.3 ± 3.4	41.7 ± 1.6	1.5
CrL	2.6 ± 0.4	32.2 ± 5.4	53.0 ± 1.5	1.6
CrA	3.4 ± 0.5	42.2 ± 6.0	60.7 ± 1.9	1.4
CrM	3.2 ± 0.5	39.7 ± 6.1	54.1 ± 1.9	1.4
CrAh	2.7 ± 0.4	33.5 ± 5.4	53.5 ± 1.8	1.6
CrF	2.7 ± 0.5	33.5 ± 6.4	58.4 ± 2.0	1.7
Average	2.7	33.5	52.2	1.6

ACKNOWLEDGEMENTS

This work was partially supported by the IAEA through the Research Contract 7/29/RB. The authors are appreciated to the chairman of NCNSRC and the members of CLERMIT for their support.

REFERENCES

- [1] UNSCEAR, United Nations Scientific Committee on the Effects of Atomic Radiation, Exposures from Natural Sources of Radiation, Forty-second session of UNSCEAR Vienna, 17 to 28 May (1993).
- [2] EL-TAHAWY, M.S. et al., Radioactive Analysis of Building Materials in Central Region of Egypt, Nuclear Science Journal 32, No.4 (1995) 322-329.
- [3] A. GHODS, et al., Determination of Uranium in Biological Materials by Laser Fluorimetry, Radiochimica Acta 50 (1990) 155-158.
- [4] MUKHTAR, O.M., GHODS A., KHANGI, F.A., Determination of Uranium in Soil and Biological Material in Sudan by Laser Fluorimetry, and Comparison with γ - Spectrometric Results for Ra-226, Radiochemica Acta 54 (1991) 201-203.
- [5] HIGGY, R.H., Measurement and Analysis of Natural Radioactivity in Building Materials and Evaluation of its Environmental Impact, PhD Thesis, Ain Shams University, Cairo (1995).



PRELIMINARY USE OF URANIUM EXPLORATION DATA IN ENVIRONMENTAL STUDIES IN GREECE

N. KARISTINEOS

Institute of Geology and Mineral Exploration,
Athens, Greece

Abstract

The UNDP/IAEA Uranium Exploration project in Northern Greece which started back in 1971, was the first source of the referred data. This car-borne survey (CBS) project covered 2/10 of the country. It was followed by a similar project of the Greek Atomic Energy Commission (GAEC) that covered the remaining 8/10. The whole country coverage took more than 12 years to be completed and the data collected were used for the delineation of potential areas for uranium exploration. After the completion of the Uranium Research project, data and personnel were transferred from GAEC to the Institute of Geology & Mineral Exploration (IGME). During the last years there was an increasing environmental awareness concerning the risks from radon emanation in buildings. Research results indicated that the referred data combined with relative geological and environmental records could be used as a good predictive tool for the definition of high radon areas. Therefore it is used for the preparation of a geologic radon potential map of Greece. The preliminary results of this effort are presented here. Furthermore additional data obtained from the follow up phases of the initial uranium exploration project are used by IGME today as a guide to specific environmental studies conducted in various parts of Greece. The most recent example is the case of uranium hydro geochemistry of the Serres basin area (northern Greece).

INTRODUCTION

The first and largest task is the establishment of radon maps using the radiometric data obtained during the Uranium Exploration Programme of Greece. The collection of data started with the UNDP-IAEA programme and was completed and financed by the Greek government.

The project started in 1971 and its aim was to delineate areas presenting a potential for uranium exploration in northern Greece. Radiometric data were collected through a car-borne survey. 41 000 km were surveyed with a car running at an average speed of 10 km/h. This corresponds to one measurement per square kilometre.

Prior to the car-borne survey (in 1980-81) attempts were also made to use airborne surveys instead of car-borne surveying. However, the results were poor due to mountainous terrains that did not allow to maintain a constant flight height.

Right from the beginning computer systems were used to express the results. The results were rather coarse with regard to current standards but then they looked great. Presenting the anomalies found, remained the goals for many years.

THE SURVEY

Regional radiometric maps were compiled. The major problem encountered in this compilation was the co-ordination system used for the initial data.

The first instrument used for the car-borne survey was the French scintillometer SPP-2 with a two inches crystal. Later it was replaced by a spectrometer equipped with a 6 inches crystal. Both instruments gave cps (count per second) values.

An area of 80 km² was surveyed with both instruments used simultaneously to allow correlation and calibration. Data were compared statistically and the results of this comparison

indicated that the two crystals represent a good correlation. When a regression with an exponential model is used, the correlation coefficient is 0.919.

An attempt has also been made to convert the CBS data into SI units. The reason for this is to be able to produce maps with the same units as those used in neighbouring countries.

The major goal of the compilation of CBS data is to produce radon maps. For this purpose additional information is needed such as geochemical information obtained through stream sediments sampling. The stream sediments were analysed for uranium and nine other elements. A radiometric reading was also taken for each sample. The number of sediments collected did not exceed 20 000. Radon samples in soils were also collected and so far amount to 1440 over the entire country.

For the compilation of the radon maps the rules which will be applied follow the general co-evaluation of four parameters:

- existing radon measurements
- radiometric data
- geology
- soil permeability and
- foundation type

A confidence index matrix similar to the one used by the USGS in the relevant US project will be applied.

RADIONUCLIDES IN WATER

In the course of the project many measurements of water samples were made. Their aim then was to determine the pathway of uranium transporting agents. No evidence was given to the environmental value of these measurements. No maximum concentration limit for uranium or radon in water were known. After adoption by the EPA in 1992 of a MCL of 20 ppb for uranium in water, all these studies are really useful for public health issues. Considering that many of the sampled wells are used also for pumping drinking water, any high values measured then must be seen today in a different light. This is the case in the Serres basin.

The Serres basin has often been referred to in this context because it was considered a model project from many points of view. The hydrogeochemistry of uranium performed in this area shows that there are many wells with water containing 30–90 ppb U. Subsequently high values were obtained for the radon contents of the water.

It must be mentioned that large parts of the areas of high radioactivity were excluded from the hydrogeochemistry sampling. Today a programme aiming at the reduction of uranium and radon contents in drinking water has been initiated.

It must be mentioned further that parts of the pilot plant used for the initial experimental treatment of uranium ore will be used today for the uranium removal from household waters of the area.

LIST OF PARTICIPANTS

Åkerblom, G.	Division of Ionizing Radiation, Swedish Radiation Protection Institute, P.O. Box 60204, S-104 01 Stockholm, Sweden
Ammar, A.A.	Nuclear Materials Authority of Egypt, P.O. Box 530, El Maadi, Cairo, Egypt
Angsuwathana, P.	Department of Mineral Resources, Ministry of Industry, Rama VI Road, Bangkok 10400, Thailand
Ball, T.K.	Kingsley Dunham Centre Keyworth, British Geological Survey, Nottingham NG12 5GG, United Kingdom
Barakat, M.B.F.	Arab Atomic Energy Agency, P.O. Box 402 Almenzah, 1004 Tunis, Tunisia
Barthel, F.	Bundesanstalt für Geowissenschaften und Rohstoffe, Postfach 510153, D-30631 Hannover, Germany
Bashir, S.S.	Jordan Phosphate Mines Co., P.O. Box 30, Amman, Jordan
Bertel, E.	Nuclear Development Division, OECD/NEA, Le Seine St. Germain, 12 Boulevard des Iles, F-92130 Issy-les-Moulineaux, France
Bojkov, I.	Committee of Energy, 8, Triadiza Str., 1040 Sofia, Bulgaria
Bourgeois, C.	CEA Valduc, Service de protection contre les rayonnements, F-21120-Is-sur-Tille, France
Cambon, R.	GME, 11 Square Esquirol, F-94000 Creteil, France
Camus, H.	CEA/B3 DAM/DDS, Bp. No. 12, F-91680 Bruyère-le-Chatel, France
Cerník, M.	AQUATEST, Jablonecká 8, 46001 Liberec, Czech Republic
Chatagnon, B.	ARPE Logging Systems, 70 Avenue des Martyres, F-3800 Grenoble, France
Chotikanatis, P.	Dept. of Mineral Resources, Economic Geology Division, Rama VI Rd., Bangkok 10400, Thailand

- Dahlkamp, F.-J. Ölbergstraße 10, Lissen,
D-53343 Wachtberg/Bonn, Germany
- Daoud, M.N. Natural Resources Authority,
Ministry of Energy and Mineral Resources,
P.O. Box 140027, Amman, Jordan
- Darnley, A.G. Geological Survey of Canada,
601 Booth Street, Ottawa, Ontario K1A 0E8, Canada
- El-Tahawy, M.S. National Centre for Nuclear Safety and Radiation Control,
P.O. Box 7551, 11762 Cairo, Egypt
- Elsirafy, A.M. Nuclear Materials Authority of Egypt,
P.O. Box 530, El Maadi, Cairo, Egypt
- Fernandez Amigot, J.A. ENUSA S.A.,
Santiago Rusiñol, 12, E-28040 Madrid, Spain
- Föhse, H.M. Dahlienstraße 4, D-53359 Rheinbach, Germany
- Grosz, A.E. United States Geological Survey,
National Center, Mail Stop 954,
Reston, VA 22092, United States of America
- Guermentchuk, M.G. Committee for Hydrometeorology,
Centre of Radiation and Environment Monitoring,
16, Komsomolskay St., Minsk, 220050, Belarus
- Höschl, V. PICODAS Praha Ltd.,
Geologická 2, 152 00 Praha 2, Czech Republic
- Jubeili, Y. Syrian Atomic Energy Commission, SAEC ,
P.O. Box 6091, Damascus, Syrian Arab Republic
- Kancheva, A.R. Airborne Geophysical Survey,
23, Sytnyakove Blvd., 1505 Sofia, Bulgaria
- Karistineos, N. Institute of Geology and Mineral Exploration, GME,
70 Messogion Str., Athens 115-27, Greece
- Kazakov, A. All-Russian Research Institute of Chemical Technology,
Kashirskoe shosse 33, 115409, Moscow, Russian Federation
- Kerbelov, L. Airborne Geophysical Surveys Limited,
23, Sytnyakovo Blvd., 1505 Sofia, Bulgaria
- Likar, B. Mine Zirovski VRH,
Todraz 1, SLO-64 224 Gorenja Vas, Slovenia

Logar, Z.	Mine Zirovski VRH, Todraz 1, SLO-64 224 Gorenja Vas, Slovenia
Lokobauer, N.	Institute for Medical Research and Occupational Health, Ksaverska cesta 2, HR-100001 Zagreb, Croatia
Mamont-Ciesla, K.A.	Central Laboratory for Radiological Protection, ul. Konwaliowa 7, PO-03-194 Warsaw, Poland
Matolín, M.	Department of Applied Geophysics, Faculty of Science, Charles University, Albertov 6, 128 43 Prague 2, Czech Republic
Medici, F.	Institute of Geophysics, ETH Hoenggerberg, CH-8092 Zurich, Switzerland
Milojević, M.	Geoinstitut, Rovinjska 12, YU-11000 Belgrade, Yugoslavia
Moupic, Z.	DIAMO, s.p., Máchova 201, Stráž pod Ralskem 471 27, Czech Republic
Munnink, J.O.	IWACO B.V., Hoofdweg 490, P.O. Box 8520, NL-3009 AM Rotterdam, Netherlands
Nath Kak, S.	Atomic Minerals Division, Department of Atomic Energy, 1-10-153/156 Begumpet, Hyderabad 500 016, India
Nicolet, J.-P.	Division of Nuclear Power and the Fuel Cycle, International Atomic Energy Agency, Wagramerstrasse 5, P.O. Box 100, A-1400 Vienna, Austria
Novák, J.	DIAMO, s.p., Máchova 201, Stráž pod Ralskem 471 27, Czech Republic
Oberlerchner, G.	Geological Survey of Austria, Rasumofskygasse 23, A-1031 Vienna, Austria
Oppon, O.C.	National Nuclear Research Institute, P.O. Box 80, Legon Ghana
Pavlik, B.	PICODAS GROUP Inc., 100 West Beaver Creed Rd., Unit 8, Richmond Hill, Ontario, L4B 1H4, Canada

- Pečcnik, M. Slovenian Nuclear Safety Administration,
Vojkova 59, SLO-1000 Ljubljana, Slovenia
- Pushkarev, A.V. State Scientific Center of Environmental Radiogeochemistry,
IGMOF, NAS Ukraine,
34 Paladina av., Kiev, Ukraine
- Renner, J. Eötvös Loránd Geophysical Institute of Hungary,
Columbus u. 17-23, H-1147 Budapest, Hungary
- Ruhrmann, G. Uranerzbergbau GmbH,
Kölner Strasse 38-44, D-50389 Wesseling, Germany
- Saad, S. Comissao Nacional de Energia Nuclear CNEN/COMAP,
Rua General Severiano, 90, Botafogo 22290-040, Brazil
- Shirav-Schwartz, M. Geological Survey of Israel,
30 Malkhei Israel St., Jerusalem 955501, Israel
- Siehl, A. Geologisches Institut, Universität Bonn,
Nußallee 8, D-53115 Bonn, Germany
- Smetana, J. DIAMO, s.p.,
Máchova 201, Stráž pod Ralskem 471 27, Czech Republic
- Stoje, V. DIAMO, s.p.,
Máchova 201, Stráž pod Ralskem 471 27, Czech Republic
- Strezelecki, R. Panstwowy Instytut Geologiczny,
Polish Geological Institute,
4, Rakowiecka, 00-975 Warsaw, Poland
- Štrumberger, V. Geoinstitut,
Rovinjska 12, YU-11000 Belgrade, Yugoslavia
- Torres de Mendonça, L.M. Instituto Geológico e Mineiro,
Estrada da Portela, P-2720 Alfragide, Portugal
- Tusveld, M.C.L. IWACO B.V.,
Hoofdweg 490, P.O. Box 8520,
NL-3009 AM Rotterdam, Netherlands
- Underhill, D.H. Division of Nuclear Power and the Fuel Cycle,
International Atomic Energy Agency,
Wagramerstrasse 5, P.O. Box 100,
A-1400 Vienna, Austria
- Urquhart, W.E. High-Sense Geophysics Ltd.,
47 Jefferson Avenue, Toronto, Ontario M6K 1Y3, Canada

Vulkan, U.	Soreq Nuclear Research Center, Yavne 81800, Israel
Wardaszko, T.	Central Laboratory for Radiological Protection, ul. Konwaliowa 7, 03-194 Warsaw, Poland
Yegani, F.-S.	Exploration Division, Atomic Energy Organization, North Kargar Ave, Tehran, Islamic Republic of Iran
Zahorowski, W.	Australian Nuclear Science and Technology ANSTO, New Illawarra RD, Menai 2234, Australia
Zettwoog, P.	Office de protection contre les rayonnements ionisants, 31, rue de l'écluse, F-78110 Le Vésinet, France